



## City Research Online

### City, University of London Institutional Repository

---

**Citation:** Wilkinson, S.A. (1989). Aspects of radiation curing. (Unpublished Doctoral thesis, City University London)

This is the accepted version of the paper.

This version of the publication may differ from the final published version.

---

**Permanent repository link:** <https://openaccess.city.ac.uk/id/eprint/7720/>

**Link to published version:**

**Copyright:** City Research Online aims to make research outputs of City, University of London available to a wider audience. Copyright and Moral Rights remain with the author(s) and/or copyright holders. URLs from City Research Online may be freely distributed and linked to.

**Reuse:** Copies of full items can be used for personal research or study, educational, or not-for-profit purposes without prior permission or charge. Provided that the authors, title and full bibliographic details are credited, a hyperlink and/or URL is given for the original metadata page and the content is not changed in any way.

ASPECTS OF  
RADIATION CURING

THE CITY UNIVERSITY, LONDON  
DEPARTMENT OF CHEMISTRY

ASPECTS OF  
RADIATION CURING

By

SUSAN ANNE WILKINSON

A thesis submitted for the degree of Doctor of Philosophy  
in the Faculty of Science of The City University, London.

(1989)

## CONTENTS

<u>Chapter 1</u>	<u>INTRODUCTION : EB CURING</u>	1
	The state of the art	5
	Radiation chemistry	9
	Interaction of photons with matter	11
	Photoelectric effect	11
	The Compton effect	12
	Pair production	13
	Interactions of charged particles	14
	Electrons	15
	Radiative processes	15
	Elastic collisions	15
	Inelastic collisions	16
	Charged particles	19
	Track structure	20
	Primary products	23
	Excited species	25
	Cations	27
	Spur processes	27
	Reactions	28
	Fragmentation and isomerisation	29
	Ion-molecule reactions	29
	Charge transfer	30
	Electrons and negative ions	30
	Spur processes	30
	Reactions	32
	Non-dissociative electron capture	32



Dissociative electron capture	33
Radiation induced polymerisation	33
Free radical polymerisation	34
Initiation	34
Propagation	35
Termination	35
Rate of polymerisation	38
Irradiation of polymers	40
Electron beam generators	43
Radiation curable materials	45
Prepolymers	46
Unsaturated polyester systems	47
Acrylated polyesters	48
Acrylated epoxy resins	49
Acrylated polyurethanes	50
Acrylated polyethers	51
Monomers/diluents	51
Vinyls	52
Acrylates	53
Formulation	55
Surface levelling	55
Mechanical properties	55
Chemical resistance	57
Gloss	57
Adhesion	58
Pigmentation	59
Cure response of a system	59
Dose of radiation, film thickness and	60

substrate relationship	
Atmosphere	62
Applications	63
References	65
<u>Chapter 2</u> QUANTITATIVE ANALYSIS OF CURE BY FTIR-PA	70
SPECTROSCOPY	
Introduction	72
Fourier Transform spectroscopy	74
Photoacoustic Spectroscopy	79
Quantitative analysis of cure using	83
FTIR-PAS	
Results and discussion	86
Conclusion	90
Experimental	91
Appendix A	94
References	101
<u>Chapter 3</u> ELECTRON BEAM INDUCED POLYMERISATION OF	103
ORGANOTINACRYLATE FILMS	
Introduction	105
Organocarboxylates	111
Synthesis	111
Structure and bonding	112
Hydrolytic stability	113
Organostannyl radicals	114
Results and Discussion	116
Conclusion	131
Acknowledgements	133
Experimental	134

<b><u>Chapter 4</u></b>	<b>ELECTRON BEAM AND UV INDUCED POLYMERISATION OF</b>	<b>148</b>
	<b>SILICON CONTAINING ACRYLATES</b>	
	Introduction	150
	Results and Discussion	156
	a) Electron beam induced	156
	polymerisation of silicon	
	containing acrylates	
	b) UV induced polymerisation of	167
	silicon containing acrylates	
	Conclusion	175
	Acknowledgements	176
	Experimental	177
	Appendix A	195
	Appendix B	201
	References	207
<b><u>Chapter 5</u></b>	<b>EFFECT OF ADDITIVES UPON ELECTRON BEAM INDUCED</b>	<b>209</b>
	<b>POLYMERISATION OF ISODECYL ACRYLATE</b>	
	Introduction	211
	Radical cations	212
	Electrons	214
	Excited states	216
	Results and Discussion	220
	Conclusion	236
	Experimental	237
	References	240

<b><u>Chapter 6</u></b>	<b>ELECTRON BEAM INDUCED POLYMERISATION OF AROMATIC</b>	<b>242</b>
	<b>ACRYLATES</b>	
	Introduction	244
	Results and discussion	249
	Conclusion	254
	Experimental	255
	References	261
<b><u>Chapter 7</u></b>	<b>INTRODUCTION: CATIONIC POLYMERISATION OF</b>	<b>262</b>
	<b>EPOXIDES</b>	
	The state of the art	265
	Cationic polymerisation	268
	Cationic initiators	272
	Protonic acids	272
	Lewis acids (Friedel Crafts catalysts)	274
	Onium salts	275
	Diazonium salts	275
	Iodonium and sulphonium salts	277
	a) Direct photolysis	278
	b) Photoinduced electron transfer	283
	between donor and onium salts	
	c) Electron transfer between nucleo-	284
	philic radicals and onium salts	
	Organometallic initiators	285
	<b>ELECTRON BEAM INDUCED POLYMERISATION OF</b>	<b>287</b>
	<b>EPOXIDES</b>	
	Introduction	287
	Factors affecting the rate and the degree	289

of polymerisation of epoxides	
Characteristics of epoxide films	290
Results and Discussion	292
Conclusion	309
Experimental	311
Appendix A	317
DIRECT AND INDIRECT UV INDUCED POLYMERISATION	322
OF EPOXIDES	
Introduction	322
Results and Discussion	324
Conclusion	331
Experimental	332
ELECTRON BEAM AND UV INDUCED POLYMERISATION OF	335
6,7-EPOXY-3,7-DIMETHYLOCTYL ACRYLATE	
Introduction	335
Results and Discussion	337
Conclusion	345
Acknowledgements	346
Experimental	347
References	350

## ACKNOWLEDGEMENTS

I would like to thank Professor R. Stephen Davidson, most sincerely, for giving me the opportunity to read for a higher degree and for all the guidance, encouragement and enthusiasm he has shown me throughout this project. I am also indebted to him for his help and patience in proof reading this script.

I would also like to thank Dr. Richard Ellis and Dr. Richard Batten for all their advice, practical help and friendship.

I am grateful to both the SERC and Wiggins Teape Research and Development Group for funding this project.

Last but not least, I would like to thank my fellow colleagues for their frien<sup>d</sup>ship and kindness.



## DECLARATION

The experimental work in this Thesis has been carried out by the author in the laboratories of the Chemistry Department of The City University, London and Wiggins Teape Research and Development Laboratories, Beaconsfield between 1st March 1984 and 31st December 1988. This work has not been presented and is not being presented for any other degree.

Susan Wilkinson

March 1989

The City University, London.

To my parents

## ABSTRACT

The electron beam induced polymerisation of dialkyltin diacrylates, as well as the UV and electron beam induced polymerisation of some novel silicon containing acrylates are discussed. The reactivity and film forming properties of these materials are compared with that of some commercial diluents such as, tripropyleneglycol diacrylate, TPGDA and trimethylolpropane triacrylate, TMPTA. Mechanistic studies concerning the initiation of free radical polymerisation of the acrylate ester, isodecylacrylate, IDA on electron beam irradiation are presented. Addition of electron and hole scavengers revealed that slow electrons contribute significantly to the initiation of electron beam induced polymerisation of acrylate esters. The film forming properties of phenyl acrylate and mono-, di- and tri- halophenyl acrylates on exposure to electron beam irradiation are evaluated in terms of their ability to produce tackfree films. The sensitivity of catechol diacrylate compared with t-butyl catechol diacrylate is also presented. Mechanistic studies concerning the initiation of both UV and electron beam induced cationic polymerisation of 3,4-epoxycyclohexylmethyl-3',4' -epoxycyclohexanecarboxylate, with the aid of diphenyliodonium hexafluorophosphate, tri-phenylsulphonium hexafluorophosphate and ( $n^5$ -2,4-cyclopentadien-1-yl) [(1,2,3,4,5,6-n) (-I-methylethyl) benzene] -iron(I+) hexafluorophosphate, as well as the radiolysis of 6,7-epoxy-3,7-dimethyloctylacrylate in the presence of diphenyliodonium hexafluorophosphate are presented. The decomposition of the salts was monitored in situ by infrared and UV spectroscopy and hydrogen fluoride is credited as the true initiator of the cationic polymerisation of epoxides in an open system. The UV photolysis of the aforementioned onium salts led to the production of volatiles, resulting in the polymerisation of thin films of 3,4-epoxycyclohexylmethyl-3',4' - epoxycyclohexanecarboxylate, providing further evidence of hydrogen fluoride evolution. The use of FTIR- photoacoustic spectroscopy was proven to be an invaluable tool in monitoring the polymerisation of thin epoxide or acrylate films on an opaque substrate.







## Chapter 1   INTRODUCTION : EB CURING

The state of the art	5
Radiation chemistry	9
Interaction of photons with matter	11
Photoelectric effect	11
The Compton effect	12
Pair production	13
Interactions of charged particles	14
Electrons	15
Radiative processes	15
Elastic collisions	15
Inelastic collisions	16
Charged particles	19
Track structure	20
Primary products	23
Excited species	25
Cations	27
Spur processes	27
Reactions	28
Fragmentation and isomerisation	29
Ion-molecule reactions	29
Charge transfer	30
Electrons and negative ions	30
Spur processes	30
Reactions	32
Non-dissociative electron capture	32
Dissociative electron capture	33
Radiation induced polymerisation	33



Free radical polymerisation	34
Initiation	34
Propagation	35
Termination	35
Rate of polymerisation	38
Irradiation of polymers	40
Electron beam generators	43
Radiation curable materials	45
Prepolymers	46
Unsaturated polyester systems	47
Acrylated polyesters	48
Acrylated epoxy resins	49
Acrylated polyurethanes	50
Acrylated polyethers	51
Monomers/diluents	51
Vinyls	52
Acrylates	53
Formulation	55
Surface levelling	55
Mechanical properties	55
Chemical resistance	57
Gloss	57
Adhesion	58
Pigmentation	59
Cure response of a system	59
Dose of radiation, film thickness and substrate relationship	60
Atmosphere	62



Applications	63
References	65

## INTRODUCTION : EB CURING

### The state of the art

The growth of the radiation-curable surface coatings industry is a direct result of several influential factors. Firstly, legislation concerning environmental pollution control, with regards to air and water pollution, and secondly, increased production costs together with limited fuel and solvent availability, all provided the necessary impetus to search for alternative methods for producing coatings. Several techniques were developed to meet the criteria of low energy consumption and negligible environmental pollution. These are collectively known as radiation curable coating systems and comprise mainly of ultraviolet (UV), electron beam (EB), infrared, radio-frequency and microwave radiation techniques. By far the most popular method of producing surface coatings is by ultraviolet radiation. The use of EB technology in this field has not yet been fully realised. The slow development of EB curing as a viable mode of producing surface coatings may be attributed to firstly, the high cost of equipment and secondly, competition from the already well established process of UV curing, both in terms of its underlying scientific principles and technology involved [1-3].

Although, the capital cost of an EB production unit is higher than equivalent UV curing equipment, the development of less expensive, energy efficient and simplified 'low

energy' EB units have helped to narrow this gap [4,5]. The high costs of EB units may however be offset by the economic gains that can be reaped from an EB production line, as opposed to conventional stoving and UV processing systems. Typical energy requirements to cure a coating of width 1m are 20 kWatts at speeds of 50 and 300mpm according to the radiation dose required by the formulation. These low energy requirements together with the ability to 'tune' the energy supply to effect complete polymerisation and crosslinking, help to minimise energy loss to the substrate. The absence of an initiator component to promote polymerisation, and insensitivity towards the UV/visible absorption characteristics of the coating enables greater latitude in formulating EB systems, consequently highly pigmented and thick films can be cured effectively. The low running costs, high production rates and the lower probability of producing defective products, in conjunction with some of the unique features of EB curing, summarised in Table I, have contributed to the increasing acceptance of EB radiation as a viable alternative to UV curing [3,6-11].

Use of EB radiation as an alternative to traditional curing methods has been demonstrated by its application to many technologies such as, the graphics and magnetic media industries [12].

Both UV and EB curing are dominated by free radical polymerisation and utilise common prepolymers and monomers in the curing process. However, the fundamental difference between EB and UV curing is the mode of initiation. UV



Table I A summary of the advantages and disadvantages of EB curing

Advantages

- High line speeds are possible
- No film thickness limitation
- Low energy consumption
- No initiator required
- Even cure throughout film
- In general pigments do not reduce rate of cure

Disadvantages

- Generally limited to flat surfaces
- Capital cost of equipment high
- Inert atmospheres are generally required for efficient surface cure

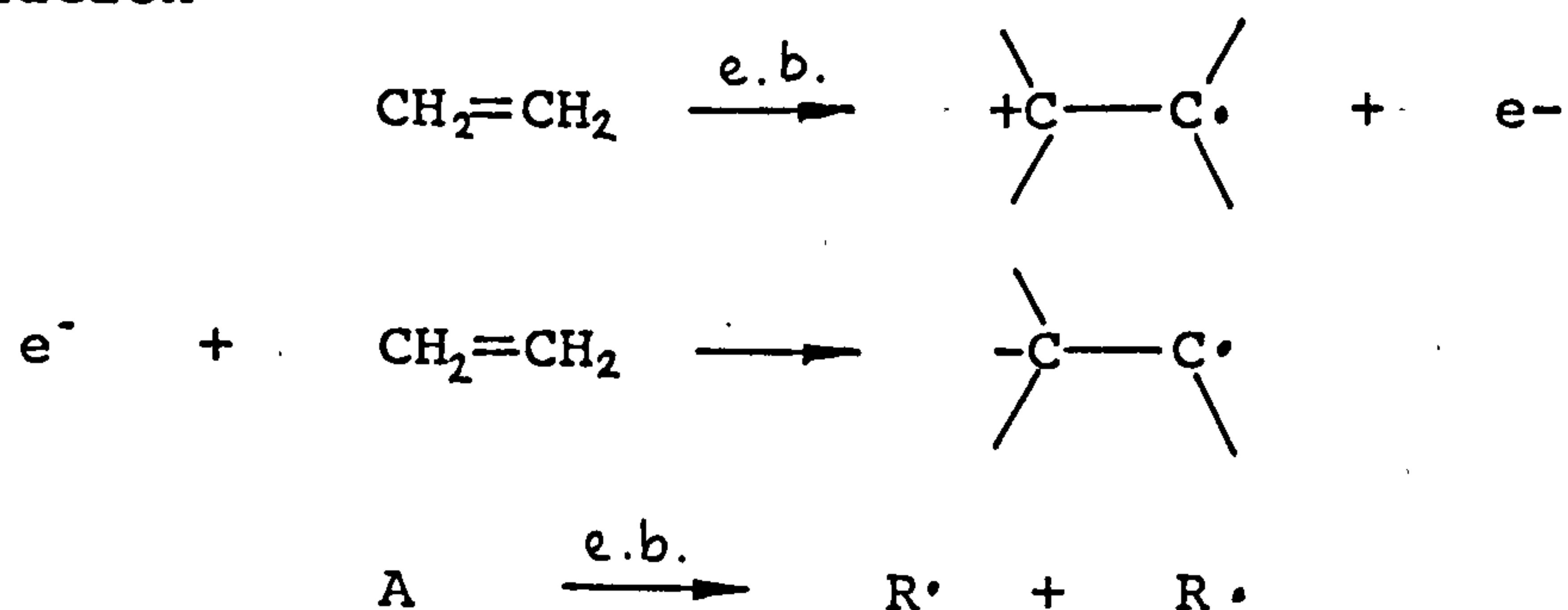
curing formulations not only consist of a prepolymer/monomer mix but also require an additive known as a photo-initiator/sensitiser that is highly reactive towards UV radiation and is capable of producing the initiating radical species required to bring about polymerisation. Conversely, EB curing requires no initiator system. On exposure to an electron beam, radicals are produced 'randomly' throughout the coating [13].

The formation of radicals on EB exposure are not the only primary species produced on irradiation. Other primary products formed on exposure to an electron beam are electrons of a range of energies, cations and anions, and excited states [14].

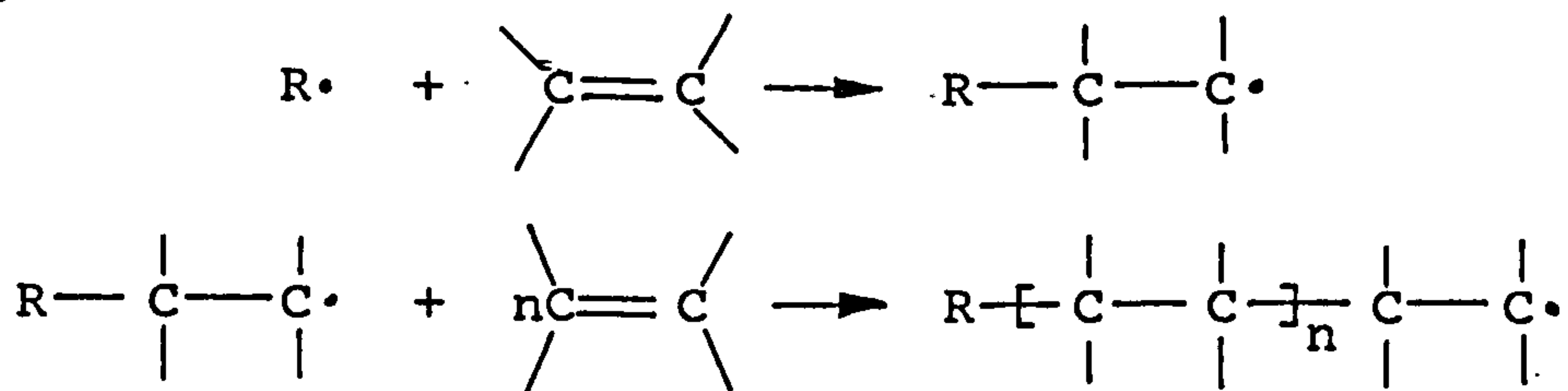
There are three basic steps in the polymerisation process. The first is the formation of 'randomly' distributed initiating radicals by ionising radiation. Once the initiating radical species have been generated it may then add to another monomer molecule giving rise to another radical, resulting in chain growth or propagation. The chain will continue to grow until termination of the growing chain occurs via a combination or disproportionation reaction of two radical chains.

### Scheme 1

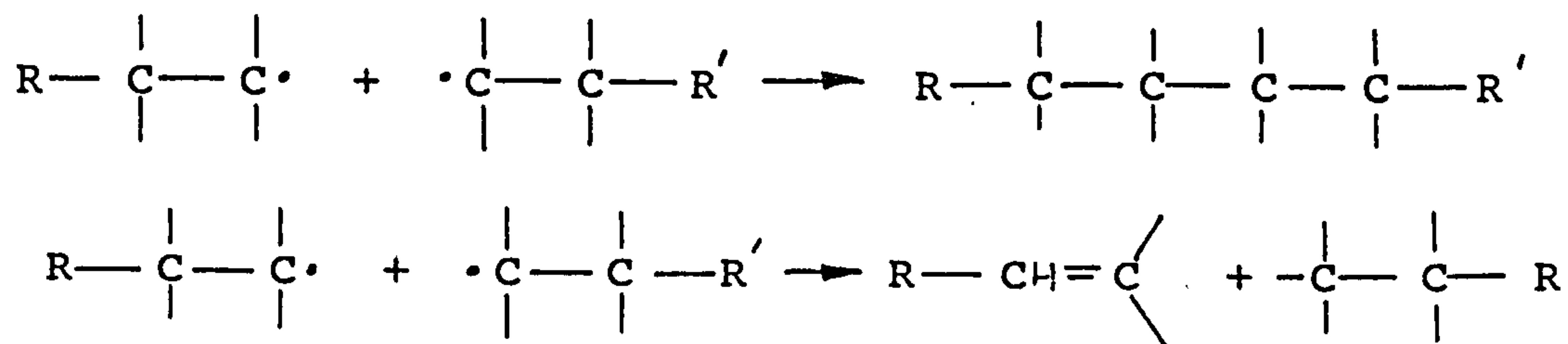
#### Initiation



#### Propagation



#### Termination



EB curable coating compositions are similar to those used by the UV industry [1-3]. They mainly consist of a two component system, comprising a reactive prepolymer and a monomer/reactive diluent. These systems are primarily based on the acrylate functionality due to their high reactivity, low volatility, good solvating powers and the diversity of materials available.

The formulation of coating compositions is very important and will govern not only wetting properties and cure response but also the final film properties. The properties of the film may be characterised by empirical techniques to evaluate chemical resistance, gloss, flexibility, adhesion and hardness [1-3]. However, cure assessments by these techniques are all subjective. Brown [17] has reviewed other objective means of cure assessment of which infrared spectroscopy is one of the most convenient and applied techniques.

### RADIATION CHEMISTRY

Several excellent general radiation chemistry texts have been published [18-21] and some authors have reviewed the radiation chemistry of monomers and polymers [22-25].

Radiation chemistry may be defined as "the interaction of energetic charged particles (electrons, protons, alpha and other heavy particles) and high energy photons (X-rays and  $\gamma$ -rays) with matter" [26]. The result of these interactions are ionisation and excitation of the medium,



hence charged particles, X-rays and  $\gamma$ -rays are appropriately called "ionising radiation".

The primary products produced on exposure to "ionising radiation" are namely, electrons of a range of energies, anions, cations and radicals. The latter species are transformed by various processes leading to the formation of radiation chemical products. The processes and species involved in such chains of events encompass the field of radiation chemistry.

Interaction of "ionising radiation" with matter results in the transfer of energy to the medium and its subsequent effect depends on the dose of radiation. The term "dose" may be applied to either the absorbed dose or the exposed dose. The dose is usually expressed in roentgens (r) or in kilogray (kGy).

The roentgen is the unit of exposed dose of X- or  $\gamma$ -radiation. One roentgen is an exposure dose of X- and  $\gamma$ -radiation such that the associated corpuscular emission per 0.001293g of air produces 1 electrostatic unit of quantity of electricity of either sign, (0.001293g of air in  $1\text{cm}^3$  of air at 760mm torr pressure).

The SI unit of absorbed dose is the Gray (Gy), defined as  $1\text{Gy} = 1\text{J/kg}$ . However, the traditional and still widely used unit is the rad, where  $1\text{Krad} = 10\text{Gy}$ .

Many methods have been established to measure the energy deposited in a medium by ionising radiation [18,19]. Absolute methods involve the direct determination of dose

and include such methods as heat produced in the irradiated medium, or measurement of the ionisation produced in gases using ionisation chambers. Relative methods are often used in practice and include such secondary techniques as chemical dosimeters.

### Interaction of photons with matter

In contrast to "non-ionising" radiation, such as infrared, visible and UV, the absorption of energy derived from "ionising" radiation is governed by the atomic composition and not by the molecular structure of the medium.

The three main processes by which X-rays or  $\gamma$ -rays interact with matter are called respectively, the photoelectric effect, Compton effect and pair production.

#### Photoelectric effect [26,27]

In the photoelectric process, X-rays or  $\gamma$ -rays give up all their energy to an inner shell electron. This results in an ejected electron, known as a photoelectron and has kinetic energy equal to the difference between the energy of the incident photon and the binding energy of the electron in the atom.

$$T = h\nu - I \quad 1$$

where,  $T$  is the acquired kinetic energy of the photoelectron,  $h\nu$  is the energy of the photon and  $I$  is the binding energy of the electron in the atom.

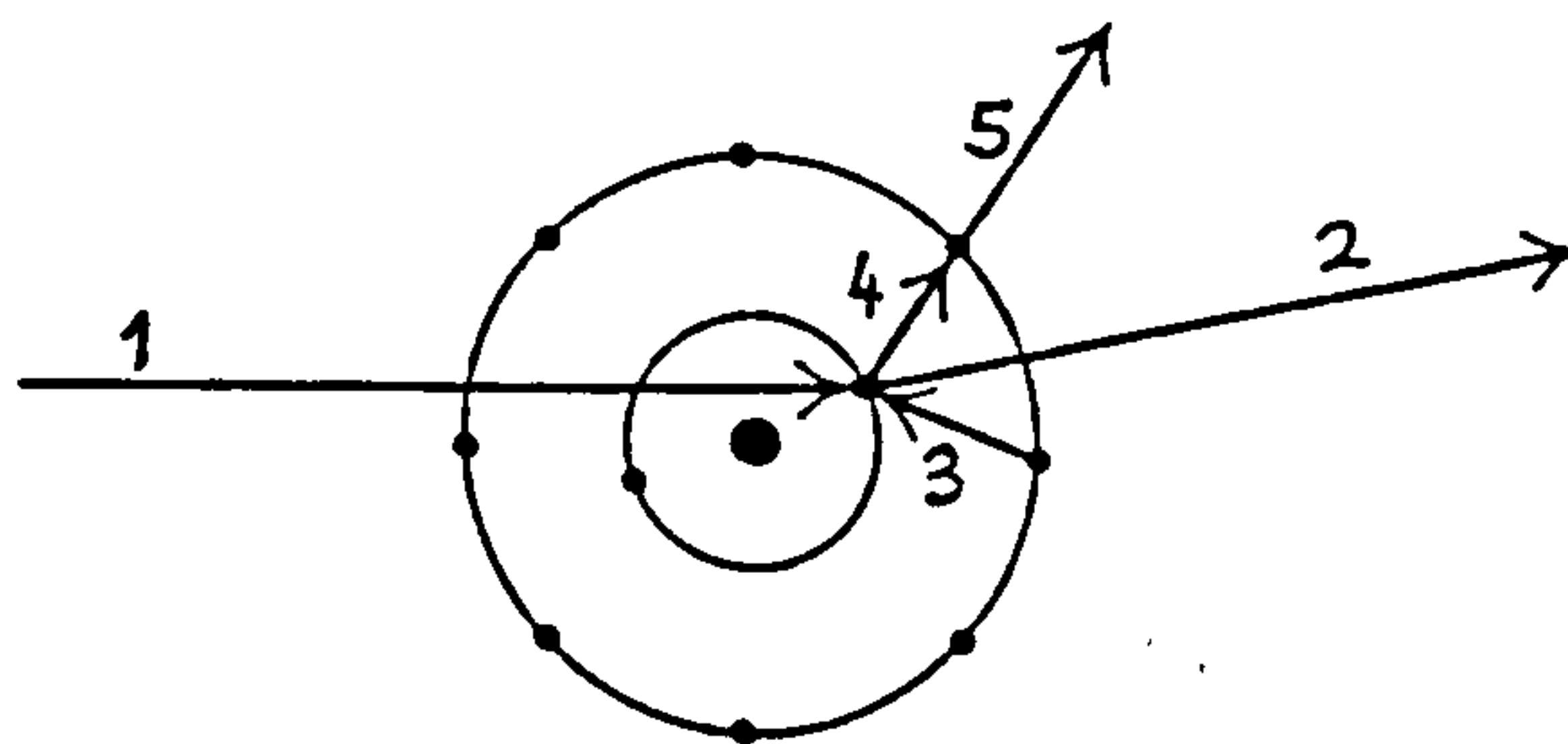
The resulting inner shell vacancy is rapidly filled by

an electron dropping in from an outer shell with expenditure of energy which appears as a photon. If the photon thus generated is of sufficient energy it may eject another electron from the atom. This process is known as the Auger effect and the expelled electron is called an Auger electron.

There is no rigorous theory to describe the photoelectric effect, however, it has been shown empirically that the probability for the photoelectric effect is greatest for atoms of high atomic number and for photons of low energies and predominates at photon energy below 0.1MeV

Photoelectrons produced in liquid and solid phase will be rapidly slowed down within the sample and will result in a 'cascade' of further ionisations.

Figure 1 Typical photoelectric absorption process (1) photon enters atom, (2) electron is ejected from inner shell, (3) vacancy filled by an outer shell electron (4) soft X-ray collides with outer electron (5) electron ejected from outer shell (Auger electron)



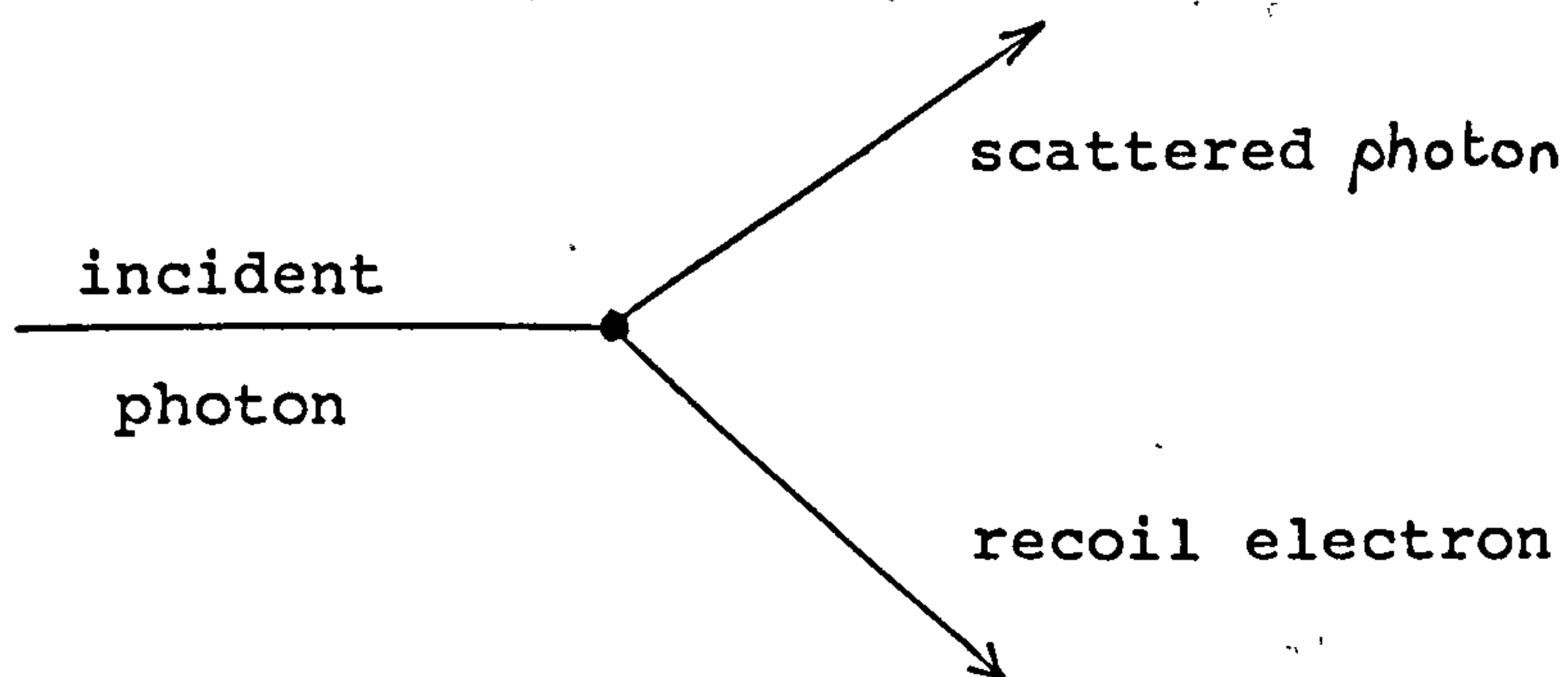
### The Compton effect [26,27]

In contrast to the photoelectric effect, the Compton



effect takes place with the more loosely bound outer shell electrons. These electrons may be considered to be "free electrons" and on absorption of part of the incident photon, are ejected. These ejected electrons are called Compton or recoil electrons. As a result of this interaction, the incident photon is deflected and continues its path with a reduced energy. The Compton effect is the major process of the interaction of photons with matter for energies between 0.1-10 MeV.

Figure 2 Compton scattering process

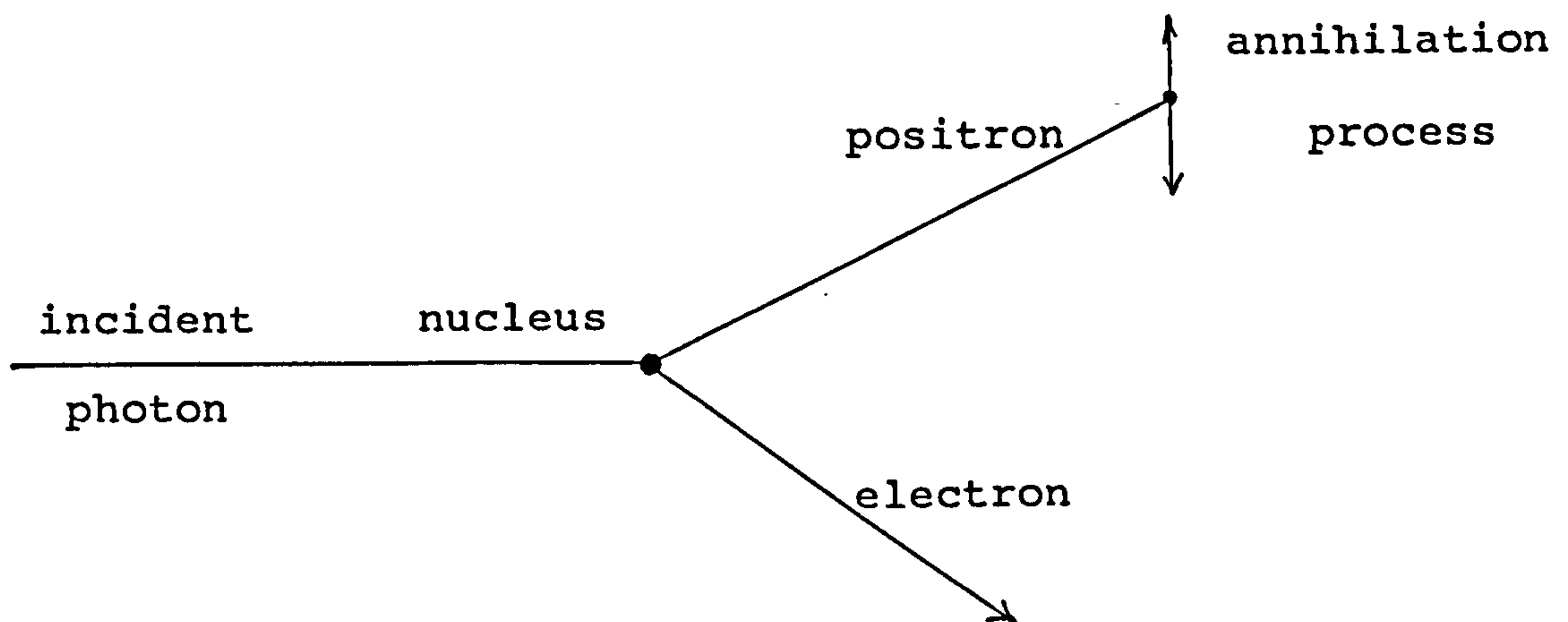


Pair production [26,27]

This process is involved with the interaction of incident photons with the nucleus. This interaction results in the complete disappearance of the incident photon and the formation of a positron-electron pair and is an example of energy being converted into matter.

For pair production to occur the minimum photon energy must be  $>1.02\text{MeV}$ . The total kinetic energy of the positron and electron pair is then the difference of the energy of the incident photon and  $1.02\text{MeV}$ . The positron and electrons

Figure 3 Pair production process



loose energy in the medium, resulting in ionisation and excitation. The annihilation of the positron with an electron has finite probability as it slows down, and usually results in the production of two photons with a combined energy of 1.02MeV.

All three processes described above, result in the generation of energetic secondary electrons which can deposit their energy to the medium in the same way as the electrons of the primary beam.

### Interactions of charged particles with matter

When a charged particle, such as an electron, or a heavy particle, such as an  $\alpha$ -particle, penetrates a medium it interacts with the molecules resulting in the ionisation and excitation of molecules along its path. The processes involved by these two classes of particles will be described

here.

### Electrons

There are three basic ways in which electrons interact with the medium:

- 1) Radiative processes (Bremstrahlung)
- 2) Inelastic collisions
- 3) Elastic collisions

The mode of interaction of a charged particle is largely determined by the energy of the particle and its distance of closest approach to the atom with which it interacts.

#### 1) Radiative Processes

An electron may interact with the field of the nucleus of an atom, resulting in the deceleration of the electron and emission of radiation known as, Bremstrahlung emission. The rate of emission of radiation,  $-(dE/dx)_{\text{rad}}$ , is proportional to  $z^2 Z^2 / m^2$ , where  $z$  and  $Z$  are the charge of the particle and the nucleus respectively and  $m$  is the mass of the particle.

Bremstrahlung emission becomes more important for materials of high atomic number and for electron energies between 10 and 100 MeV, and its energy spectrum extends from zero to the energy of the incident electron.

#### 2) Elastic collisions

When an electron passes in close proximity of the electrostatic field of a nucleus, the electron may be



scattered. This process is of some importance for electrons of low energy and materials of high atomic number.

### 3) Inelastic collisions

The passage of fast electrons through a medium will result in coulombic interactions with the material. The incident electrons slow down through inelastic collisions resulting in the excitation and ionisation of the medium and is the main process by which electrons are slowed down at electron energies below those leading to Bremstrahlung.

The deposition of energy per unit length through inelastic collisions is a very important quantity. Different methods have been used to measure electron penetration effects in solid substrates.

The depth of penetration of electrons may be evaluated empirically, based on the measurement of ionisation and excitation as a function of beam penetration or as a function of acceleration voltage. Grun measured energy dissipation versus penetration in air [28] resulting in a plot known as a depth-dose curve. Two important features may be gleaned from such a plot, Firstly he obtained the range-energy relationship

$$R_G = 4.57 E_0^{1.75} \quad 3$$

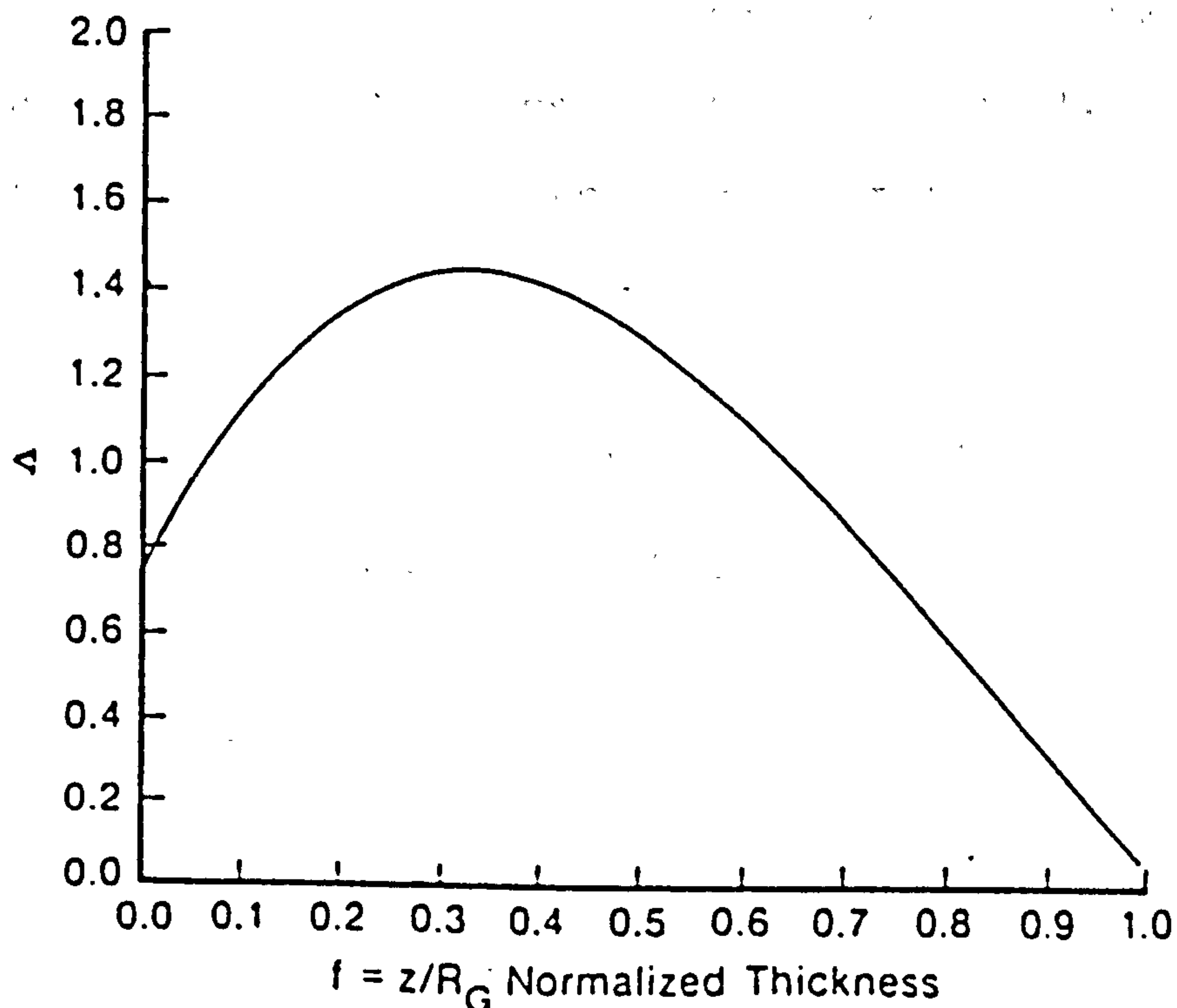
where  $E_0$  is the incident electron beam in keV, and  $R_G$  the Grun range for the electron beam in microns, valid for  $E_0$  in the range (5-25)keV and secondly he showed that the shape of the depth-dose curve is practically invariant to

the material if the penetration depth is normalised to  $R_G$  and the energy is normalised to  $E_0$  as shown in Figure 4.

Everhart and Hoff extended Gruns observation and found that identical normalised depth-dose curves were attainable for aluminium [29] and this was also found to be the case for polystyrene [30].

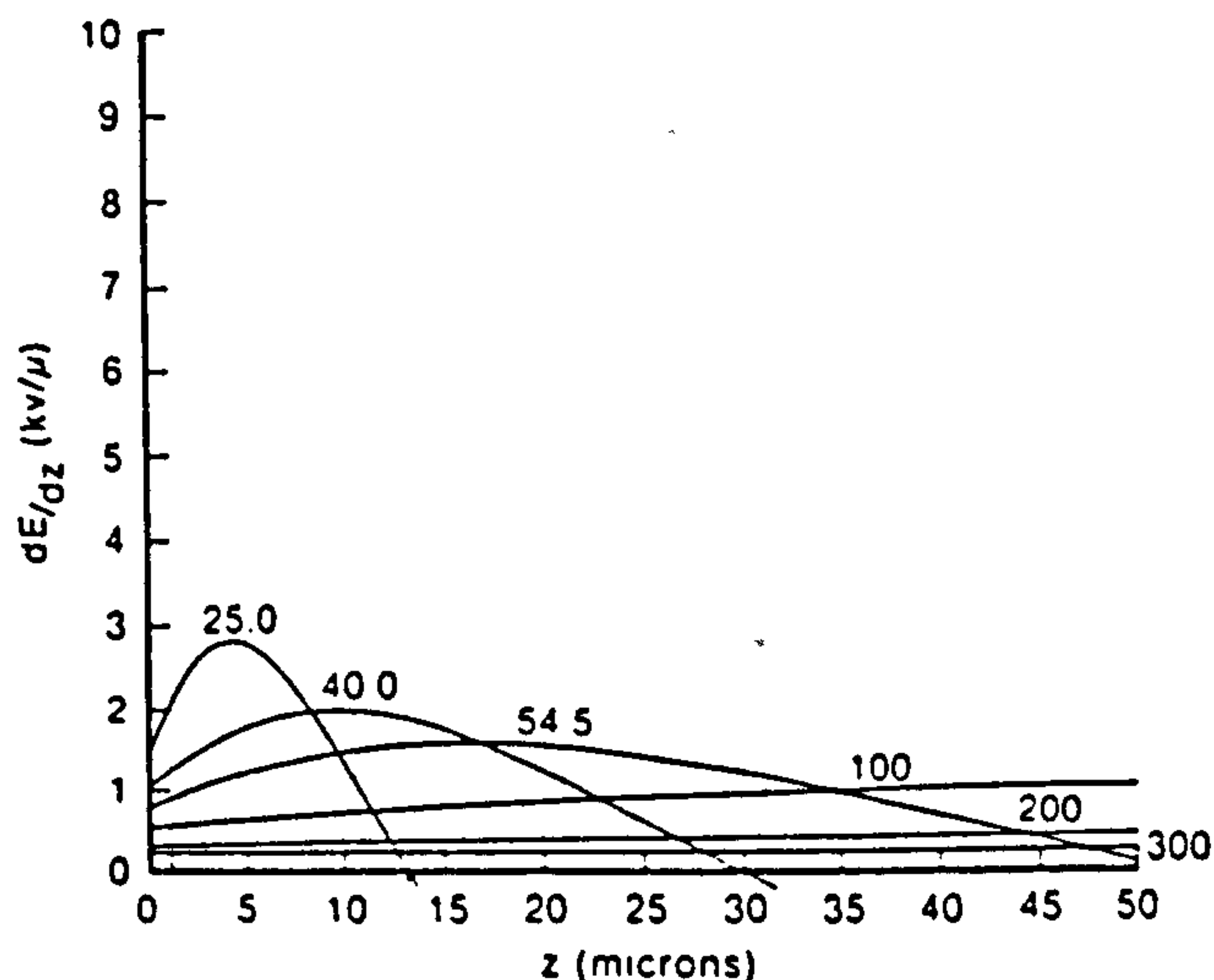
It can be seen from Figure 4 that the plot passes through a maximum at  $0.4f$  and corresponds to the depth at which maximum energy is deposited. On extrapolation of the curve to zero energy the Grun range  $R_G$ , for the penetration

Figure 4 The normalised depth-dose function  $\Lambda = \frac{d(E/E_0)}{df}$  where  $f = z/R_G$  and  $R_G$  is the Grun range



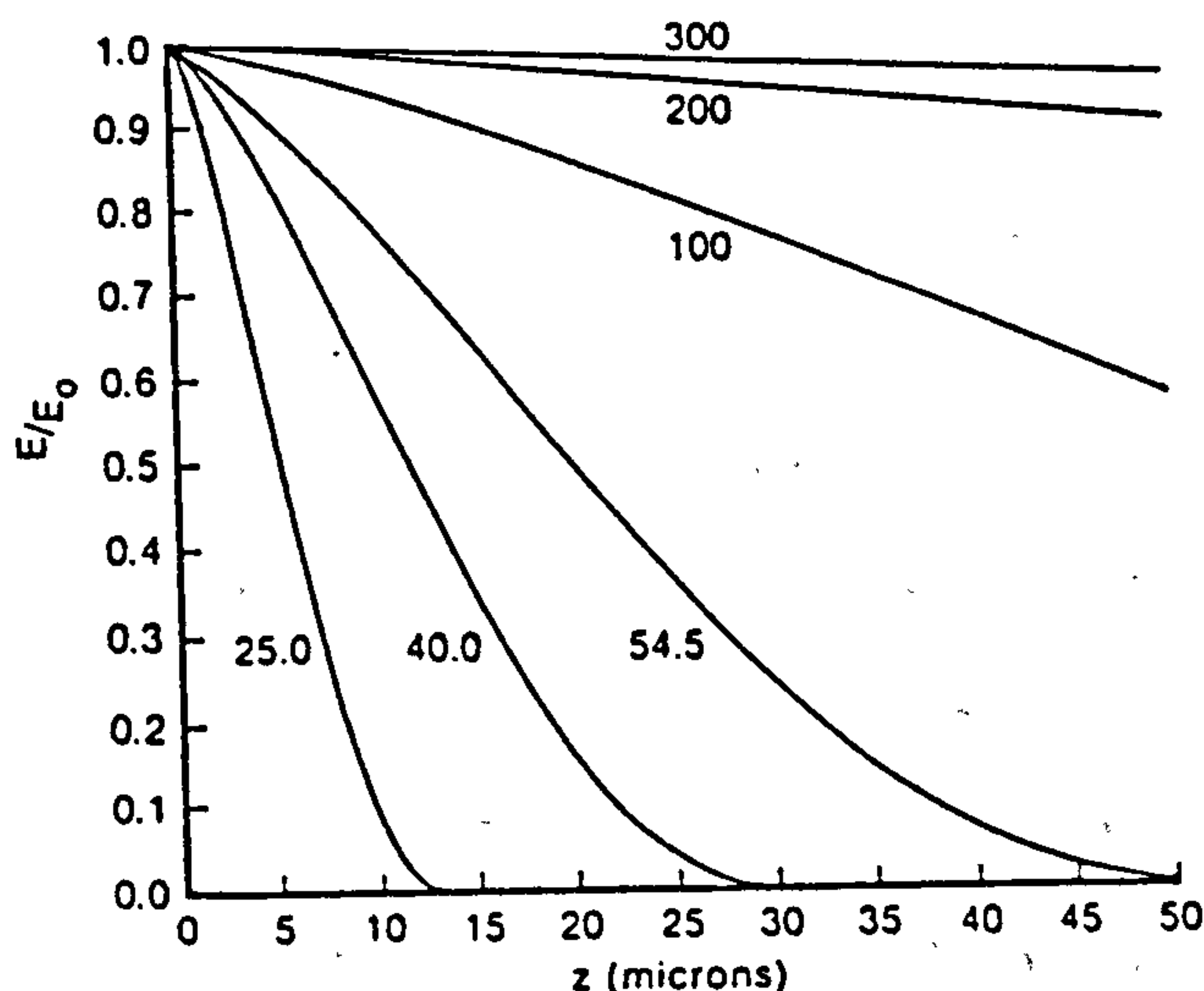
depth of the electron beam is determined. This is the point at which the electron beam has deposited most of its energy.

The rate at which energy is dissipated in the film as a function of thickness,  $dE/dz$ , for a range of incident electron beam energies is shown in Figure 5. It can be seen that as the incident energy of the electron beam increases, energy dissipation becomes constant and small. This may also be graphically illustrated by plotting the ratio of



function of thickness,  $dE/dz$ , for a range of incident electron beam energies is shown in Figure 5. It can be seen that as the incident energy of the electron beam increases, energy dissipation becomes constant and small. This may also be graphically illustrated by plotting the ratio of

Figure 6 A plot of the fractional loss in the incident electron beam energy as a function of film thickness



residual electron energy after it has penetrated a film of thickness  $z$  (Figure 6). For either case the result is the same.

In the early 1920's the application of quantum mechanics was used to determine the rate of energy dissipation in matter but with respect to the actual path of the electron in the medium. This function is called the stopping power,  $(dE/dx)_{coll}$  and provided insight as to which film parameters are responsible for the dissipation of energy. When the film thickness is small compared to  $R_G$  the stopping power,  $(dE/dx)_{coll}$ , is approximately equal to  $dE/dz$ .

The mass stopping power takes into account the density,  $p$ , of the material and is defined by

$$S_m = - \frac{dE}{dx_{coll}} \cdot \frac{1}{p}$$

For particles of  $<500\text{keV}$ , the energy loss by a charged particle is equal to the energy absorbed by the medium and the term stopping power may also be referred to as the linear energy transfer, LET [26].

### Charged particles

Charged particles, for example protons and  $\alpha$ -particles behave like electrons in losing most of their energy in matter by causing excitation and ionisation via much the same processes as described for electrons. The major dissimilarity being due to mass differences. This results in



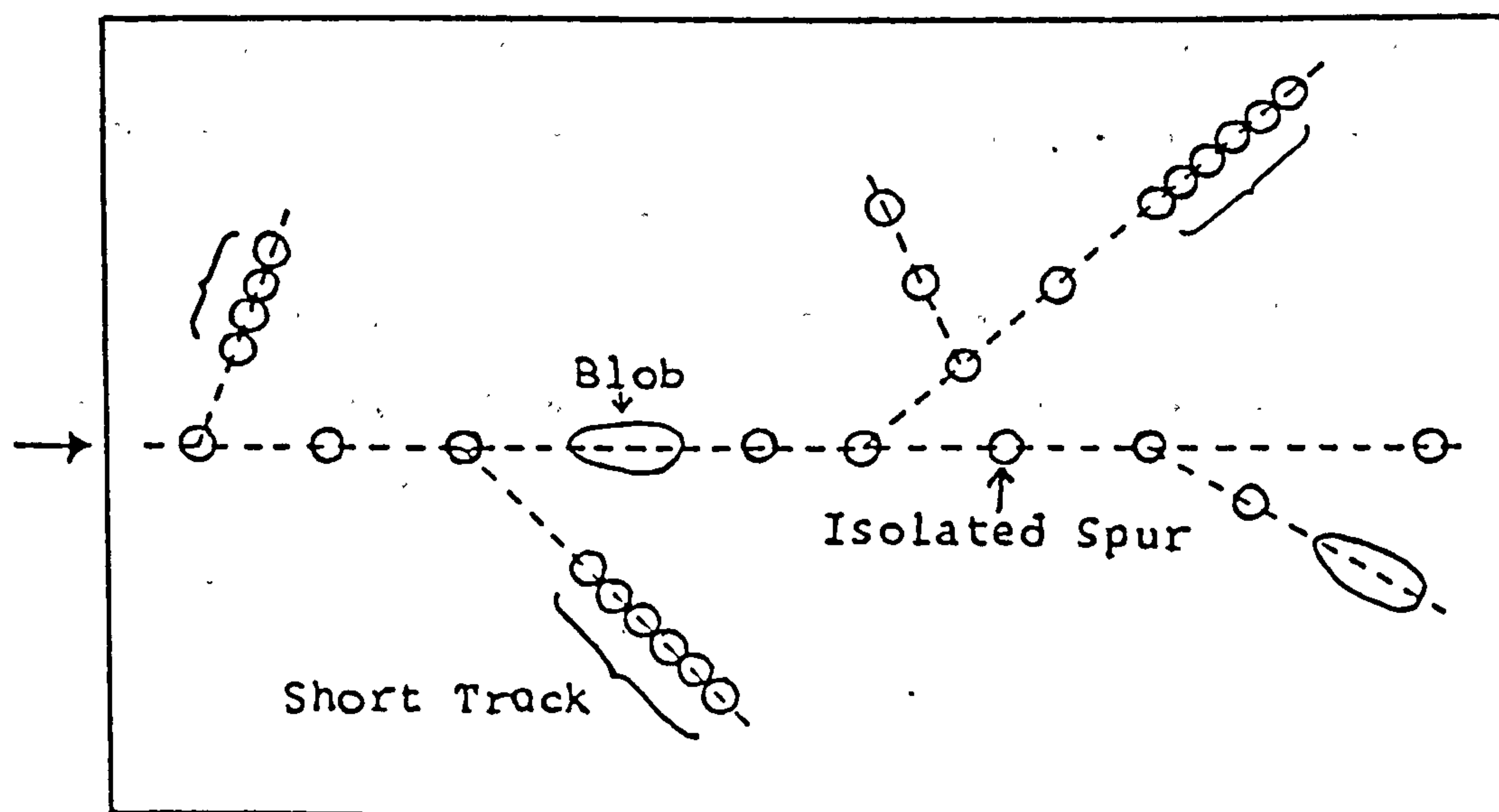
much larger values of the stopping power for heavy charged particles and results in more concentrated areas of primary products.

### Track structure

The "string of beads" model proposed by Samuel and Magee [31] has been widely used to describe the energy loss events along the trajectory of a charged particle. This model has been subsequently refined [32] and many new entities such as blobs and short tracks were defined to give a more complete picture of the track.

Energy deposited along the trajectory of the electron create track entities called spurs. The energy loss involves less than 100 eV [33] and if the incident electron has a low

Figure 7 Schematic of track entities



LET value these spurs will be widely spaced and may be considered as isolated from neighbouring spurs. However, if the LET value of the electron is high the spurs will overlap and form a continuous track entity known as a short track and involve the deposition of 500-5000eV of energy. The track entities in the 100-500eV range are known as blobs. Ionisation of the material being irradiated will simultaneously result in the production of an ejected electron. Those secondary electrons of energy greater than 5keV are also considered track forming entities and will also create spurs.

Thus according to Mozumdar and Magee [32], the partition of the energy of energetic electrons in the medium may be categorised in three ways.

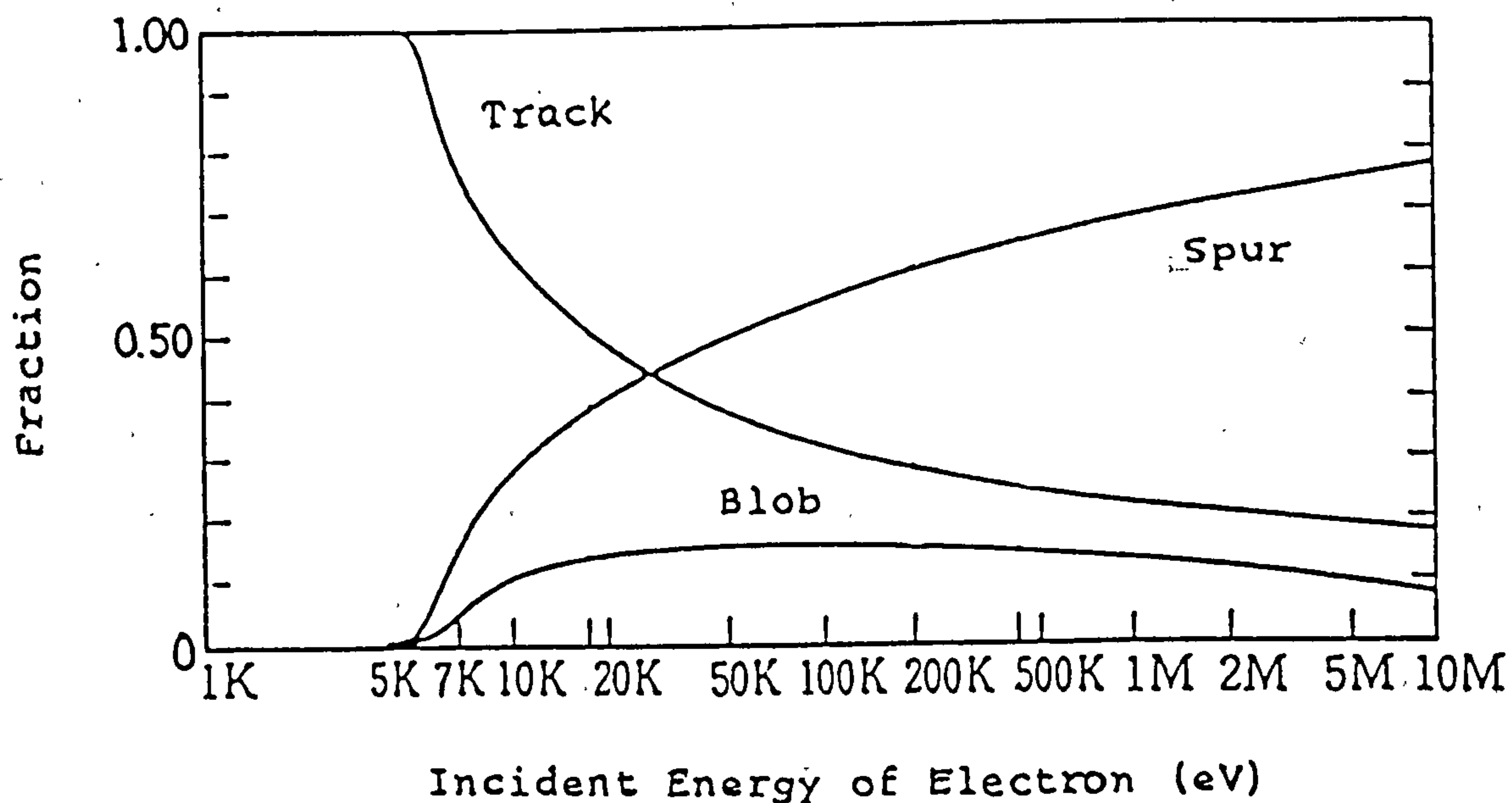
- |                 |                          |             |
|-----------------|--------------------------|-------------|
| 1) Spurs        | Energy deposited between | 6-100 eV    |
| 2) Blobs        | Energy deposited between | 100-500 eV  |
| 3) Short tracks | Energy deposited between | 500-5000 eV |

The partition of energy in the film of blobs, short tracks and isolated spurs has been calculated for water and is indicated in Figure 8.

Eventually the energy of all electrons will have been expended below a level at which they can cause ionisation or excitations. These electrons are described as being subexcitation electrons [33]



Figure 8 Energy partition between blobs, spurs and short tracks for electrons in water.



From these theoretical calculations it has be predicted [26] that high LET value particles will result in a high concentration of primary species such as electrons, ions and radicals.

## PRIMARY PRODUCTS

Deposition of energy by ionising radiation leads to the direct ionisation and excitation of the medium. The excited molecules, ion and electrons produced are called the primary species. However, the term "primary" product may encompass other species such as anions and radicals, when as stated by Burton [35] "it is claimed that the secondary process is the sole and inevitable consequence of the first under any set of conditions, there would appear to be no pragmatic value in the definition".

The statistically derived track structure of a medium [32] is a means of determining the "geometrical distribution of energy". The majority of energy is deposited in spurs [33] and involves less than 100eV. Excitation of track entities will result in the formation of highly excited states, given that photochemical excitation is to the lower excited states, when irradiated by photons of 253.7nm wavelength, corresponding to only 4.9eV. The activation process can be represented on a Jablonski energy level diagram of the type shown in photochemistry (Figure 9).

According to the Frank-Condon principle the absorption of energy and the subsequent promotion of an electron to an excited state, must take place within the order of  $10^{-15}$ s. This is very small compared with the time for a molecular vibration, which is of the order of  $10^{-13}$ s, so that during the absorption process the atomic nuclei in the molecule may be considered stationary.

Table 2 Chronology of events during radiolysis

<u>Process</u>	<u>Time/s</u>
1 MeV electron traverses molecule	$10^{-18}$
Excitation and ionisation	$10^{-17}$ - $10^{-16}$
Autoionisation of superexcited states	$10^{-14}$
Period of molecular vibration	
Dissociation of excited molecules	
Internal conversion to lowest excited state	$10^{-12}$
Electron thermalises	
Fluorescence	$10^{-9}$
Lifetime of solvated electron in presence of reactive solute $10^{-3}$ M	$10^{-7}$
Phosphorescence	$10^{-3}$

The time for a fast electron or an X-ray to traverse a molecule of a few angstroms dimension is of the order  $10^{-18}$ - $10^{-17}$ s. The deposition of energy results in the formation of excited and charged species, which may subsequently undergo secondary reactions such as de-excitation, thermalisation, neutralisation and solvation to generate the first excited singlet and triplet states, solvated electrons and cations. Some of these species react within the spur while others will diffuse out of the spur and become homogeneously distributed throughout the medium. Spur reactions may include electron capture, charge neutralisation and molecular dissociation.

The plethora of reactive species produced on irradiation of matter made the task of determining reaction mechanism



very difficult to ascertain. Methods of analysing primary products and mechanisms were developed of which the most widely applied are the use of scavengers in conjunction with pulse radiolysis. A scavenger reacts with the primary species generated, thus forming new products and from knowing their structures, that of the primary products may be deduced. In pulse radiolysis the sample is irradiated with a short intense pulse of radiation to produce high concentration of primary species which are measured via optical absorption, electron spin resonance (esr) or conductivity.

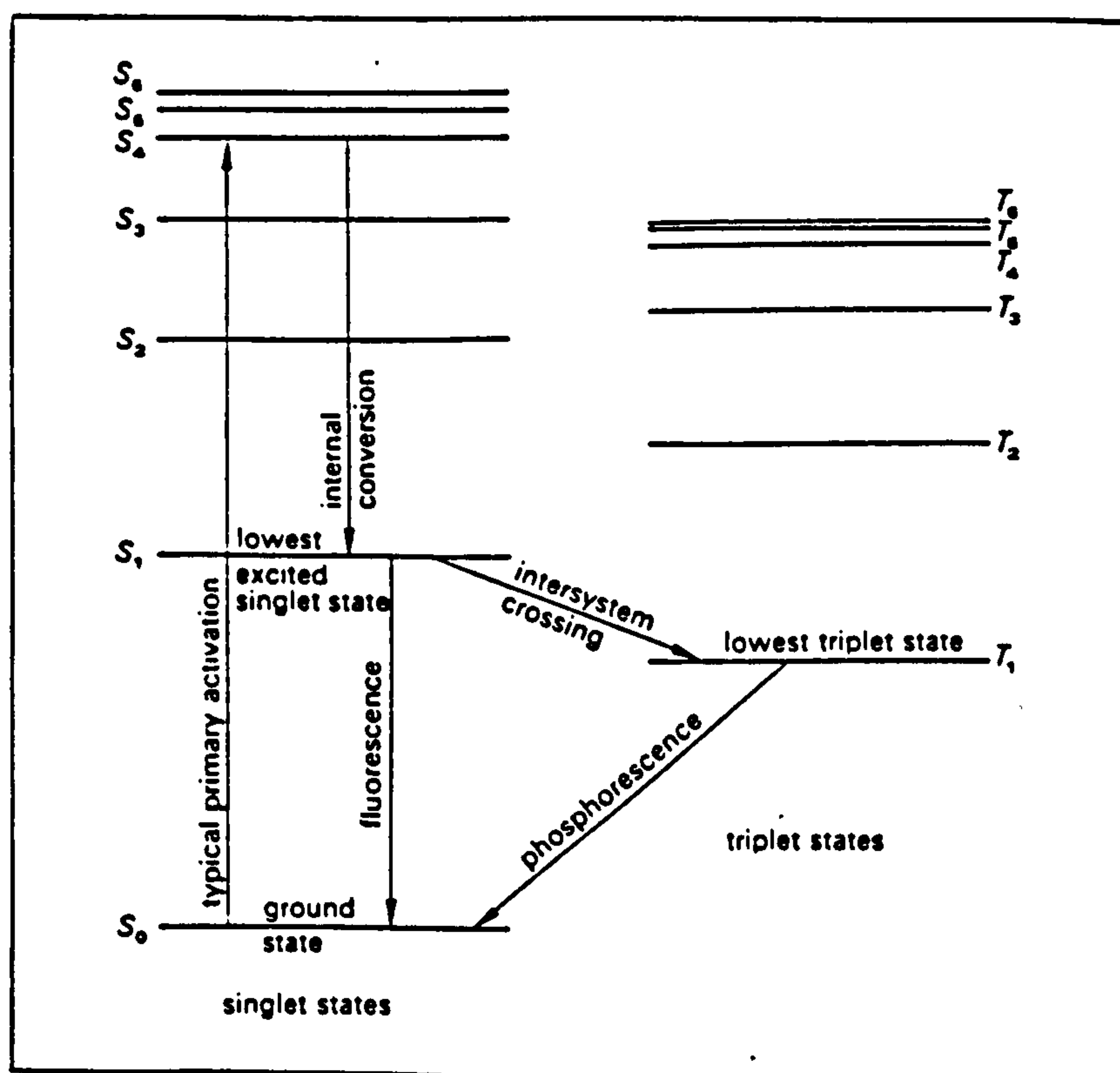
#### Excited species

The fate of highly excited states produced as a result of the passage of ionising radiation through matter are similar to those electrons promoted to the lower excited state photochemically. The physical processes and chemical changes that ensue as a result of absorption of energy encompass the subject of photochemistry and there are many excellent texts that cover this subject [36,37].

The dissipation of excitation energy from possible excitation states is best illustrated by the Jablonski diagram (Figure 9), and are seen to be of two main types - radiative and nonradiative transitions. Internal conversion IC, is a radiationless process whereby a molecule transfers from one electronic state to another of the same multiplicity, while intersystem crossing ISC, involves the transfer of an electron between states of different



Figure 9 A modified Jablonski diagram



multiplicity. Radiative energy loss in dropping from the  $S_1$  to  $S_0$  state is known as fluorescence, whilst the process  $T_1$  to  $S_0$  is known as phosphorescence.

When a molecule has been excited to a level above its ionisation potential (about 10-12eV for most molecules) it may follow one of two routes. Firstly it may promote an electron to the free state, this process is called autoionisation, or secondly, it may have a transient existence in a state above its ionisation potential and is described as being in a superexcited state. The fate of an electron in the superexcited state may lead to expulsion to

produce a free electron and an excited cation or the molecule may lose energy through dissociation to produce free radicals. The chronology of the various processes in radiation chemistry are shown in Table 2.

The processes described above involve unimolecular dissipation of excitation energy. In the condensed phase these will compete with processes which are essentially bimolecular and one of the simplest bimolecular process is transfer of excitation energy from one molecule to another.

### Cations

#### **Spur processes**

Radical cations are produced along the track of an ionising particle, along with a concomitant electron, of sufficient kinetic energy to diffuse away from the coulombic field of the cation, loosing energy as it does by collisional deactivation with molecules of the medium. If the electron has travelled a distance,  $r$ , outside the coulombic attraction of the atom it will undergo random Brownian movement. However, if the distance travelled by the

electron is less than the boundary of the electrostatic field attraction it will drift back to the cation and will recombine. Since the ionisation events produce electrons with a distribution of energy, and since the thermalisation processes are also stochastic, the ion-pair distances will also be distributed about  $n(r)$ . The number of ion-pairs escaping the coulombic field and becoming homogenously distributed are referred to as the free ion yield. This value reflects the ion pair distribution,  $n(r)$ , and the dielectric constant of the medium. In general the free ion yields will reflect the polarity of the medium and is about 0.1 ion pair/100eV for n-hexane and 2.0 in the polar methyl alcohol [33]. The total ionisation yields as determined by scavenging experiments, are in the range of 4-5 ion-pair/100eV [33]. This illustrates that for nonpolar liquids the majority of ion-pairs undergo recombination. The kinetics of these recombination processes are governed by the sum of the diffusion coefficients of the cation and the electron.

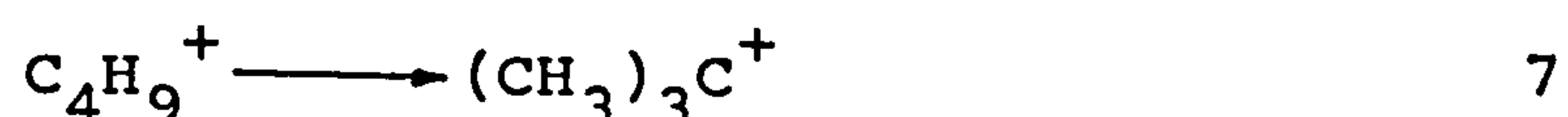
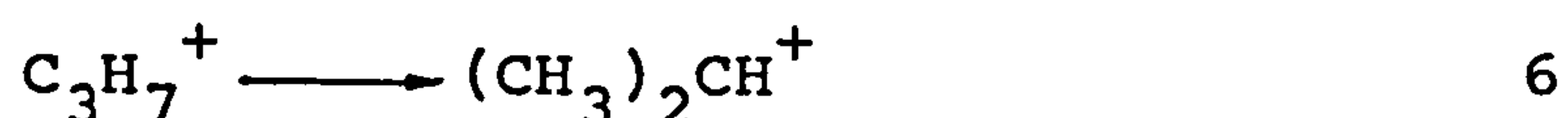
### Reactions

The reactions of positive ions have been studied extensively by mass spectroscopy. However, extrapolation of reactions observed at low gas pressures must be drawn with caution when interpreting the reactions of positive ions in the liquid phase. The reaction of positive ions are complicated for polyatomic molecules in the condensed phase and information regarding their behaviour is very sparse.

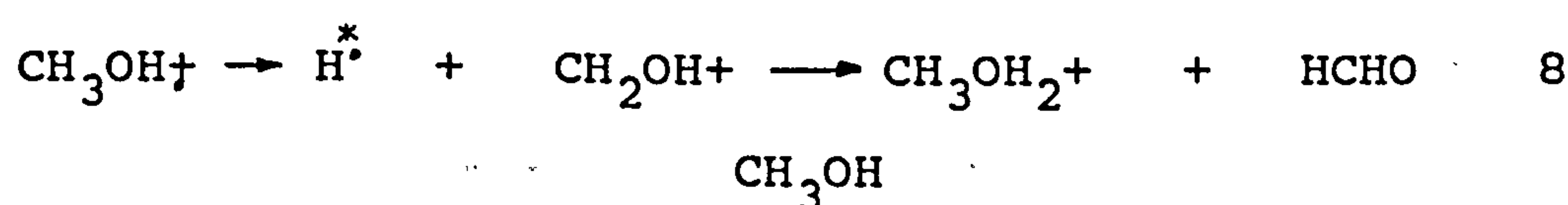


## 1. Fragmentation and Isomerisation

Due to the high collision frequencies encountered in the condensed phases, bimolecular reactions will predominate over fragmentation or isomerisation reactions. However, the radical cations,  $C_3H_7^+$  and  $C_4H_9^+$  may undergo isomerisation or rearrangement to form the most stable structure in some instances [39,40].

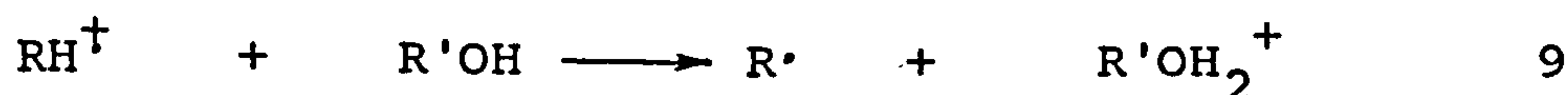


Fragmentation is also thought to be a viable reaction process in certain cases, e.g. n-alcohols are thought to fragment to ultimately yield aldehyde [33].

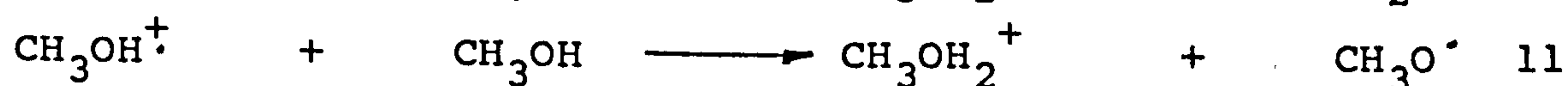


## 2. Ion-molecule reactions

Molecular ions may be considered as Bronsted acids and as such will readily transfer protons to basic molecules. For example, an alcohol in the presence of an alkane will by process of proton transfer react with the radical cation of the alkane  $RH^+$  [41],

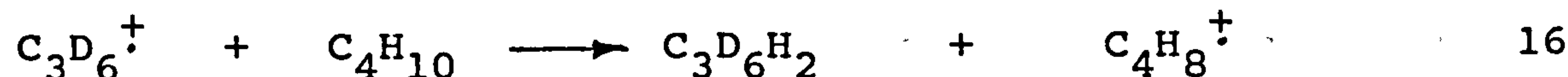
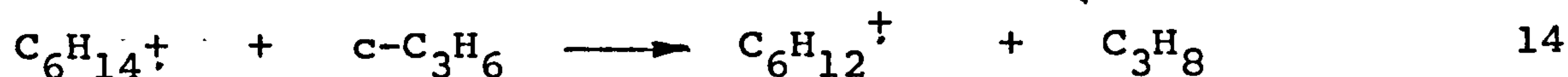
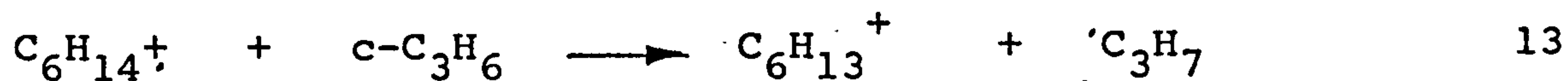
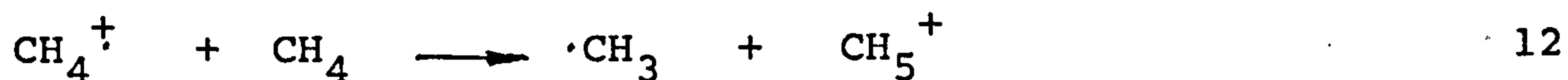


Proton transfer reactions between primary cations and the parent molecule will occur and are prevalent in hydrogen bonded systems, for example, [42],



The transfer of protons, hydrogen atoms, hydride ions,

hydrogen and hydrogen molecule anions have been studied for many gas and condensed phase hydrocarbon systems and account for many reactions of cations,



### 3. Charge transfer

This process has been demonstrated in many organic liquids and involves the transfer of an electron from a molecule of lower ionisation potential to the primary cation and is illustrated by the transfer of charge from an alkane radical cation to an aromatic amine such as N,N,N',N'-tetramethyl-1,4-phenylenediamine [33].

### Electrons and negative ions

#### **Spur processes**

Subsequent to ionisation the electron may become thermalised, undergo geminate recombination with its parent ion or form a solvated electron. If the electron possesses sufficient kinetic energy following ionisation it may escape the coulombic attractive forces of the positive ion. The electron may then undergo chemical reactions as well as energy loss processes that cause it to become thermalised. The rate of thermalisation is largely dependent on the nature of the media [44]. Rate of energy loss being greatest

for unsymmetrical or polar media [44].

If the thermalised electron has escaped the coulombic field of its counterion the electron is described as being a free electron. The probability of escape is dependent upon the dielectric constant of the liquid and the distance travelled from its geminate positive ion. The probability of escape is negligible for hydrocarbons of low dielectric constants whereas for a polar liquid it is considerably higher.

The fate of a free electron, in most media, is thermalisation and subsequent solvation of the electron. In polar media, such as an alcohol, the electron is strongly solvated, and is detectable by its absorption maximum for low molecular weight alcohols (max = 635nm for methanol [45]). For the less strongly solvated electron in higher molecular weight alcohols (max = 1075nm in t-butyl alcohol [46]). The degree of solvation of electrons in alcohols may also be followed by observing a blue shift of an absorption band in the IR with increasing solvation.

In nonpolar, low dielectric liquids such as alkanes, the electron is weakly solvated resulting in high mobility and rapid and extensive geminate recombination. The absorption maximum of  $e^-$  as expected is situated in the IR region [34]. The probability of escape to generate free ions increases with branching. Highly branched systems may be described as symmetrical and as such increased branching will also promote the mobility of the electron. For certain cases of non-polar, very symmetrical molecules, such as



tetramethylsilane the electron will be thermalised, but unsolvated or incompletely solvated, and is described as being in the quasi free state. These electrons are thus not localised and can be considered as moving in a conduction band of the liquid.

Electrons are powerful reducing agents, however, their subsequent reactions are dependent upon their state of solvation.

### Reactions

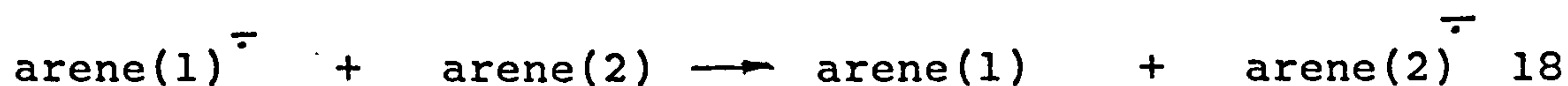
In some systems the anions rather than the electrons are regarded as the effective negatively charged primary species. This is the case for systems where the electron either undergoes electron attachment or dissociative electron attachment. Electron attachment produces a radical anion and dissociative electron attachment produces a free radical and an anion. Compounds present in the radiolytic solution that are capable of scavenging electrons will produce primary anions.

#### 1. Non-dissociative electron capture

Molecules which undergo electron capture usually possess low lying orbitals to accommodate the additional electron. Aromatic compounds, such as biphenyl and other molecules with antibonding orbitals have a strong tendency to form anions [47].

Electron capture by solid solutions of various aromatic hydrocarbons, such as biphenyl and pyrene in an organic solvent, has been shown to produce anions and on addition of a second aromatic hydrocarbon or molecule that will compete

with the original aromatic species for electrons may result in an electron transfer process at rates depending on the nature of the added solute [47].



The addition of a substance in trace amounts with a high electron affinity, may capture most slow electrons and thus have an important effect on the observed radiation chemical yields [18]. This minor component is known as a scavenger.

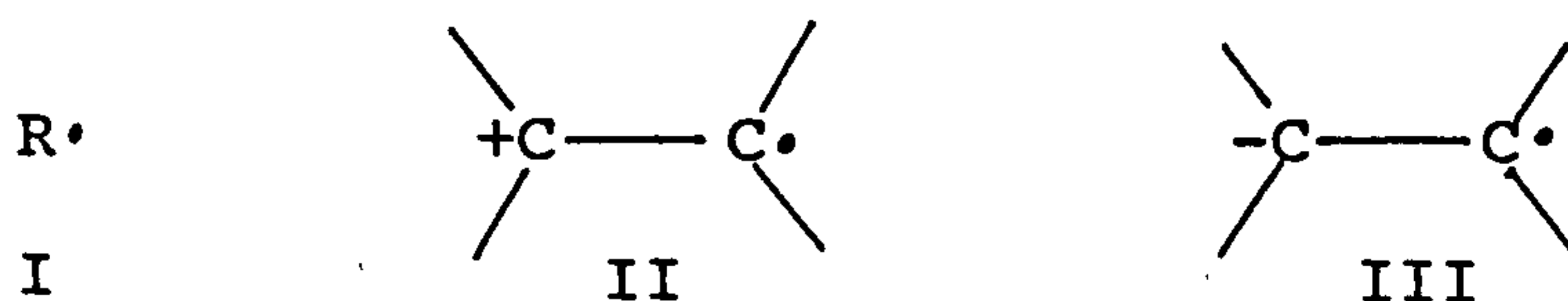
## 2. Dissociative electron capture

Dissociative electron capture usually involves a one electron reduction of a molecule containing an atom or group of atoms having electron affinity greater than their binding energy to the rest of the molecule. Molecules containing halogen groups such as the alkyl halides [48] readily undergo dissociative electron capture.



## Radiation Induced Polymerisation

Polymerisation can be initiated either by a radical or by an ion. On irradiation of unsaturated monomers, excited molecules may give rise to radicals I, radical cations II, as well as radical anions III formed by electron capture of the monomer.



All these species may be considered initiators of free radical polymerisation, whilst additionally, species II and III may promote cationic and anionic polymerisation respectively [49].

Although radiation produces ions and radicals in the primary act, the majority of polymerisations studied have been found to occur via a radical mechanism [22-25,49].

### Free radical polymerisation [15,16,43]

Free radical polymerisation is a chain reaction promoted by a free radical species and consists of a sequence of three steps - initiation, propagation and termination.

The types of system susceptible to free radical polymerisation are those containing unsaturation of which vinyl unsaturated monomers are the most important

#### **Initiation**

As mentioned previously, excited molecules may give rise to radicals, radical cations, and by way of electron capture by a neutral molecule a radical anion may also be produced. The formation of such radical and radical ions may in principle be classified as the initiators of radiation induced radical polymerisation.

The addition of a free radical species to an unsymmetrically substituted alkene will render the most stable radical. The order of stability of radicals is,



primary > secondary > tertiary.

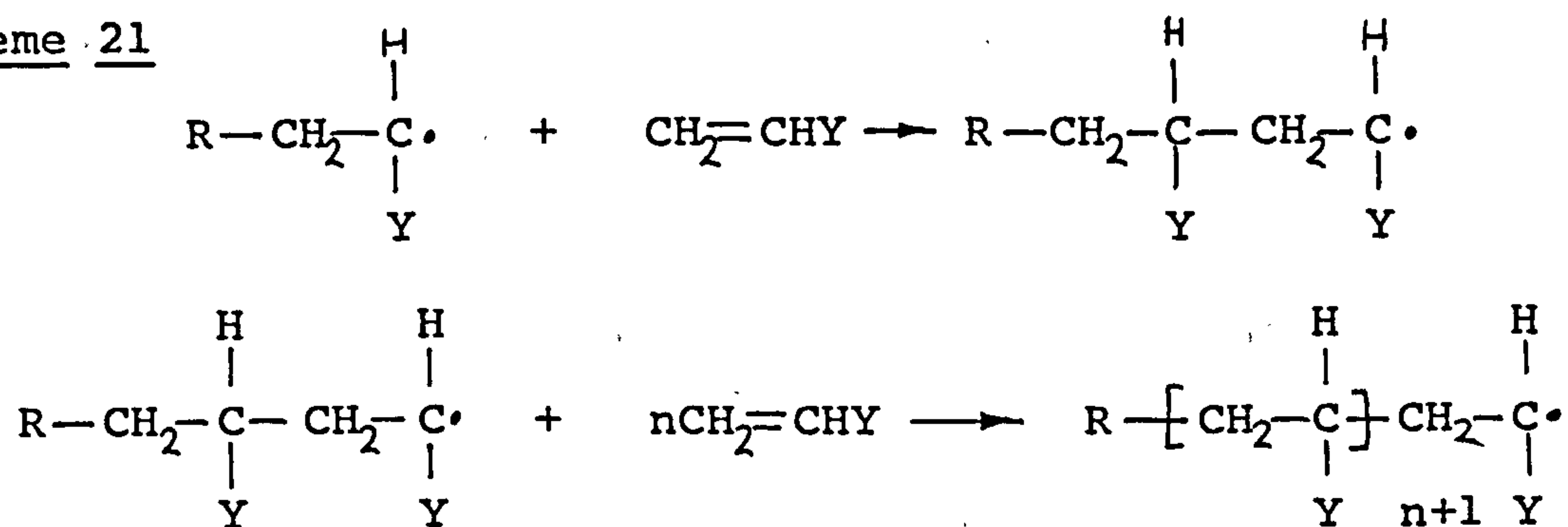
The second part of initiation involves the addition of a radical species to the double bond of the monomer to produce the initiating chain species.



### Propagation

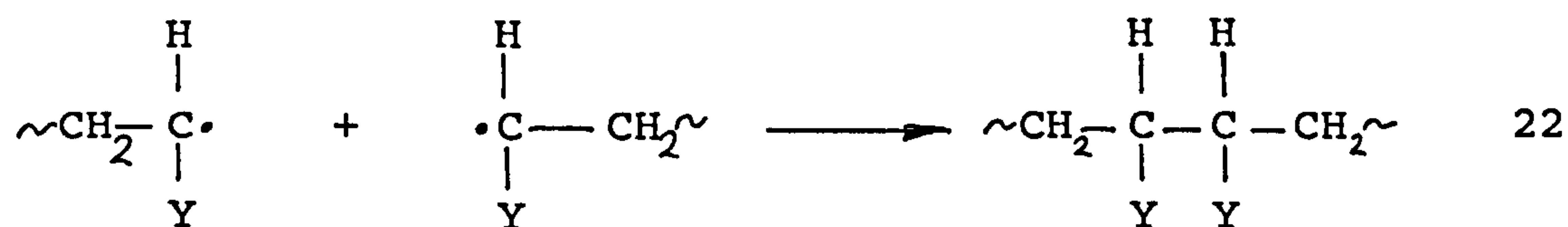
Propagation proceeds via successive additions of the monomer to the growing polymer chain.

#### Scheme 21

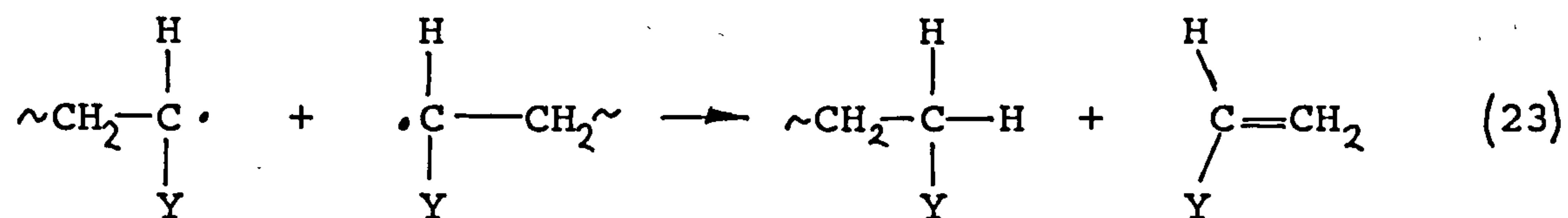


### Termination

Termination of a growing polymer chain involves a bimolecular reaction of two polymer radicals. The termination step may proceed via two mechanisms. These are combination, in which two radicals couple to form one polymer chain,



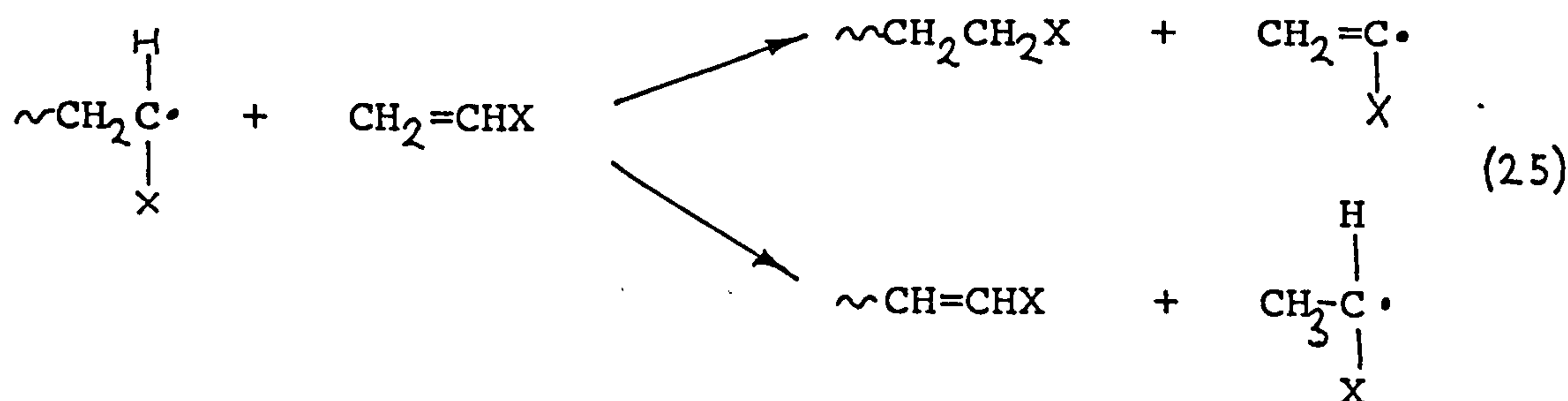
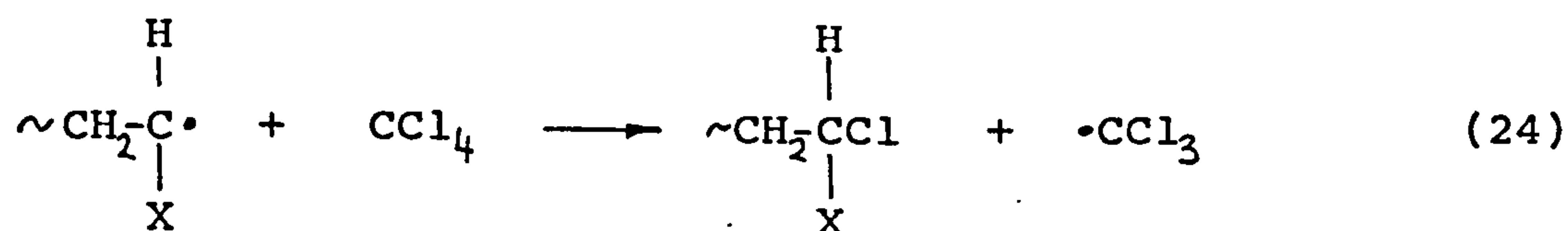
and disproportionation,

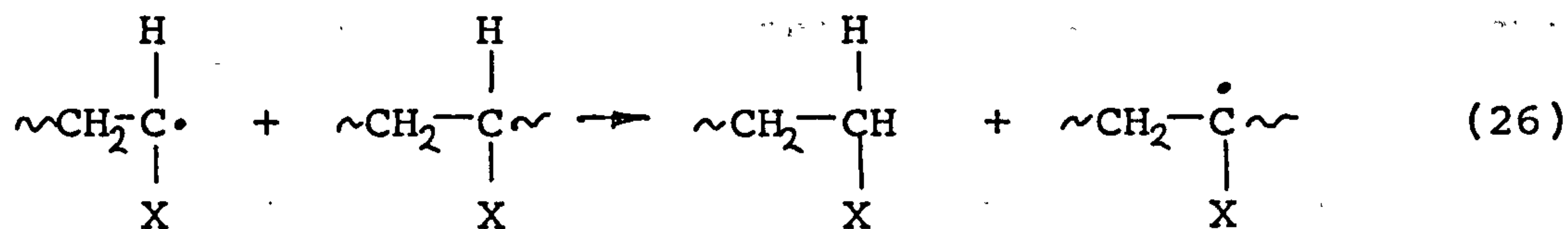


in which hydrogen transfer results in the generation of two polymer chains, with one saturated and one unsaturated end group.

Although chain polymerisation are primarily governed by the three steps of initiation, propagation and termination, other reactions may compete and hence affect the polymerisation process. These reactions involve such radical molecule reactions as chain transfer and inhibition and retardation reactions.

Chain transfer reactions results in the reactivity of a growing polymer chain being transferred to another species capable of continuing the chain reaction. Transfer reactions involves the abstraction of an atom (usually hydrogen) from solvent (24), unreacted monomer (25) or a polymer chain (26).

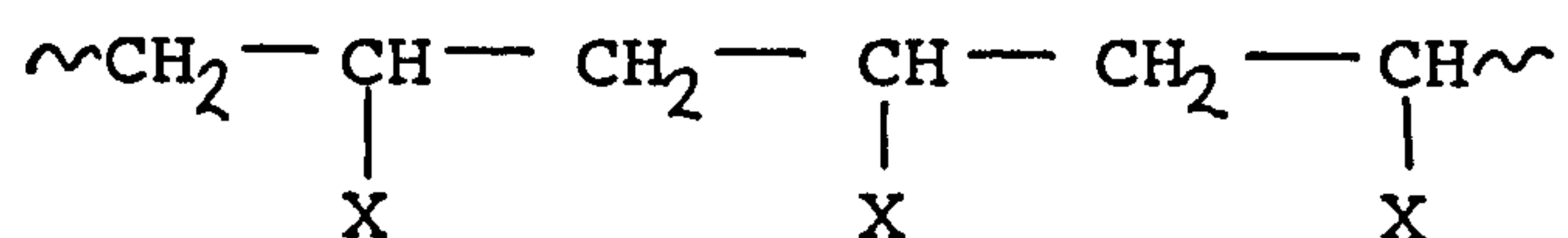




Chain transfer to a solvent molecule results in the formation of additional polymer molecules for each radical chain initiated. However, transfer to polymer and transfer to monomer with subsequent polymerisation will lead to the formation of branched molecules. The latter transfer reaction has a pronounced effect on the molecular weight distribution.

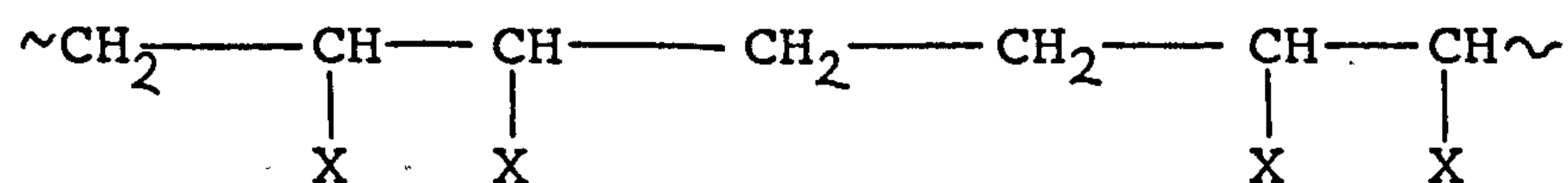
The mechanism of retardation is characterised by the reaction of a substance with a radical to form products incapable of promoting polymerisation. The action of the retarder is twofold, reducing the concentration of radicals and their average lifetime, thus limiting the length of the polymer chain. If retardation is sufficient to prevent the formation of polymer, the substance is called an inhibitor and will result in an induction period before the onset of polymerisation.

It has been previously mentioned that addition of a vinyl monomer to a free radical will lead to the more stable product being formed. Thus, for unsymmetrical vinyl monomers the most favoured configuration will be head-to-tail.





in preference to a head-to-head, tail-to-tail configuration.



The polymer chain may adopt one of three configurations. If the substituent X lies alternately above and below the plane then the configuration is said to be syndiotactic, while a random configuration of X groups denotes an atactic arrangement. Alternatively if all the substituents lie to one side of the main chain the configuration is said to be isotactic.

### Rate of polymerisation

In radiation induced polymerisation, the initiation step is brought about by the absorption of the radiation energy which will result in the production of radical species. The rate of initiation,  $R_i$ , is defined as

$$R_i = \bar{\Phi}_M I [M] \quad 27$$

where  $\bar{\Phi}_M [M]$  is the rate of production of free radicals in the monomer and I is the dose rate [23].

The overall rate of polymerisation,  $R_p$  is given by,

$$R_p = k_p k_t^{-1/2} R_i^{1/2} [M] \quad 28$$

where,  $k_p$  and  $k_t$  are the rate constants for the propagation and termination steps respectively and  $R_i$  is the rate of initiation and M is the concentration of monomer [23].

The above equations describe first order polymerisation

kinetics in which the assumption was made that all primary radicals are scavenged by the monomer and converted into growing polymer chains. However, if the dose rate increases, the concentration of primary radicals may rise to such a level that some of the primary radicals either recombine or react with the growing polymer chain.

In this case, first order kinetics no longer apply and a more detailed consideration of all free radical reactions must be adopted.

## IRRADIATION OF POLYMERS

It was not until the early 1950's when Charlesby [50] clearly showed that radiation changed polyethylene into a crosslinked, insoluble, heat resistant material, that interest in polymer radiation chemistry was shown.

The effects of ionising radiation on many other polymer types was subsequently investigated and it was observed that small chemical changes may induce large changes in the physical properties of the polymers.

Charlesby [51] and Lawton et. al. [52] both observed that polymers may either crosslink or degrade depending on their chemical composition. These processes take place simultaneously, however, in most polymers one of these predominates. If crosslinking predominates, the effect of radiation will be to form a network polymer with increased

Table 3 Predominate processes in irradiated polymers

### Group I Crosslinking

Polyethylene

Polypropylene

Poly(vinyl chloride)

Polystyrene

Polyacrylates

Polyamides

Polyesters

Polysiloxanes

### Group II Scission

Poly- $\alpha$ -methylstyrene

Polymethacrylates

Polymethacrylamides

Poly(vinylidene chloride)

Polytetrafluoroethylene

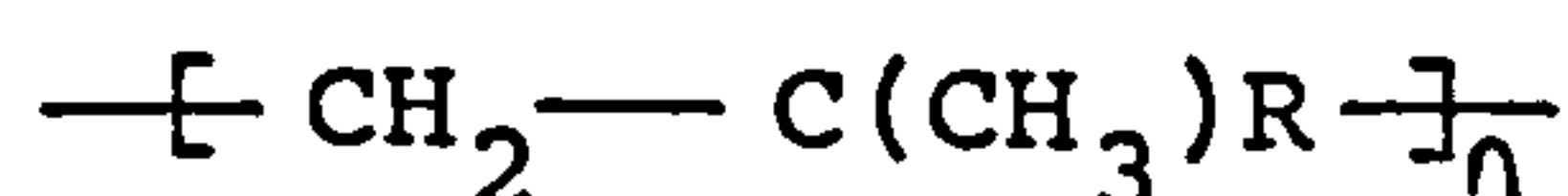


molecular weight, if degradation predominates, then a lowering of molecular weight ensues. The predominate processes of several polymers are shown in Table 3

Steric factors are thought to be at least partly responsible for the different behaviours in different polymers. For instance, in the case of vinyl polymers, it can be seen that crosslinking predominates when the polymer structure is,



but degradation predominates when the structure is of the type



This implies that the methyl group produces steric strain which weakens the backbone chain.

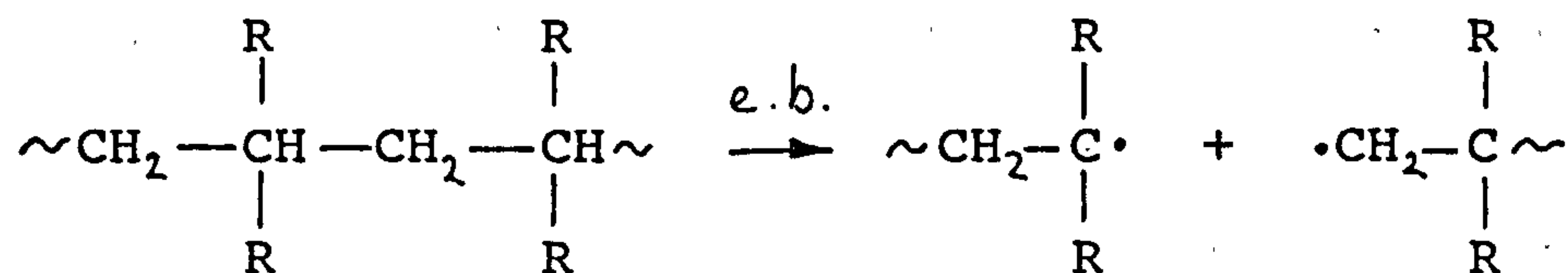
It has also been observed that the degree of unsaturation of a polymer changes on irradiation. Polymers containing some initial degree of unsaturation tend to lose a degree of unsaturation, while saturated polymers increasingly show small amounts of unsaturation.

Another chemical change is the production of hydrogen in particular, as well as, a small percentage of hydrocarbons e.g. methane.

Several theories have been developed to take into account the changes observed for irradiated polymers

The primary process on irradiating a polymer results in the formation of radicals

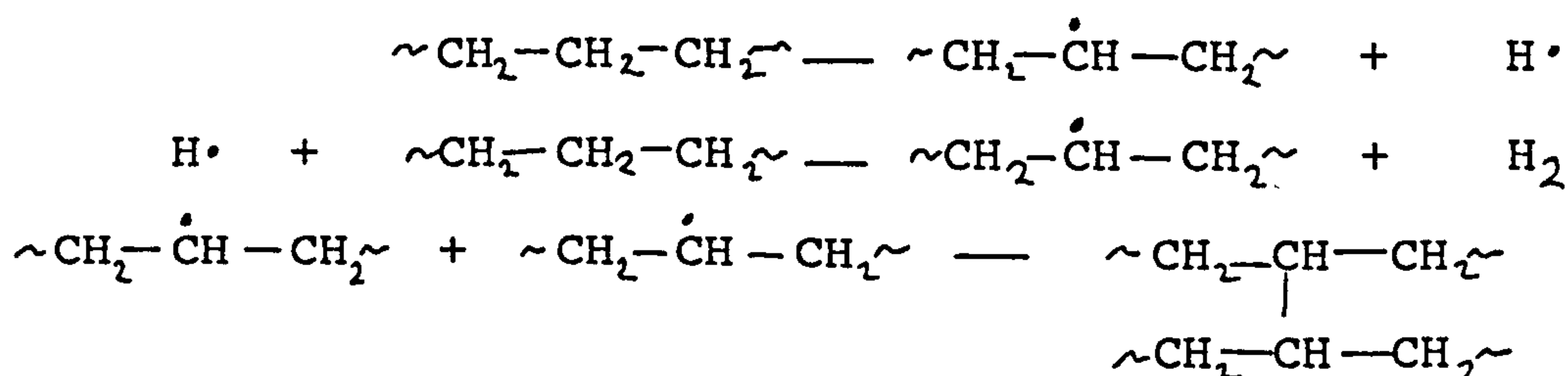
Scheme 29



The fate of these radicals may be either to recombine with disproportionation or hydrogen abstract from another molecule, alternatively they may recombine.

Chain scission tends to be more favoured in branched chain polymers, and increases with branching while, crosslinking may due to dimerisation of adjacent polymer radicals accompanied by the lose of molecular hydrogen.

Scheme 30



However, Charlesby [53] proposed that the crosslinking process would involve the formation of a polymer radical and a hydrogen atom. The hydrogen atom may then abstract a hydrogen atom from a neighbouring polymer chain, these adjacent polymer chains may then readily combine. Alternatively, the hydrogen atom formed in the primary scission step may migrate some distance before hydrogen abstraction and forming a second polymer radical. Mobility of such polymer radicals may proceed via hydrogen abstraction until recombination can occur between two

radical centres.

Irradiation of a polymer in an aerobic atmosphere will also have a profound effect on the polymer. The result of irradiating polymer in an oxygen rich atmosphere in the case of polyethylene, produces a large number of crosslinks, however, these crosslinks do not render the polymer insoluble. This is possibly due to the nature of the crosslinks formed, and under these conditions are probably peroxide bridges which will decompose on heating to produce free radicals. These radical centres may lead to the degradation of the polymer, however this method has also been used as a means of introducing radical sites along the polymer chain capable of grafting monomer to form a graft copolymer.

### ELECTRON BEAM GENERATORS

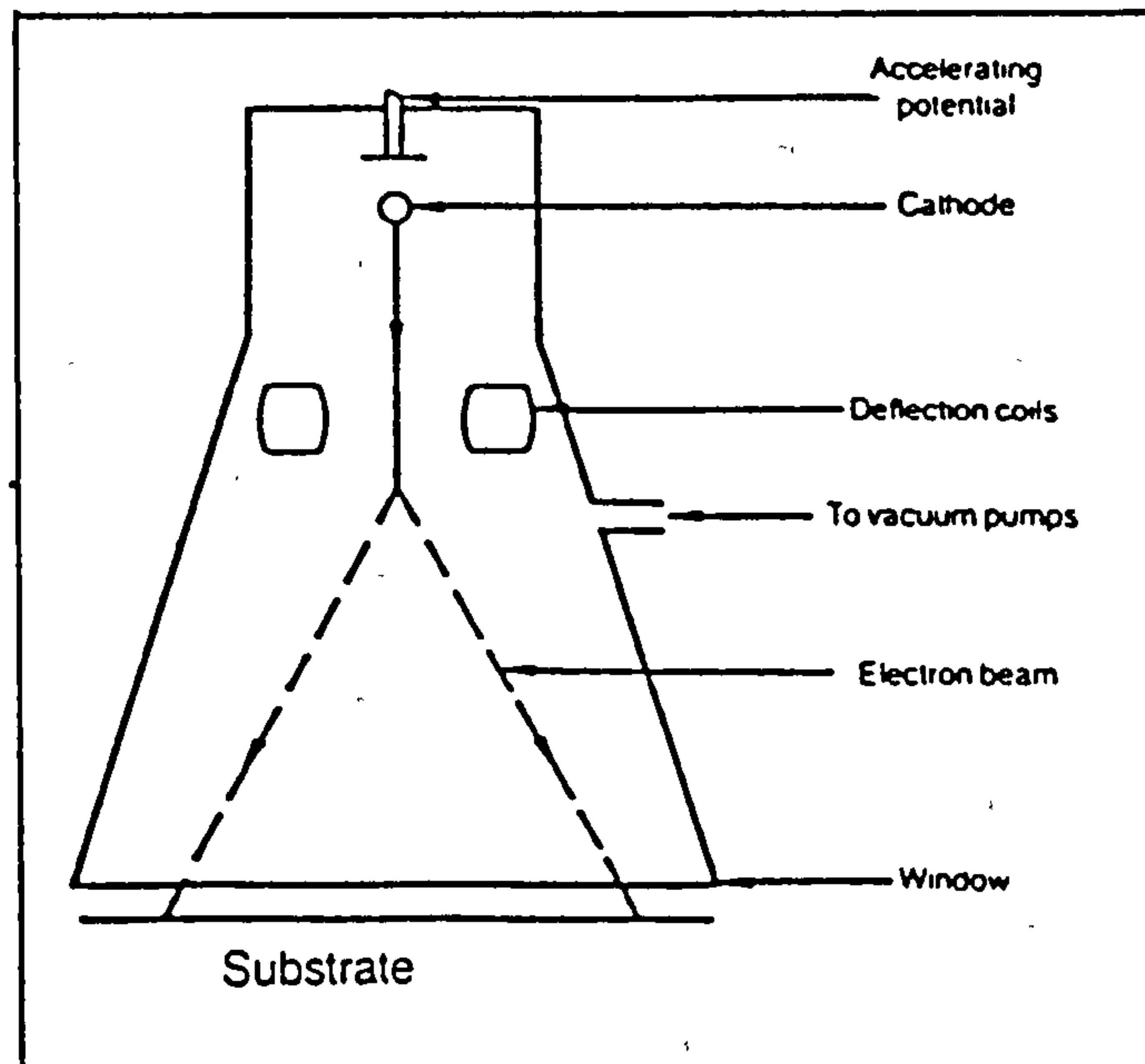
Electron beam systems used in the surface coatings industry generally utilise 'low voltages' in the range (150-300)keV and a current supply of (10-100)mA. The electron beam units used in this category all consist of a high voltage generator energising a tungsten filament which subsequently emits a stream of electrons. These electrons are then accelerated under vacuum through a thin metal foil window and projected over the coating. There are three main types of electron accelerators available for curing surface films and they are distinguished by the cathode arrangement [11].

The scanner system (Figure 10) was the first electron



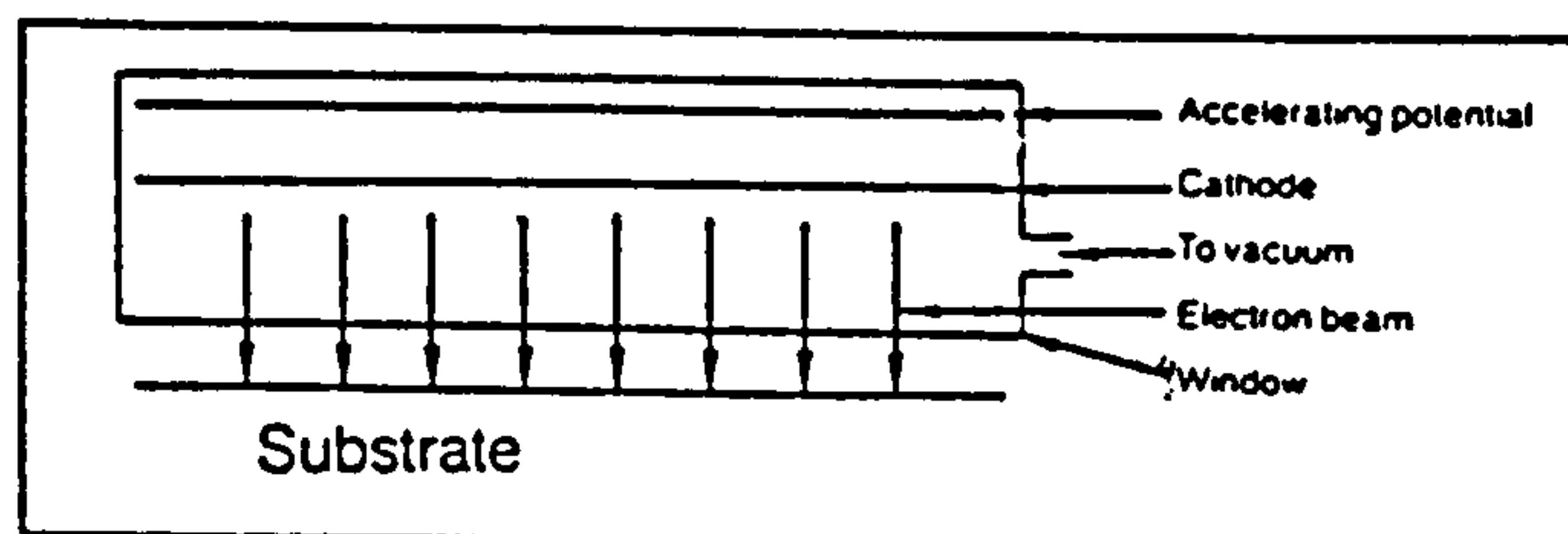
beam unit produced and produces an electron beam from a point cathode. This beam is then deflected electromagnetically over the surface coating.

Figure 10 The scanner system



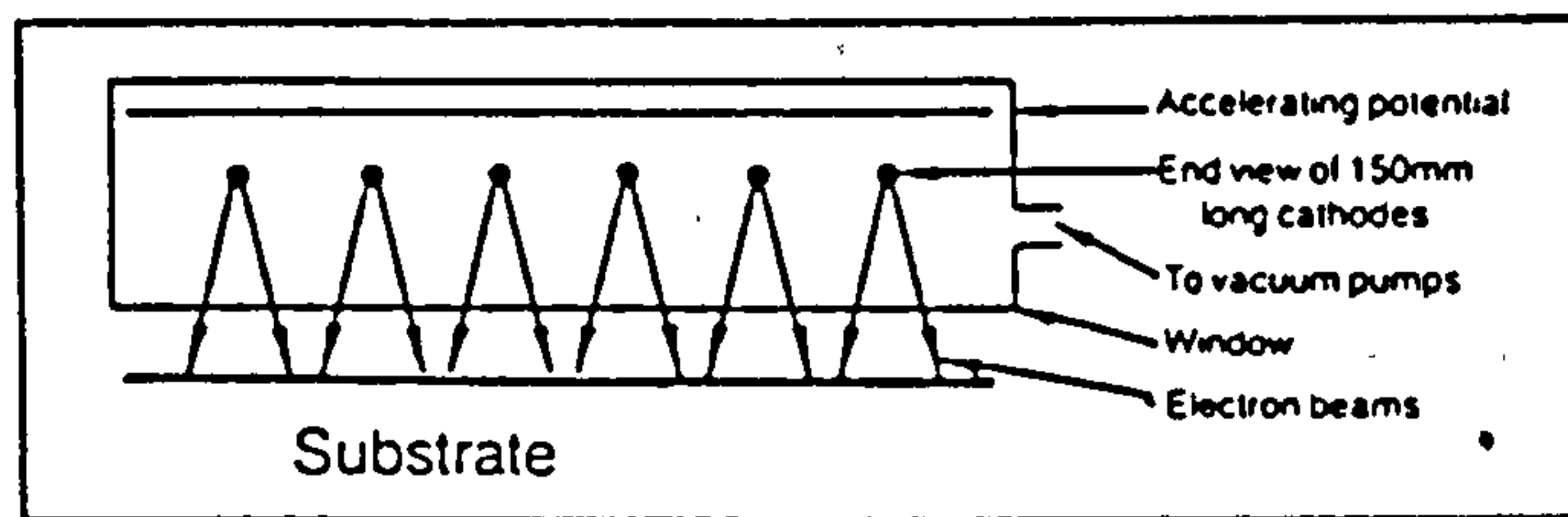
The linear cathode (Figure 11) comprises, as its name suggests, of a cathode stretched across the width of the moving web.

Figure 11 The linear cathode



The multiple cathode arrangement (Figure 12) consists of short lengths of cathode arranged in parallel to each other and the direction of the substrate.

Figure 12 The multiple cathode



One of the drawbacks associated with these EB units is the requirement of bulky lead shielding as a result of X-rays being produced on collision of the electron beam and the foil windows. It is also important to appreciate the fact that there will be energy losses of the electron beam between the power line and the coating to be cured. Energy losses may occur at the metal "window" in the electron beam unit. Although this "window" is usually very thin, of the order of 0.05mm, energy losses will be in the region of (50-60)keV [54]. Further energy losses will occur in the air gap between the window and the coating and for a typical 3.8cm air gap an energy loss of less than 10keV will occur [54].

### RADIATION CURABLE MATERIALS

Materials used for producing surface coatings by EB radiation are common to UV curable formulations [1-3]. Thus an EB formulation consists of the following components

1. Resins, e.g. a prepolymer containing double bond unsaturation.
2. Diluents, e.g. reactive monomers or unreactive

compounds that plasticize the cured film.

The first UV systems commercially used were based on the polyester-styrene systems [55]. These systems showed poor performance in terms of slow cure rates, high volatility of styrene [1-3]. Present demands on the surface coatings industry to comply with pollution regulations and the use of more energy efficient systems as characterised by fast cure response, resulted in the search of new UV- and EB-curable systems. The most successful of these are resins and diluents based on the acrylate functionality.

A radiation-curable system must fulfil several criteria. Firstly, it must display acceptable pigment wetting properties and rheology, to ensure minimum surface defects and following irradiation the cured film must display such characteristics as good adhesion to the substrate, as well as, hardness and flexibility.

### Prepolymers

Prepolymers form the backbone of a radiation curable system, and its main function are to impart such properties as good adhesion to the substrate, hardness and flexibility to the cured film. By varying the structure of the backbone certain properties of the cured film will predominate and will determine its end use. It has been shown that acrylate esters show rapid cure response compared with methacrylates, vinylethers or vinyl aromatics and so most resins used in the industry are modified to incorporate



acrylate functionality. The current trend is to replace the conventional 'two component' systems based on a viscous high molecular weight prepolymer in conjunction with a reactive diluent, by designing a very low molecular weight reactive oligomer, which would preempt the use of the more toxic and volatile reactive diluents used to date.

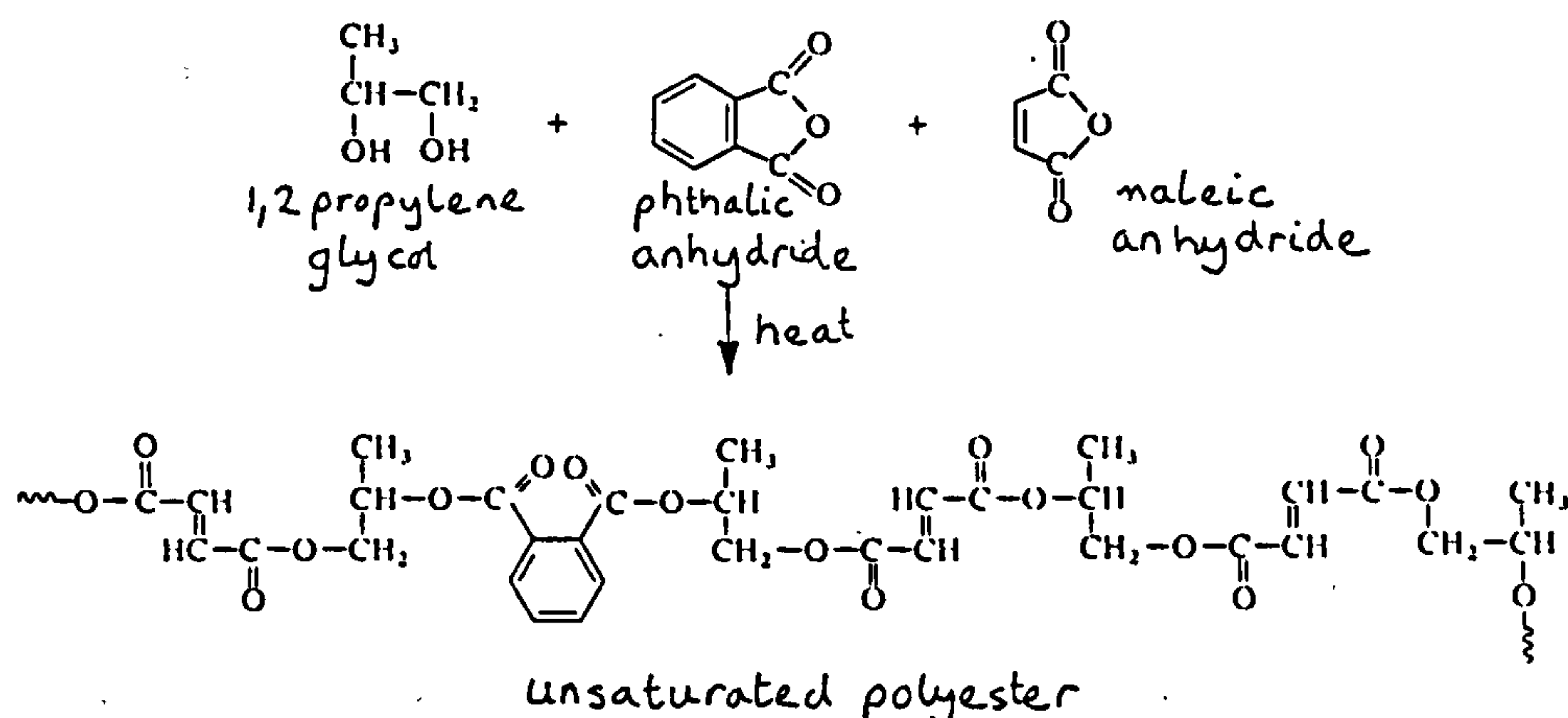
### Unsaturated Polyester systems

Some of the first UV-curable systems were based on styrene/polyester systems. However, these systems suffered from several drawbacks, such as slow cure speed, volatility of styrene and low compatibility of the polymers with styrene. These systems were primarily used as wood finishing fillers and laquers owing to their lack of adhesion and flexibility for use on metals, plastics, foils and paper.

In 1970 [56] the use of unsaturated polyester resins, in which unsaturation had been incorporated along the polyester backbone, providing sites capable of copolymerisation with vinyl monomers. Unsaturated polyesters are notably slow curing, and exhibit insufficient adhesion and flexibility for use on metals, plastics or paper. However, they produce very hard, tough and solvent resistant coatings. The unsaturated polyester resins are produced via a polycondensation reaction of dicarboxylic acids or anhydrides with polyhydric alcohols. Linear unsaturated polyesters may be formed from dibasic acids such as fumaric

acid, methylene succinic acid, phthalic acid or anhydrides such as, maleic anhydride, methyl maleic anhydride, phthalic anhydride and dibasic alcohols such as ethylene glycol or 1,2-propylene glycol. A typical unsaturated polyester may have the following composition [55].

Scheme 31



It has been shown that cure rate increases with increasing unsaturated acid content and can be increased further by replacement of styrene with acrylic monomers.

The main application of unsaturated polyester systems are for furniture finishes [1-3].

### Acrylated polyesters

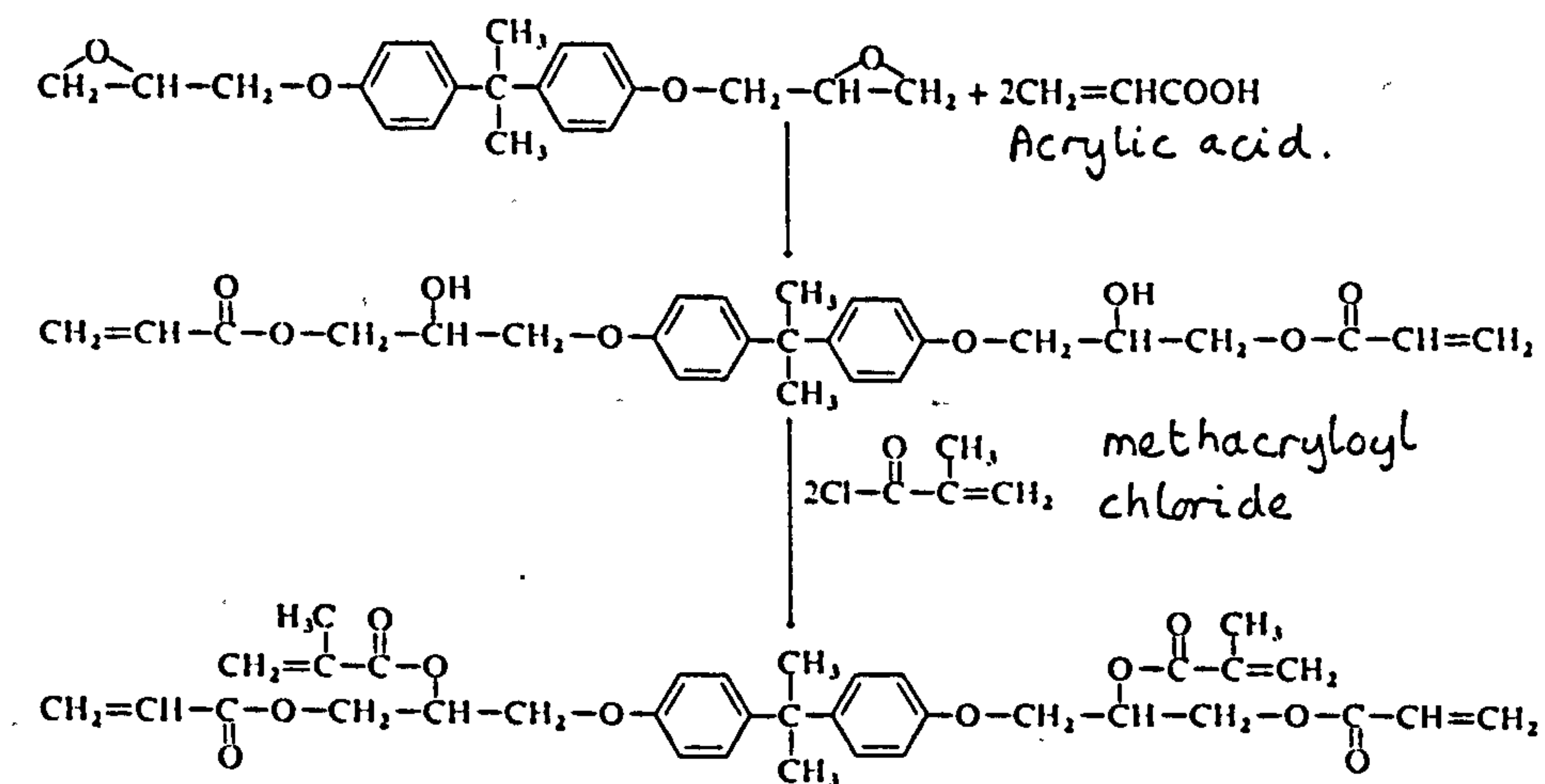
These reactive resins are prepared via esterification of a polyester containing hydroxyl groups with acrylic acid. Both the unsaturated and saturated type of polyesters have been modified this way [1-3]. These resins are widely used due to their all round performance with regards to hardness, toughness, and solvent resistance, although they are not outstanding in any particular property. However, the

structural variations of the polyester backbone together with the extent of modification by acrylation yield a wide variety of low cost prepolymers. Their wide use is also due to good wetting and formulation properties. This highly versatile group of prepolymers is used for many applications including, overprint varnishes for polyurethanes, leather, metals and inks.

### Acrylated epoxy resins

The majority of epoxy resins are based on the bisphenol-A derived epoxy resins and are formed via a condensation reaction between bisphenol-A and epichlorohydrin. Modification of the resulting epoxy resins may be accomplished by acrylation [1-3] as shown in Scheme 32

Scheme 32



### Acrylated Epoxy resin

The viscosity of such epoxy acrylates is very much greater than the parent epoxide resin and may present formulation



problems. Labana [57] showed that by reacting the hydroxyl groups present in such epoxy acrylates with acryloyl chloride, the resulting fully acrylated epoxy resin not only reduces viscosity markedly but also the reactivity of the system is increased. The outstanding properties associated with epoxy acrylates are toughness and rigidity (imparted by the bisphenol-A moiety), chemical and solvent resistance and excellent adhesion properties and as a result of the introduction acrylate functionality cure response is also good. Due to the many noble properties exhibited by epoxy acrylated resins they are used in a wide variety of radiation curable applications such as, coatings for metal, paper, plastic and wood.

### Acrylated polyurethanes

The oligomeric backbone, as well as the functionality of these acrylate modified systems dictates the properties of the finishes [1,3].

Highly branched polyurethanes prepared as a result of reacting a diisocyanate with a tri- or higher polyol, will result in the formation of a highly crosslinked, viscous material. Hydroxy containing acrylate monomers can be reacted with the polyurethane terminal isocyanate groups to produce a radiation curable acrylated polyurethane. These materials exhibit good cure speeds capable of producing a highly crosslinked and solvent resistant but inflexible coating.

Flexibility may be introduced by reacting a diisocyanate with a long chain glycol such as polyethyleneglycol or alternatively a hydroxy functional polyester, with an unsaturated hydroxy monomer [57]. However, by introducing flexibility, such properties as hardness and chemical resistance are diminished.

Acrylated urethanes are primarily used where resistance to abrasion is required and as a result have been used in the production of floor tiles, wood coatings, photopolymer printing plates and overvarnishes for paper and plastic substrates.

### Acrylated polyethers

Polyethers are formed by reacting ethylene oxide or propylene oxide with acid or basic catalysts such as  $\text{BF}_3$  or sodium hydroxide. The resulting polyether may then be esterified with acrylic acid or more successfully via a transesterification route with ethyl acrylate. Introduction of acrylate functionality tends to sacrifice film flexibility to yield very hard crosslinked films. Subsequently these systems are not recommended for finishings on metal, plastic or paper substrates.

### Monomers/reactive diluents

The prime function of a monomer is to act as a solvent

for the prepolymer and by adjusting its concentration it can be used to control viscosity. It also acts as a crosslinking agent when polyfunctional monomers are used and determines the cure response of the system. The proportion of monomer present in a system is very important as this will also reflect such film properties as film hardness, flexibility etc. The main classes of monomers are acrylates, vinyls and allylics and their cure response is in the order

acrylic > methacrylic > vinyl > allylic

The cure response is also affected by the functionality of the monomer, i.e. the number of reactive groups per molecule and increases with increasing functionality [1-3,57].

### Vinyls

The three most widely used diluents of this type are styrene (1) and its derivatives, vinyl acetate (2) and N-vinylpyrrolidine (3). All exhibit good solvent properties, however, they all suffer from several major drawbacks and have been largely replaced by the acrylate esters.

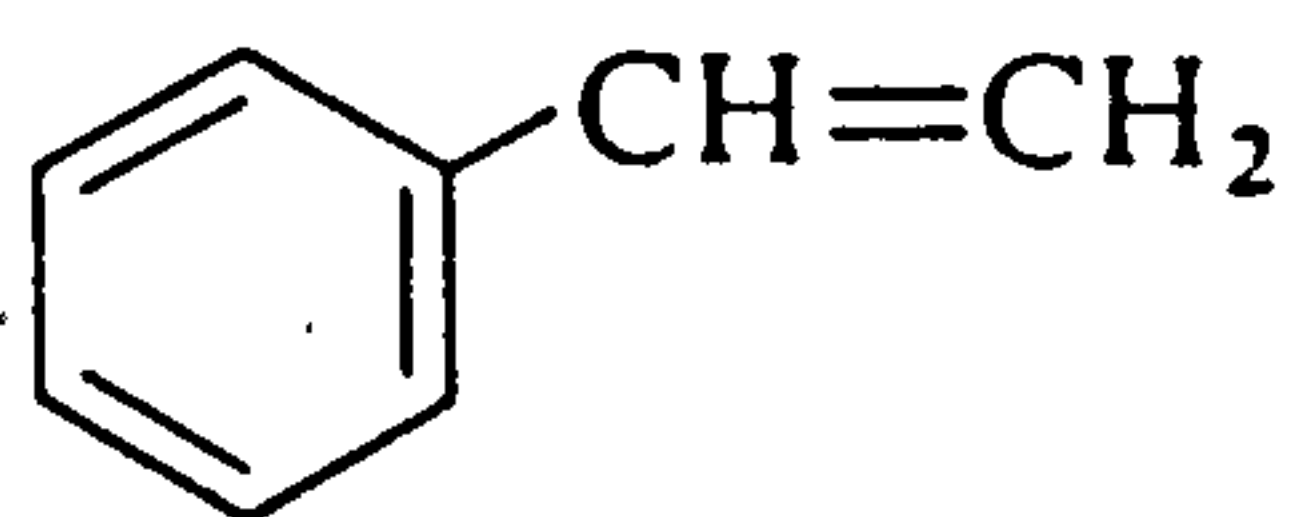
Styrene and its derivatives are very volatile and slow curing and as a result their use is in conflict with present demands for faster curing and less volatile systems. However, styrene is still a widely used monomer especially for wood finishing applications, due to its low cost.

Vinyl acetate is a slow curing and very volatile and flammable monomer and the resulting film exhibits poor

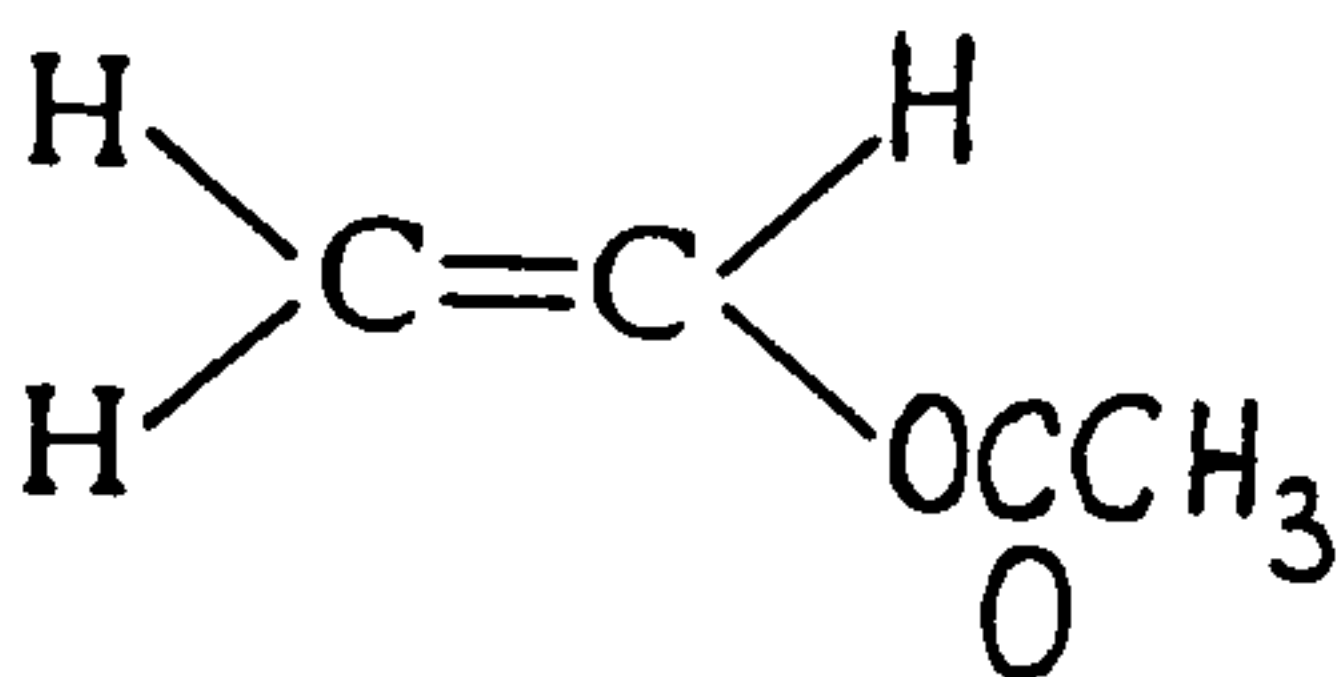


resistance to weathering.

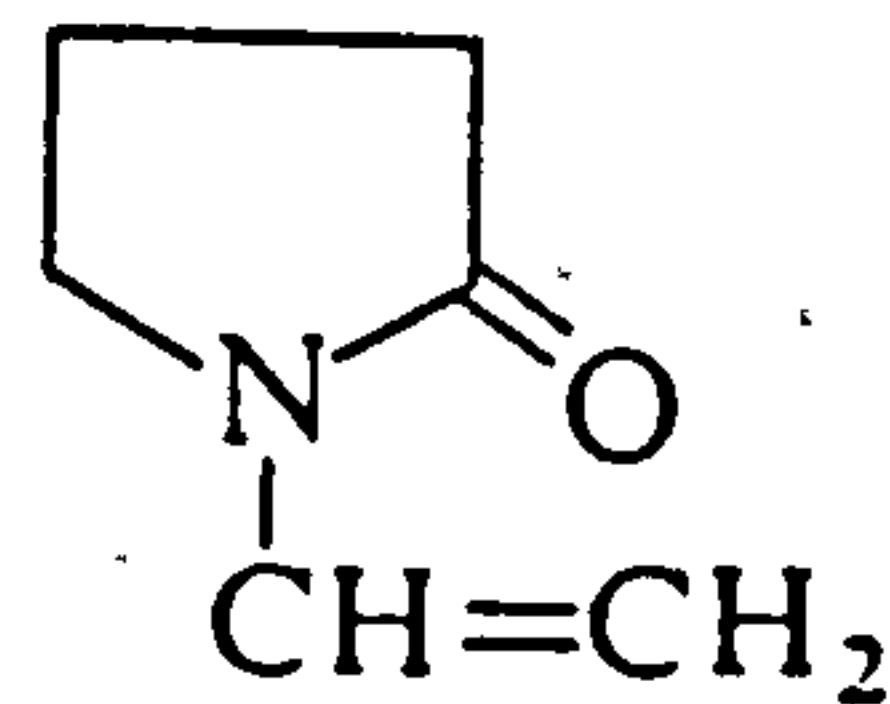
N-Vinylpyrrolidone is the most widely used of the vinyl monomers primarily due to its good solvating power and high reactivity. It also copolymerises readily with acrylates, however, it is very odiferous and this, has restricted its wide spread application.



(1)



(2)



(3)

### Acrylates

The inherent problems associated with the vinyls, are largely overcome by the acrylated esters, due to their inherently superior reactivity and reduced volatility. A range of acrylate monomers of varying functionality have been developed and a selection of which are shown in Table 4.

The wide choice of acrylate based diluents especially, in terms of their functionality enables the formulator to control not only the viscosity of the formulation but also the final film properties. In general the monoacrylates tend to be used in formulations where flexibility is required. However, they are generally odiferous and slow curing.

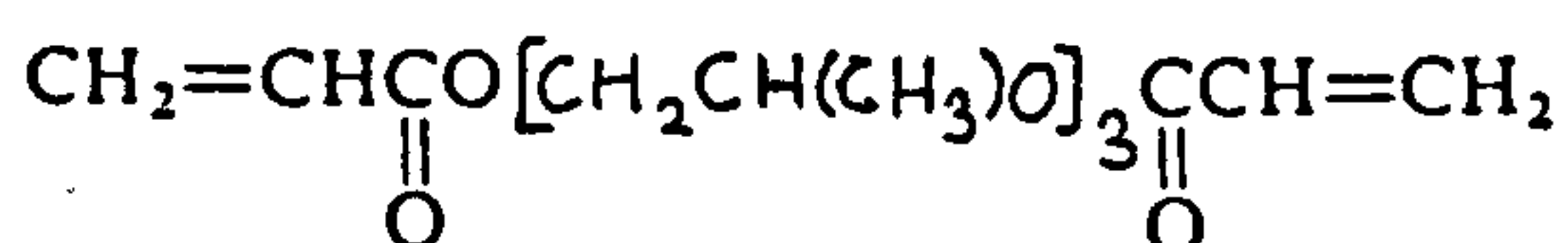
The difunctional acrylates, such as tripropylene glycol diacrylate (TPGDA), hexanediol diacrylate (HDDA) and triethylene glycol diacrylate (TEGDA) are examples of the

most widely used commercial diluents. These acrylate esters exhibit moderate crosslink density and good viscosity properties and largely avoid excessive shrinkage.

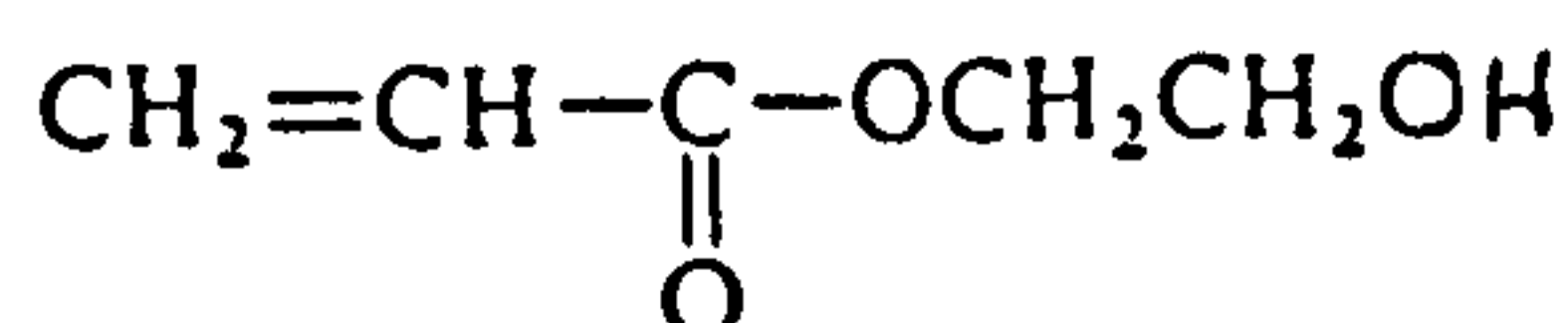
Tri-acrylates, such as trimethylolpropane triacrylate, (TMPTA), and pentaerythritol triacrylate (PETA) and the tetra acrylates, such as pentaerythritol tetraacrylate are extremely reactive and produce films which are characteristically highly crosslinked, glossy, hard and abrasion resistant. Use of these monomers may result in excessive crosslinking and shrinkage of the film resulting in poor adhesion and brittleness. However, this may be largely overcome by incorporating a monofunctional acrylate monomer into the mix thereby introducing flexibility into the system.

Despite the many virtues of acrylate esters, great care must be exercised in handling these materials as they are all classed as severe irritants and as mentioned previously this provides further impetus to the search for a reactive low molecular weight 'one component' system [1-3].

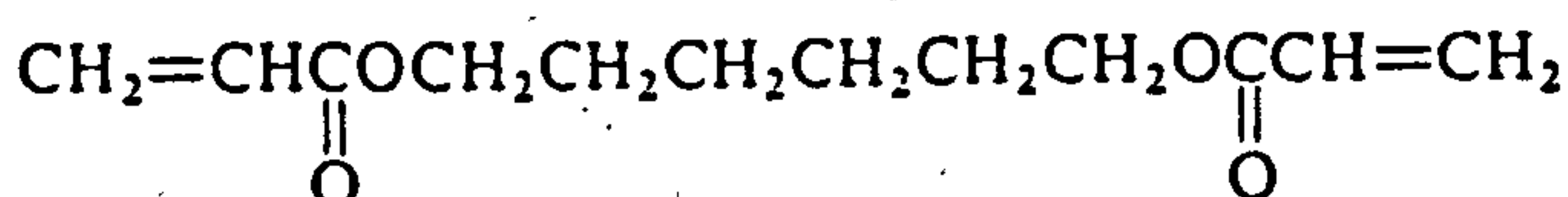
Table 4 A selection of widely used acrylate diluents



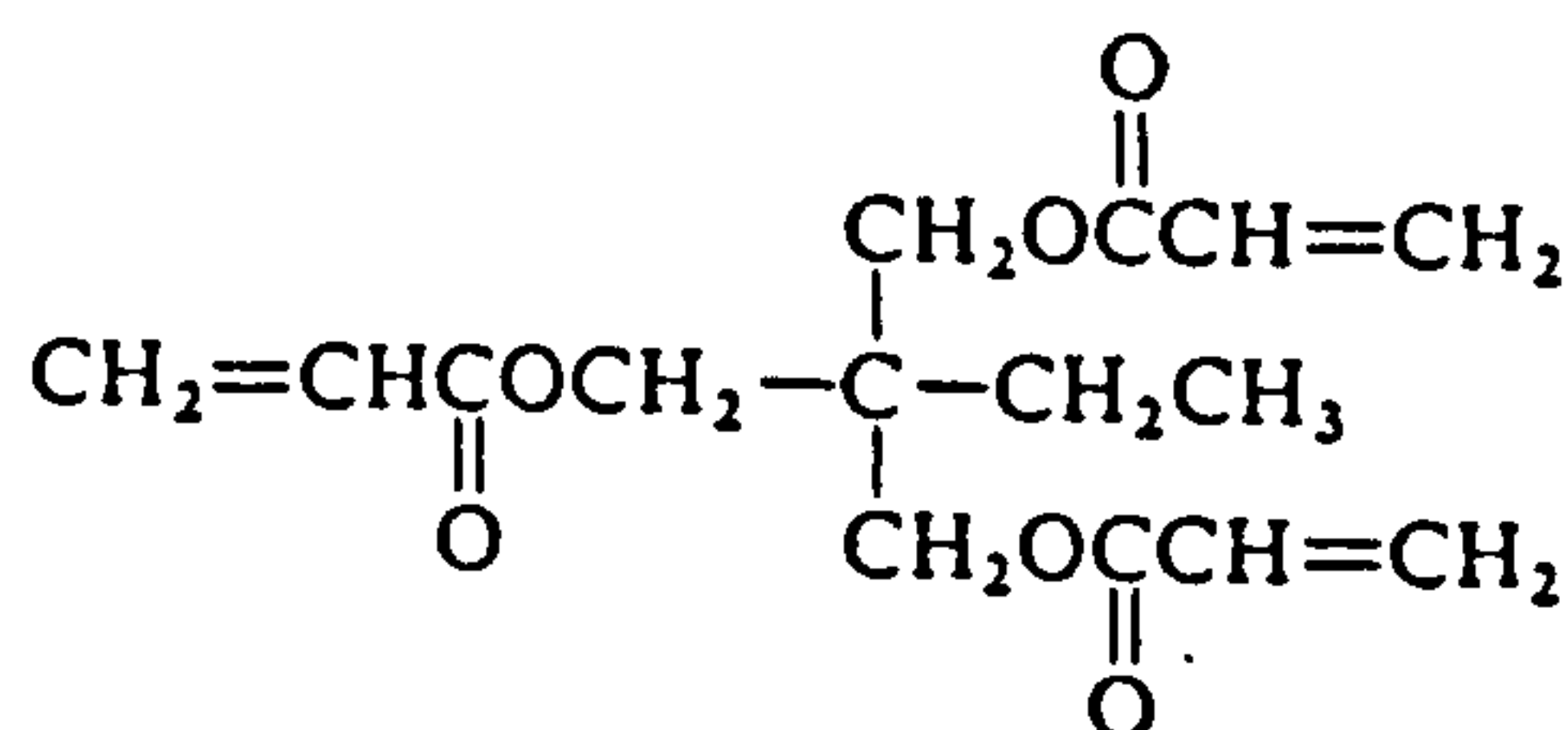
Tripropyleneglycol diacrylate (TPGDA)



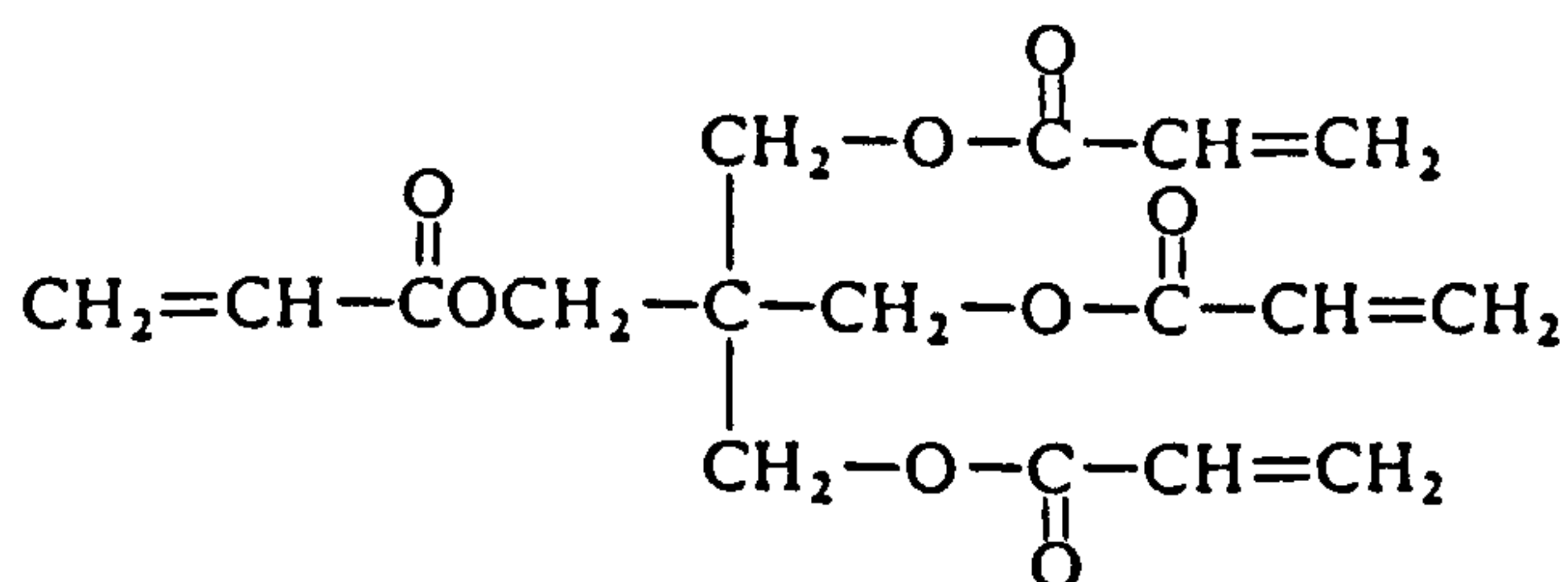
2-Hydroxyethyl acrylate (2-HEA)



Hexane diol diacrylate (HDDA)



Trimethylolpropane triacrylate  
(TMPTA)



Pentaerythritol tetra-acrylate  
(PETA).

## FORMULATION

Formulation determines such final film properties as surface characteristics, mechanical properties, chemical resistance, gloss, adhesion to the substrate and ultimately cure response [58].

### Surface levelling

Ideally a cured surface coating should be even and absent of such surface defects as cratering, blistering, reticulation or beading. Inadequate wetting of the substrate results in reticulation or beading of the film. Cratering may also occur when the time gap between application and cure is small, thus preventing levelling of the film. Both these defects may be corrected by the addition of flow agents. Blistering or beading may be caused by either entrapped solvent or air. This may be remedied by a preheat treatment to volatilise entrapped solvents or air pockets [3].

### Mechanical properties [59]

#### Hardness

Hardness is generally defined "as the ability of a film to resist surface abrasion" [3], and is the prerequisite for coatings on wood or metal surfaces. There are several ways of promoting hardness and this can be achieved by careful choice of the components of the formulation. Increasing ring



density by use of aromatic or cyclic aliphatic, increasing crosslink density, increasing  $T_g$  of the film and incorporating a post heat treatment for coatings on metal will all promote the hardness of the coating.

Acrylated epoxy resins derived from the bisphenol-A moiety produce characteristically hard surface coatings due to the presence of the aromatic rings. Resins and monomers based on acrylate functionality yield highly crosslinked networks conferring hardness. Stoving coatings on metal also promotes hardness of the film. A measurement of hardness of a film is the glass transition temperature,  $T_g$ , i.e. the temperature at which a film softens. The higher the  $T_g$  for a film the more rigid and consequently harder it becomes.

Although high crosslinking in a film encures hardness, excessive crosslink density results in brittleness. It is therefore important that toughness defined "as the ability of a surface coating to absorb energy prior to or during a fracture" is not sacrificed at the expense of hardness. Toughness is governed by the tensile strength and elongation properties of the material and is thus promoted by a depletion of restrictive crosslinks. It is therefore the requirement of a coating to achieve adequate crosslink density to impart the maximum toughness and hardness.

It is also necessary for coatings applied to metal and less rigid substrates such as paper to impart flexibility and impact resistance. Both these properties are determined by the visco-elastic character of the polymer, as well as the ability to obtain good adhesion to the substrate.

### Chemical resistance

In general chemical resistance of a cured coating improves with crosslink density. However, it is important to appreciate the inherent susceptibility of certain functional groups. For instance it has been shown that polyester/styrene systems exhibit good solvent resistance to both polar and aqueous solutions. Although, acrylates display resistance to organic solvents they are generally less resistant to aqueous solutions and are therefore not recommended for applications where hydrophilic conditions might be encountered.

### Gloss

Many coatings require either a high gloss or a matt finish [60,61]. Matt finishes may be obtained by introduction of a matting agent. However, the rheology of such systems as well as film properties must be monitored when incorporating matting agents. Gloss is obtained by careful consideration of several factors. Firstly, the nature and content of matting agents as well as the medium to which it is added. Acrylate systems tend to produce high gloss films and are difficult to modify with matting agents. Secondly, the curing of a system under aerobic or anaerobic conditions will also affect the gloss of a coating and it has been shown that gloss is markedly lower when curing is

carried out in aerobic conditions.

### Adhesion

Some important factors related to adhesion are 1) interfacial contact and surface tension, 2) curing time/temperature relation 3) shrinkage forces and 4) coating substrate interactions [59].

Good wetting of the coating is essential for the development of satisfactory adhesion. Interfacial contact is necessary in order for short-distance (i.e.  $<10\text{nm}$ ) attractive forces to operate. Adequate wetting of the surface with the coating is readily achieved at elevated temperatures and it is therefore favourable to apply a pre- or postcure heat treatment to assist adhesion forces, particularly on metal surfaces.

Rapid cure, synonymous with EB and UV cured films, will invariably be associated with shrinkage of the film. These shrinkage stresses are frequently strong enough to detach the coating from the substrate.

The topography of the substrate and physical absorption of the coating also contribute to adhesion properties. Surface roughness as well as preferential polymer absorption to the substrate than polymer/monomer interactions will both promote adhesion.

It is therefore necessary to consider the following points to optimise adhesion in radiative curable systems.

- 1) Minimise coating surface tension and maximise



- substrate energy for adequate interfacial contact.
- 2) Minimise shrinkage on curing.
  - 3) Promote association of polymer with substrate.
  - 4) Apply pre- or post- heat treatment.

### Pigmentation

As previously mentioned pigmentation of films does not affect the electron beam curing process. This may be largely attributed to the fact that EB curing is independent of the UV/visible absorption characteristics of the pigments and hence a wide range of pigmented systems may be cured by electron beam radiation.

### Cure response of a system

The measurement of cure of a system may be ascertained by the use of simple empirical tests such as tack free to the touch, the thumb twist to determine whether through cure has been obtained and scratch resistance to the fingernail, which indicates if the system is fully cured [3].

Cure assessment can also be determined by use of standardised physical test methods to evaluate film performance. The most popular of these are the solvent rub test, to determine the number of rubs with a solvent such as acetone to remove the coating and thereby giving an indication of crosslink density, the dry abrasion test to assess through cure of the film, and the pencil hardness

test to give an indication of hardness and toughness of the film. All such tests are invaluable in assessing the final film properties, however, they are empirical tests and are all subjective.

Quantitative assessment of cure, also described as measuring the 'degree of cure', of a system may be achieved by measuring the percentage change in functionality during the course of the reaction. In the case of acrylate systems the degree of cure is measured by monitoring the percentage residual carbon carbon double bonds present [62-65]. Examples of alternative methods of evaluating cure in terms of unreacted monomer are differential scanning calorimetry, dilatometry and gas liquid chromatography [66].

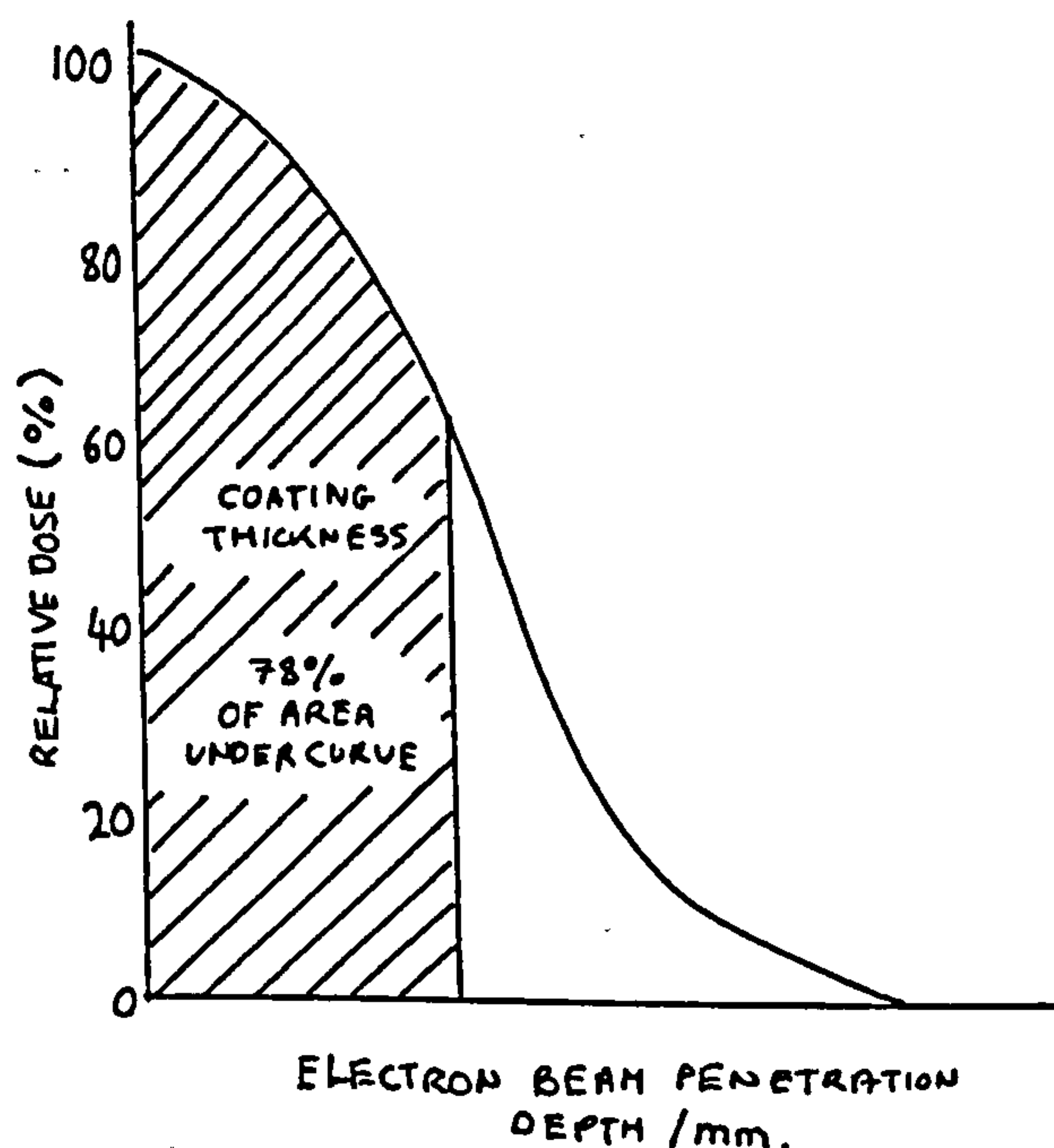
Cure response is determined by many factors including the dose of radiation applied, film thickness, type of substrate, atmosphere and chemical reactivity of the system.

#### Dose of radiation, film thickness and substrate relationship

As previously described high energy electrons will lose energy traversing a medium through elastic and inelastic collisions and emission of radiation. On exposing a radiation sensitive coating on a substrate to EB radiation absorption of the energy deposited in the coating will lead to its subsequent cure. However, the energy absorption profile throughout the coating is not uniform because of continual loss of energy. The distribution of

dose throughout a material is indicated in Figure 13 and varies considerably with film thickness as shown. It is therefore important to establish the minimum and maximum dose levels acceptable to cure the film and in order to establish which voltage will deliver the desired dose.

Figure 13 Relative dose of radiation versus electron beam penetration depth in unit density material for an electron energy of 250kV

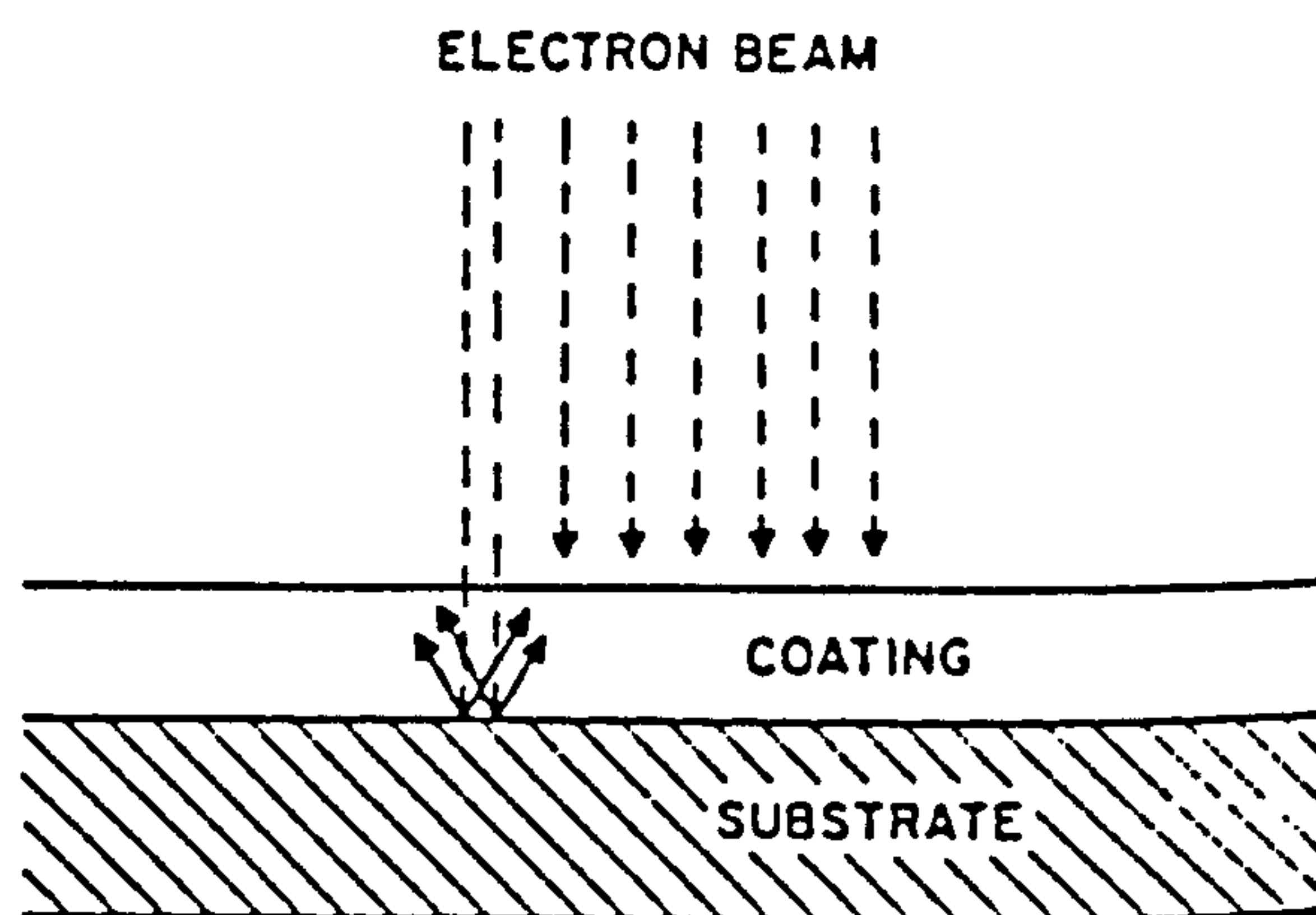


When determining dose levels required to cure a film consideration of the substrate should also be taken into consideration. If the electron beam penetrates beyond the coating and strikes a substrate with significant density, some of the electrons may be deflected via a process known as backscatter back into the coating [54] as illustrated in



the energy of the incident electron beam, they will be deflected back into the coating and account for an additional dose delivered within that portion of the coating. This effect in most instances leads to a greater dose uniformity across the coating.

Figure 14 Backscatter effects

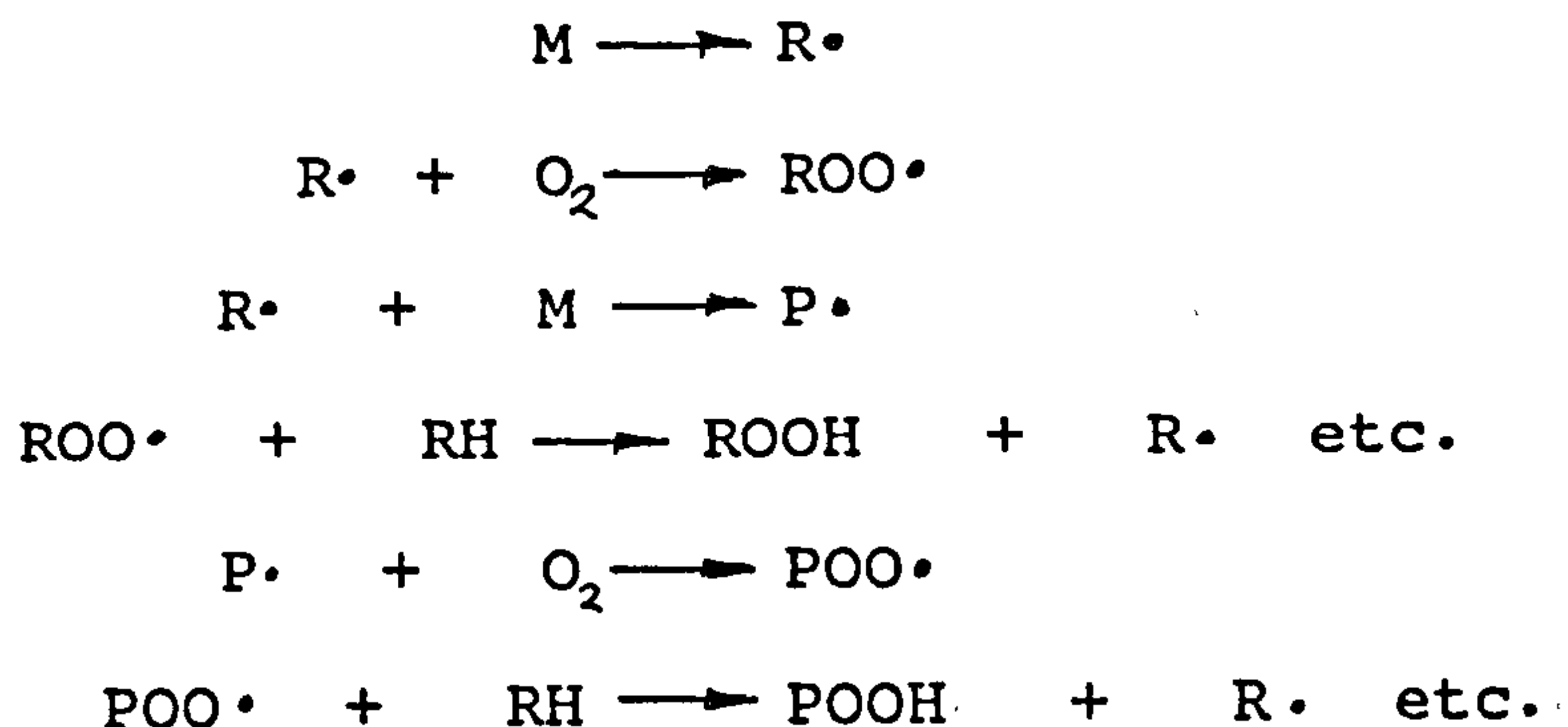


#### Atmosphere

Plews and Philips [62] have investigated the effect of air inhibition on photopolymerisable systems. Poor cure was attributed to oxygen inhibition [67,68]. The same effects have been observed for free radical polymerisation induced by EB radiation [3]. Molecular oxygen is a ground state free radical species and will react readily with free radical species. The innate reactivity of molecular oxygen towards free radical species results in effective scavenging of initiating radicals,  $R\cdot$  as well as, the growing polymer chain radicals,  $P\cdot$  yielding peroxy radicals,  $ROO\cdot$  and  $POO\cdot$ . The peroxy radicals thus formed will hydrogen abstract to generate hydroperoxide species,  $ROOH$  and  $POOH$  with the

regeneration of a radical species. The deleterious effects of generating peroxy radicals incapable of propagating polymerisation, result in the production of low molecular weight polymers and inevitable reduced film properties [69].

### Scheme 33



Several methods have been deployed to reduce the "oxygen effect" and these are blanketing the coating with an inert gas, e.g. nitrogen or the use of a polyethylene foil laminate. High dose rates can also be employed to counteract the diffusion of oxygen into the coating during the curing process [6].

### Applications of EB curing

The prime advantage of using EB curing as opposed to other radiation curing processes are due to the inherent characteristic features of EB cured films, namely, high gloss, lack of photoyellowing due to the absence of photoinitiator, pigmentation does not present a problem in terms of its absorption characteristics, and the very fast cure speeds attainable. For these reasons the electron beam

curing process has been applied to several processes, but has been primarily used for wood coatings [70] and the coating of plastic films [71].

The use of EB curing has also been applied to the graphics industry. The high gloss attainable means that a "brightening" of the overprinted graphics has attracted many applications for various packaging. Several new electron beam applications have been developed over the past few years [72]. These are primarily an adaptation of transfer coating to produce coated fabrics and other non-textile substrates to produce high gloss coatings [72]. Electron beam metallisation is a process whereby a metallised coated product is obtained. The inherent advantages of this process are due to instantaneous cure of the adhesive and the ability to make bulky or thick metallised products. The industrial application of EB to the manufacture of magnetic tape and floppy discs has also proven successful [12].



## References

- [1] S. Paul, (1986). Surface Coatings Science and Technology, Wiley-Interscience.
- [2] R. Holman, (1984). UV and EB Formulation for Printing Inks, Coatings and Paints, Sita Technology
- [3] C. G. Roffey, (1982). Photopolymerisation of Surface Coatings, Wiley-Interscience
- [4] S. V. Nablo and E. P. Tripp, (1977). Radiation Phys. Chem., 9, 325.
- [5] W. J. Rander, (1977). Radiation Phys. Chem., 9, 69.
- [6] T. A. Du Plessis and G. De Hollain, (1979). J.O.C.C.A. 62, 239.
- [7] J. Laizier, (1977). Rad. Processing, 4, 13.
- [8] A. S. Hoffman, (1971). Atomic Energy Rev., 9, 347.
- [9] S. E. Young, (1976). Prog. in Organic, 4, 225.
- [10] T. J. Miranda and T. F. Huemmer (1969). J. Paint Tech., 41, 118.
- [11] D. H. Teesdale, (1985). Coating/Curing/Converting, 1, 2.
- [12] B. S. Qunital, (1985). Proc. Radcure Conf., Basel, Switz.
- [13] Y. Tabata, (1985). Proc. Radcure Conf., Basel, Switz.
- [14] N. V. Klassen, (1987). Radiation Chemistry: Principles and Applications, Farhataziz and M. A. J. Rodgers, Eds., VCH Publishers.
- [15] F. W. Billmeyer, (1984). Textbook of Polymer, Science, 3rd Ed., Wiley-Interscience.

- [16] G. Odian, (1981). Principles of Polymerisation, 2nd Ed., Wiley-Interscience
- [17] K. H. Brown, (1977). Radiat. Curing, 4 (4), 8.
- [18] J. W. T. Spinks and R. J. Woods, (1964). An Introduction to Radiation Chemistry, Wiley-Interscience.
- [19] A. J. Swallow, (1973). Radiation Chemistry - An Introduction, longman.
- [20] Radiation Chemistry: Principles and Applications, Farhataziz and M.A.J. Rodgers, Eds., VCH Publishers.
- [21] G. Foldiak, Ed., (1981). Radiation Chemistry of Hydrocarbons, Elsevier.
- [22] A. Charlesby, (1960). Atomic Radiation and Polymers, Pergamon Press.
- [23] A. Chapiro, (1962). Radiation Chemistry of Polymer Systems, Wiley-Interscience.
- [24] A. Chapiro, (1969). Encyclopaedia of Polymer Science and Technology, Wiley-Interscience, 11, 702.
- [25] J. E. Wilson, (1974). Radiation Chemistry of Monomers, Polymers and Plastics, Marcel Dekker.
- [26] A. Chatterjee, (1987). Radiation Chemistry: Principles and Applications, Farhataziz and M. A. J. Rodgers, Eds., VCH Publishers.
- [27] K. R. Kase and W. R. Nelson, (1978). Concepts of Radiation Dosimetry, Pergamon.
- [28] J. Pacansky, (1983). Rad. Curing, August, 4.
- [29] T. E. Everhart and P. H. Hoff, (1971). J. Appl. Phys., 42, 5837.

- [30] M. Rosenstein, W. I. McLaughlin and J. Silverman,  
(1970), Electron and ion beam Science and Technology,  
R. Bakish, E., The Electronchem. Soc., p.591.
- [31] A. H. Samuel and J. L. Magee, (1953). J. Chem. Phys.,  
21, 1080.
- [32] A. Mozumder and J. L. Magee (1966). J. Radiat. Res.,  
20, 203.
- [33] G. A. Salmon, (1986). Polymeric Mat. Sci. Eng., 55,  
195.
- [34] N. V. Klassen, (1987). Radiation Chemistry:  
Principles and Applications, Farhataziz and M. A. J.  
Rodgers, Eds., VCH Publishers.
- [35] M. Burton, (1963). Faraday Discuss. Chem. Soc., 7, 1.
- [36] J. G. Calvert and J. N. Pitts, (1966). Photochemistry,  
Wiley-Interscience.
- [37] N. J. Turro, (1978). Modern Molecular Photochemistry,  
Benjamin/Cummings.
- [38] S. Lipsky, (1981). J. Chem. Ed., 58, 93.
- [39] A. A. Herod, A. G. Harrison, R. M. O'Malley, A. J.  
Fierrrer-Correia and K. R. Jennings, (1980), J. Phys.  
Chem., 74, 2720.
- [40] F. Cacace, (1982). Radiat. Phys. Chem., 20, 99.
- [41] F. S. Dainton, G. A. Salmon and P. Wardnan, (1969).  
Proc. Roy. Soc. London Ser. A, 313, 1.
- [42] D. H. Aue and M. T. Bowers, (1979). Gas Phase Ion  
Chemistry, M. T. Bowers, Ed. Academic Press.
- [43] G. C. Eastmond, Comprehensive Chemical Kinetics, C. H.  
Bamford and C. F. H. Tipper, Eds., 14A, Elsevier.



- [44] R. A. Holroyd, (1987). Radiation Chemistry:  
Principles and Applications, Farhataziz and M. A. J.  
Rodgers, Eds., VCH Publishers.
- [45] K. N. Jha, G. L. Bolton and G. R. Freeman, (1972). J.  
Phys. Chem., 76, 3876.
- [46] G. G. Teather and N. V. Klassen, (1975). Int. J.  
Radiat. Chem. 7, 475.
- [47] S. J. Swallow, (1987). Radiation Chemistry:  
Principles and Applications, Farhataziz and M. A. J.  
Rodgers, Eds., VCH Publishers.
- [48] M. Anbar, (1969). Adv. Phys. Org. Chem., 7, 115.
- [49] V. Stannett and J. Silverman, (1983). Initiation of  
Polymerisation and Catalytic Aspects of Polymers, F. E.  
Bailey, Ed., Amer. Chem. Soc., Symposium Series 212.
- [50] A. Charlesby, (1952). Proc. Roy. Soc. (London), A215,  
187
- [51] A. Charlesby, (1953), Nature, 171, 167.
- [52] E. J. Lawton, A. M. Buethel and J. S. Balwit, (1953).  
Nature, 172, 76.
- [53] A. Charlesby, (1967). Adv. in Chem., 66, Amer. Chem.  
Soc.
- [54] C. K. Schmidt, (1980). J. Rad. Curing, April, 14.
- [55] A. Lanos, S. Lynn and R. Hall, (1976). J.O.C.C.A., 59,  
193.
- [56] R. H. Chandler, (1970). The UV Curing of Unsaturated  
Polyester Laquers, Paint Technology.
- [57] K. O'Hara, (1985). Polymer Paint Colour Journal, 175,  
254.

- [58] M. De Poorter, A. Duncarme, P. Dufour and Y. Merck,  
(1978). J.O.C.C.A., 61, 195.
- [59] T. F. Huemmer, (1974). J. Rad. Curing, 1(3).
- [60] T. F. Huemmer, L. A. Wasowski and R. J. Plooy, (1972),  
J. Paint Technol. 44, 61.
- [61] A. E. Hahn, (1974). Radiat. Curing, 1 (2), 13.
- [62] G. Plews and R. J. Phillips, (1979). J. Coatings  
Tech., 51 (648), 69.
- [63] T. Nishikulso, M. Imaura, M. Mizuko and T. Takaota,  
(1974). Appl. Poly. Sci., 18, 3445.
- [64] R. Phillips, (1978). J.O.C.C.A., 61, 233.
- [65] Y. C. Chang, (1977). Phot. Sci. Eng., 21, 348.
- [66] A. Van Neerbos, (1978). J.O.C.C.A., 61, 247.
- [67] F. R. Wight, (1978). J. Polym. Sci. Polm. Letts. Ed.,  
16, 121.
- [68] J. S. Chong, (1969). J. Appl. Polm. Sci., 13, 241.
- [69] C. Dekker, (1985). Conf. Proc. Radcure, Basel, Switz.,.
- [70] C. R. Hoffman (1973). ACS, ORPL, 32, (2), 426.
- [71] E. P. Tripp and J. Weisman, (1985). Conf. Proc.  
Radcure, Basel, Switz..



[illegible]



Chapter 2    **QUANTITATIVE ANALYSIS OF CURE BY FTIR-PA  
SPECTROSCOPY**

Introduction	72
Fourier Transform spectroscopy	74
Photoacoustic Spectroscopy	79
Quantitative analysis of cure using FTIR-PAS	83
Results and discussion	86
Conclusion	90
Experimental	91
Appendix A	94
References	101

## INTRODUCTION

The term 'cure' is used to describe the phase change of a mobile liquid to a tackfree solid on irradiation. The measurement of cure may be assessed in three ways.

- 1) Cure may be measured in terms of the final film properties. The simplest of these is to test whether the irradiated film is tackfree to the touch. Other tests may relate to such mechanical properties as thumb-twist resistance, scratch resistance, pencil hardness or to such chemical properties as solvent resistance [1]. Cure assessment by these methods are subjective, however they provide a quick and practical evaluation of final film properties.
- 2) An alternative measurement of cure may be interpreted as the extent to which the resins and monomers have been incorporated into the polymeric system. Techniques for the measurement of extent of bound material are solvent extraction and weight loss on stoving [2].
- 3) Cure assessment may also be measured in terms of the percentage of conversion of functional groups and can be described as the degree of cure of the reaction. Several methods may be used to evaluate this measurement, such as infrared spectroscopy [3-5] calorimetry [6,7] and dilatometry [8]. These techniques are all objective means of evaluating cure and can be used to measure the extent of cure or monitor the progress of the reaction, if it is slow enough.



Several reviews on cure methods have been published [9,10]. Other techniques not mentioned above, include NMR, laser nephelometry and viscometry [11]. However, not all these techniques are available for measuring the cure of a polymer coating on a substrate. A technique that has been widely exploited to this end is infrared spectroscopy [12,13].

Infrared (IR) spectroscopy is a non-destructive and precise way of measuring the conversion of functional groups. The IR technique can be divided into three categories. Firstly, transmission spectroscopy, which can be used when the substrate is transparent, secondly reflectance spectroscopy for coatings on an opaque substrate and thirdly photoacoustic spectroscopy applicable for a coating on any substrate.

When a coating has been cured on a transparent substrate or if the coating remains 'wet', transmission IR spectroscopy yields excellent quality spectra and in most cases quantitative measurements can be made. For those coatings on an opaque substrate several techniques have been developed, such as diffuse reflectance [14] and attenuated reflectance [15]. These methods have been successfully applied to polymer surface studies. However, they all suffer from drawbacks that limit their application for quantitative analysis. Photoacoustic spectroscopy has only recently been available as an alternative means of obtaining an 'absorption' spectrum of solids [16]. Initial studies by Vidrine [17], Rockley [18] and Krishnan [19] have all



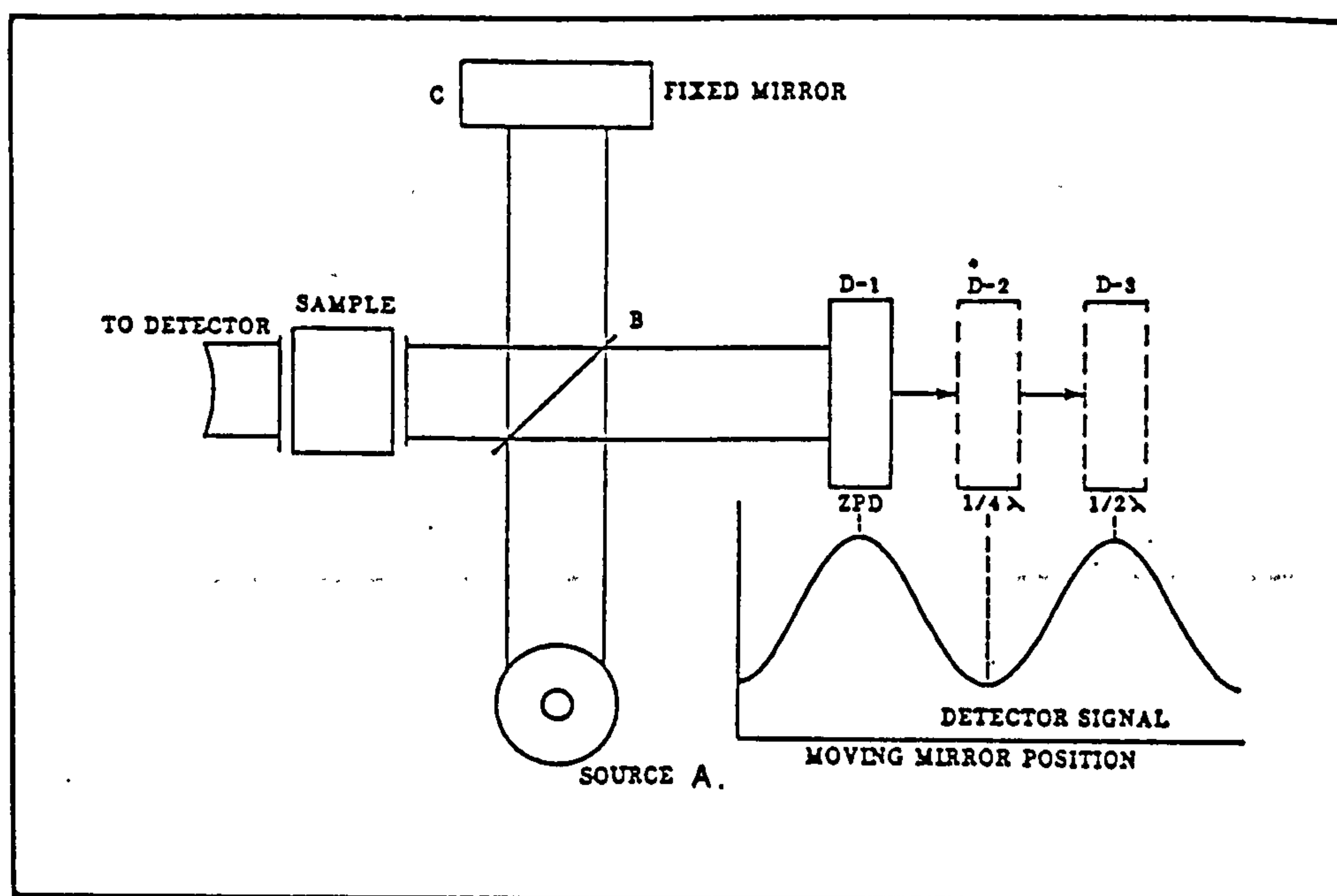
indicated the importance of the application of FTIR-PAS to polymer films.

In this chapter the use of FTIR-PAS was investigated and assessed as a quantitative means of measuring the degree of cure of thin films on a substrate. Coatings of tripropyleneglycol diacrylate, TPGDA, on aluminium foil cured at various doses of radiation were used to evaluate this technique.

### Fourier Transform Spectroscopy [20]

Fourier transform infrared (FTIR) spectroscopy is based on the use of a Michelson interferometer, rather than a monochromator used by dispersive infrared spectrometers. The Michelson interferometer, as illustrated in Figure 1, comprises of three basic parts: the beamsplitter, a fixed mirror and a moving mirror. A broad band IR source, A, projects collimated radiation into the interferometer. Approximately 50% of the beam is transmitted through the beamsplitter and directed to the fixed mirror C. The remainder of the light is reflected towards the moving mirror D. After each beam has been reflected back to the beamsplitter they recombine either constructively or destructively, depending on the position of the moving mirror relative to the fixed mirror. The resulting beam then passes through the sample and continues onto the detector.

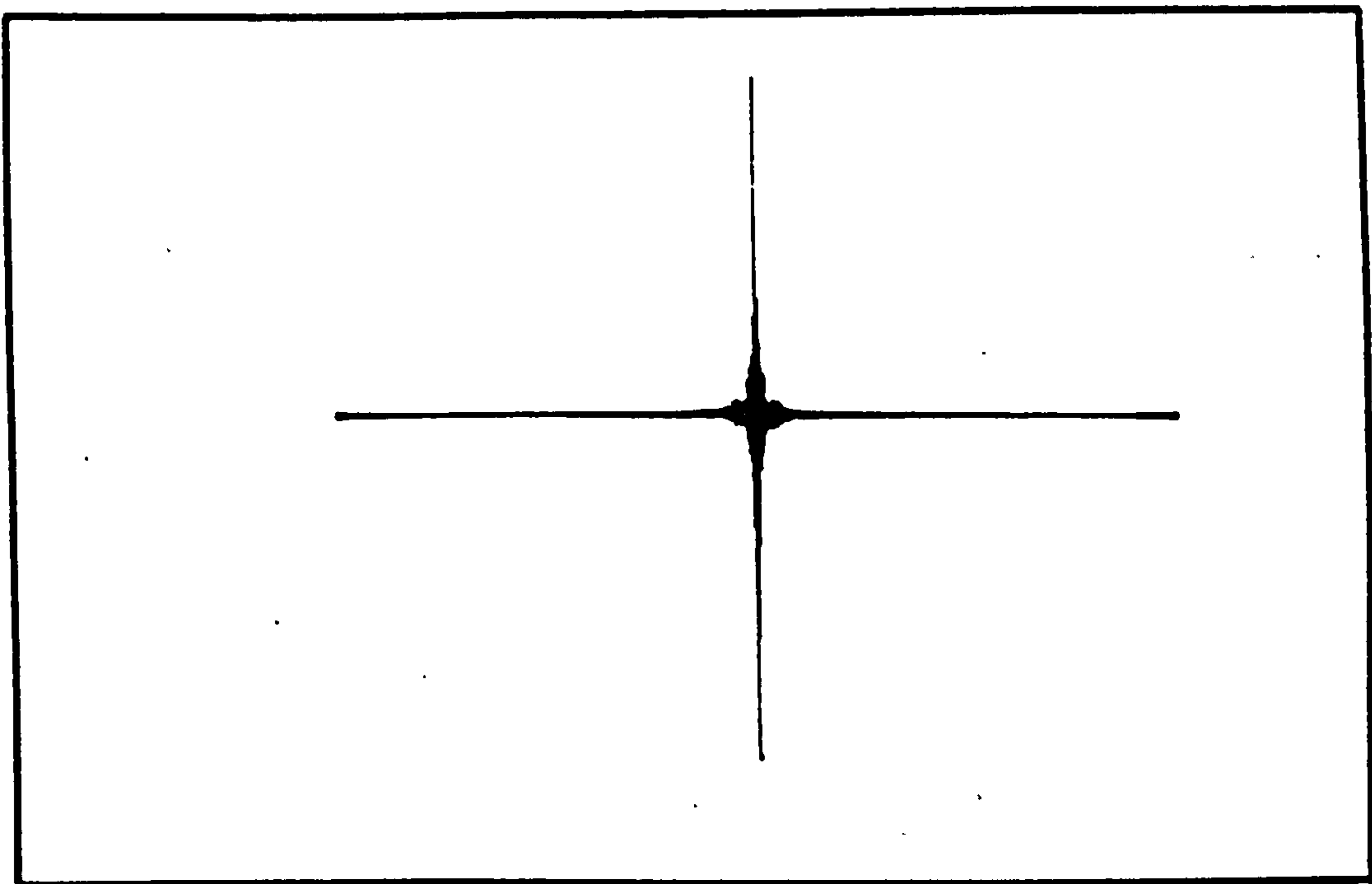
Figure 1 A Michelson Interferometer



Consider the case of a monochromatic source of radiation. When the distance between the beamsplitter and the moving mirror, B-D, and the beamsplitter and the fixed mirror, B-C, are the same then the two reflected beams would be exactly in phase with each other. At this point the beams interfere constructively so that the sum of the intensities of the beams are at a maximum. This mirror position is called the point of zero path difference, ZPD. However, when the moving mirror moves to a position, such that the total optical path difference between the two beams is an integral number of  $1/2$  wavelength, then at this point the beams will interfere destructively at the beamsplitter so that the resultant beam intensity is zero. This pattern of constructive and destructive interference will repeat itself with each subsequent  $1/4$  wavelength displacement, forming a

sine wave as shown in Figure 1. Hence the light source is said to be modulated. When a broad band IR light source is used the same process occurs for every frequency. The signal recieved by the detector is the resultant of all these modulated sine waves. The resultant detected signal is called an interferogram.

Figure 2 A typical interferogram



The interferogram is then converted by a Fourier transformation to produce a single beam spectrum as shown in Figure 3. The sample single beam spectrum is then ratioed against a single beam spectrum of the source to yield a absorbance spectrum of the sample (Figure 4).



Figure 3 Single beam spectrum of the light source

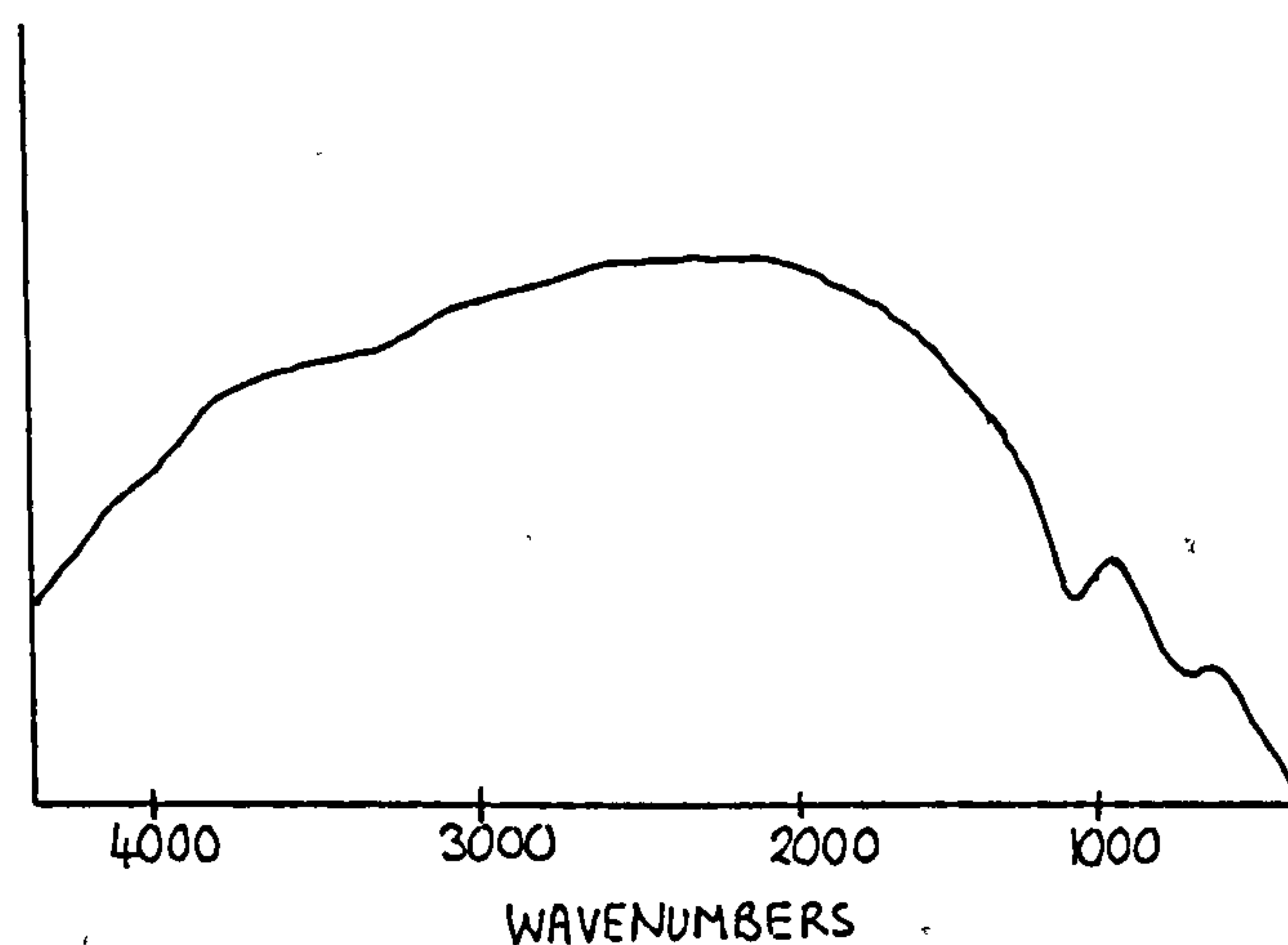
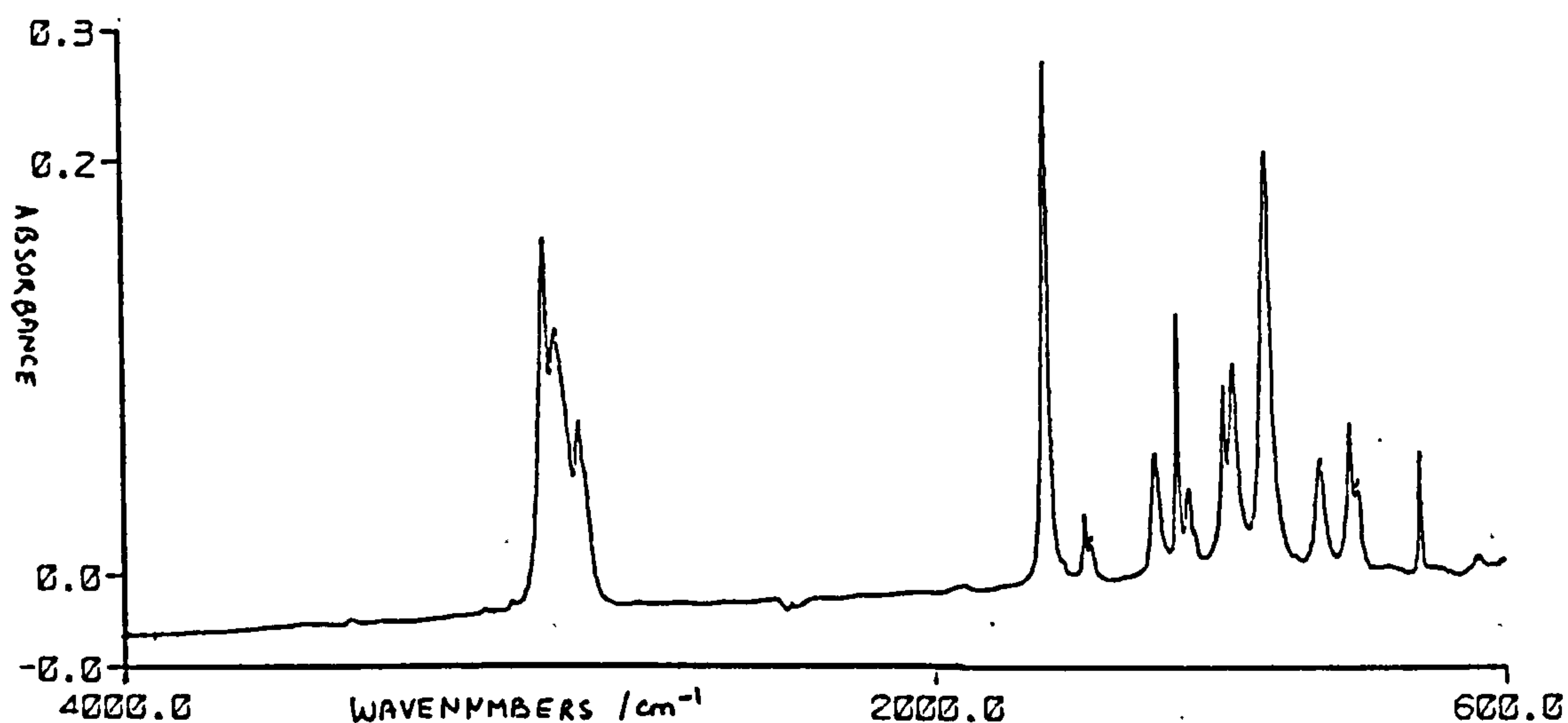


Figure 4 Absorbance spectrum of isodecyl acrylate



The main and most important features of the Michelson interferometer yield several advantageous features outlined below

- **Felgett advantage.** Data in an interferometer is collected from all spectral frequencies simultaneously throughout the duration of the measurement. The resultant signal is said to be "multiplexed" and an infrared spectrum may be obtained from one scan. The time for one scan is

approximately one second and yields a S/N ratio equivalent to that of a dispersive instrument. However, because of the very short duration of collection time, the S/N ratio may be improved substantially by addition of multiple scan measurements thus increasing the S/N ratio greatly. Fellgett's advantage (or multiplex advantage) can thus be interpreted as obtaining an infrared spectrum of equivalent S/N ratio to that of a dispersive instrument in much less time or a spectrum of superior S/N ratio using multiple scans.

- Jacquinot advantage. The optical throughput, is determined by the amount of energy that gets through the system. For dispersive instruments the throughput is largely limited by small slit widths. However, in the FTIR system there are no slits and the throughput is determined by the size of the mirrors and the interferometer itself, thus a large amount of energy gets through the system resulting in greater sensitivity

- Connes advantage. The use of an internal HeNe laser to monitor the moving mirror position means that it can also be used as an internal wavelength calibration standard. The accurately known laser frequency in turn means that wavenumbers will be within 0.01 cm<sup>-1</sup> accuracy. This is useful for very exact work and when spectral subtraction techniques are applied.

- Mechanical simplicity. The only moving part of the interferometer is the moving mirror and as such there is little 'wear out' of the spectrometer.

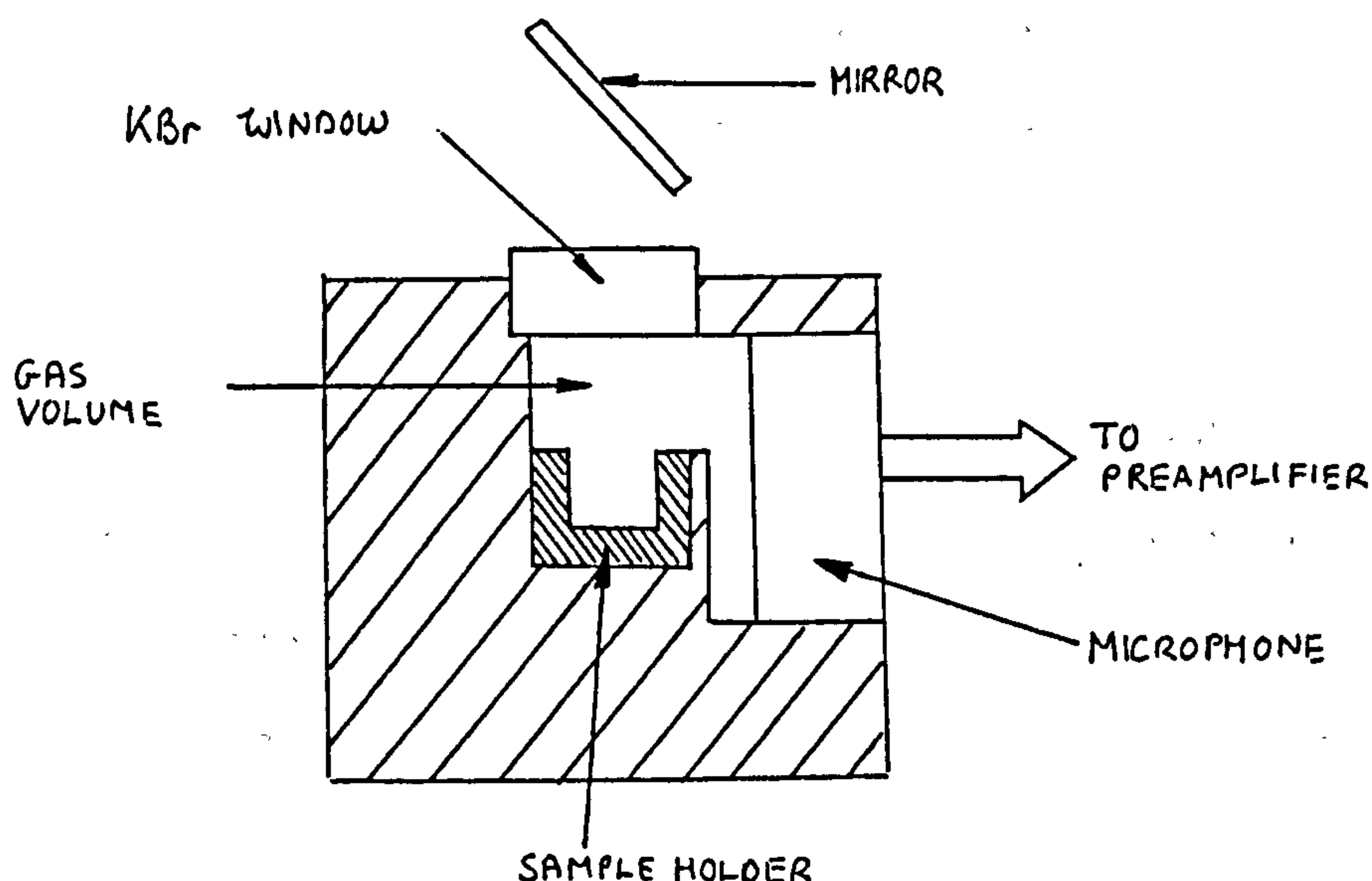
- Stray light/emission advantage. Modulation of the light source ensures that any stray light or IR emission from the sample, which is not modulated, will not be detected.

### Photoacoustic Spectroscopy (PAS) [21,22]

The photoacoustic effect was discovered by Alexander Graham Bell in the 1880's, but it was not until the advent of the microphone approximately 50 years after Bell's discovery and the subsequent application of FTIR as a modulated light source used in conjunction with PA [23], that good quality spectra of solid samples over a broad region of the IR were obtainable.

The photoacoustic cell, as illustrated in Figure 5 comprises of a sample chamber, a 'window', a microphone and a preamplifier.

Figure 5 Typical layout of a PA detector





Rosencwaig and Gersho [24] have developed a theory of the photoacoustic effect observed in solids.

When the sample inside the sample chamber is irradiated with a modulated infrared light, energy may be converted by non-radiative de-excitation processes into heat. Energy absorbed by the solid will heat its surface which conductively heats a boundary layer of air next to the solid surface. The use of a modulated light source causes intermittent expansion of this boundary layer, thus acting as an acoustic piston on the rest of the gas column. The magnitude of the periodic pressure variations in the cell is proportional to the magnitude of heat produced by the solid. The fluctuation in the acoustic pressure signal is detected by the microphone detector.

The Rosencwaig and Gersho Theory [24] shows that the photoacoustic effect is primarily attributed to the relationship between three "length" parameters of the sample

1. the thickness of the sample  $l$
2. the optical absorption length  $l_\beta$ ,
3. the thermal diffusion length  $u$ .

Where the optical pathlength is defined as,

$$l_\beta = \frac{1}{\beta} \quad , \quad \text{where } \beta = \xi C$$

$C$  = Concentration of absorbing chromophore

$\xi$  = Extinction coefficient of chromophore at the frequency of radiation

and, the thermal diffusion length, is defined as,

$$u = (2\alpha/\omega)^{1/2}$$

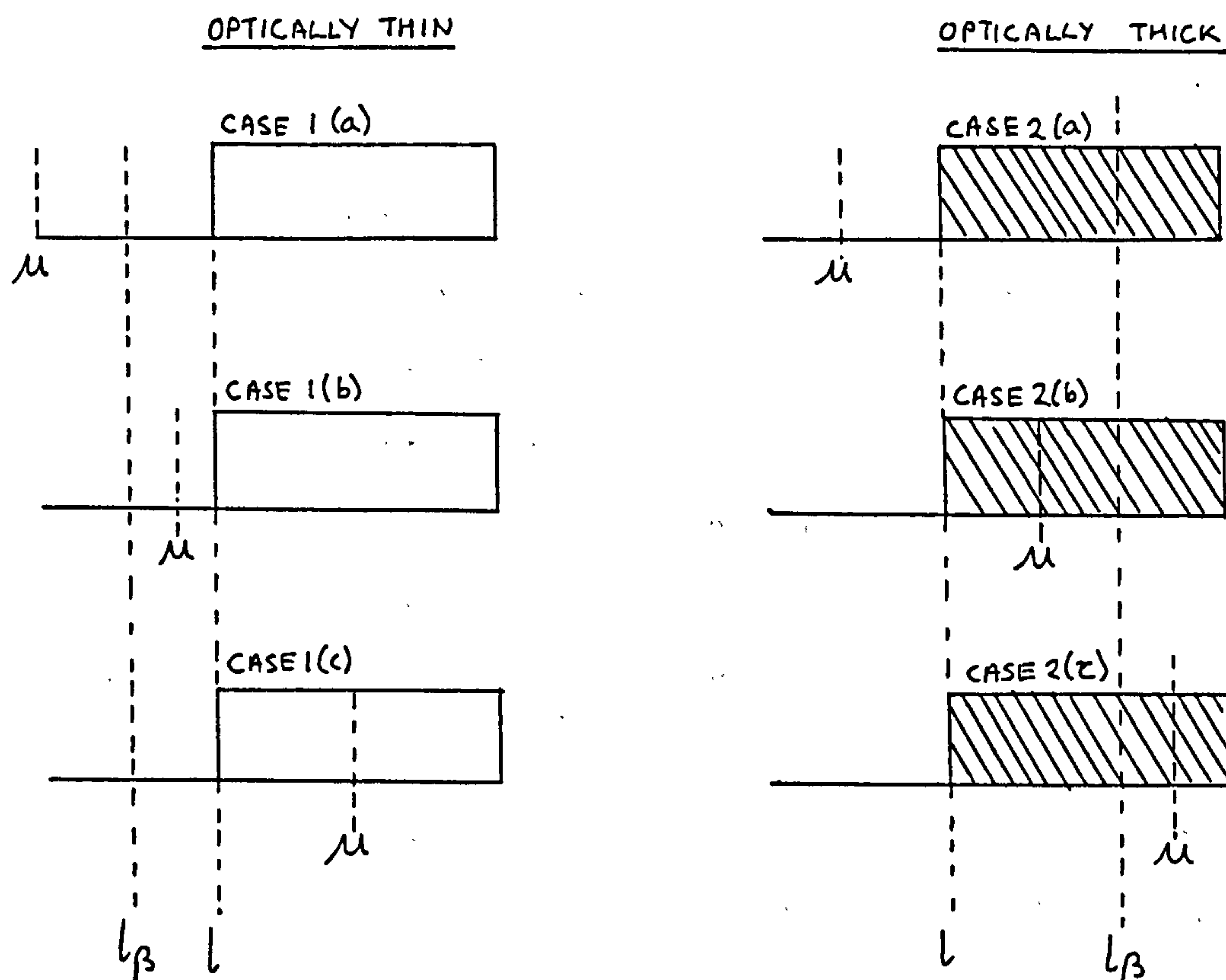
where,  $\alpha$  = thermal diffusivity of the film

$p$  = density of the film

$w$  = modulation frequency of the light source

The relative importance the above parameters play in producing the acoustic signal have been illustrated qualitatively by Rosencwaig [21], by the use of six special cases. These have been grouped according to the optical opaqueness of the solid with respect to the optical absorption length. For each category of opaqueness, different relative magnitudes of thermal diffusion length compared with the length,  $l$ , and with the optical absorption length  $l_\beta$  are considered

Figure 6 Schematic representation of special cases



## 1. Optically transparent solids ( $l_\beta > l$ )

The light is absorbed beyond the length of the sample

### Case 1(a) Thermally thin solids ( $u \gg 1; u > l_\beta$ )

The acoustic signal is proportional to  $\beta l$  therefore the thermal properties of the backing material will contribute to the acoustic signal.

### Case 1(b) Thermally thin solids ( $u > 1; u < l_\beta$ )

Again the acoustic signal is proportional to  $\beta l$  and therefore dependent on the thermal properties of the backing material.

### Case 1(c) Thermally thick solids ( $u < 1; u \ll l_\beta$ )

The acoustic signal is now proportional to  $\beta u$  and since  $u < 1$ , the thermal properties of the backing material do not contribute to the signal.

## 2. Optically opaque solids ( $l_\beta \ll l$ )

The light is being absorbed within the sample solid only

### Case 2(a) Thermally thin solids ( $u \gg 1; u \gg l_\beta$ )

In this case, the acoustic signal is independent of  $l$  and is characteristic of a blackbody absorber. The signal depends on the thermal properties of the backing material.

### Case 2(b) Thermally thick solids ( $u < 1; u > l_\beta$ )

The signal is independent of  $l$  and the backing material does contribute to the signal.

### Case 2(c) Thermally thick solids ( $u \ll 1; u < l_\beta$ )

the acoustic signal is proportional to  $\beta u$  and as in case 1(c) only the radiation absorbed within the first thermal diffusion layer contributes to the signal.



The use of FTIR-PA spectroscopy is a new mid-IR technique that requires minimal sample preparation, as the technique is essentially independent of the surface morphology of the sample. However, superior signal intensities are obtained for samples of greater surface/volume ratio, hence powdered samples and rough surfaces are actually more favourable for analysis by FTIR-PA. Vidrine [17] intimates that by varying the modulation frequency, the depth profile of a solid sample may be analysed.

#### Quantitative analysis by FTIR-PAS

In order that quantitative analysis of a polymer film can be made it is a prerequisite that absorbance of the incident light obeys the Beer-Lambert Law, defined as,

$$A = \epsilon Cl$$

Where  $\epsilon$  is the molar extinction coefficient ( $\text{l mol}^{-1} \text{cm}^{-1}$ ),  $C$  is the concentration ( $\text{mol l}^{-1}$ ) and  $l$  is the pathlength [13].

The use of FTIR-PA spectroscopy as a means of quantifying changes in specific group intensities must be determined with careful consideration of the purity of the carbon black reference and the three 'length' parameters associated with the PA signal.

From the Rosencwaig and Gersho theory [24] it can be seen that the modulation frequency  $w$ , of the interferometer described as,

$$w = 4nV\tilde{u}$$

where,  $V$  is the velocity (cm/s) and  $\tilde{u}$  is the wavenumber ( $\text{cm}^{-1}$ ), will result in a wide range of modulation frequencies across the spectral range. This will introduce a variation in  $u$  across the spectrum and since the PA signal is also a function of  $w$  this will ensure differences in signal levels across the spectra, resulting in artifacts. Ideally, spectral artifacts arising from the PA signal may be corrected for by the use of a non-resonant photoacoustic cell with a constant frequency response across the region of interest.

FTIR spectrometers are single beam instruments and accordingly photoacoustic spectroscopy will depend on the spectral output of the light source. It is therefore necessary to correct for the variation in energy output in different spectral regions to produce a spectrum where the peak heights are normalised with respect to the source output. In practice this is accomplished by ratioing the spectral output of the light source with the PA signal of the sample. The spectral output of the light source is obtained by recording a reference single beam spectrum of a blackbody absorber, which acts as an optically opaque thermally thin solid, and therefore yields a signal proportional to the incident light intensity.

Lew and Parodi [25] remarked that it is important to obtain a reference spectrum devoid of water vapour or carbon dioxide, as these features would perturb any reduced spectrum of the sample using this reference. Interference

from water and carbon dioxide absorbed on the surface of carbon black may be overcome by use of a drying agent in the chamber of the sample cell as suggested by Rockley and Delvin [26]. By use of a reference, the sample spectrum signal amplitude is compensated at all wavenumbers across the region of interest.

As pointed out before, the modulation frequency of the incident light will vary across the spectral range and since the thermal diffusion length is also frequency dependent sampling depth variation will also be wavenumber dependent. Vidrine [17] suggests that by adjusting the mirror velocity so that the modulation frequency is constant across the spectrum a composite spectrum may be produced where the sampling depth will be constant for all wavenumbers. However, the impracticality of obtaining a constant modulation frequency across the spectrum to compensate for variation in depth profile may be overcome by careful consideration of the three length parameters that determine the signal intensity.

The variation in signal intensity for a polymer film was illustrated by Gardella [27], who measured the differences in spectral output in terms of relative intensities of the absorption peaks for films of different thickness. The spectral inaccuracies obtained for the higher coatweight films were attributed to saturation of highly absorbing peaks, such as the carbonyl band at  $1735\text{cm}^{-1}$ . Saturation of this peak occurred when the thickness of the film was increased to a point at which the polymer films



represented transition from optically thin to optically opaque and from thermally thin to thermally thick cases. However, Gardella [27] also showed that weaker bands exhibit no such saturation.

It therefore follows that quantitative analysis of spectral changes for a given system may be made using FTIR-PAS, provided consideration of the sample's opacity and thermal properties are realised.

## RESULTS AND DISCUSSION

The cure response of tripropyleneglycol diacrylate, TPGDA, was evaluated using the technique of FTIR-PA spectroscopy. Application of this technique to measure the degree of cure of polymer films requires consideration of those parameters of the sample that contribute to the PA signal. As described by Rosencwaig [21] in a set of six special cases, saturation effects will prevail in certain cases. It is a prerequisite that spectra are recorded out of saturation in order to 'quantify' the measurement of cure in terms of double bond consumption.

For optically transparent polymer films, where the sample thickness is less than the optical path length at a given wavenumber, or, for an optically opaque film, where the thermal diffusion length is less than its optical path length, saturation can be avoided. The extent of cure

evaluated from those absorbance peaks associated with the acrylate functionality which meet the above criteria may be quantified.

The double bond functionality of TPGDA is characterised by the absorption peak at  $810\text{cm}^{-1}$  due to the CH deformation mode of the vinyl group,  $1640\text{cm}^{-1}$  due to the C=C stretching bond of vinyl groups and  $1620\text{cm}^{-1}$  due to the overtone frequency at  $810\text{cm}^{-1}$  [4,5,28]. The use of an internal standard is required to compensate for slight variation in film thickness and/or thermal diffusion length of a sample. The application of the ratio method is also very important in systems in which chemical reactions are monitored, such as the polymerisation reaction studied here. Polymerisation reactions not only result in a change of the double bond content of the polymer film, but also incur a change in thermal properties of the material, u, as the radiation dose increases.

The ratio method requires the use of an internal standard which is unaffected by the polymerisation process and is out of saturation. One such peak that meets this criteria is the  $\text{CH}_3$ - bend at  $1380\text{cm}^{-1}$ . The average thickness of the polymer film investigated here was approximately  $12.5\text{gm}^{-2}$ . It may therefore be assumed that a strongly absorbing group such as that associated with the carbonyl stretching frequency at  $1730\text{cm}^{-1}$  may exhibit a degree of opaqueness. It is therefore desirable to select a weak absorbance peak for use as an internal standard. This was not always possible for the diluents studied in subsequent

chapters (see chapters 3,4 and 7) and use of the carbonyl stretching frequency was evaluated by comparison with those results obtained using the methyl stretch at  $1380\text{cm}^{-1}$ . The use of both the  $\text{CH}_3$ - absorbance band at  $1380\text{cm}^{-1}$  and the carbonyl stretching frequency at  $1730\text{cm}^{-1}$  were investigated as internal standards for measuring the extent of cure as monitored by the decrease in intensity of the  $1640/1620\text{ cm}^{-1}$  absorption doublet and the  $810\text{cm}^{-1}$  peak.

In order to obtain good quality spectra for the low surface area polymer films produced here, very long scan times were required in order to compensate for the low signal to noise ratio.

A selection of spectra of TPGDA cured at various doses of radiation are shown in Appendix A. As can be seen from the spectra obtained for TPGDA cured at various doses of radiation, saturation of the carbonyl peak at  $1730\text{cm}^{-1}$  was not visually discernable.

For each dose of radiation three spectra were run and the average percentage cure was calculated and are collated in Table I.

As can be seen from Table I the variation in percentage cure as evaluated using all four combinations of acrylate absorbance peaks with internal standards was small. These results provide evidence that both the carbonyl stretching frequency at  $1730\text{cm}^{-1}$  and the  $\text{CH}_3$ - bend at  $1380\text{cm}^{-1}$  could be used as an internal standard to evaluate the percentage degree of cure for a polymer films of TPGDA.

The use of the carbonyl stretching frequency at  $1730\text{cm}^{-1}$



does not appear to introduce any measurable perturbations in determining the percentage degree of cure when compared with those results obtained using the small internal standard absorbance peak at  $1380\text{cm}^{-1}$ , was unexpected. This result may reflect the use of polymer films of similar low coatweights, and constant surface areas such that the extent of

Table I The percentage degree of cure of TPGDA at various doses of radiation using FTIR-PA spectroscopy

Dose of Radiation /kGy	Percentage degree of cure measured using the specified wavenumber and internal standard			
	1640/1730	1640/1380	810/1730	810/1380
0	0	0	0	0
5	41±2	38±2	45±3	46±3
10	66±2	66±2	61±2	62±2
20	89±2	88±1	92±2	91±2
40	95±1	95±1	97±2	97±2
100	99±1	98±1	99±1	97±1
200	100	100	100	100

saturation, if any, of the carbonyl absorbance band was similar for all the spectra recorded. Evidence to justify the use of the carbonyl absorbance band as an internal standard comes from the method of spectral subtraction. On subtracting a film cured at 200 kGy, which comprises of 100% polymer, from a spectrum of a partly cured polymer film of

TPGDA, a difference spectrum of the monomer is obtained. When one compares the difference spectrum of the monomer with that of the pure monomer all the relative intensity information is preserved over the spectral range  $4000\text{cm}^{-1}$  to  $600\text{cm}^{-1}$ . Since good spectral subtraction depends on 'quantitative' accuracy, this further justifies the use of the  $1730\text{cm}^{-1}$  carbonyl stretch as an internal standard.

In conclusion, use of FTIR-PA spectroscopy has been shown to be a most invaluable means of measuring the degree of cure of glossy polymer films on an opaque substrate.

## EXPERIMENTAL

### Materials

Tripropyleneglycol diacrylate (TPGDA), (Cray Valley Products Ltd.) was used as received.

Aluminum foil (0.051mm gauge) (BDH Chemicals Ltd.) was used as a substrate for all coatings.

### Instrumentation

The diluent was coated onto a moving web via a Dixon coater unit.

Electron beam curing was carried out using an Otto Durr ESH 150/130 electron beam unit under a nitrogen blanket. The operating voltage was maintained at 150kV and the beam current was adjusted for each applied dose.

Infrared spectroscopic data were obtained using a Digilab FTS-60 Fourier transform infrared spectrometer. The moving mirror velocity in the interferometer was  $0.16\text{cm}^{-1}$  and the spectra reported here were recorded at  $8\text{cm}^{-1}$  resolution. All spectra were recorded as a photoacoustic spectrum using a Digilab photoacoustic detector for 4096 scans.

### Preparation of thin films of TPGDA

All polymer films were coated onto aluminum foil using a Dixon 164 coater. Even coatweights of about  $12.5\text{gm}^{-2}$  were obtained using a forward spinning smoothing roller at a setting of 32psi. The coatings were then passed



under the electron beam. For all doses of radiation (0-100)kGy the moving web was maintained at  $20\text{mmmin}^{-1}$ , but for a dose of 200kGy the machine speed was reduced to  $10\text{mmmin}^{-1}$ .

All samples were bottled and stored at  $-5^{\circ}\text{C}$ .

#### Analysis of spectra obtained by Fourier transform infrared spectroscopy

All cured films of TPGDA yielded tackfree films.

The technique of multiple internal reflectance spectroscopy was initially looked into for obtaining spectra of cured films of TPGDA on an opaque substrate. This method was found to give inconsistent results due to the difficulty in obtaining uniform contact and pressure of the polymer film and the caesium bromide crystal. Although the quality of spectra was good it was deemed ineffective as a quantitative means of determining the percentage unsaturation.

The relatively new technique of diffuse reflectance infrared (DRIFTS) was also investigated and as expected poorly defined spectra were obtained due to the spectral reflectance of the highly glossy films produced.

The use of FTIR in conjunction with a photoacoustic detector was subsequently investigated and was found to give good quality spectra. Examples of spectra recorded by this technique are shown in Appendix A.

Spectra recorded of films of TPGDA cured at various doses of radiation should not be compared directly due to

variation in film thickness. It is therefore a prerequisite to apply the ratio method [29] to compensate for these differences. This method involves the measurement of the area or heights of the peak of interest ratioed against the area or height of a peak which remains constant throughout the process being studied.

#### Analysis of infrared spectra obtained for films of TPGDA

The FTIR-PA spectra obtained for TPGDA were of excellent quality and examples of which are shown in Appendix A. On exposure to electron beam irradiation the consumption of carbon carbon double bonds of the acrylate group was monitored by the peak at  $810\text{cm}^{-1}$  associated with the CH deformation of the vinyl group and the doublet at  $1640\text{cm}^{-1}$  and  $1620\text{cm}^{-1}$  associated with the carbon carbon double bond stretch and the overtone frequency at  $810\text{cm}^{-1}$  respectively [5,28,29].

The use of an internal standard was employed to determine the percentage degree change associated with the aforementioned peaks. The peak at  $1380\text{cm}^{-1}$  due to the  $\text{CH}_3$ - bond [29] together with the use of the carbonyl stretching frequency at  $1730\text{cm}^{-1}$  were chosen to assess their value as internal standard.

The area associated with each peak was computed given a predefined baseline, and from which the peak ratio's were evaluated and the percentage change of a given peak calculated.

## APPENDIX A

A selection of spectra of TPGDA cured at various doses of radiation were recorded using the technique of photoacoustic spectroscopy, in conjunction with FTIR and are illustrated overleaf. The degree of unsaturation was measured by monitoring the area associated with the peak at  $810\text{cm}^{-1}$  and the doublet at  $1640/1620\text{cm}^{-1}$ . The absorption peak at  $810\text{cm}^{-1}$  is characteristic of the acrylate group and is associated with the CH deformation mode [5,28]. The absorbance band at  $1640\text{cm}^{-1}$  is due to the C=C stretching frequency of the vinyl group and the peak at  $1620\text{cm}^{-1}$  is relevant to the overtone frequency of the  $810\text{cm}^{-1}$  CH deformation [5,28].

The reference absorbance bands utilised here, were the  $1380\text{cm}^{-1}$  band attributable to the symmetric methyl bending vibration and the  $1730\text{cm}^{-1}$  peak due to the carbonyl stretching vibration [29].



Figure 1 The FTIR photoacoustic spectrum of a thin film of TPGDA monomer recorded at  $8\text{cm}^{-1}$  resolution for 4096 scans

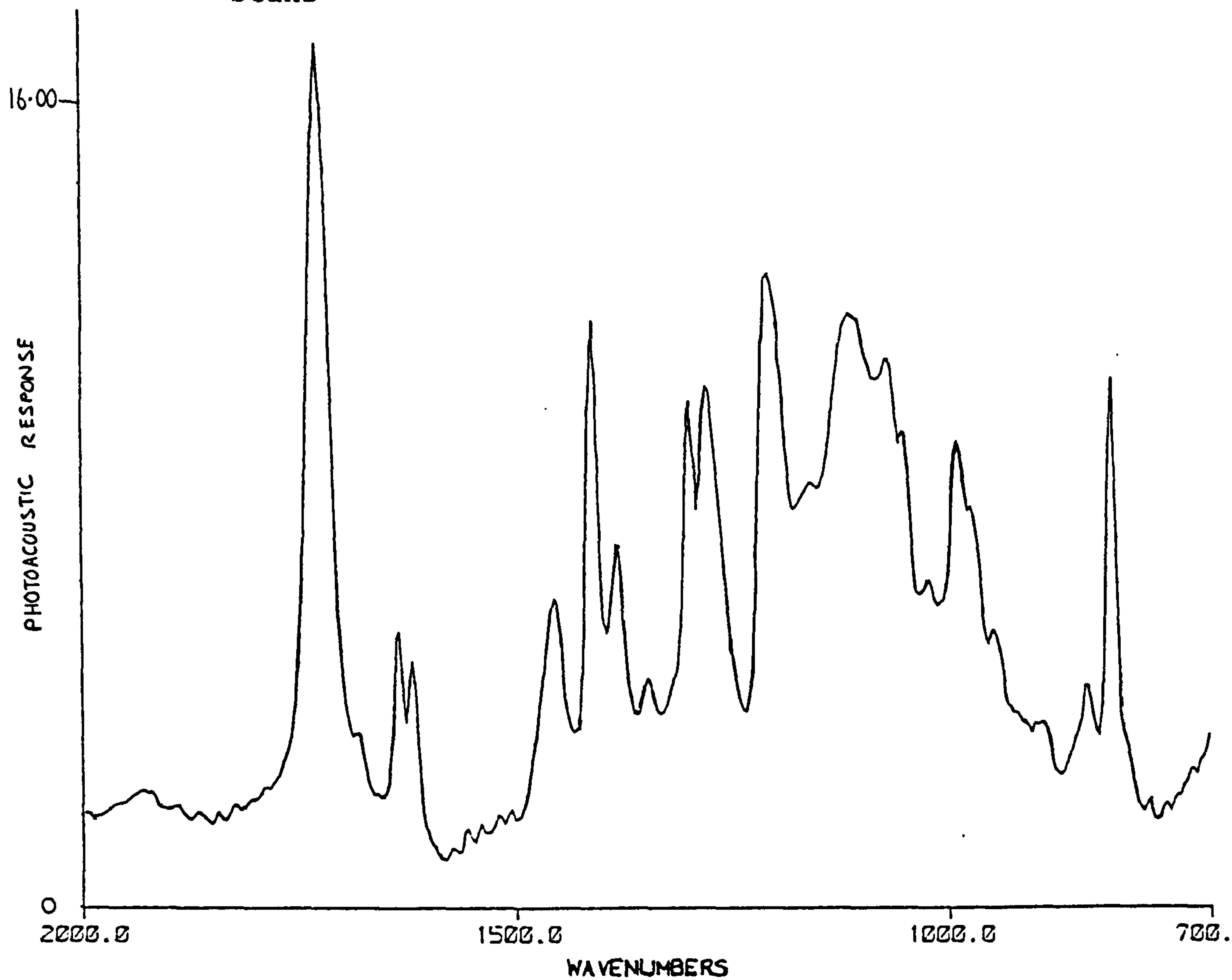
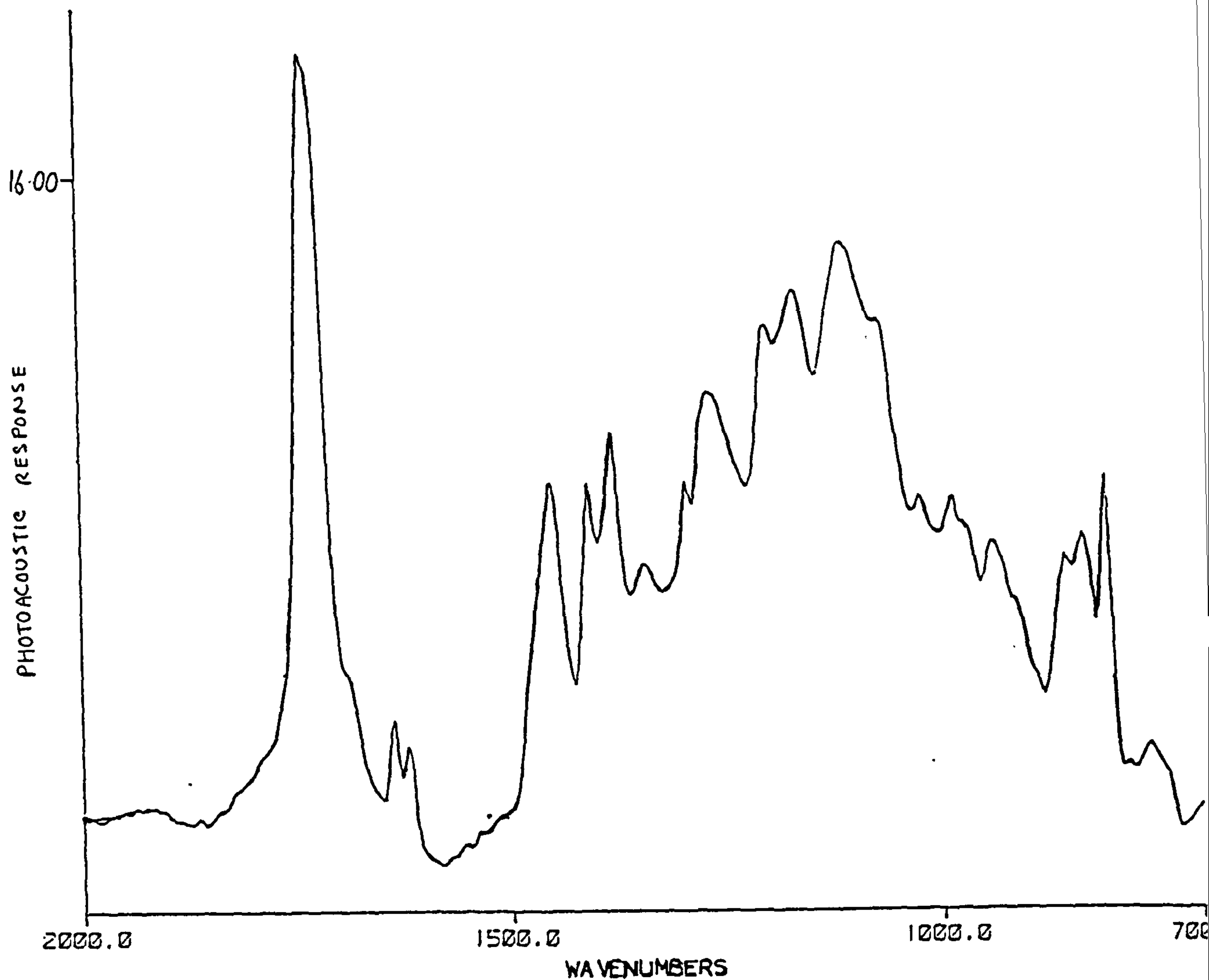


Figure 2 The FTIR photoacoustic spectrum of a thin film of TPGDA cured at 5kGy recorded at  $8\text{cm}^{-1}$  resolution for 4096 scans



**PAGE**

**NUMBERING**

**AS ORIGINAL**



Figure 3 The FTIR photoacoustic spectrum of a thin film of TPGDA cured at 20kGy recorded at  $8\text{cm}^{-1}$  resolution for 4096 scans

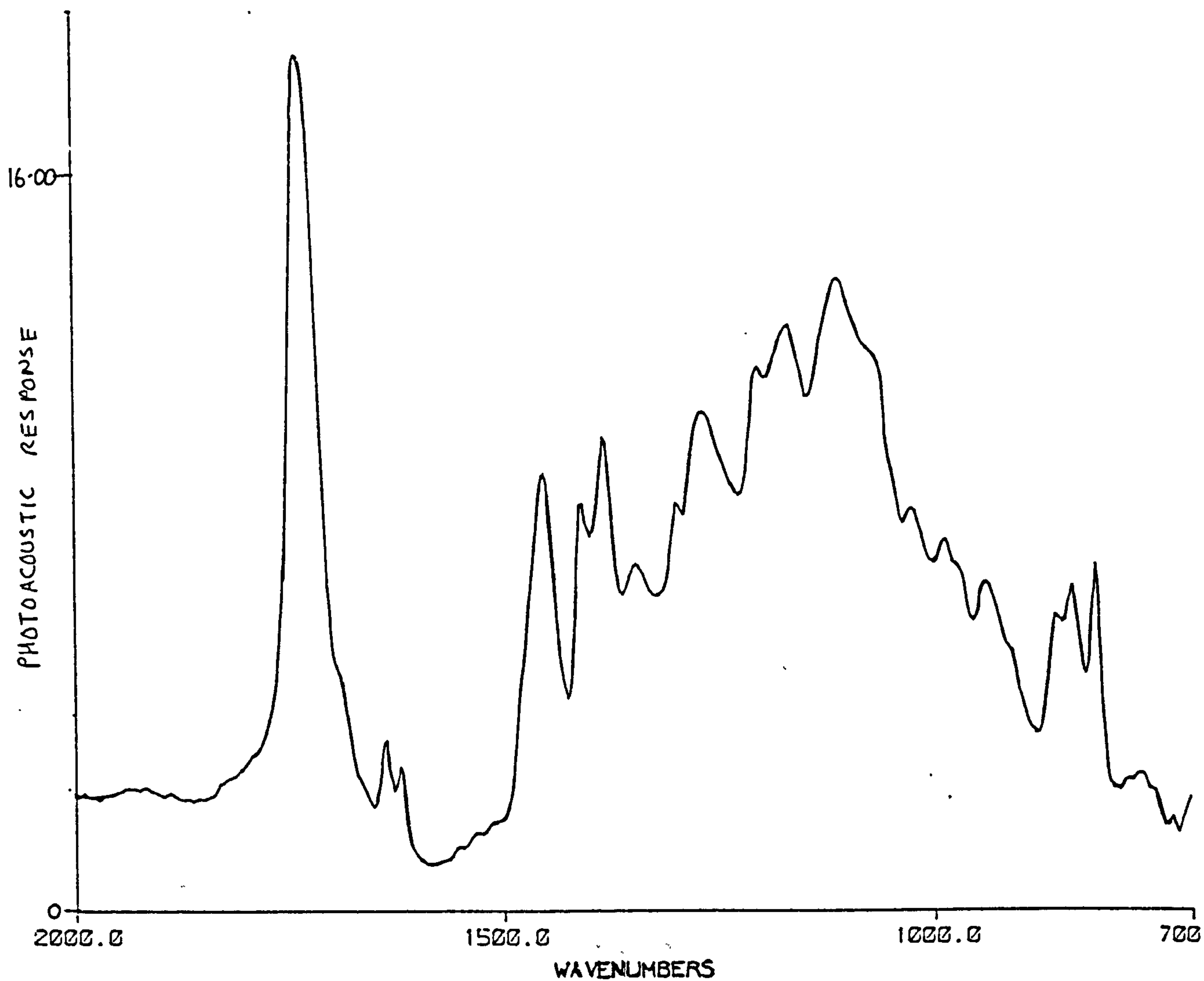


Figure 4 The FTIR photoacoustic spectrum of a thin film of TPGDA cured at 40kGy recorded at  $8\text{cm}^{-1}$  resolution for 4096 scans

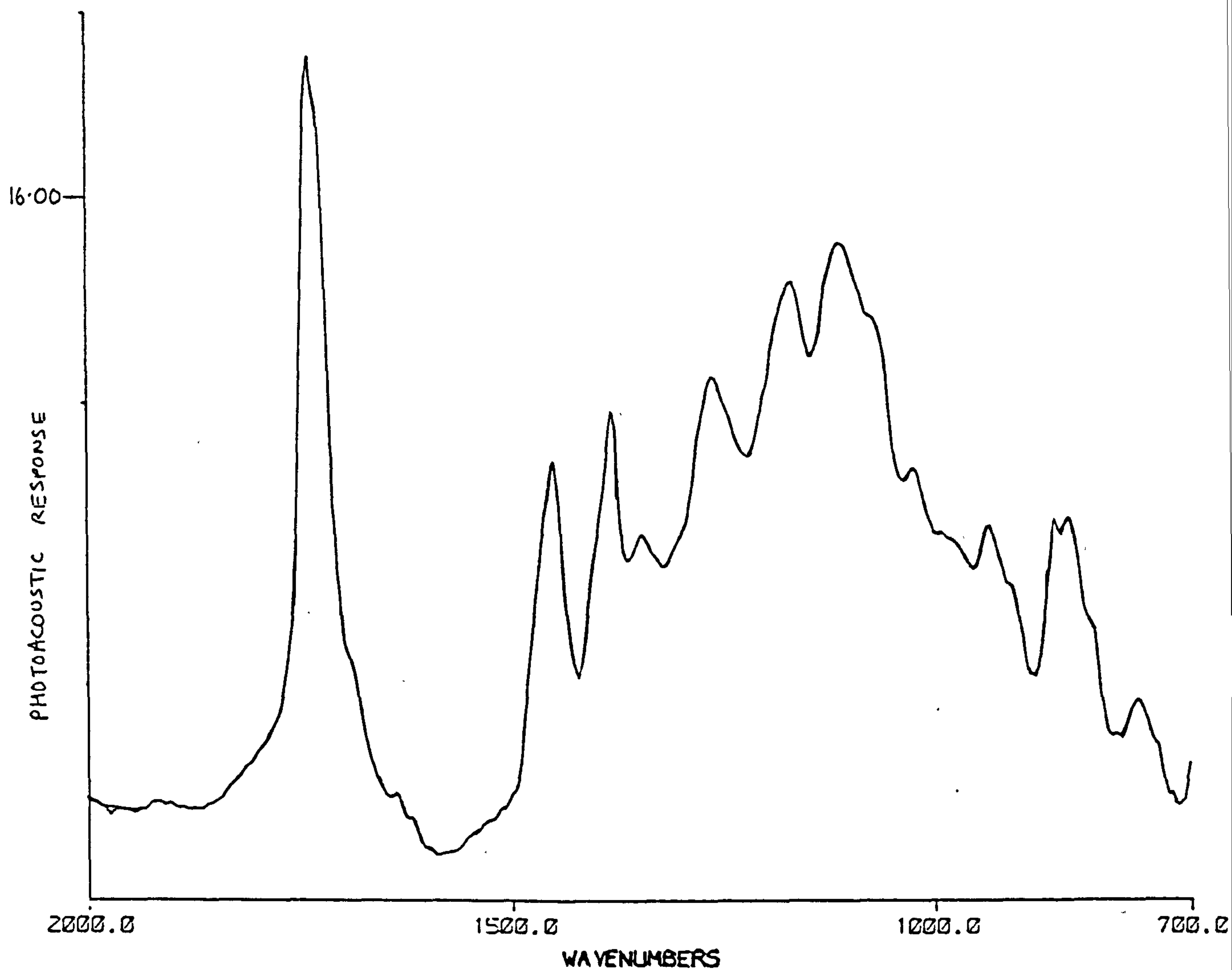
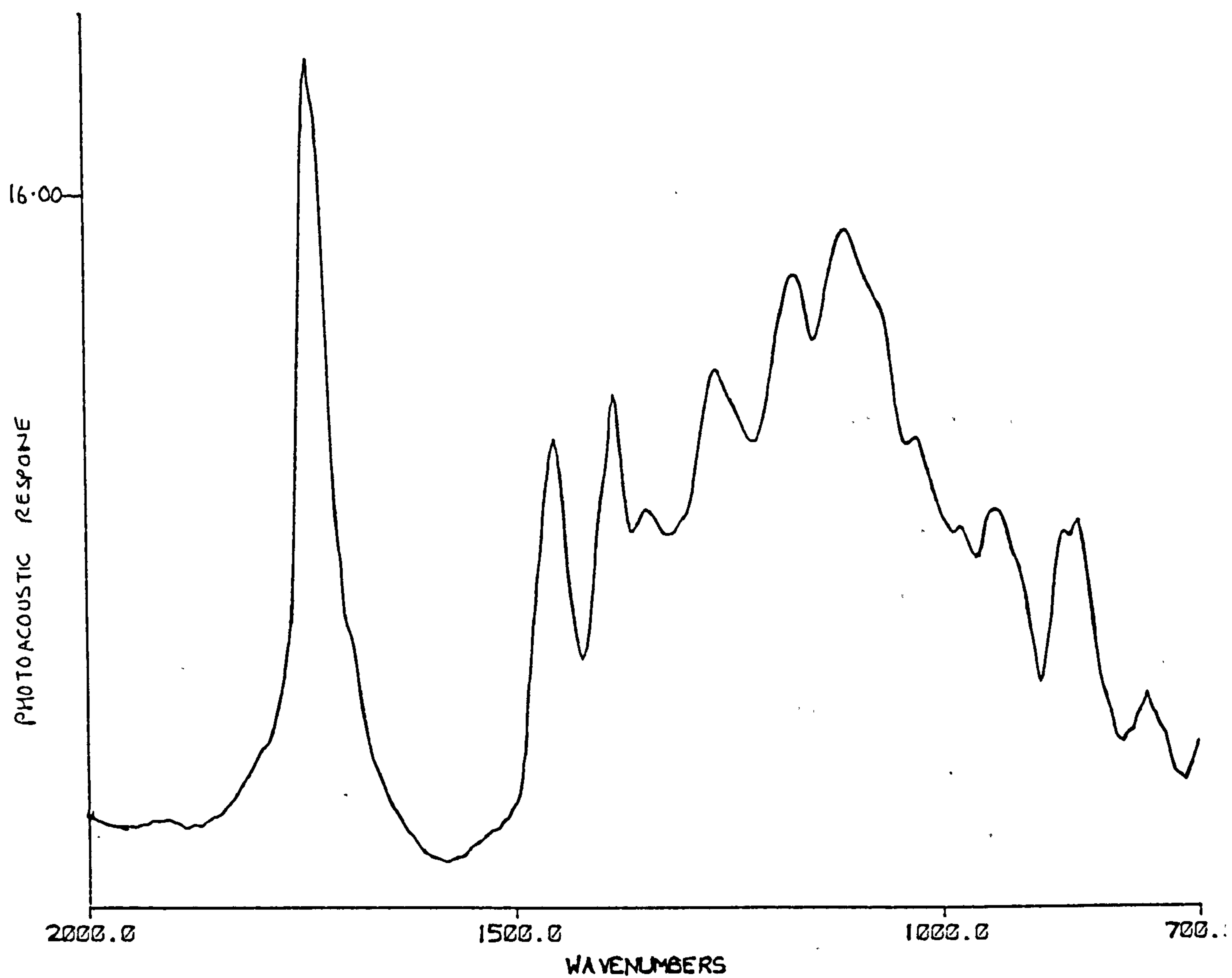


Figure 5 The FTIR photoacoustic spectrum of a thin film of TPGDA cured at 200kGy recorded at  $8\text{cm}^{-1}$  resolution for 4096 scans





## REFERENCES

- [1] C. G. Roffey, (1982). Photopolymerisation of Surface Coatings, Wiley-Interscience.
- [2] J. J. Krajewski, E. S. Packer and T. Yamazaki, (1976). J. Coat. Technol. 48 (623), 43; Met. Finish., 74 (11), 58.
- [3] Y. C. Chang, (1977). Photograph. Sci. Eng., 21 (6), 348.
- [4] R. Phillips, (1978). J.O.C.C.A., 61(7), 233.
- [5] G. Plews and R. Phillips, (1979). J. Coat. Technol., 51, 69.
- [6] J. E. Moore, (1978). UV Curing : Science and Technology, S. P. Pappas, Ed., Technology Marketing Corp. Chap. 3.
- [7] R. W. Bush, A. D. Ketley, C. R. Morgan and D. G. Whit, (1980). J. Radiation Curing, 7(2), 20.
- [8] V. D. Mc Guiniss and R. M. Holsworth, (1975). J. Appl. Polym. Sci., 19 (8), 2243.
- [9] K. H. Brown, (1977). Radiation Curing, 4 (4), 8.
- [10] J. L. Barrett, (1979). J. Radat. Curing, 6 (4), 20.
- [11] C. Decker, J. Faure and M. Fizet, (1980). ACS Div. Org. Coat. Plast. Chem. Preprints, 42, 710.
- [12] G. L. Collins, D. A. Young and J. R. Costanza, (1976). J. Technol., 48, 48.
- [13] R. T. Conley, (1972). Infrared Spectroscopy, 2nd Ed., Allyn and Bacon.
- [14] W. W. Wendlandt and H. G. Hecht, (1966). Reflectance

Spectroscopy, Wiley-Interscience.

- [15] P. A. Wilks and T. Hirschfield, (1968). Appl. Spectroscopy Rev., 1, 99.
- [16] A. Rosencwaig, (1975). Anal. Chem., 47 (6), 592A.
- [17] D. W. Vidrine, (1980). Appl. Spect., 34, 314.
- [18] M. G. Rockley, (1980). Appl. Spect., 34, 405.
- [19] K. Krishnan (1981) Appl. Spect., 35, 549.
- [20] P. R. Griffiths, (1975). Chemical Infrared Fourier Transform Spectroscopy, Wiley-Interscience.
- [21] A. Rosencwaig, (1980). Photoacoustics and Photoacoustic Spectroscopy, Wiley-Interscience.
- [22] Optoacoustic Spectroscopy and detection, (1977). Yoh-Han Pao, Ed., Academic Press.
- [23] M. G. Rockley, (1979). Chem Phys. Lett., 68, 455.
- [24] A. Rosencwaig and A. Gersho, (1975). Science, 190, 556; *ibid.* (1976). J. Appl. Phys., 47, 64.
- [25] Y. C. Teng and B. S. H. Royce, (1982). Appl. Optics, 21(1), 1982.
- [26] M. G. Rockley and J. P. Delvin, (1980). Appl. Spect. 34, 40.
- [27] J. A. Gardella, G. L. Grobe, W. L. Hopson and E. M. Eyring, (1984). Anal. Chem., 56, 1169.
- [28] W. O. George. D. V. Hassid, W. C. Harris and W. F. Maddams, (1975). J. C. S. Perkin II, 392.
- [29] R. T. Conley, (1972). Infrared spectroscopy, 2nd Ed., Allyn and Bacon.



[illegible]

00000001, 00000002, 00	10, 04 00, 00 00000000 11100000, 000000 00000000, 0000, 00000000 000000 00000000, 00, 00	00000000, 00000000
------------------------	--	--------------------

DATE	DESCRIPTION	AMOUNT	CHECK NO.	BANK	INTEREST	TOTAL	REMARKS
12/01/2023	DEPOSIT	1000.00		CHASE		1000.00	INITIAL DEPOSIT
12/05/2023	PAYROLL	500.00	1001	CHASE		500.00	PAYROLL DEBIT
12/10/2023	RENT	250.00	1002	CHASE		250.00	RENT DEBIT
12/15/2023	SALES	750.00		CHASE		750.00	SALES CREDIT
12/20/2023	UTILITIES	100.00	1003	CHASE		100.00	UTILITIES DEBIT
12/25/2023	SALES	600.00		CHASE		600.00	SALES CREDIT
12/30/2023	SALES	400.00		CHASE		400.00	SALES CREDIT
	TOTAL					2900.00	

51219119700	11444049435	34495515164	22418737339	14301416887	33031807095	37274718800	37294403514	40451612795	04437772229	33541777779	54339943455	37274718800	04437772229	44651200005	54337772229	14479444444	40130315100	70144442279	35349199900	51377915555	23444010015	37274718800	70144442279	44223425515	21122655515	04453315111	39554401009	553447222
-------------	-------------	-------------	-------------	-------------	-------------	-------------	-------------	-------------	-------------	-------------	-------------	-------------	-------------	-------------	-------------	-------------	-------------	-------------	-------------	-------------	-------------	-------------	-------------	-------------	-------------	-------------	-------------	-----------



<u>Chapter 3</u>	ELECTRON BEAM INDUCED POLYMERISATION OF ORGANOTINACRYLATE FILMS	
	Introduction	105
	Organocarboxylates	111
	Synthesis	111
	Structure and bonding	112
	Hydrolytic stability	113
	Organostannyl radicals	114
	Results and Discussion	116
	Conclusion	131
	Acknowledgements	133
	Experimental	134
	Appendix A	141
	References	145

# EB INDUCED POLYMERISATION OF ORGANOTIN ACRYLATE FILMS

## Introduction

The introduction of environmental regulations and demands for energy conservation resulted in the rapid development of the radiation curing industry, and the production of radiation curable monomers and resins. The class of radiation curable compounds that have been developed and exploited the most are the acrylate esters. The widespread use of these compounds is primarily due to their characteristic properties, namely, good solvating power, low volatility, high reactivity, and good film forming properties [1]. However, it is important to note that although propagation of polymerisation is via a free radical mechanism common to both UV and EB curing, the initiation step of the polymerisation process is very different for the two processes. This may be attributed to the difference in energies utilised by the two techniques and their subsequent mode of interaction with matter.

In general, most acrylate esters used in the industry do not absorb wavelengths of light longer than 254nm, energy equivalent of 4.9eV. However, it is a general requirement of UV-induced chemical reactions to comply with two basic laws of photochemistry, known as the Grotthus-Draper Law which states that only light which is absorbed is capable of initiating a photochemical process and the Stark-Einstein Law, which states that when a molecule undergoes a



photochemical change it is the result of the absorption by the molecule of a single photon of energy. It is therefore a prerequisite of UV curable formulations to incorporate a component that will absorb radiation energy in the region of the light source and as a result lead to the formation of a primary reactive species capable of chain propagation. This component is called a photoinitiator/sensitiser.

The depth of cure that can be achieved by UV curing is therefore dependent upon the absorption characteristics of the initiator, the absorption properties of the oligomer/diluent, inhibition of cure at the surface by oxygen, and when pigments are incorporated into the formulation, the optical properties of the pigments used will also affect the depth of cure attainable by UV curing [1-6]. The depth of a photocured film may therefore exhibit undercure at the surface, due to oxygen inhibition and undercure at the coating/substrate interface due to the optical opacity of the film at these depths. The maximum film thickness that can be cured is therefore limited by these factors.

EB curing utilises a source of 'high energy' electrons, in the range of 150-300keV for coating purposes [7]. On exposure of an electron beam, 'primary species', such as radicals, ions and electrons are produced along the tracks of the incident electrons [8]. The radical species produced on exposure to an electron beam are capable of initiating free radical polymerisation and as a result EB induced polymerisation do not require an initiator component.

From the rate equation shown in Chapter 1, the rate of



initiation is directly proportional to the efficiency of radical production in the monomer,  $\Phi_M[M]$ , and the dose rate  $I$ , for a given energy.

Increasing the dose rate will therefore result in a proportional increase of concentration of initiating radical species. However, at very high dose rates it may be perceived that a situation is soon reached when some of the primary radicals escape the scavenging process by the monomer and either recombine or react with a growing polymer chain [8].

The efficiency of radical production in the monomer for a given energy also depends on the sensitivity of the monomer towards the absorbed energy. It is known that certain functional groups either exhibit a protective action towards radiation or are susceptible to a variety of processes leading to the formation of radical species. The production of radical species has been outlined in Chapter 1. Some important examples of those materials which show greatest susceptibility are those containing bonds most prone to homolytic bond cleavage, e.g., tertiary C-H bonds [9], or, materials containing halogen groups leading to dissociative electron capture to produce a radical and a halide ion [10].

The distribution of radicals is also a function of the energy of the electron beam. Low LET radiation (>500keV) will result in the formation of isolated concentrations of radicals while high LET radiation (150-200keV) will result in a high random concentration of radicals [7,11]. High LET

radiation will be promoted by minimising the energy of the electron beam as well as using materials of high stopping value.

It is an important facet of EB curing that electron beam energies may be adjusted in order to penetrate the complete depth of the coating, thereby ensuring an even cure profile across the coatings of various thicknesses.

EB formulations have largely adopted those utilised by the UV curing industry and primarily comprise of the acrylate esters. Although these compounds have been shown to cure very rapidly on exposure to an electron beam, by utilising materials with increased stopping power and containing bonds labile to homolysis, superior cure response is predicted.

Some organometallic polymers have recently received attention for potential application as resist materials. Examples of resist systems that have been reported are polymers derived from trimethylstannyl styrene [12] and poly(trimethylstannylalkyl) methacrylates [13]. The high reactivity of these materials, was ascribed to the presence of the tin atom. The incorporation of tin was perceived to increase the energy absorbed by the material as a result of its larger cross section/high stopping power, as well as, leading to the rupture of the weak tin carbon bond, generating radical sites capable of crosslinking.

Other tin containing polymers that have been widely

used commercially are the unsaturated triorganostannyl ester monomers [14,15]. The class of most significance are the triorganotin acrylates and methacrylates. The polymerisation of these monomers has been carried out using peroxides or other free radical initiators. The resulting polymers are of importance industrially, as they are the active ingredients in biocidal paints [16].

In this chapter, some dialkyltin diacrylates esters were investigated as materials for electron beam coating purposes and their performance were compared with standard commercial diluents (Figure 1). It was predicted that these materials would readily cure on account of,

- 1) increased energy absorption, due to the incorporation of tin, and,
- 2) homolysis of weak tin carbon bonds, producing radicals capable of crosslinking or initiating polymerisation.

The cure response of these materials was determined primarily by obtaining the minimum dose of radiation required to produce a tackfree film, as well as by use of such standard physical tests, as the solvent rub test, pencil hardness, brittleness, and acid/alkali rub resistance tests. The evaluation of cure efficiency of D-n-BTDA compared with TPGDA, HDDA and TMPTA was also measured quantitatively using FTIR-PA spectroscopy (See Chapter 2). The ability of these organotin diluents to control the viscosity of formulations was also investigated and the cure responses of these systems were measured in terms of their

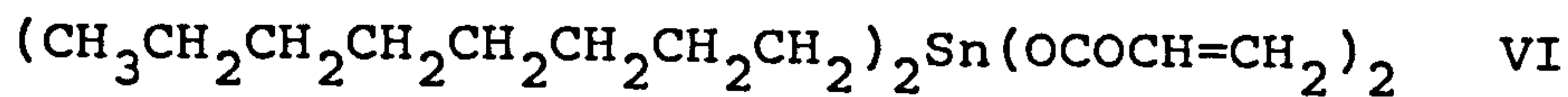
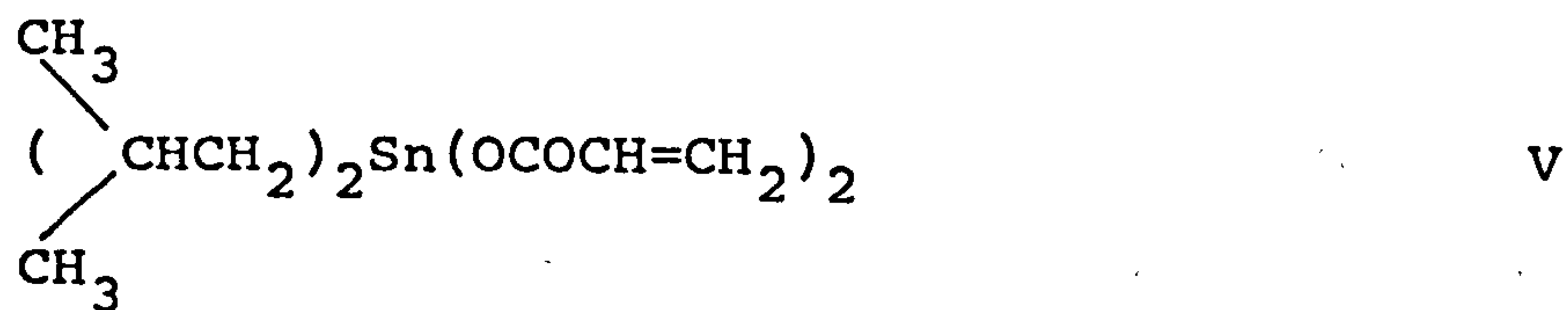
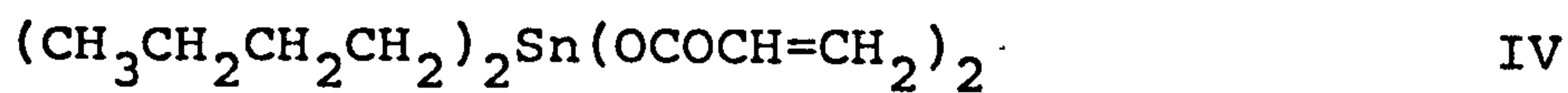
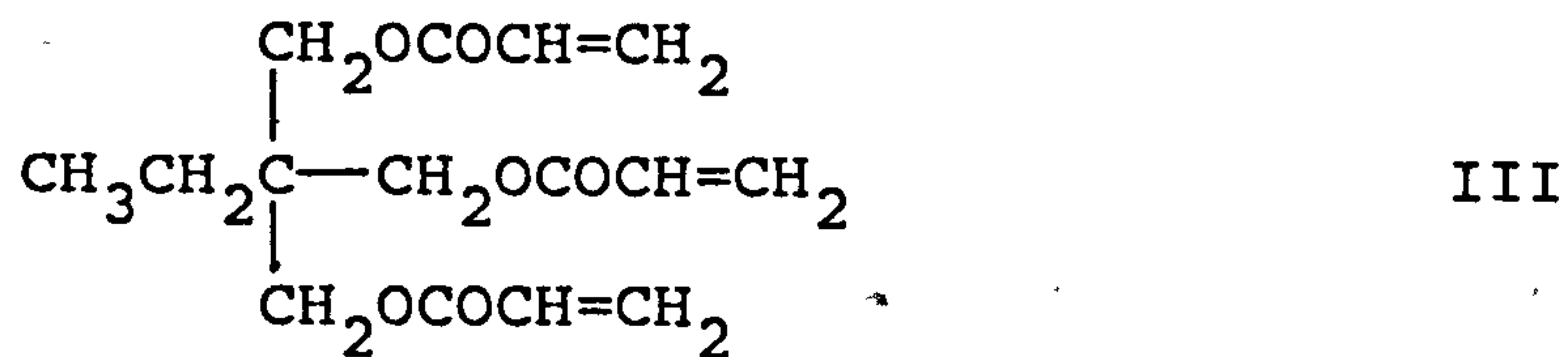
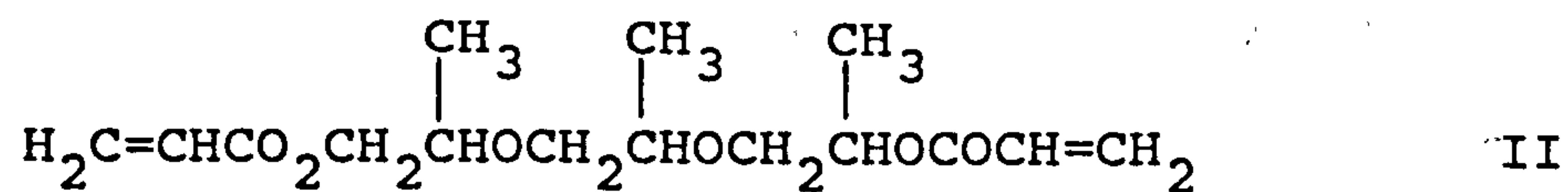
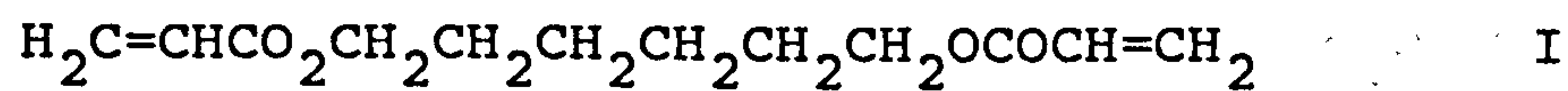


final film properties.

Figure 1 The diluents to be compared

I = HDDA, II = TPGDA, III = TMPTA, IV = D-n-BTDA,

V = D-i-BTDA, VI = D-n-OTDA

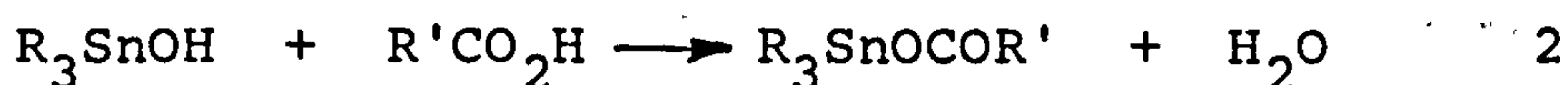
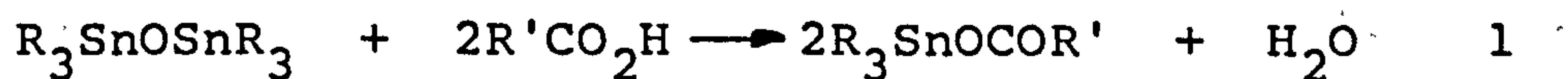


## Organotin Carboxylates

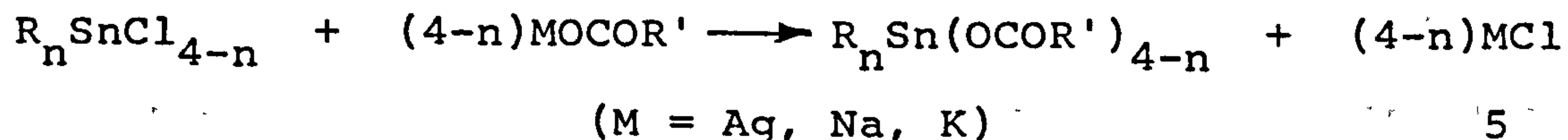
The chemistry of this group has been reviewed by several workers [17,18].

### Synthesis

The most popular method of preparing organotin carboxylates is via esterification of the organotin oxide or hydroxide with a carboxylic acid, achieved by azeotropic dehydration of the reactants in either boiling benzene or toluene using a Dean-Stark separator for 1-2 hours (equation 1-4).

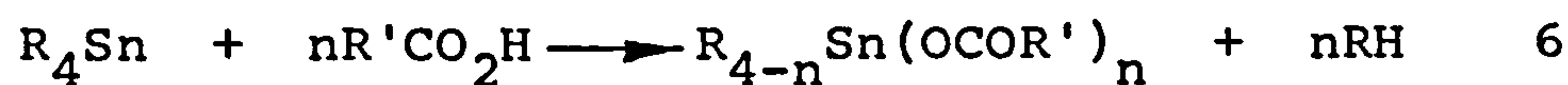


Another general method involves the conversion of organotin chlorides to the esters by heating with carboxylates in suitable solvent.



Organotin esters may also be prepared by the direct reaction of tetraorganotins with carboxylic acids. Vinyl groups are cleaved more readily than saturated alkyl groups,

but less readily than phenyl groups.

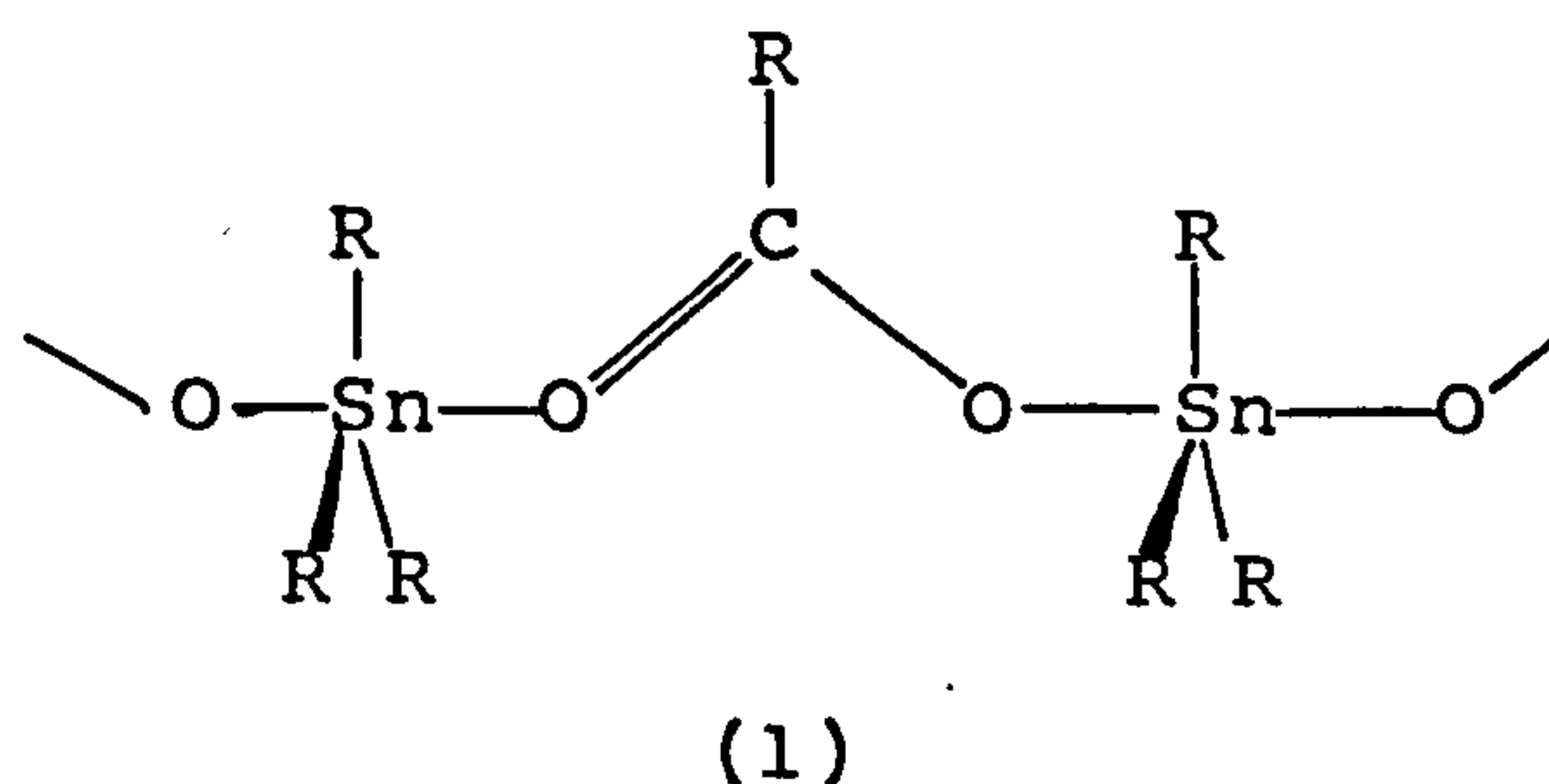


A considerable amount of work has been carried out on the synthesis of unsaturated triorganostannyl ester monomers, most commonly the triorganotin acrylates or methacrylates [19]. Organotin acrylates

or methacrylates have been largely synthesised by the first method described here. This is primarily due to the ready availability of organotin oxides or hydroxides.

### Structure and Bonding

The structure and bonding of triorganotin carboxylates have been widely investigated [17]. Their general very low solubility in organic solvents has been attributed to their polymeric associated structure (1)[17].

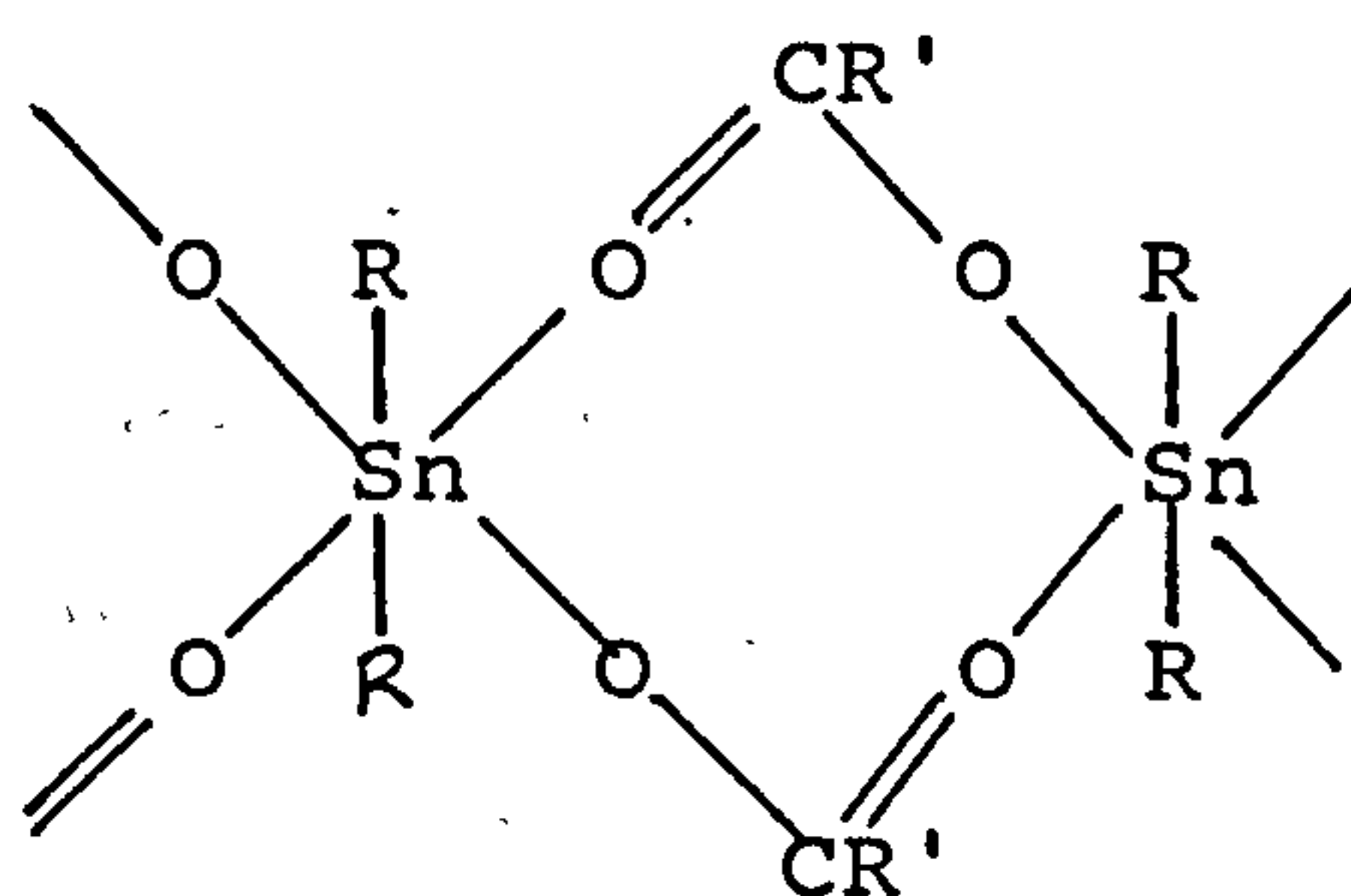


However, on dilution the associated triorganotin carboxylates usually produce monomeric species containing tetrahedral tin atoms and free ester carbonyl groups [17,20,21].

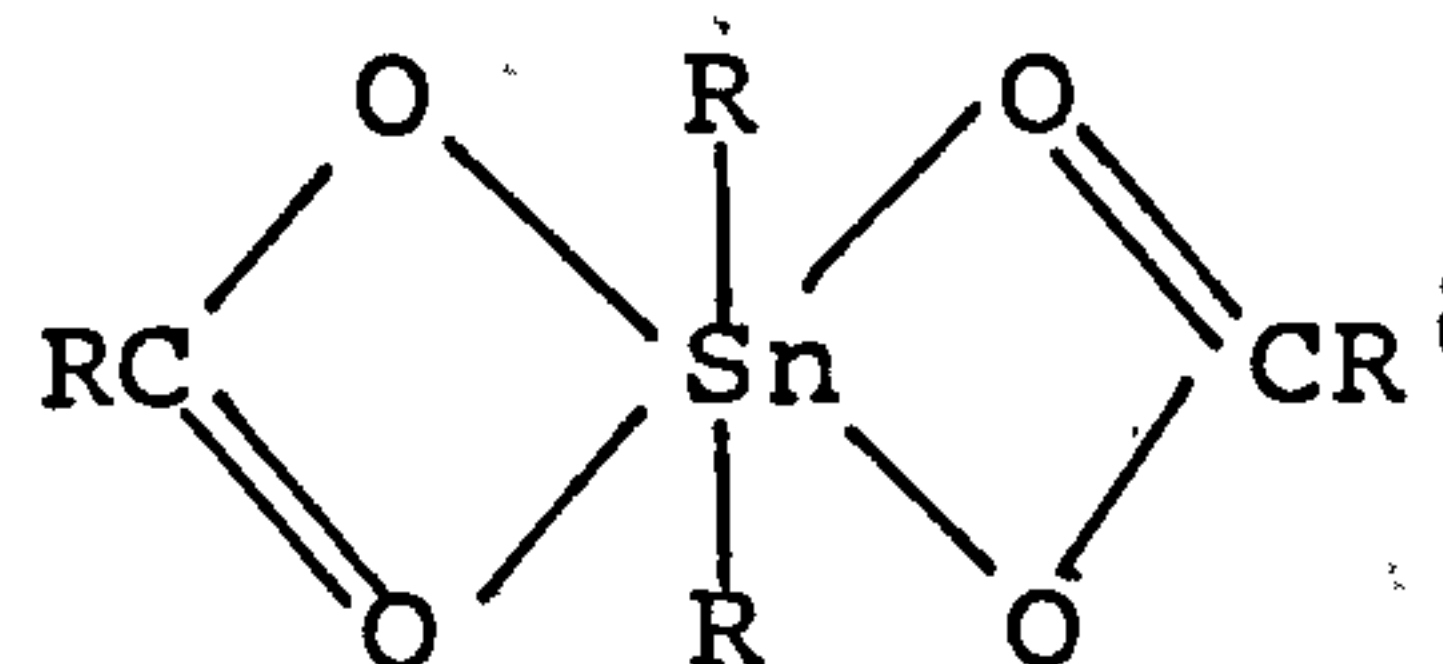
The infrared data of dialkyltin dicarboxylates suggest that in the neat liquid or solid state, these compounds



adopt a polymeric structure (2) with intermolecularly bridging carboxylate groups and an octahedral trans- $R_2SnX_4$  tin atom geometry [17,22]. However, in solution these compounds exist as monomers and it has been proposed that intramolecular chelated species, also possess an octahedral configuration (3) [17,22].

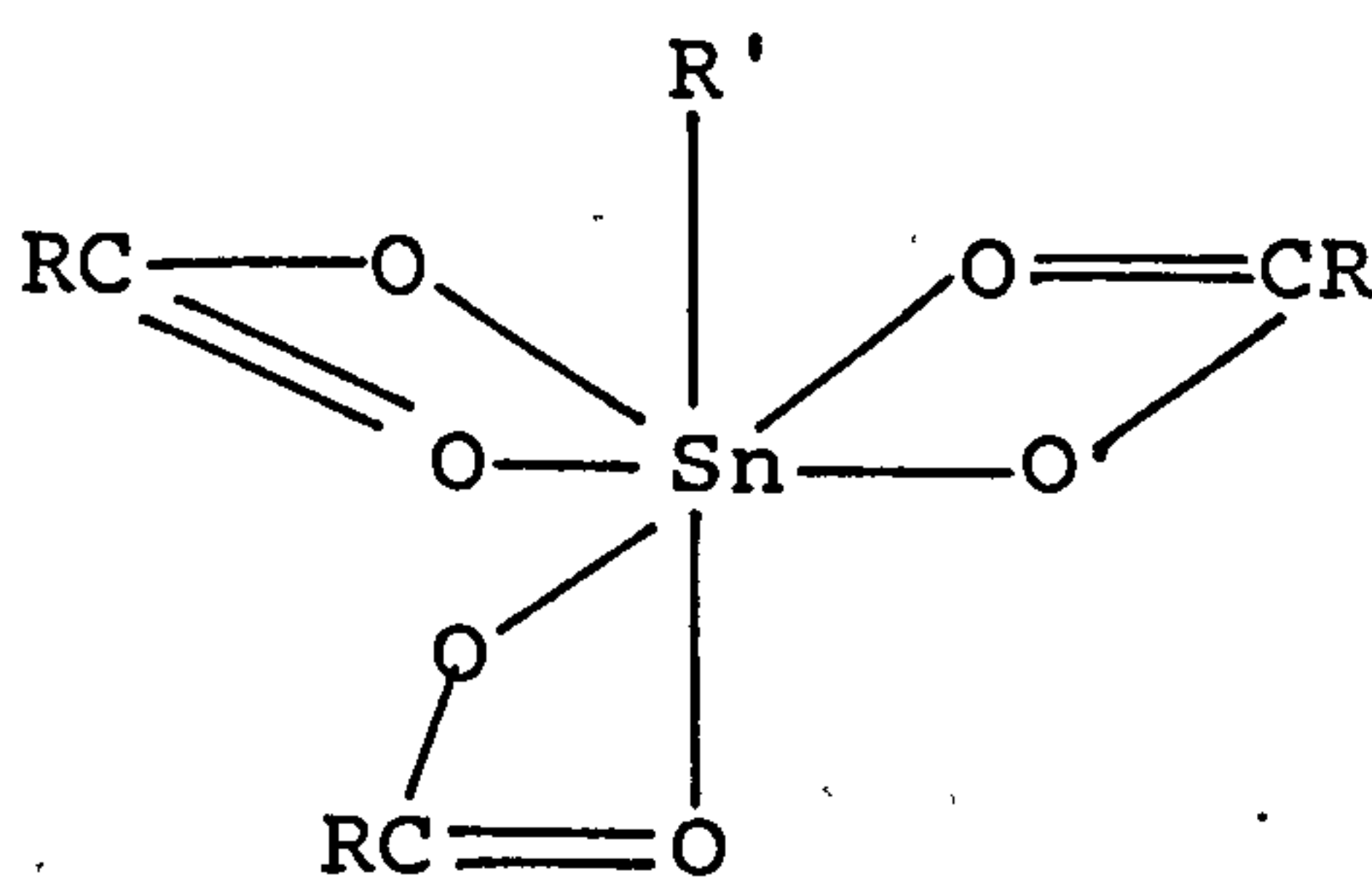


(2)



(3)

The infrared spectra <sup>of</sup> monoorganotin tricarboxylates have been shown to exhibit coordinated carboxyl stretching bands on solvation. This is <sup>an</sup> indication of seven coordinated tin atom geometry for these compounds (4).



(4)

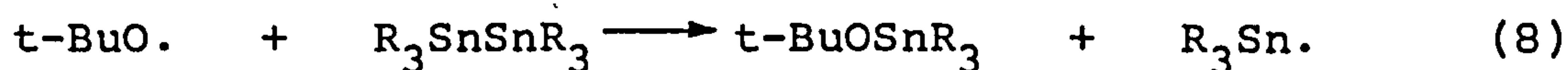
### Hydrolytic stability

The triorganotin carboxylates are hydrolytically stable, whereas the diorganotin dicarboxylates are prone to

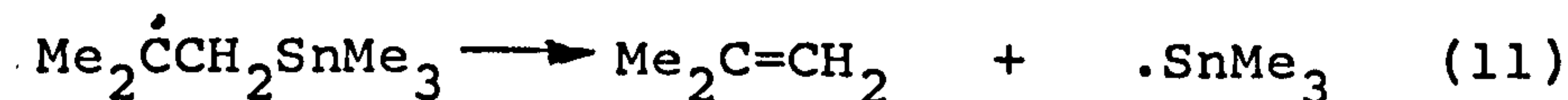
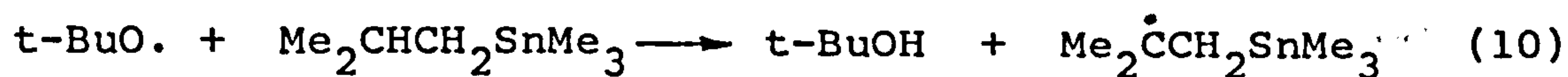
hydrolysis to form the dimeric distannoxanes  $R_2Sn(OCOR')-OSnR_2(OCOR')$  and  $R_2Sn(OCOR')OSnR_2OH$  [17,23]. The monoorganotin tricarboxylates are readily hydrolysed to form the monoorganotin oxycarboxylates [24].

### Organostannyl radicals [18,25]

The seven electron organotin(III) radicals,  $R_3Sn\cdot$ , may be generated by some organotin compounds, e.g.  $R_3SnSnR_3$ , by unimolecular photolysis or thermolysis (equation 7), however, tin centred radicals are usually generated from organotins by a bimolecular reaction with some other radical (equations 8,9)

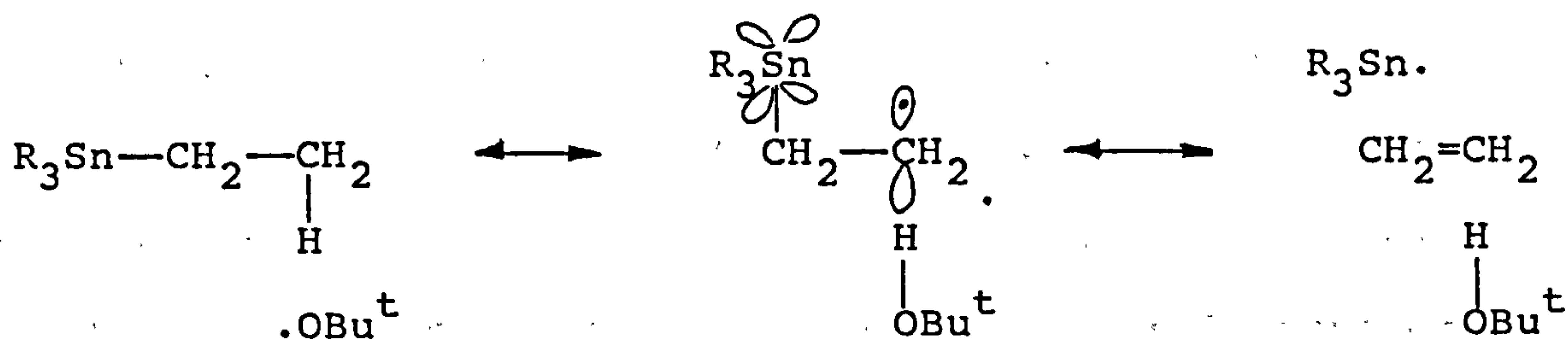


Trialkyltin radicals are also formed by  $\beta$ -scission of a variety of  $\beta$ -stannylalkyl radicals, (equations 10-11)[26].

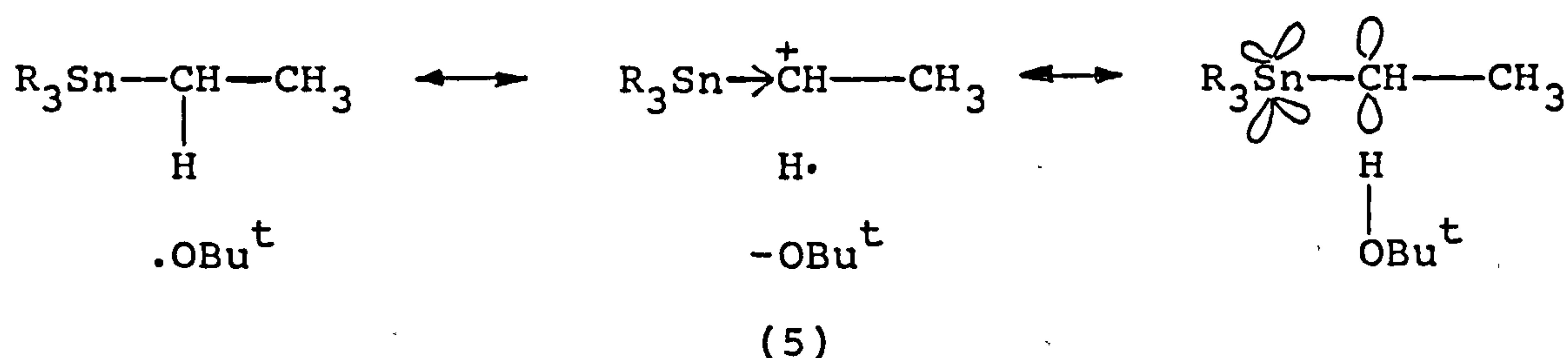


The  $\beta$ -stannylalkyl radicals, may also be formed in the irradiation of organotin compounds [27]. Davies [25,26] ascribed the reactivity of  $\beta$ -stannylalkyl radicals to hyperconjugation between the p-electron and the carbon tin.

bond as well as contribution from  $p\pi$  and  $\pi$  homoconjugation.



The CH group in the  $\alpha$  position to tin is even more reactive and was been attributed to conjugation between the singly occupied p orbital on carbon and the 5d orbital on tin, as well as, hyperconjugation between the singly occupied 2p orbital and the three tin-alkyl bonds and the resonance form (5), being stabilised by an inductive electron release by the tin.



The most important reactions of trialkyltin radicals are halogen abstraction from an alkyl halide and addition to an alkene [25,8].



## Results and Discussion

A comparison of cure response of di-n-butyltin diacrylate (D-n-BTDA), di-i-butyltin diacrylate (D-i-BTDA), and di-n-octyltin diacrylate (D-n-OTDA) with three widely used commercial diluents was investigated. The three commercial diluents chosen were two difunctional monomers, hexanediol diacrylate (HDDA), tripropyleneglycol diacrylate, (TPGDA), and a trifunctional diluent trimethylolpropane triacrylate (TMPTA).

Cure response of the aforementioned diluents was initially evaluated by determining the minimum dose of radiation required to produce a tackfree film. All resulting films, with the exception of TMPTA which produced pitted films, were tested for solvent resistance, pencil hardness, brittleness and resistance to acid and alkali solutions. The results of these tests are shown in Tables 1-5. The films of TPGDA, HDDA and D-n-TGDA used to obtain the results shown in Tables 1,2,3 and those of TMPTA were examined by FTIR-PA spectroscopy. The results were recorded as the percentage of residual double bonds remaining after electron beam irradiation. The absorption band at  $\sim 810\text{cm}^{-1}$ , characteristic of the acrylate group was used to monitor residual double bond content. The carbonyl stretch at  $1730\text{cm}^{-1}$  was used as an internal standard for all calculations (See Chapter 2). The viscosities of TPGDA, D-n-BTDA and D-n-OTDA as a function of temperature were recorded (Figure 2) and their ability to produce low

viscosity formulations suitable for coating applications was investigated and summarised in Figures 3 and 4. The prepolymers used for this study were an epoxidised soya bean oil and a polyurethane acrylate. Formulations containing the above prepolymers were subsequently cured at various doses of radiation and the resulting films were evaluated using the standard physical test methods mentioned above and are collated in Tables 7-14 in Appendix A.

D-n-BTDA, D-i-BTDA and D-n-OTDA rendered tackfree films at 0.5kGy while the three standard diluents all required a minimum dose of 2.5kGy to obtain the tackfree state. The ability of the dialkyltin diacrylates to render tackfree films at low doses indicates that these materials readily crosslink under electron beam irradiation.

Physical tests such as solvent rub, pencil hardness and brittleness were used to assess the relative crosslink density of these films. Careful interpretation of physical test data must be applied as variation in coatweights may produce anomolous results. It is therefore a prerequisite to compare test results for coatings of similar coatweights. For all materials investigated here each test was repeated at least twice and for all cases the general trends were consistent.

Comparison of the physical test results for TPGDA and HDDA (shown in Tables 1 and 2 respectively) with those for D-n-BTDA, D-i-BTDA and D-n-OTDA (collated in Tables 3, 4 and 5 respectively), clearly provide evidence that the

dialkyltin diacrylates all produce hard highly crosslinked films as depicted by their superior solvent resistance and their innate brittleness, even at low doses of radiation.

Table 1 Physical test results for TPGDA

<u>Radiation</u>	<u>Coatweight</u>	<u>Solvent</u>	<u>Pencil</u>	<u>Brittleness</u>	<u>Alkali</u>	<u>Acid</u>
<u>Dose/kGy</u>	<u>gm<sup>2</sup></u>	<u>Rub</u>	<u>Hardness</u>		<u>Rub</u>	<u>Rub</u>
2.5	31.3	36	HB	1	>30	>30
5	30.7	74	2H	2	>30	>30
10	27.3	52	2H	2/3	>30	>30
20	25.7	175	>4H	2/3	>30	>30
40	24.5	437	>4H	2/3	>30	>30
60	31.4	>500	>4H	3/4	>30	>30

Table 2 Physical test results for HDDA

<u>Radiation</u>	<u>Coatweight</u>	<u>Solvent</u>	<u>Pencil</u>	<u>Brittleness</u>
<u>Dose/kGy</u>	<u>gm<sup>2</sup></u>	<u>Rub</u>	<u>Hardness</u>	
2.5	17.4	32.5	H	1
5	18.8	55	H	2
10	11.1	75	2H	2
20	20.0	500	2H	2/3
40	10.0	>500	2H	2/3
60	19.4	>500	>3H	3/4



Table 3 Physical test results for D-n-BTDA

<u>Radiation</u>	<u>Coatweight</u>	<u>Solvent</u>	<u>Pencil*</u>	<u>Brittleness</u>	<u>Alkali</u>	<u>Acid</u>
<u>Dose/kGy</u>	<u>gm<sup>2</sup></u>	<u>Rub</u>	<u>Hardness</u>		<u>Rub</u>	<u>Rub</u>
2.5	21.4	226	>2H	5	<1	<1
5	28.4	261	>2H	5	<1	<1
10	25.5	>500	>2H	5	<1	<1
20	29.2	>500	>3H	5	<1	<1
40	29.6	>500	>3H	5	<1	<1
60	26.3	>500	>3H	5	<1	<1

\* Maximum value before film scattered

Table 4 Physical test results for D-i-BTDA

<u>Radiation</u>	<u>Coatweight</u>	<u>Solvent</u>	<u>Pencil*</u>	<u>Brittleness</u>
<u>Dose/kGy</u>	<u>gm<sup>2</sup></u>	<u>Rub</u>	<u>Hardness</u>	
2.5	25.2	495	>H	5
5	30.6	>500	>2H	5
10	26.8	>500	>3H	5
20	19.3	>500	>2H	5
40	16.8	>500	>2H	5
60	27.6	>500	>3H	5

\* Maximum value before film scattered

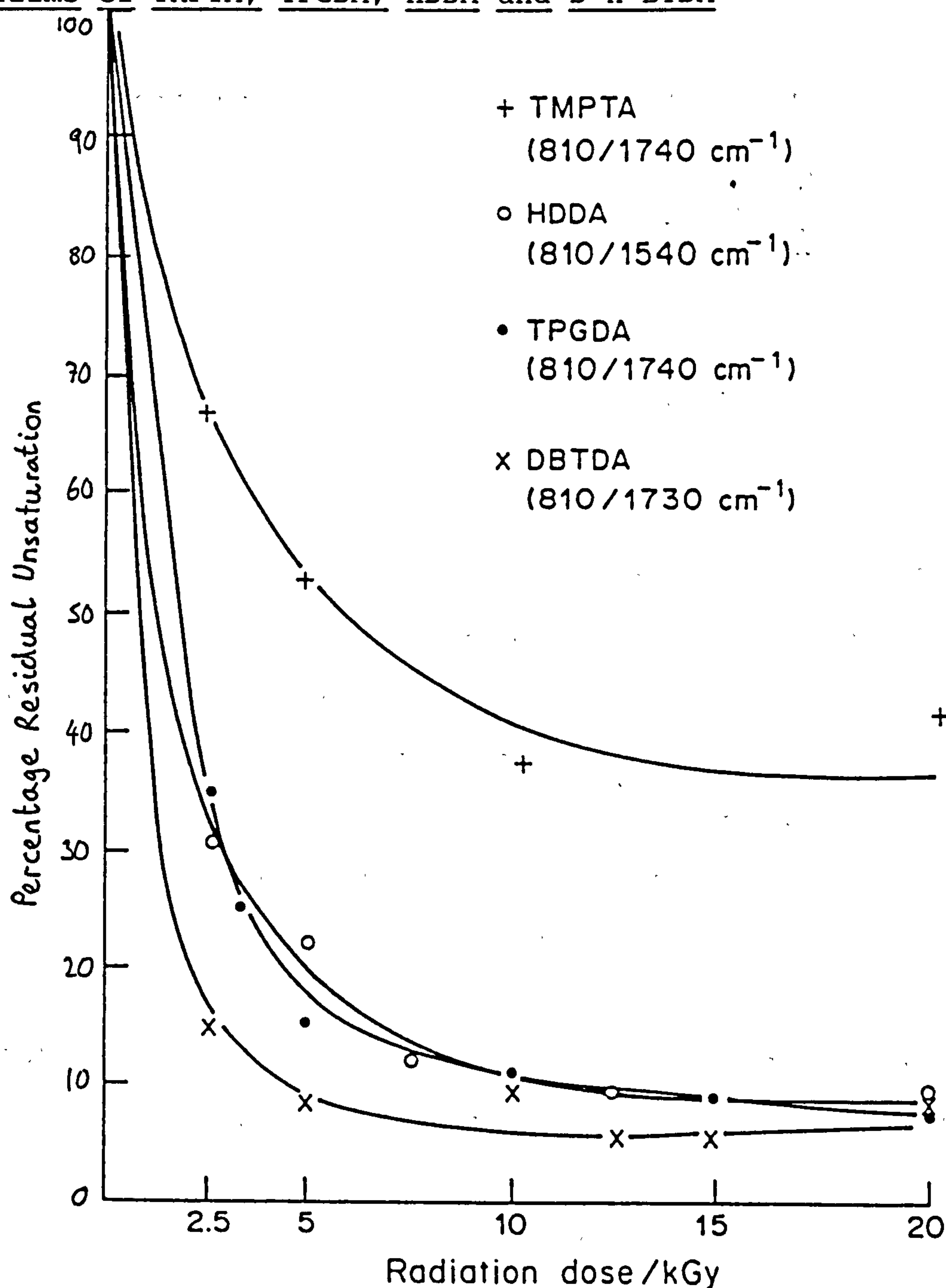
Table 5 Physical test results for D-n-OTDA

<u>Radiation</u>	<u>Coatweight</u>	<u>Solvent</u>	<u>Pencil</u>	<u>Brittleness</u>	<u>Alkali</u>	<u>Acid</u>
<u>Dose/kGy</u>	<u>gm<sup>2</sup></u>	<u>Rub</u>	<u>Hardness</u>		<u>Rub</u>	<u>Rub</u>
2.5	17.6	10	4H	5	6.5	10
5	12.3	12	>4H	3/4	5	10
10	20.4	280	>4H	3/4	5	21
20	46.7	>500	>4H	5	2	20
40	33.9	>500	>4H	4	9	30
60	30.5	>500	>4H	3/4	7	25

The cure response of D-n-BTDA, TPGDA, HDDA and TMPTA was also assessed by calculating the percentage residual unsaturation from the photoacoustic spectra obtained for these films. The out of plane C-H deformation centred at  $810\text{cm}^{-1}$  for TPGDA, HDDA and TMPTA [28] and located at  $830\text{cm}^{-1}$  for D-n-BTDA was used to monitor residual unsaturation. The carbonyl stretching band at  $1730\text{cm}^{-1}$  was used as an internal standard [29].

The trends observed from physical test data are reiterated when one compares the cure response of D-n-BTDA with HDDA, TPGDA and TMPTA as evaluated by the percentage double bonds consumed and summarised in Figure 1. This provides further quantitative evidence that D-n-BTDA polymerises far more readily than the di- and tri-functional commercial diluents.

Figure 1 The percentage residual unsaturation for cured films of TMPTA, TPGDA, HDDA and D-n-BTDA



The observed rapid cure of the tin acrylates may be attributed to the far greater stopping power of these compounds, as calculated using Bragg's additivity rule [29] and listed in Table 6 compared with the standard commercial diluents.



Table 6 Stopping power of D-n-BTDA, D-n-OTDA, TPGDA, HDDA and TMPTA for a high energy electron beam (1MeV)

Compound	Stopping Power / $\text{MeVcm}^2\text{g}^{-1}$
DBTDA	0.0425
DOTDA	0.0352
TPGDA	0.0149
HDDA	0.0147
TMPTA	0.0150

The spurs produced by an electron beam of high LET will tend to overlap, forming short tracks. These track entities consist of high concentrations of reactive intermediates (excited and/or ionised species, radicals). The fate of these primary species will be thermalisation, transformation and reaction and diffusion away from the track to produce a homogenous distribution of these species.

These track entities may be regarded as the sites of initiation of polymerisation and as such cure efficiency will increase, the denser these regions of high local concentration are distributed.

It is therefore be postulated that the tin acrylates will produce a higher random concentration of initiating radicals, on account of their greater LET values, compared with TPGDA, HDDA and TMPTA, and reflected by their ability to cure faster as measured in terms of double bond consumption and crosslink density.

The superior reactivity of the tin acrylates may also be attributed in part to the variety of initiating species that may be formed on electron beam irradiation.

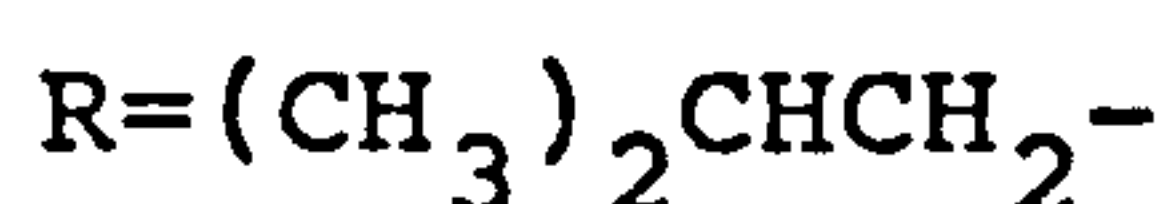
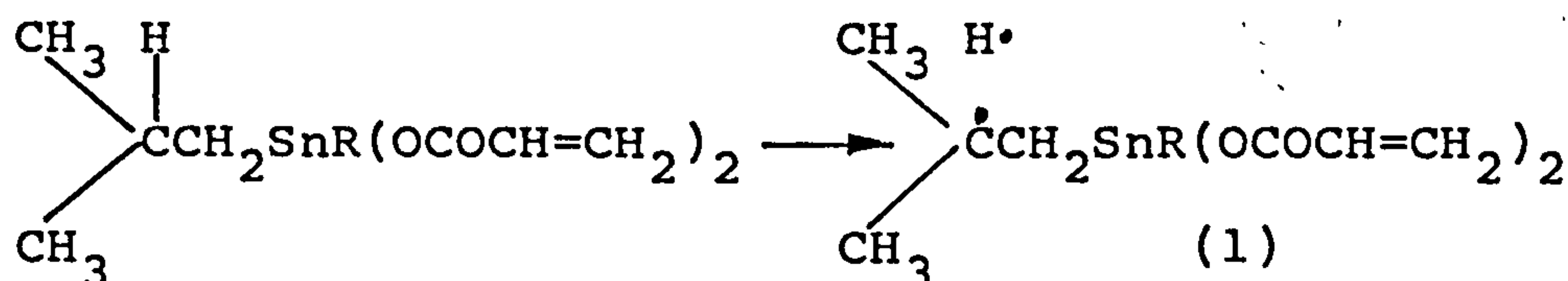
The weak tin carbon bond, whose approximate average bond energy is  $193\text{kJmol}^{-1}$  [30], compared with the covalent bond energy of  $356\text{kJmol}^{-1}$  [30] for a carbon carbon single bond, will be prone to rupture, generating tin and carbon centred radicals capable of crosslinking or initiating polymerisation. This is consistent with those results obtained by Lloyd and Rogers [27] who showed that the rupture of tin-carbon bonds by  $^{60}\text{Co}$  radiation to be a facile process for small molecules of the type  $(\text{CH}_3)_n\text{SnCl}_{4-n}$ , where  $n = 1, 2, 3, 4$ . Labadie et al [13] also explained superior sensitivity of resist materials such as trimethylstannyl styrene polymers, due to their ability to rupture weak tin-carbon bonds creating radical sites which lead to crosslinking

It was also observed from the physical test data of these materials that D-i-BTDA exhibited greater solvent resistance compared with D-n-BTDA. It is known that the reactivity of C-H bonds decreases with increasing bond strength [9] and consequently, tertiary C-H bonds are more easily broken than secondary or primary C-H bonds. The reactivity of  $\beta$ -C-H bonds may also be enhanced as a result of homoconjugation between the singly occupied 2p orbital on carbon and the 5d orbital on tin ( $p\pi$ - $d\pi$  homoconjugation), as well as hyperconjugation between the p-electron and the

carbon tin bond [25,26].

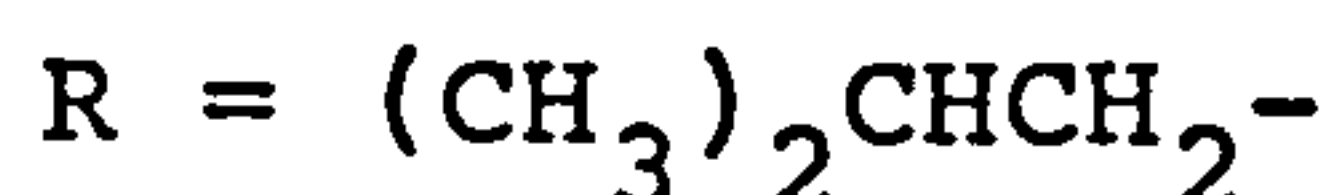
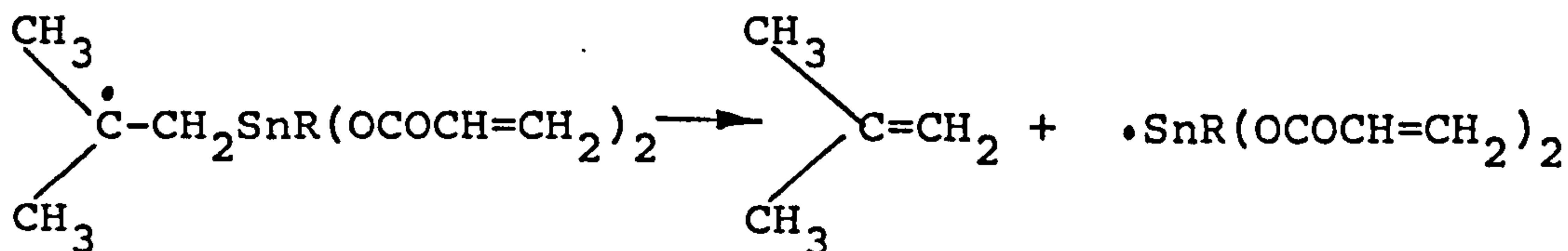
On this basis D-i-BTDA would be expected to form a  $\beta$ -stannylalkyl radical (1) which may initiate polymerisation or form crosslinks with a neighbouring polymer chain

Scheme 1



radical. Alternatively, the  $\beta$ -stannylalkyl radical may generate an alkene and an organostannyl radical (Scheme 1) capable of promoting polymerisation or crosslinking reactions.

Scheme 2



The crosslink density of the dialkyltin diacrylate diluents and the standard commercial diluents, as evaluated by solvent resistance, pencil hardness and brittleness (Table 1-5) was shown to increase in the order,



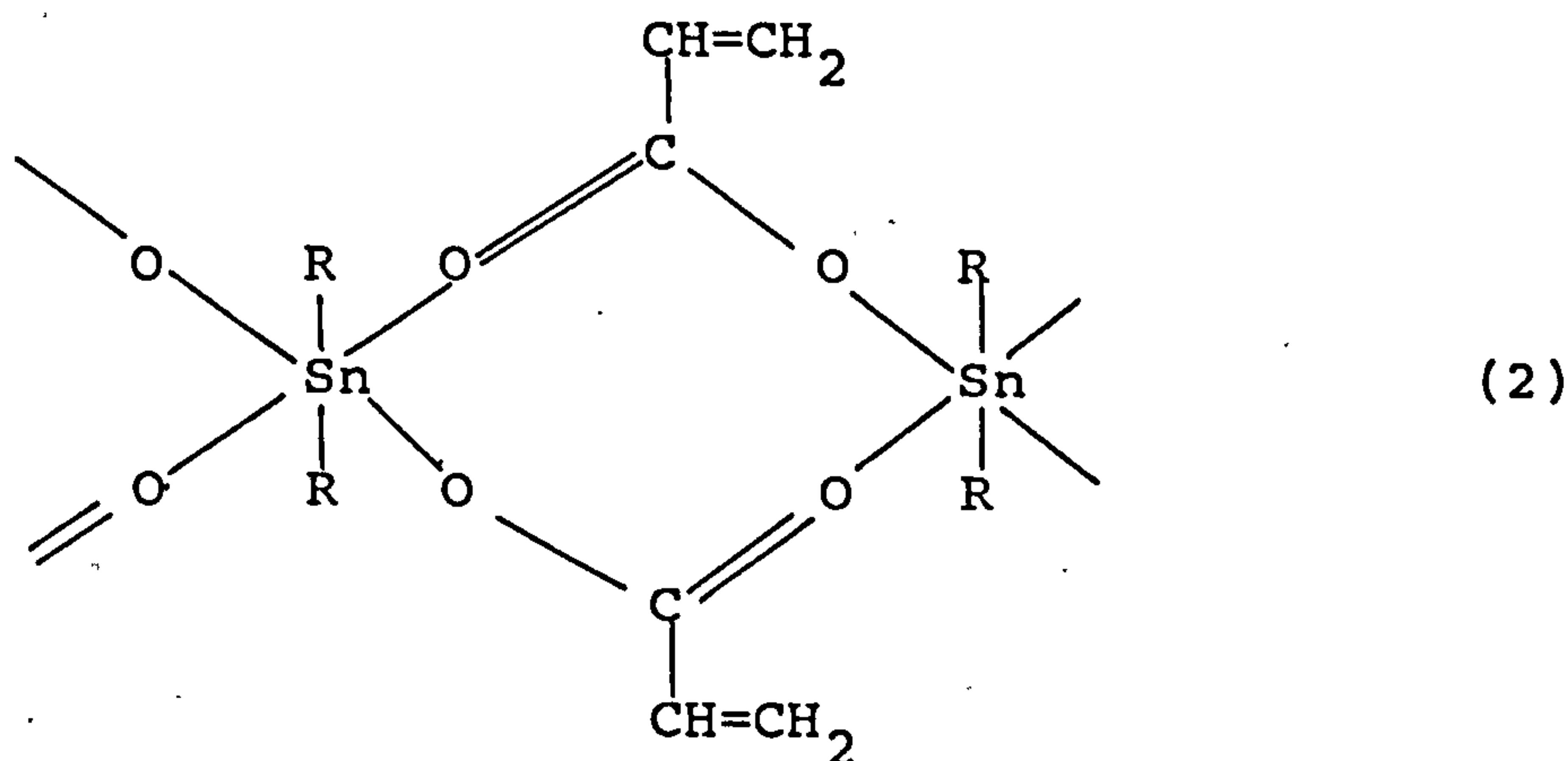
The solvent resistance of the polymer films derived from D-n-OTDA were significantly lower than those of the dibutyltin diacrylates. The former coatings also exhibited greater



flexibility compared with the dibutyltin diacrylates as indicated by their lower brittleness ratings. The D-n-OTDA films were of comparable flexibility to those polymer films derived from TPGDA and HDDA. The lower crosslink density and resulting increased flexibility of D-n-OTDA relative to D-n-BTDA and D-i-BTDA may be expected on account of its slightly lower stopping power and concomitant reduction in radical production, as well as, the considerably greater alkyl content of these films capable of imparting flexibility.

However, all three tin containing polymers exhibited greater crosslink density, as evaluated from the solvent rub test and greater or similar degrees of flexibility, compared with TPGDA or HDDA.

The final film properties of the dialkytin diacrylates may also be due in part, to the ability of D-n-BTDA, D-i-BTDA and D-n-OTDA to form a polymeric structure with intermolecularly bridging carboxylate groups (2)



where R = n-C<sub>4</sub>H<sub>9</sub>-, i-C<sub>4</sub>H<sub>9</sub>-, C<sub>8</sub>H<sub>17</sub>-

Evidence for this coordinated structure comes from the observation that the tin based diluents all exhibit strong

absorbance peaks at  $\sim 1560\text{cm}^{-1}$  and  $\sim 1415\text{cm}^{-1}$ . This is consistent with the IR data of a number of dialkyltin dicarboxylates [17,22]

It is known that diorganotin dicarboxylates undergo partial hydrolysis to form the dimeric distannanoxanes  $\text{R}_2\text{Sn}(\text{OCOR}')\text{OSnR}_2(\text{OCOR}')$  and  $\text{R}_2\text{Sn}(\text{OCOR}')\text{OSnR}_2\text{OH}$  [17,23]. The acid and alkali resistance of DBTDA, DOTDA and TPGDA films are shown in Table 1,3,5. Films of TPGDA were found to be resistant to hydrolysis under our experimental conditions. However, cured films of D-n-BTDA immediately hydrolysed on contact with both alkaline (1M sodium hydroxide) and acidic solutions (1M hydrochloric acid) resulting in the formation of a white precipitate consistent with the hydrolysis product of di-n-butyltin oxide. Cured films of dioctyltin diacrylate afforded greater resistance to hydrolysis due to the greater alkyl content of D-n-OTDA producing a film of increased hydrophobicity, as well as, causing steric inhibition of ester hydrolysis.

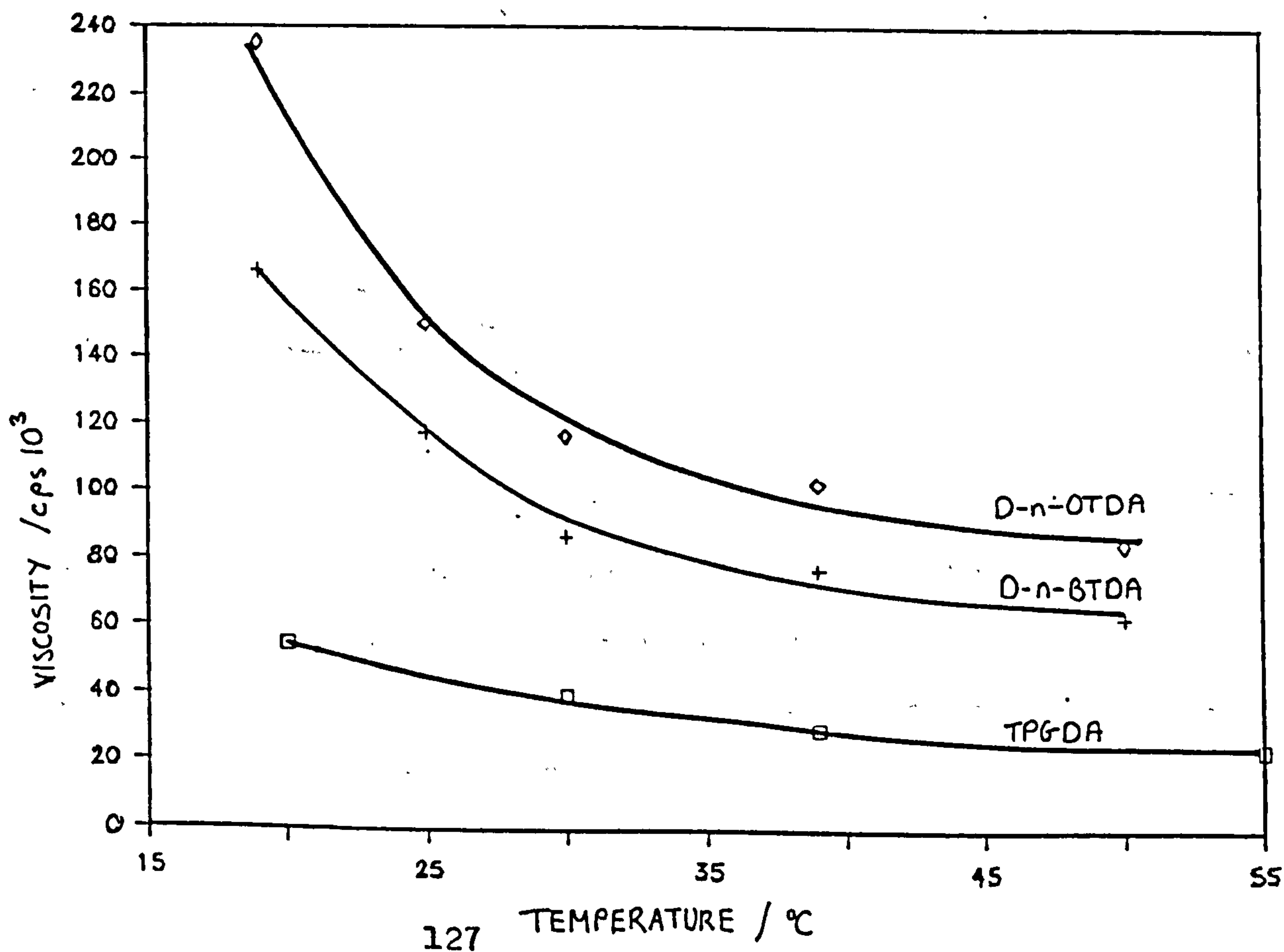
One of the prime functions of low molecular weight diluents is their ability to solvate a prepolymer in order to produce a low viscosity formulation capable of coating a substrate. The viscosity of a radiation curable system may also be adjusted by varying the percentage of the diluent present [1]. TPGDA and HDDA have been shown to display excellent solvating ability, as well as, exhibiting good cure response and final film properties [1,31]. The di-

alkyltin diacrylates were evaluated as rheological control agents of radiation curable systems. As can be seen from the temperature/viscosity curves for neat TPGDA, D-n-BTDA and D-n-OTDA shown in Figure 2, the viscosity of these materials was found to increase in the order

$$\text{TPGDA} < \text{D-n-OTDA} < \text{D-n-BTDA}$$

The above trend provides further evidence of the associated nature of these materials. It was therefore expected that these materials would also exhibit low solubility/compatibility and poor thinning action with viscous prepolymers. This was indeed found to be the case.

Figure 2 Viscosity versus temperature plots for TPGDA, D-n-BTDA and D-n-OTDA

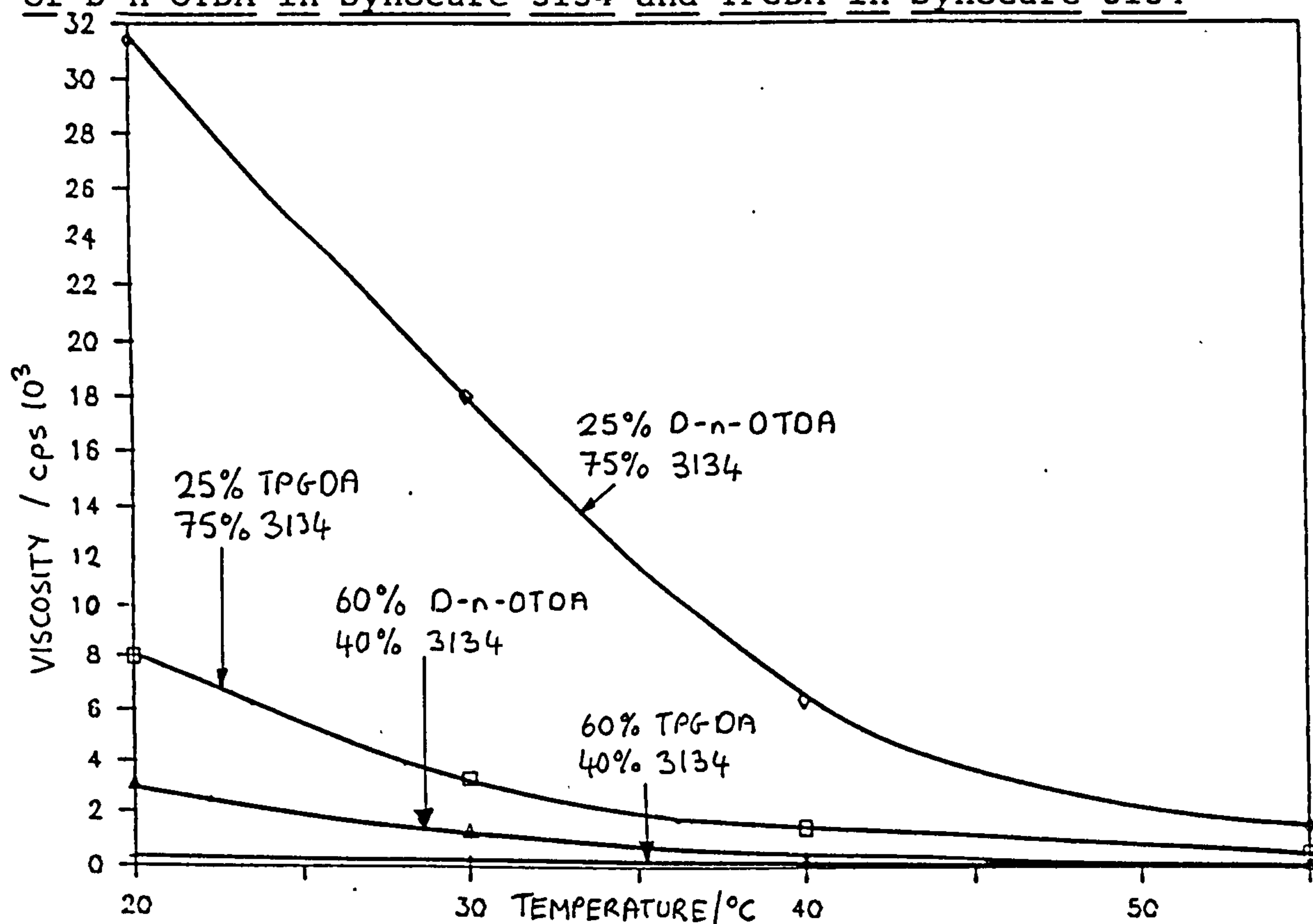




The choice of prepolymer was restricted to those compatible with the tin containing diluents, again providing further evidence of the 'polymeric' associated structure of these compounds.

The ability of D-n-OTDA to reduce the viscosity of two prepolymers, an epoxidised soya bean (Synocure 3111) and a urethane acrylate (Synocure 3134) was assessed. The

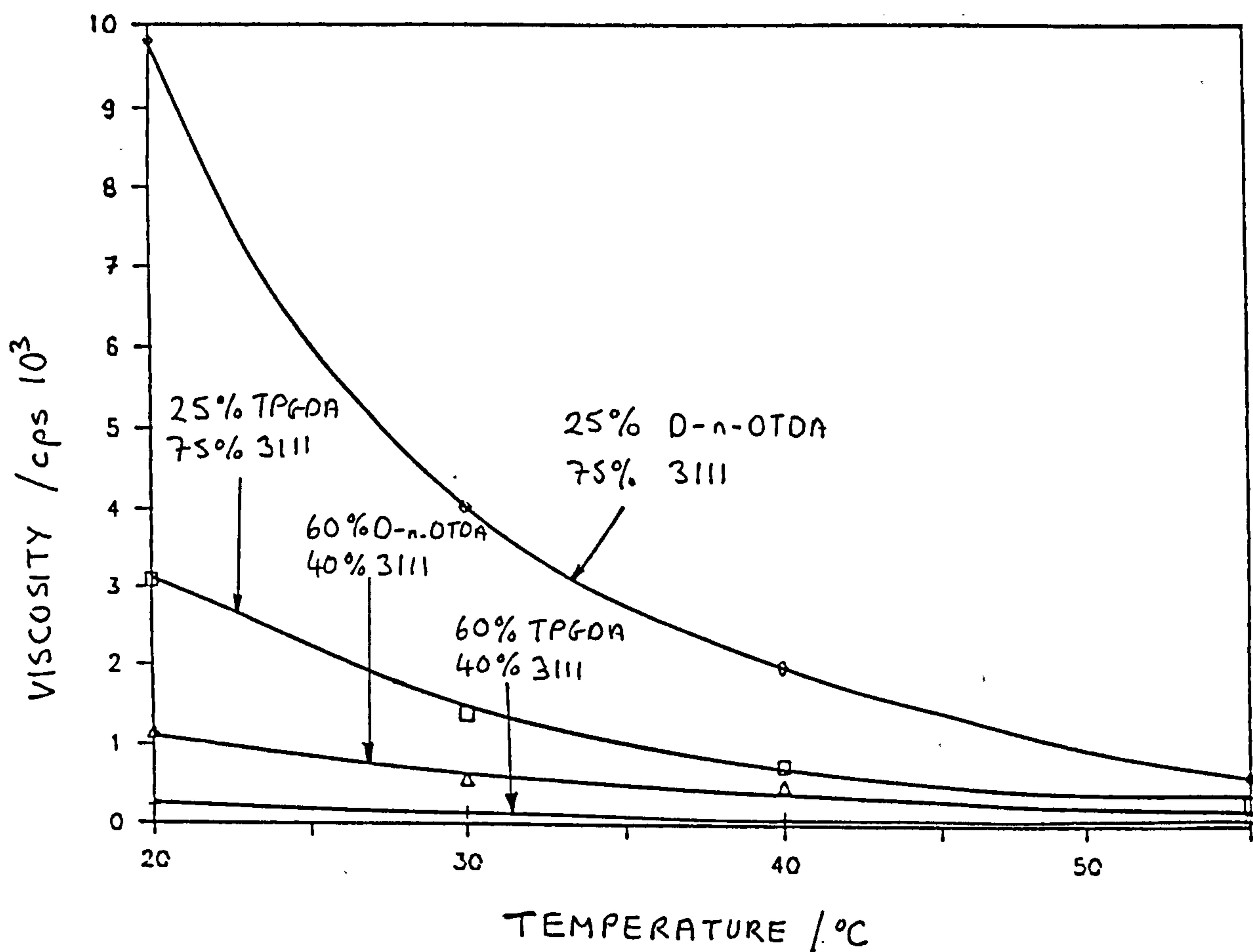
Figure 3 Viscosity versus temperature plots for formulations of D-n-OTDA in Synocure 3134 and TPGDA in Synocure 3134



The viscosity of formulations containing 25% and 60% D-n-OTDA were investigated and compared with formulations in which D-n-OTDA had been substituted by TPGDA. As can be seen from Figures 3 and 4, D-n-OTDA was shown to be a less effective diluent than TPGDA in producing low viscosity

formulations for each type of prepolymer investigated. Formulations of D-n-OTDA, D-n-BTDA and TPGDA containing the above prepolymers were subsequently cured over a range of doses and the resulting films were assessed in terms of solvent resistance, pencil hardness, brittleness and resistance towards aqueous alkali and acid solutions.

Figure 4 Viscosity versus temperature plots for formulations of D-n-OTDA in Synocure 3111 and TPGDA in Synocure 3111



The results of the solvent rub, pencil hardness and brittleness tests for formulations containing, one third

prepolymer by weight and two thirds diluent, cured at 5, 10 and 20kGy have been collated in Tables 7-14 in Appendix A.

It was observed that formulations in which TPGDA were progressively substituted by D-n-BTDA, were accompanied by a significant increase in solvent resistance (see Table 7 and 11). Increased solvent resistance was also accompanied by increased brittleness for the formulations containing the epoxidised soya bean oil (Table 12). However, this trend was not observed for formulations containing the acrylated polyurethane (Table 8). The brittleness observed for formulations of D-n-BTDA and the epoxidised soya bean oil may be explained in terms of the poor crosslinking ability of the oligomer in question. It may be perceived that an oligomer devoid of acrylate functionality will not crosslink efficiently with the homopolymer of D-n-BTDA. The resulting polymer film will thus contain 'islands' of oligomer and 'islands' of the highly crosslinked D-n-BTDA polymer. As the D-n-BTDA content increases the resulting polymer matrix would be expected to exhibit brittleness associated with polymer films of neat D-n-BTDA. Conversely, prepolymers containing some acrylate functionality, such as the acrylated polyurethane, Synocure 3134, will crosslink efficiently with the diluent to produce a polymer network of structural uniformity. The resulting polymer film would be expected to be inherently more flexible as was found to be the case for the acrylated polyurethane and D-n-BTDA formulations.

Formulations containing 33% prepolymer and varying



amounts of TPGDA and D-n-OTDA produced films of similar good flexibility (Tables 10 and 14). However, by increasing the D-n-OTDA content, cured films exhibited a significant concomitant increase in solvent resistance. (Tables 9 and 13).

Enhanced solvent resistance was observed for all films in which TPGDA had been substituted by D-n-BTDA and D-n-OTDA. Once again this may be attributed to the innate chelated polymeric structure of the dialkyltin dicarboxylates, as well as their crosslinking ability as described previously for neat films of these diluents.

The hydrolytic stability of films containing D-n-OTDA and D-n-BTDA were improved and were found to be resistant to both acid and alkali solution under our experimental conditions. This may be attributed to the innate hydrophobicity of the cured films.

### CONCLUSION

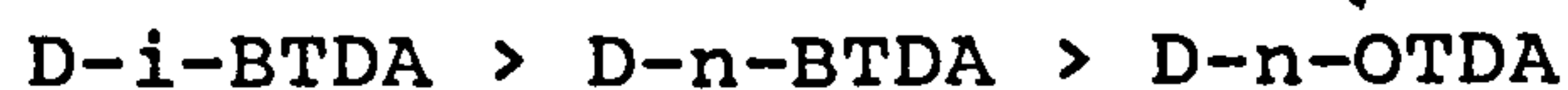
The superior reactivity, in terms of minimum dose required to form a tackfree film, crosslink density and double bond consumption of the dialkyltin diacrylates, compared with standard commercial diluents is ascribed to

- 1) the greater stopping power of these materials due to the presence of the tin atom,
- 2) homolysis of the weak tin carbon bond, thus producing radicals capable of crosslinking or initiating

polymerisation, and,

- 3) the ability of these materials to form an intermolecularly associated structure.

The order of crosslink density exhibited by these diorganotin diacrylates was shown to be,



The enhanced crosslink density of D-i-BTDA is thought to be due to the ability of this material to form a -stannyl-alkyl radical, arising from the homolysis of the tertiary C-H bond. The greater crosslink density shown by both D-i-BTDA and D-n-BTDA compared with D-n-OTDA is attributed to the lower stopping power of the latter material, as well as its greater alkyl content, thus imparting greater flexibility and solubility.

Although the cured films of the title materials are hydrolytically unstable their resistance was markedly improved when incorporated in an electron beam formulation. The final film properties of these formulations were shown to exhibit both greater crosslink density as measured by solvent resistance with respect to the corresponding formulations containing TPGDA and improved flexibility compared with the neat polymeric films of the diluent in question.

In conclusion, the final film performance of the dialkyltin diacrylates showed several favourable attributes compared with such commercial diluents as TPGDA, HDDA and TMPTA and may be exploited as a new class of acrylate diluent.

## ACKNOWLEDGEMENTS

I would like to thank C. Malde, at Wiggins Teape Research and Development Group, for carrying out the physical test results presented here. I would also like to thank Dr. R. Ellis who helped with the task of measuring peak heights many times over. The viscosity measurements carried out by S. Herlihy are also gratefully acknowledged.



## EXPERIMENTAL

### Instrumentation

All formulations were coated onto a moving web via a Dixon 164 coater unit.

Electron beam curing was carried out using an Otto Durr ESH 150/130 electron beam unit under a nitrogen blanket. The operating voltage was maintained at 150kV and the beam current was adjusted for each applied dose.

Infrared spectra of prepared monomers were analysed using a Perkin Elmer Infrared Spectrometer model no. 599.

Proton NMR spectra were obtained using a Jeol NMR spectrometer model no. JNM-MH-100 and referenced against TMS.

All elemental analysis was carried out using a Carlo Erba Strumentazione Elemental Analyzer Mod 1106.

Analysis of cured films were carried out using a Nicolet 60-SX fourier transform infrared spectrometer in conjunction with a Princeton photoacoustic cell model no 6005. The spectra obtained at 4cm<sup>-1</sup> resolution for 500 scans.

### Materials

#### Resins and diluents

Tripropyleneglycol diacrylate, TPGDA (Cray Valley Products Ltd.), trimethylolpropane triacrylate, TMPTA (Cray Valley Products Ltd.), hexanediol diacrylate, HDDA (Cray Valley Products Ltd.), Synocure 3111 (Cray Valley Products

Ltd.), Synocure 3131 (Cray Valley Products Ltd.) and Synocure 3134 (Cray Valley Products Ltd.) were all used as received.

### Chemicals for synthesis

Benzene (BDH Chemicals Ltd.) was dried by addition of sodium wire, 24 hours before use.

Dibutyltin oxide (Schering AG), dioctyltin oxide (Schering AG), 1-iodo-2-methylpropane (Aldrich Chemicals Co.), acrylic acid (Aldrich Chemical Co.), 2-ethoxyethanol (Aldrich Chemical Co.), lithium bromide (BDH Chemicals Ltd.), tin (Aldrich Chemical Co.) were all used as received.

Gateway natural tracing paper (Wiggins Teape Group Ltd.) was used as a substrate for all coatings.

### Synthesis

#### Di-(3-methylbutyl)tin oxide [32]

#### Method

Lithium bromide ( $1.08^g_A$ ; 0.011moles) was added to a mixture of 1-iodo-2-methyl propane (13.62ml; 0.11moles) and 2-ethoxyethanol (5.43g; 0.056moles). Granulated tin (5.93g; 0.05g-atom) was then added and the mixture was heated under reflux for 3.5 hours. The unreacted tin was removed by filtration and the filtrate stripped of excess 1-iodo-2-methylpropane. The residue was dissolved in ethanol (100ml) and the solution was added to a stirred solution of caustic soda (25g) in water (100ml). The resulting precipitate of di-(isobutyl)tin oxide was

collected by filtration, washed first with ethanol, then water and dried at 80° C to constant weight. (13.1g;95%) Mpt > 300° C

### Di-n-butyltin diacrylate

#### Method

A mixture of dibutyltin oxide (24.9g;0.1moles), acrylic acid (14.4g;0.2moles) and 2 drops of concentrated sulphuric acid in dry benzene (500ml) was refluxed until 1.8ml of water (0.1moles) had been removed azeotropically. The reaction mixture was dried with sodium sulphate and the solvent was removed over a rotary evaporator. The clear colourless residue was di-n-butyltin diacrylate (34.1g;91%)

Infrared (Liquid film) : 2961, 2930, 2875, 2865, 1730, 1649, 1638, 1590-1540, 1430-1405, 1383, 1365, 1262, 1184, 1047, 983, 962, 915, 880, 829 (out of plane bend =CH<sub>2</sub>), 719, 700-670, 630cm<sup>-1</sup>.

<sup>1</sup>H NMR (CDCl<sub>3</sub>) : δ (0.7-1.8) (multiplet, 18H, C<sub>4</sub>H<sub>9</sub>-), (5.50-6.40)(multiplet, 6H, CH<sub>2</sub> and CH of acrylate)

Analysis calculated for C<sub>14</sub>H<sub>24</sub>O<sub>4</sub>Sn : C, 44.83; H, 6.45;

Found : C, 44.97; H, 6.45

### Di-i-butyltin diacrylate

#### Method

A mixture of di-i-butyltin oxide (12.9<sup>9</sup><sub>1</sub>;0.05moles), acrylic acid (7.2g;0.1moles) and 2 drops of concentrated sulphuric acid in dry benzene (200ml) was refluxed until 0.9ml of water (0.05moles) had been removed azeotropically.



The reaction mixture was dried with sodium sulphate and the solvent was removed over a rotary evaporator. The clear colourless residue was di-i-butyltin diacrylate (16.9g; 90%).  
Infrared (Liquid film) : 2960, 2935, 2875, 1732, 1650, 1640, 1545-1580, 1415, 1365, 1339, 1262, 1185, 1079, 1049, 985, 965, 918, 880, 829, 700, 682, 630 $\text{cm}^{-1}$ .  
 $^1\text{H}$  NMR ( $\text{CDCl}_3$ ) :  $\delta$  (0.9-1.6) (multiplet, 18H,  $\text{C}_4\text{H}_9$ -), (5.7-6.5) (multiplet, 6H, CH and  $\text{CH}_2$  of acrylate);  
Analysis calculated for  $\text{C}_{14}\text{H}_{24}\text{O}_4\text{Sn}$  : C, 44.83; H, 6.45;  
Found : C, 45.00; H, 6.61.

#### Di-n-octyltin diacrylate

##### Method

A mixture of di-n-octyltin oxide (18.1g; 0.05 moles), acrylic acid (7.2g; 0.1 moles) and 2 drops of concentrated sulphuric acid in dry benzene (200ml) was refluxed until 0.9ml of water (0.05 mole) had been removed azeotropically. The reaction mixture was dried with sodium sulphate, and the solvent was removed over a rotary evaporator. The clear colourless residue was di-n-octyltin diacrylate (21g; 86%).

Infrared (Liquid film) : 2959, 2930, 2855, 1731, 1650, 1640, 1550-1590, 1415, 1362, 1337, 1261, 1183, 1049, 985, 965, 918, 829, 728, 699, 680, 625 $\text{cm}^{-1}$ .

$^1\text{H}$  NMR ( $\text{CDCl}_3$ ) :  $\delta$  (0.80-1.9) (multiplet, 34H,  $\text{C}_8\text{H}_{17}$ -) (5.7-6.5) (multiplet, 6H, CH and  $\text{CH}_2$  of acrylate).

Analysis calculated for  $\text{C}_{22}\text{H}_{40}\text{O}_4\text{Sn}$  : C, 54.23; H, 8.28.  
Found : C, 54.00; H, 8.28.

### Preparation of films of the acrylate esters

All formulations were coated onto aluminium foil via a Dixon 164 coater using a forward spinning smoothing roller at a setting of 32psi. The coatings were then passed under the electron beam. For all doses of radiation the moving web was maintained at  $20\text{mm}^{-1}$ .

### Analysis of spectra obtained by Fourier transform infrared spectroscopy

The FTIR-PA spectra obtained for all films were of good quality. As discussed in Chapter 2 the spectra of films should not be directly compared due to variation in film thickness.

It was therefore necessary to use an internal standard to compensate for variation in coatweights. From the results obtained in Chapter 2, and from spectra obtained here, a suitable internal standard was found to be the carbonyl stretching frequency at  $1730\text{cm}^{-1}$  [29] and was used as an internal standard for all calculations.

### Analysis of infrared spectra obtained for films of TPGDA, HDDA, TMPTA and D-n-BTDA

For films of TPGDA, HDDA and TMPTA the peak at  $810\text{cm}^{-1}$  associated with the CH out of plane deformation of the acrylate functionality [28] was used to monitor residual unsaturation in the film. The out of plane deformation associated with the acrylate group in D-n-BTDA was centred at  $830\text{cm}^{-1}$ . The carbonyl stretching frequency for D-n-BTDA

were centred at  $1730\text{cm}^{-1}$  (weak intensity) and  $1570\text{cm}^{-1}$  (very strong) and possibly  $1420\text{cm}^{-1}$  (strong). The infrared of D-n-BTDA has not been investigated, however, the infrared spectrum of a similar material, dibutyltin diacetate has been assigned [22]. It was found that neat dibutyltin diacetate yielded strong absorbances at  $1605\text{cm}^{-1}$ ,  $1570\text{cm}^{-1}$  and  $1425\text{cm}^{-1}$ . The former two peaks were associated with the carbonyl asymmetric stretching frequency. The appearance of the  $1570\text{cm}^{-1}$  peak and the enhancement of the  $1425\text{cm}^{-1}$  absorbance band were attributed to the coordination of the acetoxy groups to the tin atom. This coordinated structure was used to explain similar absorbance bands present in the spectrum of D-n-BTDA.

#### Physical test methods

These were carried out on all films, with the exception of coatings derived from TMPTA, which produced pitted films due to reticulation. These tests are all subjective and results will vary for different coatweights of the material examined. It is therefore necessary to evaluate the film properties of coatings of similar coatweights. This was sometimes difficult to achieve due to differences in the flow properties of the materials investigated. These tests were carried out at least twice for films of similar coatweights in order that a fair comparison of film properties could be made. All coatweights were calculated from the weight of a coating over a  $(10 \times 10)\text{cm}^2$  surface area.



## Physical test methods

### Solvent rub test

This method is based on the ASTM(D3363)27. A felt pad soaked in acetone was mechanically rubbed backand forth across the surface of the sample under test held flat under tension on a SATRA rub tester. The load on the felt pad was 0.5kg and the pad was kept saturated with acetone. The number of "double rubs" required before the acetone broke through the coating was recorded.

### Pencil hardness

The pencil hardness of the film was assessed by drawing the coated substrate under the lead using a Rotring pencil with changeable 0.5mm flat ended leads. This was repeated using lead types of HB, H, 2H, 3H and 4H and the pointat which the film was etched was recorded.

### Brittleness

This test involved folding a coated substrate through 180 and assessing the amount of debris along the crease. An arbitrary scale from 1 (no debris, flexible) to 5 (large amount of debris, very brittle) was used to assess brittleness.

### Acid/Base rub test

The procedure for the measurement of acid/base rub resistance was carried out as described for the solvent rub test above, substituting<sup>for</sup> the organic solvent for hydrochloric acid (1M) and sodium hydroxide (1M) respectively.

# APPENDIX A

Table 7 Solvent rub test results for D-n-BTDA/Synocure 3134 (acrylated polyurethane)

<u>Dose of</u>	<u>Formulation</u>		
<u>Radiation</u>	33% 3134	33% 3134	33% 3134
<u>/kGy</u>	67% TPGDA	33% TPGDA	67% D-n-BTDA
		34% D-n-BTDA	
5	5 (39.9)	-	16.5 (39.5)
10	20 (39.7)	37 (26.9)	61 (24.0)
20	26 (43.4)	-	75 (24.3)

Table 8 Pencil hardness (P.H) and brittleness test results for D-n-BTDA/Synocure 3134 (acrylated polyurethane)

<u>Dose of</u>	<u>Formulation</u>			
<u>Radiation</u>	33% 3134	33% 3134	33% 3134	
<u>/kGy</u>	67% TPGDA	33% TPGDA	67% D-n-BTDA	
		34% D-n-BTDA		
	<u>P.H</u>	<u>Brittle-</u>	<u>P.H.</u>	<u>Brittle-</u>
		<u>ness</u>		<u>ness</u>
5	>4H	1	-	>4H 1
10	>4H	1	>4H 1	>4h 2
20	>4H	1	-	>4H 1

Coatweights in parenthesis

Table 9 Solvent rub test results for D-n-OTDA/Synocure 3134  
(acrylated polyurethane)

<u>Dose of</u>	<u>Formulation</u>		
<u>Radiation</u>	33% 3134	33% 3134	33% 3134
<u>/kGy</u>	67% TPGDA	33% TPGDA 34% D-n-OTDA	67% D-n-OTDA
5	5 (39.9)	9 (25.2)	12.5 (46.2)
10	20 (39.7)	9 (27.6)	30 (40.4)
20	26 (43.4)	27 (34.3)	-

Table 10 Pencil hardness (P.H) and brittleness test  
results for DOTDA in Synocure 3134

<u>Dose of</u>	<u>Formulation</u>		
<u>Radiation</u>	33% 3134	33% 3134	33% 3134
<u>/kGy</u>	67% TPGDA	33% TPGDA 34% DOTDA	67% DOTDA
	<u>P.H</u> <u>Brittle-</u>	<u>P.H.</u> <u>Brittle-</u>	<u>P.H.</u> <u>Brittle-</u>
	<u>ness</u>	<u>ness</u>	<u>ness</u>
5	>4H 1	>4H 1	>4H 1
10	>4H 1	>4H 2/3	>4H 2
20	>4H 1	>4H 1	-



Table 11 Solvent rub test for D-n-BTDA in Synocure 3111  
(epoxidised soya bean oil)

<u>Dose of</u>	<u>Formulation</u>		
<u>Radiation</u>	33% 3111	33% 3111	33% 3111
<u>/kGy</u>	67% TPGDA	33% TPGDA	67% D-n-BTDA
		34% D-n-BTDA	
5	2.5 (18.3)	15 (17.4)	23 (35.2)
10	8.5 (23.5)	24 (21.7)	88 (29.1)
20	12.5 (18.6)	62 (22.7)	>500 (34.7)

Table 12 Pencil hardness (P.H.) and brittleness test results  
for D-n-BTDA in Synocure 3111 (epoxidised soya bean oil)

<u>Dose of</u>	<u>Formulation</u>					
<u>Radiation</u>	33% 3111		33% 3111		33% 3111	
<u>/kGy</u>	67% TPGDA		33% TPGDA		67% D-n-BTDA	
			34% D-n-BTDA			
	<u>P.H</u>	<u>Brittle-</u>	<u>P.H.</u>	<u>Brittle-</u>	<u>P.H.</u>	<u>Brittle-</u>
		<u>ness</u>		<u>ness</u>		<u>ness</u>
5	>4H	2/3	>4H	2	>4H	5
10	>4H	2	>4H	2/3	>4H	4
20	>4H	3	>4H	3	>4H	5

Table 13 Solvent rub test results for D-n-OTDA/Synocure 3111  
(epoxidised soya bean oil)

<u>Dose of</u>	<u>Formulation</u>		
<u>Radiation</u>	33% 3111	33% 3111	33% 3111
<u>/kGy</u>	67% TPGDA	33% TPGDA	67% D-n-OTDA
		34% D-n-OTDA	
5	2.5 (18.3)	-	15.0 (23.7)
10	8.5 (23.6)	25 (18.5)	-
20	12.5 (18.6)	31 (20.4)	19.5 (17.8)

Table 14 Physical test results for D-n-OTDA/Synocure 3111  
(epoxidised soya bean oil)

<u>Dose of</u>	<u>Formulation</u>		
<u>Radiation</u>	33% 3111	33% 3111	33% 3111
<u>/kGy</u>	67% TPGDA	33% TPGDA	67% D-n-OTDA
		34% D-n-OTDA	
	<u>P.H</u> <u>Brittle-</u>	<u>P.H.</u> <u>Brittle-</u>	<u>P.H.</u> <u>Brittle-</u>
	<u>ness</u>	<u>ness</u>	<u>ness</u>
5	>4H 2/3	-	>4H 2
10	>4H 2	>4H 2/3	-
20	>4H 3	>4H 3	>4H 3

## REFERENCES

- [1] C. G. Roffey, (1982). Photopolymerisation of Surface coatings, Wiley-Interscience.
- [2] UV Curing : Science and Technology (1980), S. P. Pappas, Ed., Technology Marketing Corp.
- [3] J. Guthrie, M. B. Jeganathan, M. S. Otterburn and J. Woods, (1986). Polymer Bulletin, 15, 51.
- [4] UV and EB Curing Formulations for Printing Inks Coatings and Paints, (1984). R. Holman, Ed., Sita Technology.
- [5] S. P. Pappas, (1985). Radiat. Phys. Chem., 25, (4-6), 633.
- [6] B. L. Brann, (1985). J. Rad. Curing, 12 (3), 4.
- [7] Radiation Chemistry - Principles and Applications, (1987). Farhataziz and M. A. J. Rodgers, Eds., VCH Publishers, Chap. 20.
- [8] A. Chapiro, (1962). Radiation Chemistry of Polymeric Systems, Wiley-Interscience.
- [9] Radiation Chemistry of Hydrocarbons (1981). G. Foldiak, Ed., Elsevier.
- [10] N. Kimura and s. takamuku, (1985). Radiat. Phys. Chem., 29 (3), 179.
- [11] Y. Tabata, (1985). Conf. Proc. Radcure, Basel, Switz..
- [12] S. A. MacDonald, H. Ito and C. G. Wilson, (1983). Microelectro. Eng., 1, 269.
- [13] J. W. Labadie, S. A. MacDonald and C. G. Wilson, (1986). J. Imaging Sci., 30 (4), 169.



- [14] M. C. Henry and W. Davidsohn, (1972). Organotin Compounds, A. K. Sawyer, Ed., Dekker.
- [15] R. V. Subramanian and B. K. Garg, (1978). Polym. Plast. Technol. Eng., 11, 81.
- [16] P. Smith and L. Smith, (1975). Chemistry in Britain, 11, 208.
- [17] R. Okawara and M. Wada, (1971). organotin Compounds, A. K. Sawyer, Ed., Dekker.
- [18] A.G. Davies and P. J. Smith, (1982). Comprehensive Organometallic Chemistry, G. Wilkinson, F. G. A. Stone and E. W. Abel, Eds., Pergamon Press.
- [19] J. C. Montermoso, T. M. Andrews and L. P. Marinelli, (1958). J. Polym. Sci., 32 (125), 523.
- [20] W. Mc Farlane and R. J. Wood, (1972). J. Organomet. Chem. 40, C17.
- [21] P. B. Simons and W. A. Graham, (1967). J. Organomet. Chem., 8, 479.
- [22] Y. Maeda and R. Okowara, (1867). J. Organomet. Chem., 10, 247.
- [23] D. L. Alleston, A. G. Davies, M, Hancock and R. F. M. White, (1963). J. Chem. Soc., 5469.
- [24] A. G. Davies, L. Smith and P. J. Smith, (1972). J. Organometal. Chem., 39, 279.
- [25] A. G. Davies, (1976). Adv. Chem. Ser., 157, 26.
- [26] A. G. Davies, B. P. Roberts and M. W. Tse, (1978). J. Chem. Soc., Perkin Trans., 2, 145.
- [27] R. V. Lloyd and M. T. Rodgers, (1978). J. A. C. S., 95 (8), 2459.

- [28] G. Plews and R. J. Phillips, (1979). J. Coatings Technol., 51, 69.
- [29] R. T. Conley, (1972). Infrared spectroscopy, 2nd Ed., Allyn and Bacon.
- [30] Handbook of Chemical and Physics, Handbook of Chemistry and Physics, Chemical Rubber Co., 47th Ed..
- [31] S. Paul, (1985). Surface Coatings Science and Technology, Wiley-Interscience.
- [32] V. Oakes and R. E. Hutton, (1965). J. Organometal. Chem., 3, 472.



UNIVERSITY OF WISCONSIN LIBRARY MAR 20 1968

CHAPTER 4

UV AND ELECTRON BEAM

INDUCED POLYMERISATION OF

SILICON CONTAINING ACRYLATES

UNIVERSITY OF WISCONSIN LIBRARY MAR 20 1968



Chapter 4 **ELECTRON BEAM AND UV INDUCED POLYMERISATION OF  
SILICON CONTAINING ACRYLATES**

Introduction	150
Results and Discussion	156
a) Electron beam induced polymerisation of silicon containing acrylates	156
b) UV induced polymerisation of silicon containing acrylates	167
Conclusion	175
Acknowledgements	176
Experimental	177
Appendix A	195
Appendix B	201
References	207

# ELECTRON BEAM AND UV INDUCED POLYMERISATION OF SILICON CONTAINING ACRYLATES

## Introduction

Radiation curing by means of both electron beam and UV irradiation has been exploited and gained wide acceptance in the surface coatings industry [1-3]. The growth of this industry may in part be ascribed to the development of diluents and prepolymers containing the acrylate functionality. It is also recognised that analogous methacrylated monomers and prepolymers may be produced and although it is known that these resins are of lower reactivity than their acrylate counterparts, their reduced toxicological ratings often favour the use of these materials [1].

The 'ubiquitous' application of acrylate systems may be primarily attributed to their low cost, high reactivity, low volatility and good film forming properties [1-3]. Use of such highly sensitive UV and electron beam formulations will result in the rapid formation of a polymer film. While those parameters pertaining to the utilisation of incident radiation to generate radical species capable of promoting polymerisation must not be overlooked (see chapter 1 and 3), systems characterised by exceedingly high cure rates will result in the formation of a cured film primarily governed by the structure and functionality of the radiation curable components.

Mono(meth)acrylates can polymerise to give linear



polymers, whereas polyfunctionalised (meth)acrylates will produce a crosslinked network which will be inherently harder and more rigid than for a system comprising of monoacrylates.

Oraby and Walsh [4] proposed that the initial high reaction rates associated with polyfunctional viscous oligomers resulting in rapid gelation was due to a decrease in termination reactions arising from radical radical recombination or disproportionation. These workers also noticed that the observed initial high reaction rates was greatest for low molecular weight oligomers due to the high concentration of the double bonds. However, on decreasing the molecular weight of the oligomer one may forfeit initial high cure rates for incomplete consumption of double bonds. This situation may arise as a result of yielding a film of reduced conformational mobility thereby retarding the polymerisation process with the advanced degree of overall reaction rate. The formation of such highly crosslinked films may concurrently result in film shrinkage and ultimately poor adhesion to the substrate and brittleness.

Radiation curable silicones consist of a silicone backbone which has been subsequently modified by acrylate functionality thus enabling such oligomers to be incorporated into radiation curable systems. This class of reactive prepolymer has received recent attention for potential application as adhesive coating materials [5] or as a component of magnetic recording medium [6]. The obvious advantage of incorporating acrylate functionality into a



silicone is primarily to improve compatibility of the silicone towards radiation curable formulations, as well as enabling the prepolymer to become bound into the polymer matrix.

The effects of  $\gamma$  and electron beam irradiation on polysiloxanes e.g. polydimethylsiloxane, polydiphenylsiloxane and polymethylphenylsiloxane have been studied. Main chain scission of these materials has been shown to be negligible [7], while crosslinking reactions have been observed to occur. A detailed investigation of electron beam and radiolysis of polydimethylsiloxane has been shown to render crosslinks of the type  $\equiv\text{Si-Si}\equiv$ ,  $\equiv\text{Si-CH}_2\text{-CH}_2\text{-Si}\equiv$  and  $\equiv\text{Si-CH}_2\text{-Si}\equiv$  [7]. The reduced crosslinking reaction and gas evolution of polymethylphenylsiloxane and polydiphenylsiloxane compared with polydimethylsiloxane have been attributed to the protective action of the aromatic group [7].

The silicone resins are characterised by their outstanding thermal stability attributable to their relative high bond strengths (see Table 1) and their hydrophobic nature arising from the sheath of organo- substituents encasing the polymer backbone.

Table 1 Bond energies of various carbon and silicon bonds[8]

Bond	Bond energy $\text{kJ/mol}^{-1}$	Bond	Bond energy $\text{kJ/mol}^{-1}$
Si-O	444	Si-C	318
C-H	414	Si-H	318
C-O	360	Si-Si	222
C-C	348		

Table 2 The diluents to be tested using  
electron beam radiation

Compound	Acronym
$\text{Si}(\text{OCH}_2\text{CH}_2\text{OCOCH}=\text{CH}_2)_4$	STEA *
$\text{C}_6\text{H}_5\text{CH}_2\text{Si}(\text{OCH}_2\text{CH}_2\text{OCOCH}=\text{CH}_2)_3$	BSTEА *
$4\text{-ClC}_6\text{H}_4\text{CH}_2\text{Si}(\text{OCH}_2\text{CH}_2\text{OCOCH}=\text{CH}_2)_3$	CBSTEА
$(\text{C}_6\text{H}_5)_2\text{CHSi}(\text{OCH}_2\text{CH}_2\text{OCOCH}=\text{CH}_2)_3$	BHSTEА
$\text{C}_{12}\text{H}_{25}\text{Si}(\text{OCH}_2\text{CH}_2\text{OCOCH}=\text{CH}_2)_3$	DSTEА *
$\text{CH}_3\text{Si}(\text{OCH}_2\text{CH}_2\text{OCOCH}=\text{CH}_2)_3$	MSTEА *
$\text{C}_{18}\text{H}_{37}\text{Si}(\text{OCH}_2\text{CH}_2\text{OCOCH}=\text{CH}_2)_3$	ODSTEА
$\text{C}_8\text{H}_{17}\text{Si}(\text{OCH}_2\text{CH}_2\text{OCOCH}=\text{CH}_2)_3$	OSTEА *
$\text{C}_6\text{H}_5\text{Si}(\text{OCH}_2\text{CH}_2\text{OCOCH}=\text{CH}_2)_3$	PSTEА *
$\text{CH}_2=\text{CHSi}(\text{OCH}_2\text{CH}_2\text{OCOCH}=\text{CH}_2)_3$	VSTEА
$(\text{CH}_3)_2\text{Si}(\text{OCH}_2\text{CH}_2\text{OCOCH}=\text{CH}_2)_2$	DMSDEА
$(\text{C}_6\text{H}_5)_2\text{Si}(\text{OCH}_2\text{CH}_2\text{OCOCH}=\text{CH}_2)_2$	DPSDEА *
$\text{CH}_3(\text{C}_6\text{H}_5)\text{Si}(\text{OCH}_2\text{CH}_2\text{OCOCH}=\text{CH}_2)_2$	MPSTEА *
$\text{Si}\{[\text{O}(\text{CH}_2)_5\text{CO}]_2\text{OCH}_2\text{CH}_2\text{OCOCH}=\text{CH}_2\}_4$	STT
$\text{C}_6\text{H}_5\text{CH}_2\text{Si}\{[\text{O}(\text{CH}_2)_5\text{CO}]_2\text{OCH}_2\text{CH}_2\text{OCOCH}=\text{CH}_2\}_3$	BSTT
$\text{CH}_3\text{Si}\{[\text{O}(\text{CH}_2)_5\text{CO}]_2\text{OCH}_2\text{CH}_2\text{OCOCH}=\text{CH}_2\}_3$	MSTT *
$\text{C}_6\text{H}_5\text{Si}\{[\text{O}(\text{CH}_2)_5\text{CO}]_2\text{OCH}_2\text{CH}_2\text{OCOCH}=\text{CH}_2\}_3$	PSTT *
$(\text{C}_6\text{H}_5)_2\text{Si}\{[\text{O}(\text{CH}_2)_5\text{CO}]_2\text{OCH}_2\text{CH}_2\text{OCOCH}=\text{CH}_2\}_2$	DPSTT
$\text{CH}_2=\text{CHCO}_2[\text{CH}_2\text{CH}(\text{CH}_3)\text{O}]_3\text{COCH}=\text{CH}_2$	TPGDA
$\text{CH}_2=\text{CHCO}_2(\text{CH}_2)_6\text{OCOCH}=\text{CH}_2$	HDDA
$\text{CH}_3\text{CH}_2\text{C}(\text{CH}_2\text{OCOCH}=\text{CH}_2)_3$	TMPTA

\* = selected diluents

In this chapter the electron beam curing of a number of silicon containing acrylates shown in Table 2 were investigated. The cure response of these materials was initially measured in terms of minimum dose of radiation required to obtain a tackfree coating to the touch. The cure response of selected silicon containing acrylates were evaluated by such physical test methods as the solvent rub, pencil hardness and brittleness tests.

The effect of structure and functionality of such silicon containing acrylates listed in Table 3 was also investigated and assessed in terms of gel content and consumption of double bonds as measured by FTIR.

Table 3 Silicon containing acrylates and commercial diluents to be compared in terms of structure and functionality

$\text{CH}_3\text{Si}(\text{OCH}_2\text{CH}_2\text{OCOCH}=\text{CH}_2)_3$	MSTEA
$(\text{CH}_3)_2\text{Si}(\text{OCH}_2\text{CH}_2\text{OCOCH}=\text{CH}_2)_2$	DMSDEA
$(\text{CH}_3)_3\text{SiOCH}_2\text{CH}_2\text{OCOCH}=\text{CH}_2$	TMSEA
$\text{HOCH}_2\text{CH}_2\text{OCOCH}=\text{CH}_2$	2-HEA
$\text{CH}_3\text{Si}(\text{OCH}_2\text{CH}_2\text{CH}_2\text{CH}_2\text{OCOCH}=\text{CH}_2)_3$	MSTBA
$(\text{CH}_3)_2\text{Si}(\text{OCH}_2\text{CH}_2\text{CH}_2\text{CH}_2\text{OCOCH}=\text{CH}_2)_2$	DMSDBA
$(\text{CH}_3)_3\text{SiOCH}_2\text{CH}_2\text{CH}_2\text{CH}_2\text{OCOCH}=\text{CH}_2$	TMSBA
$\text{HOCH}_2\text{CH}_2\text{CH}_2\text{CH}_2\text{OCOCH}=\text{CH}_2$	4-HBA
$\text{CH}_2=\text{CHCO}_2[\text{CH}_2\text{CH}(\text{CH}_3)\text{O}]_3\text{COCH}=\text{CH}_2$	TPGDA
$\text{CH}_3\text{CH}_2\text{C}(\text{CH}_2\text{OCOCH}=\text{CH}_2)_3$	TMPTA



The UV curing of a number of silicon containing acrylates and methacrylates (see Table 4) compared with standard diluents using 2-hydroxy-2,2-dimethylacetophenone (Darocure <sup>®</sup> 1173) as photoinitiator is also reported here. Cure speeds were established in terms of the number of passes required to produce a tackfree to the touch film. Cured films were subsequently assessed by use of standard physical test methods as well as by infrared measurement of double bond consumption.

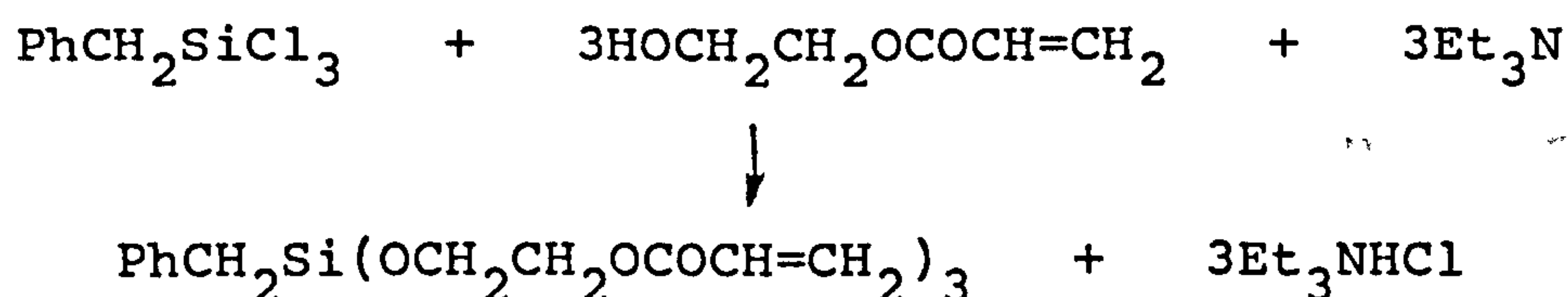
Table 4 UV curing of silicon containing acrylates and methacrylates compared with commercial diluents

$C_6H_5CH_2Si(OCH_2CH_2OCOCH=CH_2)_3$	BSTEA
$C_6H_5CH_2Si[OCH_2CH_2OCOC(CH_3)=CH_2]_3$	BSTEMA
$(C_6H_5)_2CHSi(OCH_2CH_2OCOCH=CH_2)_3$	BHSTEA
$(C_6H_5)_2CHSi[OCH_2CH_2OCOC(CH_3)=CH_2]_3$	BHSTEMA
$C_{12}H_{25}Si(OCH_2CH_2OCOCH=CH_2)_3$	DSTEA
$CH_3Si(OCH_2CH_2OCOCH=CH_2)_3$	MSTEA
$C_6H_5Si(OCH_2CH_2OCOCH=CH_2)_3$	PSTEA
$C_6H_5Si[OCH_2CH_2OCOC(CH_3)=CH_2]_3$	PSTEMA
$(C_6H_5)_2Si(OCH_2CH_2OCOCH=CH_2)_2$	DPSTEA
$(C_6H_5)_2Si[OCH_2CH_2OCOC(CH_3)=CH_2]_2$	DPSTEMA
$(C_6H_5)_2Si(OCH_2CH_2CH_2CH_2OCOCH=CH_2)_2$	DPSDBA
$CH_2=CHSi(OCH_2CH_2OCOCH=CH_2)_3$	VSTEA
$CH_2=CHCO_2[CH_2CH(CH_3)O]_3COCH=CH_2$	TPGDA
$CH_2=CHCO_2(CH_2)_6OCOCH=CH_2$	HDDA
$CH_3CH_2C(CH_2OCOCH=CH_2)_3$	TMPTA
$CH_2=C(CH_3)CO_2(CH_2)_6OCOC(CH_3)=CH_2$	HDDMA
$CH_3CH_2C[CH_2OCOC(CH_3)=CH_2]_3$	TMPTMA

## RESULTS AND DISCUSSION

### a) Electron beam induced polymerisation of silicon containing acrylates

The new silicon containing acrylates were prepared by reaction of a hydroxymonoacrylate with the appropriate silyl chloride in the presence of base [9,10], e.g.,



The silicon containing diluents listed in Table 2 were all prepared by this method and were found to render tackfree films at the low dose of radiation of 2.5kGy. A comparison of the cure response of selected tetra-, tri-, and di-functional silicon containing acrylates indicated in Table 2, with three commercial diluents was investigated. The three commercial diluents chosen were two difunctional monomers, hexanediol diacrylate HDDA and tripropyleneglycol diacrylate TPGDA, and a trifunctional monomer trimethylolpropane triacrylate TMPTA. The cure performance of these selected diluents were assessed in terms of their solvent resistance, pencil hardness and brittleness. The results of these tests are shown in Tables 5-16 in Appendix A.

The effect of the structure and functionality of those silicon based diluents listed in Table 3 on cure response was also examined and measured in terms of gel content of cured films (see Table 17). The cured films were

subsequently analysed using FTIR to assess the percentage residual unsaturation. The absorption doublet at  $1640/1620\text{cm}^{-1}$  due to the carbon carbon double bond stretch and  $810\text{cm}^{-1}$  overtone frequency respectively, was used to monitor residual unsaturation. The carbonyl stretch at  $1730\text{cm}^{-1}$  was chosen as an internal standard for all calculations (see Chapter 2). The results of these measurements are summarised in Figures 1 and 2.

The commercially available tetraacrylate, pentaerythritol tetraacrylate PETA, is known to be a very reactive diluent and forms a very brittle highly crosslinked network [1-3]. The tetraacrylate tetakis(2-hydroxyethyl)silane, tetraacrylate ester STEA, was observed to cure at the low dose of  $0.5\text{kGy}$  and readily formed a highly crosslinked polymer film, as indicated by its solvent resistance shown in Table 16. The presence of electropositive silicon atoms might be expected to lead to dipole interactions with neighbouring chains resulting in a brittle and rigid polymer coating. However, contrary to PETA, polymer films of STEA resulted in highly flexible coatings as indicated by their low brittleness ratings. Although both compounds are tetrafunctional, the flexibility exhibited by cured films of STEA may be accounted for in terms of its greater molecular weight and hence lower acrylate concentration, thus producing a coating inherently more flexible as a result of reduced crosslink density. The flexibility of these materials may also be due to the large Si-O-Si bond angle



which permits very free rotation about the Si-O bond, thus close packing and hence the formation of a rigid structure is not possible. It may also be perceived that the complete utilisation of all double bonds in PETA is not possible at moderate doses of radiation due to the rapid decrease in mobility of residual acrylate functionality preventing the maximum possible crosslink density. Conversely, STEA would be expected to utilise a greater number of its acrylate groups on account of the molecular conformations possible about its central silicon atom.

The triacrylated silicon containing compounds:-  
tris(2-hydroxyethyl)phenylsilane, triacrylate ester PSTEA,  
benzyltris(2-hydroxyethyl)silane, triacrylate ester BSTEA,  
tris(2-hydroxyethyl)methylsilane, triacrylate ester MSTEA,  
and tris(2-hydroxyethyl)octylsilane, triacrylate ester OSTEAs rendered tackfree films at doses of radiation less than the minimum dose of radiation required to cure TPGDA, HDDA, TMPTA and 2-HEA. The ability of these silicon trifunctional monomers to yield tackfree films at low doses of radiation indicates that these materials readily crosslink under electron beam irradiation.

Physical tests such as solvent rub, pencil hardness and brittleness were used to assess the relative crosslink density of these films. It is important to compare such test data of films of similar coatweights. Uniform film thickness for the materials investigated here was difficult to achieve, primarily due to the use of an electron beam curing unit more suited for production use than for small scale

scientific experiments. Variation in viscosity and the rheology of these materials also contributed to inconsistent coatweights. Therefore, the physical test data collated in Tables 5-15 in Appendix A can at best indicate some general trends of the cured films investigated.

TMPTA produces severely<sup>e</sup> reticulated films and hence could not be tested for solvent resistance or pencil hardness. The performance of the trifunctional silicon containing compounds was thus compared with two difunctional materials HDDA and TPGDA. Comparison of physical test results for TPGDA and HDDA shown in Tables 5 and 6 respectively with those for PSTEA, BSTEA, MSTEA and OSTEa (collated in Tables 7-10), suggest that the latter group of materials are of comparable if not slightly higher crosslink density as indicated by their similar or improved solvent rub resistance and pencil hardness. It was also noticed that the trifunctional acrylate TMPTA produces very brittle films, while both TPGDA and HDDA produced coatings of moderate flexibility, however, the trifunctional silicon acrylates, PSTEA, BSTEA, MSTEA and OSTEa all rendered hard but very flexible films.

The similar or enhanced solvent rub resistance displayed by the above silicon containing diluents compared with HDDA and TPGDA may be ascribed to the increased functionality of the former class of compounds. However, the superior flexibility of the silicon diluents might be once again interpreted on account of the greater degree of freedom of those groups attached to the silicon atom.



The difunctional acrylates bis(2-hydroxyethyl)silane, diacrylate ester DPSDEA and bis(2-hydroxyethyl)methylphenylsilane, diacrylate ester MPSDEA also rendered tackfree films at doses of radiation below that required to cure the standard commercial diluents and once again would indicate that these materials readily crosslink under electron beam radiation. However, the solvent resistance and pencil hardness of these films as shown in Tables 12 and 13 do not exhibit superior test results compared with HDDA or TPGDA, and presumably reflect the lower crosslink density of these silicon containing materials.

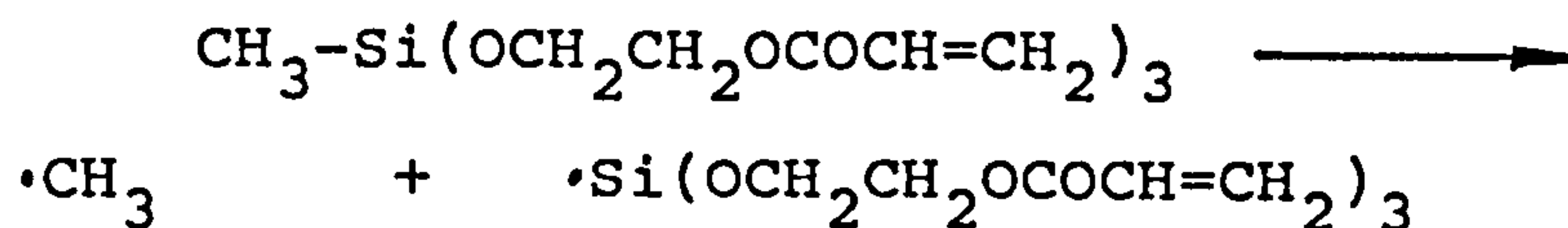
Examination of Tables 7 and 12 shows that PSTEA and DPSTEA produce films of enhanced and comparable solvent resistance respectively compared with TPGDA and HDDA. The improved solvent resistance of PSTEA may be attributed to the that compound being a trifunctional acrylate whereas DPSDEA and the two commercial diluents are all difunctional. It is generally accepted that increasing the functionality of a material will lead to the production of a polymer matrix of increased crosslink density, as reflected by its solvent resistance. The observed result that PSTEA exhibits improved solvent compared with DPSDEA, TPGDA and HDDA collaborates this explanation.

It was also noted that both MSTT and PSTT (see tables 14 and 15) exhibited poor solvent resistance compared with MSTEA and PSTEA. This may be explained in terms of the increase in size of the groups attached to the central silicon atom. Presumably, increasing the size of the



attached groups will lead to a decrease in the density of the polymer formed and hence the low solvent rub resistance reflects the more open structure of these films as well as the solubility of the ester chain between the silicon atom and the acrylate group.

It has been demonstrated that the silicon based diluents all showed superior reactivity, in terms of minimum dose required to produce a tackfree coating compared with HDDA, TPGDA and TMPTA. This noticeable enhanced reactivity may be attributable to the homolysis of the C-Si bonds whose approximate average bond energy is  $318\text{kJmol}^{-1}$  [8] generating silicon and carbon centred radicals capable of crosslinking or initiating polymerisation



This is consistent with those results obtained by Miller [7,11] who showed that homolysis of C-Si bonds in polydimethylsiloxane occurs on electron beam and gamma radiolysis.

However, the greater reactivity shown by the silicon containing diluents may also be attributed to the basic star shaped structure about a silicon nucleus of these compounds. This may indicate the importance of the large number of molecular conformations possible about the central silicon atom thus enabling greater mobility of the reactive

sites required to give a high crosslink density.

The effect of the structure and molecular weight of several silicon containing diluents was investigated and evaluated in terms of the gel content and consumption of

Table 17 Gel content of ten diluents irradiated at 20 kGy

Compound	Percentage gel
MSTEA	84
DMSDEA	63
TMSEA	0
2-HEA	76
MSTBA	82
DMSDBA	52
TMSBA	0
4-HBA	66
TPGDA	79
TMPTA	85
Blank	2

double bonds of the resultant polymer films for the series of diluents listed in Table 3.

These ten diluents were all irradiated at 20kGy and the gel content of the cured materials were measured and are collated in Table 17.

Both groups of silicon containing diluents derived from 2-hydroxyethyl acrylate, 2-HEA and 4-hydroxybutylacrylate,

4-HBA are of similar acrylate content, however, the functionality increases from 1 to 3 in both cases. It was therefore predicted the the gel content of the irradiated films would increase with a concomitant increase in functionality and indeed from examination of Table 5, this was found to be the case for both series. The gel content of both the triacrylates MSTEA and MSTBA were of comparable magnitude to that obtained for the commercial triacrylate TMPTA. However, the gel content of the diacrylates DMSDEA and DMSDBA was markedly less than for TPGDA. This may indicate that the crosslink density of both DMSDEA and DMSDBA is less than for TPGDA or that the former materials produce a more open polymer network enabling dissolution of the polymer film to occur more readily.

Both monofunctional silicon containing diluents TMSEA and TMSBA resulted in wet coatings, contrary to 2-HEA and 4-HBA which were observed to yield tackfree films at the low dose of 2.5kGy. The poor film forming properties of TMSEA and TMSBA may be ascribed to the inability of these compounds to form hydrogen bonds thus adopting a less ordered packing structure compared with both 2-HEA and 4-HBA. It was also noticed that 2-HEA and the silicon diluents based on this hydroxymonoacrylate resulted in films of greater gel content than their counterparts based on 4-HBA. Once again this may reflect the higher crosslink density of the series based on 2-HEA compared with those based on 4-HBA.

Figure 1 shows the percentage degree of cure of TMPTA,

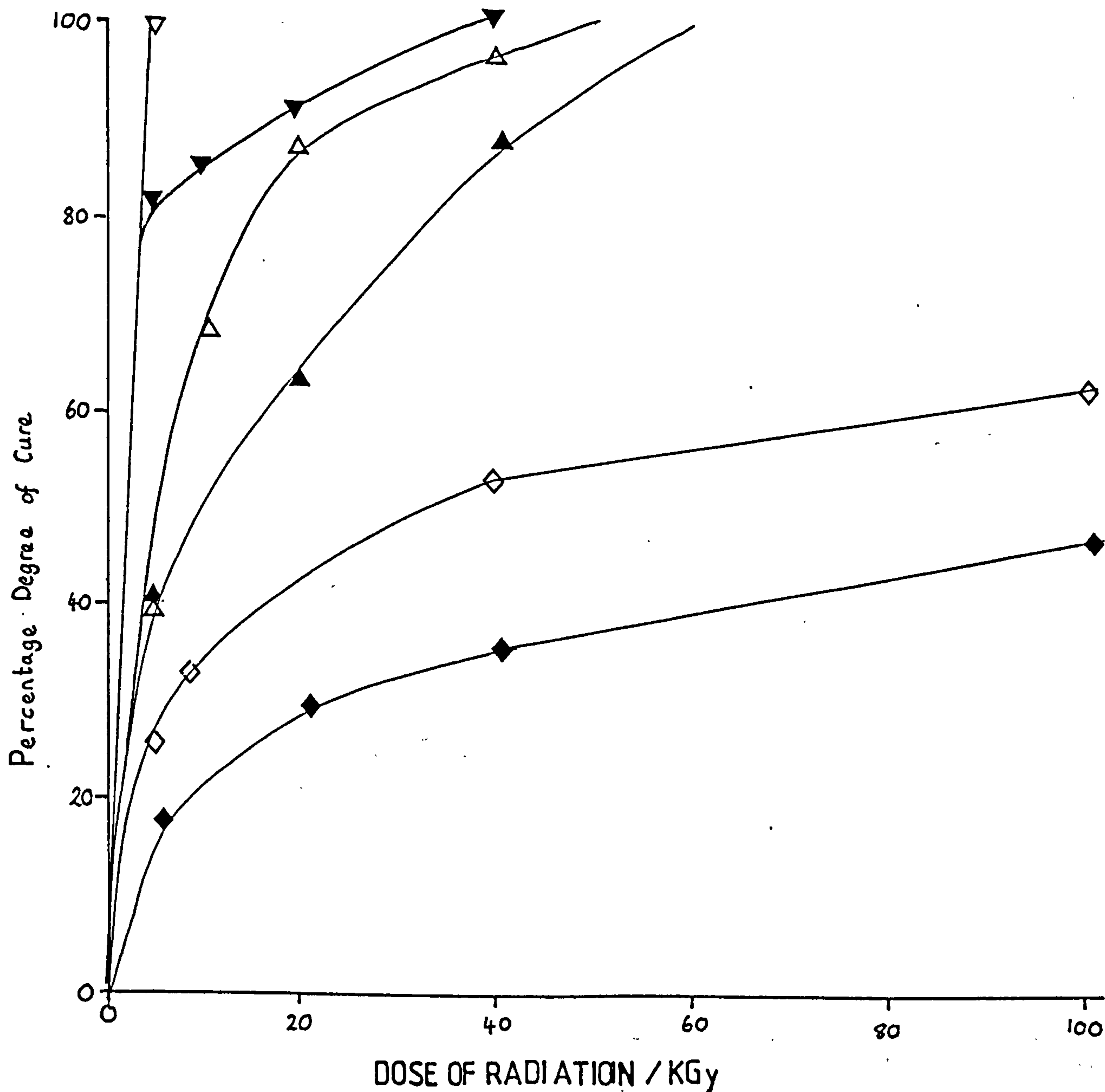


TPGDA, 2-HEA, TMSEA, DMSDEA and MSTEA. All curves show rapid initial consumption of double bonds which levels off as the dose of radiation increases. The order in terms of double bond consumption was observed to be

2-HEA > DMSDEA > TPGDA > MSTEA > TMPTA > TMSEA

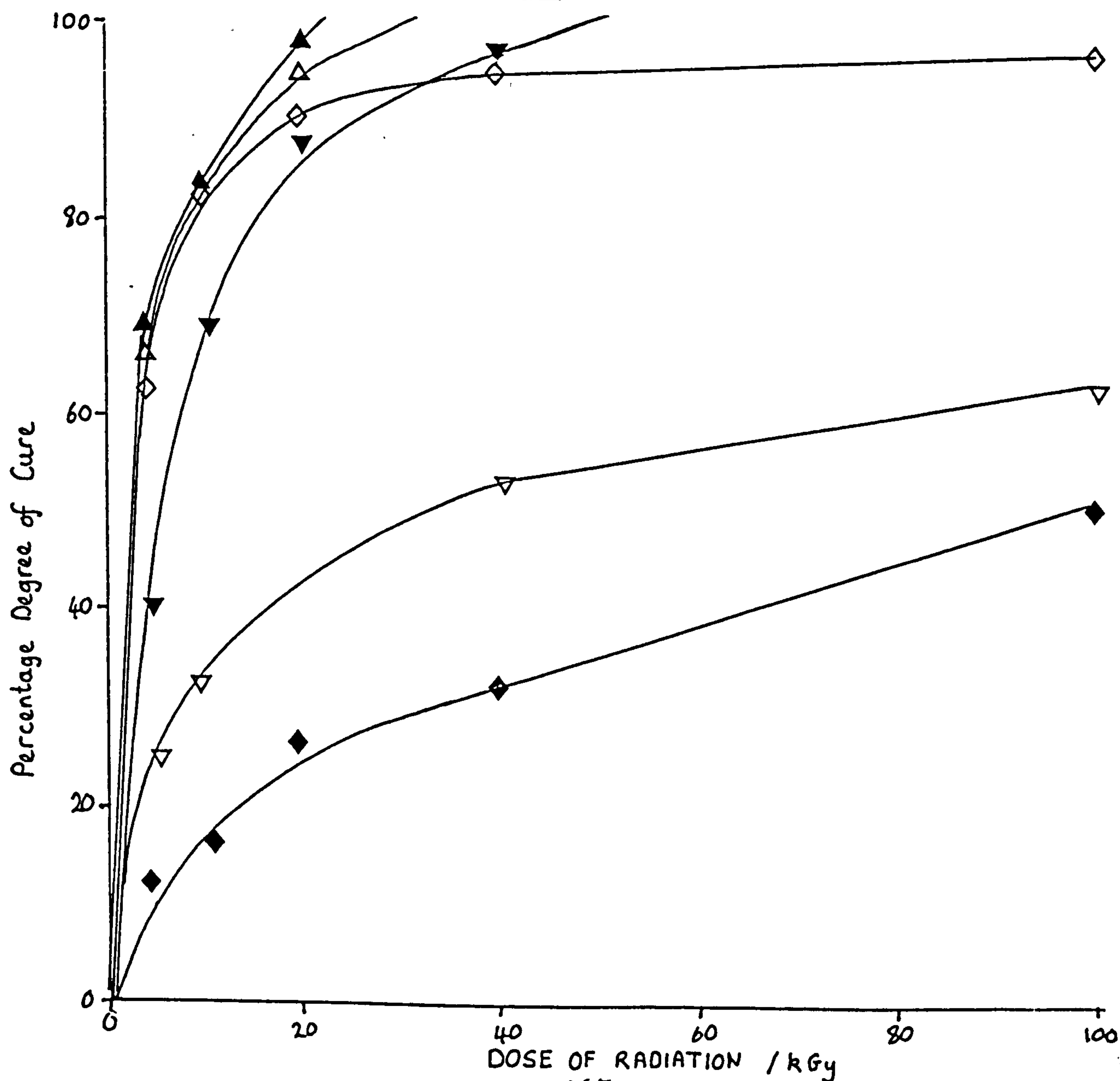
This would indicate, with the exception of TMSEA, that by increasing functionality one restricts the mobility of the

Figure 1 Percentage degree of cure of 2-HEA ( $\nabla$ ), TMSEA ( $\blacklozenge$ ), DMSDEA ( $\blacktriangledown$ ), MSTEA ( $\blacktriangle$ ), TPGDA ( $\triangle$ ) and TMPTA ( $\diamond$ ) cured at various doses of radiation.



double bonds with the advancement of the cure process. The low reactivity shown by TMSEA is consistent with the inability of this material to form a tackfree coating and once again may reflect the lack of attaining a favourable packing arrangement enabling the promotion of polymerisation. Figure 2 also confirms the greater reactivity of both DMSDEA and MSTEA compared with their commercial counterparts TPGDA and TMPTA respectively. As mentioned previously this may either reflect homolysis of C-Si bonds

Figure 2 Percentage degree of cure of 4-HBA ( $\blacktriangle$ ), DMSDBA ( $\triangle$ ), MSTBA ( $\diamond$ ), TPGDA ( $\blacktriangledown$ ), TMPTA ( $\nabla$ ) and TMSBA ( $\blacklozenge$ ) cured at various doses of radiation.



to create silicon and carbon centred radicals capable of promoting polymerisation or a more open mobile structure thus enhancing the extent of double bond consumption.

Figure 2 depicts the residual unsaturation of those silicon containing diluents based on 4-HBA compared with TMPTA and TPGDA. The order in terms of double bond consumption was observed to be



Once again the low reactivity of TMSBA, as with TMSEA, may be attributed to an unfavourable packing arrangement of this compound due to the lack of hydrogen bonding. Differentiation between residual unsaturation for 4-HBA, DMSDBA and MSTBA for a given dose of radiation is small and probably is not significant. This would indicate that for both DMSDBA and MSTBA, the chain length between the central silicon atom and the acrylate group enables comparable mobility of the reactive sites with that of 4-HBA, resulting in similar high reaction rates for these compounds compared with TPGDA and TMPTA.



## b) UV induced polymerisation of silicon containing acrylates

The performance of the new acrylated silicon containing materials was compared with that of hexane-1,6-diol diacrylate HDDA, tripropyleneglycol diacrylate TPGDA and trimethylolpropane triacrylate TMPTA, while the cure response of the methacrylated silicon containing materials was compared with hexane-1,6-diol dimethacrylate and trimethylolpropane trimethacrylate. The samples were coated onto sheets of GNT paper using an automatic coating unit in conjunction with a no. 5 K bar to produce even coatweights of about  $12\text{gcm}^{-2}$  and subsequently passed under a Colordry medium pressure mercury lamp ( $80\text{Wcm}^{-1}$ ) on a conveyor belt. The speed of the belt was varied as well as the concentration of the photoinitiator (2-hydroxy-2-methyl-1-phenylpropane-1-one, Darocur <sup>®</sup> 1173) and the number of passes under the lamp to achieve a tackfree coating to the touch was determined. The results are shown in Tables 18 and 19 in Appendix B. Further testing of the films was carried out by examining the solvent resistance of selected films (Table 20).

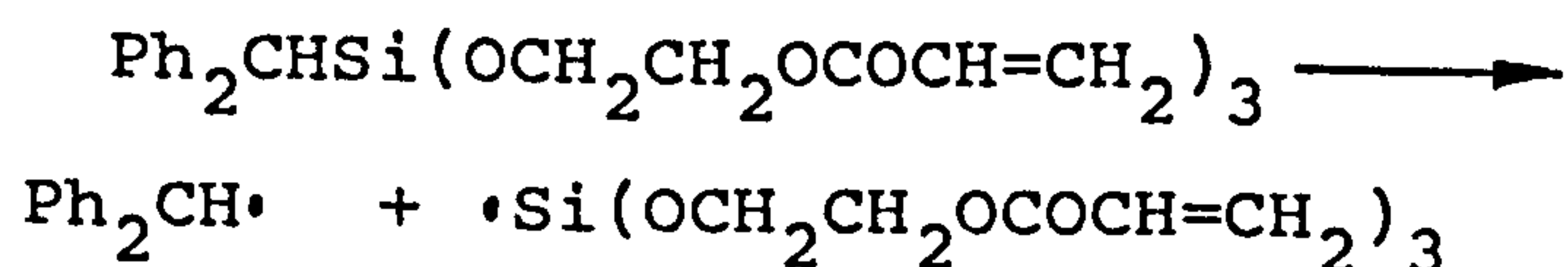
Since the silicon acrylates are often more reactive than materials such as TPGDA an investigation was then carried out to determine whether silicon containing methacrylates would cure at acceptable speeds (Table 21).

In order to compare the reactivity of the methacrylates with the acrylates, films of the materials were applied to potassium bromide discs then subjected to UV curing. The

results are presented in Figures 3 and 4.

Examination of Tables 18 and 19 in Appendix B shows that PSTEA, BSTEA, BHSTE and PSTT cure to give tackfree films faster than either TPGDA, HDDA and TMPTA. VSTE and DPDEA cured at comparable rates to TPGDA and TMPTA. The increase in reactivity, where observed, may be attributed to the compounds being trifunctional whereas two of the reference materials are difunctional. Certainly the greater the degree of functionality will lead to more rapid crosslinking and hence should lead to a more rapid attainment of a tackfree coating. The finding that DPSDEA cures more slowly than PSTEA is in agreement with this assumption. However, it should be noted that TMPTA, a tri-functional acrylate shows similar reactivity to TPGDA and HDDA, therefore the functionality of a diluent is only partly responsible for the greater reactivity of the trifunctional silicon containing compounds. The superior reactivity of these materials may also be due in part to the increased conformational mobility about the silicon atom which is required to give a high crosslink density.

The most reactive compound, in terms of yielding a tackfree coating, was shown to be benzhydryltris-(2-hydroxyethyl)silane, triacrylate ester (Table 19). This would indicate that reactions of the following type may occur.



Whether or not the stabilised benzhydryl radical can initiate polymerisation is not known. The reactivity of BSTEA may also be in part due to photoinduced homolysis of the benzyl silicon bond. The reactivity of this compound is similar to PSTEA in which homolysis of a silicon carbon bond is much less likely to occur.

One factor which must affect the film forming characteristics is the size of the groups attached to the

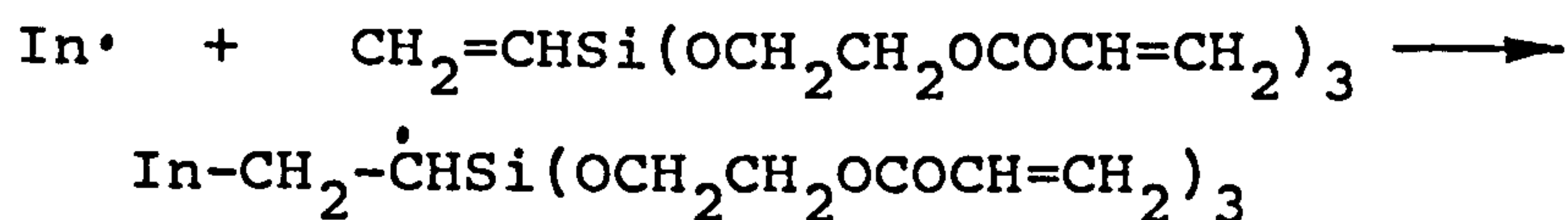
Table 20 Solvent rub test for UV cured films

Monomer	% Initiator	Belt speed m/min	No. of passes	No. of passes to cause failure in rub test
TPGDA	4	5	15	40
	6	10	17	15
HDDA	4	5	19	>500
	6	10	30	>500
DSTEa	4	5	20	90
	6	10	17	95
PSTEa	1	5	21	>500
	2	10	30	>500
	4	20	21	>500
	6	40	6	>500
BSTEA	1	5	20	>500
	2	10	14	>500
	4	20	26	>500
	6	40	8	>500



silicon atom. Presumably, increasing the size of the attached groups will lead to a decrease in the density of the polymer formed and as can be seen from Table 20 DSTEAs rendered films of very poor solvent resistance. Solvent resistance is partly a measure of the extent of crosslinking in the film but it is also affected by the solubility of the polymer backbone and pendant groups. Thus, the films produced by TPGDA which contain ether groups in the backbone has a poor solvent resistance. The low solvent resistance of DSTEAs no doubt reflects the more open structure of the film due to the presence of the dodecyl group and the solubilising effect that the latter group will have. Similarly the slow cure and poor solvent resistance of films produced for PSTT is probably due to both the more open structure of the film and the solubilising contribution of the ester groups.

The cure result which does not accord with the above rationale is the relatively low reactivity of the VSTEAs. With this compound there is the possibility that the vinyl group traps some of the initiating radicals to give a radical, which for steric reasons is inefficient at propagating polymerisation.



The silicon containing diluents rendered highly flexible coatings on UV irradiation, as was seen to be the case for

electron beam cured films. The superior flexibility of the silicon diluents might be once again interpreted in terms of the greater degree of freedom of those groups attached to the silicon atom as well as the slightly reduced acrylate concentration of these compounds compared with TMPTA or even HDDA.

Not suprisingly curing of the methacrylates to give

Table 21 Number of passes required under the UV lamp to produce a tackfree coating of methacrylates

Compound	Belt speed m/min	% Initiator			
		1	2	4	6
$\text{PhSi}(\text{OCH}_2\text{CH}_2\text{OCOC}(\text{Me})=\text{CH}_2)_3$	5	*	*	*	15 (12.0)
	10	*	*	*	28 (12.0)
	20	*	*	*	*
	40	*	*	*	*
$\text{PhCH}_2(\text{OCH}_2\text{CH}_2\text{OCOC}(\text{Me})=\text{CH}_2)_3$	5	*	*	*	16 (12.0)
	10	*	*	*	30 (12.0)
	20	*	*	*	*
	40	*	*	*	*

tackfree films (Table 21) was a much slower process than for the corresponding acrylates. Even the silicon materials were retarded to a considerable degree and the only satisfactory results were obtained with PSDEMA.

Following the rate of double bond consumption of the acrylates and methacrylates upon exposure to UV radiation in the presence of a photoinitiator proved to be very informative (Figure 3 and Figure 4). For all the acrylates one pass leads to a very high percentage of the double bonds available for consumption being utilised. If one takes 10 passes as leading to almost complete cure it can be seen that the number of residual double bonds is dependent upon the structure and the functionality of the diluent.

The order of initial cure rate and maximum consumption of double bonds was observed to be,

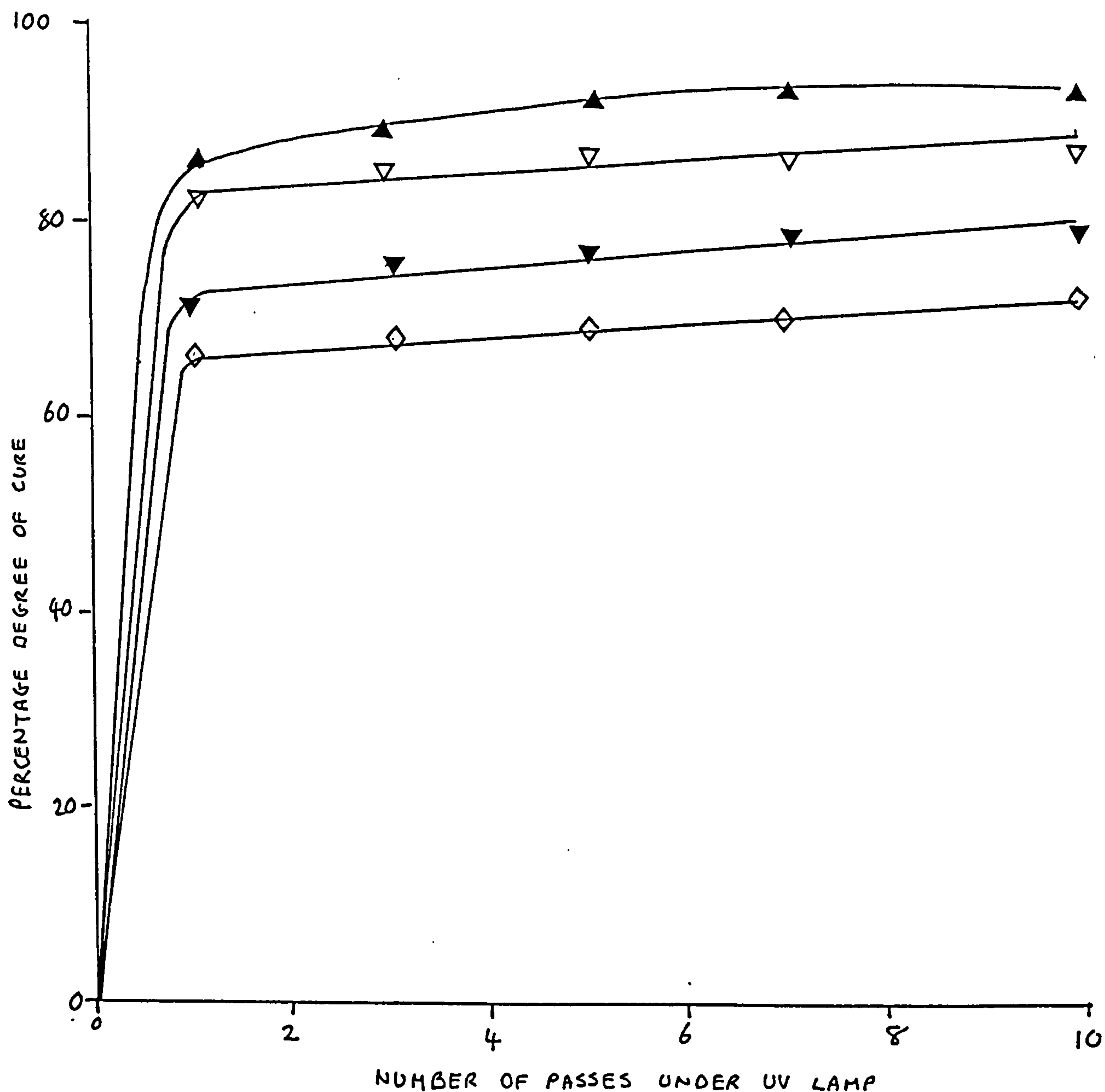


The order of reactivity of the silicon acrylates and TMPTA based on double bond consumption is different to the rate of cure to give a tackfree film (Table 18 and 19). In accord with previous work (also see Chapter 3), the diacrylates led to greater double bond consumption as well as faster initial cure rates upon irradiation compared with the triacrylates. The curing of BSTEA resulted in significantly less residual unsaturation compared with TMPTA. Once again these results would indicate that the silicon containing acrylates are able to render a greater number of molecular conformations about the silicon atom thus enabling greater mobility of the



reactive sites required to give a high crosslink density. Consequently, materials of reduced conformational mobility, give tackfree films which often contain high concentrations of unreacted double bonds.

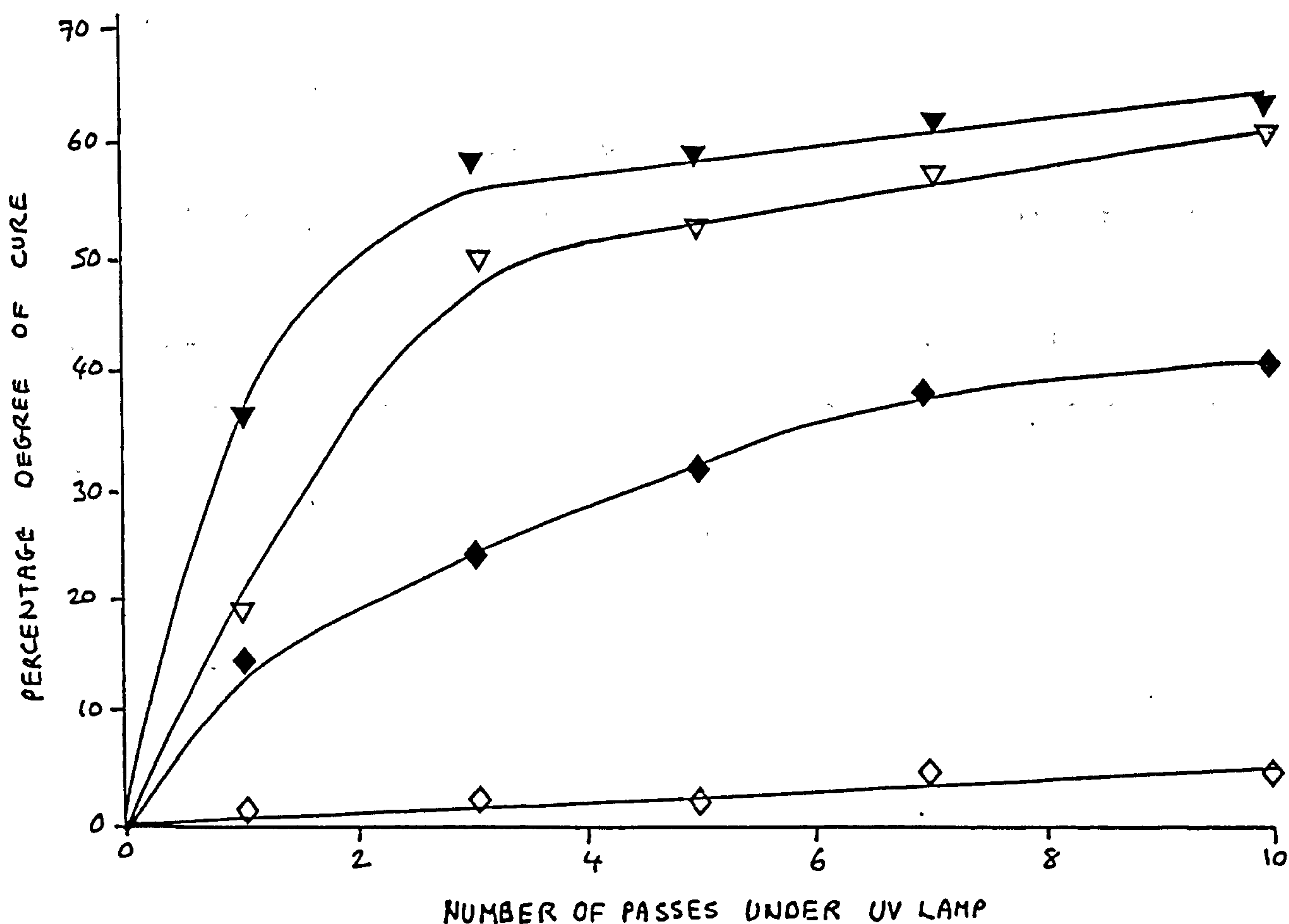
Figure 3 The percentage degree of cure of DPSDEA (▲), DPSDBA (▽), BSTEA (▼) and TMPTA (◇) upon UV irradiation



It will be noted that DPSBA showed<sup>a</sup> slightly lower rate of double bond consumption than DPSDEA. Further work using more carefully controlled conditions is required to confirm the reactivity order of these two closely related compounds.

UV induced polymerisation of the methacrylates led to

Figure 4 The percentage degree of cure of DPSDEMA (▼), BHSTEMA (▽), BSTEMA (◆) and TMPTMA (◇) upon UV irradiation



very slow double bond consumption thereby explaining why such materials require long exposure periods in order to give tackfree films (Figure 4). However the results show the greater reactivity of the silicon containing compounds as indicated by the following reactivity order for the methacrylated materials

DPSDEMA > BHSTEMA > BSTEMA > TMPTMA

### CONCLUSION

The above results show that electron beam and UV induced polymerisation of the silicon containing di-, tri- and tetra-acrylates give tackfree films more rapidly than commercially used di- and tri- acrylates. This may in part be due to the silicon containing acrylates acting as radical sources as a result of light induced carbon silicon bond cleavage but more importantly, the silicon atoms appears to allow more molecular conformations which are required to promote double bond consumption and maximum crosslink density.



## ACKNOWLEDGEMENTS

I would like to thank C. Malde at Wiggins Teape Research and Development Group for carrying out the physical tests presented here.

I would also like to thank S. Tudor who monitored the UV polymerisation of the silicon acrylates by infrared spectroscopy. The task of solvent extraction of polymer films by J. Abrahams is also gratefully acknowledged.

## EXPERIMENTAL

### Instrumentation

Electron beam curing was carried out using an Otto Durr ESH 150/130 electron beam unit under a nitrogen blanket. The operating voltage was maintained at 150kV and the beam current was adjusted for each applied dose.

UV curing of thin films was carried out using a Colordry UV curing unit. The medium pressure mercury lamp, ( $80\text{Wcm}^{-1}$  and 23cm in length) was situated 15cm above a moving belt which was calibrated in  $\text{mmmin}^{-1}$ .

Infrared spectra of prepared monomers, as well as films cured on a KBr disc were analysed using a Perkin Elmer Infrared spectrometer model no. 599.

Proton NMR spectra were obtained using a Jeol NMR spectrometer model no. JNH-MH-100 and referenced against TMS.

All elemental analyses were carried out using a Carlo Erba Strumentazione Elemental Analyzer Model 1106.

Analysis of films cured on an opaque substrate was obtained using a Digilab FTS-60 Fourier transform infrared spectrometer. The moving mirror velocity in the interferometer was  $0.16\text{cm}^{-1}$  and the spectra reported here were recorded at  $8\text{cm}^{-1}$  spectral resolution. Liquid samples were analysed using transmission infrared for 16 scans, while tackfree films were recorded using a Digilab photoacoustic detector for 4096 scans.

## Materials

### Resins and diluents

Tripropyleneglycol diacrylate, TPGDA (Cray Valley Products Ltd.), trimethylolpropane triacrylate, TMPTA (Cray Valley Products Ltd.), 1,4-butanediol diacrylate, BDDA (BASF), 1,4-butanediol monoacrylate, 4-HBA (BASF), 2-hydroxyethyl acrylate, 2-HEA (Fluka AG), hexanediol diacrylate, HDDA (Cray Valley Products Ltd.), hexanediol dimethacrylate, HDDMA (Cray Valley Products Ltd.), trimethylolpropane trimethacrylate, TMPTMA (Cray Valley Products Ltd.) and the caprolactone based acrylate, TONE-100 (Union Carbide) were all used as received.

### Chemicals for synthesis

Diethylether (BDH Chemicals Ltd.) was distilled from lithium aluminium hydride and stored over molecular sieves, 4Å.

Tetrahydrofuran (Rathburn Chemical Co.) HPLC grade was stabilised with hydroquinone (<0.025%).

The following commercial samples obtained from Aldrich Chemical Co. were used without further purification: benzyl chloride, 4-chlorobenzyl chloride, benzophenone, cyclohexyltrichlorosilane, dichlorodimethylsilane, dichloromethylphenylsilane, dichlorodiphenylsilane, 2-hydroxymethacrylate, methyltrichlorosilane, octadecyltrichlorosilane, octyltrichlorosilane, phenyltrichlorosilane, tetrachlorosilane, trichlorosilane, triethylamine, tri-n-propylamine.

The following commercial samples obtained from Fluka AG were used without further purification: dodecyltri-



chlorosilane, vinyltrichlorosilane.

Gateway natural tracing paper, GNT (Wiggins Teape Group Ltd.), aluminium foil, gauge 0.051mm (BDH Chemicals Ltd.) and polyester sheets (Wiggins Teape Group Ltd.) were all used as substrates for all coatings.

## Synthesis

### Benzyltrichlorosilane [12]

#### Method

Trichlorosilane (30.40ml;0.30moles) was added to a mixture of benzyl chloride (23.00ml;0.20moles) and tri-n-propylamine (38.11ml;0.20moles). The mixture was refluxed for 20 hour at 56-90° C. On addition of diethyl ether, tri-n-propylamine hydrogenchloride precipitated and was removed by filtration. The solvent was removed over a rotary evaporator. The crude product was distilled at 70° C at 3.0mmHg (Lit. [13], 213-214° C/760mmHg) and afforded the title compound in 60% yield .

### 4-Chlorobenzyltrichlorosilane [12]

#### Method

Trichlorosilane (30.40ml;0.30moles) was added to a mixture of p-chlorobenzylchloride (32.21g;0,20moles) and tri-n-propylamine (38.11ml;0.20moles). The mixture was refluxed for 20 hours at 140° C. On addition of diethyl ether tri-n-propylamine hydrogenchloride precipitated and was removed by filtration. The solvent was removed over a rotary evaporator. The crude product was distilled at 75° C/0.5mmHg

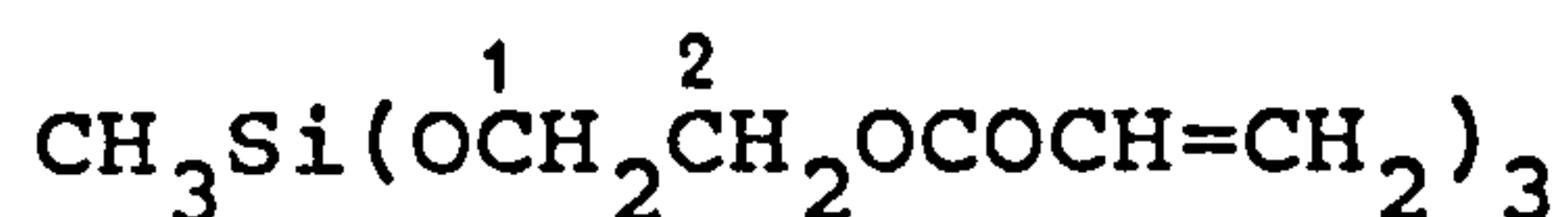
(Lit. [14], 80°C/10mmHg) and afforded the title product in 70 % yield.

### Benzhydryltrichlorosilane [15]

#### Method

Trichlorosilane (30.40ml;0.30moles) was added to a mixture of benzophenone (18.22g;0.10moles) and tri-n-propylamine. The mixture was refluxed for 1 hour at 55-75° C. On addition of pentane, tri-n-propylamine hydrogenchloride precipitated and was removed by filtration. The solvent was removed over a rotary evaporator. The crude product was distilled at 116° C at 0.5mm Hg (Lit. 141-145° C/2.5mmHg) and afforded the title product in 57% yield.

### Tris(2-hydroxyethyl)methylsilane, triacrylate ester (MSTEA)



#### Method

Trichloromethylsilane (3.50ml;0.03moles) diluted with dry diethyl ether (20ml) was slowly added to an ice cooled mixture of 2-hydroxyethylacrylate (10.34ml;0.09moles), triethylamine (12.55ml;0.09moles) and dry diethyl ether (200ml). The mixture was maintained at <5° C and stirred until the reaction was complete. The precipitate of triethylamine hydrogenchloride was filtered off and the solution was dried over anhydrous sodium sulphate. The solvent was removed by evaporation under reduced pressure to give a clear colourless liquid (Yield = 86%). Vacuum

distillation of the title compound resulted in decomposition of the product upon heating and therefore further purification of this material was not undertaken.

Infrared (Liquid film) : 3050, 3040, 3020, 2960, 1728, 1638, 1620, 1455, 1410, 1300, 1275, 1200, 1130, 1100, 1060, 970, 810cm<sup>-1</sup>.

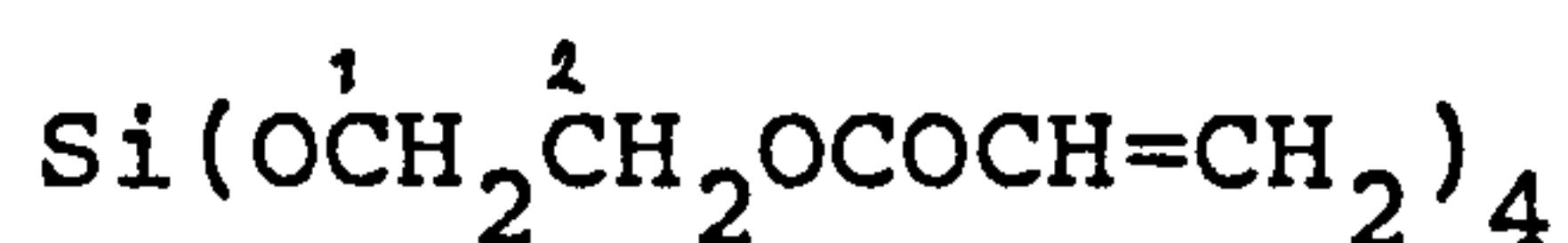
<sup>1</sup>H nmr (CDCl<sub>3</sub>) : δ 0.2 (singlet, 3H, methyl group), 3.90 (triplet, J=6Hz, 6H, CH<sub>2</sub> at C-1), 4.2 (triplet, J=6Hz, 6H, CH<sub>2</sub> at C-2), (5.70-6.50) (multiplet, 9H, acrylate group)

Analysis calculated for C<sub>16</sub>H<sub>24</sub>O<sub>9</sub>Si : C, 49.47; H, 6.23

Found : C, 49.40; H, 6.20.

The silicon containing diluents described forthwith were prepared in a similar way to that described above [9].

Tetrakis(2-hydroxyethoxy)silane, tetraacrylate ester (STEA)



Clear colourless liquid. (Yield = 84%)

Infrared (Liquid film) : 2960, 2890, 1640, 1620, 1410, 1300, 1275, 1200, 1130, 1105, 1065, 1040, 980, 850, 810, 670cm<sup>-1</sup>.

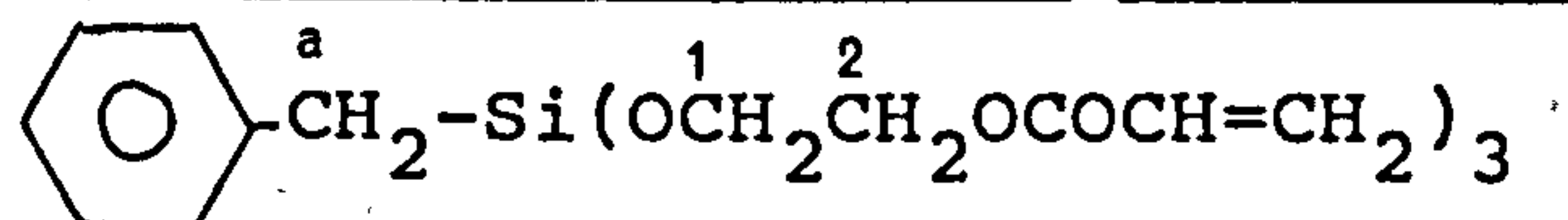
<sup>1</sup>H nmr (CDCl<sub>3</sub>) : δ 3.84 (triplet, J=6Hz, 8H, CH<sub>2</sub> at C-1), 4.08 (triplet, J=6Hz, 8H, CH<sub>2</sub> at C-2), (5.44-6.30) (multiplet, 12H, acrylate group).

Analysis calculated for C<sub>20</sub>H<sub>28</sub>O<sub>12</sub>Si : C, 49.17; H, 5.78

Found : C, 48.89 ; H, 5.92.



Benzyltris(2-hydroxyethoxy)silane, triacrylate ester (BSTEA)



Clear colourless liquid. (Yield = 79%)

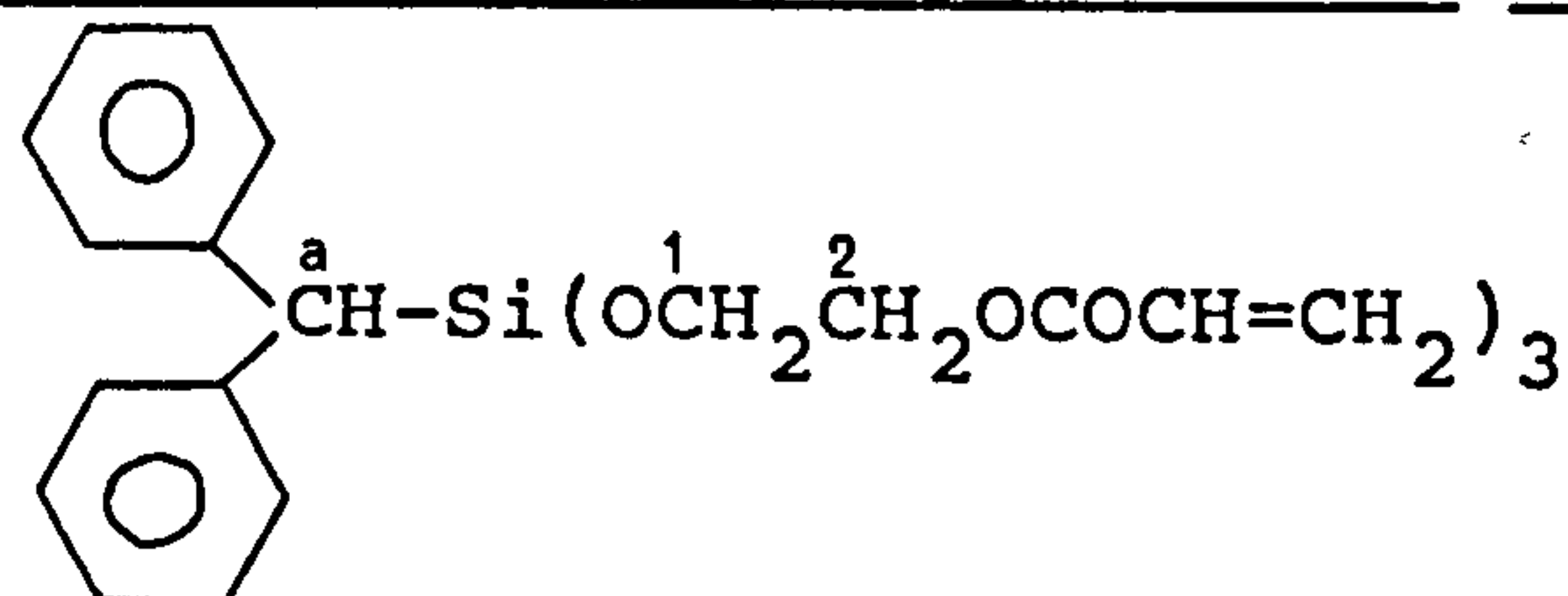
Infrared (Liquid film) : 3110, 3090, 3060, 3030, 2950, 2890, 1725, 1640, 1620, 1600, 1495, 1410, 1300, 1275, 1200, 1140-1100, 1060, 970, 810, 760, 740, 700cm<sup>-1</sup>.

<sup>1</sup>H nmr (CDCl<sub>3</sub>) : δ 2.19 (singlet, 2H, CH<sub>2</sub> at C-a), 3.80 (triplet, J=6Hz, 6H, CH<sub>2</sub> at C-1), 4.10 (triplet, J=6Hz, 6H, CH<sub>2</sub> at C-2), (5.60-6.40) (multiplet, 9H, acrylate group), (6.95-7.20) (multiplet, 5H, C<sub>6</sub>H<sub>5</sub>-)

Analysis calculated for C<sub>22</sub>H<sub>28</sub>O<sub>9</sub>Si : C, 60.54 ;H, 6.47

Found : C, 60.49; H, 6.57.

Benzhydryltris(2-hydroxyethoxy)silane, triacrylate ester



(BHSTEa)

Clear colourless liquid. (Yield = 72%)

Infrared (Liquid film) : 3110, 3090, 3060, 3030, 2950, 1725, 1640, 1620, 1600, 1495, 1450, 1410, 1300, 1275, 1195, 1165-1080, 1065, 1035, 980, 845, 910, 790, 755, 735, 705cm<sup>-1</sup>

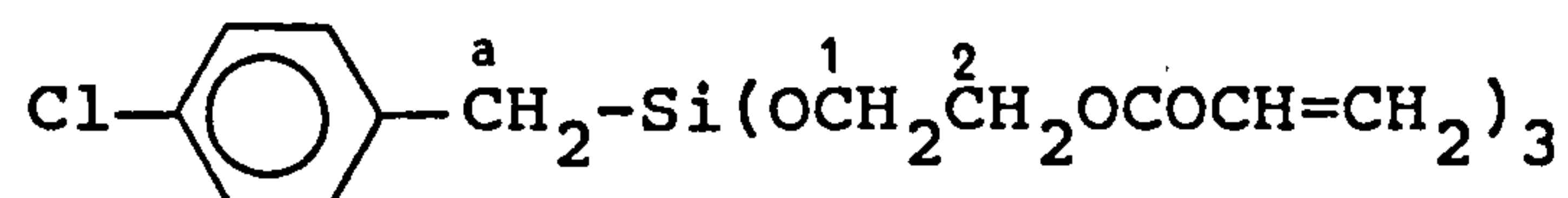
<sup>1</sup>H nmr (CDCl<sub>3</sub>) : δ 3.80 (triplet, J=6Hz, 6H, CH<sub>2</sub> at C-1), 4.15 (triplet, J=6Hz, 6H, CH<sub>2</sub> at C-2), 4.35 (singlet, 1H, CH at C-a), (5.60-6.50)(multiplet, 9H, acrylate group), (6.90-7.20)(multiplet, 10H, C<sub>6</sub>H<sub>5</sub>-)

Analysis calculated for : C<sub>28</sub>H<sub>32</sub>O<sub>9</sub>Si : C, 62.21; H, 5.97

Found : C, 60.32; H, 5.99

p-Chlorobenzyltris(2-hydroxyethoxy)silane, triacrylate ester

(CBSTEA)



Clear colourless liquid. (Yield = 76%).

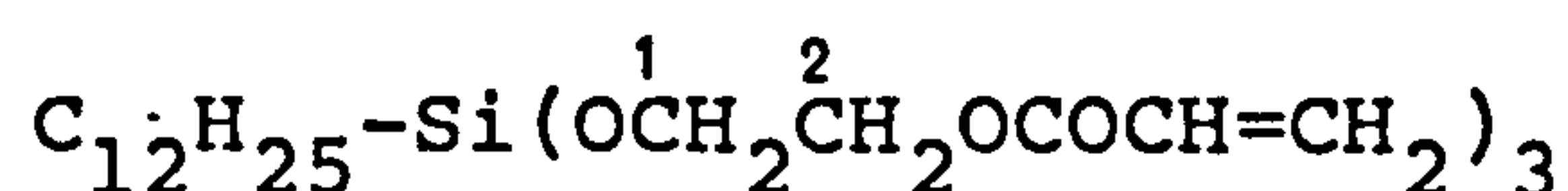
Infrared (Liquid film) : 3100, 3040, 2960, 2890, 1725, 1640, 1620, 1490, 1455, 1410, 1300, 1275, 1200, 1135, 1100, 1065, 1015, 985, 835, 810, 760, 715 cm<sup>-1</sup>

<sup>1</sup>H nmr (CDCl<sub>3</sub>) : δ 2.20 (singlet, 2H, CH<sub>2</sub> at C-a), 3.92 (triplet, J=6Hz, 6H, CH<sub>2</sub> at C-1), 4.22 (triplet, J=6Hz, 6H, CH<sub>2</sub> at C-2), (5.70-6.60) (multiplet, 9H, acrylate group), (6.90-7.20) (multiplet, 4H, Cl-C<sub>6</sub>H<sub>4</sub>-).

Analysis calculate for C<sub>22</sub>H<sub>27</sub>O<sub>9</sub>ClSi : C, 52.95; H, 5.45

Found : C, 51.89; H, 5.70

Dodecyltris(2-hydroxyethoxy)silane, triacrylate ester (DSTEa)



Clear colourless liquid. (Yield = 82%).

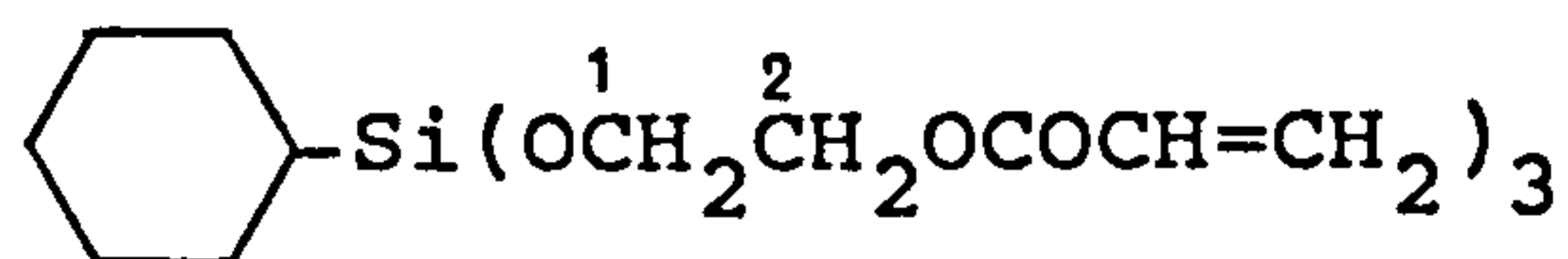
Infrared (Liquid film) : 2930, 2855, 1730, 1640, 1620, 1460, 1410, 1298, 1271, 1192, 1130, 1100, 1065, 985-965, 810, 670 cm<sup>-1</sup>

<sup>1</sup>H nmr (CDCl<sub>3</sub>) : δ (0.50-1.40) (multiplet, 25H, C<sub>12</sub>H<sub>25</sub>-), 3.90 (triplet, J=6Hz, 9H, CH<sub>2</sub> at C-1), 4.18 (triplet, J=6Hz, 6H, CH<sub>2</sub> at C-2), (5.60-6.30) (multiplet, 9H, acrylate group)

Analysis calculated for C<sub>27</sub>H<sub>46</sub>O<sub>9</sub>Si : C, 59.75; H, 8.54

Found : C, 59.62; H, 8.73.

c-Hexyl(2-hydroxyethoxy)silane, triacrylate ester (CHSTEA)



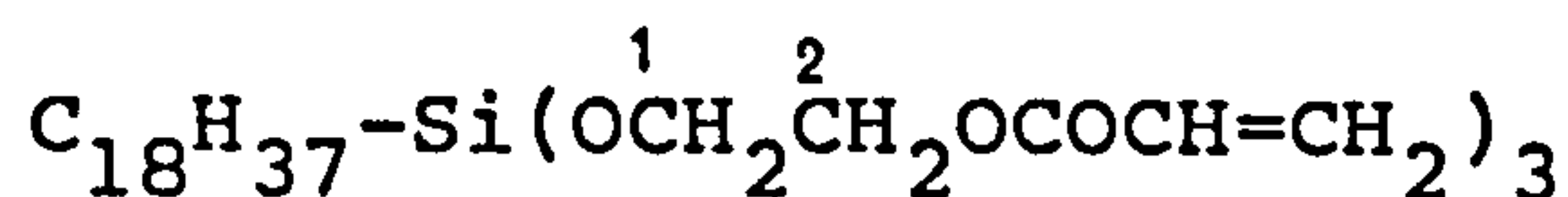
Infrared (liquid film) : 3090, 3070, 3050, 3020, 2940, 2870, 1725, 1640, 1620, 1595, 1485, 1445, 1400, 1295-1270, 1130-1030, 970, 870, 850, 810, 790, 712, 700,  $660\text{cm}^{-1}$

$^1\text{H}$  nmr ( $\text{CDCl}_3$ ) :  $\delta$  (0.60-1.70)(multiplet, 11H,  $\text{C}_6\text{H}_{11}$ -group); 3.80 (triplet,  $J=6\text{Hz}$ , 6H,  $\text{CH}_2$  at C-1), 4.05 (triplet,  $J=6\text{Hz}$ , 6H,  $\text{CH}_2$  at C-2), (5.50-6.50) (multiplet, 9H, acrylate group)

Analysis calculated for  $\text{C}_{21}\text{H}_{32}\text{O}_9\text{Si}$  : C, 55.25; H, 7.06

Found : C, 55.01; H, 7.29

Tris(2-hydroxyethoxy)octadecylsilane, triacrylate ester  
(ODSTEA)



Clear colourless liquid. (Yield = 78%)

Infrared (liquid film) : 2960, 2930, 2850, 1730, 1640, 1620, 1460, 1410, 1300, 1270, 1200, 1130, 2200, 1060, 980,  $960, 810\text{cm}^{-1}$ .

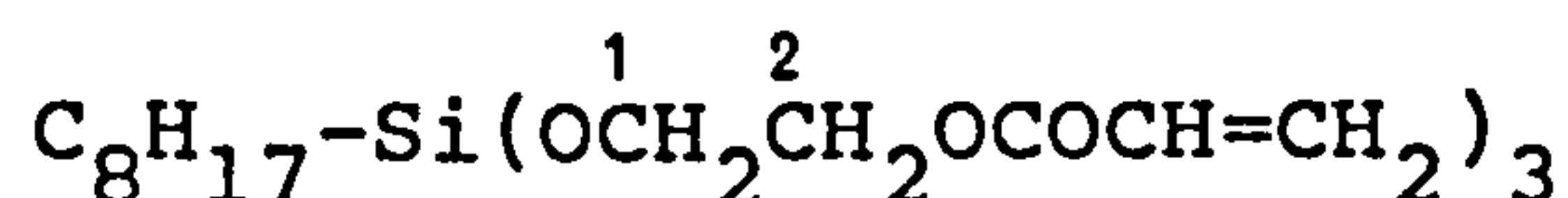
$^1\text{H}$  nmr ( $\text{CDCl}_3$ ) :  $\delta$  (0.70-1.40)(multiplet, 37H,  $\text{C}_{18}\text{H}_{37}$ -), 3.90 (triplet,  $J=6\text{Hz}$ , 6H,  $\text{CH}_2$  at C-1), 4.10 (triplet,  $J=6\text{Hz}$ , 6H,  $\text{CH}_2$  at C-2), (5.60-6.40)(multiplet, 9H, acrylate group)

Analysis calculated for  $\text{C}_{33}\text{H}_{58}\text{O}_9\text{Si}$  : C, 63.23; H, 9.33

Found : C, 63.12; H, 9.73



Tris(2-hydroxyethoxy)octylsilane, triacrylate ester (OSTEA)



Clear colourless liquid. (Yield = 81%)

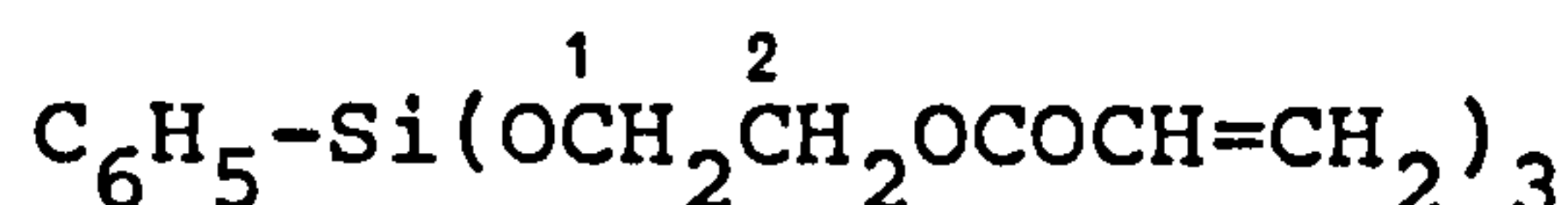
Infrared (liquid film) : 3050, 3040, 3020, 2960, 1725, 1640, 1620, 1460, 1410, 1300, 1275, 1200, 1130, 1100, 1060, 970, 810 $\text{cm}^{-1}$

$^1\text{H}$  nmr ( $\text{CDCl}_3$ ) :  $\delta$  (0.60-1.80)(multiplet, 17H,  $\text{C}_8\text{H}_{17}$ -), 4.00 (triplet,  $J=6\text{Hz}$ , 6H,  $\text{CH}_2$  at C-1), 4.30 (triplet,  $J=6\text{Hz}$ , 6H,  $\text{CH}_2$  at C-2), (5.70-6.50) (multiplet, 9H, acrylate group)

Analysis calculated for  $\text{C}_{23}\text{H}_{38}\text{O}_9\text{Si}$  : C, 56.77; H, 7.87

Found : C, 56.54; H, 8.05.

Tris(2-hydroxyethoxy)phenylsilane, triacrylate ester (PSTEa)



Pale yellow clear liquid. (Yield = 83%)

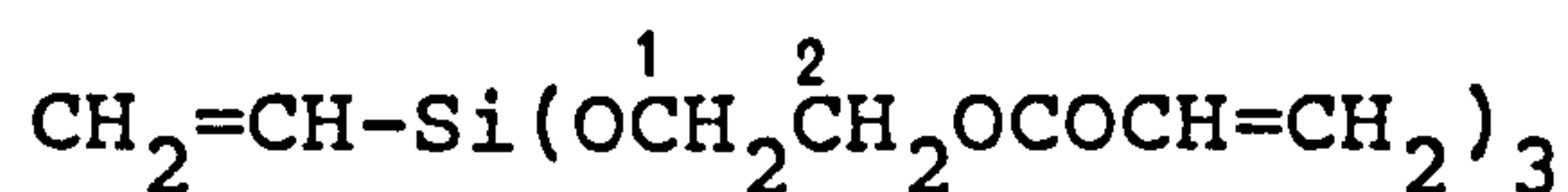
Infrared (Liquid film) : 3080, 3040, 2950, 2870, 1725, 1640, 1620, 1410, 1300, 1270, 1190, 1130, 1100, 1060, 970, 810, 740, 700 $\text{cm}^{-1}$

$^1\text{H}$  nmr ( $\text{CDCl}_3$ ) :  $\delta$  4.00 (triplet,  $J=6\text{Hz}$ ,  $\text{CH}_2$  at C-1), 4.20 (triplet,  $J=6\text{Hz}$ ,  $\text{CH}_2$  at C-2), (5.60-6.40) (multiplet, 9H, acrylate group), (7.00-7.25) (multiplet, 5H,  $\text{C}_6\text{H}_5$ -)

Analysis calculated for  $\text{C}_{21}\text{H}_{26}\text{O}_9\text{Si}$  : C, 55.99; H, 5.82

Found : C, 56.09; H, 5.90

Tris(2-hydroxyethoxy)vinylsilane, triacrylate ester (VSTEA)



Pale yellow clear liquid. (Yield = 83%)

Infrared (Liquid film) : 2960, 2930, 2880, 1725, 1640, 1620, 1410, 1300, 1275, 1200, 1130, 1100, 1060, 980, 810 $\text{cm}^{-1}$ .

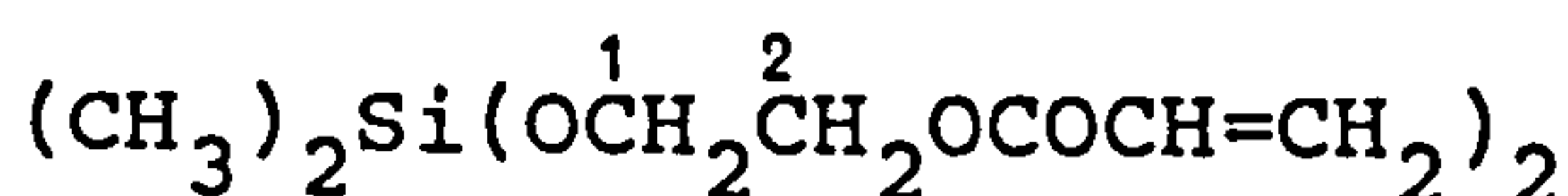
$^1\text{H}$  nmr ( $\text{CDCl}_3$ ) :  $\delta$  3.80 (triplet,  $J=6\text{Hz}$ , 6H,  $\text{CH}_2$  at C-1)  
4.10 (triplet,  $J=6\text{Hz}$ , 6H,  $\text{CH}_2$  at C-2), (5.40-6.30)  
(multiplet, 12H, acrylate and vinyl group)

Analysis calculated for  $\text{C}_{17}\text{H}_{24}\text{O}_9\text{Si}$  : C, 50.98; H, 6.04

Found : C, 50.87; H, 6.28

Bis(2-hydroxyethoxy)dimethylsilane, diacrylate ester

(DMSDEA)



Clear colourless liquid. (Yield = 78%)

Infrared (Liquid film) : 2960, 2880, 1727, 1637, 1620, 1410, 1298, 1260, 1190, 1130, 1100, 1061, 965, 840, 806 $\text{cm}^{-1}$

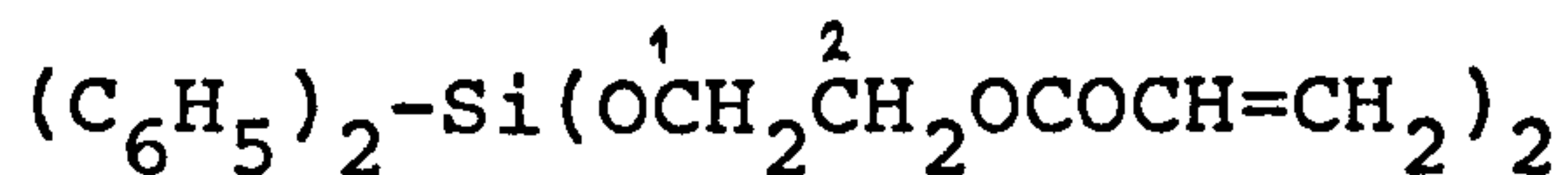
$^1\text{H}$  nmr ( $\text{CDCl}_3$ ) :  $\delta$  0.20 (singlet, 6H, methyl group), 3.90  
(triplet,  $J=6\text{Hz}$ , 4H,  $\text{CH}_2$  at C-1), 4.20 (triplet,  $J=6\text{Hz}$ , 4H,  
 $\text{CH}_2$  at C-2), (5.74-6.50) (multiplet, 6H, acrylate)

Analysis calculated for  $\text{C}_{12}\text{H}_{20}\text{O}_6\text{Si}$  : C, 49.98; H, 6.99

Found : C, 49.92; H, 7.16

Bis(2-hydroxyethoxy)diphenylsilane, diacrylate ester

(DPSDEA)



Pale yellow and clear liquid. (Yield = 83%)

Infrared (Liquid film) : 3080, 3050, 2950, 2930, 2880, 1725, 1640, 1620, 1595, 1430, 1410, 1300, 1275, 1200, 1130, 970, 810, 740, 720, 700cm<sup>-1</sup>.

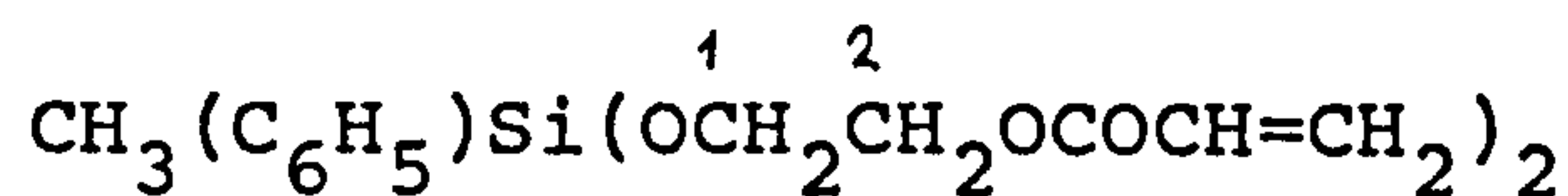
<sup>1</sup>H nmr (CDCl<sub>3</sub>) : δ 3.80 (triplet, J=6Hz, 4H, CH<sub>2</sub> at C-1), 4.10 (triplet, J=6Hz, 4H, CH<sub>2</sub> at C-2), (5.40-6.30) (multiplet, 6H, acrylate group), (6.80-7.50) (multiplet, 10H, C<sub>6</sub>H<sub>5</sub>-).

Analysis calculated for : C<sub>22</sub>H<sub>24</sub>O<sub>6</sub>Si : C, 64.06; H, 5.86

Found : C, 64.08; H, 6.04

Bis(2-hydroxyethoxy)methylphenylsilane, diacrylate ester

(MPSDEA)



Pale yellow clear liquid. (Yield = 83%)

Infrared (Liquid film) : 3070, 3050, 1725, 1640, 1620, 1590, 1430, 1410, 1300, 1275, 1200, 1120, 970, 810, 740, 720, 700cm<sup>-1</sup>.

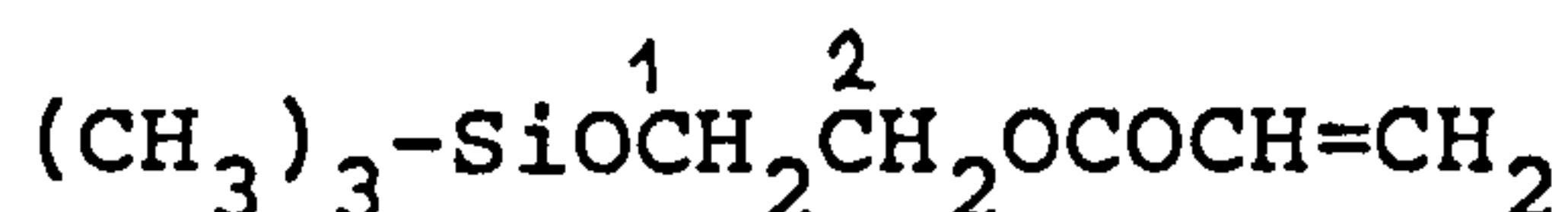
<sup>1</sup>H nmr (CDCl<sub>3</sub>) : δ 0.30 (singlet, 3H, CH<sub>3</sub>-), 3.80 (triplet, J=6Hz, 4H, CH<sub>2</sub> at C-1), 4.10 (triplet, J=6Hz, 4H, CH<sub>2</sub> at C-2), (5.50-6.30) (multiplet, 6H, acrylate group), (6.95-7.50) (multiplet, 5H, C<sub>6</sub>H<sub>5</sub>-)

Analysis calculated for C<sub>17</sub>H<sub>22</sub>O<sub>6</sub>Si : C, 58.27; H, 6.33

Found : C, 58.30 ; H, 6.49



(2-Hydroxyethoxy)trimethylsilane, acrylate ester (TMSEA)



Clear colourless liquid. (Yield = 86%)

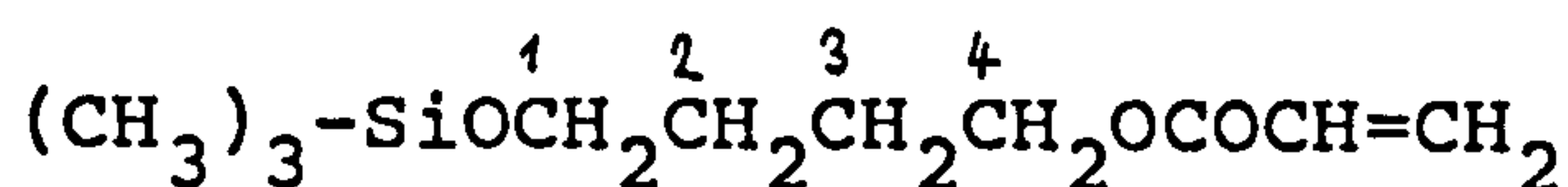
Infrared (Liquid film) : 2963, 2882, 1728, 1638, 1620, 1448, 1408, 1296, 1261, 1190, 1093, 1060, 985, 871, 841, 810, 740 $\text{cm}^{-1}$ .

$^1\text{H}$  nmr ( $\text{CDCl}_3$ ) :  $\delta$  0.10 (singlet, 9H,  $\text{CH}_3$ -) 3.80 (triplet,  $\text{J}=6\text{Hz}$ , 2H,  $\text{CH}_2$  at C-1), 4.10 (triplet,  $\text{J}=6\text{Hz}$ , 2H,  $\text{CH}_2$  at C-2), (5.60-6.30) (multiplet, 3H, acrylate group)

Analysis calculated for  $\text{C}_8\text{H}_{16}\text{O}_3\text{Si}$  : C, 51.03; H, 8.56

Found : C, 61.33; H, 8.69.

(4-Hydroxybutoxy)trimethylsilane, acrylate ester (TMSBA)



Clear colourless liquid. (Yield = 84%)

Infrared (Liquid film) : 2963, 2882, 1728, 1638, 1620, 1448, 1408, 1296, 1261, 1190, 1093, 1060, 985, 871, 841, 810, 740 $\text{cm}^{-1}$ .

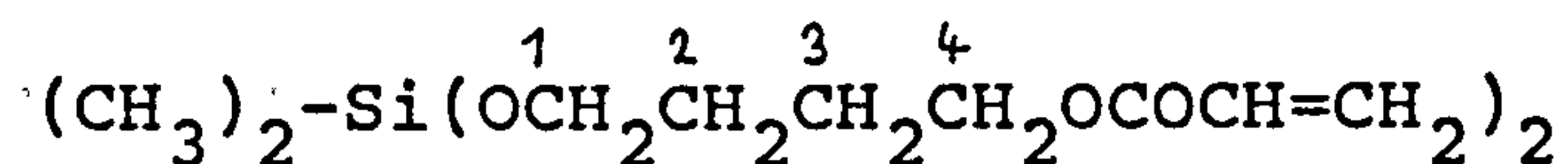
$^1\text{H}$  nmr ( $\text{CDCl}_3$ ) :  $\delta$  0.10 (singlet, 9H,  $\text{CH}_3$ -) 1.80 (multiplet, 4H,  $\text{CH}_2$  at C-2 and C-3), 3.80 (triplet, 2H,  $\text{CH}_2$  at C-4), 4.20 (triplet, 2H,  $\text{CH}_2$  at C-4), (5.60-6.30) (multiplet, 3H, acrylate group)

Analysis calculated for  $\text{C}_{10}\text{H}_{20}\text{O}_3\text{Si}$  : C, 55.52; H, 9.32

Found : C, 55.60; H, 9.39

Bis(4-hydroxybutoxy)dimethylsilane, diacrylate ester

(DMSDBA)



Clear colourless liquid. (Yield = 88%)

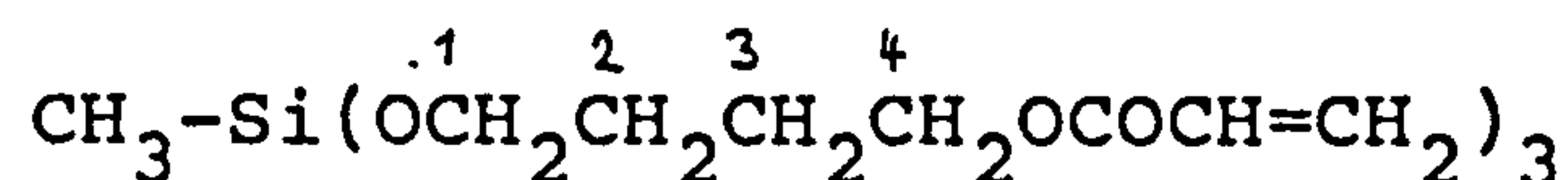
Infrared (Liquid film) : 2963, 2936, 2870, 1728, 1636, 1620, 1455, 1412, 1296, 1265, 1192, 1060, 1038, 987, 899, 849, 810cm<sup>-1</sup>.

<sup>1</sup>H nmr (CDCl<sub>3</sub>) : δ 0.20 (singlet, 6H, CH<sub>3</sub>-), 1.80 (multiplet, 8H, CH<sub>2</sub> at C-2 and C-3), 3.80 (triplet, 4H, CH<sub>2</sub> at C-1), 4.20 (triplet, 4H, CH<sub>2</sub> at C-4), (5.60-6.30) (multiplet, 6H, acrylate group)

Analysis calculated for C<sub>16</sub>H<sub>28</sub>O<sub>6</sub>Si : C, 55.79; H, 8.19

Found : C, 55.90; H, 8.25

Tris(4-hydroxybutoxy)methylsilane, triacrylate ester (MSTBA)



Clear colourless liquid. (Yield = 84%)

Infrared (liquid film) : 2955, 2874, 1728, 1635, 1620, 1455, 1411, 1300, 1269, 1190, 1065, 987, 899, 849, 810cm<sup>-1</sup>.

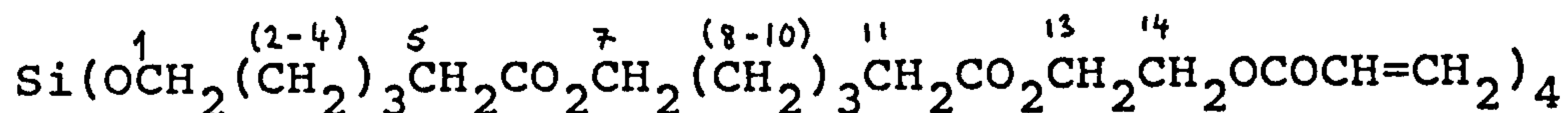
<sup>1</sup>H nmr (CDCl<sub>3</sub>) : δ 0.20 (singlet, 3H, CH<sub>3</sub>-), 1.80 (multiplet, 12H, CH<sub>2</sub> at C-2 and C-3), 3.80 (triplet, 6H, CH<sub>2</sub> at C-1), 4.20 (triplet, 6H, CH<sub>2</sub> at C-4), (5.65-6.40) (multiplet, 9H, acrylate)

Analysis calculated for C<sub>22</sub>H<sub>36</sub>O<sub>9</sub>Si : C, 55.91; H, 7.68

Found : C, 55.98; H, 7.71.

Tetrakis{5-[5-(2-hydroxyethoxycarbonyl)pentoxycarbonyl]-  
pentoxy}silane, tetraacrylate ester (STT)

5-[5-(2-hydroxyethoxycarbonyl)pentoxycarbonyl]pentoxy will from now on be referred to by its trade name, TONE-100.



Clear colourless liquid. (Yield = 76%)

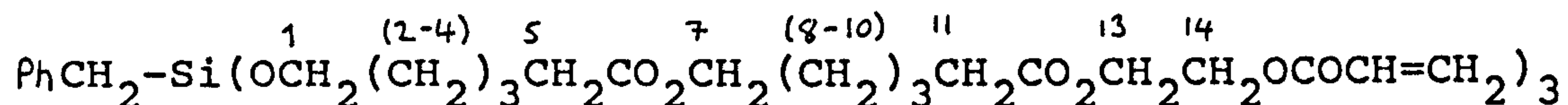
Infrared (liquid film) : 2950, 2880, 1730, 1640, 1620, 1460, 1413, 1280, 1200-1160, 1100, 990, 815, 740cm<sup>-1</sup>.

<sup>1</sup>H nmr (CDCl<sub>3</sub>) : δ (1.20-1.90) (multiplet, 48H, CH<sub>2</sub> at C-(2-4), C-(8-10), (2.24-2.60) (multiplet, 16H, CH<sub>2</sub> at C-5, C-11), (3.75-4.60) (multiplet, 32H, CH<sub>2</sub> at C-1, C-7, C-13, C-14), (5.50-6.50) (multiplet, 12H, acrylate group)

Analysis calculated for C<sub>68</sub>H<sub>108</sub>O<sub>28</sub>Si : C, 58.26; H, 7.76

Found : C, 58.12; H, 8.02

Benzyltris(TONE-100)silane, triacrylate ester (BSTT)



Clear colourless liquid. (Yield = 80%)

Infrared (Liquid film) : 2943, 2867, 1732, 1635, 1620, 1602, 1494, 1455, 1409, 1354, 1297, 1274, 1191, 1095, 986, 810, 700cm<sup>-1</sup>.

<sup>1</sup>H nmr (CDCl<sub>3</sub>) : δ (1.10-1.90) (multiplet, 36H, CH<sub>2</sub> at

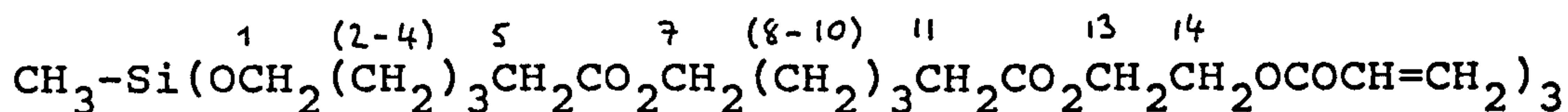


C-(8-10), C(2-4)), (2.20-2.60) (multiplet, 14H, CH<sub>2</sub>, at C-5, C-11), (3.60-4.60) (multiplet, 24H, CH<sub>2</sub> at C-1, C-7, C-13, C-14), (5.60-6.40) (multiplet, 9H, acrylate group), 7.20 (multiplet, 5H, C<sub>6</sub>H<sub>5</sub>-)

Analysis calculated for C<sub>58</sub>H<sub>88</sub>O<sub>21</sub>Si : C, 60.60; H, 7.71

Found : C, 60.30; H, 7.92

Methyltris(TONE-100)silane, triacrylate ester (MSTT)



Clear colourless liquid. (Yield = 84%)

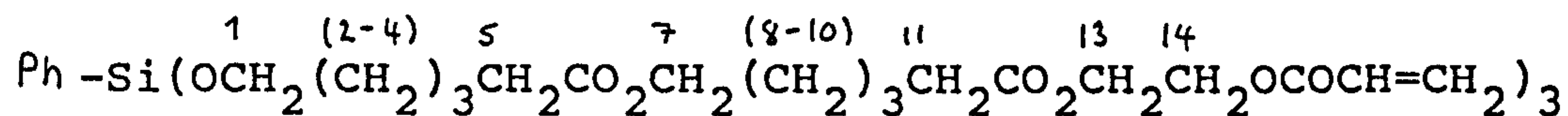
Infrared (Liquid film) : 2940, 2870, 1730, 1640, 1620, 1460, 1410, 1270, 1200-1160, 1100, 990, 850, 810cm<sup>-1</sup>

<sup>1</sup>H nmr (CDCl<sub>3</sub>) : δ 0.12 (singlet, 3H, CH<sub>3</sub>-), (1.16-1.85) (multiplet, 36H, CH<sub>2</sub> at C-(8-10), C-(2-4)), (2.15-2.55) (multiplet, 12H, CH<sub>2</sub> at C-5, C-11), (3.50-4.40) (multiplet, 24H, CH<sub>2</sub> at C-1, C-7, C-13, C-14), (5.70-6.50) (multiplet, 9H, acrylate group)

Analysis calculated for C<sub>52</sub>H<sub>84</sub>O<sub>21</sub>Si : C, 58.19; H, 7.88

Found : C, 58.13; H, 8.15

Phenyltris(TONE-100)silane, triacrylate ester (PSTT)



Clear colourless liquid. (Yield = 74%)

Infrared (Liquid film) : 2943, 2868, 1730, 1636, 1619,

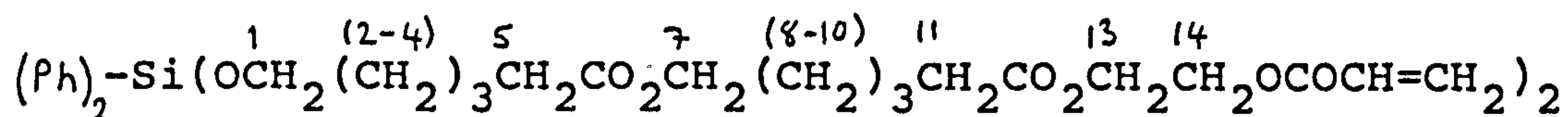
1594, 1456, 1431, 1410, 1354, 1294, 1275, 1235, 1190, 1130, 1094, 986, 810, 742, 702cm<sup>-1</sup>.

<sup>1</sup>H nmr (CDCl<sub>3</sub>) : δ (1.10-1.90) (multiplet, 36H, CH<sub>2</sub> at C-(2-4), C(8-10)), (2.20-2.60) (multiplet, 12H, CH<sub>2</sub>, at C-5, C-11), (3.60-4.60) (multiplet, 24H, CH<sub>2</sub> at C-1, C-7, C-13, C-14), (5.60-6.40) (multiplet, 9H, acrylate group), 7.20 (multiplet, 5H, C<sub>6</sub>H<sub>5</sub>-)

Analysis calculated for C<sub>57</sub>H<sub>86</sub>O<sub>21</sub>Si : C, 50.98; H, 6.04

Found : C, 50.87; H, 6.28

Diphenylbis(TONE-100)silane, diacrylate ester (DPSDT)



Clear colourless liquid (Yield = 81%)

Infrared (liquid film) : 3070, 3049, 2943, 2868, 2320, 1731, 1635, 1619, 1592, 1456, 1430, 1409, 1353, 1297, 1274, 1235, 1189, 1117, 1094, 985, 810, 742, 719, 702cm<sup>-1</sup>

<sup>1</sup>H nmr (CDCl<sub>3</sub>) : δ (1.10-1.90) (multiplet, 24H, CH<sub>2</sub> at C-(2-4), C(8-10)), (2.20-2.60) (multiplet, 8H, CH<sub>2</sub>, at C-5, C-11), (3.60-4.60) (multiplet, 16H, CH<sub>2</sub> at C-1, C-7, C-13, C-14), (5.60-6.40) (multiplet, 6H, acrylate group), 7.20 (multiplet, 10H, C<sub>6</sub>H<sub>5</sub>-)

Analysis calculated for C<sub>46</sub>H<sub>64</sub>O<sub>14</sub>Si : C, 63.57; H, 7.42

Found : C, 63.68; H, 7.60

### Preparation of films cured by electron beam irradiation

All formulations were coated onto GNT paper and aluminium foil via a Dixon 164 coater using a forward spinning smoothing roller at a setting of 32psi. The coatings were then passed under the electron beam. For doses of radiation (0-100kGy) the moving web was maintained at  $20\text{mmmin}^{-1}$ , but for a dose of 200kGy the machine speed was reduced to  $10\text{mmmin}^{-1}$ .

### Preparation of films cured by UV irradiation

All materials were coated onto GNT sheets via an automatic K-bar coater unit using a weighted coating bar (no. 5). The coatings were then passed under the UV lamp. The minimum number of passes required to produce a tackfree to the touch coating was recorded for a given belt speed and initiator level.

### Preparation of films cured by UV irradiation (for infrared analysis).

All diluents were coated onto a KBr disc using a K-bar (no. 1). The coatings were then passed under the UV lamp.

### Physical Tests

Solvent rub resistance, brittleness and pencil hardness tests were carried out on all tackfree coatings on GNT paper with the exception of those coatings exhibiting surface defects due to reticulation. The procedure for these tests is as described in Chapter 3.



### Solvent extraction of cured films

Solvent extraction of cured films of 4-HBA, 2-HEA, TPGDA, TMPTA, TMSEA, DMSDEA, MSTEA, TMSBA, DMSDBA and MSTBA on GNT paper as well as a blank of uncoated paper was carried out as follows.

Four (10x10)cm<sup>2</sup> templates of a cured coating on GNT of known coatweights were extracted using tetrahydrofuran (50ml) for 24 hours. The solvent was removed over a rotary evaporator and the amount of extract was recorded and calculated as the percentage extract.

### Analysis of spectra obtained by Fourier transform infrared

The transmission and photoacoustic infrared spectra obtained for all films were of excellent quality. The residual unsaturation of all films were evaluated by monitoring the dis-appearance of the doublet at 1640/1620cm<sup>-1</sup> due to the carbon carbon double bond stretch of the vinyl group and the 810cm<sup>-1</sup> overtone frequency respectively [16, 17, 18]. Compensation for sample thickness was considered by use of the ratio method. The internal standard used for all calculations was that of the carbonyl stretching frequency at 1730cm<sup>-1</sup> [18].

The area associated with each peak was computed given a predefined baseline and from which the peak ratio's were calculated and the percentage change of a peak evaluated.

APPENDIX A

Table 5 Physical test data for TPGDA

<u>Dose of</u> <u>radiation</u> <u>/kGy</u>	<u>Coatweight</u> <u>/gm<sup>-2</sup></u>	<u>Solvent</u> <u>Rubs</u>	<u>Pencil</u> <u>Hardness</u>	<u>Brittleness</u>
2.5	31.3	36	HB	1
5	30.7	74	2H	2
10	27.3	52	2H	2/3
20	25.7	175	>4H	2/3
40	24.5	437	>4H	2/3
60	31.4	>500	>4H	2/3

Table 6 Physical test data for HDDA

<u>Dose of</u> <u>radiation</u> <u>/kGy</u>	<u>Coatweight</u> <u>/gm<sup>-2</sup></u>	<u>Solvent</u> <u>Rubs</u>	<u>Pencil</u> <u>Hardness</u>	<u>Brittleness</u>
2.5	17.4	32.5	H	1
5	18.8	55	H	2
10	11.1	75	2H	2
20	20.0	500	2H	2/3
40	10.0	>500	2H	2/3
60	19.4	>500	>3H	3/4

Table 7 Physical test data for PSTEA

<u>Dose of</u> <u>radiation</u> <u>/kGy</u>	<u>Coatweight</u> <u>/gm<sup>-2</sup></u>	<u>Solvent</u> <u>Rubs</u>	<u>Pencil</u> <u>Hardness</u>	<u>Brittleness</u>
2.5	25.7	95	>4H	1
5	29.0	100	>4H	1
10	21.0	180	>4H	1
20	20.8	333	>4H	1
40	24.5	>500	>4H	1
60	15.0	>500	>4H	2

Table 8 Physical test data for BSTEA

<u>Dose of</u> <u>radiation</u> <u>/kGy</u>	<u>Coatweight</u> <u>/gm<sup>-2</sup></u>	<u>Solvent</u> <u>Rubs</u>	<u>Pencil</u> <u>Hardness</u>	<u>Brittleness</u>
2.5	49.3	465	>4H	1
5	54.2	>500	>4H	2
10	25.4	>500	>4H	2
20	44.4	>500	>4H	2
40	56.3	>500	>4H	2
60	45.3	>500	>4H	2



Table 9 Physical test data for MSTEa

<u>Dose of</u> <u>radiation</u> <u>/kGy</u>	<u>Coatweight</u> <u>/gm<sup>-2</sup></u>	<u>Solvent</u> <u>Rubs</u>	<u>Pencil</u> <u>Hardness</u>	<u>Brittleness</u>
2.5	36.0	>500	H	2
5	41.6	>500	2H	1
10	22.1	>500	2H	2
20	22.4	>500	3H	2
40	18.8	>500	3H	2
60	17.9	>500	>3H	1

Table 10 Physical test data for OSTEA

<u>Dose of</u> <u>radiation</u> <u>/kGy</u>	<u>Coatweight</u> <u>/gm<sup>-2</sup></u>	<u>Solvent</u> <u>Rubs</u>	<u>Pencil</u> <u>Hardness</u>	<u>Brittleness</u>
2.5	47.4	142.5	H	1
5	41.4	111	2H	1
10	43.0	>500	2H	2
20	44.4	>500	3H	1
40	40.3	>500	3H	2
60	40.1	>500	>4H	2

Table 11 Physical test data for DSTEA

<u>Dose of</u> <u>radiation</u> <u>/kGy</u>	<u>Coatweight</u> <u>/gm<sup>-2</sup></u>	<u>Solvent</u> <u>Rubs</u>	<u>Pencil</u> <u>Hardness</u>	<u>Brittleness</u>
2.5	29.0	>500	H	2
5	38.8	>500	2H	1
10	29.3	>500	2H	2
20	20.0	>500	3H	1
40	22.2	>500	3H	2
60	42.9	>500	>3H	3

Table 12 Physical test data for DPSDEA

<u>Dose of</u> <u>radiation</u> <u>/kGy</u>	<u>Coatweight</u> <u>/gm<sup>-2</sup></u>	<u>Solvent</u> <u>Rubs</u>	<u>Pencil</u> <u>Hardness</u>	<u>Brittleness</u>
2.5	25.6	14.5	-	1
5	30.4	-	-	-
10	29.2	31	-	1
20	22.3	95	-	-
40	25.1	97.5	-	-
60	36.2	126	-	-

Table 13 Physical test data for MPSDEA

<u>Dose of</u> <u>radiation</u> <u>/kGy</u>	<u>Coatweight</u> <u>/gm<sup>-2</sup></u>	<u>Solvent</u> <u>Rubs</u>	<u>Pencil</u> <u>Hardness</u>	<u>Brittleness</u>
2.5	53.9	18	-	1
5	47.2	25	-	2
10	53.9	89	-	2
20	56.0	47	-	-
40	68.4	>500	-	-
60	49.1	373	-	-

Table 14 Physical test data for MSTT

<u>Dose of</u> <u>radiation</u> <u>/kGy</u>	<u>Coatweight</u> <u>/gm<sup>-2</sup></u>	<u>Solvent</u> <u>Rubs</u>	<u>Pencil</u> <u>Hardness</u>	<u>Brittleness</u>
2.5	38.6	2.5	2H	2
5	62.6	13.5	4H	2
10	50.3	40.5	>4H	3
20	53.3	29	>4H	3



Table 15 Physical test data for PSTT

<u>Dose of</u> <u>radiation</u> <u>/kGy</u>	<u>Coatweight</u> <u>/gm<sup>-2</sup></u>	<u>Solvent</u> <u>Rubs</u>	<u>Pencil</u> <u>Hardness</u>	<u>Brittleness</u>
2.5	21.8	4	3H	1
5	32.0	22	>4H	2
10	18.5	32	>4H	3
20	30.3	50	>4H	3

Table 16 Physical test data for STEA

<u>Dose of</u> <u>radiation</u> <u>/kGy</u>	<u>Coatweight</u> <u>/gm<sup>-2</sup></u>	<u>Solvent</u> <u>Rubs</u>	<u>Pencil</u> <u>Hardness</u>	<u>Brittleness</u>
2.5	47.8	>500	H	2
5	49.7	>500	3H	1
10	39.6	>500	3H	2
20	33.2	>500	3H	1
40	29.2	>500	3H	1
60	41.0	>500	>3H	1

## APPENDIX B

Table 18 Number of passes required of the coated paper under the lamp to render a tackfree film using TPGDA, HDDA and TMPTA

	Belt speed	% Initiator			
	m/min	1	2	3	4
TPGDA	5	*	*	15 (12.1)	8 (12.5)
	10	*	*	*	17 (11.6)
	20	*	*	*	30 (12.5)
	40	*	*	*	*
HDDA	5	*	*	19 (11.5)	11 (11.8)
	10	*	*	*	30 (11.9)
	20	*	*	*	*

Coatweights given in parenthesis /gm<sup>-2</sup>

\* indicates not cured to give a touch dry coating after 30 passes

Table 18 contd. Number of passes required of the coated paper under the lamp to render a tackfree film using TPGDA, HDDA and TMPTA

	Belt speed		% Initiator			
	m/min	1	2	3	4	
TMPTA	5	*	*	11	4	
				(12.0)	(13.2)	
	10	*	*	19	7	
				(11.6)	(12.8)	
	20	*	*	*	11	
					(12.8)	
	40	*	*	*	15	
					(12.0)	

Coatweights given in parenthesis /gm<sup>-2</sup>

\* indicates not cured to give a touch dry coating after 30 passes



Table 19 Number of passes required of paper coated with silicon acrylates under the lamp in order to produce a tackfree coating

Belt speed		% Initiator			
	m/min	1	2	3	4
DSTEА	5	*	*	20	6
				(11.8)	(12.5)
	10	*	*	*	17
					(12.1)
	20	*	*	*	25
					(11.8)
	40	*	*	*	*
PSTEА	5	21	14	4	1
		(13.2)	(13.2)	(12.3)	(12.8)
	10	*	30	10	3
			(12.8)	(12.4)	(12.9)
	20	*	*	21	5
				(12.5)	(12.7)
	40	*	*	30	6
				(12.7)	(12.3)

Coatweights given in parenthesis /gm<sup>-2</sup>

\* indicates not cured to give a touch dry coating after 30 passes

Table 19 contd. Number of passes required of paper coated with silicon acrylates under the lamp in order to produce a tackfree coating

Belt speed		% Initiator			
	m/min	1	2	3	4
PSTT	5	*	15 (10.8)	16 (10.8)	8 (11.6)
	10	*	*	27 (11.2)	17 (11.2)
	20	*	*	9 (10.8)	25 (11.6)
	40	*	*	30 (11.2)	30 (10.2)
DPSDEA	5	*	*	21 (48.8)	5 (59.2)
	10	*	*	30 (54.4)	6 (53.2)
	20	*	*	*	14 (56.8)
	40	*	*	*	15 (57.2)

Coatweights given in parenthesis /gm<sup>-2</sup>

\* indicates not cured to give a touch dry coating after 30 passes

Table 19 contd. Number of passes required of paper coated with silicon acrylates under the lamp in order to produce a tackfree coating

	Belt speed		% Initiator			
	m/min	1	2	3	4	
VSTEA	5	*	*	19	5	
				(11.2)	(10.8)	
	10	*	*	*	12	
					(10.8)	
	20	*	*	*	28	
				(10.4)		
	40	*	*	*	*	
BSTEA	5	20	14	6	1	
		(11.9)	(13.1)	(13.0)	(13.1)	
	10	*	*	18	3	
				(12.8)	(13.0)	
	20	*	*	26	6	
				(12.6)	(13.0)	
	40	*	*	*	8	
				(12.2)		

Coatweights given in parenthesis /gm<sup>-2</sup>

\* indicates not cured to give a touch dry coating after 30 passes



Table 19 contd. Number of passes required of paper coated with silicon acrylates under the lamp in order to produce a tackfree coating

Belt speed		% Initiator			
	m/min	1	2	3	4
BHSTE A	5	4	3	2	2
		(13.2)	(13.2)	(14.4)	(14.0)
	10	9	6	4	2
		(13.2)	(12.4)	(13.6)	(12.8)
	20	15	8	5	3
		(14.4)	(13.2)	(13.2)	(12.8)
	40	19	11	7	3
		(14.0)	(12.0)	(12.8)	(14.8)

Coatweights given in parenthesis /gm<sup>-2</sup>

\* indicates not cured to give a touch dry coating after 30 passes

## REFERENCES

- [1] C. G. Roffey, (1982). Photopolymerisation of Surface Coatings, Wiley-Interscience.
- [2] S. Paul, (1986). Surface coatings: Science and Technology, Wiley-Interscience.
- [3] UV and EB Curing Formulations for printing Inks, Coatings and Paints, (1984). R. Holman, Ed., Sita Technology.
- [4] W. Oraby and W. K. Walsh, (1979). J. Appl. Polym. Sci., 23, 3227.
- [5] US patent no. 4,306,050. (1981 to Goldschmidt AG).
- [6] US patent no. 4,434,210. (1984 to Sony Corporation).
- [7] Comprehensive Chemical Kinetics, (1976). C. H. Bamford and C. F. H. Tipper, Eds., Vol. 14, Elsevier.
- [8] K. J. Saunders, (1988). Organic Polymer Chemistry, 2nd Ed., Chapman and Hall.
- [9] Comprehensive Organometallic Chemistry, (1981). G. Wilkinson, F. G. A. Stone and E. W. Abel, Eds., Pergamon Press.
- [10] A. E. Pierce, (1968). Silylation of Organic compounds, Pierce Chemical co..
- [11] E. D. Roberts, (1973). J. Electrochem. Soc., 120, 1716.
- [12] R. A. Benkeser, J. M. Gaul and W. E. Smith, (1969). J.A.C.S., 91, 3666.
- [13] N. Hagihara, M. Kumada and R. Okawara, (1968). Handbook of Organometallic Compounds, Benjamin.
- [14] Handbook of Organosilicon Compounds, (1973). V.

Bazant, V. Chvalosky and J. Rathousky, Eds., Vol 1-4, A Series, Marcel Dekker.

[15] R. A. Benkeser and W. E. Smith, (1969). J.A.C.S., 91, 1556.

[16] G. Plews and R. Phillips, (1979). J. Coat. Techn., 51, 69.

[17] W. O. George, D. V. Harris and W. E. Maddams, (1975). J. C. S. Perkin II, 392.

[18] R. T. Conley, (1972). Infrared spectroscopy, 2nd Ed., Allyn and Bacon.



---

## CHAPTER 5

EFFECT OF ADDITIVES UPON

ELECTRON BEAM INDUCED

POLYMERISATION OF

ISODECYL ACRYLATE

---

**Chapter 5 EFFECT OF ADDITIVES UPON ELECTRON BEAM INDUCED  
POLYMERISATION OF ISODECYL ACRYLATE**

Introduction	211
Radical cations	212
Electrons	214
Excited states	216
Results and Discussion	220
Conclusion	236
Experimental	237
References	240

## INTRODUCTION

The most widely used class of radiation curable systems are those based on the acrylate functionality. Whilst it is generally accepted that the polymerisation of these unsaturated monomers is propagated by a radical species [1-3], the nature of the initiating species produced as a result of electron beam irradiation is unclear.

Exposure of matter to an electron beam of high energy,  $>500\text{eV}$ , will result in the formation of highly excited states. These excited states may lose energy through collisional deactivation, autoionisation to produce radical cations and electrons, or, they may have a transient existence ultimately leading to, either the expulsion of an electron or, dissociation to generate free radicals. The fate of the expelled electron depends primarily on its kinetic energy. Electrons that do not travel beyond the coulombic attractive forces of its parent ion will be drawn back to its geminate radical cation and recombine to form an electronically excited state. In principle therefore, many photochemical processes may ensue. However, if the expelled electron has sufficient kinetic energy to escape the electrostatic attractive forces of its parent ion it may cause further ionisations. The electrons produced by all these events can also produce excited states by direct excitation [4]. Electrons of  $<12\text{eV}$  may result in the formation of triplet states, while electrons of  $5\text{-}20\text{eV}$  may generate excited singlet states [4]. Thermalised or



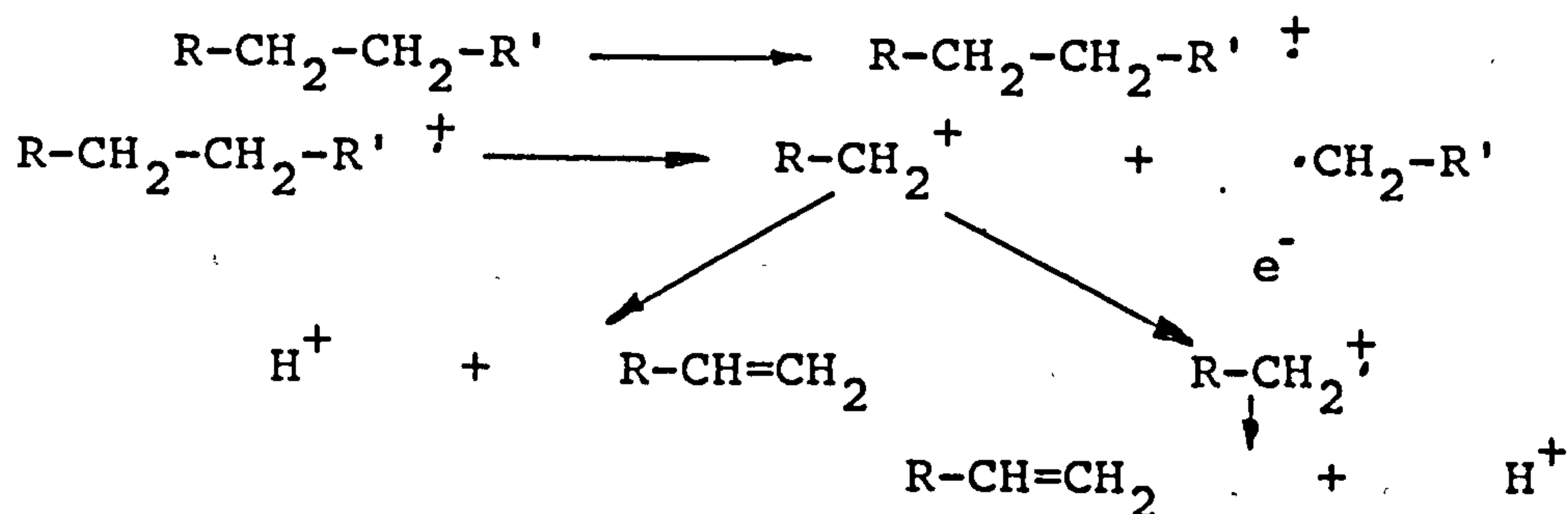
electrons of low energy may also undergo electron attachment to produce a radical anion [5,6].

Thus irradiation of thin films of alkylacrylate esters will primarily generate radical cations, electrons of a distribution of energies and excited singlet and triplet states. The importance of each of these entities in relation to generating species capable of initiating the polymerisation of alkylacrylate esters will now be discussed.

### Radical cations

Radical cation production will occur 'randomly' [7] throughout the medium. For the vast majority of radical cations produced, radical cation-electron recombination to generate an excited state is expected to occur [8]. If a radical cation is formed along the alkyl chain, radical generation may ensue as a result of fragmentation of the radical cation to produce a carbonium ion and a carbon centred radical capable of initiating polymerisation [9]. The former product may subsequently fragment to yield a proton and an alkene, alternatively, it may scavenge an electron to ultimately generate an alkene and a hydrogen

### Scheme 1





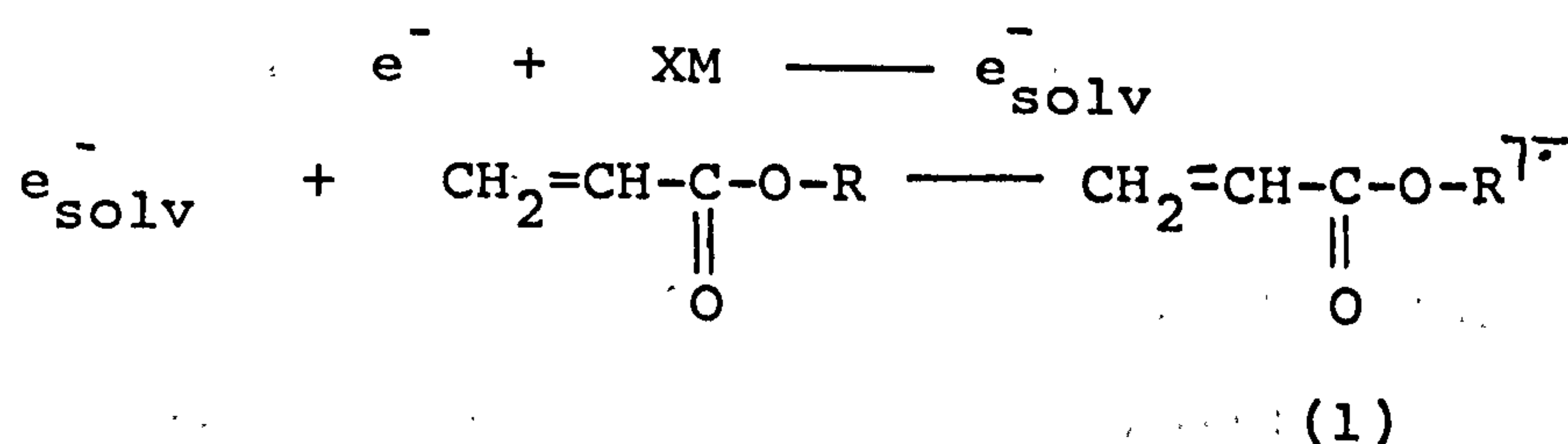
Pyrene may also be expected to behave as a hole scavenger, however, polycyclic aromatics are also known to be effective electron scavengers and interpretation of the effect of pyrene on the polymerisation process requires due consideration of the dual nature [9] displayed by this class of compound.

### Electrons

Electrons of a range of energies will be produced within the film as a result of ionisation of matter and thermalisation of the incident electron beam [11].

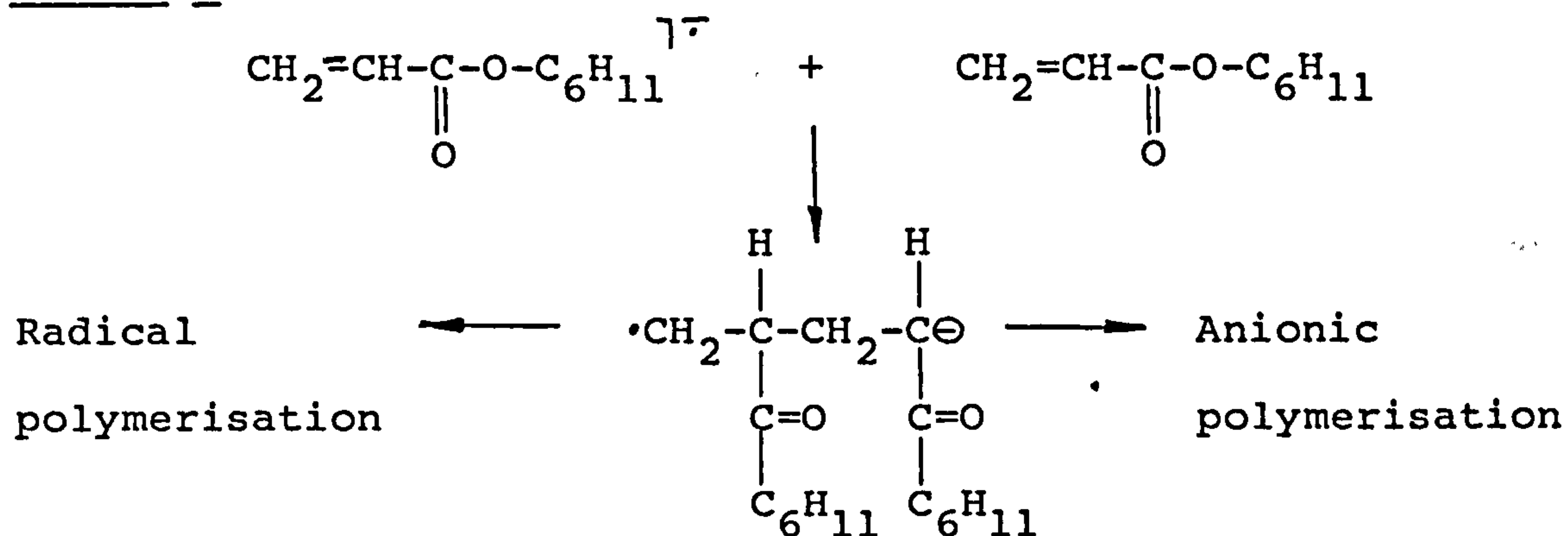
Eventually all electrons will become thermalised. The fate of these subexcitation electrons will be solvation and scavenging by the monomer to form a radical anion as shown below

### Scheme 3



Evidence for the formation of the radical anion (1) comes from the observation that, on irradiation at low temperatures, a solvated electron will add to a carbonyl group to produce a radical anion [12]. Roger et al [13] proposed that on irradiation of cyclohexylacrylate, a radical anion is produced, resulting in simultaneous radical and anionic polymerisation.

Scheme 3 contd.



These workers provided evidence for the involvement of a radical anion in the initiation process from the observation that, addition of proton donors, such as an alcohol, inhibited the formation of the high molecular weight fraction associated with anionic polymerisation.

If slow electrons are important in generating the initiating species then any additive having a lower reduction potential than the acrylate ester will act as an electron scavenger and quencher of the curing process. The effect of such effective electron acceptors as m-dinitrobenzene [14], azobenzene [14] and pyrene [10] (see Table 1 for their respective reduction potentials) on the polymerisation of an acrylate ester was therefore investigated here. Although m-dinitrobenzene is generally regarded as an inhibitor or retarder of radical polymerisation, Kice [15] showed that m-dinitrobenzene has little effect on the polymerisation of the acrylate ester, methyl acrylate. The first and second halfwave reduction potentials of m-dinitrobenzene are -0.9V and -1.25V respectively [14] and <sup>it</sup> is therefore expected to behave as an



effective electron scavenger. Addition of azobenzene to an alkylacrylate is of particular relevance to the commercial user as a large majority of dyes used by the industry are derived from azobenzene. The first and second halfwave potential of azobenzene are  $-1.41\text{V}$  and  $-1.76\text{V}$  [14] respectively, which suggest that azobenzene may also be classified as an efficient electron scavenger.

Haloaromatics are also readily reduced [16], however, the radical anion formed will fragment to produce an aryl radical capable of initiating polymerisation and a halide ion [17,18]. These electron scavengers would thus be expected to promote radical polymerisation. The effect of 1,3,5-trichlorobenzene on the polymerisation of an acrylate ester was also investigated here.

#### Excited states

As mentioned previously excited states may be produced as a result of direct excitation by low energy electrons, radical cation and electron recombination, or via an energy transfer process. If recombination of the radical cation and its geminate electron are important in the generation of excited states and ultimately radical formation, then addition of a solute of high electron affinity will once again retard the polymerisation process. The addition of an aromatic species, such as pyrene, may also be expected to inhibit polymerisation of an acrylate ester, if excited states are important in generating initiating radicals due

to the protective action that aromatic compounds exhibit (see Chapter 6).

It is also known that superexcited states will be formed on electron beam irradiation of matter. The fate of which may be autoionisation, unimolecular dissipation of excitation energy, or monomolecular detachment of hydrogen atoms capable of initiating polymerisation in conjunction with its carbon centred radical [19].

Homolytic fragmentation of C-H bonds has been proposed [20] to be the most important method of generating radicals required to initiate the free radical polymerisation of acrylate esters.

Although the addition of benzoquinone would be expected to inhibit or retard the polymerisation of an alkylacrylate ester [20], the low reduction potential of benzoquinone (see

Table I Electrochemical data of selected compounds  
[10,14,16]

Reduction potentials

<u>Compound</u>	<u>Solvent/supporting electrolyte</u>	<u>Working reference</u>	<u>Electrochemical result, <math>E_{1/2}^0/V</math></u>
Benzoquinone	MeCN; 0.1M TEAP	SCE	-0.52
			-1.14
m-Dinitro-benzene	MeCN; 0.1M TEAP	SCE	-0.90
			-1.25
Azobenzene	MeCN; 0.1M TEAP	SCE	-1.41
			-1.76

Table 1 contd.

<u>Compound</u>	<u>Solvent/supporting electrolyte</u>	<u>Working reference</u>	<u>Electrochemical result, <math>E_{1/2}/V</math></u>
1,3,5-Trichloro-benzene	MeCN; 0.1M TEABr	SCE	-1.99
Pyrene	MeCN; 0.1M TEAP	SCE	-2.49
<u>Oxidation potentials</u>			
1,3,5-Trimethoxy-benzene	MeCN; 0.1M TPAP	SCE	+1.49
Pyrene	MeCN; 0.1M TEAP	Pt wire	+1.25

SCE = Saturated calomel electrode

TEABr = Tetraethylammonium bromide

TPAP = Tetrapropylammonium phosphate

TEAP = Tetraethylammonium phosphate

Table 1) would also suggest that addition of this quinone will also act as a very effective electron scavenger. The effect of the well known radical inhibitor, benzoquinone, on the polymerisation of thin films of the alkylacrylate ester was also investigated.

By monitoring the cure response of an acrylate ester in the presence of these additives, the relevance of those primary products, generated as a result of electron beam irradiation, capable of promoting radical polymerisation of acrylates may be indicated.

Apart from the fundamental interest in radiation induced polymerisation, there is considerable practical significance of these experiments with regards to the

commercial user of electron beam formulations. Radiation curable formulations can be complex and the effect each component has on the cure response of the system is not easily discernible by investigating such systems. It is therefore of relevance to evaluate the effect of an additive on the cure of a simple alkylmonoacrylate ester. The unsaturated monomer used to monitor cure efficiency was isodecyl acrylate. The cure response of such a two component systems was determined 'quantitatively' using transmission FTIR spectroscopy [21]. The results of such an investigation may provide information with regards to predicted cure response on addition of those components that comprise a radiation curable formulation.



## RESULTS AND DISCUSSION

In order to make a valid assessment of the cure performance of isodecyl acrylate, IDA, in terms of residual double bonds remaining after electron beam irradiation, it was deemed necessary to firstly evaluate the accuracy of recording the extent of cure by transmission infrared for a given sample. The results of this initial investigation are collated in Table 2. Secondly, the reproducibility of attaining a given dose of radiation using the Otto Durr electron beam line was also assessed. This was carried out by recording the percentage degree of cure of a series of films of IDA cured over the dose range (0-100)kGy on five different occasions. These results are presented in Table 3. The absorbance peaks associated with the double bond content of IDA used to monitor the extent of cure were, the  $1640/1620\text{cm}^{-1}$  band, associated with the carbon carbon double bond symmetric stretching frequency and the  $810\text{cm}^{-1}$  overtone frequency respectively, as well as the  $810\text{cm}^{-1}$  peak due to the C-H deformation of the acrylate group. In both cases the internal standard at  $1380\text{cm}^{-1}$  associated with the  $\text{CH}_3$ - twist was used to correct for differences in film thickness. As can be seen from Table 2, excellent reproducibility of results using transmission infrared can be achieved and all results are within  $\pm 2\%$  error. It was also found that reproducibility of the extent of cure of IDA for a given dose of radiation on different test runs (see table 3) was also consistent within  $\pm 3\%$  error.

Table 2 The average percentage degree of cure of IDA at various doses of radiation for 5 samples

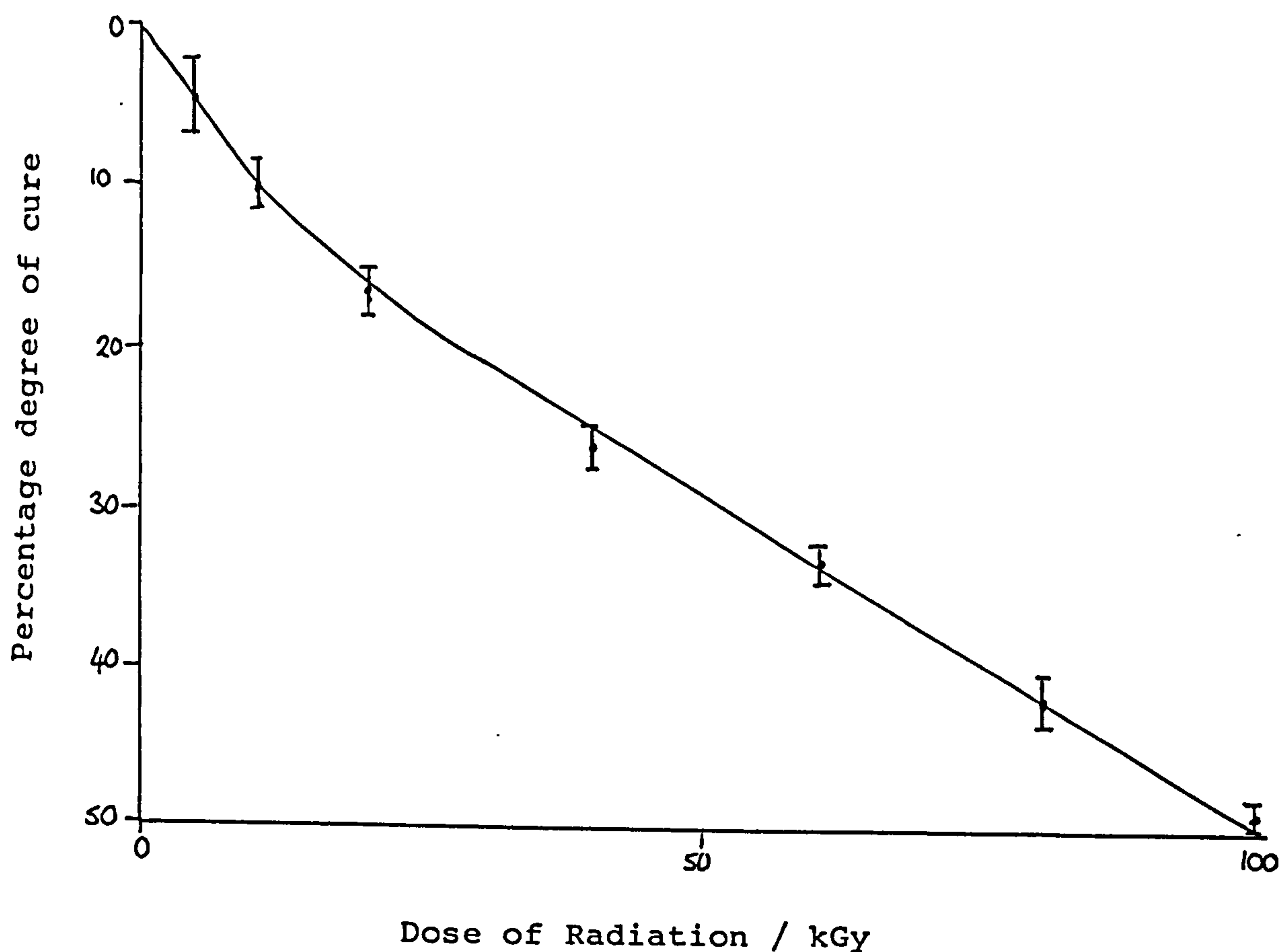
Dose of radiation /kGy	Average % unsaturation using 1640cm <sup>-1</sup>	σ	Average % unsaturation using 810cm <sup>-1</sup>	σ
0	0		0	
5	6	0.632	4	0.748
10	11	0.632	9	0.748
20	18	0.748	16	1.166
40	27	1.020	25	1.020
60	35	0.748	32	1.414
80	43	1.020	40	0.837
100	52	1.166	49	0.748

Table 3 The percentage degree of cure of IDA cured on 5 different test runs.

Dose of radiation /kGy	Average % unsaturation using 1640cm <sup>-1</sup>	σ	Average % unsaturation using 810cm <sup>-1</sup>	σ
0	0		0	
5	4	2.280	2	1.020
10	10	0.632	6	1.166
20	16	1.414	13	2.280
40	26	1.020	24	1.414
60	33	0.748	30	1.747
80	41	1.743	40	0.632
100	49	1.743	48	1.414

Examination of Figure 1 shows that IDA cures at a slightly faster rate initially. This observed slight deviation from linearity may be genuine, however, it is more likely that this effect is the result of selecting an appropriate baseline for the internal standard absorbance

Figure 1 The percentage degree of cure of IDA at various doses of radiation.

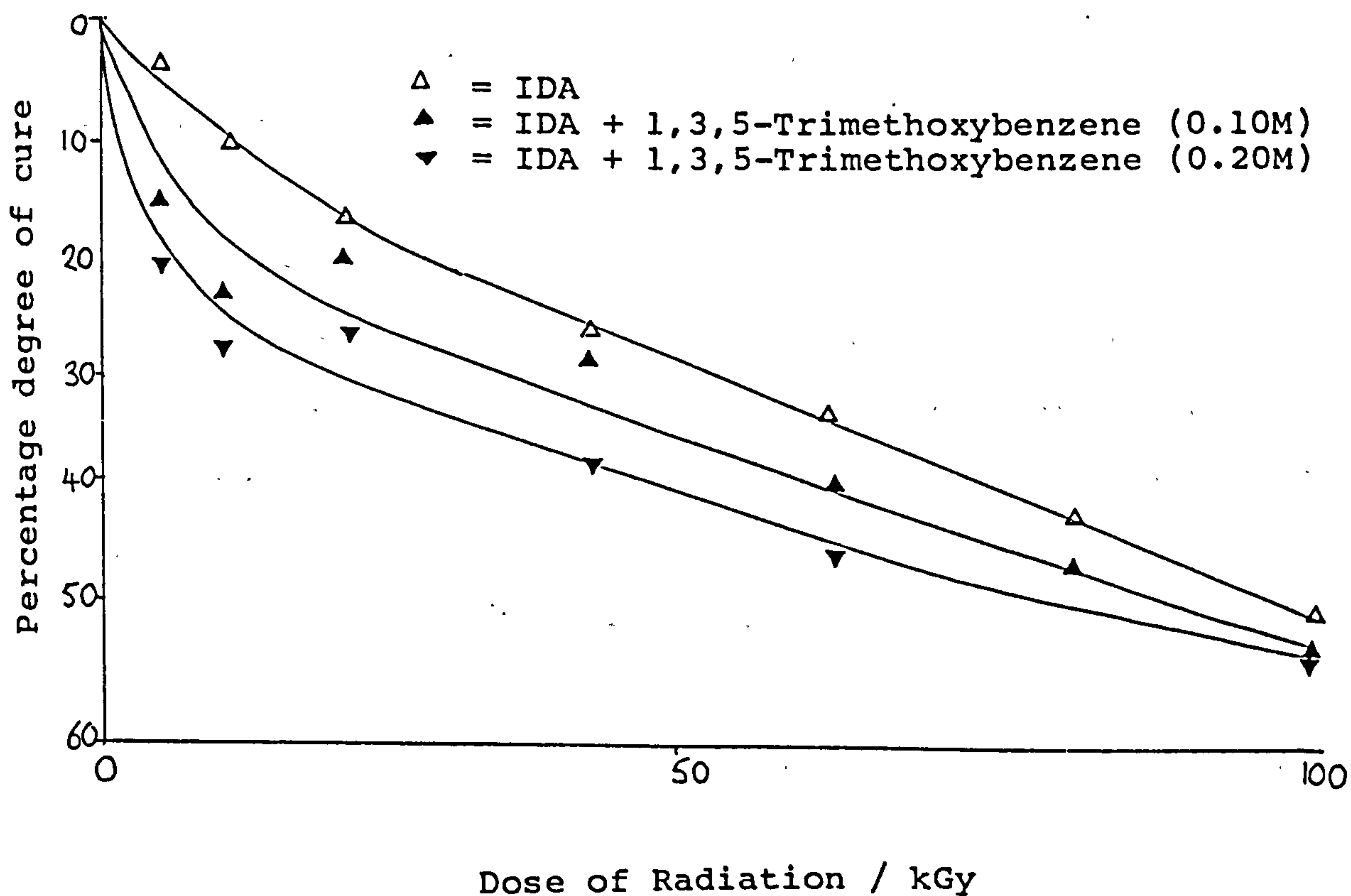


peak at  $1380\text{cm}^{-1}$ . The  $1380\text{cm}^{-1}$  absorbance band overlapped slightly with neighbouring peaks, which may have resulted in a small deviation of baseline definition, and in turn reflected by the measured cure response.

Calculations of the percentage cure of IDA in the presence of the additives studied here, required the use of the technique of spectral subtraction. This was essential in order to eliminate interference of those absorbance bands associated with the additive and the absorbance peaks of IDA, required to evaluate percentage degree of cure.

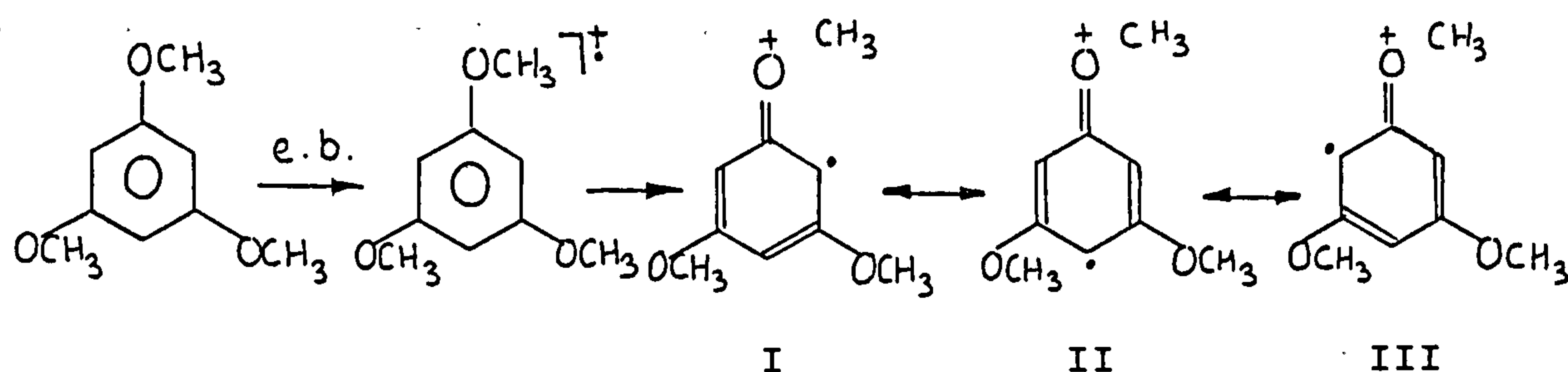
Addition 1,3,5-trimethoxybenzene was shown to enhance the extent of cure of IDA significantly on increasing the amount of the additive (Figure 2).

Figure 2 Percentage degree of cure of IDA in the presence of 1,3,5-trimethoxybenzene at various doses of radiation





It has been shown from electrochemical studies of aryl ethers [10] such as, 1,3,5-trimethoxybenzene, that these compounds are readily oxidised to form a radical cation and are therefore predicted to scavenge holes. The ease with which 1,3,5-trimethoxybenzene gives up an electron is primarily due to the lone pair interaction of the methoxy groups with the ring, shown by the classical resonance structures I, II and III.

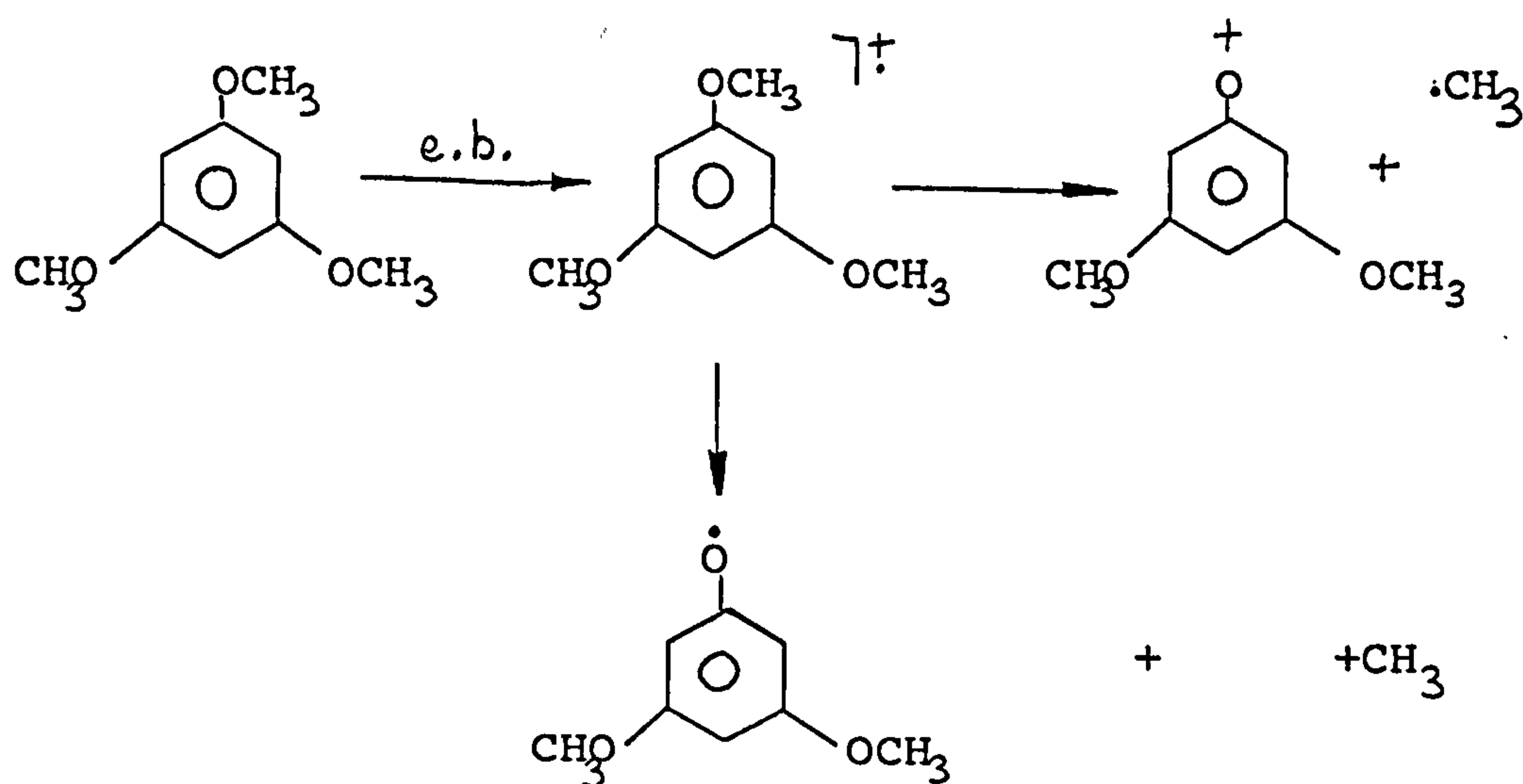


Thus the radical cation of 1,3,5-trimethoxybenzene retains aromatic character due to the contribution of the oxygen lone pair. The observed increase in cure rate of IDA in the presence of 1,3,5-trimethoxybenzene (Figure 2) indicates that radical cations are not important in the initiation of polymerisation of acrylate esters. This result was not unexpected as it is known [8] that the majority of primary radical cations will recombine with their geminate electron to form an excited state molecule. In fact the observed result may indicate the importance slow electrons and ultimately radical anions play in the initiation process. This result is consistent with those results obtained by Roger [13].

However, it was observed that there was a significant

reduction in the extent of cure at higher dose rates. A possible explanation for this observed trend may be gleaned from the fragmentation patterns of methoxybenzene derived from mass spectroscopy experiments [22]. The decomposition of methoxybenzene in the gas phase was shown to yield the phenoxy radical as one of its products, which will act as a chain terminator and thus retard the polymerisation process. The initial cure enhancement of IDA may also be due to the coproduction of a methyl radical capable of promoting polymerisation.

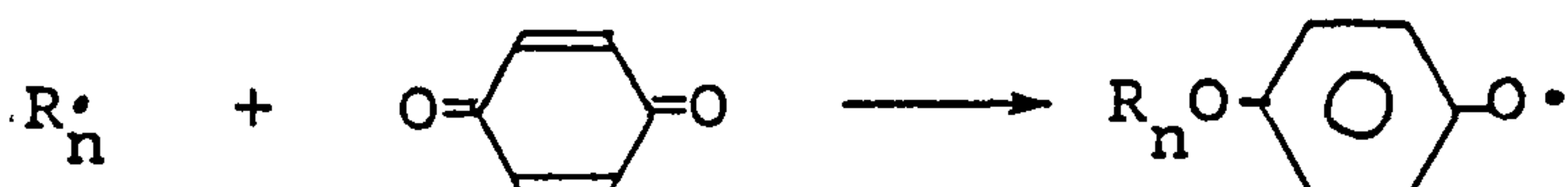
Scheme 1



1,4-Benzoquinone was found to be a very effective inhibitor of the polymerisation of IDA (Figure 3). This is not surprising since 1,4-benzoquinone is a very effective radical scavenger and is known to inhibit and/or retard the polymerisation of acrylate derivatives [20]. Inhibition of the polymerisation of IDA in the presence of benzoquinone may be the result of addition of the propagating radical to

the oxygen of the quinone,

Scheme 2



The unreactive phenoxy radical thus formed may terminate another propagating chain as follows

Scheme 3

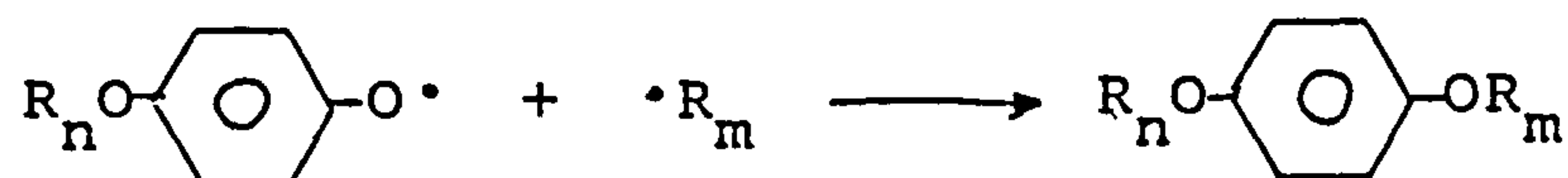
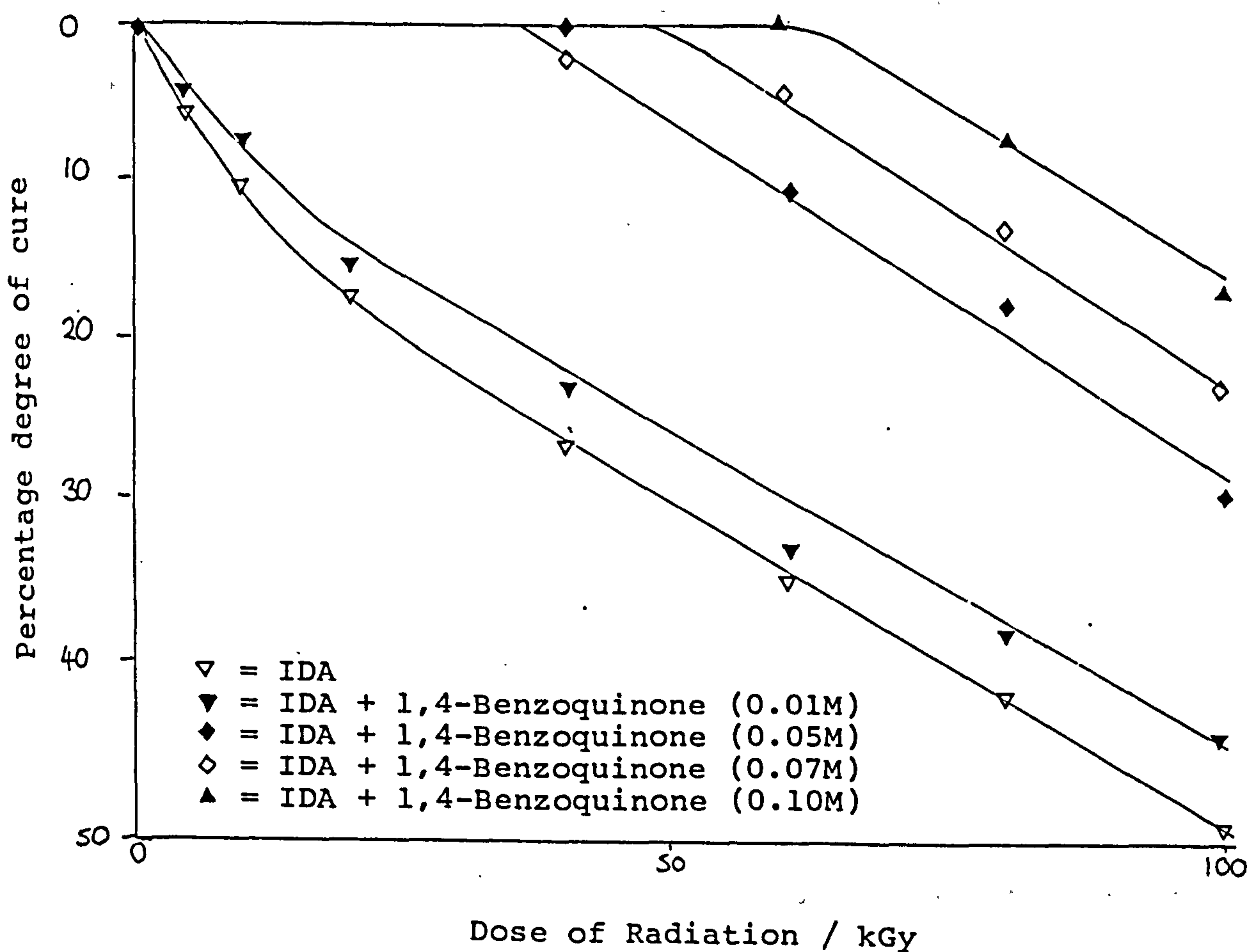
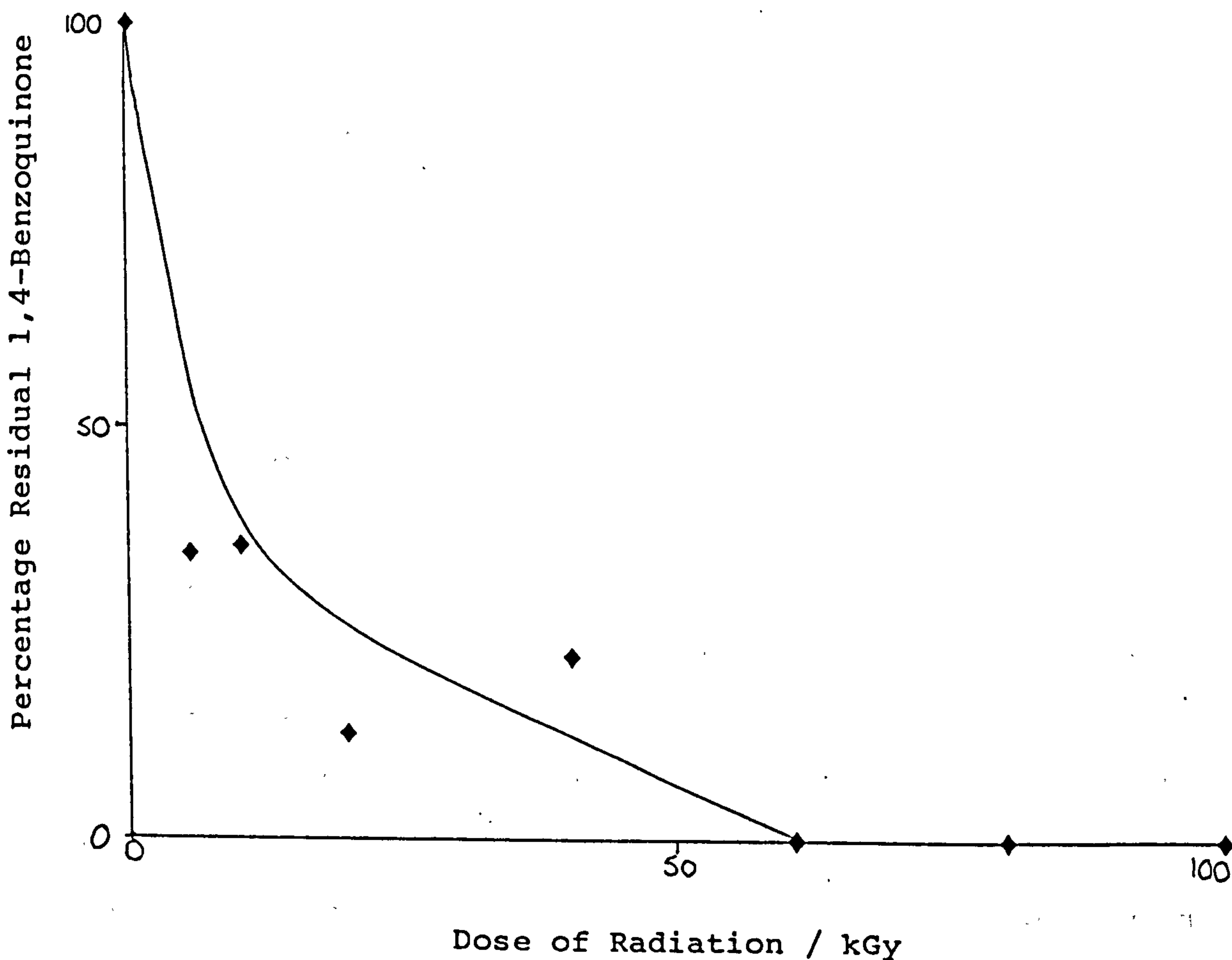


Figure 3 Percentage degree of cure of IDA in the presence of 1,4-benzoquinone at various doses of radiation



By use of spectral subtraction it was possible to monitor the decomposition of 1,4-benzoquinone at its highest concentration of approximately 0.1M. The decomposition of 1,4-benzoquinone was evaluated by monitoring the peak associated with the C=O stretching frequency at  $1628\text{cm}^{-1}$ . As can be seen from Figure 4 the decomposition of 1,4-benzoquinone was found to be complete at 60kGy, the dose at which polymerisation of IDA is initiated.

Figure 4 The percentage residual benzoquinone in films of IDA cured in the presence of benzoquinone (0.10M)

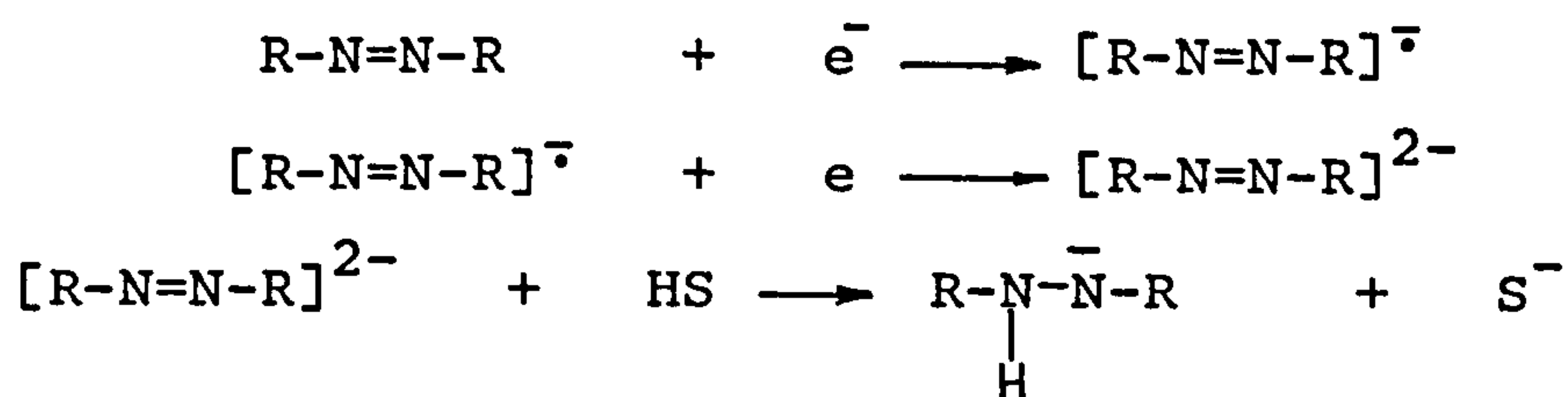




Azobenzene, pyrene and 1,3-dinitrobenzene were used to determine the effect additives of high electron affinities, as evaluated from their polagraphic data, have on the efficiency of electron beam induced polymerisation of IDA.

As can be seen, from Figure 5 the cure of IDA was markedly inhibited and retarded by the addition of azobenzene. Azobenzene will undergo electroreduction in two one electron step additions, the first of which results in the formation of a radical anion and the second electron transfer process being followed by a fast chemical reaction consisting of a protonation step of the dianion to produce a monoanionic state [14]

Scheme 4



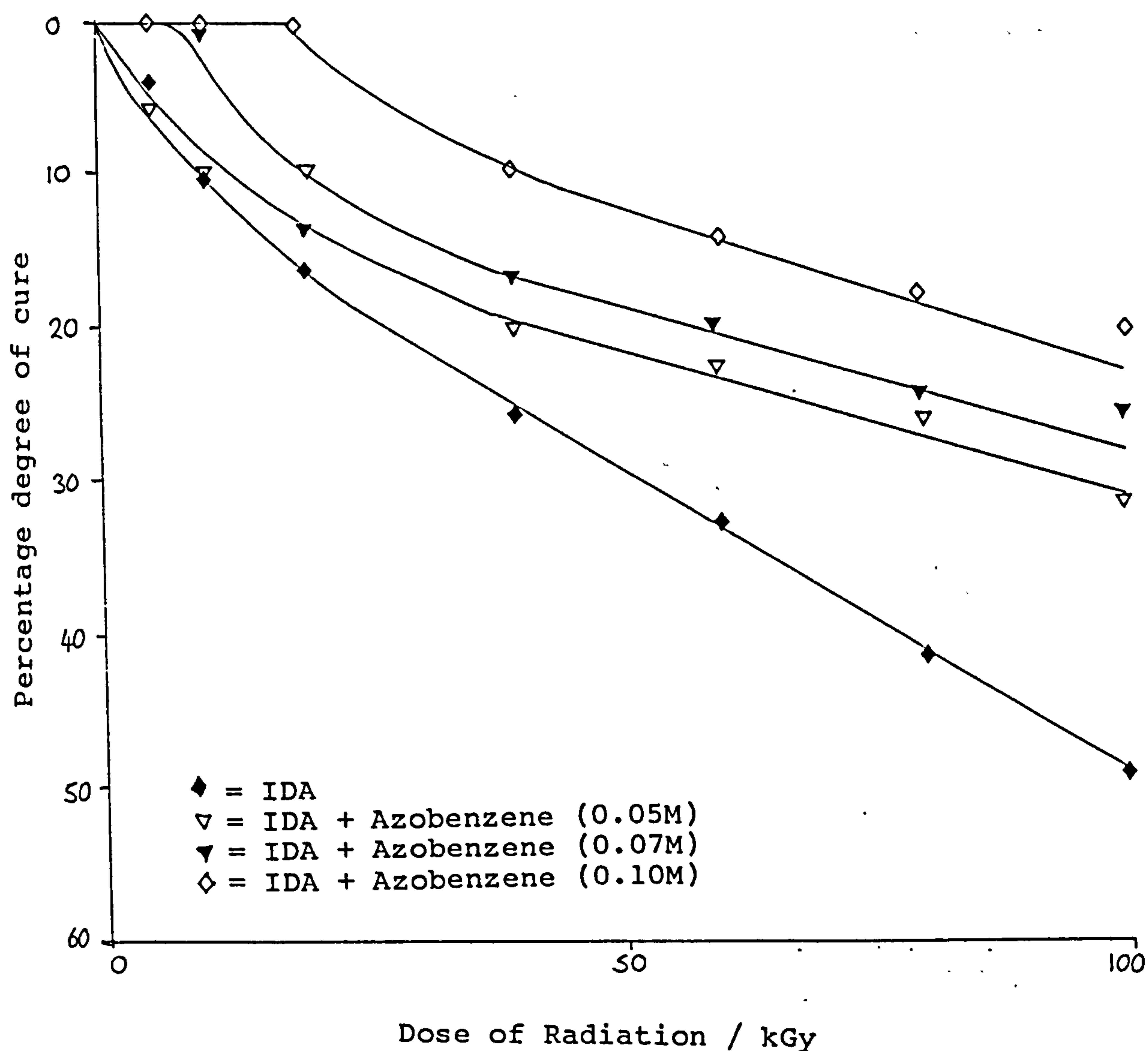
where HS is a source of protons.

The observed result indicates that azobenzene is acting as an effective electron scavenger and thus inhibiting either recombination of an electron with its parent cation to form an excited state or preventing electron capture by the acrylate to generate a radical anion capable of promoting both radical and anionic polymerisation. The contribution of the anionic polymerisation of IDA is not expected to be of significance under our experimental conditions, as this process will be effectively quenched as a result of protonation of the propagating chain due to

moisture present in the nitrogen blanket.

This result illustrates the importance slow electrons play in the initiation of polymerisation.

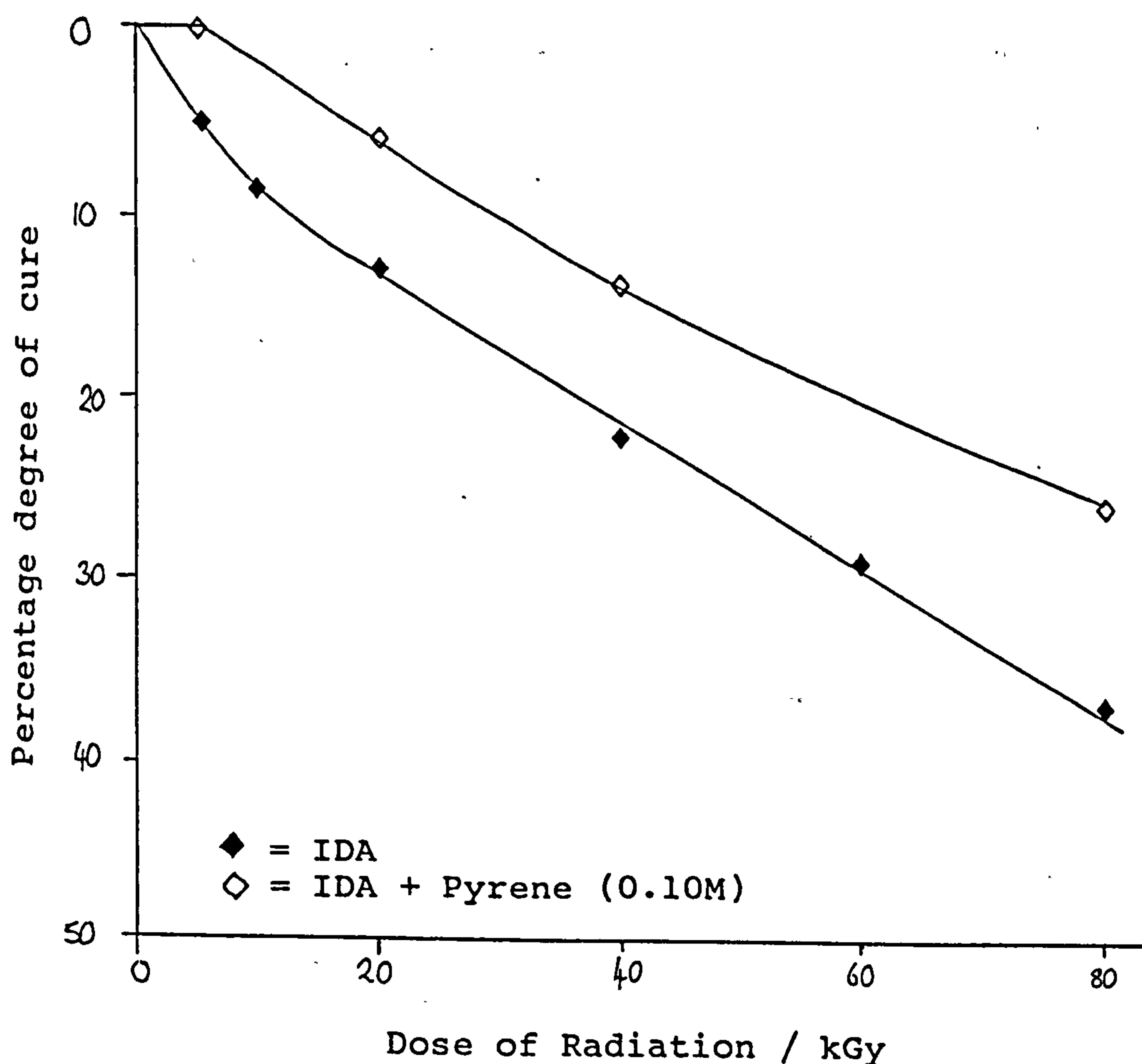
Figure 5 Percentage degree of cure of IDA in the presence of azobenzene at various doses of radiation



The addition of pyrene to IDA also resulted in inhibition of cure of IDA. This would indicate that pyrene is acting as a electron scavenger and may undergo rapid formation of a radical anion, followed by the addition of a

second electron to yield a dianionic radical. Such two electron radical anions are expected to undergo protonation as shown from electrochemical data of polycyclic aromatics [20]. Once again this provides evidence that slow electrons are important in the cure process.

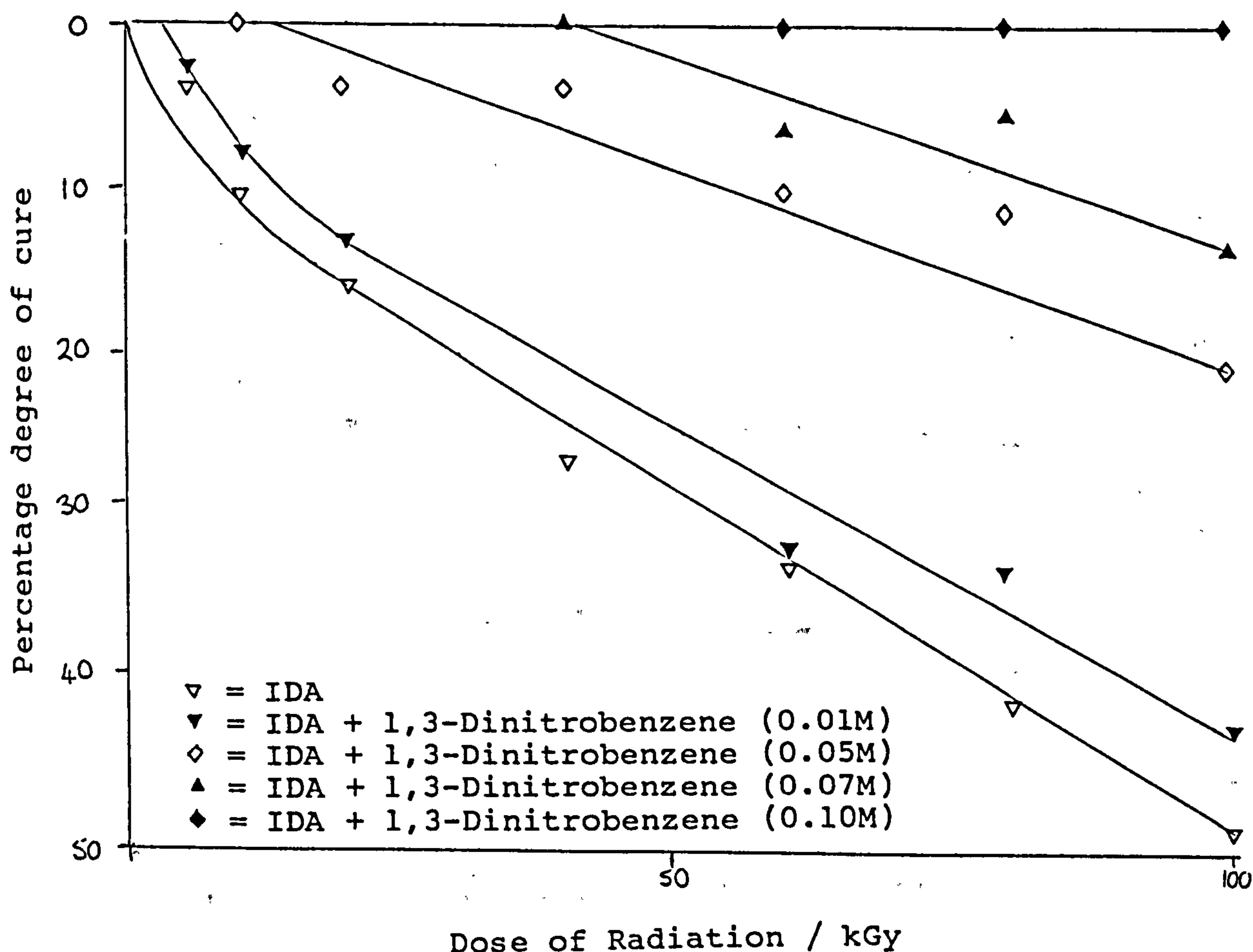
Figure 6 Percentage degree of cure of IDA in the presence of pyrene at various doses of radition



Addition of 1,3-dinitrobenzene to IDA resulted in considerable inhibition and slight retardation of polymerisation of IDA (See Figure 7). Aromatic nitro compounds are an important class of retarders, although they

are generally less effective than quinones [20]. However, Kice [15] has shown that m-dinitrobenzene has very little effect upon the polymerisation of methyl acrylate. This is in direct conflict with the result obtained here, which suggests that m-dinitrobenzene is not only an effective inhibitor/retarder but is more effective than p-benzoquinone.

Figure 7 Percentage degree of cure of IDA in the presence of 1,3-dinitrobenzene at various doses of radiation

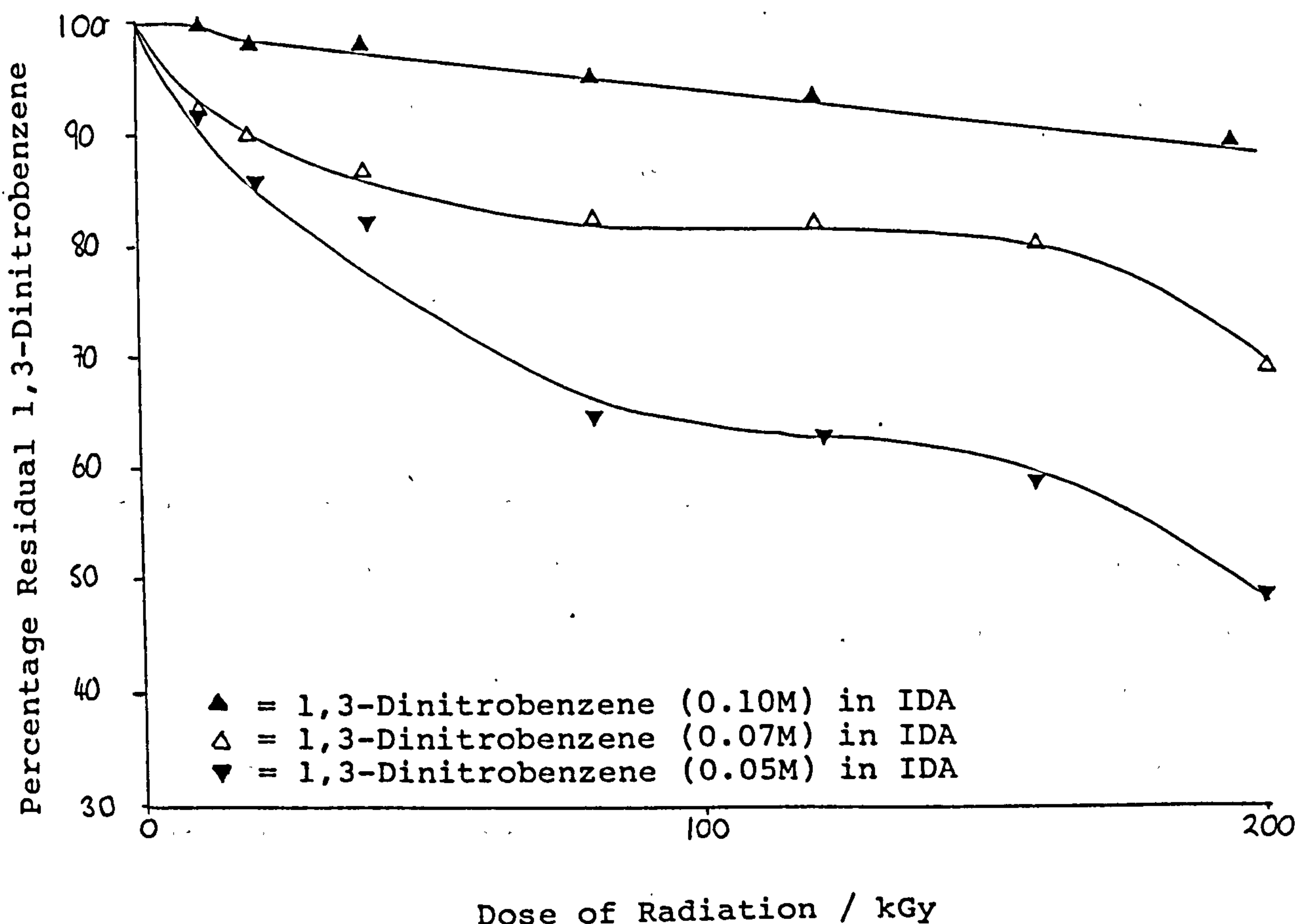


It was also noticed that films of IDA containing m-dinitrobenzene turned progressively yellow on increasing



the dose of radiation and from examination of the transmission spectra of these films it was also noticed that the nitro asymmetric stretching frequency at  $1540\text{cm}^{-1}$  decreased in intensity in conjunction with the simultaneous growth of a neighbouring peak centred at  $1534\text{cm}^{-1}$  (see Figure 8). The observed absorbance band at  $1534\text{cm}^{-1}$  may be indicative of the attack of a propagating radical on the aromatic ring generating an alkyl substituted dinitro-aromatic, thus conferring a perturbation of the nitro stretching frequency [22].

Figure 8 Percentage residual 1,3-dinitrobenzene at various concentrations in IDA over a range of doses of radiation

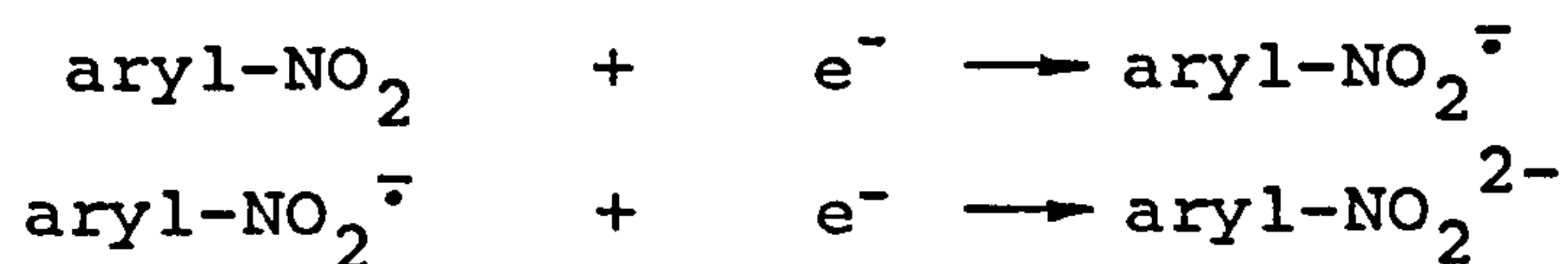


However, it is unlikely that alkylsubstituted dinitrobenzene compounds would exhibit the observed significant colour change. Since most alkyl substituted dinitrobenzene compounds do not absorb light beyond the UV range [22].

Whilst the potential of m-dinitrobenzene to act as an inhibitor of acrylate polymerisation must not be overlooked an alternative explanation may be gleaned from the fact that m-dinitrobenzene is readily reduced as indicated from its polagraphic data shown in Table 1 and may thus be classified as an effective electron scavenger. It is therefore proposed that m-dinitrobenzene primarily acts as an electron scavenger thus reflecting the importance that slow electrons play in the polymerisation process.

Aromatic nitro compounds have been studied polagraphically in aprotic solvents and have been shown to undergo two one electron reductions

Scheme 5

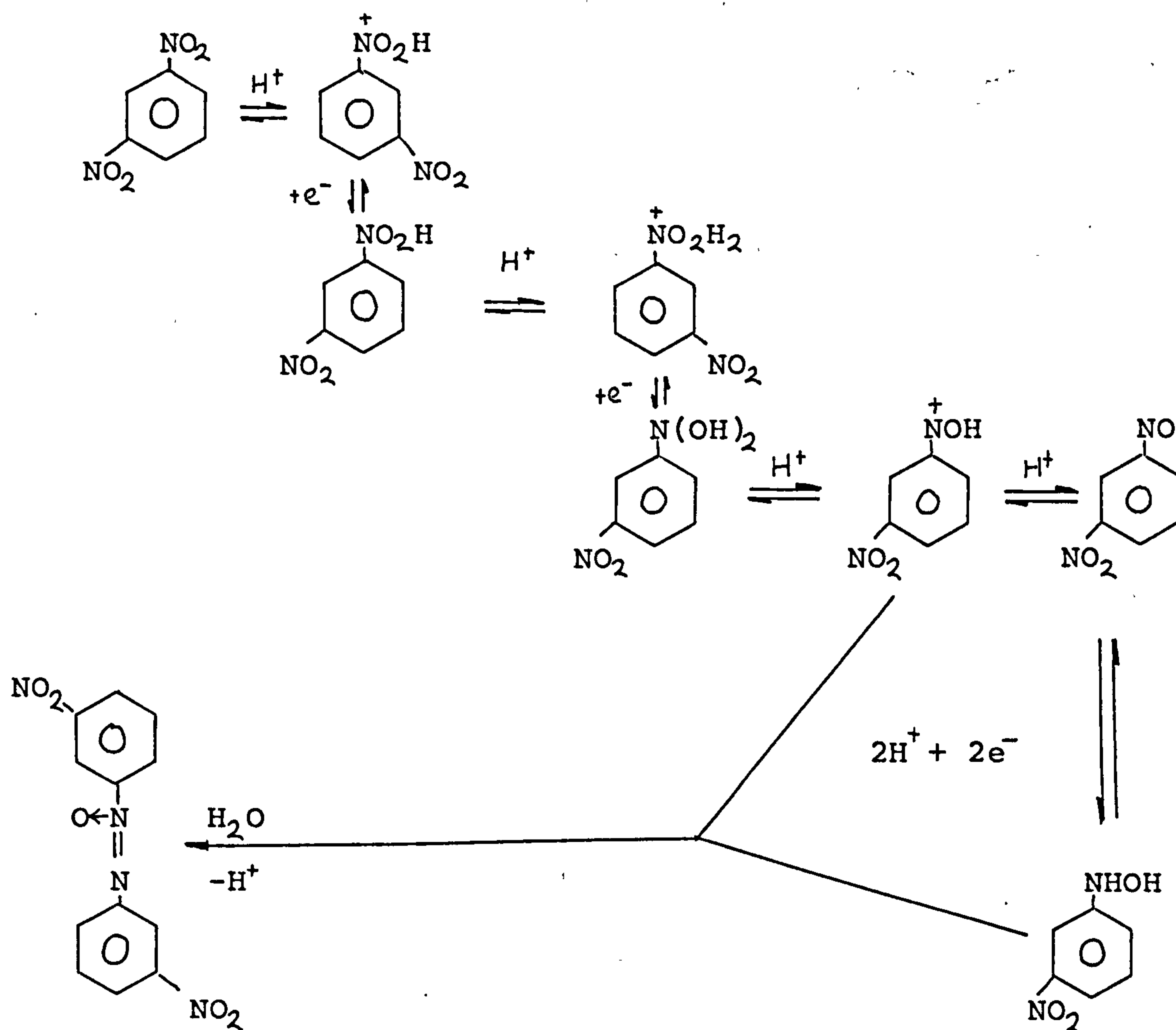


Reduction of nitroaromatics in protonic systems is very complex. Since, moisture is expected to be present under our experimental conditions the reduction of m-dinitrobenzene may ultimately produce m,m'-dinitroazoxybenzene as depicted in Scheme 6. The formation of an azoxybenzene derivative would account for the yellowing observed for cured films of IDA containing m-dinitrobenzene, since, these compounds are known to be highly coloured [23].

Since the chemistry of these additives didn't fall

within the remit of the project, further work was not undertaken. However, these findings may provide the basis of a further worthwhile project.

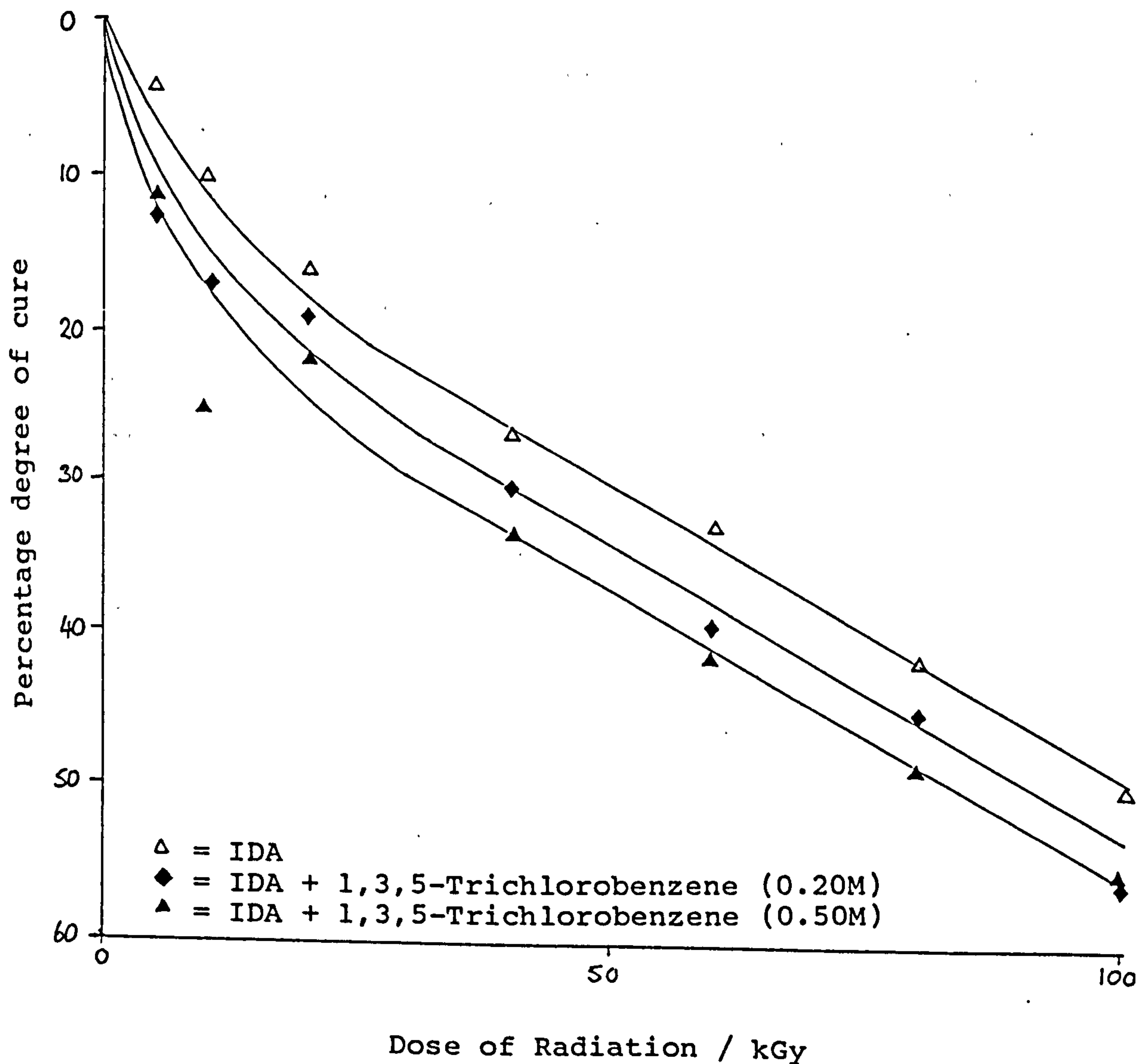
Scheme 6



The effect of 1,3,5-trichlorobenzene upon the efficiency of cure of IDA was also investigated. 1,3,5-Tri-chlorobenzene also has a low reduction potential (see Table 1) and is known that haloaromatics are easily reduced to generate the radical anion in which the charge is delocalised in the aromatic ring, and finally localised in the halogen atom dissociated [17]. The observed increase in

the extent of polymerisation may be attributed to the production of aryl radicals, created as a result of the dissociative electron capture, which may initiate polymerisation. When more than one halogen atom is present the polyhaloaromatic has the potential to yield more than one radical and promote crosslinks.

Figure 9 Percentage degree of cure of IDA in the presence of 1,3,5-trichlorobenzene at various doses of radiation





## CONCLUSION

It has been shown that additives, such as 1,4-dinitrobenzene and azobenzene, which are readily reduced to form radical anions, inhibit the polymerisation of IDA. This indicates that the role of slow electrons is important in the polymerisation process and from which it may be inferred that addition of a component of greater electron affinity than the monomer may inhibit polymerisation, either by preventing geminate radical cation - electron recombination or, the formation of a radical anion.

Addition of a polyhaloaromatic was shown to enhance the cure of IDA and would indicate that dissociative electron capture was responsible for promoting polymerisation of the acrylate ester.

The role of radical cations upon the initiation of polymerisation was more difficult to assess, however, addition of 1,3,5-trimethoxybenzene, which is readily oxidised, resulted in significant cure enhancement of IDA. This indicates that radical cations do not play a significant role in the initiation of polymerisation.

## EXPERIMENTAL

### Materials

Isodecylacrylate, IDA (BASF) was used as received.

The following commercial compounds obtained from Aldrich Chemical Co. were all used as received: 1,3,5-trichlorobenzene, 1,3,5-trimethoxybenzene, 1,2-dinitrobenzene, pyrene, azobenzene, 1,4-benzoquinone.

Aluminum foil (0.051mm gauge) (BDH Chemicals Ltd.) was used as a substrate for all coatings.

### Instrumentation

The diluent was coated onto a moving web via a Dixon coater unit.

Electron beam curing was carried out using a Otto Durr ESH 150/130 electron beam unit under a nitrogen blanket. The operating voltage was maintained at 150kV and the beam current was adjusted for each applied dose.

Infrared spectroscopic data were obtained using a Digilab FTS-60 Fourier transform infrared spectrometer. The moving mirror velocity in the interferometer was  $0.16\text{cm}^{-1}$  and the spectra reported here were recorded at  $8\text{cm}^{-1}$  resolution. All spectra were recorded as a photoacoustic spectrum using a Digilab photoacoustic detector for 4096 scans.

### Preparation of thin films of IDA

All polymer films were coated onto aluminum foil

using a Dixon 164 coater. Even coatweights of about  $10\text{gm}^{-2}$  were obtained using a forward spinning smoothing roller at a setting of 32psi. The coatings were then passed under the electron beam. For doses of radiation (0-100)kGy the moving web was maintained at  $20\text{min}^{-1}$ .

All samples were bottled and stored at -5 C.

Analysis of spectra obtained by Fourier transform transmission infrared spectroscopy.

All electron beam films of IDA resulted in wet films. On exposure to electron beam radiation the acrylate group was reduced in size due to the consumption of carbon carbon double bonds. The disappearance of this group was monitored by the peak at  $810\text{cm}^{-1}$  associated with the CH out of plane deformation of the acrylate group [2,4,25] and the peaks at 1620 and  $1640\text{cm}^{-1}$  associated with the carbon carbon double bond stretch and  $810\text{cm}^{-1}$  overtone frequency respectively, of the acrylate group [4,25].

The use of an internal standard was employed to determine percentage change associated with the aforementioned peaks. The peak at  $1380\text{cm}^{-1}$  due to the  $-\text{CH}_3$  bend [26] was chosen as the internal standard as this group was largely unaffected by irradiation.

The area associated with each peak was computed given a predefined baseline, and from which peak ratios were evaluated and the percentage change of a given peak calculated.

Reproducibility of spectra obtained from a given sample was investigated by analysing 5 spectra acquired

from each sample at a given dose of radiation and evaluating the error in measured percentage cure.

Reproducibility of spectra obtained for a given dose of radiation was also investigated. The spectra of 5 individual samples each run at the same dose on different trial runs were recorded and the error in percentage cure was determined.

In order to evaluate the percentage degree of cure of IDA containing an additive it was deemed necessary to subtract the spectrum of the additive superimposed on that of IDA. In order to subtract the spectra of the additive from that of IDA containing the additive, a suitable reference spectrum of the additive must be obtained. The reference spectrum of the additive was achieved by subtracting a spectrum of IDA from that of IDA plus the additive recorded for liquid films of similar pathlength.



## REFERENCES

- [1] A. Charlesby, (1960). Atomic Radiation and Polymers, Pergamon Press.
- [2] A. Chapiro, (1962). Radiation Chemistry of Polymeric Systems, Wiley-Interscience.
- [3] A. J. Swallow, (1973). Radiation Chemistry - An Introduction, Longman.
- [4] A. Kuppermann, W. E. Flucker and O. A. Mosher, (1979). Chemical Reviews, 79 (1), 77.
- [5] R. S. Davidson to be published.
- [6] K. D. Jordan and P. D. Burrow, (1978). Aus. Chem. Revs., 11, 341.
- [7] Y. Tabata, (1985). Proc. Radcure Conf., Basle, Switzerland.
- [8] G. A. Salmon, (1986). Polymeric Mat. Sci. Eng., 55, 195.
- [9] G. Foldiak, Ed., (1981). Radiation chemistry of hydrocarbons, Elsevier.
- [10] A. J. Bard and H. Lund, (1978). Encyclopedia of Electrochemistry of the Elements. Organic section, Vol. XI, Marcel Dekker.
- [11] Farhataziz and M. A. J. Rodgers, Eds., (1987). Radiation Chemistry: Principles and applications, VCH publishers.
- [12] S. Arai. D. A. Grev and L. V. Dortman, (1967). J. Chem. Phys., 46, 2572; T. Shida, S. Iwata and Imanura, (1974). J. Phys. Chem., 78, 741.

- [13] R. Roger, M. H. Rao and K. N. Rao, (1986). Radiat. Phys. Chem., 28 (2), 161.
- [14] A. J. Bard and H. Lund, (1978). Encyclopedia of Electrochemistry of the Elements. Organic section, Vol. XIII, Marcel Dekker.
- [15] J. L. Kice, (1956). J. Polymer Sci., 19, 123.
- [16] A. J. Bard and H. Lund, (1978). Encyclopedia of Electrochemistry of the Elements. Organic section, Vol. XIV, Marcel Dekker.
- [17] N. Kimura and S. Takamuku, (1987). Radiat. Phys. Chem., 29 (3), 179.
- [18] V. G. Plotnikov, (1985). Radiat. Phys. Chem., 26 (5), 519.
- [19] J. E. Wilson, (1974). Radiation chemistry of Monomers Polymers and Plastics, Marcel Dekker.
- [20] Comprehensive Chemical Kinetics, C. H. Bamford and C. F. H. Tipper, Eds., (1976), Vol.14, Elsevier.
- [21] P. R. Griffiths, (1975). Chemical Infrared Fourier Transform Spectroscopy, Wiley-Interscience.
- [22] Sadtler Standard Spectra (Ultraviolet), (1978), Heyden.
- [23] I. L. Finar, (1981). Organic Chemistry, Vol I, 6th Ed., Longman.
- [24] W. O. George, D. V. Hassid, W. C. Harris and W. E. Maddams, (1975). J.C. S. Perkin II, 392.
- [25] G. Plews and R. Phillips, (1979). J. Coat. Technol., 51, 69.
- [26] R. T. Conley, (1972). Infrared spectroscopy, 2nd Ed., Allyn and Bacon.

---

CHAPTER 6

ELECTRON BEAM INDUCED

POLYMERISATION

OF AROMATIC ACRYLATES

---

## Chapter 6 ELECTRON BEAM INDUCED POLYMERISATION OF AROMATIC

### ACRYLATES

Introduction	244
Results and discussion	249
Conclusion	254
Experimental	255
References	261



# Electron beam induced polymerisation of aromatic acrylates

## Introduction

Aromatic compounds afford "protection" towards high energy radiation as illustrated by their low radiation chemical yields. The stability displayed by these materials in comparison to their aliphatic counterparts, has been attributed to the highly conjugated  $\pi$ -electron system. Thus the energy absorbed by an aromatic molecule as a result of exposure to a high energy source of radiation will be readily redistributed over the whole molecule due to the non-localised  $\pi$ -electrons. The high resistance to radiation may also be interpreted in terms of the greater efficiency of radiative or collision induced decay processes by the conjugated  $\pi$ -electrons compared with other classes of compounds [1].

Exposure of aromatic hydrocarbons to an electron beam of high energy will result in the formation of highly excited states. These excited states, as with other classes of compounds will give rise to positive ions and electrons. The production of excited states may also be brought about by geminate recombination of molecular ions with electrons, interaction of secondary electrons and charge neutralisation of positive ions by negative ions.

The chief difference between aromatics and alkanes, with respect to the formation of primary products, is the relative proportions of charged and neutral intermediates.

The superexcited states produced on irradiation of aromatic compounds will generally lead to internal conversion, while saturated hydrocarbons exhibit a higher probability of undergoing autoionisation and the generation of molecular ions.

The behaviour of alkyl substituents in alkylbenzene upon radiolysis will result in the formation of products consistent with its aliphatic chain. However, its reactivity is markedly reduced by the protective action of the benzene ring.



In this way aromatic compounds protect alkanes and hence reduce their sensitivity towards electron beam irradiation [2].

As with benzenoid compounds the radiolysis of alkylbenzene will generally undergo those primary processes similar to that of benzene and hence will give rise to excited states in considerably greater yield than molecular ions [1].

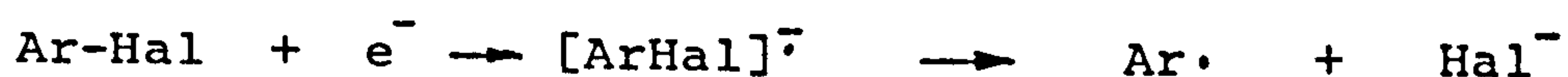
The radiolysis of liquid phase alkylbenzenes results in the formation of gaseous hydrocarbon products governed by the structure of the side chain, and it has been shown that the most important product is methane, except for the case of butylbenzenes, where rupture of the C-C bond in the  $\beta$ -position with respect to the ring is most prevalent [1].

It may also be perceived that for the case of

alkylsubstituted aromatics the electron donating character of the hydrocarbon chain will lower the ionisation potential of the compound and may promote molecular ion yields.

It may therefore be assumed that the sensitivity of oligomers containing aromatic units towards electron beam radiation will be reduced due to the protective action of the aromatic unit. It was therefore proposed to study the reactivity of the difunctional aromatic, catechol diacrylate, compared with its alkylsubstituted analogue, 4-t-butylcatechol diacrylate, assessed by means of obtaining a dry coating. By introducing an alkyl substituent into the aromatic ring the reactivity of 4-t-butylcatechol diacrylate is expected to be enhanced compared with catechol diacrylate, in accord with the greater sensitivity of the alkylbenzenes.

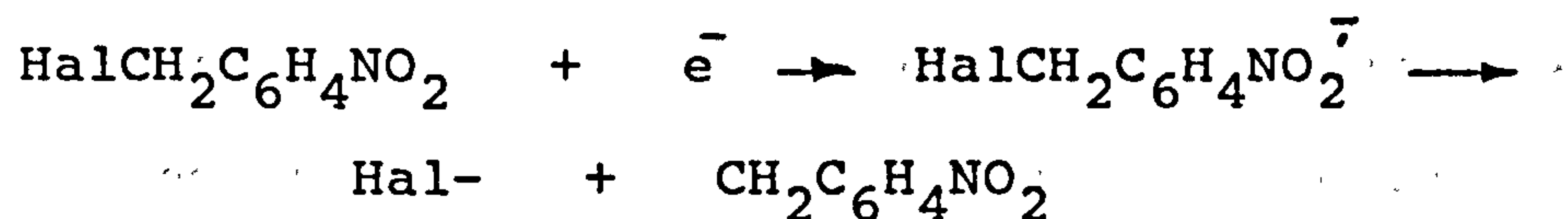
Aromatic compounds will also undergo electron attachment to generate a radical anion. This process is promoted by the presence of electron withdrawing groups about the aryl ring. The haloaromatics readily undergo one electron reduction which immediately leads to the formation of an aryl radical and halide ion. This process is known as dissociative electron capture [3,4].



Behar and Neta [5-9] have shown that when the molecule contains such electrophilic substituents as NO<sub>2</sub> or CN, the



initial radical anion has a finite lifetime before releasing the halide



This process has been interpreted as an intramolecular electron transfer mechanism when an electron associated with the  $\text{NO}_2$  or  $\text{CN}$  groups and the conjugated  $\pi$  system is transferred to the halogen atom to cause scission. These workers also showed that the rates of dehalogenation proceed in the order



The rate of dehalogenation was also shown to depend on the relative position of the halogen atom with respect to the other substituent and proceeded in the order



Datta and Rao [10] have investigated the kinetics of radiation induced polymerisation of phenyl acrylate and showed that this material polymerises readily, however, the molecular weight of the resultant polymer is low. This was attributed to a chain transfer process in which the propagating chain radical abstracts a hydrogen atom from the vinyl group of the monomer. Thus resulting in termination of the propagating chain and generation of an initiating monomer radical.

However, by introduction of a halogen atom about the aryl ring the generation of aryl radicals may be perceived



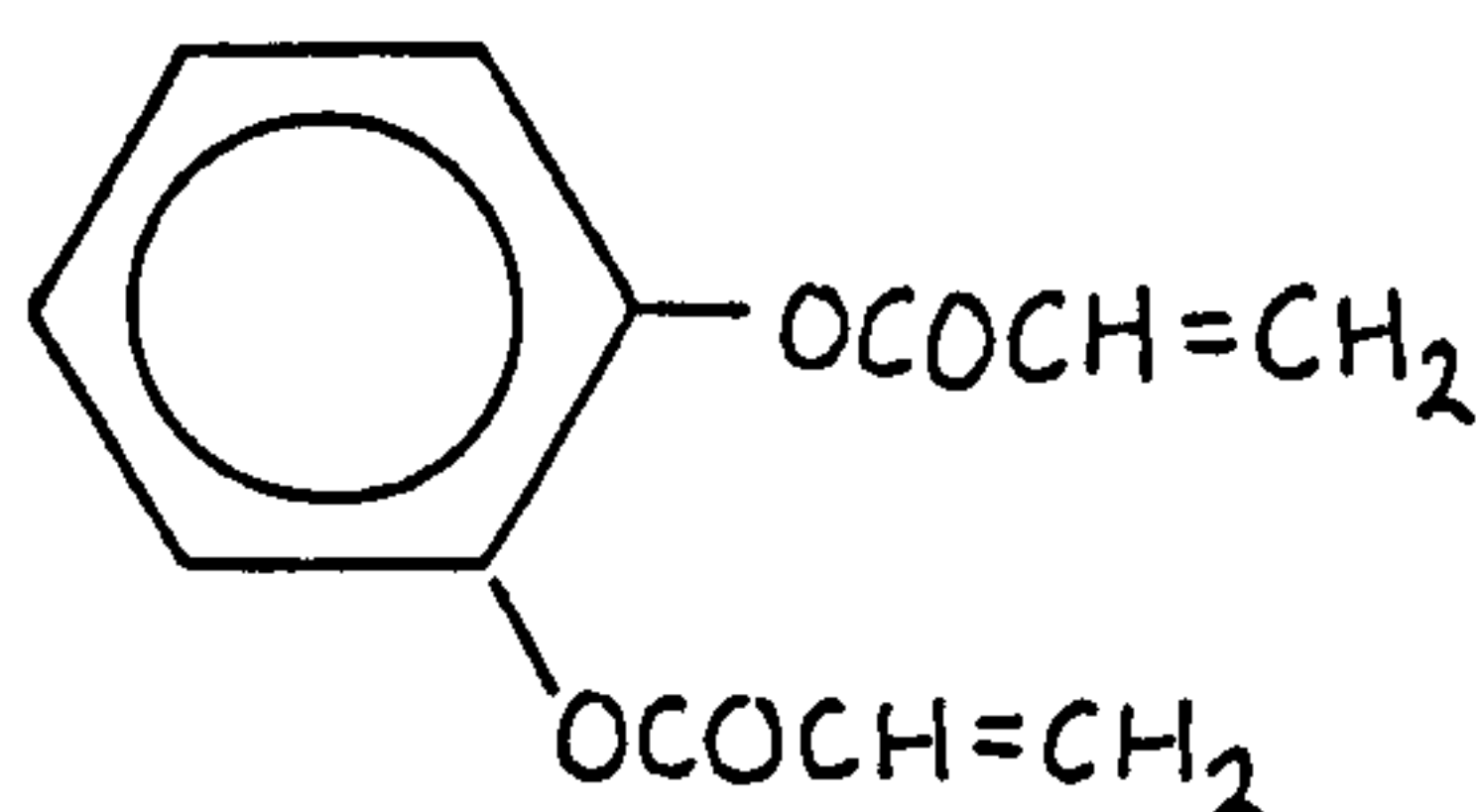
to promote crosslinks or polymerisation, as indicated by the radiolysis of isodecyl acrylate in the presence of 1,3,5-trichlorobenzene (see Chapter 5).

The cure performance of phenyl acrylate compared with mono-, di- and tr-halophenyl acrylates (see Figure 1), as well as the effect substitution patterns play in promoting cure response was undertaken. The cure response of these materials was primarily assessed in terms of producing a touch dry coating and for the case of 1,3,5-trichlorophenyl triacrylate elemental analysis of the film cured at 5 and 40kGy was determined.

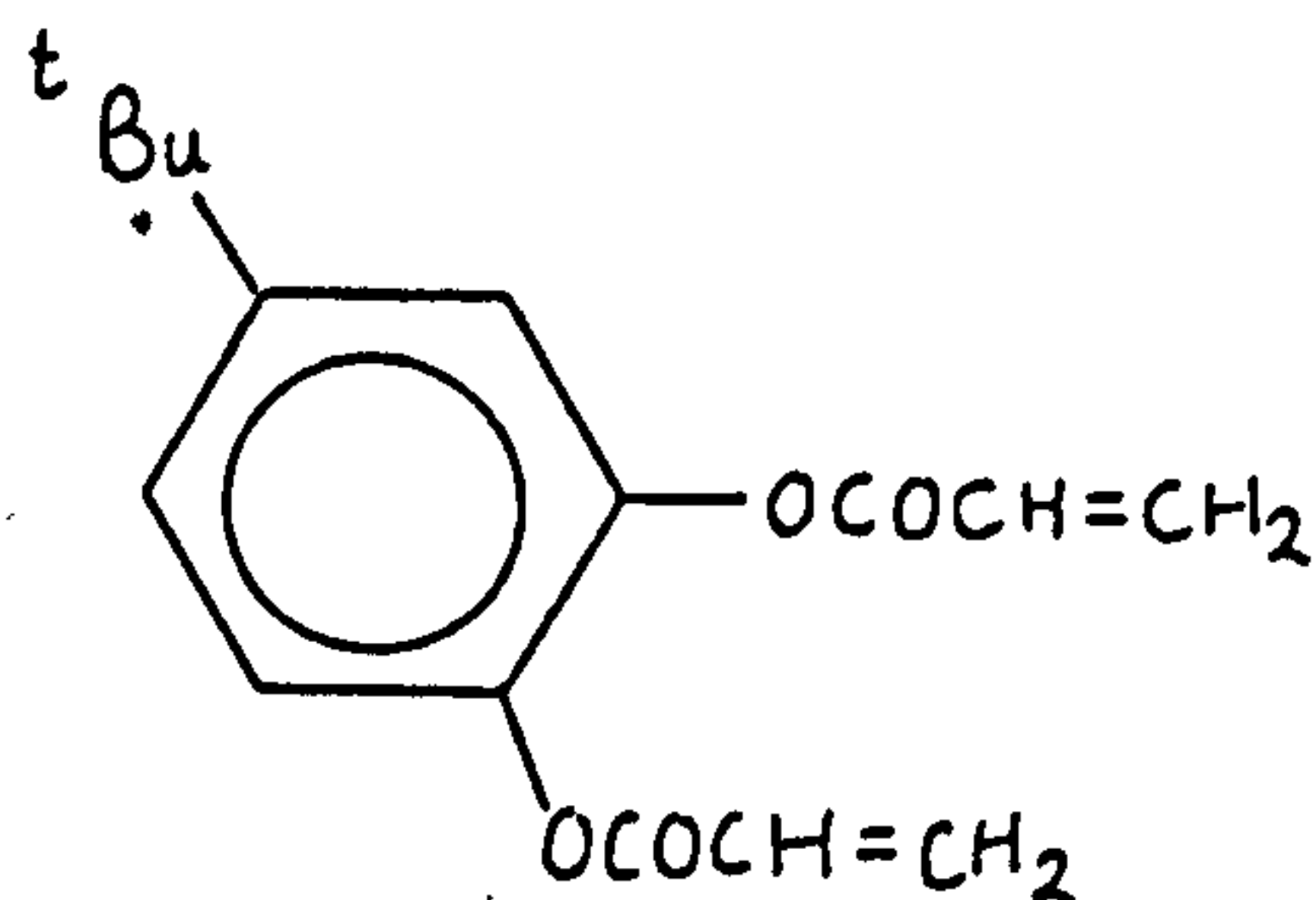
The behaviour of the diacrylate, resorcinol diacrylate, 4-chlororesorcinol diacrylate and 4-bromoresorcinoldiacrylate were investigated to assess the nature of the halogen upon cure response.

## Results and discussion

The two difunctional compounds, catechol diacrylate (I) and 4-*t*-butylcatechol diacrylate (II) were found to

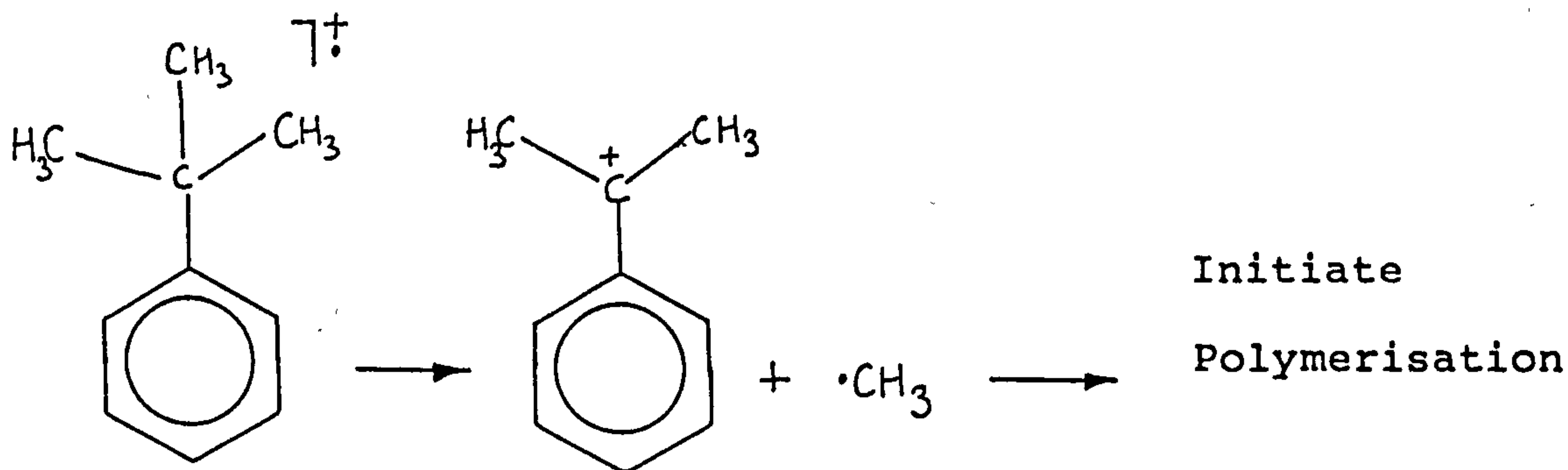


I



II

produce tackfree coatings at a minimum dose of 30kGy and 10kGy respectively. This result illustrates the increased sensitivity of the alkyl<sup>l</sup>substituted catechol diacrylate compared with catechol diacrylate. This may be due to the alleviating effect that an electron donating group can have upon the protective action of aromatics towards electron beam irradiation. Alkyl substituted materials may thus undergo fragmentation resulting in radical and cation production



Examination of Table 1 shows that phenyl acrylate did

not render tackfree coatings even at the high dose of 160kGy. This is consistent with those findings by Datto and Rao [10] who showed that although phenyl acrylate readily polymerised, only low molecular weight polymer was produced.

Table 1 The cure response of halosubstituted phenyl acrylates upon electron beam irradiation

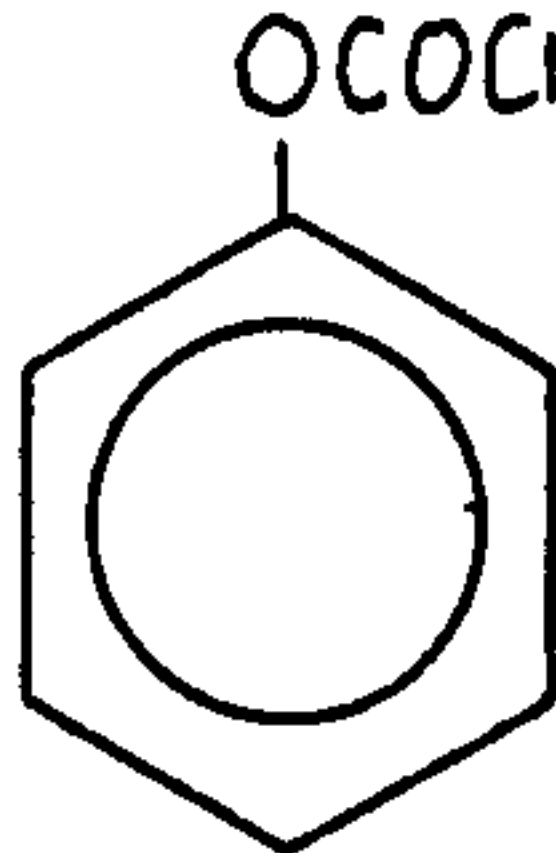
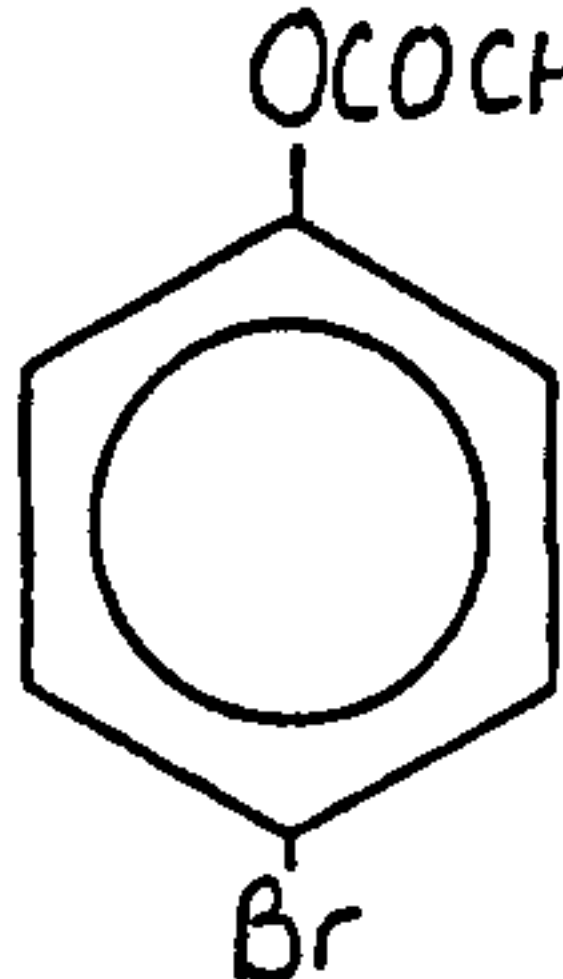
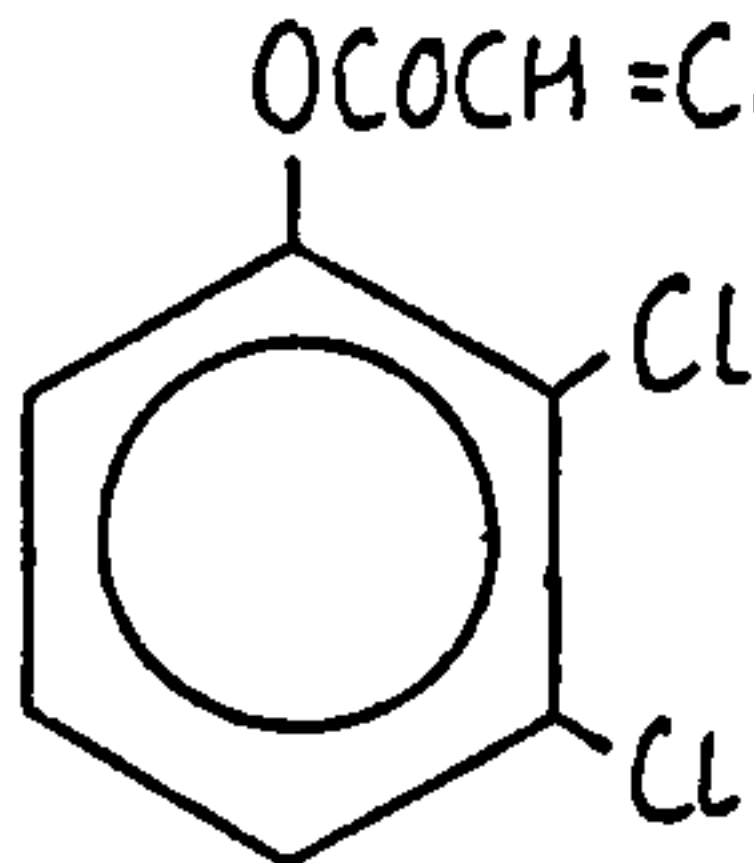
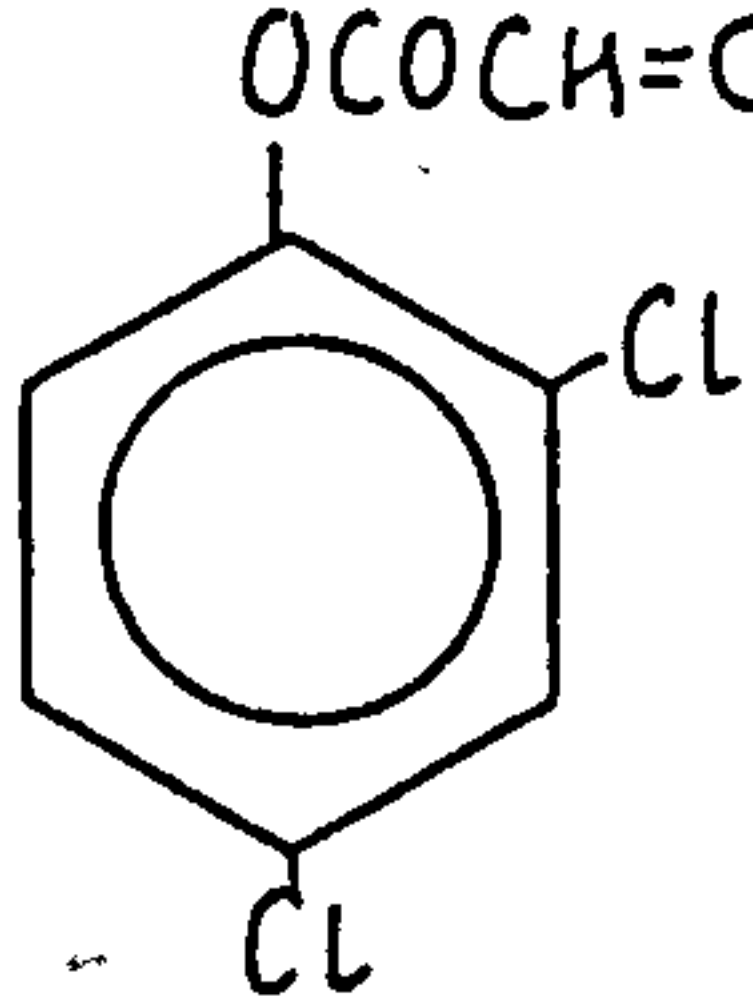
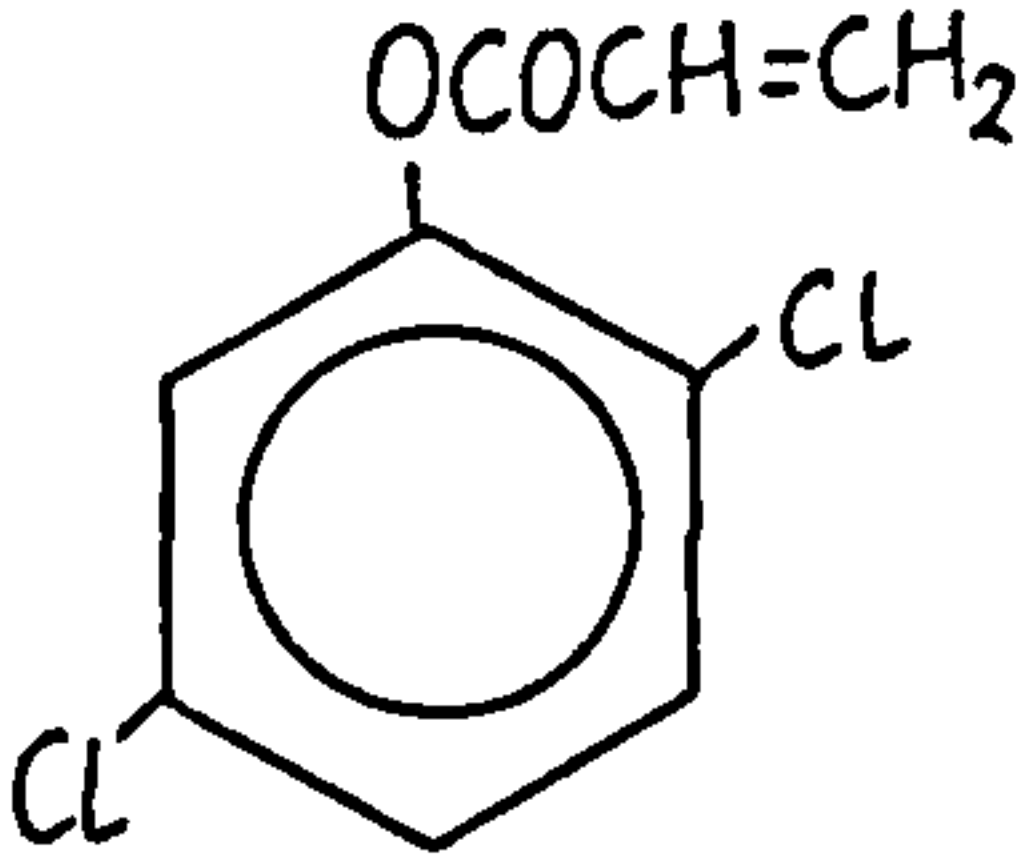
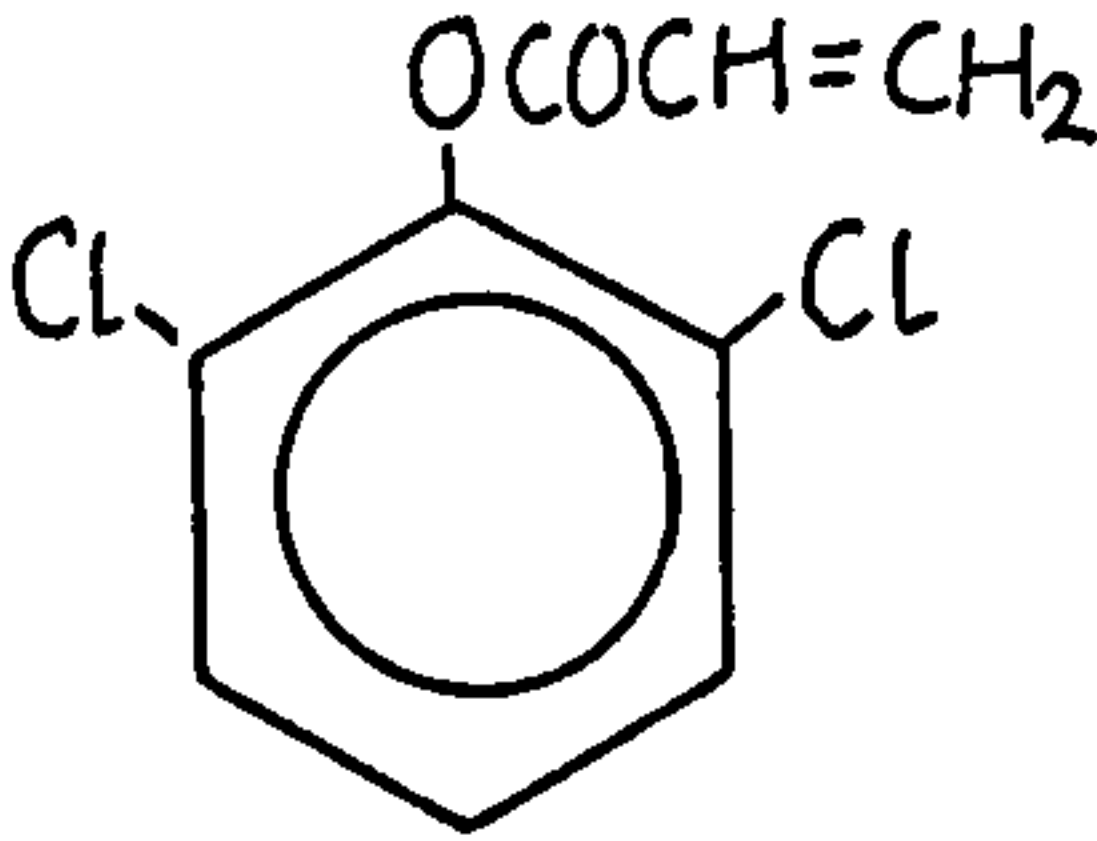
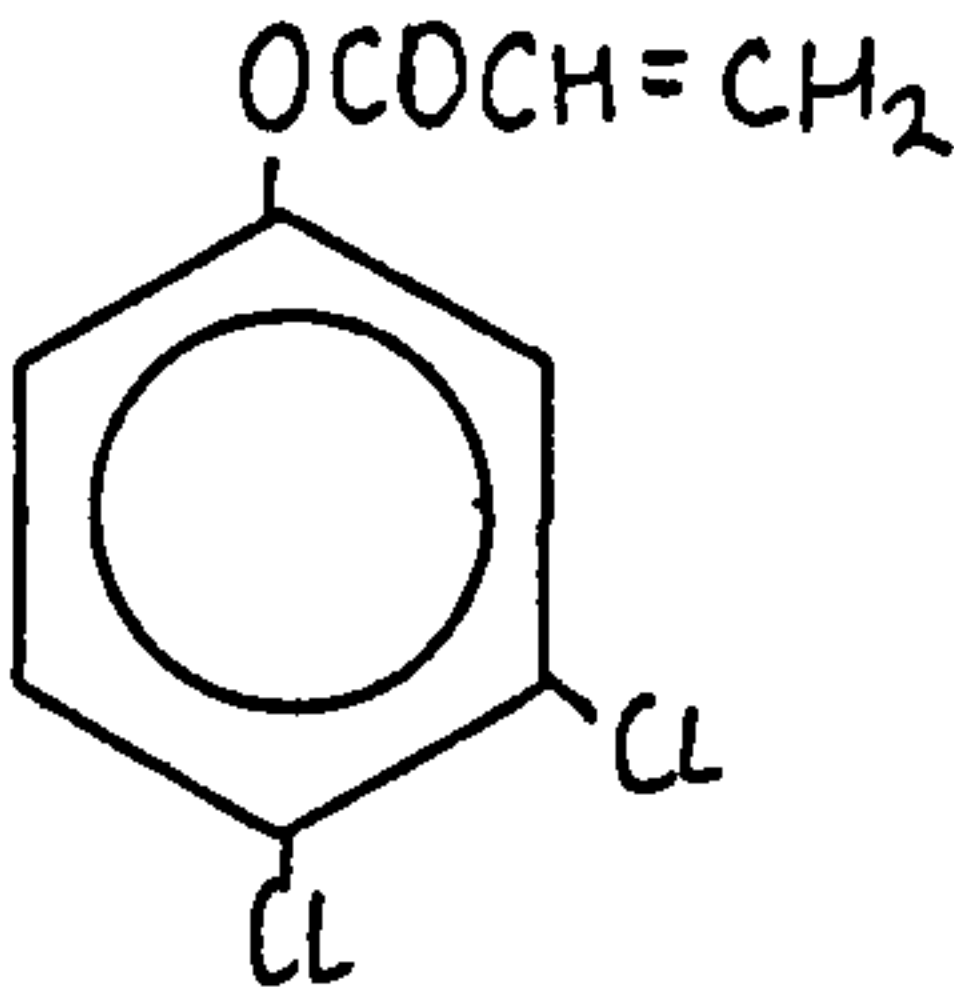
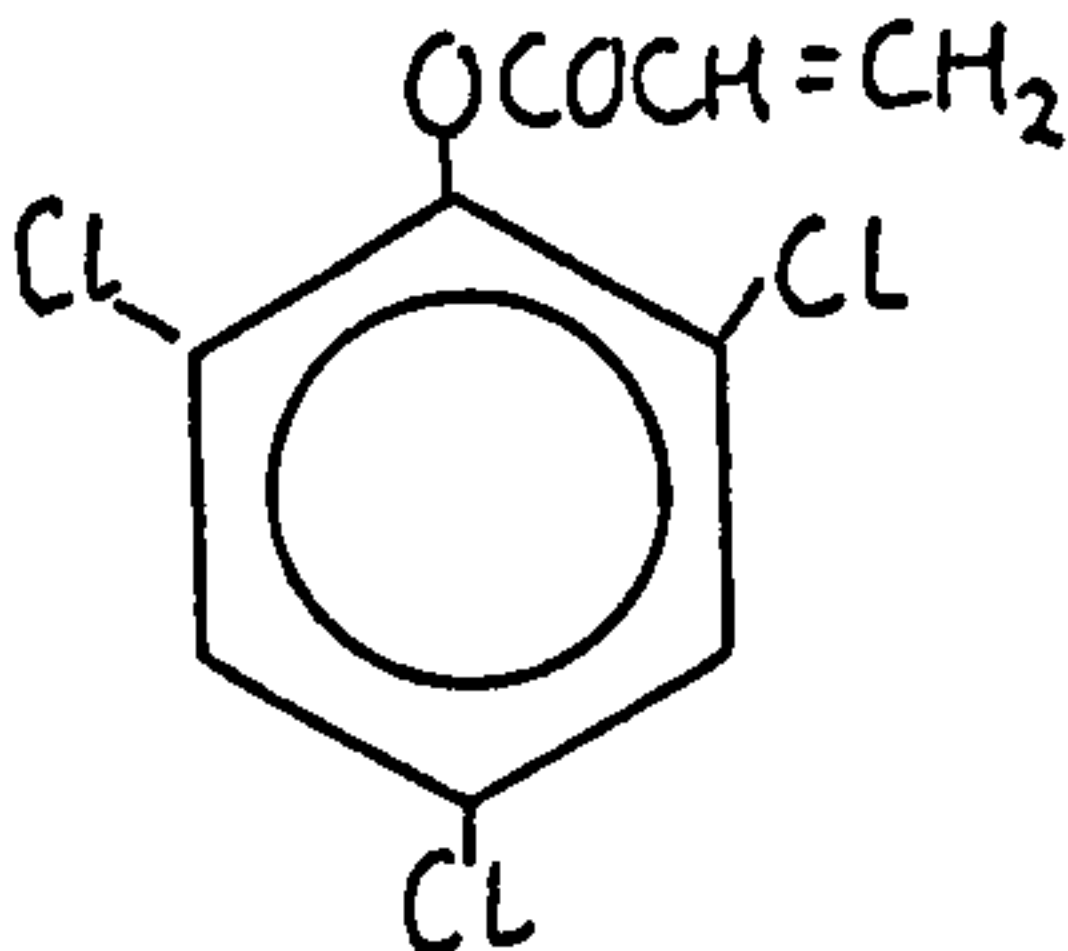
Compound	Dose of radiation/kGy					
	2.5	5	10	20	60	160
	*	*	*	*	*	*
	*	*	*	*	*	*
	*	*	Cured	Cured	Cured	Cured
	*	*	Cured	Cured	Cured	Cured

Table 1 contd. The cure response of halosubstituted phenyl acrylates upon electron beam irradiation

Compound	Dose of radiation/kGy					
	2.5	5	10	20	60	160
	*	*	Cured	Cured	Cured	Cured
	Cured	Cured	Cured	Cured	Cured	Cured
	*	*	*	Cured	Cured	Cured
	Cured	Cured	Cured	Cured	Cured	Cured

\* = wet to the touch

The cure response of the monohalosubstituent, 4-bromophenylacrylate was also ineffective in producing a tackfree coating within the dose range investigated. However, the series of dihaloaromatic acrylates were able to render dry films at considerably reduced doses of radiation



compared with phenyl acrylate and 4-bromophenyl acrylate. This observation provides evidence that dissociative electron capture is operative and enables the production of sufficient crosslinks to occur in order to yield dry coatings.

This mechanism is again corroborated by the rapid formation of a tackfree film upon irradiation of 1,3,5-trichlorophenyl acrylate. The elemental analysis of polymer films of 1,3,5-trichlorophenyl acrylate cured at 5kGy and 40kGy as indicated in Table 2, illustrates the

Table 2 Micro analysis of films of 1,3,5-trichlorophenyl acrylate cured at 5kGy and 40kGy

<u>Dose of radiation</u>		<u>Percentage of</u>		
<u>/kGy</u>		C	H	Cl
0	Expected	42.98	2.00	42.29
	Observed	42.89	1.96	42.73
5	Observed	45.40	2.34	36.88
40	Observed	45.86	2.48	35.28

considerable reduction in halogen content of these coatings compared with the original monomer. Once again this provides evidence that dissociative electron capture is occurring to a significant extent, thereby generating aryl radicals capable of forming crosslinks.

Further examination of Table 1 with respect to the order of reactivity of the dihalophenyl acrylates, suggests that these materials are sensitive to the relative position of the halogen atom in relation to the acrylate moiety. The order of reactivity was shown to occur as follows



The above ratings indicate that when the halogen atom is located in the ortho position the material is more reactive than when situated in either the meta or para positions. This is consistent with those findings of Neta and Behar [5-9] who showed that the rates of dehalogenation of nitrobenzylhalides were dependent on the relative position of the halide group to that of the nitro group, and proceeded in the order of (o > p > m). Neta and Behar [8] also indicated that nitrophenylhalides will not undergo the process of dehalogenation as these compounds form very stable radical anions which may not undergo fragmentation. These workers also showed that by replacing the nitro group by a substituent of lower electron affinity the release of halide ions will be enhanced. It is proposed that the haloaromatic acrylates undergo dehalogenation unlike the

halonitroaromatics due to the lower electron affinity of the acrylate substituent compared with the nitrogroup, thus facilitating the release of halide ions.

### CONCLUSION

The film forming properties of phenylacrylate have been shown to be greatly improved with increasing substitution of halogen atoms about the aryl ring. This can be attributed to the process of dissociative electron capture and it has been shown that the extent of crosslinking was related to the substitution pattern of the halogen atoms with respect to the acrylate group, and shown to proceed in the order  $o > p, m$ .

The sensitivity of catechol diacrylate was also shown to increase as a result of introducing an alkyl substituent. This effect is attributed to the alleviating effect that an electron donating group can have upon the protective action of aromatics towards electron beam irradiation.

## EXPERIMENTAL

### Instrumentation

All formulations were coated onto a moving web via a Dixon 164 coater unit.

Electron beam curing was carried out using an Otto Durr ESH 150/130 electron beam unit under a nitrogen blanket. The operating voltage was maintained at 150 kV and the beam current was adjusted for each applied dose.

Infrared spectra of prepared monomers were analysed using a Perkin Elmer Infrared spectrometer model no. 599.

Proton NMR spectra were recorded using a Jeol NMR spectrometer model no. JNM-MH-100 and referenced against TMS.

All elemental analysis were carried out using a Carlo Erba Strumentazione Elemental Analyzer Mod. 1106.

### Materials

The following commercial samples obtained from Aldrich Chemical co. were used without further purification : catechol, 4-tertbutylcatechol, phenol, 2,3-dichlorophenol, 2,4-dichlorophenol, 2,5-dichlorophenol, 2,6-dichlorophenol, 3,4-dichlorophenol, 2,4,6-trichlorophenol, acryloyl chloride, triethylamine.

Diethylether (BDH Chemicals Ltd.) was distilled from lithium aluminium hydride and stored over molecular sieves, 4A.

Gateway Natural Tracing paper, GNT (Wiggins Teape Group



Ltd.) was used as a substrate for all coatings.

## Synthesis

### Phenylacrylate [11]

#### Method

Acryloyl chloride (4.1ml; 0.05 moles) diluted with dry diethyl ether (20ml) was slowly added to an ice cooled solution of phenol (4.7g; 0.05 moles), triethylamine (7.0ml; 0.05 moles) and dry diethyl ether (200ml). The mixture was maintained at  $<5^{\circ}\text{C}$  and stirred until the reaction was complete. The precipitate of triethylamine hydrochloride was filtered off and the solution was dried over anhydrous sodium sulphate. The solvent was removed by evaporation under reduced pressure to give a clear colourless oil (Yield = 85%). Vacuum distillation of the product thus obtained resulted in decomposition of the product upon heating and therefore purification of this material was not undertaken.

Infrared (Liquid film) : 3068, 3042, 2917, 1740, 1631, 1592, 1491, 1455, 1404, 1294, 1251, 1198, 1165, 1150, 1070, 1025, 983, 921, 883, 801, 754, 691, 656,  $615\text{cm}^{-1}$ .

$^1\text{H}$  nmr ( $\text{CDCl}_3$ ):  $\delta$  (5.60-6.40) (multiplet, 3H, CH and  $\text{CH}_2$  of the acrylate group), (6.80-7.20) (multiplet, 5H, aromatic protons).

Analysis calculated for  $\text{C}_9\text{H}_8\text{O}_2$  : C, 72.96; H, 5.44

Found : C, 73.02; H, 5.48.

The following aromatic acrylates were prepared in <sup>a</sup> similar way to that described above.

4-Bromophenylacrylate

Infrared (Liquid film) : 3095, 1746, 1633, 1584, 1483, 1404, 1297, 1248, 1201, 1166, 1150, 1100, 1069, 1012, 982, 939, 899, 839, 803, 707, 674,  $\text{cm}^{-1}$ .

<sup>1</sup>H nmr (CDCL<sub>3</sub>) :  $\delta$  (5.60-6.50)(multiplet, 3H, CH and CH<sub>2</sub> of the acrylate group), 7.30 (quartet, 4H, phenyl group).

Analysis calculated for C<sub>9</sub>H<sub>7</sub>O<sub>2</sub>Br : C, 47.61; H, 3.11.

Found : C, 47.50; H, 3.00.

2,3-Dichlorophenylacrylate

Infrared (Liquid film) : 3080, 3036, 1750, 1630, 1576, 1450, 1431, 1404, 1293, 1226, 1190, 1135, 1104, 1070, 1052, 1020, 982, 919, 901, 866, 798, 779, 743, 714, 676, 622 $\text{cm}^{-1}$ .

<sup>1</sup>H nmr (CDCl<sub>3</sub>) :  $\delta$  (5.50-6.30)(multiplet, 3H, CH and CH<sub>2</sub> due to acrylate group), (6.4-7.20)(multiplet, 3H, aromatic protons).

Analysis calculated for C<sub>9</sub>H<sub>6</sub>O<sub>2</sub>Cl<sub>2</sub> : C, 49.80; H, 2.79

Found : C, 49.84; H, 2.79.

### 2,4-Dichlorophenylacrylate

Infrared (Liquid film) : 3093, 3035, 1754, 1631, 1585, 1474, 1403, 1384, 1293, 1238, 1218, 1134, 1098, 1058, 1016, 982, 895, 865, 811, 798, 754, 705, 665cm<sup>-1</sup>.

<sup>1</sup>H nmr (CDCl<sub>3</sub>) :  $\delta$  (5.60-6.40)(multiplet, 3H, CH and CH<sub>2</sub> of acrylate group), (6.70-7.20)(multiplet, 3H, phenyl group).

Analysis calculated for C<sub>9</sub>H<sub>6</sub>O<sub>2</sub>Cl<sub>2</sub> : C, 49.80; H, 2.79.

Found : C, 49.72; H, 2.76.

### 2,5-Dichlorophenylacrylate

Infrared (liquid film) : 3093, 3033, 1752, 1631, 1574, 1469, 1397, 1292, 1238, 1217, 1142, 1091, 1056, 1017, 982, 917, 889, 850, 811, 798, 736, 694, 668cm<sup>-1</sup>.

<sup>1</sup>H nmr (CDCl<sub>3</sub>) :  $\delta$  (5.60-6.50)(multiplet, 3H, CH and CH<sub>2</sub> of the acrylate group), (6.70-7.10)(multiplet, 3H, phenyl protons).

Analysis calculated for C<sub>9</sub>H<sub>6</sub>O<sub>2</sub>Cl<sub>2</sub> : C, 49.80; H, 2.79.

Found : C, 49.77; H, 2.78,

### 2,6-Dichlorophenylacrylate

Infrared (Liquid film) : 3082, 3037, 1755, 1634, 1622, 1574, 1446, 1404, 1294, 1246, 1220, 1136, 1100, 1069, 1012, 981, 891, 837, 799, 774, 730, 718, 665cm<sup>-1</sup>.

<sup>1</sup>H nmr (CDCl<sub>3</sub>) :  $\delta$  (5.60-6.30)(multiplet, 3H, CH and

CH<sub>2</sub> of the acrylate), (6.50-7.00)(multiplet, 3H, phenyl group).

Analysis calculated for C<sub>9</sub>H<sub>6</sub>O<sub>2</sub>Cl<sub>2</sub> : C, 49.80; H, 2.79.

Found : C, 49.77; H, 2.76.

### 3,4-Dichlorophenylacrylate

Infrared (Liquid film) : 3094, 3036, 1750, 1631, 1584, 1473, 1403, 1384, 1294, 1238, 1218, 1133, 1098, 1059, 1016, 982, 895, 864, 798, 754, 705, 665cm<sup>-1</sup>

<sup>1</sup>H nmr (CDCl<sub>3</sub>) : δ (5.60-6.40)(multiplet, 3H, CH and CH<sub>2</sub> of acrylate group), (6.60-7.10)(multiplet, 3H, phenyl protons).

Analysis calculated for C<sub>9</sub>H<sub>6</sub>O<sub>2</sub>Cl<sub>2</sub> : C, 49.80; H, 2.79.

Found : C, 49.70; H, 2.75.

### 2,4,6-Trichlorophenylacrylate

Infrared (Liquid film) : 3082, 3030, 1755, 1634, 1622, 1576, 1446, 1403, 1294, 1240, 1220, 1136, 1100, 1069, 1012, 981, 890, 837, 800, 730, 565cm<sup>-1</sup>.

<sup>1</sup>H nmr (CDCl<sub>3</sub>) : δ (5.60-6.30)(multiplet, 3H, acrylate protons), 7.10 (singlet, 2H, phenyl protons).

Analysis calculated for C<sub>9</sub>H<sub>5</sub>O<sub>2</sub>Cl<sub>3</sub> : C, 42.98; H, 2.00.

Found : C, 42.89; H, 1.96.



### Catechol diacrylate

Infrared (Liquid film) : 3105, 3070, 3040, 1750, 1660, 1595, 1490, 1460, 1405, 1295, 1245, 1150, 1100, 1015, 980, 895, 885, 850, 800, 755cm<sup>-1</sup>.

<sup>1</sup>H nmr (CDCl<sub>3</sub>) :  $\delta$  (5.60-6.50)(multiplet, 6H, acrylate protons), 7.05 (multiplet, 4H, phenyl protons)

Analysis calculated for C<sub>18</sub>H<sub>10</sub>O<sub>4</sub> : C, 66.05; H, 4.61

Found : C, 65.85; H, 4.78

### 4-tert-Butylcatecholdiacrylate

Infrared (Liquid film) : 3025, 1753, 1634, 1600, 1460, 1294, 1240, 1184, 1136, 1100, 1069, 1012, 980, 895, 830, 803, 707, 675cm<sup>-1</sup>.

<sup>1</sup>H nmr (CDCl<sub>3</sub>) :  $\delta$  1.25 (singlet, 9H, butyl group), (5.65-6.55)(multiplet, 6H, CH and CH<sub>2</sub> of acrylate), (6.95-7.2)(multiplet, 3H, phenyl group).

Analysis calculated for C<sub>16</sub>H<sub>18</sub>O<sub>4</sub> : C, 76.44; H, 7.90.

Found : C, 76.30; H, 7.70.

The cure responses of the above diluents were recorded in terms of producing a tackfree to the touch coating.

## REFERENCES

- [1] G. Foldiák, (1981). Radiation chemistry of Hydrocarbons, Elsevier.
- [2] J. K. Thomas and I. Mani, (1969). J. Chem. Phys., 51, 1834.
- [3] V. G. Plotnikov, (1985). Radiat. Phys. Chem., 26 (5), 519.
- [4] N. Kimura and S. Takamuku, (1987). Radiat. Phys. Chem. 29 (3), 179.
- [5] P. Neta and D. Behar, (1980). J.A.C.S., 102, 4798.
- [6] D. Behar and P. Neta, (1981). J. Phys. Chem., 85, 690.
- [7] P. Neta and D. Behar, (1981). J.A.C.S., 103, 103.
- [8] P. Neta and D. Behar, (1981). J.A.C.S., 103, 2280.
- [9] J. P. Bays, S. T. Blumer, S. Baral-Tosh, D. Behar and P. Neta, (1983). J.A.C.S., 105, 320.
- [10] R. K. Datta and K. N. Rao, (1979). Radiat. Phys. Chem., 13, 65.
- [11] Sonntag, (1953). Chem. Revs., 52, 237.

---

## CHAPTER 7

# UV AND ELECTRON BEAM INDUCED POLYMERISATION OF EPOXIDES

---

**Chapter 7 INTRODUCTION: CATIONIC POLYMERISATION OF  
EPOXIDES**

The state of the art	265
Cationic polymerisation	268
Cationic initiators	272
Protonic acids	272
Lewis acids (Friedel Crafts catalysts)	274
Onium salts	275
Diazonium salts	275
Iodonium and sulphonium salts	277
a) Direct photolysis	278
b) Photoinduced electron transfer	283
between donor and onium salts	
c) Electron transfer between nucleo- philic radicals and onium salts	284
Organometallic initiators	285

**ELECTRON BEAM INDUCED POLYMERISATION OF EPOXIDES**

Introduction	287
Factors affecting the rate and the degree of polymerisation of epoxides	289
Characteristics of epoxide films	290
Results and Discussion	292
Conclusion	309
Experimental	311
Appendix A	317



**DIRECT AND INDIRECT UV INDUCED POLYMERISATION  
OF EPOXIDES**

Introduction	322
Results and Discussion	324
Conclusion	331
Experimental	332

**ELECTRON BEAM AND UV INDUCED POLYMERISATION OF 335  
6,7-EPOXY-3,7-DIMETHYLOCTYL ACRYLATE**

Introduction	335
Results and Discussion	337
Conclusion	345
Acknowledgements	346
Experimental	347
References	350

## INTRODUCTION: CATIONIC POLYMERISATION OF EPOXIDES

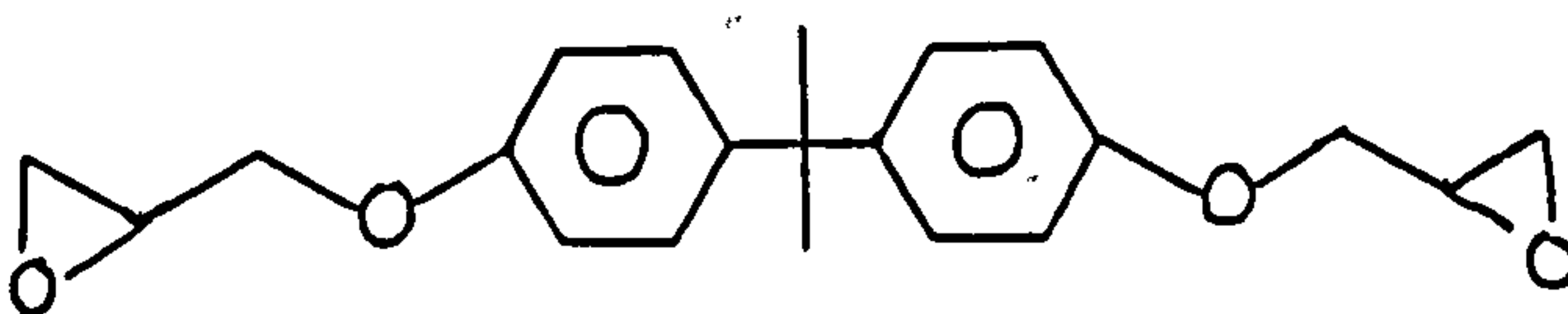
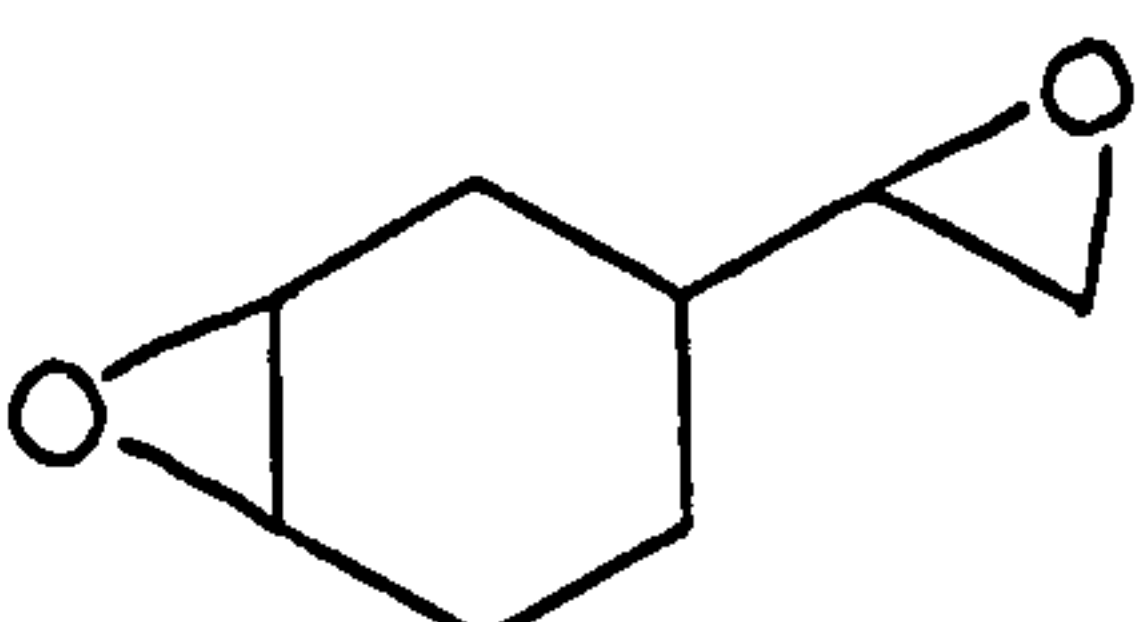
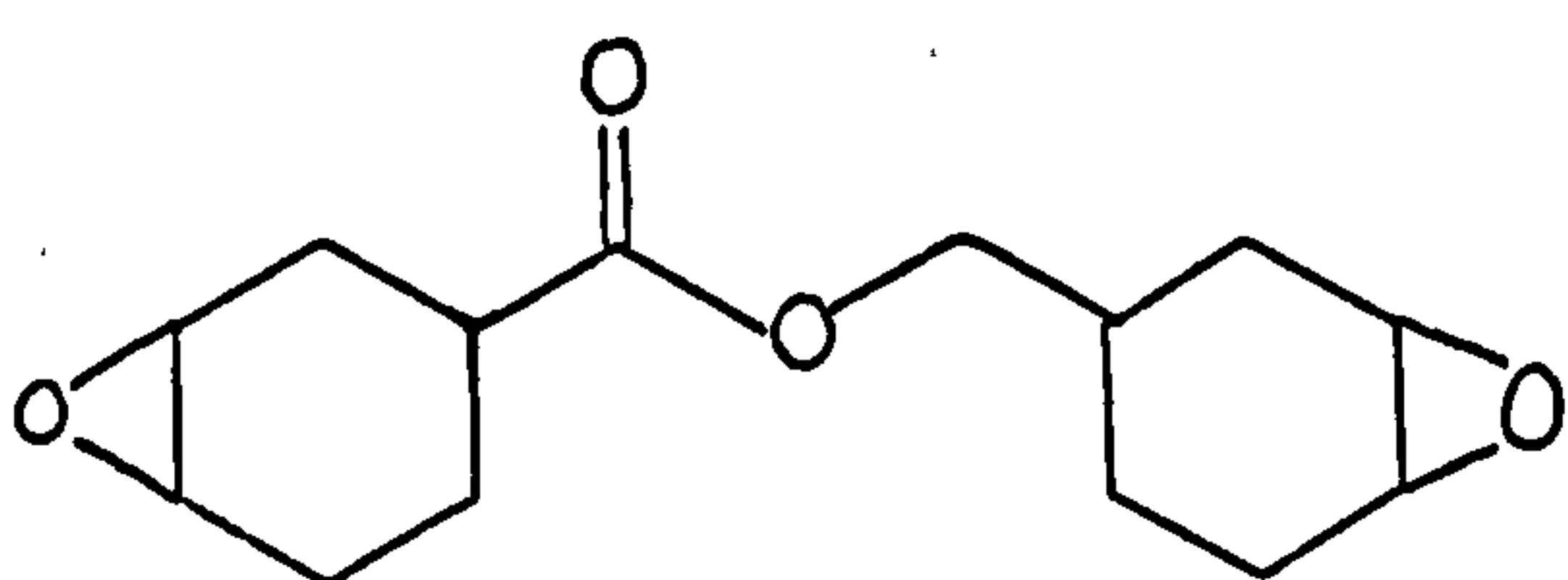
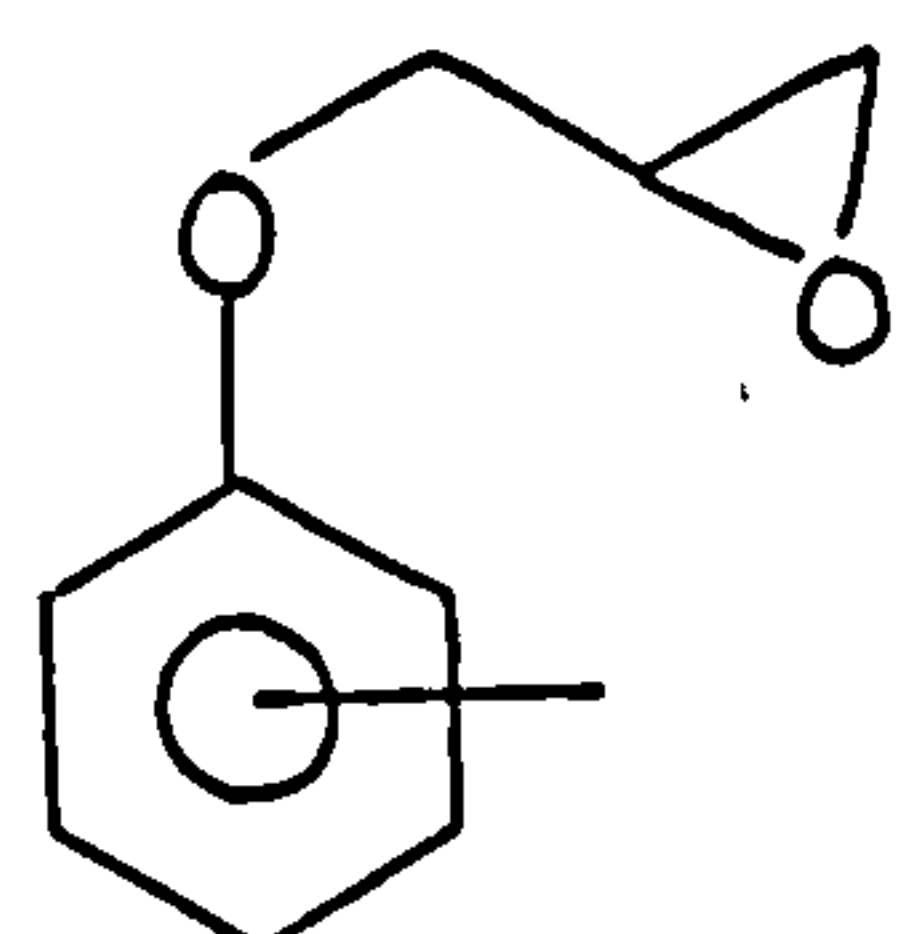
### The State of the Art

During the past decade there has been much interest in the development of UV induced cationic polymerisation of epoxides. This recent interest in the use of epoxide systems in the surface coatings industry has been spurred on by the development and commercial availability of the onium salts, notably the iodonium and sulphonium salts [1] and more recently the iron arene complexes [2].

Some of the main advantages of using epoxy based resins over unsaturated based resins, such as the acrylates, are due to good flow properties, no significant colour or odour and low shrinkage on cure [3]. Epoxides are also insensitive to oxygen and hence nitrogen blanketing is not required [4]. They also exhibit the phenomena of "living polymerisation", that is, on removal of the radiation source these systems continue to polymerise thermally and are capable of consuming all functional groups present. The resulting film properties of most epoxides exhibit good substrate adhesion, high chemical and solvent resistance and good impact and flexibility [3].

However, epoxy resins only represent a small portion of the UV-curable resin market [1]. This is partly due to the high cost of epoxides and available photoinitiators, as well as competing with other UV-curable resins, namely the acrylates.

Table 1 Some typical commercial epoxy resins

<u>Epoxy resin</u>	<u>Structure</u>
Diglycidyl-bisphenol-A	
4-Vinylcyclohexene dioxide	
3,4-Epoxycyclohexylmethyl-3',4'-epoxycyclohexane carboxylate	
Cresyl glycidyl ether	

The first epoxy resins based on bisphenol-A were introduced commercially by Greenlee [3] in 1939 for coating applications and have gained wide acceptance for this end use. The outstanding properties associated with bisphenol-A epoxy resins are toughness, rigidity and elevated temperature performance, (imparted by the bisphenol-A moiety), chemical and solvent resistance (associated with the ether linkages) and the excellent adhesion

properties (due to the epoxy and hydroxyl groups formed during the course of the reaction). In the late 1960's Union Carbide developed a range of cycloaliphatic epoxides [3]. These resins showed improved weatherability, and light stability, but reduced flexibility, adhesion and chemical resistance compared with bisphenol-A derived epoxy resins. The subsequent production of multifunctional epoxy cresol novolaks were introduced by Ciba, Celanese, Shell and Union Carbide in the mid 1960's to improve on specific properties, such as high temperature performance. Ciba in the 1970's developed epoxy resins based on hydantoin [3], shown to have excellent electrical and weatherability properties.

A selection of some commercial epoxy resins available are listed in Table 1.

In 1974, Watt [5] was the first to describe the use of UV-curable epoxide formulations in the production of films. A year later the appearance of the diphenyliodonium salts and onium salts of Groups Va and VIa as photoinitiators of cationic polymerisation were described in the patent literature [6-11]. Crivello and Lam [12] demonstrated the use of the diphenyliodonium salts as photoinitiators of olefins, lactones and cyclic ethers. In 1978, the triphenylsulphonium salts were also shown to cure various epoxy resins [13]. The isolation of an inexpensive photoinitiator on reaction of potassium hexafluorophosphate with "mixed aromatic sulphonium chlorides" in water, yielded a product capable of absorption above 300nm. These "mixed



aromatic sulphonium hexafluorophosphates" (acronym MASH) resulted in the rapid cure of epoxy resins [1].

The commercial introduction of these photoinitiators led the way for the development of epoxy resins to be used for the production of UV-curable films. The class of epoxy resins found to be suitable for this purpose are the cycloaliphatic epoxide resins, largely due to their superior cure speeds with these photoinitiators, compared with glycidyl epoxy resins.

### Cationic polymerisation

Cationic polymerisation can be defined as "chain growth reactions promoted by active species possessing electrophilic character: carbonium, oxonium, sulphonium, ammonium, phosphonium ions ..." [14].

There are two types of system susceptible to cationic polymerisation. These are olefinic monomers, e.g. styrene, isobutylene, and vinyl ethers and the cyclic types such as the epoxides. The cationic polymerisation of cyclic ethers will be the only class discussed here.

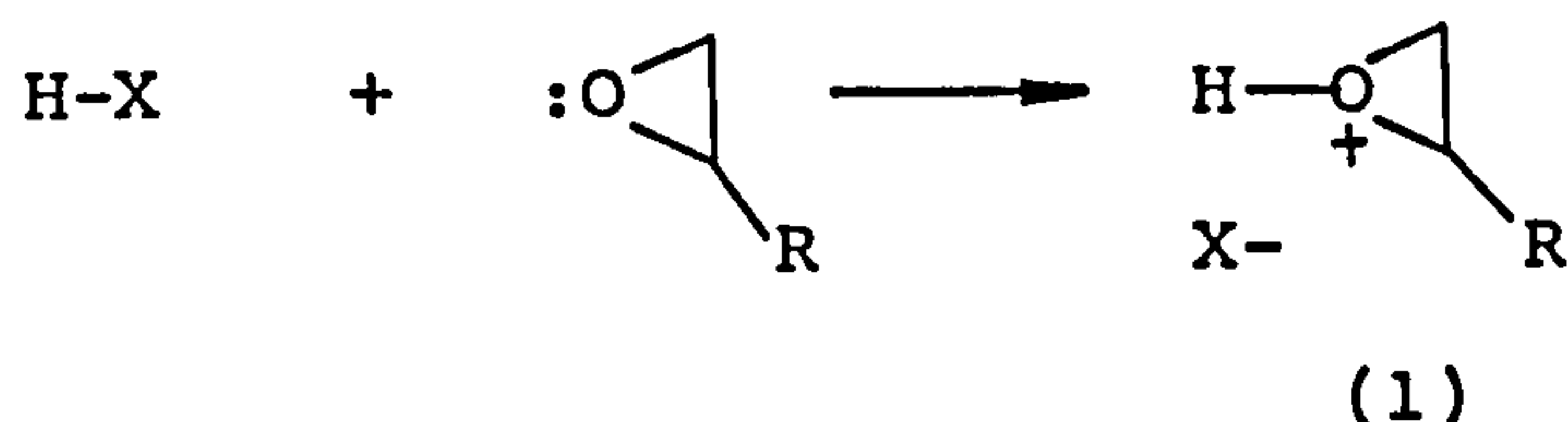
Ionic polymerisations in general are not as well understood as radical polymerisations because of the difficulties encountered in their study, due to their fast rates of cure and extreme susceptibility to trace amounts of impurities. The polymerisation of cyclic ethers, like other chain growth reactions involves three stages, initiation, propagation and termination reactions.

## Initiation

The initiation step requires the formation of an active site, and in the case of cyclic ethers this is a tertiary oxonium ion (1)[15].

The formation of the tertiary oxonium ion is the result

Scheme 1

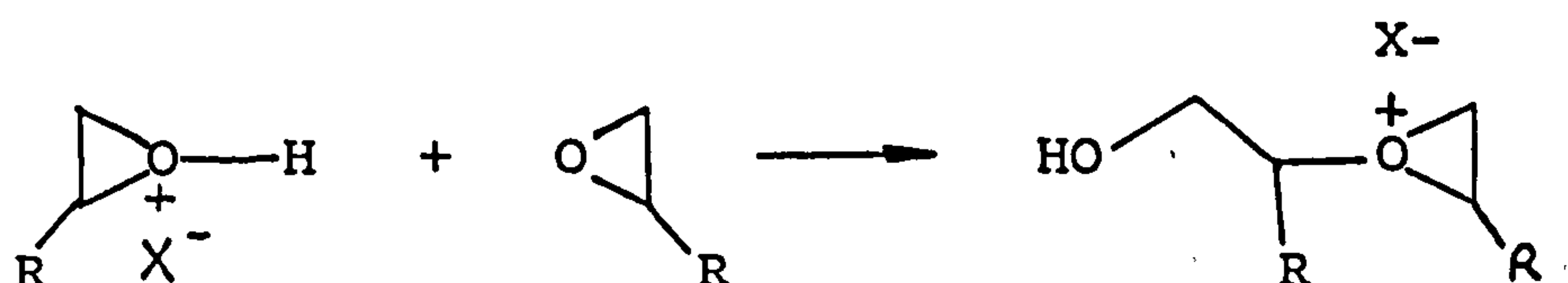


of nucleophilic attack of the lone pair of electrons on the oxygen atom of the ether toward the initiating species.

## Propagation

Propagation in cationic polymerisation of cyclic ethers, proceeds via a tertiary oxonium ion [15].

Scheme 2



The  $\alpha$ -carbon of the oxonium ion is electron deficient and is susceptible to nucleophilic attack by the oxygen of another monomer molecule.

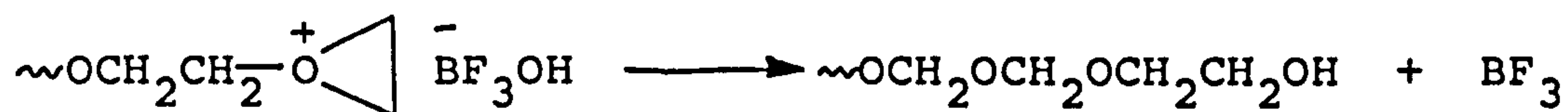
These oxonium ions may exist in various forms of ionic aggregates, as paired macroions or free macrocations [16]. The three factors influencing the reactivities of these macroion pairs and macrocations are, solvation, size of

anions and the resulting interaction with the cation [16]. The concentration of free macrocations is generally smaller than ion pair concentration and reflects the polarity of the media. However, for efficient polymerisation of epoxides or other cyclic ethers to occur a complex counteranion e.g.  $\text{AsF}_6^-$ ,  $\text{SbF}_6^-$  is required and in this case, it can be assumed for the most part that, reactivity of paired and free macroions are the same [16].

### Termination

True termination reactions of cationic polymerisations are scarce in very pure systems. Generally they involve combination of the counteranion or an anionic fragment of the counteranion with the oxonium ion [15].

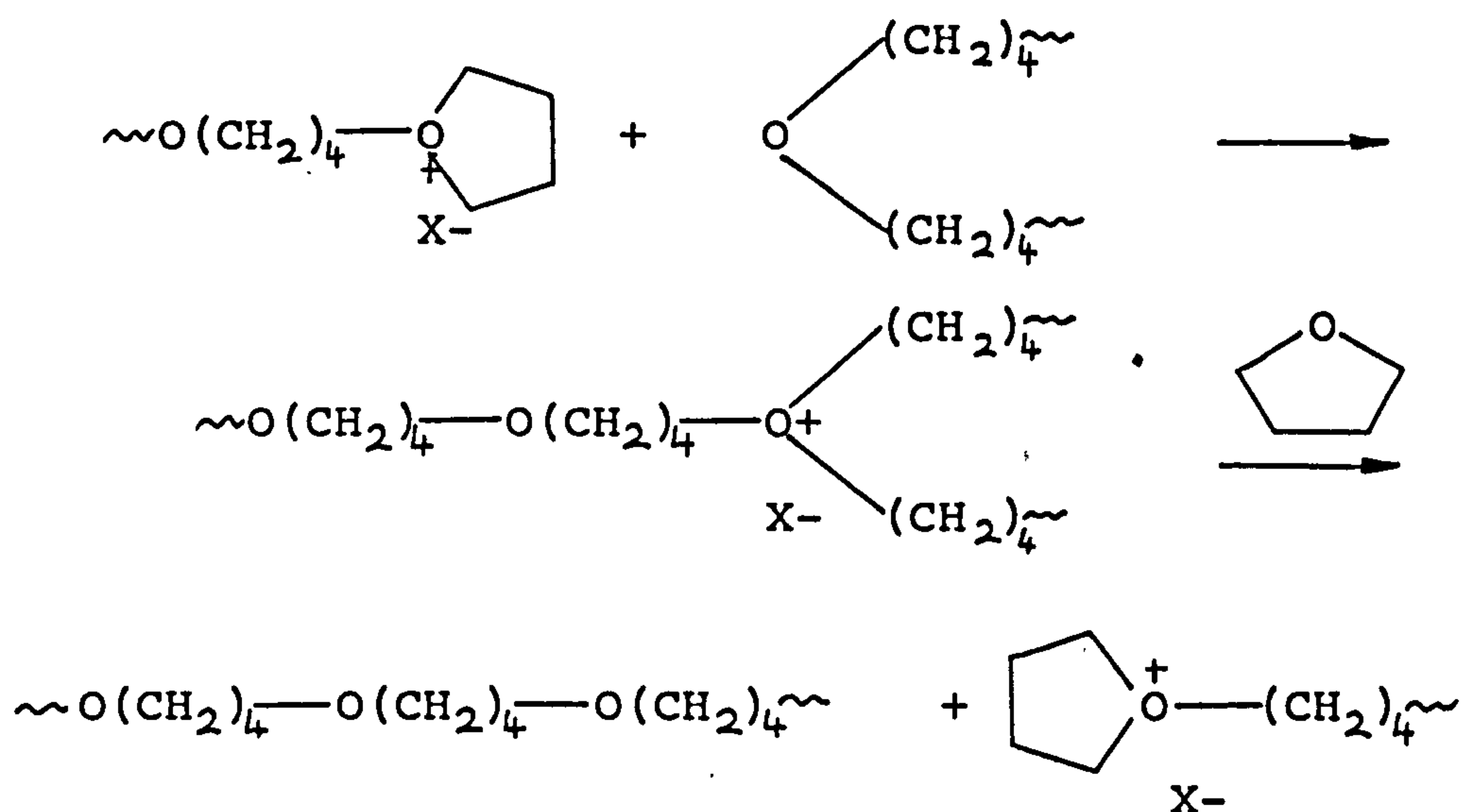
#### Scheme 3



Chain transfer reactions, terminate the growth of one polymer chain with concurrent initiation of another, leading to a lowering of molecular weight of the resulting polymer.

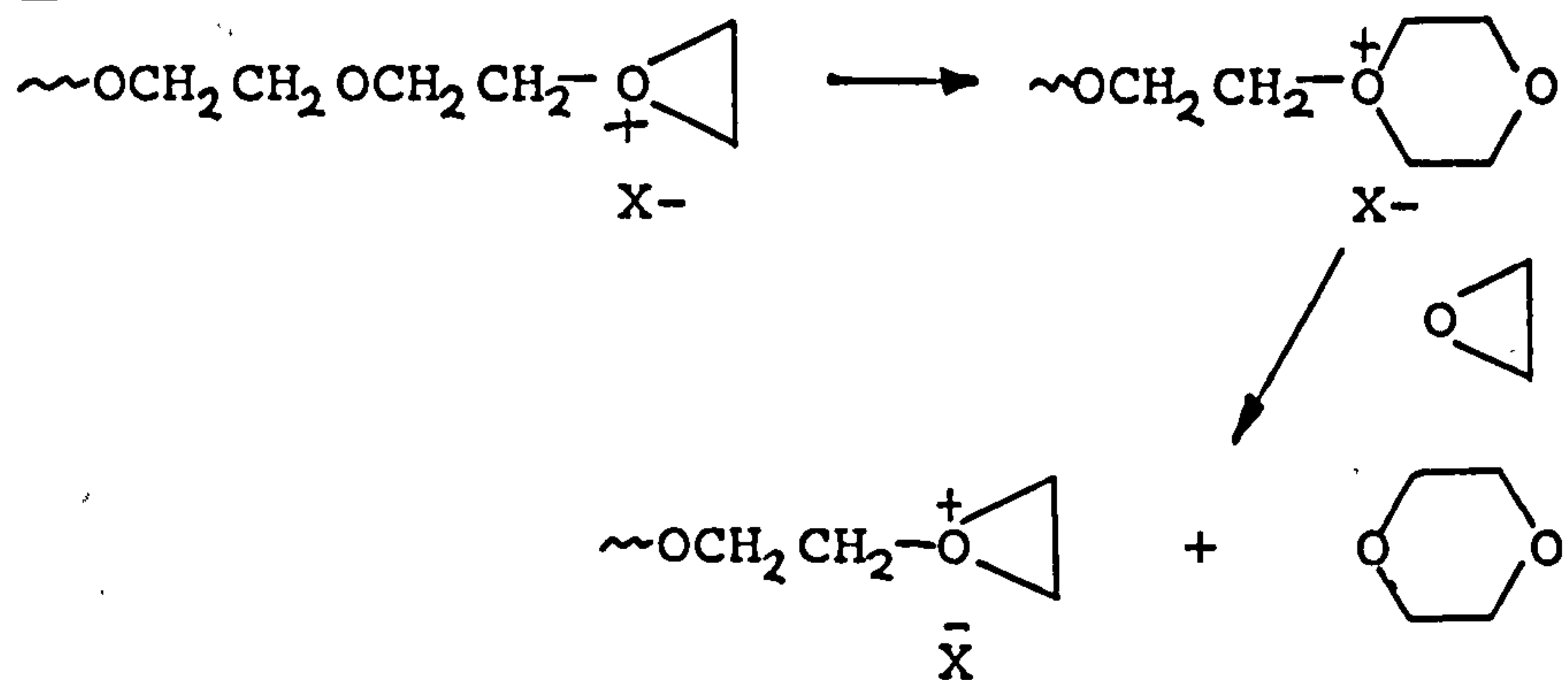
Chain transfer to polymer via alkyl exchange involves an alkyl exchange reaction between the oxonium ion and an ether oxygen of a polymer chain [15].

Scheme 4



Backbiting reactions readily occur, where an oxygen atom in the polymer chain attacks the  $\alpha$ -carbon of the oxonium ion. The resulting larger sized cyclic oxonium ion is then displaced by monomer [15]. This reaction accounts for the depolymerisation of polymers on excessive heating as illustrated in Scheme 5 [15].

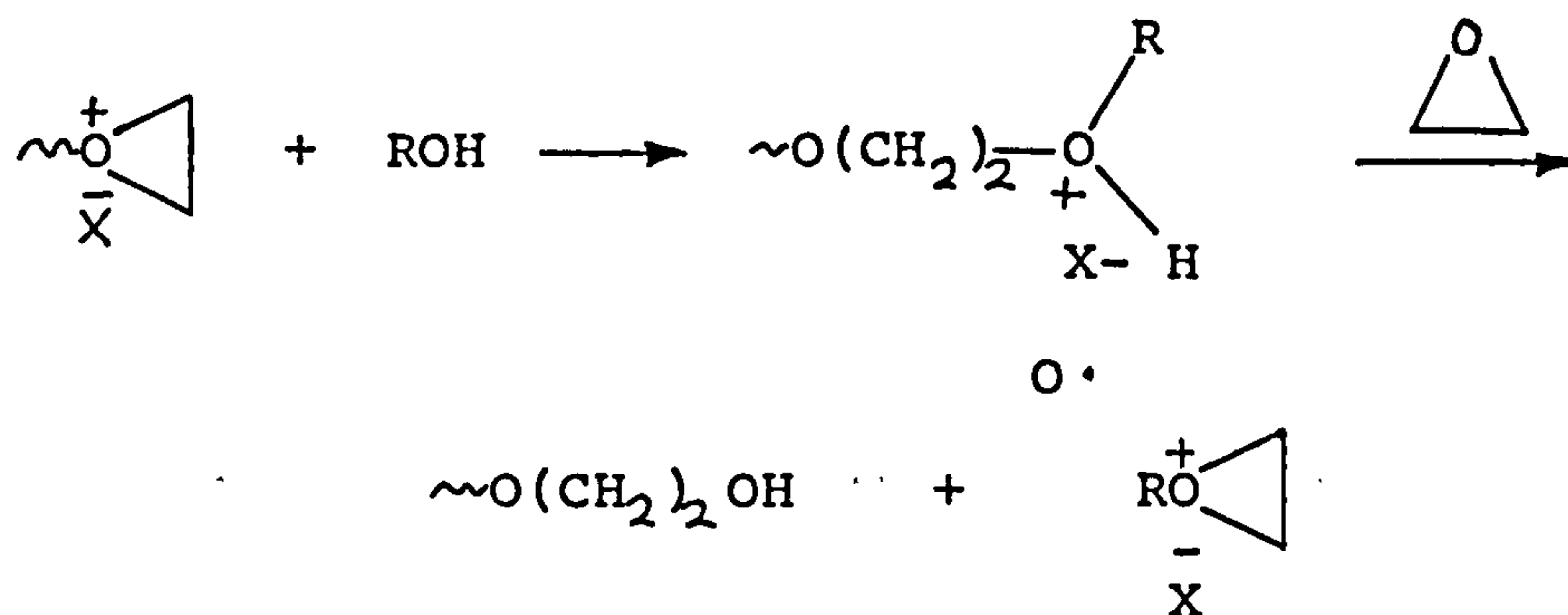
Scheme 5



Another chain transfer reaction may involve water or alcohol [15]. Watt has shown that the moisture content of paper substrates can influence the time to cure UV-curable epoxide films [1].



Scheme 6



### Cationic initiators

The cationic polymerisation of cyclic ethers can be initiated in many ways and there are several excellent reviews on this subject [1,16,17].

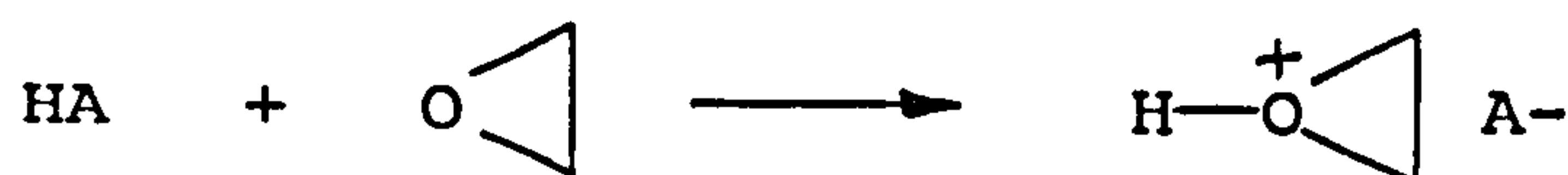
The initiators of most significance can be categorised as follows:

- 1) Protonic acids (Brønsted acids),
- 2) Lewis acids (Friedel Crafts catalysts),
- 3) Onium salts,
- 4) Organometallic initiators.

### Protonic acids

Protonic acids with non-complex anions of the type Cl<sup>-</sup>, HSO<sub>4</sub><sup>-</sup>, SO<sub>3</sub>F<sup>-</sup> will undergo heteroconjugation with cyclic ethers [16], to generate an oxonium ion.

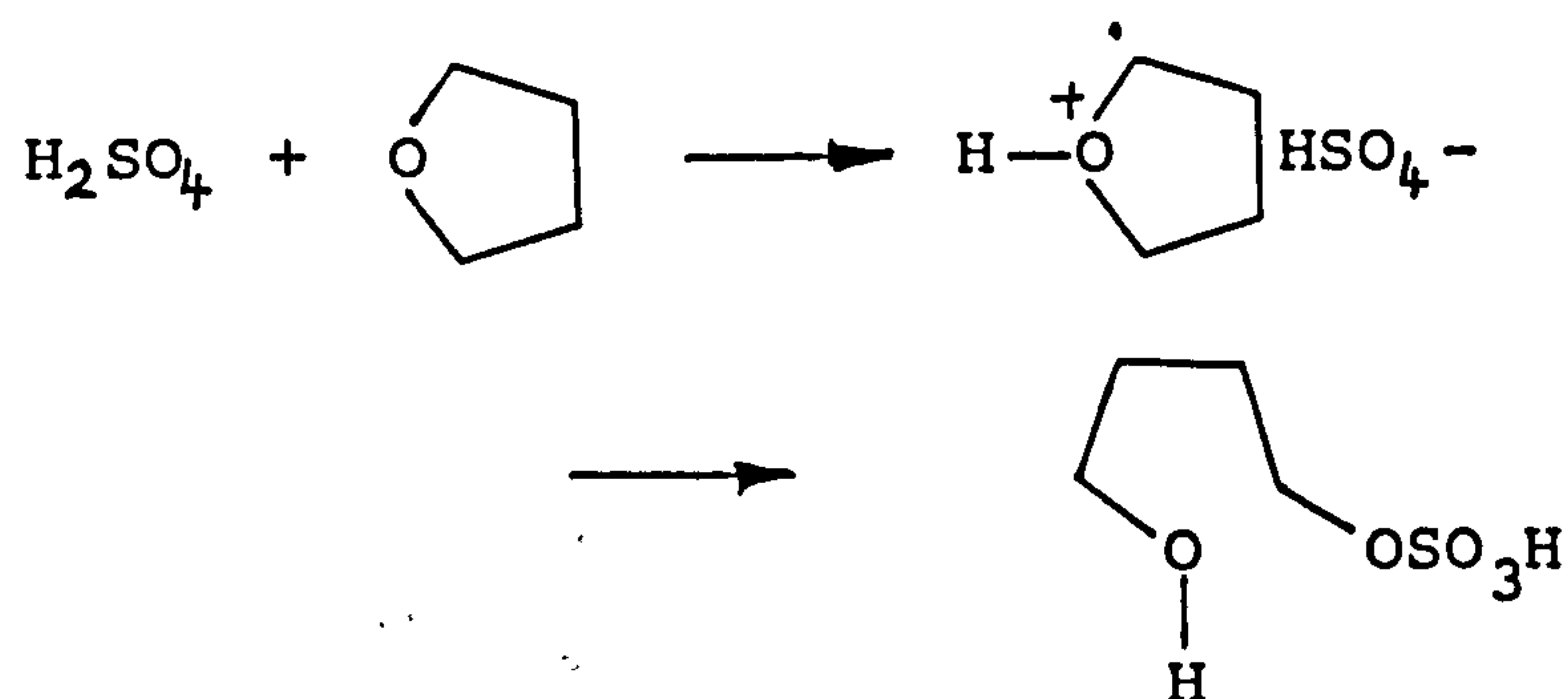
Scheme 7



However, the degree of polymerisation depends on the nucleophilicity of the monomer compared to that of the

anion. If, as in the case of tetrahydrofuran in the presence of sulphuric acid, the anion is a stronger nucleophile than the monomer, it competes successfully with the oxonium ion [18] as shown in Scheme 8.

Scheme 8



However, fluorosulphuric acid and chlorosulphuric acid, whose anion is less nucleophilic than the bisulphate anion, are capable of a certain degree of polymerisation.

Protonic acids with complex anions are believed to be formed as a result of combination of e.g. HF with a Lewis acid, e.g.  $\text{BF}_3$  and  $\text{SbF}_5$  [16].

Scheme 9

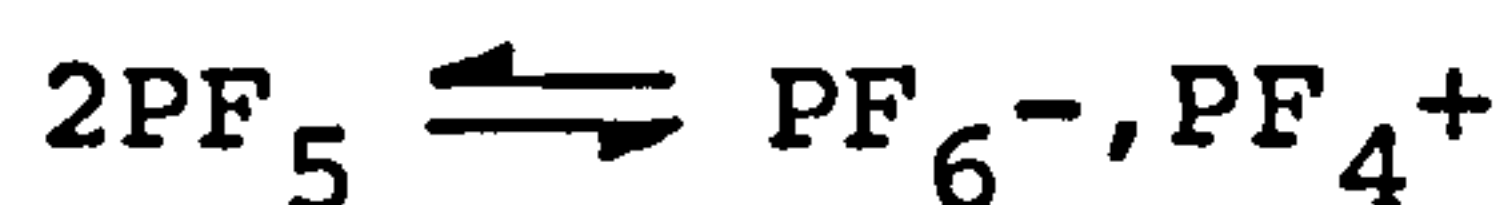


Acids with complex anions can only exist in the ionised form and therefore stabilisation of the proton by solvation in the presence of a suitable nucleophile is required [16]. Little is known as to the exact nature of these systems, however, they are among the strongest acids known and are most effective initiators of cationic polymerisation of cyclic ethers.

### Lewis acids (Friedel Crafts catalysts)

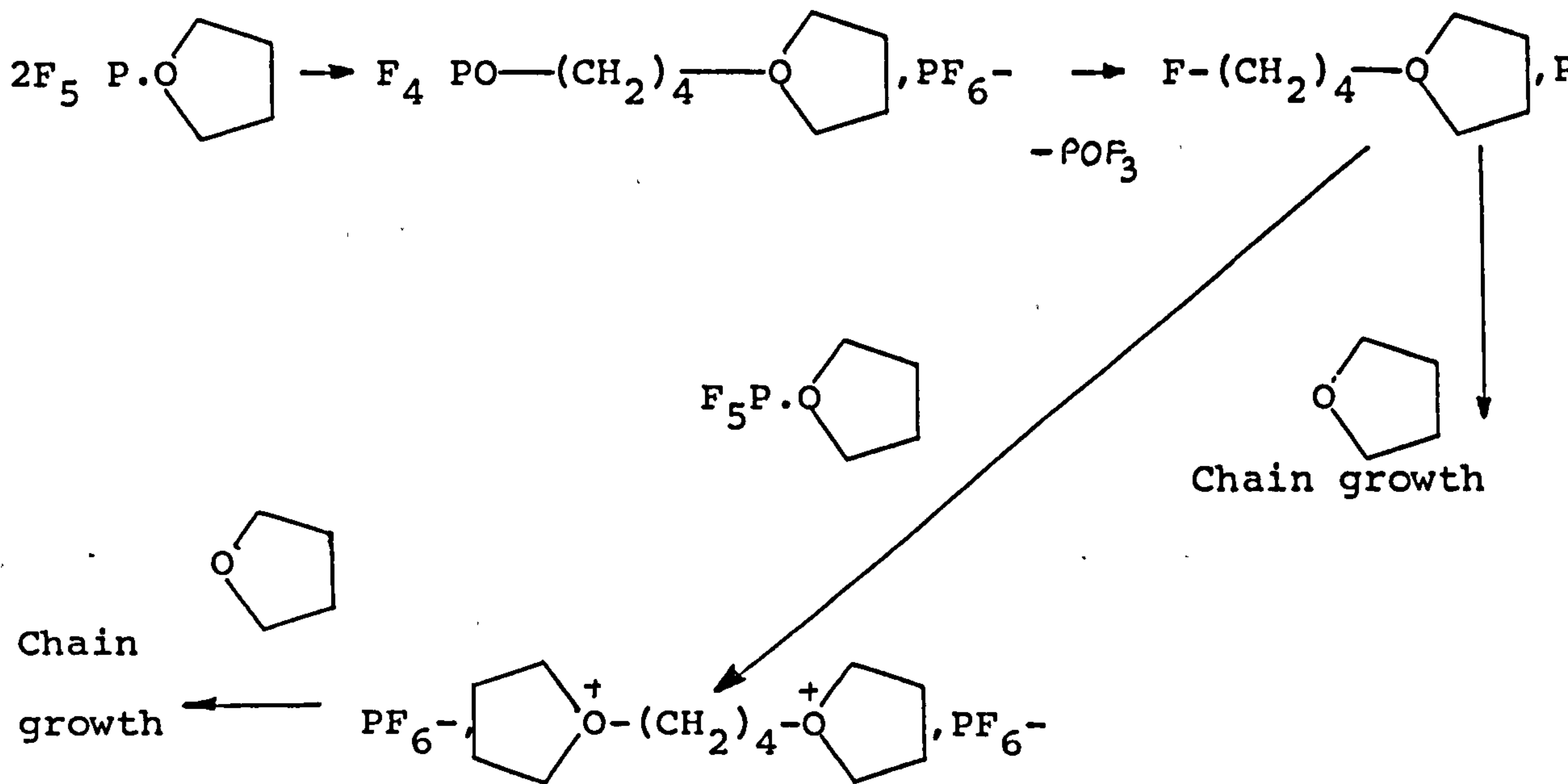
It has been suggested that some Lewis acids may initiate polymerisation alone, as a result of self-ionisation resulting in the formation of the first propagating species [15].

#### Scheme 10



The mechanism of initiation was studied for the  $\text{PF}_5/\text{THF}$  system [19,20] using  $^{31}\text{P}$ -NMR and the following mechanism was proposed.

#### Scheme 11



However, Evans et al. [21] showed that the purest  $\text{BF}_3$  doesn't initiate the polymerisation of isobutylene, but on addition of a protogen ( $\text{H}_2\text{O}$ ) to anhydrous  $\text{BF}_3/\text{isobutylene}$  immediately produced high molecular weight polymer. In the wake of this now classical "stopping experiment" it has been

demonstrated that the addition of  $\text{H}_2\text{O}$  significantly increased the polymerisation rate [22] of tetrahydrofuran/ $\text{BF}_3$ . The proposed initiator generated in this system, in the presence of very little water, is the result of forming a complex acid " $\text{H}+\text{BF}_3\text{OH}^-$ " [4].

Lewis acids are not used widely as initiators for the cationic polymerisation of cyclic ethers, mainly due to low efficiency, slow rate of reaction and the production of side products [16]

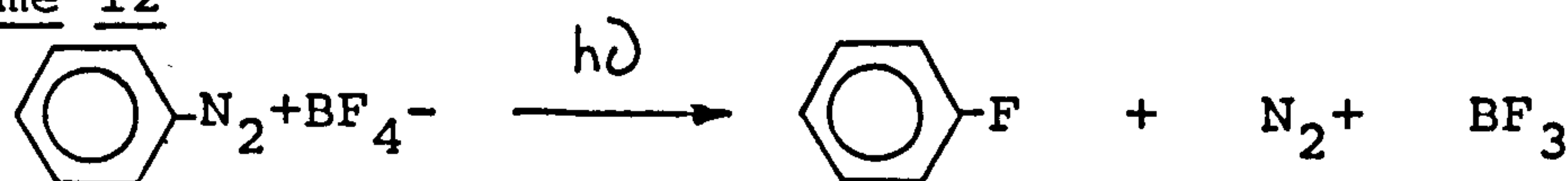
#### Onium salt

#### Diazonium salts

The use of diazonium salts as curatives of epoxides were first demonstrated photochemically by Licari and Crepeau [23], and thermally by Dreyfuss and Dreyfuss [24,25]. However, it was not until the 1970's that Schlesinger [26,27] demonstrated the range and versatility of diazonium salts as photoinitiators of epoxides.

The mechanism by which these salts initiate cationic polymerisation of cyclic ethers has been attributed to the Schiemann reaction [28].

Scheme 12



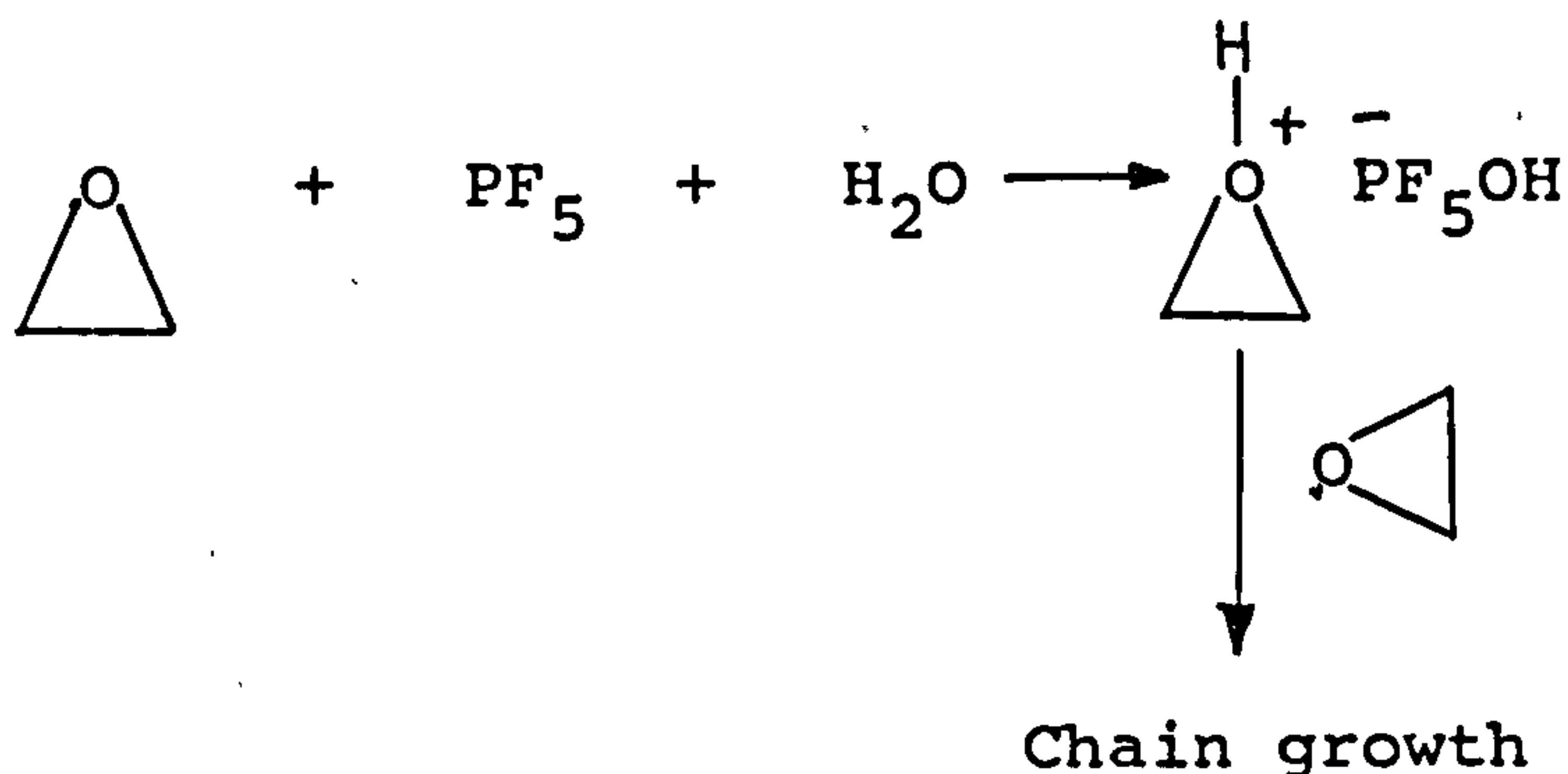
The Lewis acid formed was shown by Meutters [29] to initiate polymerisation of cyclic ethers to high molecular weight.

The mechanism by which  $\text{BF}_3$  or  $\text{PF}_5$  initiate the



polymerisation of epoxides is depicted in Scheme 13 [30].

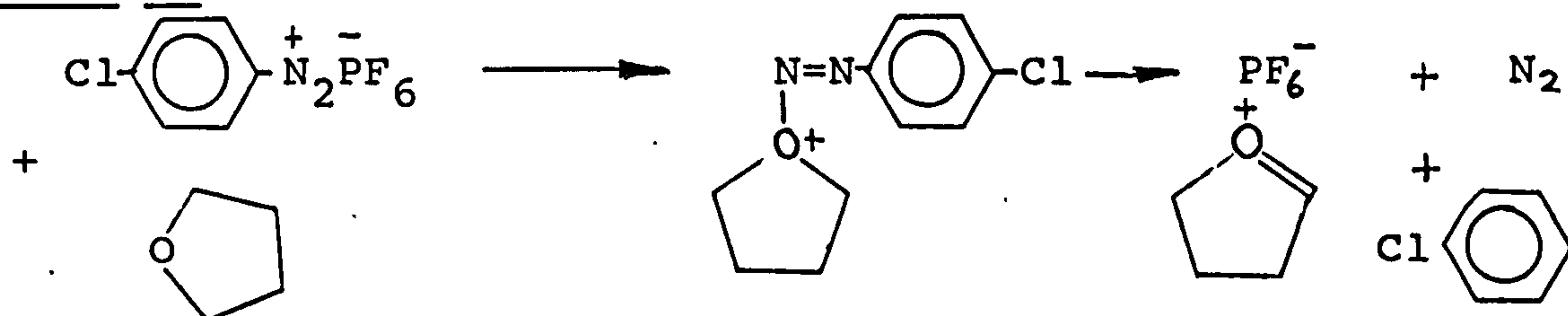
Scheme 13



The photolysis of pure crystalline diazonium salts with  $\text{BF}_4^-$  or  $\text{PF}_6^-$  counter anions produced the expected products of aryl fluoride and Lewis acid [31], although in different proportions to when the salt is treated thermally. It was therefore postulated it was unlikely that these reactions proceeded by an exclusive mechanism through a common intermediate [31].

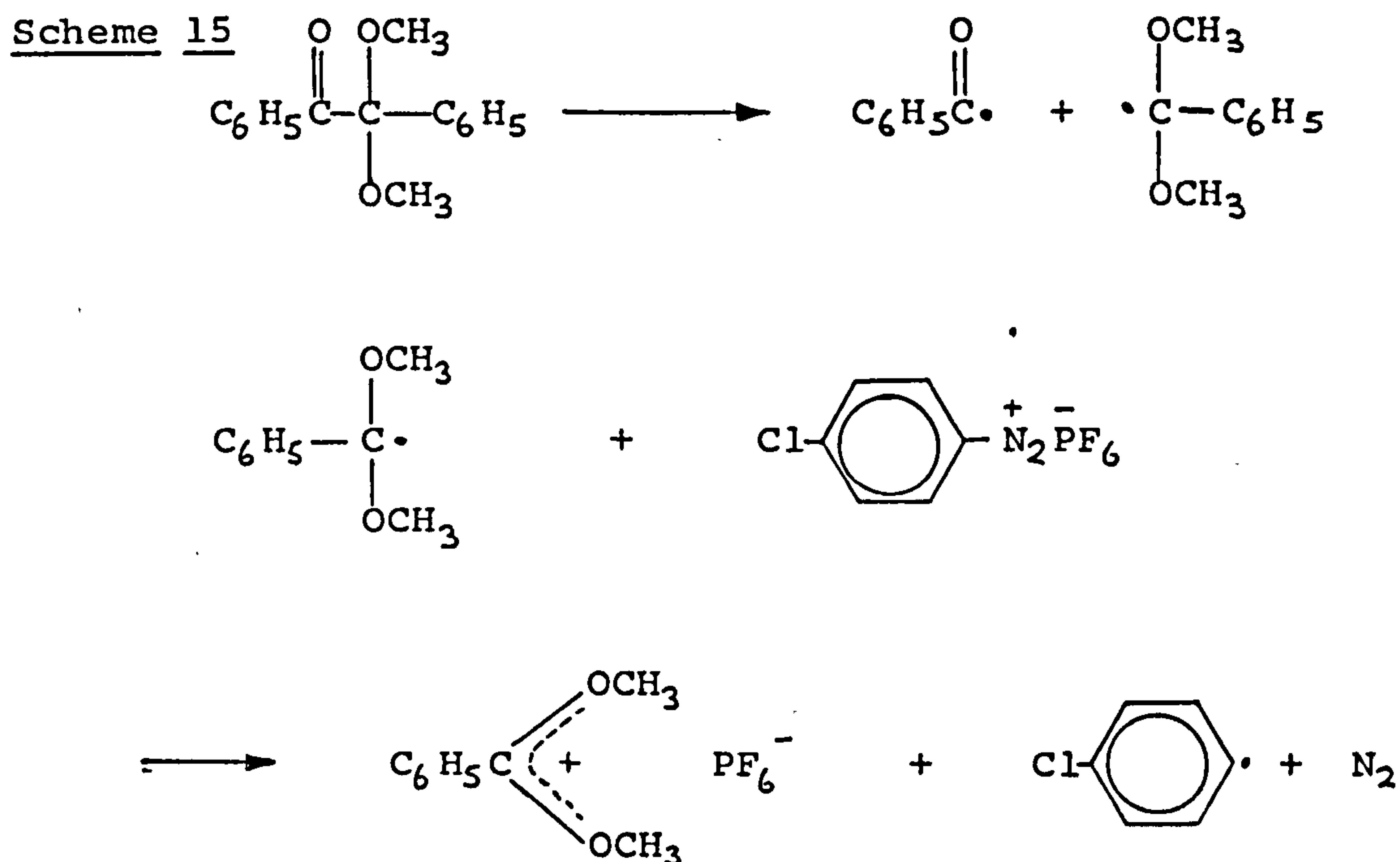
Dreyfuss and Dreyfuss [25] postulated that thermal polymerisation of tetrahydrofuran involves hydride abstraction.

Scheme 14



Ledwith et al. [32] subsequently proposed that the photolysis of tetrahydrofuran and p-chlorodiazonium hexafluorophosphate in the presence of various free radical initiators would result in the formation of an initiating cation without the requirement of hydrogen abstraction from

the monomer, illustrated in Scheme 15.



The main advantage in the use of diazonium salts as initiators is their wide range of absorption characteristics [26]. However, mixtures containing diazonium salts and epoxides generally undergo "dark reactions", resulting in restricted shelflife of formulations and the evolution of nitrogen limits the thickness of the coating to be cured.

#### Iodonium and Sulphonium salts

The major advantage of the iodonium and sulphonium salts compared with the diazonium salts, is their increased thermal stability.

The diphenyliodonium salts were the first discovered as effective curatives of cationic polymerisable monomers by Crivello and coworkers [33-35] followed by the successful development of triphenyl sulphonium salts [36-38].

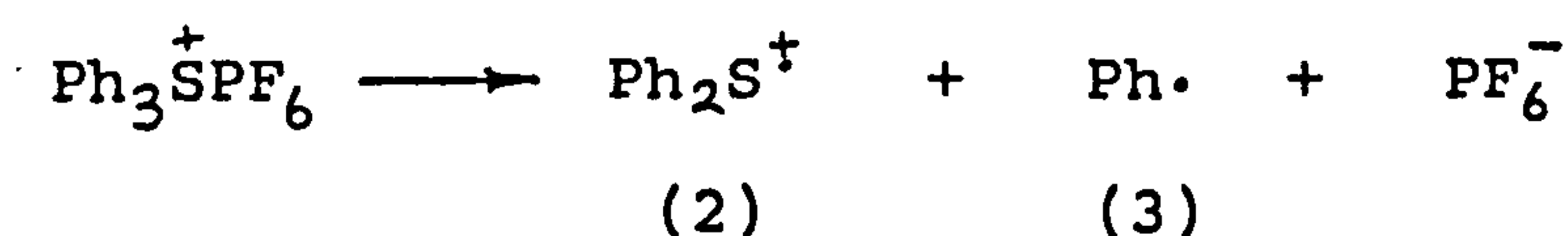
The mechanisms by which iodonium and sulphonium salts decompose to give rise to effective cationic and radical initiators can be categorised as follows [39]:

- a) direct photolysis of onium salts,
- b) photoinduced electron transfer between donor and onium salt,
- c) electron transfer between nucleophilic radicals and onium salts.

a) Direct Photolysis of onium salts

The mechanism of photolysis of diphenyliodonium salts in solution in alcohols was investigated by Knapczek and McEwen [40] and Knapczak et al.[41]. It was found from their examination of photolyses products that the primary photochemical step was homolytic bond cleavage to yield the phenyliodonium radical cation, (2) and a phenyl radical (3).

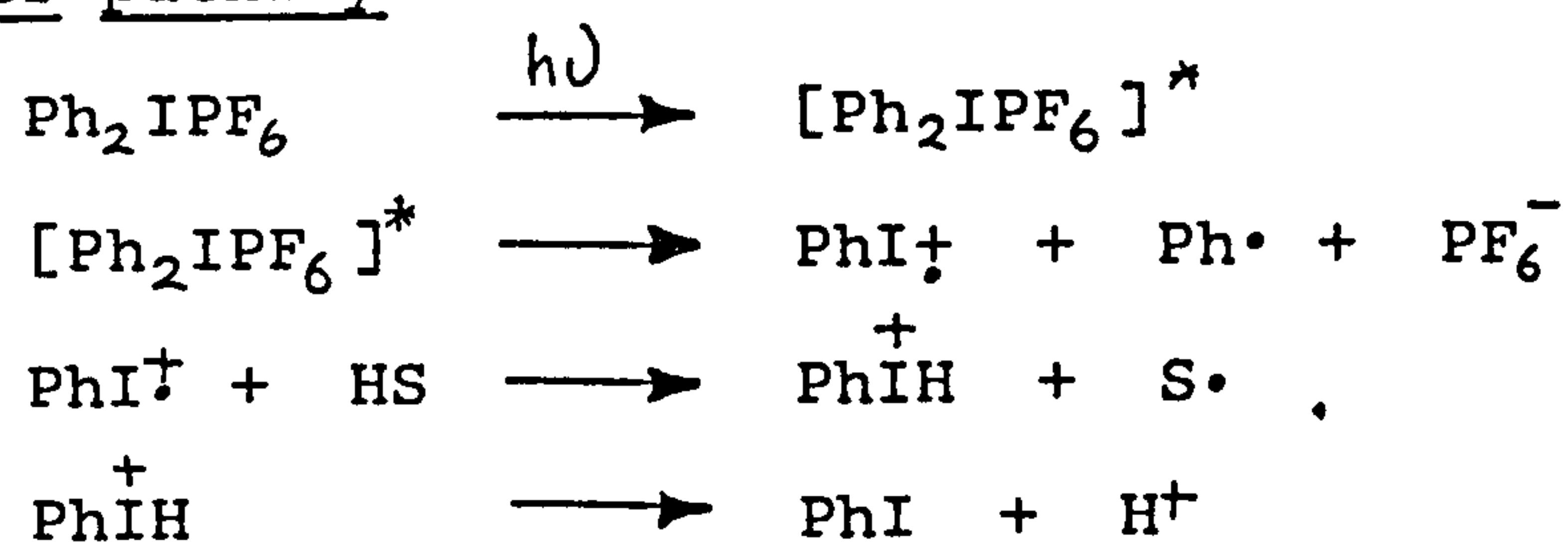
Scheme 16



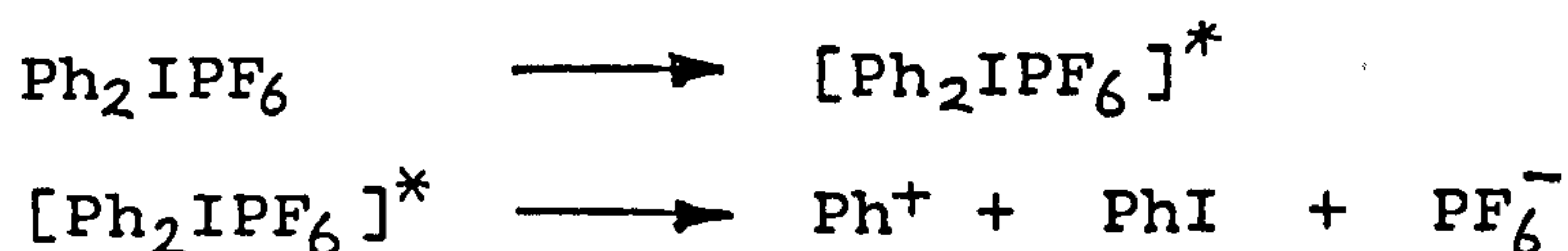
Crivello and Lam [33,34] reinvestigated the photolysis of these salts in acetonitrile, acetone, ethanol/water or acetone and on the basis of their findings and those of Knapczak proposed the following photolytic mechanism illustrated in Scheme 17

### Scheme 17

#### Major pathway



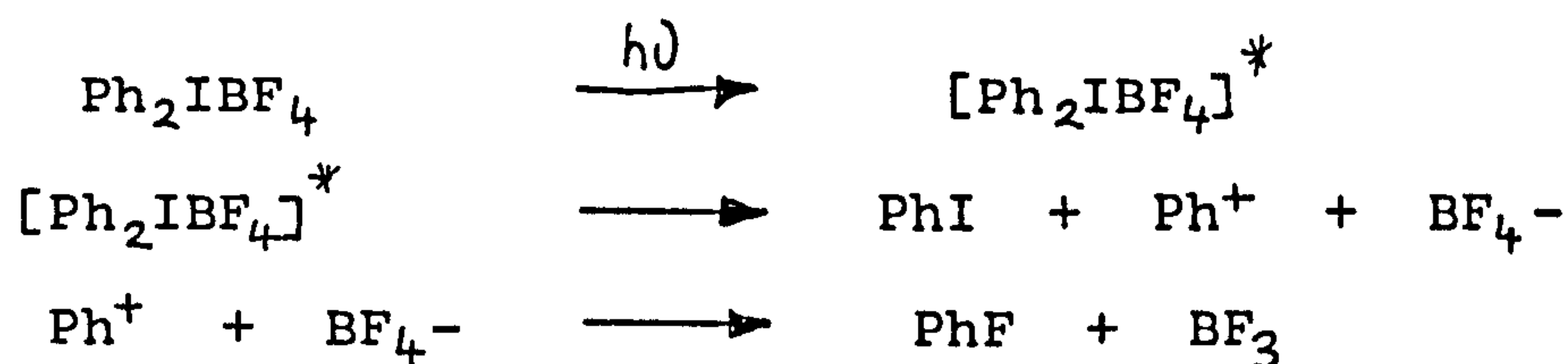
#### Minor pathway



Evidence that supports the above mechanism are firstly the absence of aryl fluorides and secondly anions in the series  $\text{BF}_4^-$ ,  $\text{PF}_6^-$ ,  $\text{AsF}_6^-$ ,  $\text{SbF}_6^-$ , have little effect on the quantum yields of phenyl iodides formed. The evidence for the formation of the true initiator, i.e. acids such as  $\text{HBF}_4$ ,  $\text{HPF}_6$ ,  $\text{HAsF}_6$ ,  $\text{HSbF}_6$ , has been obtained by irradiating diphenyl iodonium salts prior to the addition of monomer and still inducing polymerisation [42].

However, Davidson and Goodin [43] reported significant yields of fluorobenzene formed on irradiation of diphenyl-iodonium tetrafluoroborate in methanol. To account for these findings it was proposed that the photodecomposition of these salts may follow a photoinduced ionic process shown in Scheme 18.

### Scheme 18





The formation of anisole also suggests that the decomposition of the excited salt gives rise to phenyl cations.

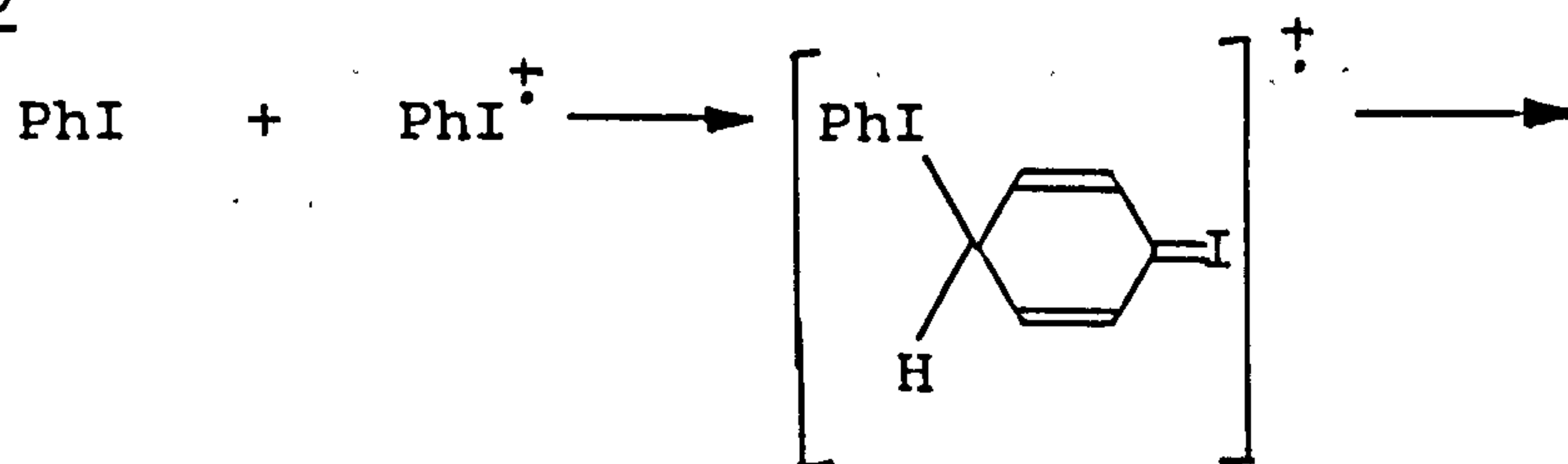
Scheme 19

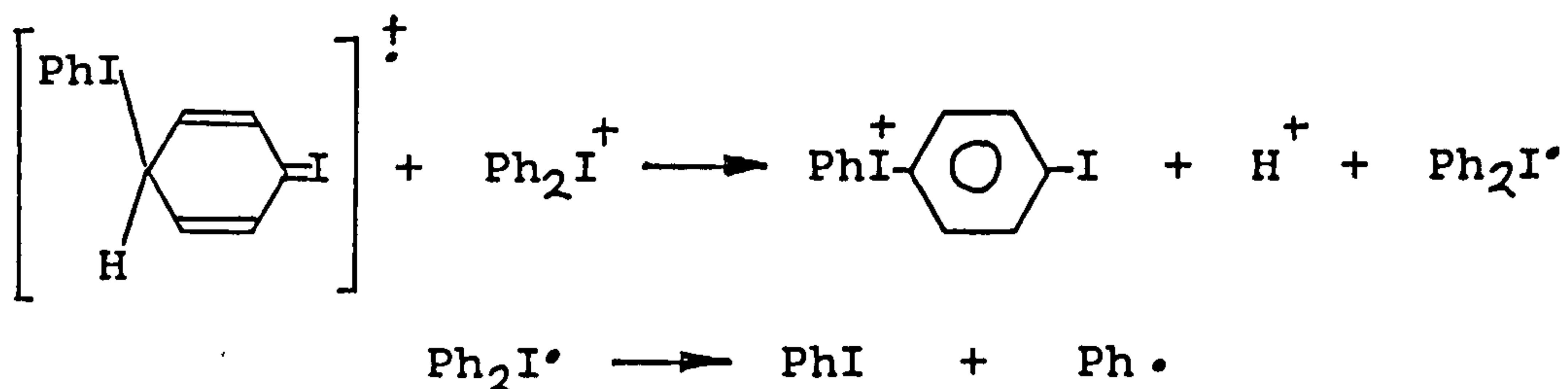


Although it is generally accepted that Brönsted acids are the primary species responsible for initiating polymerisation, these studies have all been conducted in polar media, where free ions predominate, and it has been suggested by Ledwith [44] that the photofragmentation pattern of these salts in polar media may not be valid in nonpolar media where aggregates will predominate.

Knapczak [41] made the observation that in the case of diphenyliodonium tetrafluoroborate, the quantum yield of acid was far greater than expected and was attributed to the solvolysis of  $\text{BF}_4^-$ . Pappas [45] also noted greater yields of acids than expected in the case of diphenyliodonium hexafluoroarsenate. The mechanism shown in scheme 20 was postulated by Pappas to account for these high yields of acid relative to iodobenzene.

Scheme 20





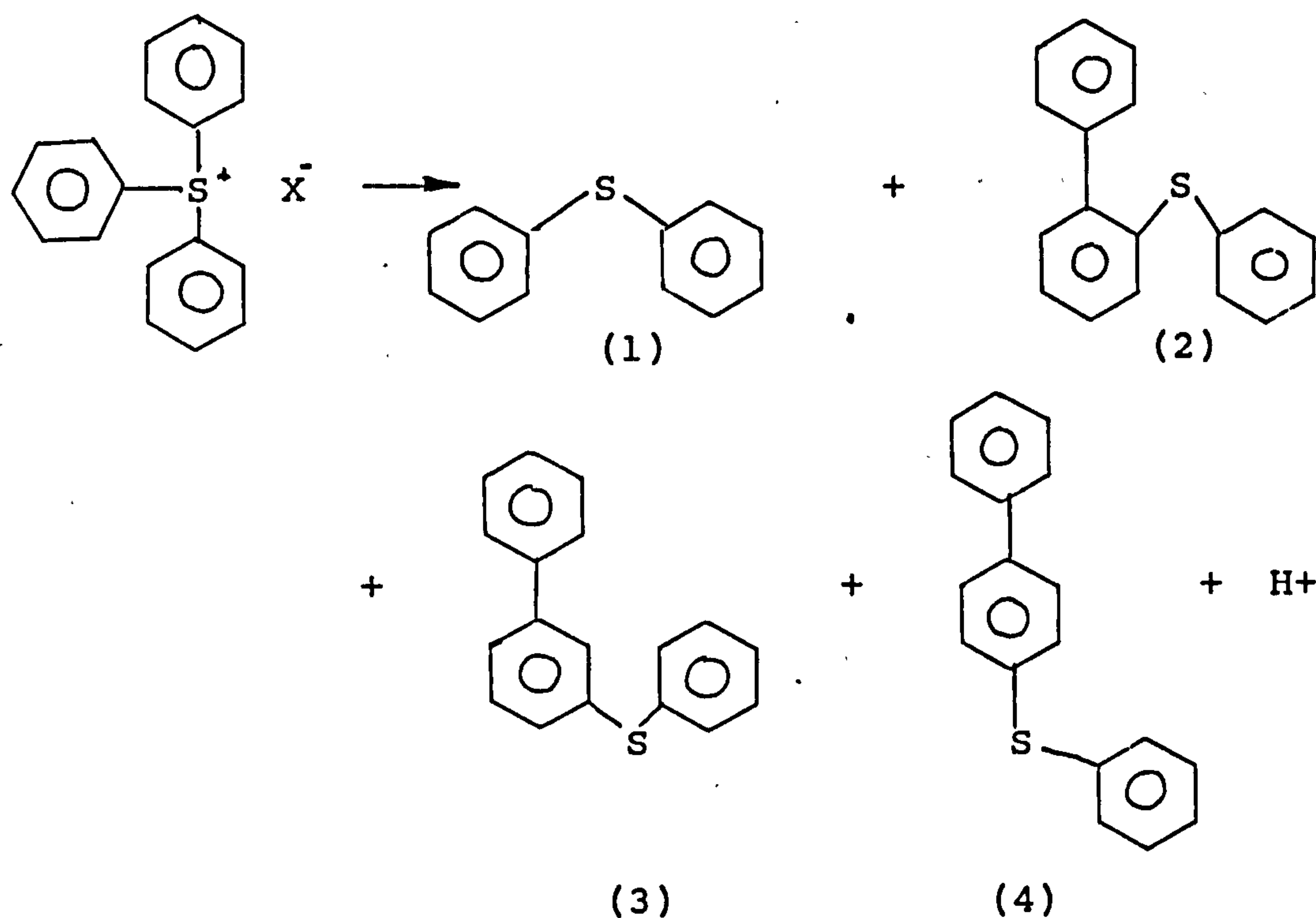
Pappas [45] also suggested that because  $\text{PhI}^{\dagger}$  was highly reactive towards cyclohexeneoxide ( >10 times more reactive than with an alcohol, ether or water), that this species may be a primary initiating species with highly reactive epoxides such as 3,4-epoxycyclohexylmethyl-3',4'-epoxycyclohexane carboxylate.

Photolysis of sulphonium salts also produced greater than expected acid yields and Pappas [46] again explained these findings via an analogous mechanism to that proposed in Scheme 20 for the iodonium salts.

The reactivity of  $\text{Ph}_2\text{S}^{\dagger}$  towards cyclohexene oxide has not yet been recorded, but evidence that  $\text{Ph}_2\text{S}^{\dagger}$  is involved in the initiation process was obtained from spectroscopic data obtained by Ledwith [47]. This revealed that p-alkoxydiphenyl sulphide end groups exist in poly(cyclohexene oxide) using diphenyl-4-thiophenoxyphenyl sulphonium as initiator. It was also proposed that  $\text{PhI}$  would be capable of initiating polymerisation by a similar mechanism.

Dektar and Hacker [48] proposed a new mechanism for acid formation. On photolysis of the triphenyl sulphonium salt a range of products were isolated

Scheme 21

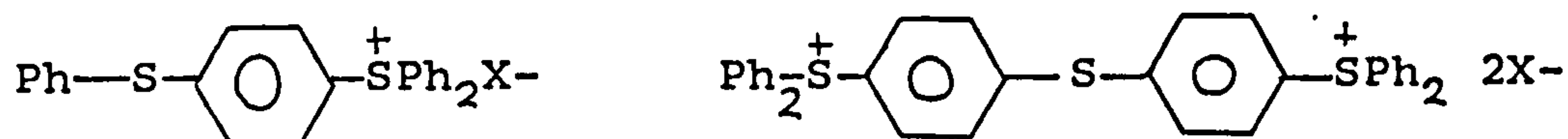


From this and the measurement of acid yields it was proposed that isomers (2)-(4) were the result of recombination by molecular rearrangement of the phenyl cation with diphenylsulphide or the phenyl radical cation with a diphenylsulphonium radical cation.

Diphenyliodonium and triphenylsulphonium salts absorb strongly in the region 230-260nm with little absorbance above 300nm. The application of these photoinitiators in thick films or pigmented systems will have obvious drawbacks. The products of the photolysis of these salts having similar absorption spectra to their parent compound,

will also compete for radiation.

In the case sulphonium salts this was overcome by using a complex sulphonium salt with a larger chromophore [49-51]. The commercially available "triphenyl sulphonium" salts called MASH (Mixed Aromatic Sulphonium Hexafluorophosphates) and are of the type shown below



MASH absorbs beyond 300nm due to the presence of extended chromophores.

Alternatively, a photosensitiser may be used, which will absorb radiation at longer wavelenghts.

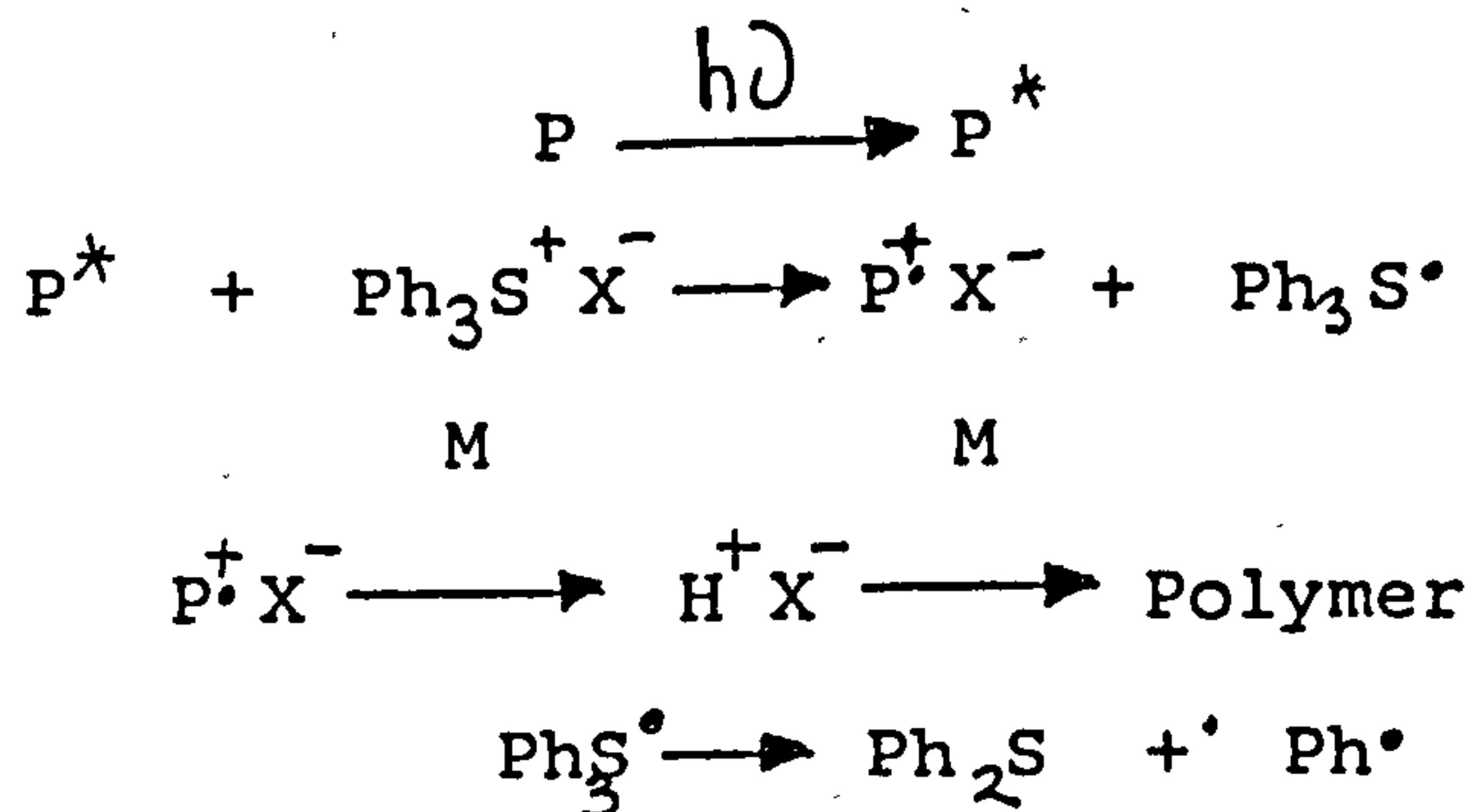
Crivello and Lam [52] showed that dyes such as acridine orange, benzoflavin could be used as photoactivators in systems containing iodonium salts. Perylene [53] was found to be a successful dye in the activation of systems containing the sulphonium salt. The mechanism by which these dyes operate will be illustrated in the following section.

#### b) Photoinduced electron transfer between donor and onium salts

Pappas and Jilek [54] studied the photosensitisation of onium salts and provide evidence that the process involves electron transfer from the excited state photosensitiser to the onium salts as shown in Scheme 22.



Scheme 22



Energy requirement:  $[E^*(P) - E^{\text{ox}}(P)] > E^{\text{red}}(\text{O}^+)$

The success of a photosensitiser/onium salt system is based on the requirement that for electron transfer to be energetically favourable the excitation energy of the photosensitiser must be greater than the sum of the energy required to oxidise the photosensitiser and the energy required to reduce the onium salt, as shown in Scheme 22.

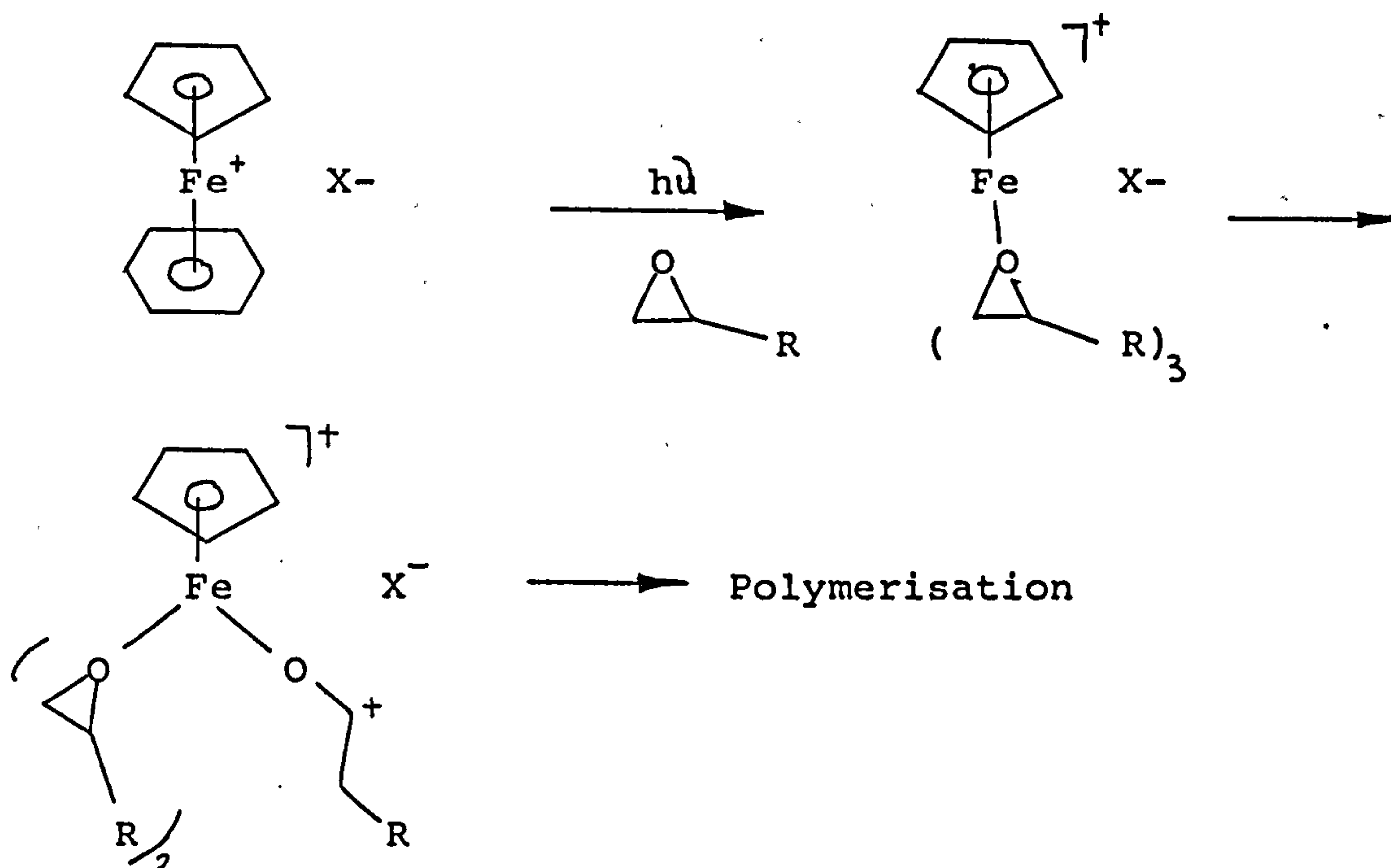
Iodonium salts with small reduction potentials are more susceptible to decomposition by photosensitisers than sulphonium.

c) Electron transfer between nucleophilic radicals and onium salts

Ledwith [32,55] demonstrated that free radicals formed photochemically in the presence of onium salts are capable of generating the carbenium salts which can initiate cationic polymerisation. The free radical photoinitiator 2,2-dimethoxyphenyl acetophenone was used in conjunction with diphenyl iodonium salts and was shown to induce cationic polymerisation of cyclic ethers, alkyl vinyl ethers



It was then proposed that the Lewis acid formed would rapidly coordinate with three epoxides, leading to ring opening and initiation of polymerisation as depicted in Scheme 26.



However, it was also noted that the iron cation is less reactive in epoxide polymerisation compared with Brönsted acids produced from iodonium or sulphonium salts, and a heat treatment was required to promote the reaction [2].

# ELECTRON BEAM INDUCED POLYMERISATION OF EPOXIDES

## Introduction

The introduction of environmental pollution regulations and the concern for energy conservation resulted in the search of methods of producing surface coatings with the minimum energy consumption and with negligible pollution to the environment. Several techniques have been developed to overcome the unacceptable problems associated with solvent based systems, and these are, infrared, microwave and radiofrequency, electron beam and ultraviolet radiation. By far the most popular method of producing surface coatings is by UV radiation. The use of electron beam radiation in this field has not been fully realised. Two main reasons for its slow development are, firstly, the high cost of equipment and secondly, competition from the already well established process of UV curing.

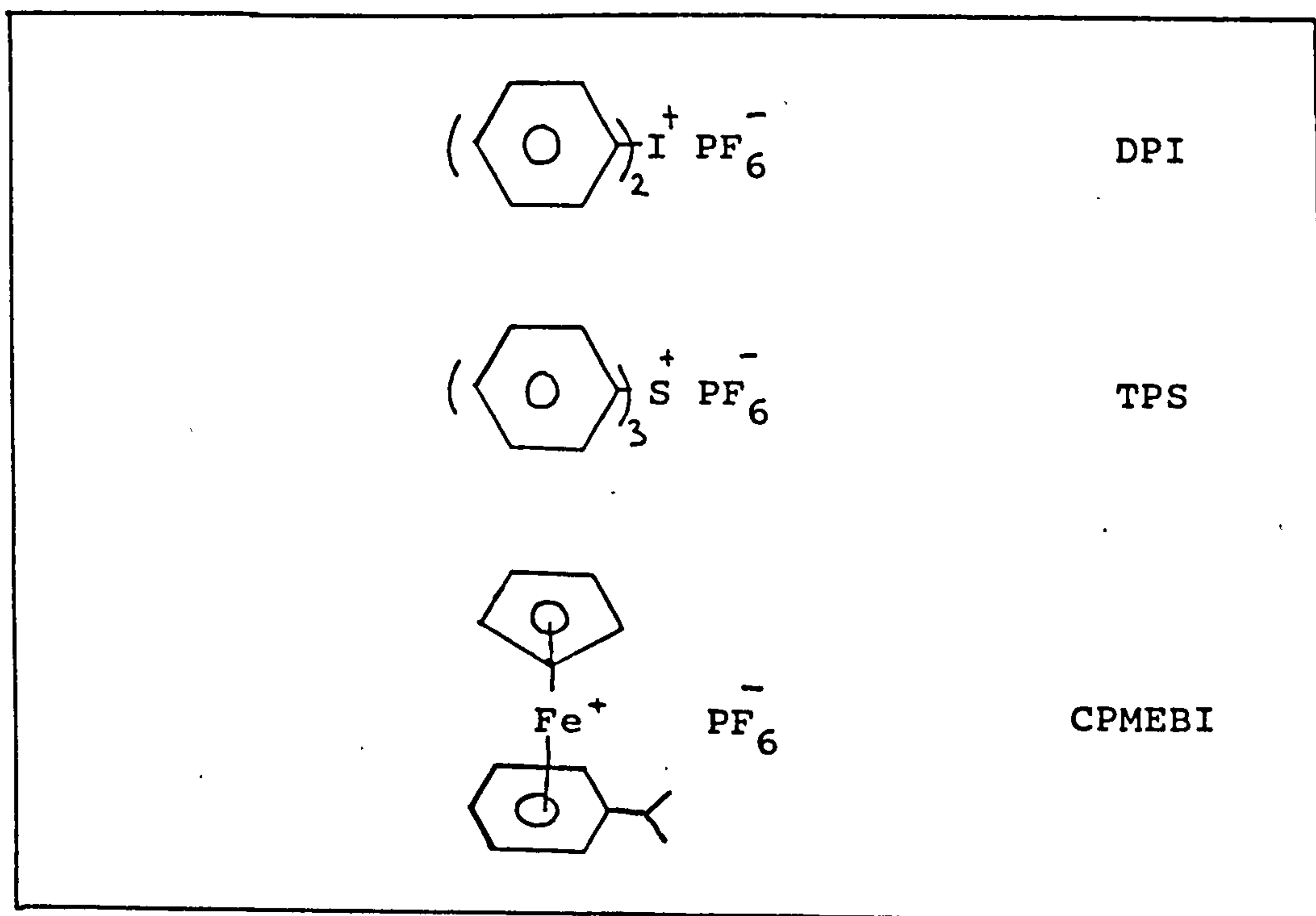
The materials primarily used for UV curing and electron beam curing are dominated by the unsaturated type of resin/diluent, namely the acrylates. The application of cationically polymerisable materials such as the vinyl ethers and epoxides has only recently been added to the list of potential UV-curable systems. The introduction of these materials to the surface coatings industry was as a result of the discovery that onium salts with nonnucleophilic anions [12,13] were effective photoinitiators of epoxide polymerisation.



The use of epoxy systems in producing surface coatings by electron beam has not been fully investigated, although Watt [1] briefly mentioned that p-methoxybenzenediazonium hexafluorophosphate and triphenylsulphonium hexafluorophosphate can cure an epoxy system under electron beam radiation. It is interesting to note that the electron beam curing of epoxides requires the presence of a photoinitiator to promote polymerisation, contrary to the electron beam induced polymerisation of acrylates which proceed via a free radical mechanism in the absence of a photoinitiator.

In this chapter a comparative study of the performance of some commercial cationic initiators, namely the iodonium and sulphonium salts and the iron arene complex (Figure 1), and sulphonium salts and the iron arene complex (Figure 1),

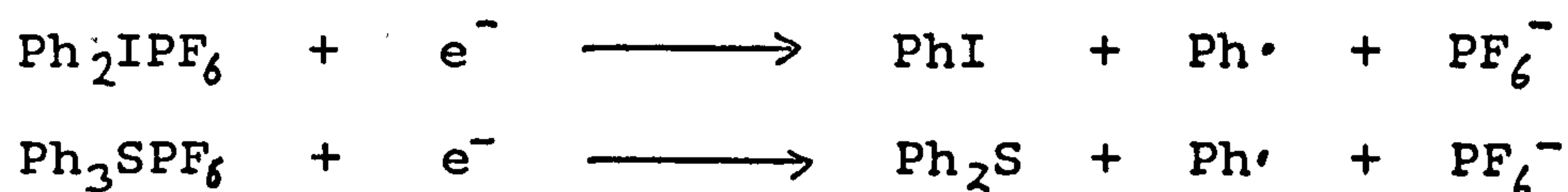
Figure 1 The coinitiators to be compared



as coinitiators of epoxide films exposed to electron beam radiation was undertaken. The epoxide chosen to study these systems, was the cycloaliphatic diepoxide, 3,4-epoxycyclohexylmethyl-3',4'-epoxycyclohexane carboxylate. The changes in composition of the diepoxide film were also monitored.

Interestingly, Yamoto et al [59], have recently investigated the use of radiolysis induced polymerisation of tetrahydrofuran with diphenyliodonium and triphenylsulphonium hexafluorophosphates and proposed that decomposition of the salts was as a result of electron capture

#### Scheme 27



The oxonium ion capable of initiating the cationic polymerisation of tetrahydrofuran was produced as a result of forming a radical cation which then undergoes a hydrogen abstraction reaction with another tetrahydrofuran molecule.

It is known that the cationic polymerisation of epoxides is notably sensitive to several factors, such as, the structure of the epoxide, temperature and the presence of contaminants.

#### Factors affecting the rate of cure and the degree of polymerisation of epoxides

Epoxy resins based on the glycidyl structure are generally less reactive than non-glycidyl epoxy resins in

the presence of catalysts [1]. The rate of polymerisation is also much greater for resins of high epoxy value [1]. The presence of bulky groups close to the heteroatom may also inhibit the interaction.

The effect of temperature on the rate of cure and the degree of polymerisation will generally always result in an increase in the rate of cure or the time taken to obtain a tackfree coating [1,15]. However, excessive heating may lead to a decrease in molecular weight, due to an increase in termination by backbiting [15].

It is known that the presence of even minute quantities of impurities such as amines or powerful nucleophiles will react with either the acid initiator or with a propagating cation [1], which may inhibit polymerisation.

Watt [1] also showed that the substrate e.g. polyamide film, may also effect the rate or degree of polymerisation of epoxides.

Water is known as a inhibitor of epoxide polymerisation and it has been shown by Watt [1] that high humidity decreases the rate of polymerisation of UV-curable epoxide coatings.

#### Characteristics of epoxide films

The polymerisation of epoxides can be monitored by observing the disappearance of either the peak at  $\sim 900\text{cm}^{-1}$  or  $\sim 800\text{cm}^{-1}$  indicative of the epoxide structure [60]. The ring opening reaction of epoxides may also be followed by measuring the growth of the aliphatic ether absorption at

$\sim 1050\text{cm}^{-1}$  [60]. However, this is complicated by the fact that it is a broad peak and is superimposed on other peaks. The measurement of the disappearance of the absorption peak associated with the epoxide have shown that the polymerisation process continues long after irradiation [25]. The fate of the photoinitiators, on exposure to UV radiation has been monitored by Pobiner [61], for aryldiazonium salts of complex anions. These photoinitiators display an absorption band at 280-403nm due to the diazonium chromophore and on exposure to UV radiation, this band disappears. From a calibration curve it was possible to determine the quantity of residual photoinitiator.



## RESULTS AND DISCUSSION

A comparison of the cure performance of a cycloaliphatic diepoxide in the presence of diphenyliodonium hexafluorophosphate (DPI), 'triphenylsulphonium' hexafluorophosphate (TPS), and (n5-2,4-cyclopentadien-1-yl)-[(1,2,3,4,5,6-n)(-1-methylethyl)-benzene]-iron(1+) hexafluorophosphate (CPMEBI) on exposure to electron beam radiation was investigated.

Cure response of the diepoxide was determined by measuring the actual conversion of epoxide functionality and growth of hydroxyl content in the presence of the aforementioned coinitiators/initiators. The ring opening reaction of the epoxide group was monitored by measuring the area associated with the  $795\text{cm}^{-1}$  peak, ascribed to the C-H deformation of an epoxide group. The area associated with the C-H stretching frequencies at around  $3000\text{cm}^{-1}$  was used as an internal standard [60].

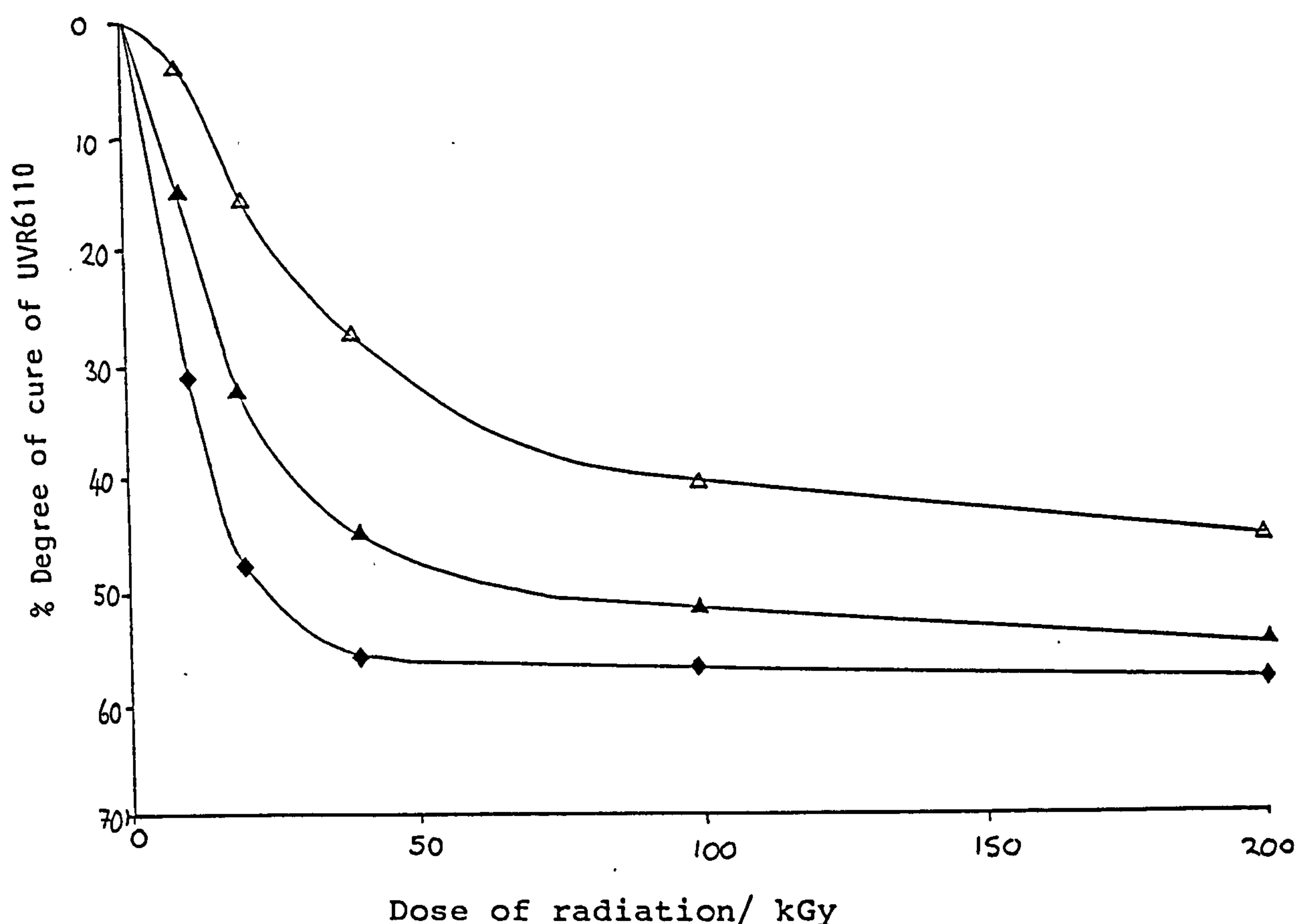
As can be seen from Figure 1 the order of reactivity of the initiator/coinitiators studied was found to be :-



The observed order of reactivity of the iodonium and sulphonium salts is in agreement with those results obtained from the  $\gamma$ -radiolysis of tetrahydrofuran in the presence of these salts and with those findings obtained by Kobunshi et al [62]. The cure efficiency using these salts

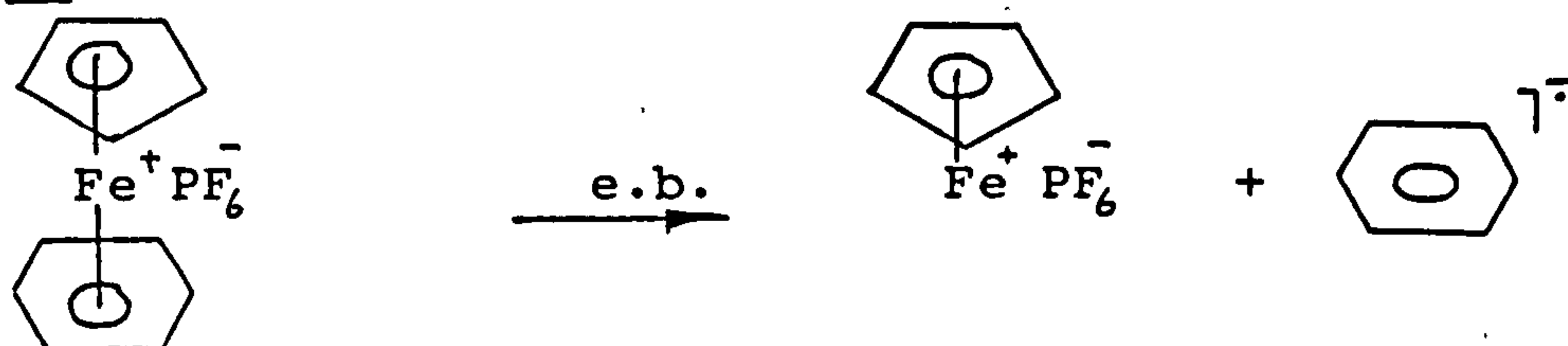
may indicate that they are being decomposed by electron capture.

Figure 1 Percentage degree of cure of the diepoxide in the presence of DPI ( $0.047\text{molkg}^{-1}$ )( $\blacklozenge$ ), TPS ( $0.048\text{molkg}^{-1}$ )( $\blacktriangle$ ) and CPMEBI ( $0.047\text{molkg}^{-1}$ )( $\triangle$ )



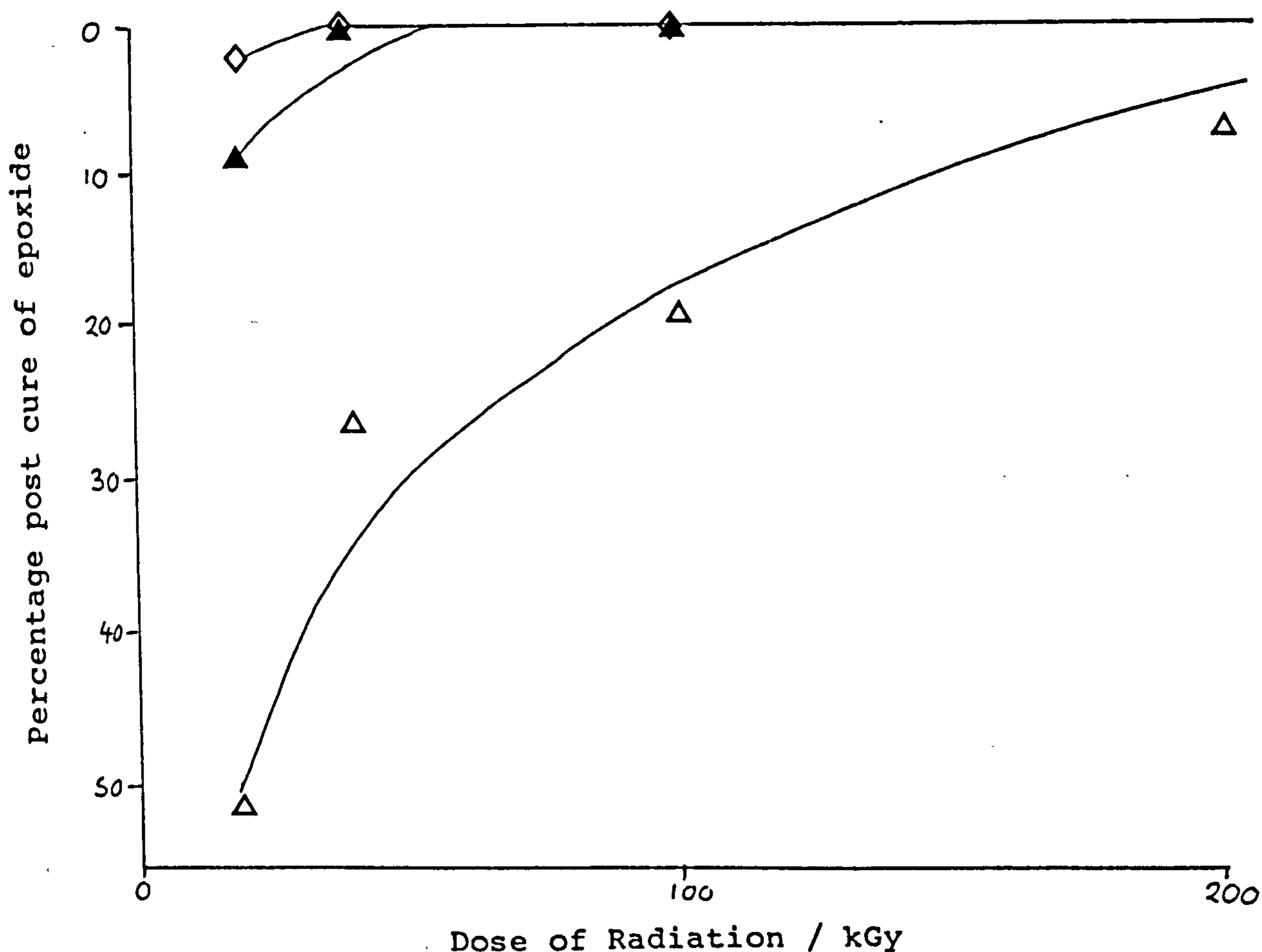
That the iron arene complex is also capable of initiating polymerisation of the diepoxide on exposure to electron beam radiation would also indicate that it is being decomposed and may occur via an electron capture process.

Scheme 28



The slower rate of cure using the iron arene complex has been attributed to the fact that the iron cation is less reactive than the Brönsted acids produced by the onium salts. These systems therefore require a heat treatment after irradiation. Figure 2 illustrates the effect of post

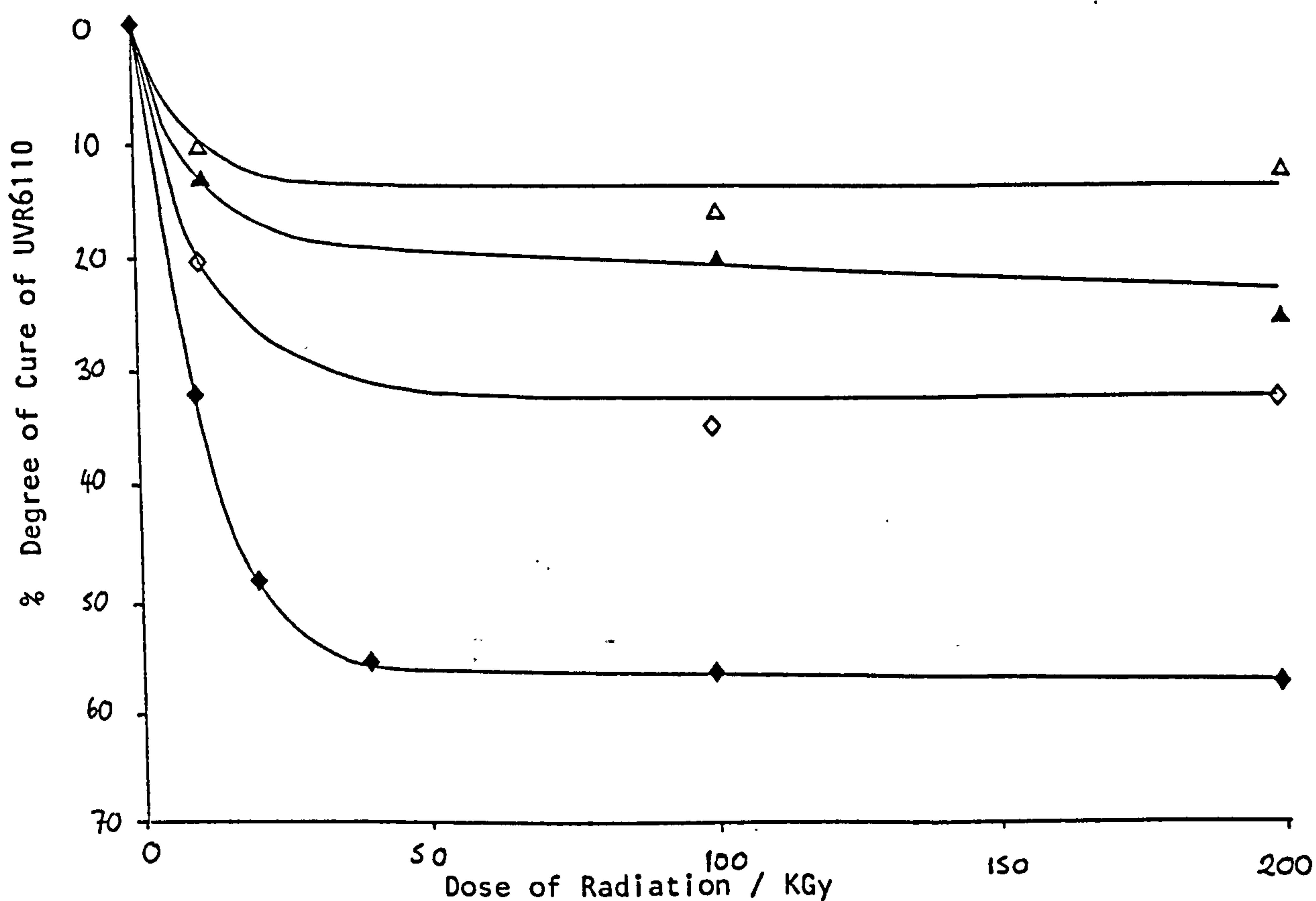
Figure 2 Percentage post cure following a post heat treatment at 70° C of the diepoxide films containing DPI (0.047molkg<sup>-1</sup>)(◇), TPS (0.048molkg<sup>-1</sup>)(▲), CPMEBI (0.047molkg<sup>-1</sup>)(Δ) cured at various doses of radiation



heat treatment at  $70^{\circ}\text{C}$  of the diepoxide containing the coinitiator/initiators, DPI, TPS, and CPMEBI cured at various doses of radiation. In the case of CPMEBI, a post heat treatment was very beneficial, however, for both DPI and TPS the effect was far less marked, especially for those films irradiated at high doses of radiation.

Figure 3 shows that the degree of cure is closely related to concentration of the iodonium salt employed which suggests that under our experimental conditions the rate of cure is related to the efficiency of electron capture which in turn is related to the concentration of the iodonium salt.

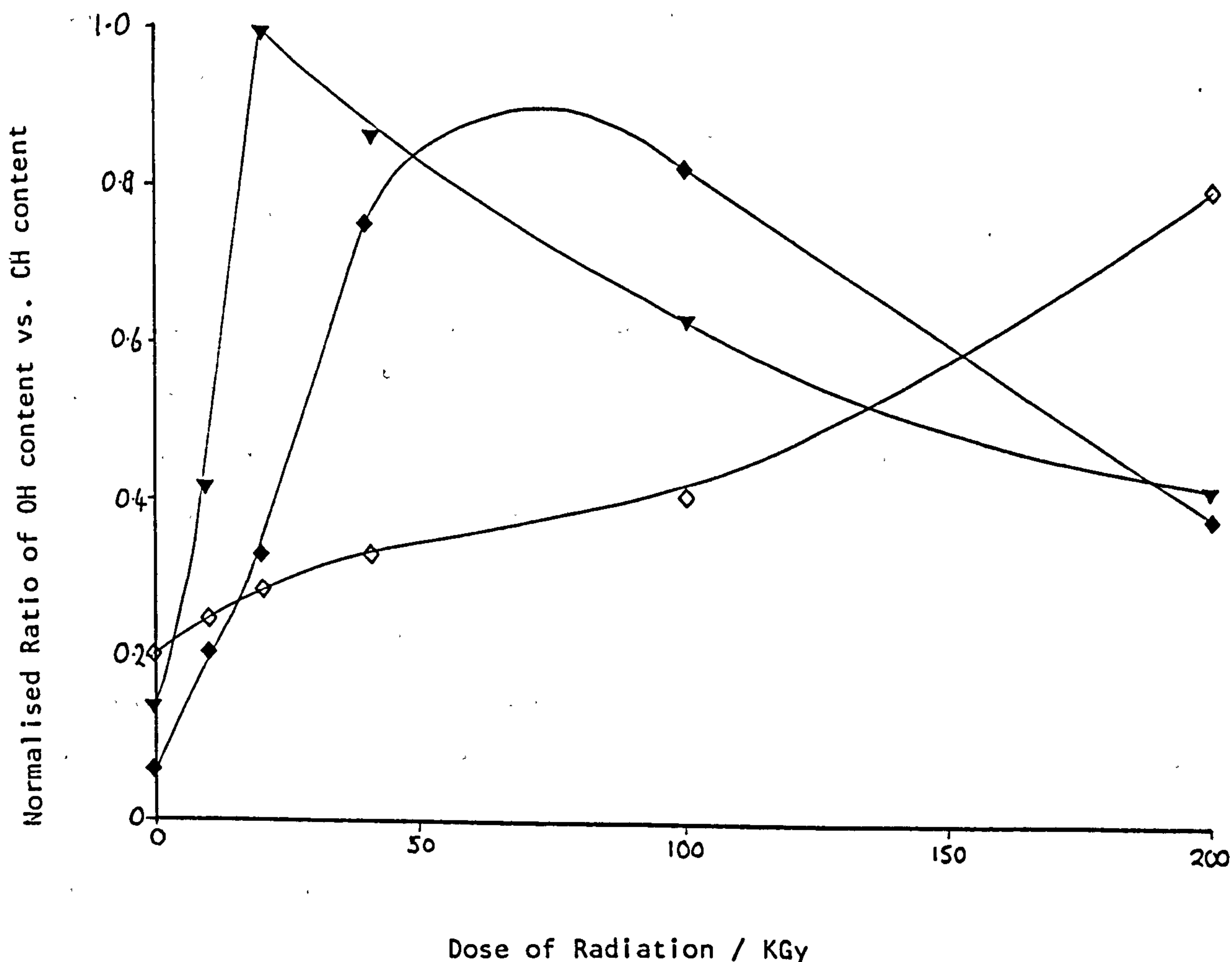
Figure 3 Percentage degree of cure of diepoxide containing DPI at various concentrations, ( $0.047\text{molkg}^{-1}$   $\blacklozenge$ ), ( $0.034\text{molkg}^{-1}$   $\diamond$ ), ( $0.016\text{molkg}^{-1}$   $\blacktriangle$ ), ( $0.008\text{molkg}^{-1}$   $\triangle$ )





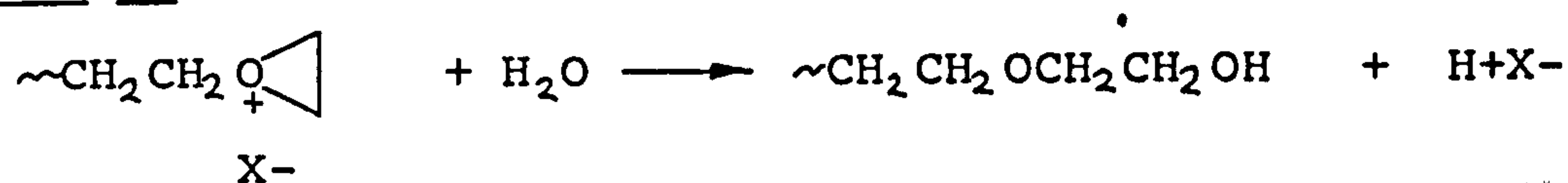
The appearance of the absorption band associated with the hydroxyl group was monitored and it was observed that the hydroxyl content grew in magnitude relative to the chosen internal standard at low doses, but began to diminish in intensity at higher doses of radiation, in the case of DPI and TPS. In the case of CPMEBI only an increase in the hydroxyl content was observed. In the absence of chain transfer agents the formation of free hydroxyl groups

Figure 4 Hydroxyl content of diepoxide films exposed to electron beam radiation in the presence of DPI (0.047molkg<sup>-1</sup> ▼ ), TPS (0.048molkg<sup>-1</sup> ◆ ), CPMEBI (0.047molkg<sup>-1</sup> ◇ )



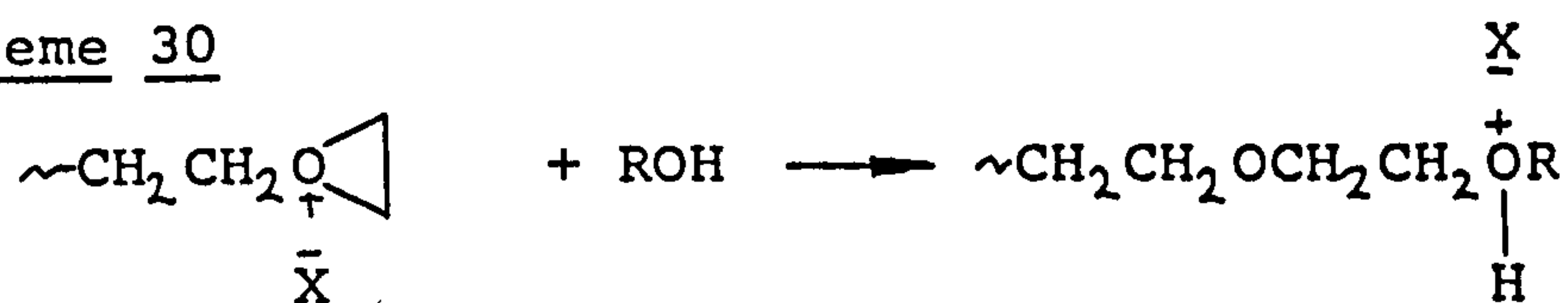
should not occur. However, if water is present even to a small extent in the nitrogen blanket the growing polymer chains will be terminated by traces of water to give alcohols.

Scheme 29



As the degree of cure proceeds the film presumably becomes less permeable to water and the active centre will undergo chain transfer reactions with previously formed alcohol groups. The result will be a reduction in the intensity of the hydroxyl group absorption band.

Scheme 30



The use of polyols as chain transfer agents has been described by Crivello [63], and it was shown possible to obtain films of varying flexibility and molecular weight according to the amount of transfer agent in the system.

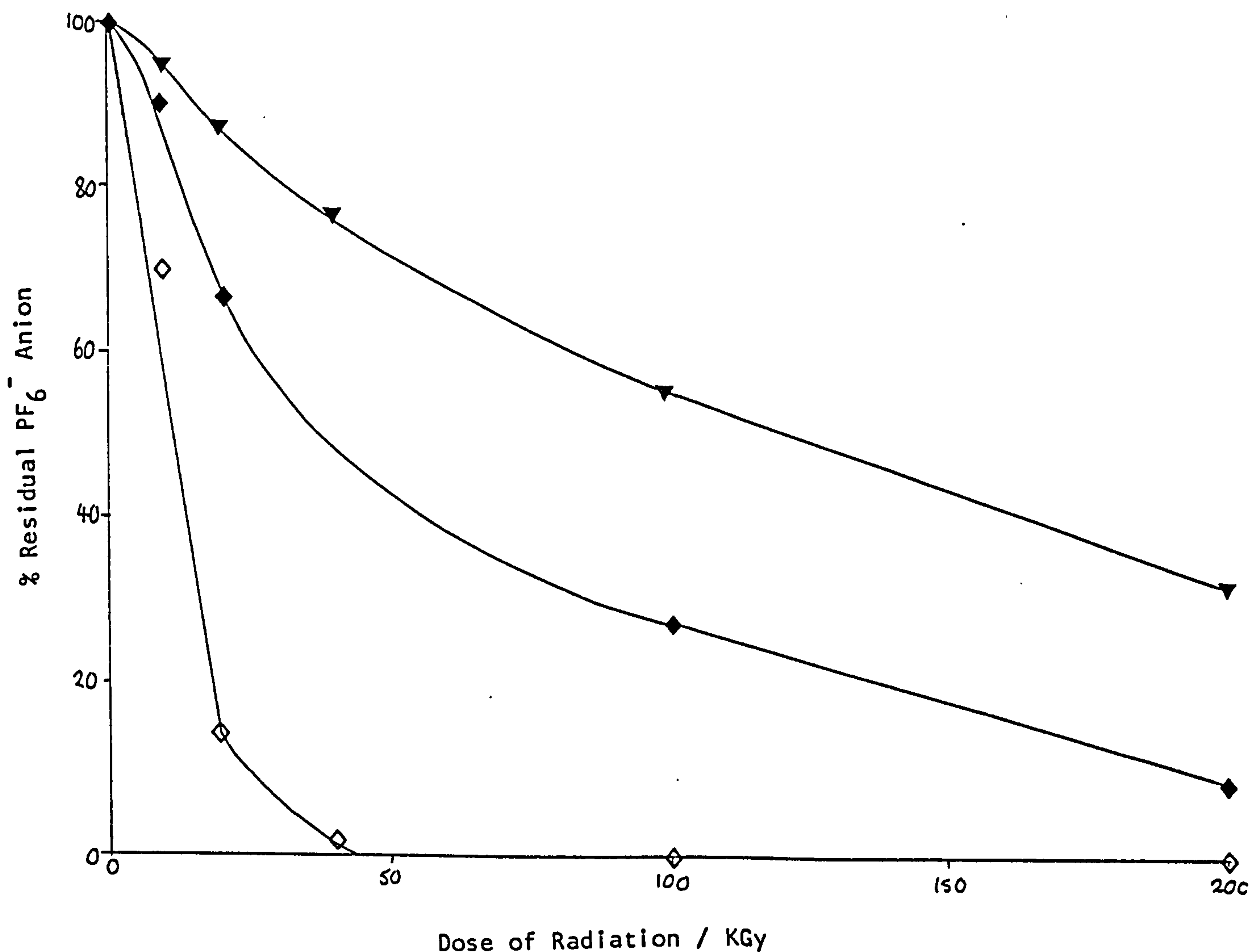
Inspection of the infrared spectra of the diepoxide films cured by electron beam radiation revealed another interesting feature of the polymerisation process. The peak at  $844\text{cm}^{-1}$  associated with the absorption peak of the hexafluorophosphate anion [64] was found to decrease in

intensity and the extent of decomposition of the  $\text{PF}_6^-$  anion was found to occur in the order:-

$\text{DPI} > \text{TPS} > \text{CPMEBI}$

As can be seen from Figure 5 the extent of decomposition of the counteranion corresponds well with the rate of cure of the diepoxide.

Figure 5 Percentage residual hexafluorophosphate anion on curing the diepoxide in the presence of DPI ( $0.047\text{molkg}^{-1}$   $\diamond$ ) TPS ( $0.048\text{molkg}^{-1}$   $\blacklozenge$ ), CPMEBI ( $0.047\text{molkg}^{-1}$   $\blacktriangledown$ )

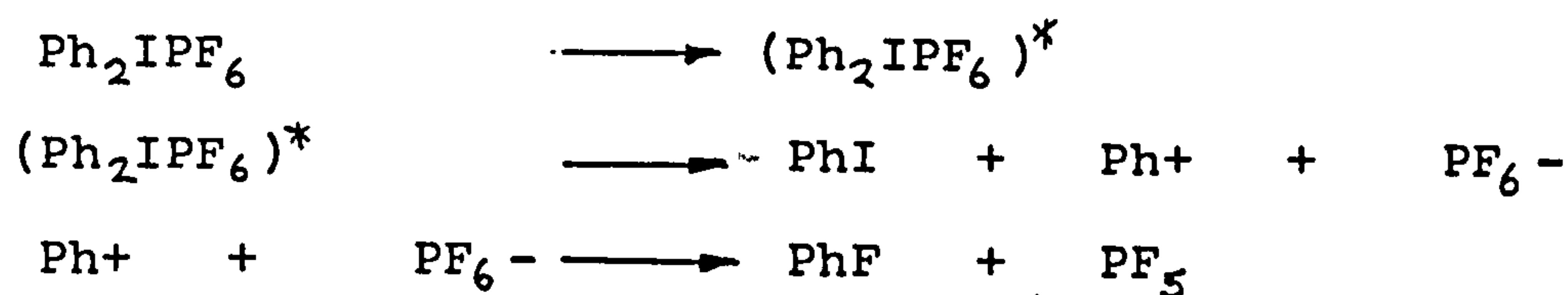


It has always been assumed that the hexafluorophosphate anion remains intact during the photolysis of these salts and forms the stable non-nucleophilic counteranion associated with the active centre [16].

To account for this anomaly the fate of the counter anion may be interpreted as follows.

Firstly, Davidson and Goodin [43] reported significant yields of fluorobenzene on irradiation of diphenyliodonium tetrafluoroborate in methanol. This observation was explained in terms of a heterolytic reaction of the diphenyliodonium cation followed by nucleophilic attack of the tetrafluoroborate anion towards the phenyl cation. An analogous reaction may account for the dis-appearance of the absorption peak associated with  $\text{PF}_6^-$  under electron beam radiation.

Scheme 32



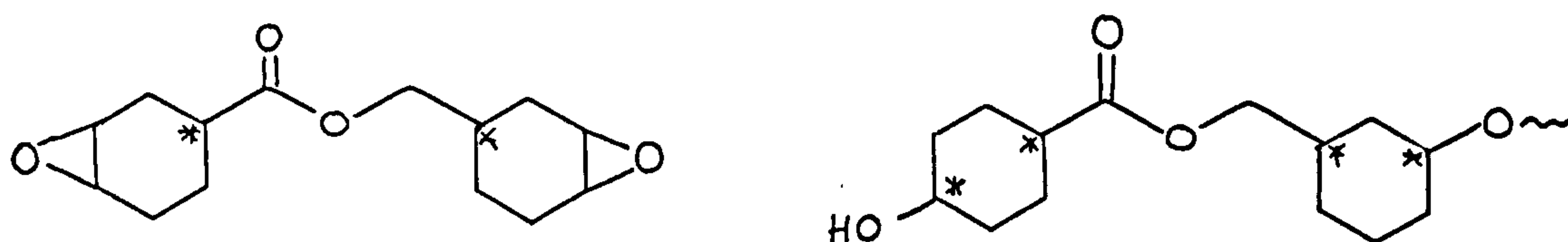
An alternative explanation may involve the fate of the initiating species,  $\text{HPF}_6$ , generated as a result of homolytic cleavage of the excited state of the salt. Acids such as  $\text{HPF}_6$ , are unstable in the absence of a nucleophile, and will form hydrogen fluoride and pentafluorophosphate [16].

However, under electron beam radiation an alternative route to generate the acid  $\text{HPF}_6$  may be involved. It was observed as seen in Figure 6a 6b that an absorption peak at



1780cm<sup>-1</sup> developed and is consistent with a carbonyl stretch of a six membered ring ketone [60], or a vinyl ester [60]. Formation of either a ketone or a vinyl ester may be the result of, firstly, the production of tertiary radicals at various sites on the monomer or polymer as indicated below, which may subsequently be oxidised by the iodonium salt to produce protons.

Scheme 32



\* C-H homolysis may occur at these sites

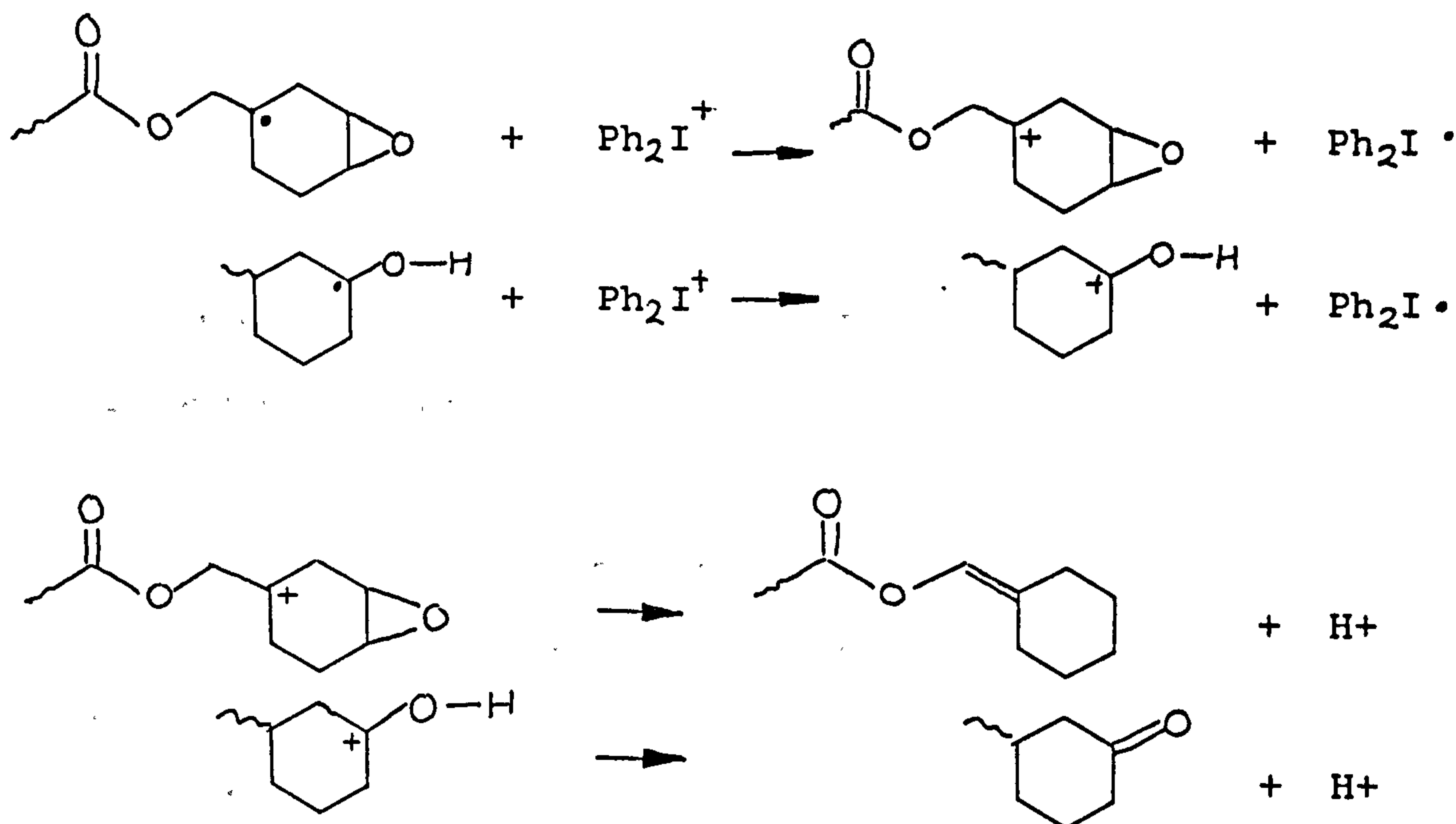
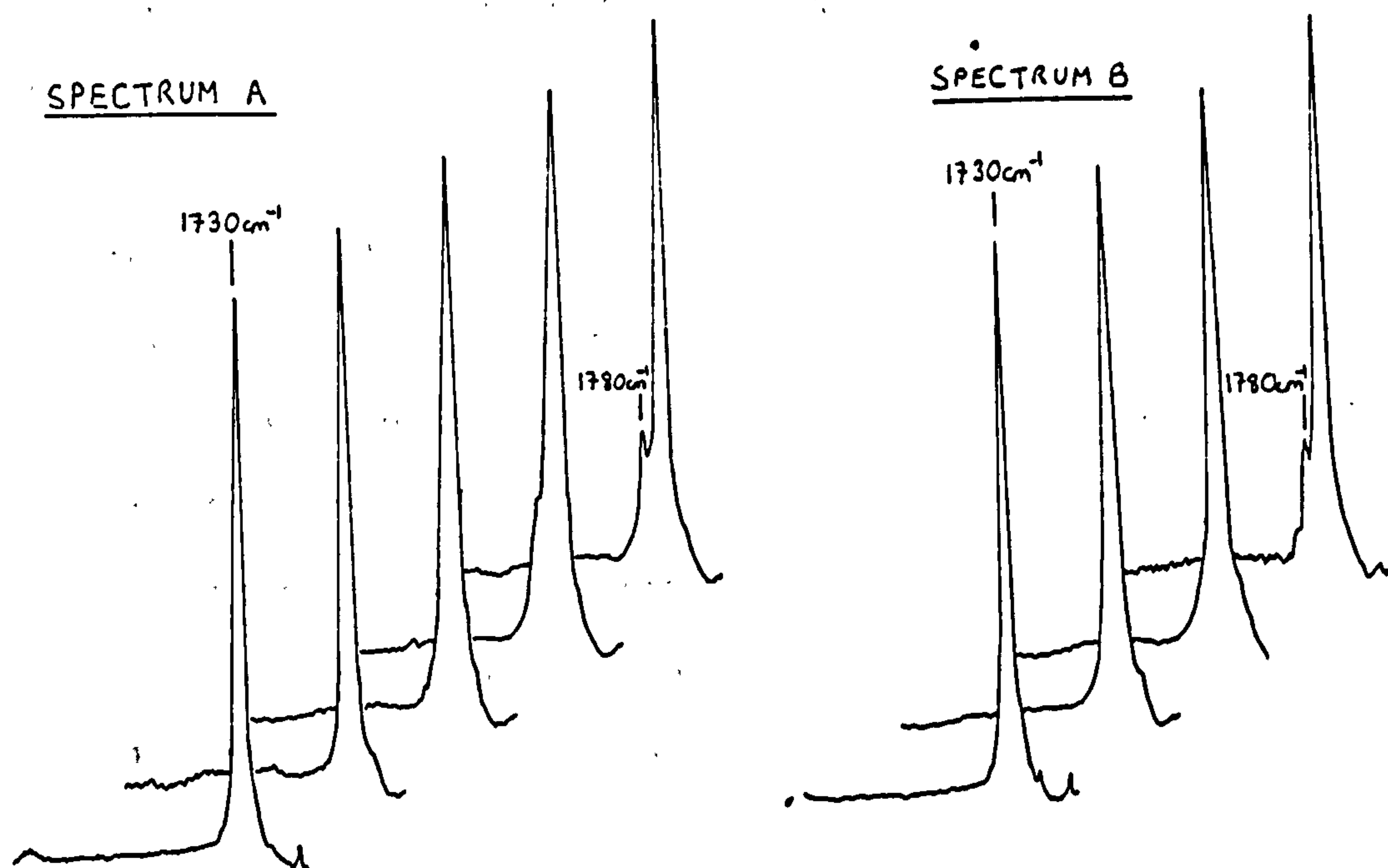
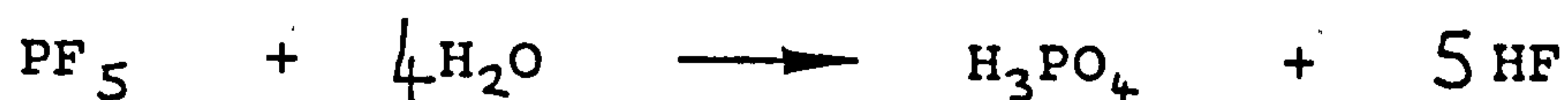


Figure 6 a and b Spectra of diepoxide cured in the presence of DPI (0.047molkg<sup>-1</sup> A) and TPS (0.048molkg<sup>-1</sup> B) cured at various doses of radiation



Absorption peaks associated with the production of PF<sub>5</sub> were not observed. This, would not be surprising on two accounts, firstly, PF<sub>5</sub> is a gas and would probably escape into the atmosphere and secondly PF<sub>5</sub> is readily hydrolysed to yield phosphoric acid and hydrofluoric acid [65].

Scheme 33



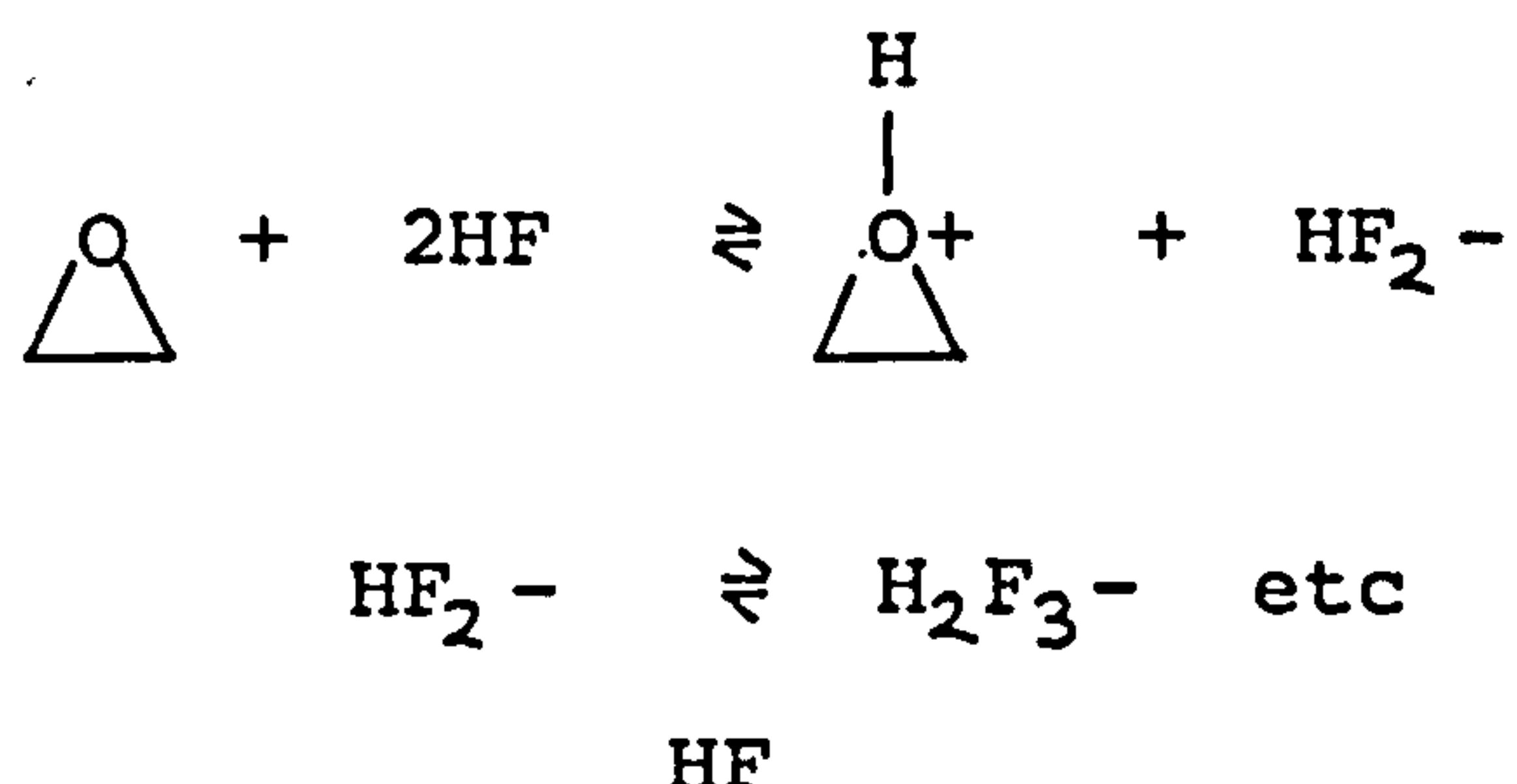
Since all experiments were carried out in an open environment the hydrolysis of PF<sub>5</sub> would occur to a significant extent.

The degree of cure of the diepoxide slows down and eventually levels off at higher doses of radiation. This levelling off process occurs when the decomposition of the anion is almost complete. This may reflect the effect the decomposition products, HF and  $\text{H}_3\text{PO}_4$ , have on the active site.

Firstly, HF has been observed to polymerise cycloaliphatic epoxides quite effectively [66]. This may be due to the fact that  $\text{F}^-$  is a weak nucleophile as a result of the strength of the H-F bond and the very high heat of solvation required to solvate the fluoride ion.

In the presence of an epoxide which has some nucleophilic capacity, HF may undergo heteroconjugation.

#### Scheme 34

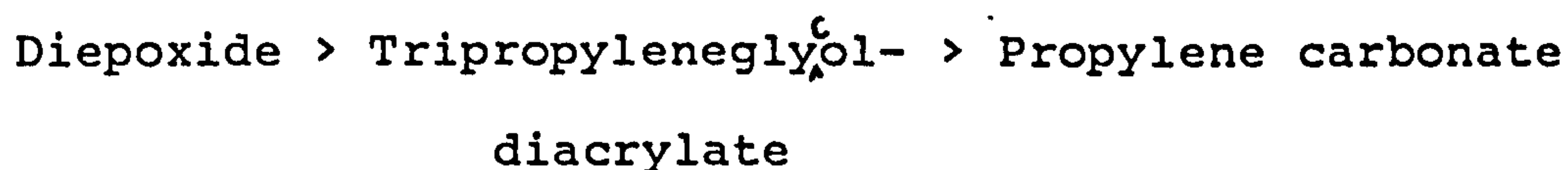


The formation of the hydrogen bonded anions provide a suitably weakly nucleophilic counter anion to allow a certain degree of polymerisation to occur.

It is therefore postulated that HF may infact be the true initiating species of the cationic polymerisation of an epoxide, when using an onium salt under electron beam radiation in an open system. A decrease in the polymerisation rate which eventually levels off was

observed and starts at a point at which the onium salt has been decomposed completely. This may reflect the role  $\text{PF}_5$  generated on decomposition of the salt, plays in the polymerisation process. As discussed previously,  $\text{PF}_5$  is hydrolytically unstable and on reaction with moisture will form  $\text{HF}$  and  $\text{H}_3\text{PO}_4$ , and it is the phosphoric acid produced that may well act as a chain terminator by nucleophilic attack at the active centre. Termination of the active centre may also be brought about by combination of  $\text{F}^-$  ion with the tertiary oxonium ion.

The extent of decomposition of the  $\text{PF}_6^-$  anion was monitored for the iodonium salt, DPI, in media of varying ionisation potential as can be seen in Figure 7. The rate of decomposition of the salt in media of increasing ionisation potential was found to be



It therefore appears that the electron beam induced decomposition of the anion is related to the ease with which the media undergoes electron detachment when subjected to electron beam radiation.

Scheme 35

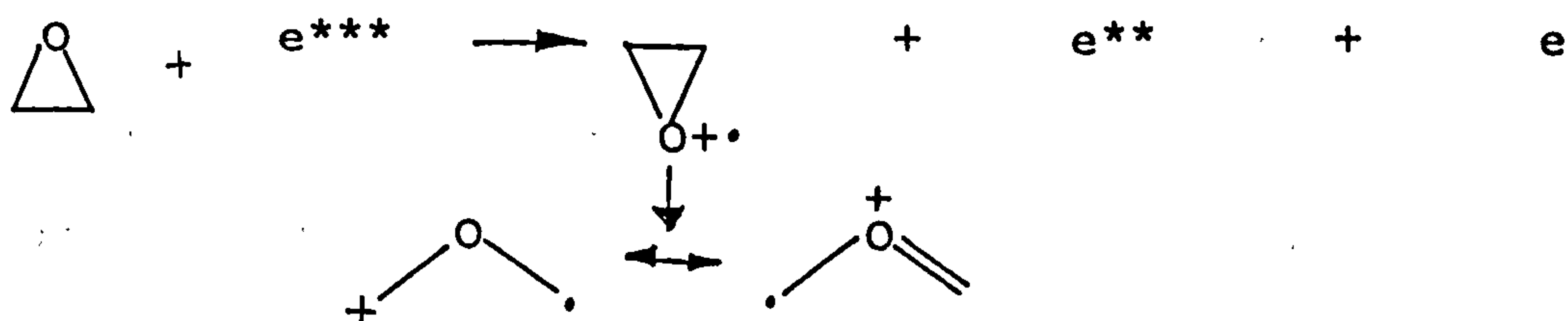
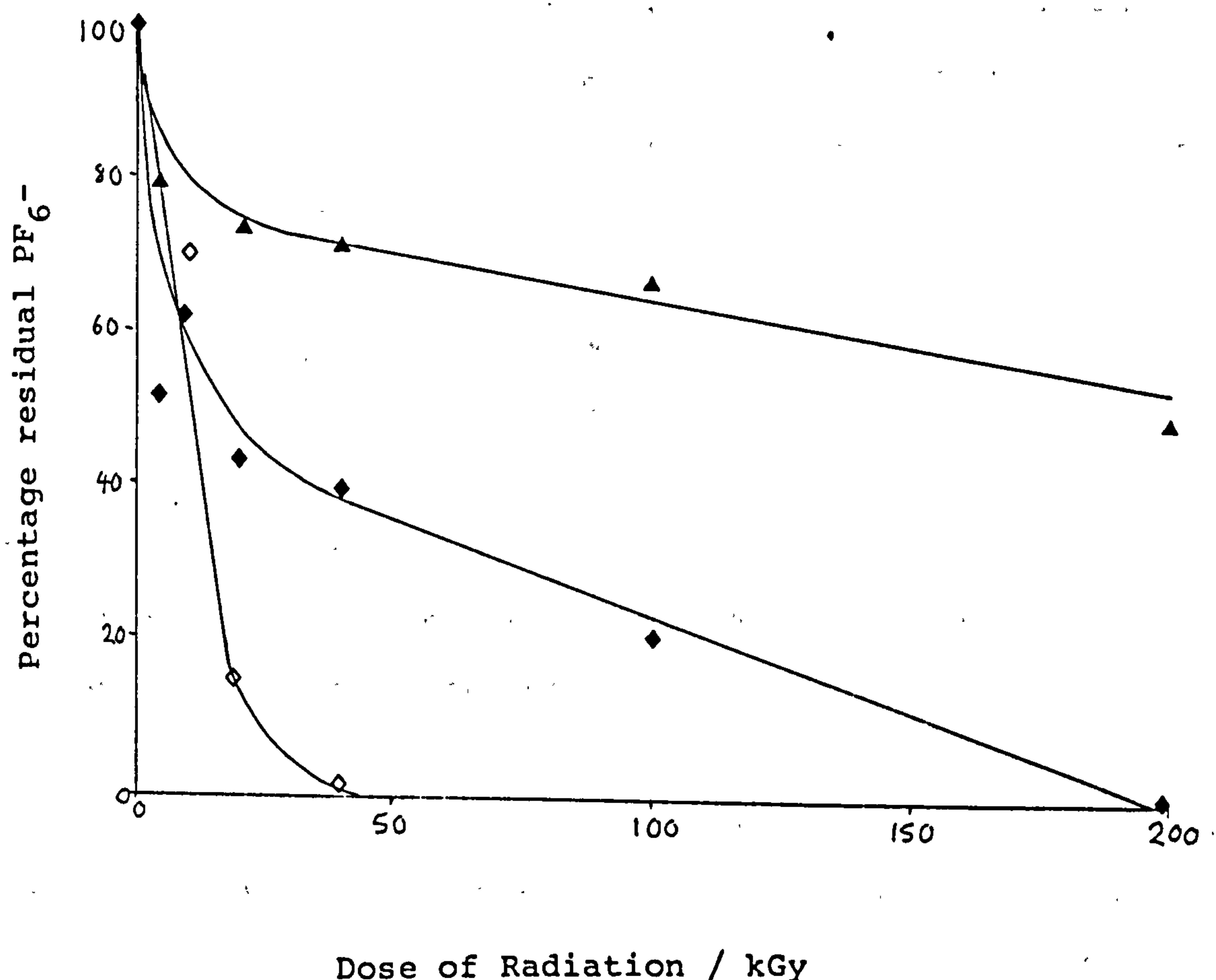




Figure 7 Percentage residual  $\text{PF}_6^-$  on curing the diepoxide ( $\diamond$ )  
TPGDA ( $\blacklozenge$ ), and propylene carbonate ( $\blacktriangle$ ) in the presence of  
DPI ( $0.047\text{molkg}^{-1}$ ).

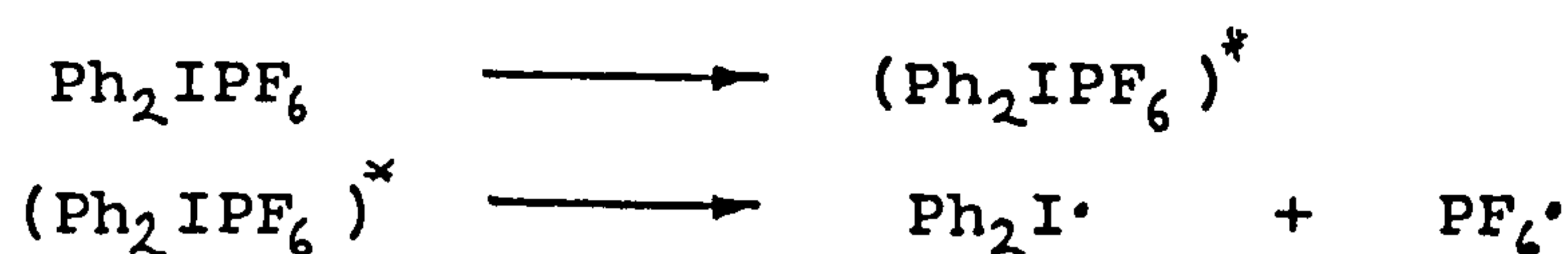


Propylene carbonate probably has a fairly high ionisation potential compared with epoxides and will therefore be a poorer source of slow electrons.

However, an alternative explanation for the decomposition of, as well as extent of decomposition of, DPI in various media may in fact be due to not only the solvating power of the media, but also its ability to generate radicals, which are subsequently oxidised by  $\text{Ph}_2\text{I}^+$

to produce protons as depicted in Scheme 32. It may be assumed that higher aggregates of the salt will form in media of low polarity such as the epoxide, while solvents of high polarity such as propylene carbonate will be effective in solvating the ions. The media in which the salts are poorly solvated may favour the decomposition of these salts by an electron transfer process from the anion to the cation to generate the radical,  $\text{PF}_6^\cdot$ .

Scheme 37



The  $\text{PF}_6^\cdot$  radical may then in turn either abstract a hydrogen atom from a suitable donor to form HF and  $\text{PF}_5$  or oxidise the solvent, tertiary radical or react with a slow electron to regenerate  $\text{PF}_6^-$ .

A source of hydrogen atoms may arise from one of several tertiary hydrogens present within the cycloaliphatic diepoxide and its resultant polymer. TPGDA and propylene carbonate also have tertiary hydrogens but presumably these are less prone to C-H homolysis.

Knapczyk et al [40] obtained evidence for this process from the observation that for the iodonium salts containing the anions  $\text{Cl}^-$ ,  $\text{Br}^-$ ,  $\text{I}^-$  the order of reactivity increased with the ease with which the anion can give up an electron. However, the same workers [41] showed that there was no difference in the reactivity as measured by product yields for the series  $\text{BF}_3^-$ ,  $\text{NO}_3^-$  and  $\text{Cl}^-$ . This may indicate that

an electron transfer process from the anion to counter anion is not important for less readily oxidisable anions. However, it may be significant that these experiments were conducted in highly polar solvents.

From these results, and those of many others [12,31,43,48], a variety of mechanisms <sup>have been proposed</sup> by which the onium salts decompose. The subsequent decomposition of the anion shown here, may explain the marked difference in the post heat treatment of films described earlier. Little postcure at 70°C was observed for films cured using DPI or TPS compared with CPMEBI. The lack of reactivity of films cured by DPI and TPS provides further evidence that the counteranion has decomposed to HF and H<sub>3</sub>PO<sub>4</sub>.

The decomposition of the onium salts and the iron arene complex can be followed, albeit less satisfactorily by UV spectroscopy. Figures 8 and 9 show the spectra for the decomposition of the iodonium salt in the diepoxide and propylene carbonate respectively.

The decomposition product iodobenzene, competes with the iodonium salt in the UV spectra. However, at high doses of radiation no absorption corresponding to this decomposition product was observed. This was attributed to the fact that both iodobenzene and benzene may have been flushed out by the nitrogen blanket. The decomposition of the iodonium salt in propylene carbonate followed by UV

Figure 8 UV spectra of dosed films of the diepoxide in the presence of DPI (0.48molkg<sup>-1</sup>)

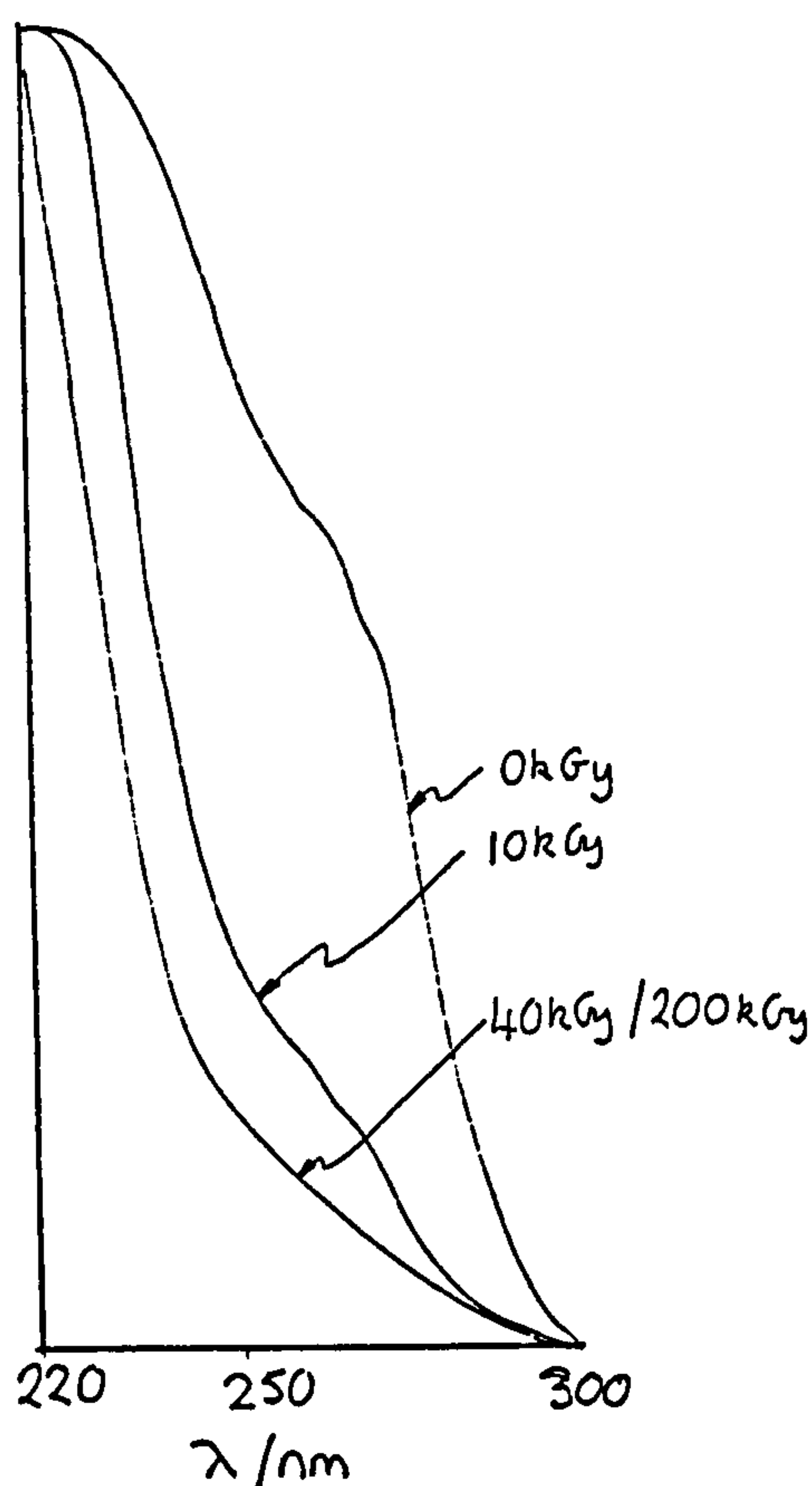
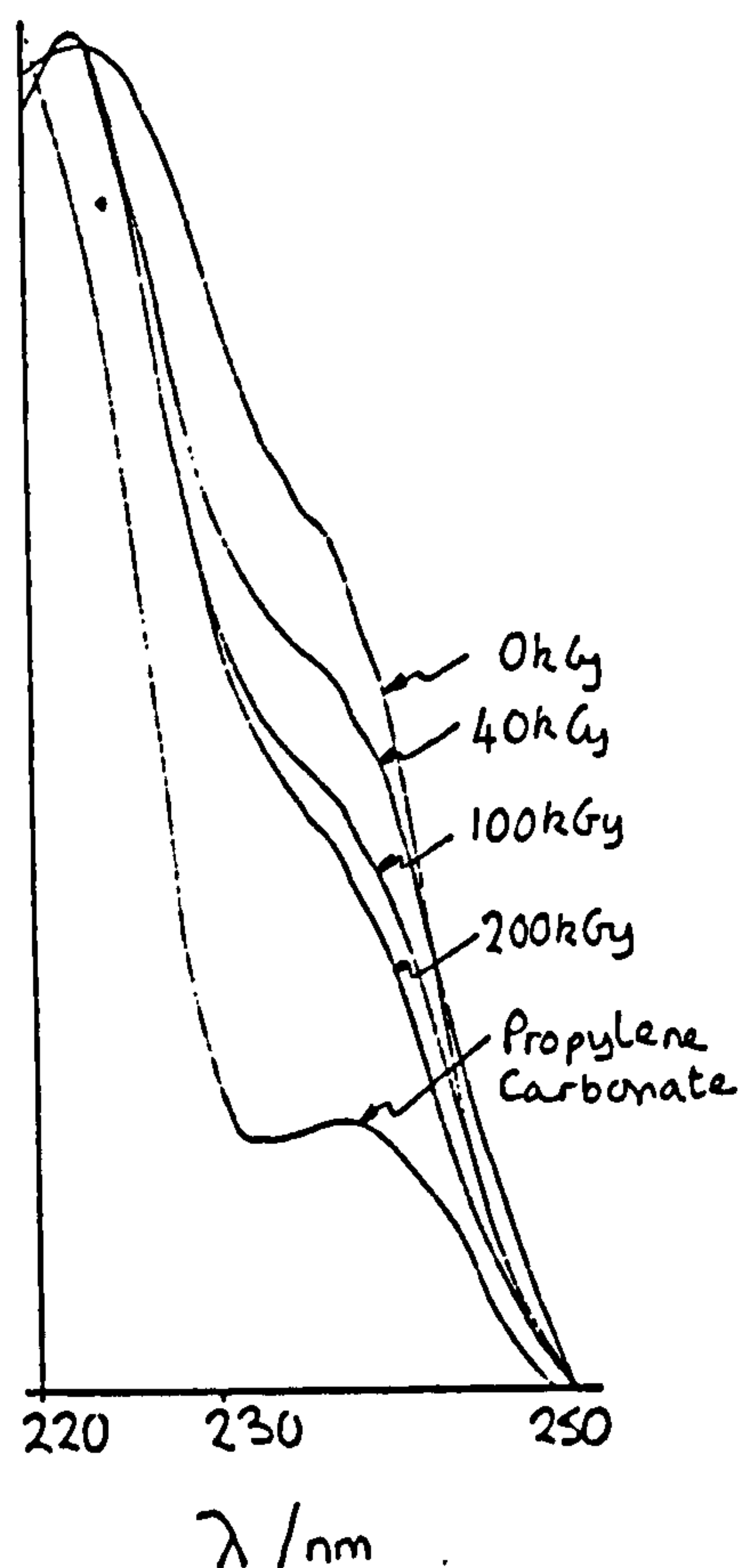


Figure 9 UV spectra of propylene carbonate in the presence of DPI (0.50molkg<sup>-1</sup>)



spectroscopy was found to be considerably slower than in the diepoxide which corresponds well with the extent of degradation of the  $\text{PF}_6^-$  anion as monitored by infrared spectroscopy.

The picture for the sulphonium salt as seen in Figure 10 is not so clear. However, it can be seen at higher doses of radiation the spectrum of a typical aryl sulphide is obtained. In this case the sulphide is far less volatile than corresponding decomposition products of the iodonium salt, and will therefore remain in the film.



Figure 10 UV spectra of dosed films of the diepoxide in the presence of TPS ( $0.047\text{molkg}^{-1}$ )

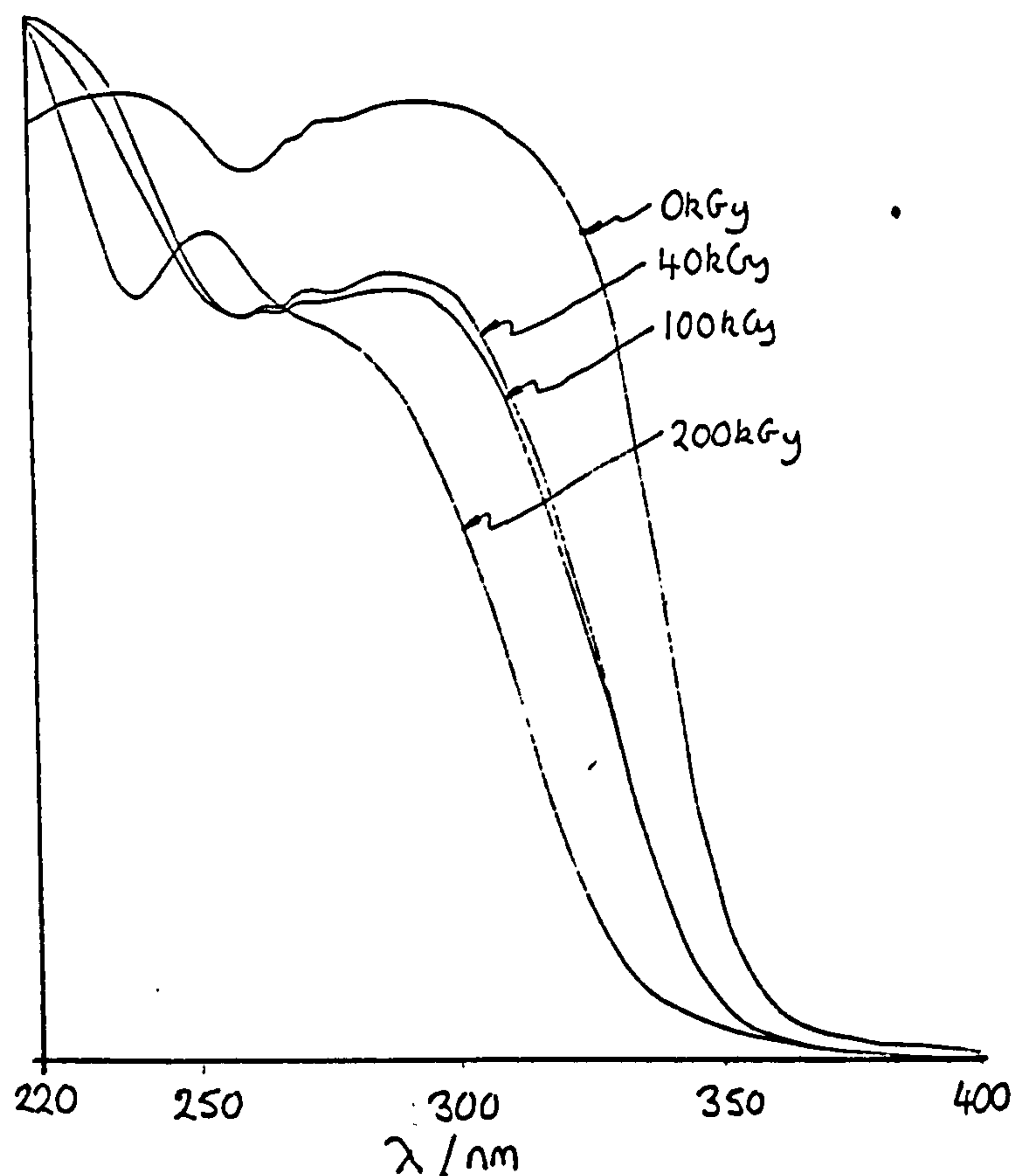
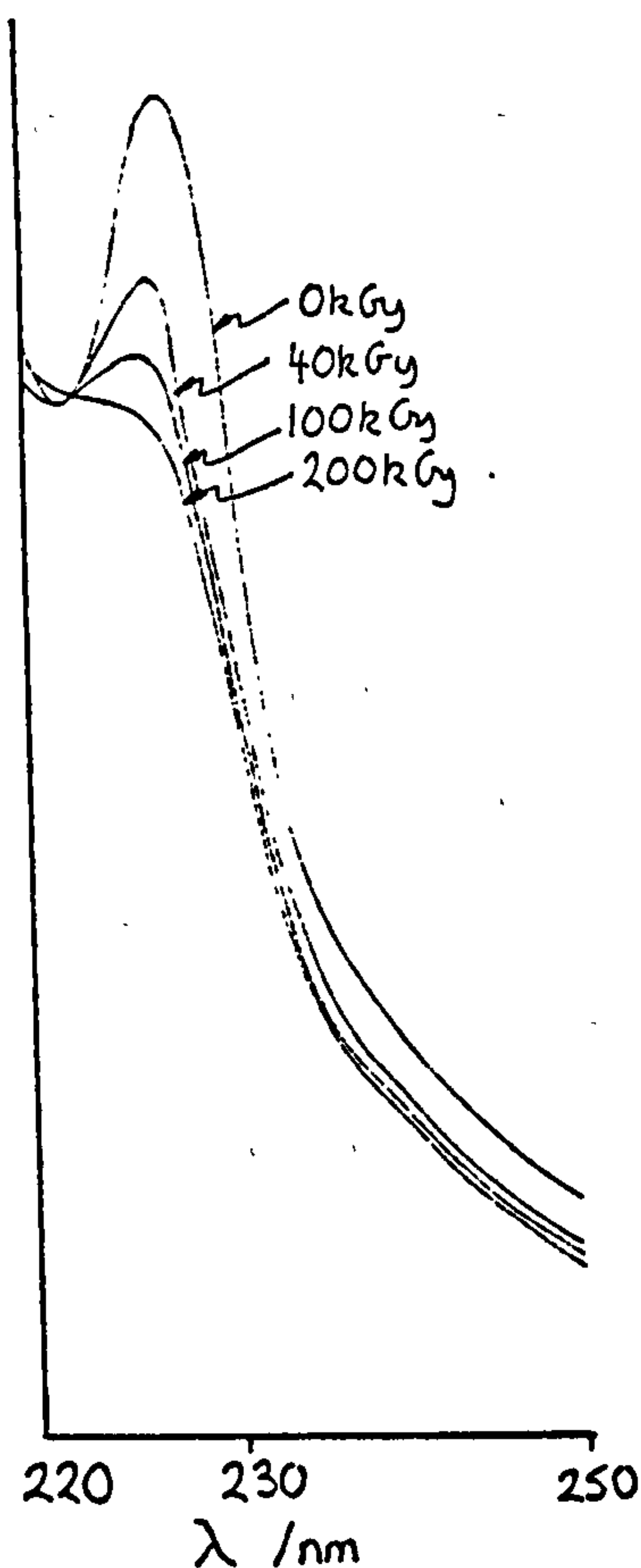


Figure 11 shows the UV spectra of the diepoxide films cured in the presence of the iron arene complex and illustrates a gradual decrease of the iron arene complex with increased radiation.

Although no quantitative data were obtained from the UV spectra of these films, it can be seen that the decomposition of the chromophore is closely related to the decomposition of its corresponding counteranion.

Figure 11 UV Spectra of dosed films of the diepoxide in the presence of CPMEBI ( $0.047\text{molkg}^{-1}$ )



### CONCLUSION

The decomposition of the onium salts and iron arene complex under electron beam radiation in epoxide films has been shown not only to involve the cation portion of the salt but also its counteranion, namely  $\text{PF}_6^-$ . The reactivity of DPI, TPS and CPMEBI under electron beam radiation suggest decomposition is related to the efficiency of electron capture.

It has also been shown that degradation of  $\text{PF}_6^-$  occurs and has been accounted for in terms of its instability in acid form, and that the initiating species may not be the acid  $\text{HPF}_6$  but due to one of its decomposition products,  $\text{HF}$ .

The role of the medium has been shown to greatly influence the rate of degradation of these salts and may be explained in terms of its ability to supply slow electrons to effect decomposition of the salt, although its solvating power and structure may also play a part.

The decomposition of the cation and its counteranion have been shown to be closely allied and may reflect the inherent instability of  $\text{HPF}_6$  produced and/or the involvement of an electron transfer process between the anion and the chromophoric cation.

## EXPERIMENTAL

### Materials

Diphenyliodonium hexafluorophosphate (Ciba Geigy), 'triphenyl sulphonium' hexafluorophosphate (Ciba Geigy) and  $(n^5-2,4\text{-cylcopentadien-1-yl})[(1,2,3,4',5,6\text{-n})$  (-1-methylethyl) benzene]-iron(1+)-hexafluorophosphate)(1-) (CG 24-61, Ciba Geigy) were all used as received.

3,4-Epoxy cyclohexylmethyl-3',4'-epoxy cyclohexane carboxylate (Cyracure Diluent UVR6110, Union Carbide), propylene carbonate (Aldrich), tripropyleneglycol diacrylate (Cray Valley Products Ltd.) were all dried over molecular sieves, 4A, (BDH Chemicals Ltd.)

Aluminium foil (0.051mm gauge) (BDH Chemicals Ltd.) was used as a substrate for all coatings.

### Instrumentation

Electron beam curing was carried out using an Otto Durr ESH 150/130 electron beam unit under a nitrogen blanket. The operating voltage was maintained at 150kV and the beam current was adjusted for each applied dose. All formulations were coated onto a moving web via a Dixon 164 coater unit.

UV curing was carried out using a Colourdry UV curing unit. The medium pressure lamp (80Wcm<sup>-1</sup> and 23cm in length) was situated 15cm above a moving belt which was calibrated in mmin<sup>-1</sup>.

Infrared spectroscopic data were obtained using a Digilab



FTS-60 Fourier transform infrared spectrometer. The moving mirror velocity in the interferometer was 0.16cm-1 and most of the spectra reported here were recorded at 8cm-1 spectral resolution. Liquid samples were analysed using transmission infrared for 16 scans, while 'sticky' and tackfree films were recorded using a Digilab photoacoustic detector for 4096 scans.

UV spectroscopic data were obtained using a UV-visible Perkin Elmer spectrophotometer Lambda 5 model with an integrating sphere attachment.

#### Criteria for the selection of an epoxide system to be examined

The selection of a suitable epoxide system to monitor its behaviour under electron beam radiation was determined by several criteria. The assessment of several epoxide systems rendered the cycloaliphatic diepoxide 3,4-epoxycyclohexylmethyl-3',4'-epoxy-cyclohexane carboxylate the most suitable system, primarily due to its ability to produce uniform films, low volatility and moderate cure speed under electron beam irradiation and, most importantly its relatively uncomplicated infrared spectra.

#### Formulation of cycloaliphatic diepoxide containing initiators

Initial inspection of UV spectra of diphenyliodonium hexafluorophosphate and the iron arene complex were consistent with authentic<sup>t</sup> samples shown in the literature

[2,34]. However, the UV spectrum of triphenylsulphonium hexafluorophosphate was not consistent with literature sources [1], and exhibited appreciable absorbance above 300nm. The spectra of the 'triphenylsulphonium' hexafluorophosphate was infact very similar to that of the commercial 'triphenylsulphonium' salts (appropriately labelled MASH) [1].

In order to make a valid comparison of the electron beam response of the diepoxide containing one of the three types of initiator, it was deemed necessary to express all concentrations in terms of hexafluorophosphate concentration. The following procedure was carried out to achieve this. Firstly, the ratio of peak area associated with the P-F stretch at  $844\text{cm}^{-1}$  [64] to peak area associated with the C-H stretches at  $3000\text{cm}^{-1}$  [60] was obtained for the formulation containing a known concentration of diphenyliodonium hexafluorophosphate. Equivalent amounts of hexafluorophosphate could then be obtained for solutions containing the 'triphenylsulphonium' salts by matching its ratio value with that evaluated from the formulation containing a known amount of hexafluorophosphate anion.

Dissolution of the salts in the diepoxide required prolonged gentle heating. This was overcome by dissolving the salt in a polar solvent, such as acetone or acetonitrile, prior to the addition of the diepoxide. The solvent was then removed over a rotary evaporator.

### Preparation of thin films of the diepoxide

All formulations were coated onto aluminium foil using the Dixon 164 coater. Even coatweights of about 10gm-l were obtained using a forward spinning smoothing roller at a setting of 32psi. The coatings were then passed under the electron beam. For doses of radiation (0-100)kGy the moving web was maintained at 20min-l, but for a dose of 200kGy the machine speed was reduced to 10min-l.

All samples were bottled and stored at -5°C.

### Analysis of infrared spectra obtained for films of the diepoxide and TPGDA with coinitiator

The spectra obtained by both transmission and photoacoustic infrared are of excellent quality, and examples of which are shown in Appendix A. On exposure to electron beam radiation the ring opening of the epoxide group was monitored by the peak at 795 cm<sup>-1</sup> associated with the C-H deformation of the epoxide group [60]. This peak was chosen in preference to the peak at 910 cm<sup>-1</sup> [60] as the latter absorption peak was of lower intensity and overlapped greatly with a neighbouring peak.

The growth of the hydroxyl content of the diepoxide film was monitored by the broad peak centred at 3500cm<sup>-1</sup> relevant to the O-H stretching frequency [60].

The peak centred at 844cm<sup>-1</sup> associated with the P-F stretching frequency [64] of the hexafluorophosphate anion was also measured. This absorption peak overlapped to



a small extent with the neighbouring peak at 850cm<sup>-1</sup>. In order to resolve the 844cm<sup>-1</sup> peak the technique of spectral subtraction was employed.

The use of an internal standard was employed to determine percentage change associated with the aforementioned peaks and to compensate for variation in film thickness. The peak at 3000cm<sup>-1</sup> associated with both symmetric and asymmetric C-H stretching vibrations [60], was used as an internal standard for films of the diepoxide and the peak at 1380cm<sup>-1</sup> associated with the -CH<sub>3</sub> twist was selected as an internal standard for the films of TPGDA.

The area associated with each peak was computed. given a predefined baseline. From which peak ratio's were evaluated and the percentage change of a given peak calculated.

#### Infrared analysis of films of propylene carbonate containing initiator

All these films were wet after irradiation and it was also noted that at high doses of radiation, ie >100kGy, evaporation of propylene carbonate had occurred. Therefore in order to evaluate percentage decomposition of hexafluorophosphate anion in this media, in which no internal standard could be used, the following procedure was undertaken. Firstly, the films were removed by washing with acetone from a given area and the solvent subsequently removed over a rotary evaporator. The addition of a weighed amount of KBr doped with a known concentration of KSCN was



then added and KBr discs were made up and the infrared spectra recorded. The peak at  $2140\text{cm}^{-1}$  associated with the  $\text{C}\equiv\text{N}$  stretching frequency [60] was used as an internal standard for evaluating hexafluorophosphate anion content

#### Analysis by UV spectroscopy

The UV spectra in the range of 200-500nm in the reflection mode was obtained for each panel and referenced against an uncoated aluminium sheet.

## APPENDIX A

The quality of spectra recorded using transmission and photoacoustic spectroscopy are illustrated overleaf. The series shown is that of the diepoxide containing diphenyliodonium hexafluorophosphate (0.048 molkg<sup>-1</sup>) cured at various doses of radiation.

The peaks of interest indicated on the spectra are associated with the following molecular vibrations.

- A = 3500cm<sup>-1</sup> = O-H Stretching vibration
- B = 3000cm<sup>-1</sup> = C-H Asymmetric and symmetric stretching  
of methylene and methine groups
- C = 844cm<sup>-1</sup> = P-F Stretching vibration of hexafluorophosphate anion
- D = 795cm<sup>-1</sup> = C-H Vibration of epoxide group

Figure 1 Photoacoustic spectra of the diepoxide in the presence of DPI (0.048molkg<sup>-1</sup>)

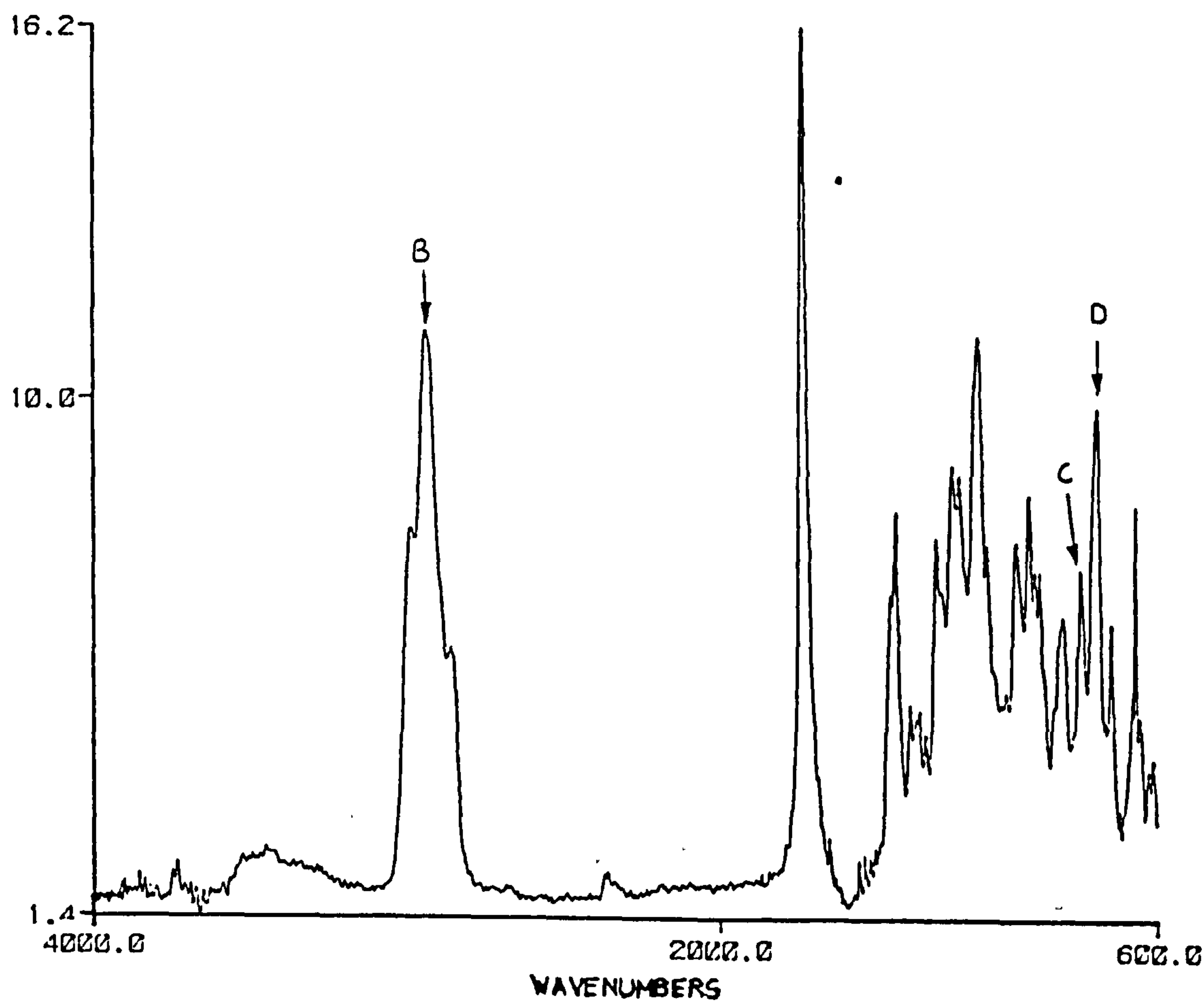


Figure 2 Photoacoustic spectra of the diepoxide in the presence of DPI (0.048molkg<sup>-1</sup>) cured at 40kGy

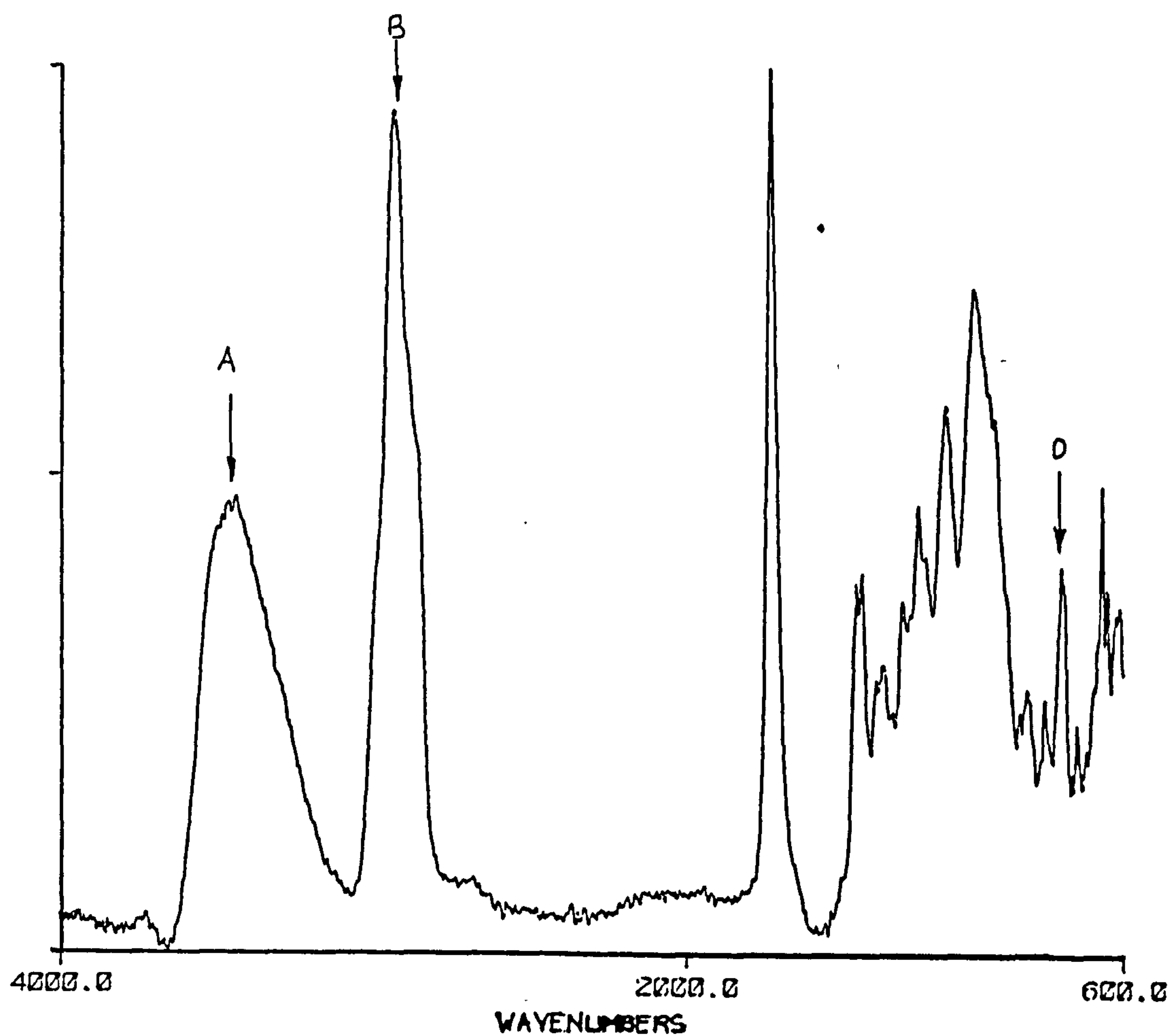




Figure 3 Photoacoustic spectra of the diepoxide in the presence of DPI (0.048molkg<sup>-1</sup>) cured at 100kGy

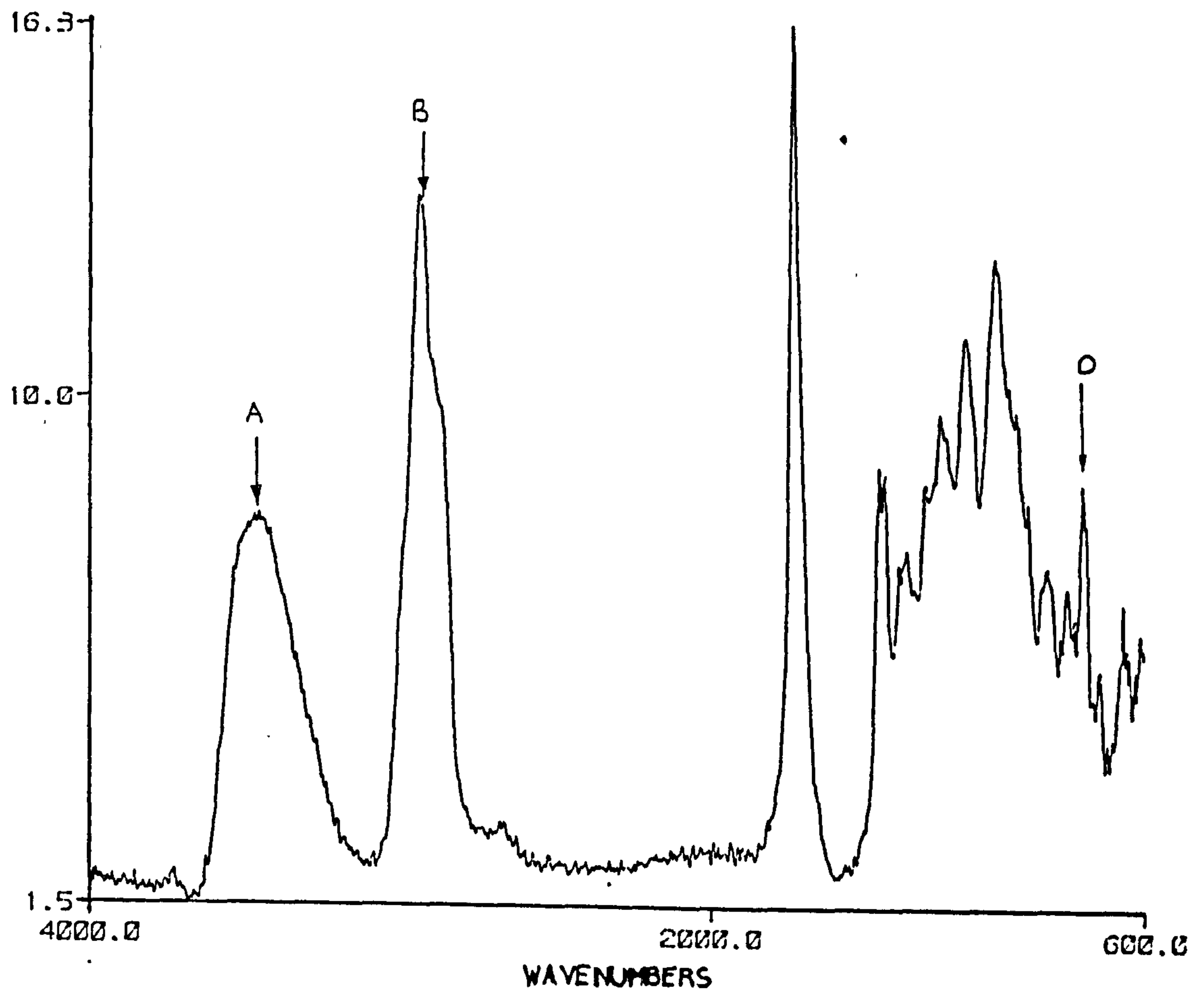
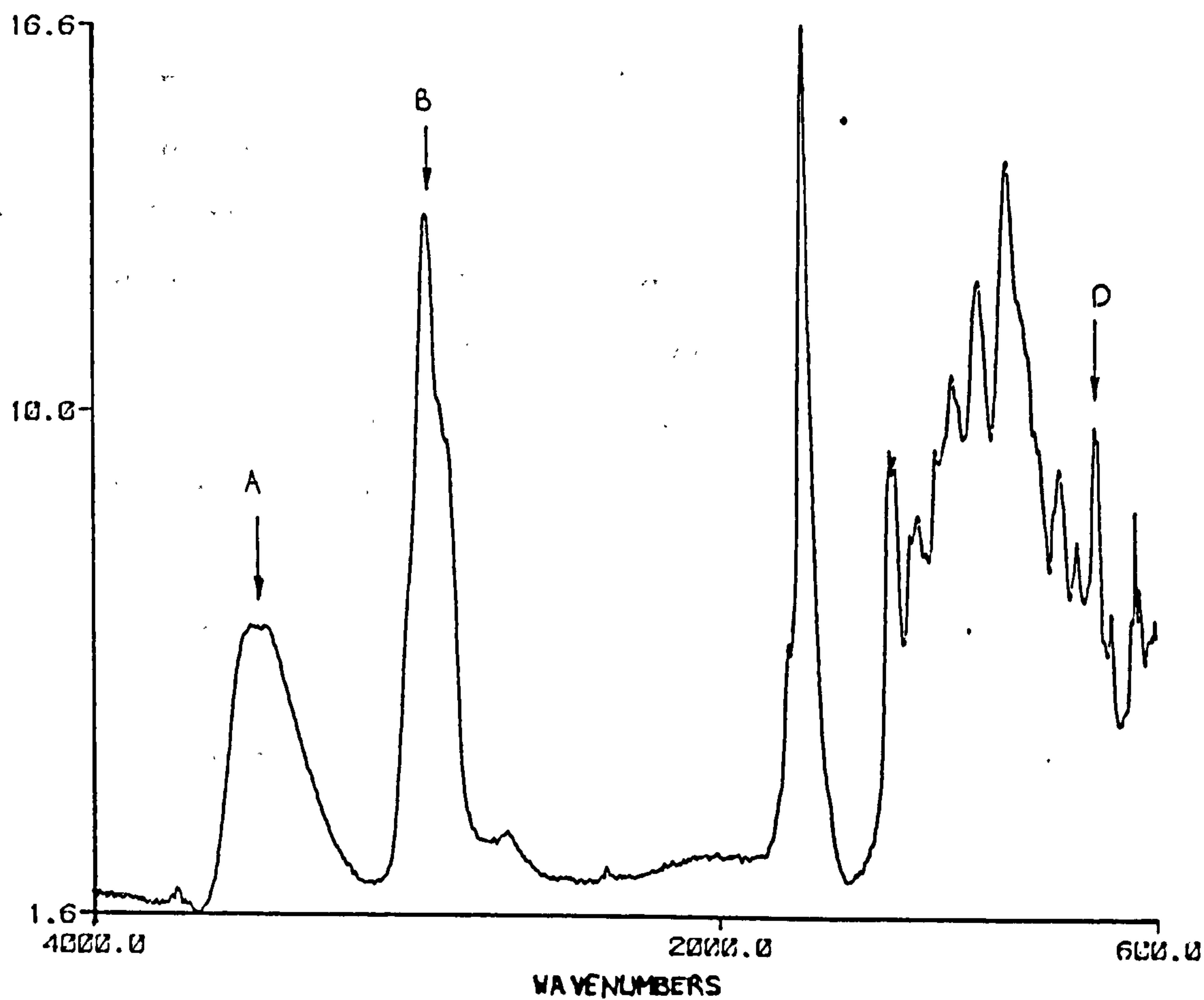


Figure 4 Photoacoustic spectra of the diepoxide in the presence of DPI ( $0.048\text{molkg}^{-1}$ ) cured at 200kGy



Introduction

The photodecomposition of the onium salts in solution has been subject to many investigations [33-38]. The proposed mechanisms for the photodecomposition involve homolytic and heterolytic reactions from the excited state of the onium salt. Both pathways ultimately produce a Brönsted acid containing a complex anion, responsible for the polymerisation of epoxides. Stabilisation of the acids in question, namely,  $\text{HBF}_4$ ,  $\text{HPF}_6$ ,  $\text{HSbF}_6$  is possible in the presence of a nucleophilic species, producing in the case of an epoxide, a tertiary oxonium ion in conjunction with a nonnucleophilic anion  $\text{BF}_4^-$ ,  $\text{PF}_6^-$ ,  $\text{SbF}_6^-$  capable of initiating polymerisation

However, it has been shown [67] that the complex counterion does not remain intact during the electron beam radiolysis of thin epoxide films containing an onium salt in an 'open' system. The disappearance of the complex counterion was ascribed to the decomposition of the acid produced to yield  $\text{HF}$  and  $\text{PF}_5$ .

A preliminary examination of the behaviour of these salts dissolved in an epoxide and exposed to UV radiation as thin films was investigated

Ledwith et al [68] showed that the degree of dissociation of several onium salts at a salt concentration

of  $10^{-5}$  M in dichloromethane will be approximately 50% and since much higher concentrations of the onium salt are used in the polymerisation of epoxides 'the degree of dissociation will be drastically reduced and further, higher aggregates of ions will be formed'.

A system in which aggregates predominate may favour decomposition of the acid to yield HF and PF<sub>5</sub>. It was therefore proposed that photolysis of crystalline onium salts may reflect a more accurate photodecomposition pattern of the salts in an epoxide film, than when investigated in such polar media as methanol, where the salts will be dissociated to a much greater extent. The fate of the onium salts were investigated by irradiating crystalline films of iodonium and sulphonium hexafluorophosphate and sulphonium hexafluoroantimonate.

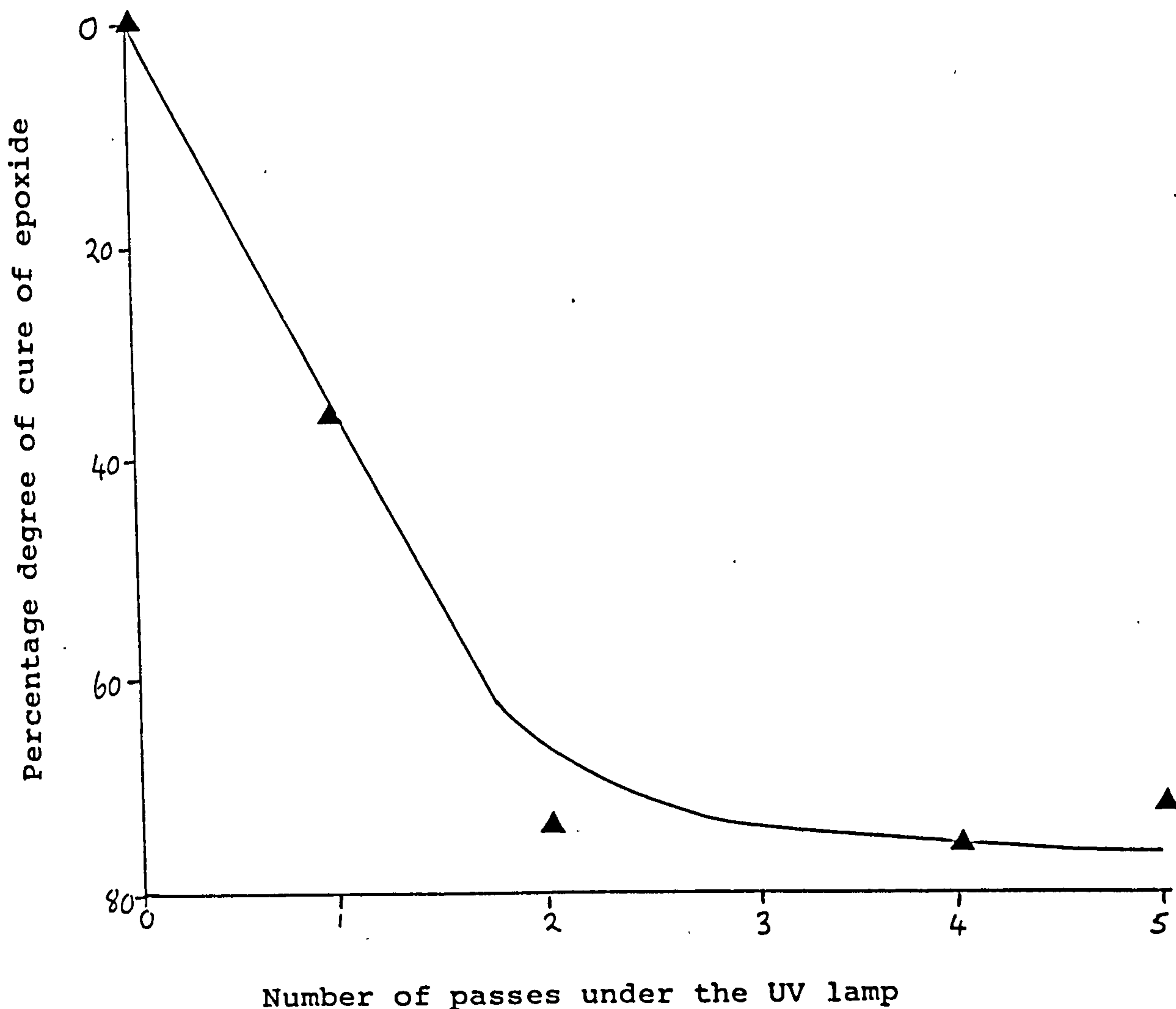
If on photolysis of crystalline onium salts containing hexafluorophosphate as its counterion, such volatiles as HF and PF<sub>5</sub> are produced, an epoxide film in the presence of such gases would be expected to undergo polymerisation. This 'three phase' or indirect process of inducing polymerisation of an epoxide was also investigated.



## RESULTS AND DISCUSSION

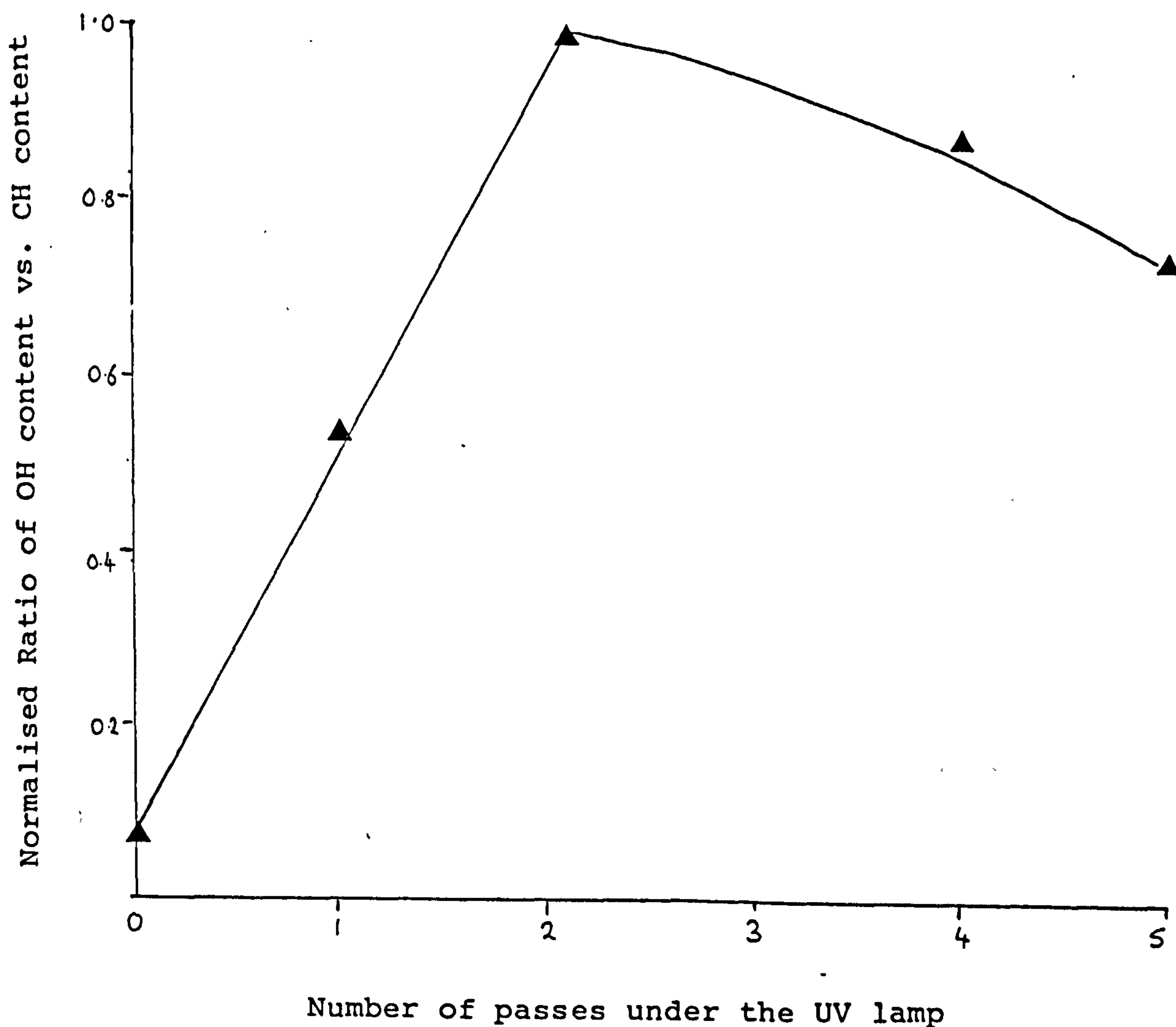
The polymerisation of the cycloaliphatic epoxide 3,4-epoxycyclohexylmethyl-3',4'-epoxycyclohexane carboxylate in the presence of the iodonium salt, diphenyliodonium-hexafluorophosphate (DPI), by UV radiation was monitored and as shown in Figure 1 the degree of polymerisation proceeds readily at first and then levels off after 2 passes.

Figure 1 Percentage degree of cure of diepoxide in the presence of DPI ( 0.047 molkg<sup>-1</sup> ) exposed to UV radiation.



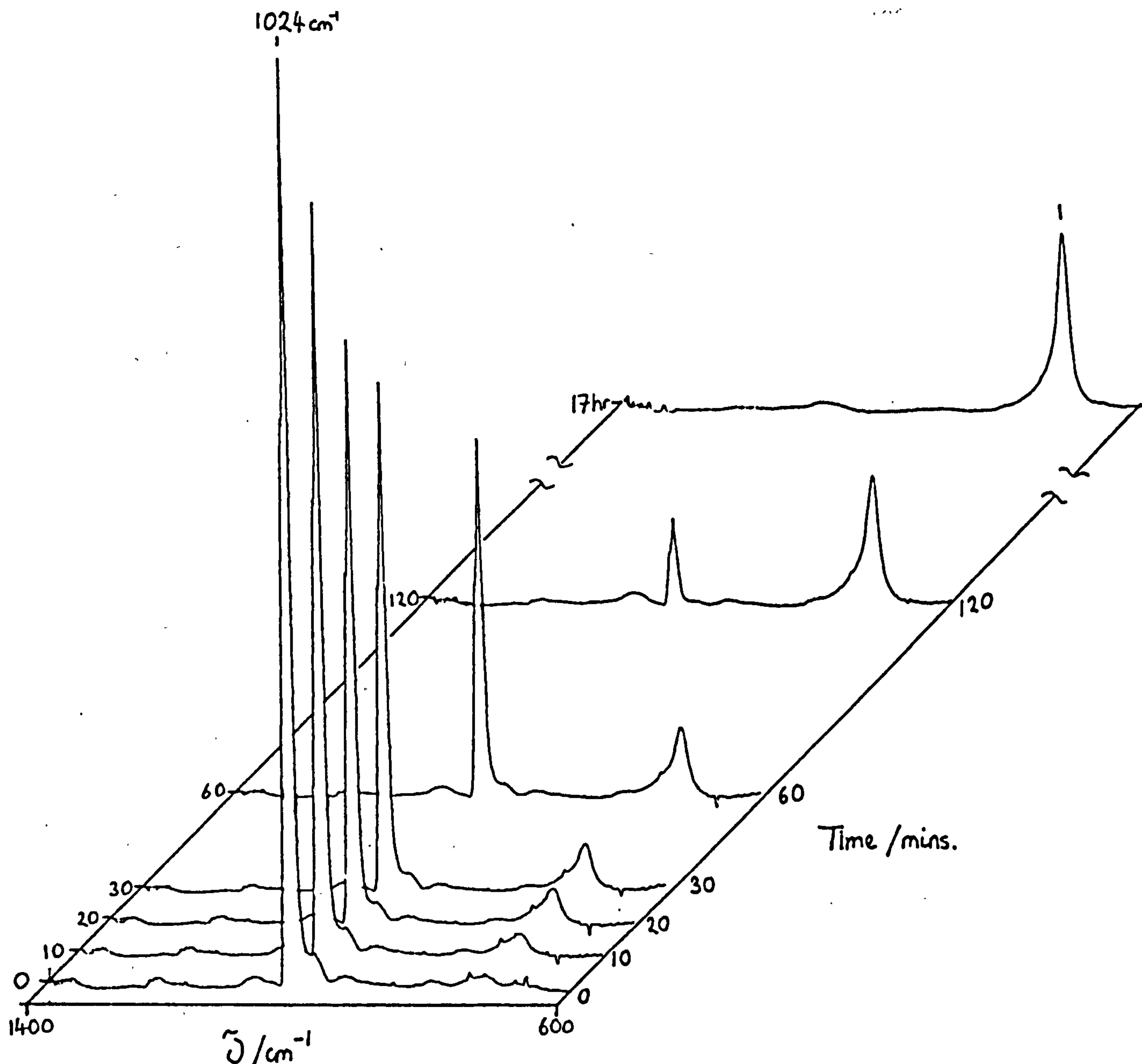
The hydroxyl content was also monitored and was shown to increase steadily as shown in Figure 2. The peak at  $844\text{cm}^{-1}$  associated with the hexafluorophosphate anion decreased after 1 pass, but on subsequent exposure to UV radiation, its fate was obscured by the growth of a neighbouring peak.

Figure 2 Hydroxyl content of diepoxide cured in the presence of DPI (  $0.047\text{molkg}^{-1}$  ) exposed to UV radiation.



UV irradiation of the crystalline salts under a nitrogen atmosphere in a quartz tube produced volatiles which were analysed by transmission infrared ( Figure 3 ), Absorption peaks at 1032, 1024, 1017 $\text{cm}^{-1}$  were found and were

Figure 3 Spectrum of volatiles produced on UV exposure of crystalline DPI



identified by comparison with an authentic sample of  $\text{SiF}_4$ . It is proposed that under our experimental conditions and those in which epoxide films containing these onium salts are produced, photolysis firstly generates an acid, such as  $\text{HPF}_6$ , which on rearrangement will form  $\text{HF}$  and  $\text{PF}_5$ . Despite careful drying of all apparatus, there will be residual moisture present which will react with  $\text{PF}_5$  to generate hydrogen fluoride and phosphoric acid [65].

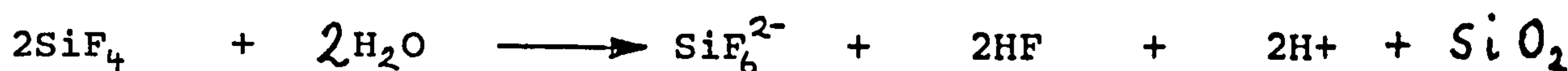
Hydrogen fluoride readily attacks glass to form  $\text{SiF}_4$  [65]

Scheme 1



which in turn is hydrolysed to form the hexafluorosilicate anion [65]. The simultaneous disappearance of  $\text{SiF}_4$  and appearance of  $\text{SiF}_6^{2-}$  ion was observed in the gas cell over a period of 2 hours

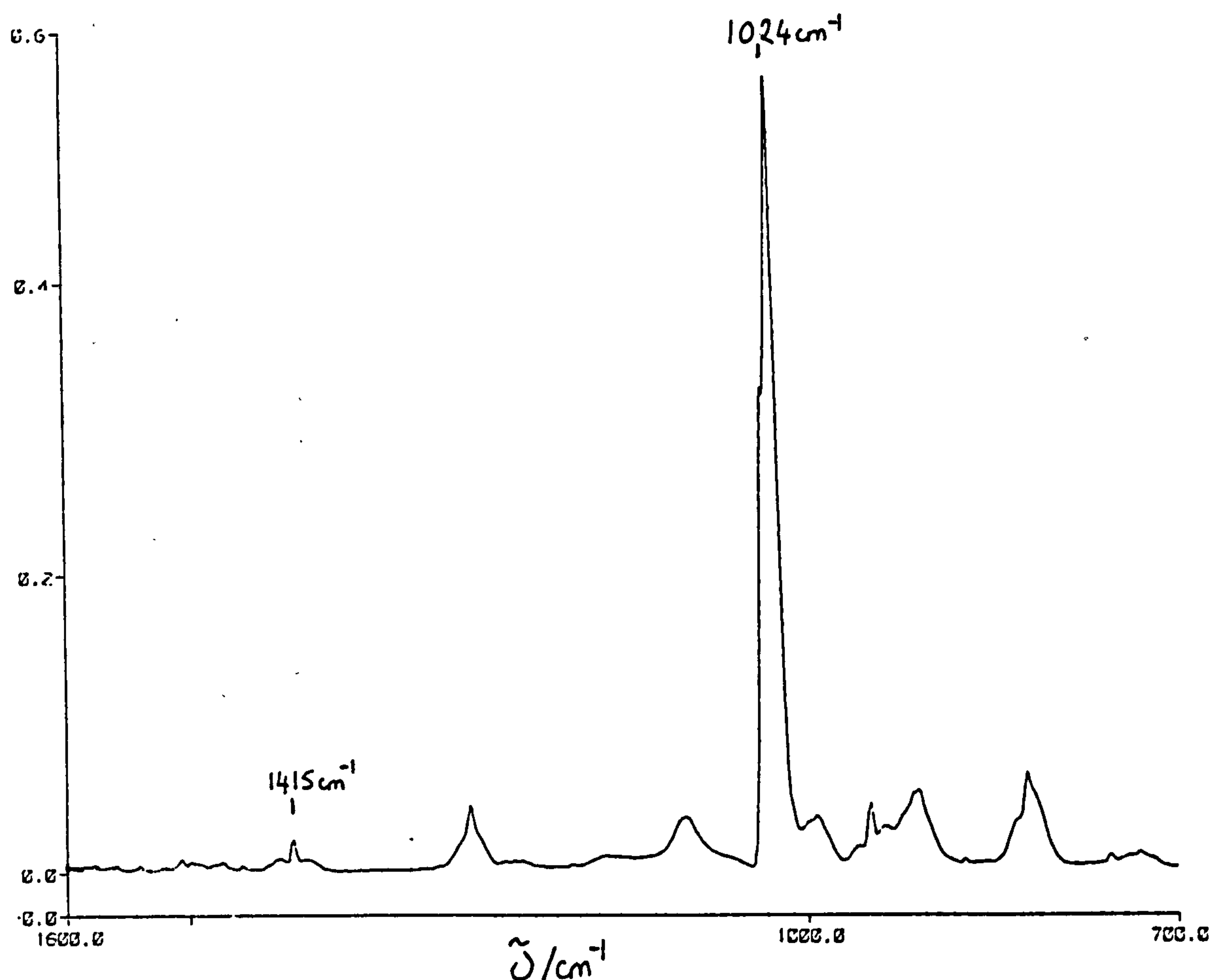
Scheme 2



When all glassware was baked at  $120^\circ\text{C}$  for 24 hours, an absorption peak centred at  $1415\text{ cm}^{-1}$  associated with  $\text{POF}_3$  [69] in the gas phase was detected (Figure 4), and provides further evidence for the proposed sequence of events described above. UV exposure of a cycloaliphatic diepoxide in the presence of DPI was also shown to generate  $\text{SiF}_4$  but in considerably smaller proportions, which might be expected as the volatiles produced, namely  $\text{HF}$  would be largely trapped within the film.



Figure 4 Spectra of volatiles produced on UV exposure of DPI when all glassware was baked at 120° C for 24 hours



UV exposure of 'triphenylsulphonium' hexafluorophosphate also produced similar gas phase spectra to those obtained in the case of DPI. UV irradiation of crystalline 'triphenylsulphonium' hexafluoroantimonate yielded comparatively small amounts of  $\text{SiF}_4$  and this may be ascribed, firstly to the fact that  $\text{SbF}_5$  is a polymeric liquid at room temperature and secondly  $\text{SbF}_5$  is hydrolytically more stable

than gaseous  $\text{PF}_5$  [65].

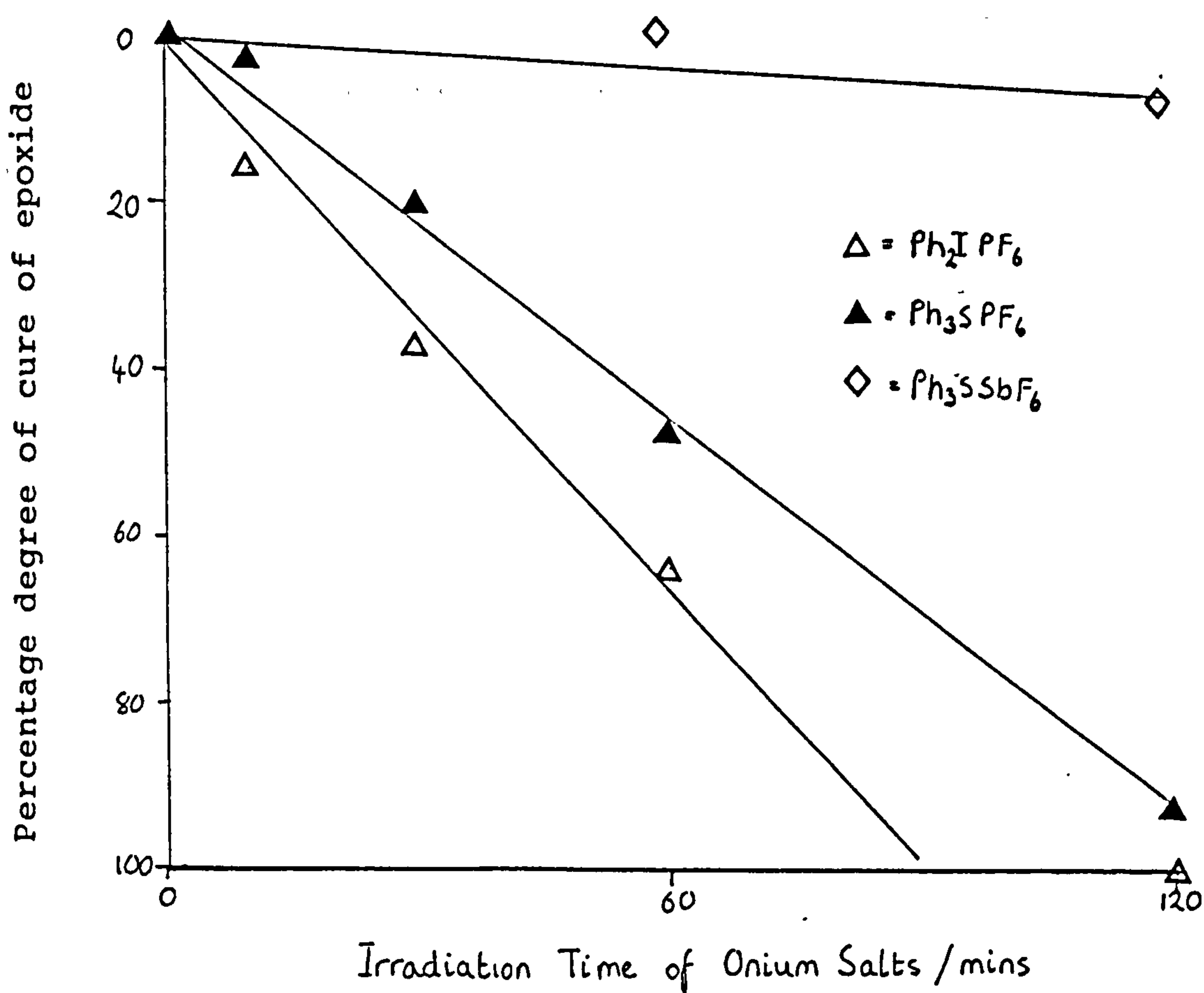
Irradiation of  $\text{Ph}_2\text{IPF}_6$  and  $\text{Ph}_3\text{SPF}_6$  resulted in an unidentified orange/yellow solid. Only slight yellowing of  $\text{Ph}_3\text{SSbF}_6$  was noted. Speculation as to the nature of this material may in fact be derived from the mechanism of acid production put forward by Dektar and Hacker [48]. It is claimed that if the phenyl radical or phenyl cation, produced by homolysis or heterolysis of the sulphonium salt respectively, does not escape from the solvent cage, recombination by molecular rearrangement will result in the formation of 3-phenylthiobiphenyl isomers. It can be envisaged that when the crystalline salts are irradiated that recombination of the phenyl radical or phenyl cation may involve not only the parent compound but also neighbouring ones, thus forming an extended chromophoric network.

HF has been observed to polymerise certain cycloaliphatic epoxides readily [66]. The polymerisation of a film of the cycloaliphatic diepoxide studied here, was coated onto an aluminium sheet and situated directly above but not incontact with a crystalline film of the salt in a nitrogen atmosphere in a quartz tube. The salt was then irradiated with a medium pressure mercury lamp and the percentage of cure of the epoxide film was monitored and the rate of cure was found to occur in the order



as shown in Figure 5. This is consistent with the ease with which HF can be generated from  $\text{Ph}_2\text{IPF}_6$  and  $\text{Ph}_3\text{SPF}_6$  compared with  $\text{Ph}_3\text{SSbF}_6$ . Although  $\text{SiF}_4$  is seen as the major product produced on photolysis of these salts it is thought unlikely to be a primary initiating species.

Figure 5 Percentage cure of an epoxide film exposed to the volatiles produced on UV irradiation of the onium salts



## CONCLUSION

The UV curing of epoxide films containing DPI showed that the counterion  $\text{PF}_6^-$  decomposed, as was observed for electron beam cured films.

Photolysis of the crystalline salts of DPI and TPS were shown to decompose to generate HF and  $\text{PF}_5$ , which, under our experimental conditions resulted in the formation of  $\text{SiF}_4$  and  $\text{SiF}_6^{2-}$ .

It was also shown that an epoxide film may be cured in the presence of the UV irradiated crystalline onium salts. This '3 phase' or indirect UV induced curing process was explained in terms of HF production.



## EXPERIMENTAL

### Materials

Diphenyliodonium hexafluorophosphate (Ciba Geigy)  
'tri- phenylsulphonium' hexafluorophosphate (Ciba Geigy)  
and 'triphenylsulphonium' hexafluorophosphate (Ciba Geigy)  
were all used as received.

3,4-Epoxycyclohexylmethyl-3',4'-epoxycyclohexane carb-  
oxylate was dried over molecular sieves, 4A, (BDH Chemicals  
Ltd.).

Aluminium foil (0.051mm gauge) (BDH Chemicals Ltd.) was  
used as a substrate for all coatings.

### Instrumentation

UV curing of thin films was carried out using a Colordry  
curing unit. The medium pressure lamp ( $80\text{Wcm}^{-1}$  and 23cm in  
length) was situated 15 cm above a moving belt which was  
calibrated in  $\text{min}^{-1}$ .

UV irradiation of the crystalline onium salts was  
carried out by irradiating the salts in a quartz tube,  
rotated around a water cooled medium pressure mercury lamp  
(Applied Photophysics Ltd. 450 Watts) for a given period of  
time.

Infrared spectroscopic data obtained using a Digilab  
FTS-60 Fourier transform infrared spectrometer. The moving  
mirror velocity in the interferometer was  $0.16\text{cm}^{-1}$  and most  
of the spectra reported here were recorded at  $8\text{cm}^{-1}$  spectral  
resolution. Liquid samples were analysed using transmission

infrared for 16 scans, while 'sticky' and tackfree films were recorded using a Digilab photoacoustic detector for 4096 scans. Gas samples were analysed in a Beckman gas cell, of 10cm pathlength, using transmission infrared for 16 scans at a spectral resolution of 1cm-1.

#### Formulation of cycloaliphatic diepoxide containing onium salts

The preparation of this solution has been described in the previous section of this chapter.

#### Preparation of thin films for UV curing

All formulations were coated onto aluminium foil using a hand K-bar coating unit. The coatings were then passed under the UV lamp. The belt speed was maintained at 80mmmin-1.

#### UV irradiation of the onium salts

The onium salts were irradiated as crystalline films on aluminium foil placed inside a quartz tube, previously dried at 120°C for 2 hour, and purged with dry nitrogen. The films were deposited by evaporation of solutions of the salts in acetonitrile or methanol at 50°C using a vacuum oven. The volatiles produced on photolysis of the salts were identified by a comparison of transmission spectra of authentic samples.

Polymerisation of the cycloaliphatic diepoxide by the volatiles produced on irradiation of the onium salts

Thin films of the diepoxide were coated onto aluminium foil sheets using a hand K-bar coating unit. These coatings were then placed above, but not in contact with, a crystalline film of the salts inside a quartz tube. This was then purged with dry nitrogen and the diepoxide coating was shielded from exposure to UV irradiation. All glassware had been previously baked at 120° C.

ELECTRON BEAM AND UV INDUCED POLYMERISATION OF  
6,7-EPOXY-3,7-DIMETHYLOCTYL ACRYLATE

Introduction

The mechanism by which the onium salts decompose, as proposed by Crivello [35] produces not only protonic acids capable of initiating cationic polymerisation but also radical species capable of promoting free radical polymerisation.

Smith [70] illustrated the use of the iodonium salts as free radical initiators. Subsequently, Kunenda et al [71] described the use of a suphonium salt for the photopolymerisation of methyl methacrylate and styrene. Several workers [72] have reported the simultaneous polymerisation of hybrid systems containing a mixture of acrylates and epoxides in the presence of the onium salts. The advantage of using this type of system is claimed to be rapid polymerisation of thick sections. Crivello [73] showed that these mixtures lead to a mixture of the homopolymers obtained by simultaneous free radical and cationic polymerisations, and illustrated the advantage of using a one component system such as, glycidyl acrylate which can produce a crosslinked system.

Investigation of a one component hybrid system of higher molecular weight, and presumably therefore less toxic than that of glycidyl acrylate was investigated, both under electron beam and UV radiation. Its cure performance and the

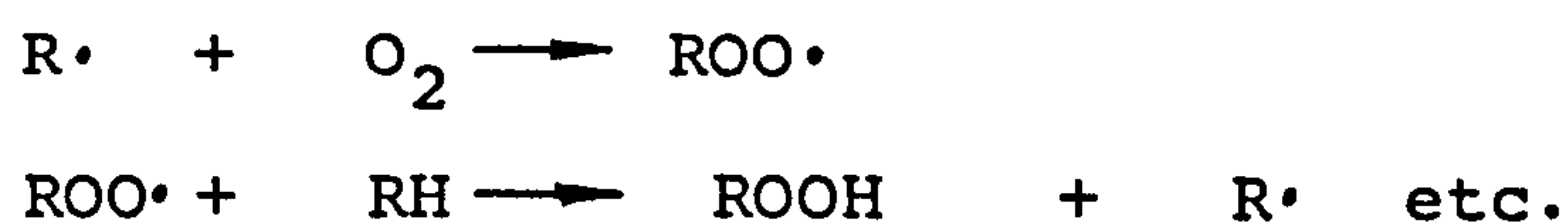


decomposition of the  $\text{PF}_6^-$  anion of the iodonium salt was also monitored.

The effect of oxygen on the cure of thin films of the title compound by UV was also investigated.

The oxygen molecule which exists as a ground state free radical, will react with intermediate free radicals in the photopolymerisation process, giving rise to a peroxy radical, a non-effective chain initiator [74].

Scheme 1



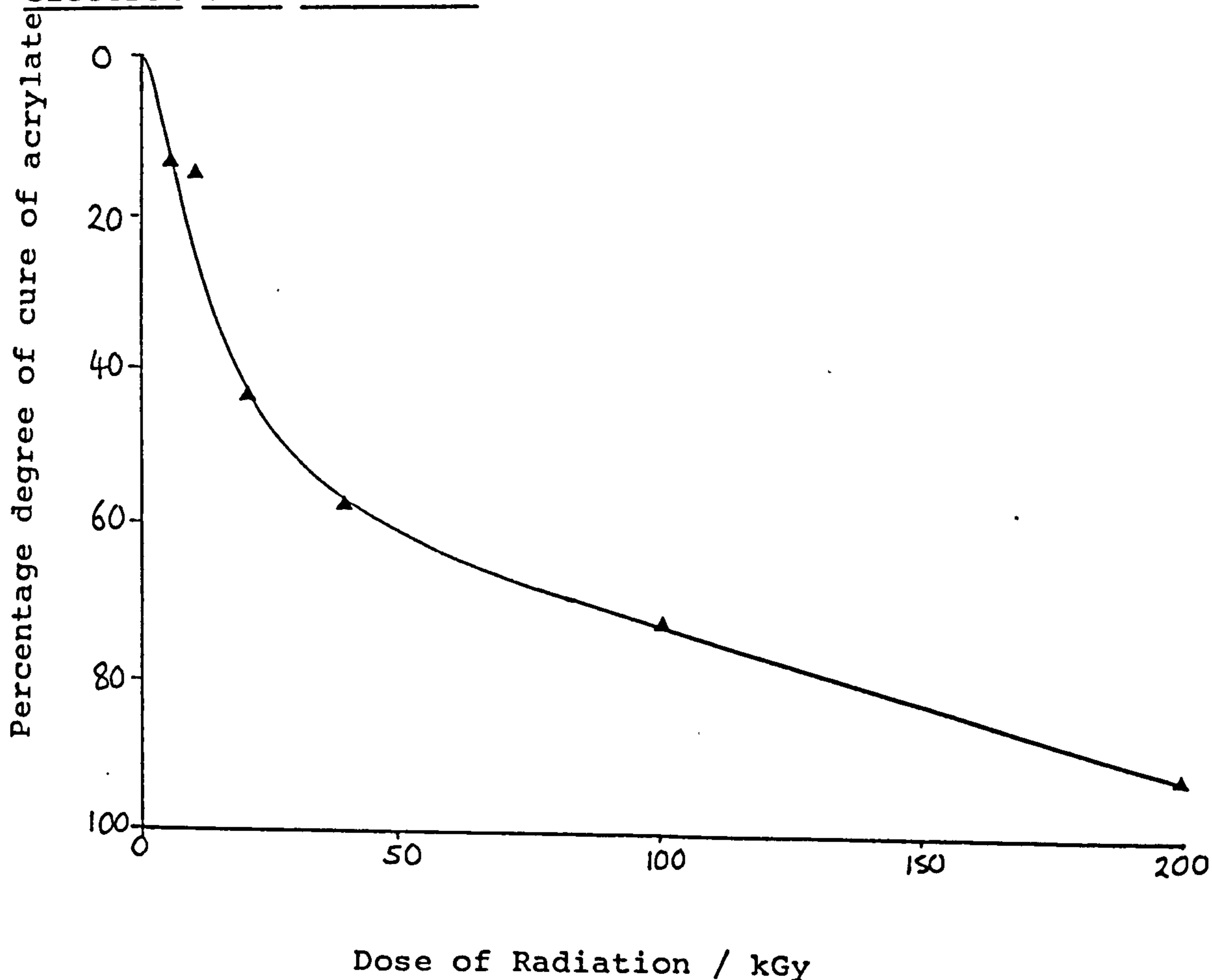
The presence of oxygen on curing films notably results in poor surface properties as a result of undercure due to the inhibiting effect of oxygen. Several techniques can be applied to overcome the detrimental effects of oxygen in producing films. Examples of some methods to overcome oxygen inhibition at the surface are:-

- 1) curing under an inert atmosphere, e.g.,  $\text{N}_2$
- 2) application of a surface/air barrier, e.g., paraffin
- 3) addition of synergists or coinitiators to accelerate surface cure, e.g., use of amines.

## RESULTS AND DISCUSSION

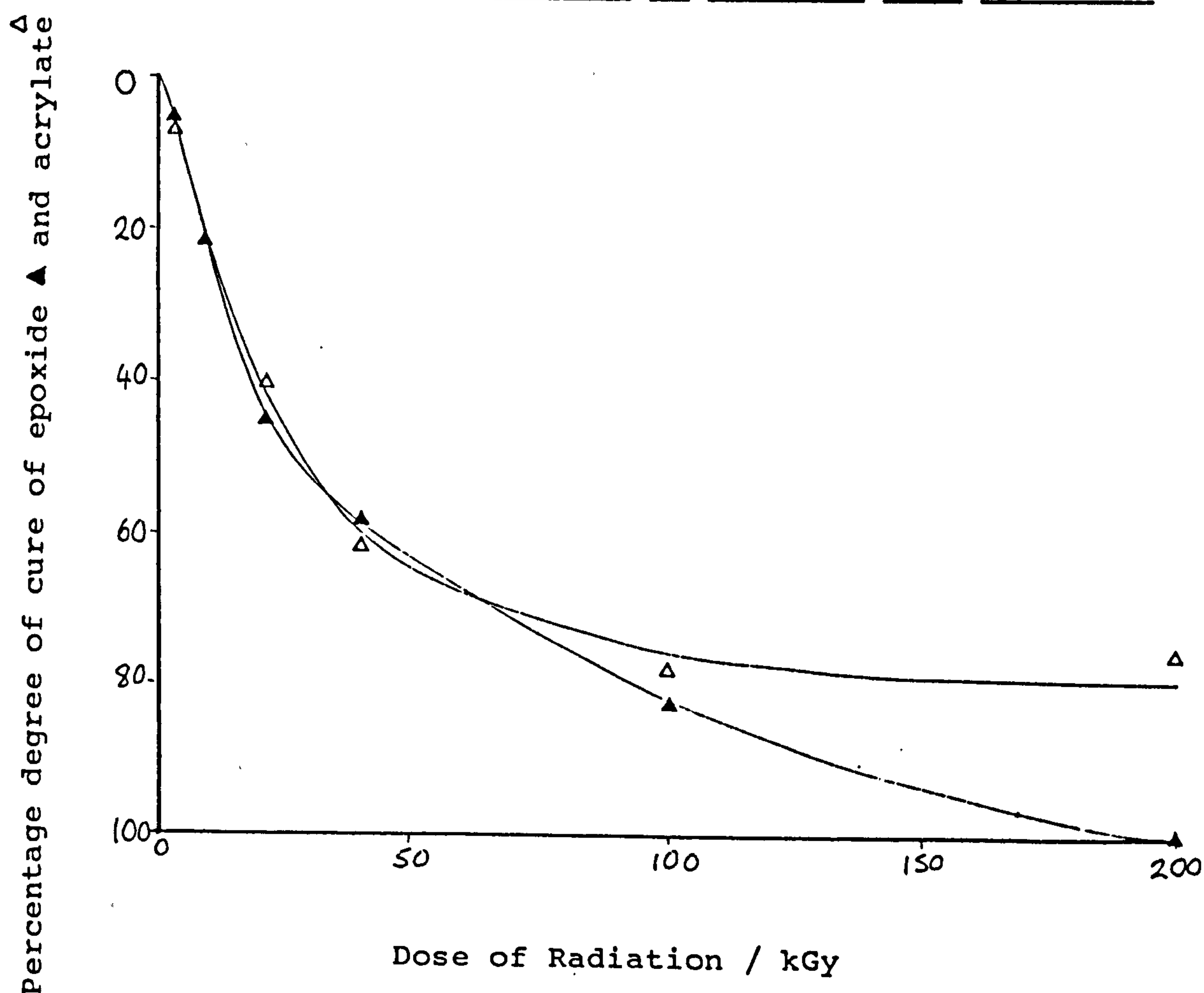
The electron beam polymerisation of 6,7-epoxy-3,7-dimethyloctylacrylate (EDMOA) in the absence of the iodonium salt was monitored and as shown in Figure 1 no polymerisation of the epoxide functionality was observed, but the acrylate component was found to cure readily.

Figure 1 Percentage degree of cure of EDMOA exposed to electron beam radiation



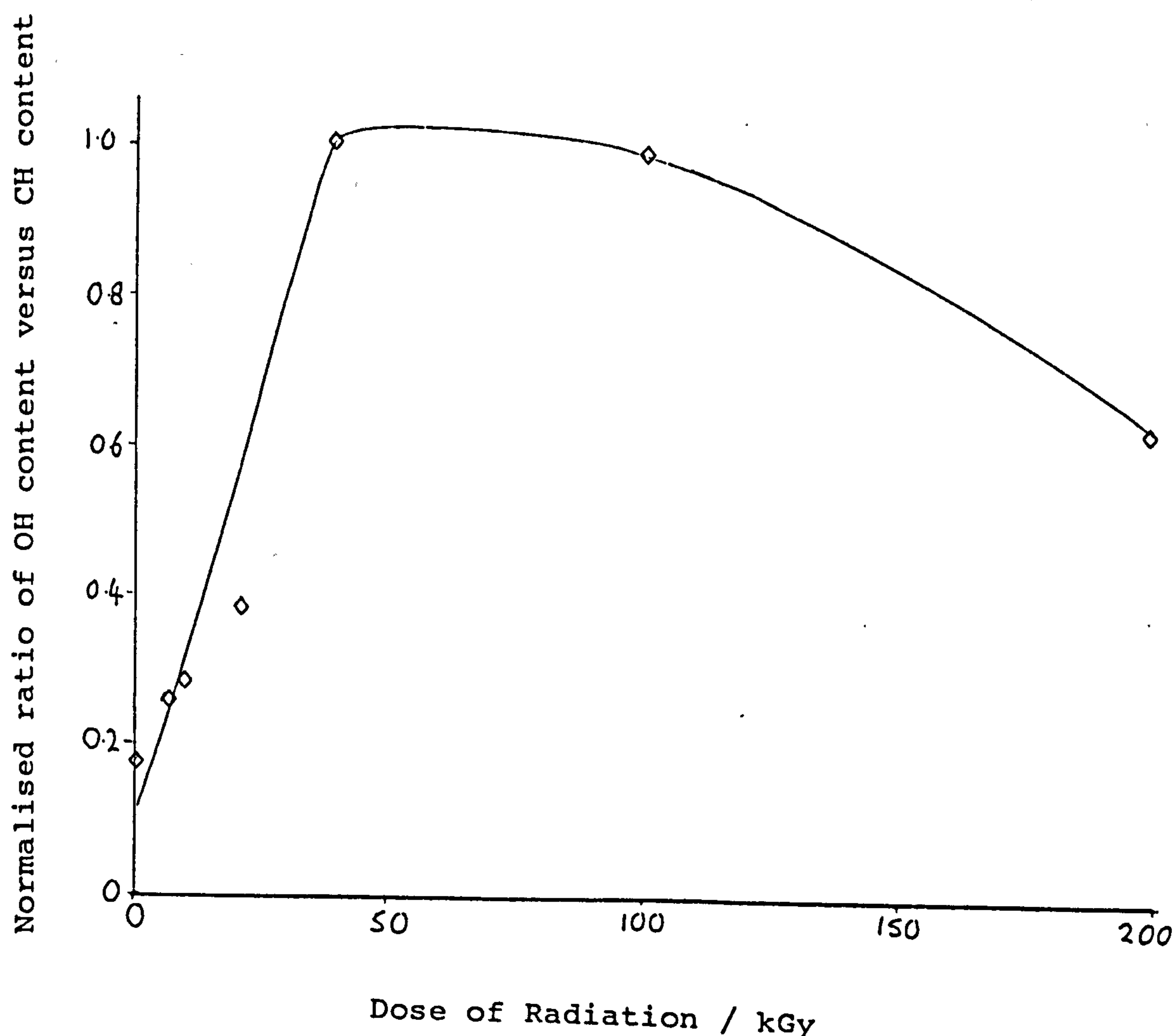
The polymerisation of this system resulted in wet films even at 200 kGy. It was only on addition of the onium salt, diphenyliodonium hexafluorophosphate, DPI, that tack free films were achieved at the low dose of 20 kGy. By monitoring the reaction by infrared it was found that both the acrylate and epoxide components polymerised readily to form a crosslinked network (see Figure 2)

Figure 2 Percentage degree of cure of EDMOA in the presence of DPI ( 0.047 molkg<sup>-1</sup> ) exposed to electron beam radiation



A comparison of the cure response of the acrylate component in the presence and absence of the onium salt was found to be very similar. At first sight addition of the onium salt which has a low reduction potential,  $-0.2V$  [75], would be expected to result in an induction period or inhibition of the acrylate polymerisation process. This was not observed and may be explained by the fact that decomposition of the onium salt results in the production of free radical species capable of initiating polymerisation.

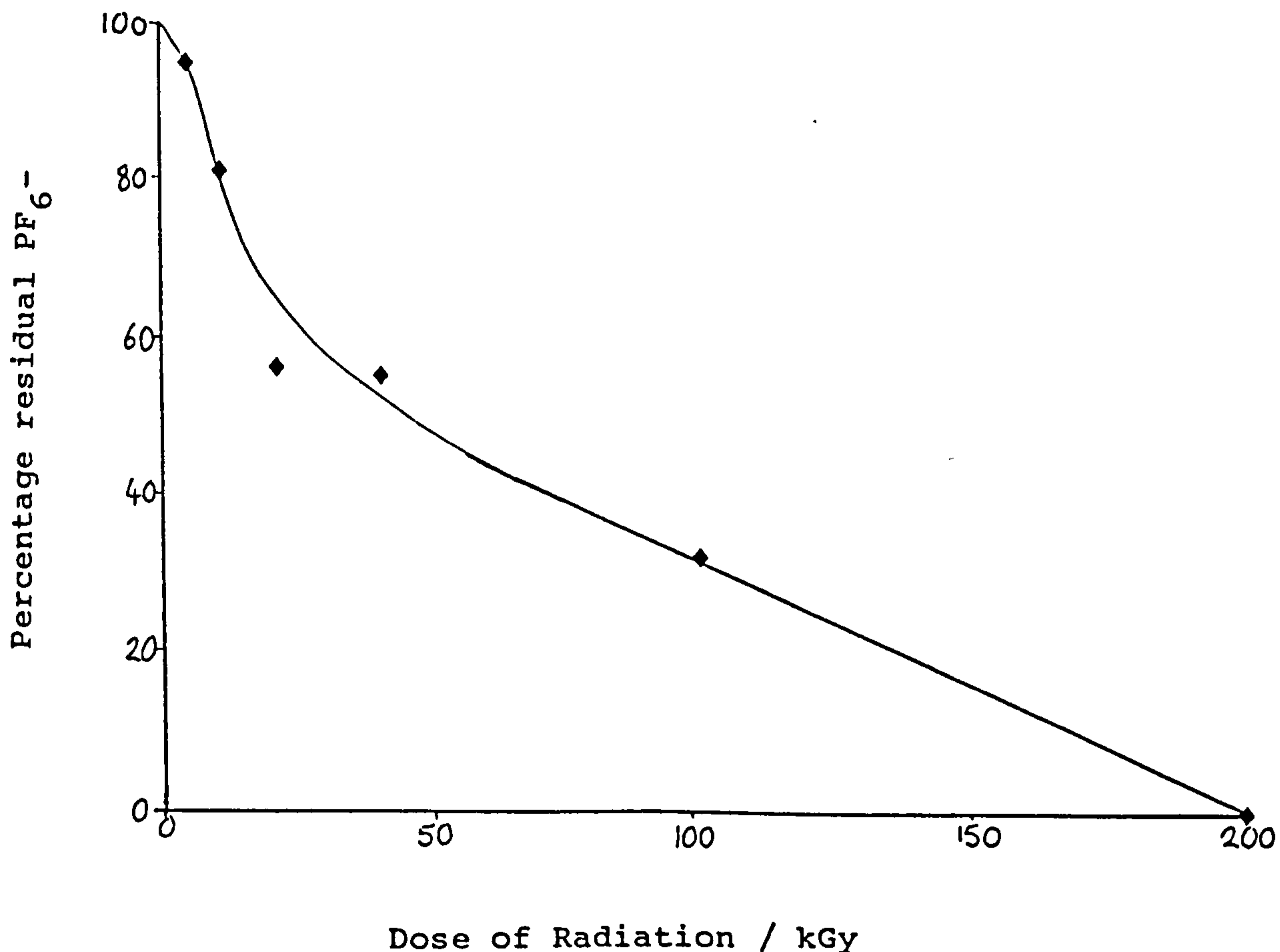
Figure 3 Hydroxyl content of EDMOA cured in the presence of DPI (  $0.047\text{molkg}^{-1}$  )





Figures 3 and 4 show the growth of hydroxyl content and dis-appearance of the counterion  $\text{PF}_6^-$  respectively. Again it was observed that hydroxyl content increased at low doses and decreased at the higher doses of radiation. Once again this may reflect the role water plays in the polymerisation process. Firstly, at low doses it causes termination of the growing polymer chain leading to the production of alcohols, but at higher doses of radiation termination of the active site may occur via previously formed alcohols. The decomposition of  $\text{PF}_6^-$  was found to be slower in EDMOA compared with its decomposition in the cycloaliphatic diepoxide and reflects the important role that the media plays in the decomposition of these salts.

Figure 4 Percentage residual hexafluorophosphate anion on curing EDMOA in the presence of DPI ( 0.047molkg<sup>-1</sup> )



The UV cure performance of EDMOA was also investigated. Under aerobic conditions all films were wet up to 10 passes under the UV lamp. The epoxide response was monitored and was found to proceed to high yields of conversion as shown in Figure 5. The acrylate functionality was unaffected under these conditions. The hydroxyl content was found to increase steadily and may reflect the ability of atmospheric moisture to penetrate the wet films produced, and hence promote chain transfer reactions with the active centre.

Figure 5 Percentage degree of cure of EDMOA in the presence of DPI ( 0.048molkg<sup>-1</sup> ) initiated by UV radiation.

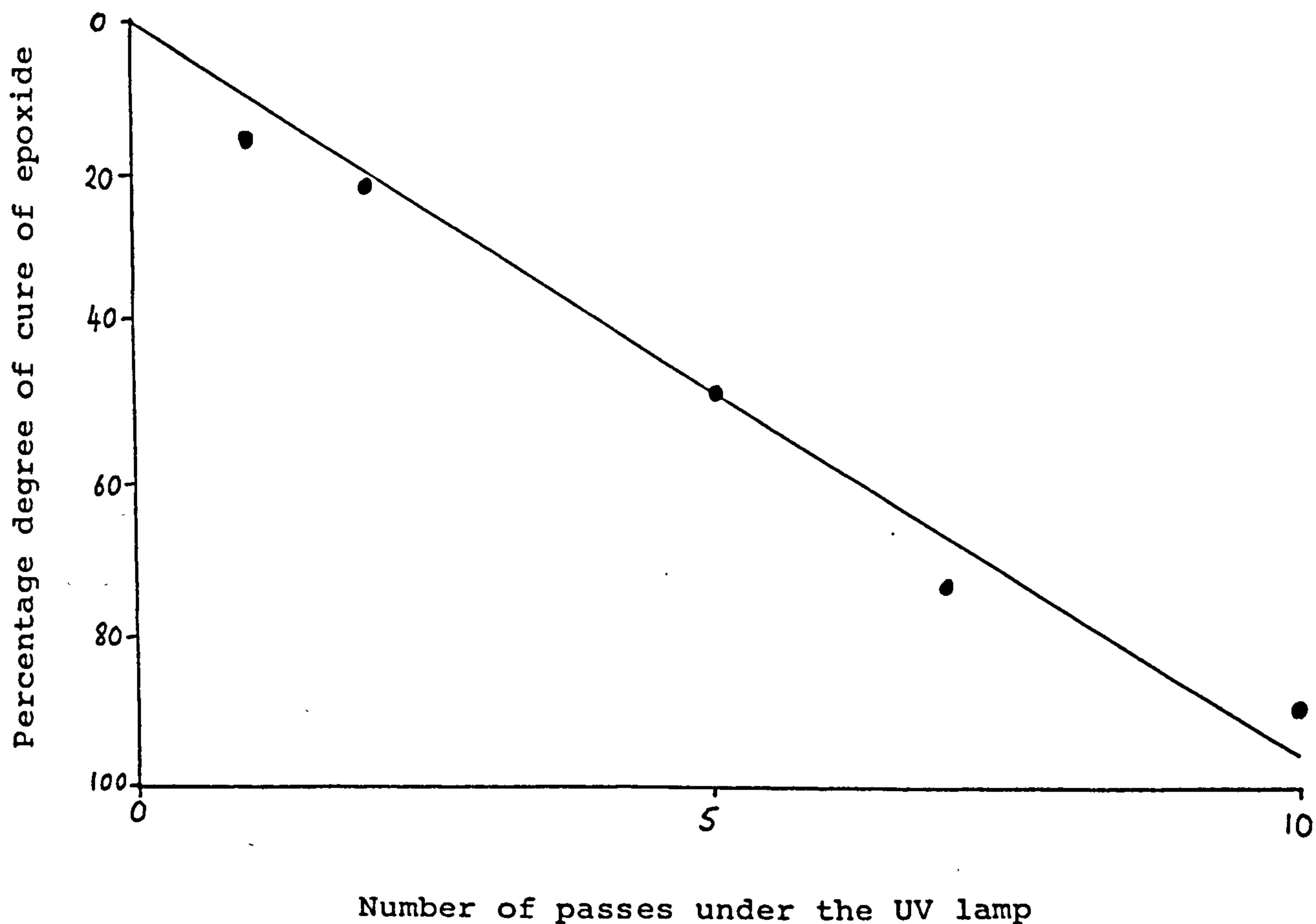
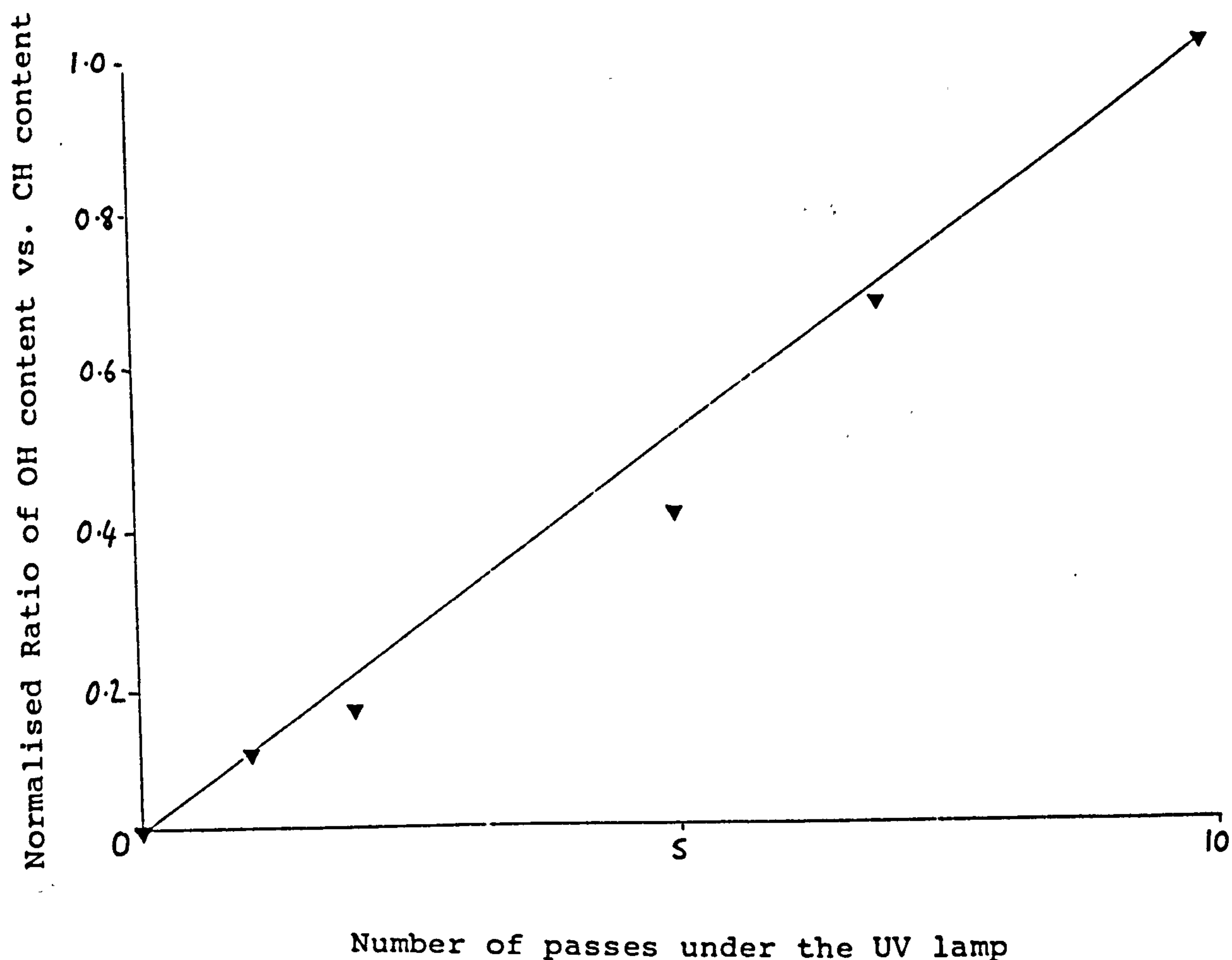


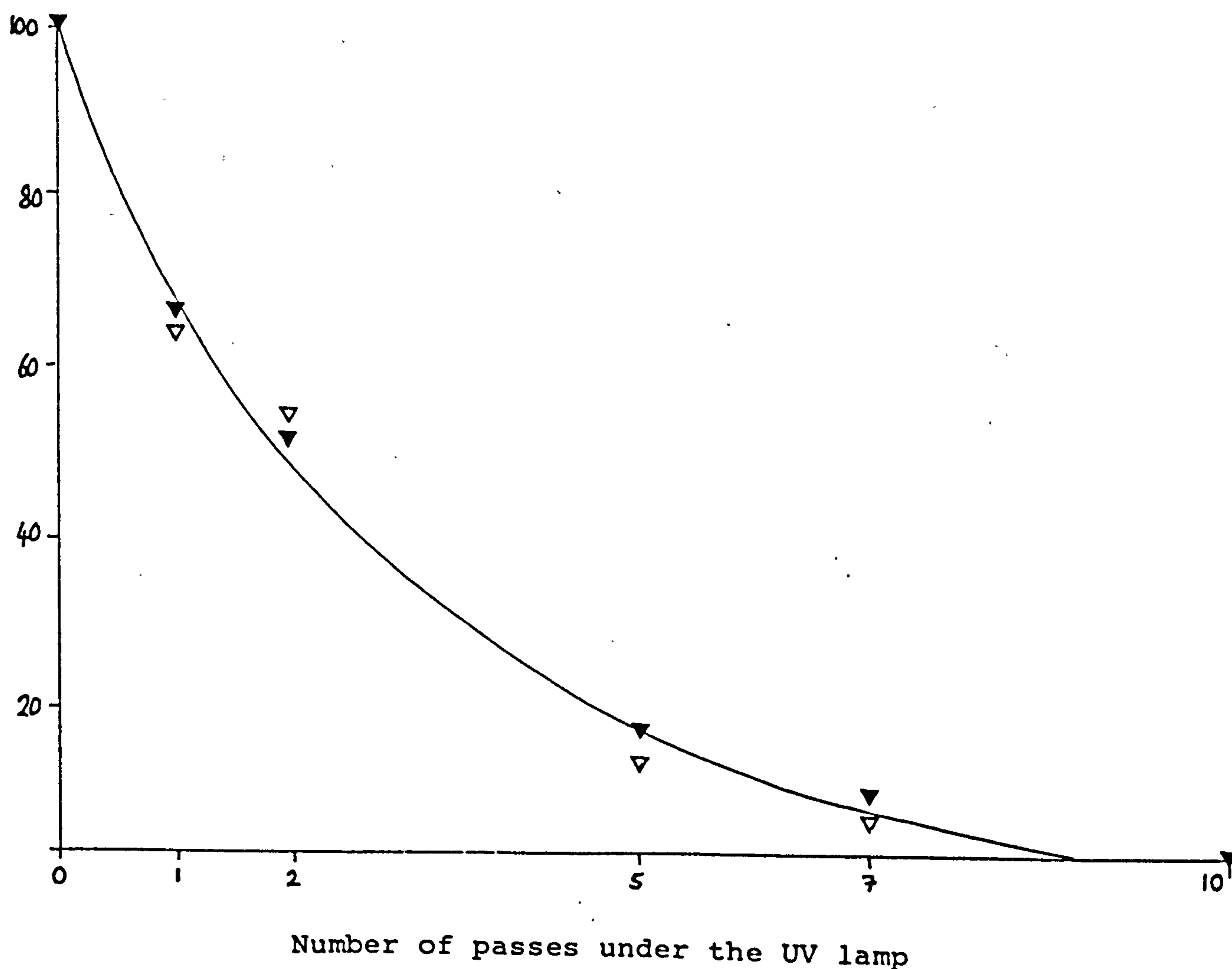
Figure 6 Hydroxyl content of EDMOA cured in the presence of  
DPI ( 0.048 molkg<sup>-1</sup> ) by UV radiation



The disappearance of the  $\text{PF}_6^-$  anion was also shown to decrease readily under UV radiation as illustrated in Figure 7. The decomposition of the hexafluorophosphate anion was monitored by measuring the percentage change associated with both the  $844\text{cm}^{-1}$  and the  $740\text{cm}^{-1}$  peaks relevant to the anion in question [64].

As indicated in previous sections this would once again indicate that under our conditions formation of  $\text{HPF}_6$  as a result of either homolytic or heterolytic decomposition of the salts, leads to the rapid decomposition of the acid to form  $\text{HF}$  and  $\text{PF}_5$ . This result therefore suggests that the true initiating species for the polymerisation of the epoxide may be that of  $\text{HF}$  formed as a result of direct decomposition of the acid as well as from the hydrolysis of  $\text{PF}_5$ .

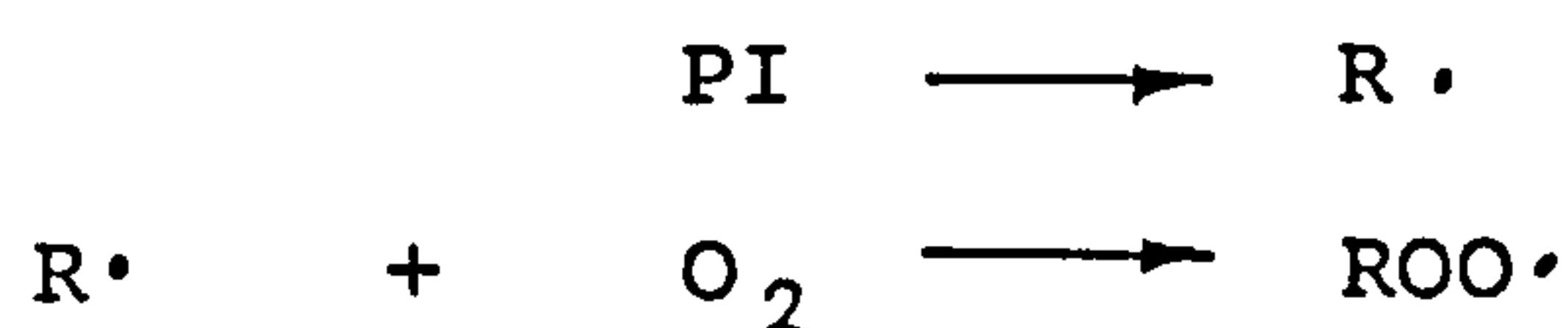
Figure 7 Percentage residual hexafluorophosphate content on UV curing EDMOA in the presence of DPI (0.047 mol kg<sup>-1</sup>)





The lack of reactivity of the acrylate group under these conditions was probably due to the presence of oxygen which is known to react with free radicals leading to the production of inactive products (probably peroxides and hydroperoxides) [74]

Scheme 2



The most common method of suppressing the detrimental effects of oxygen on the cure process has been by use of amines. However, the use of amine synergists would have obvious drawbacks when used in conjunction with systems containing epoxides. An effective method of promoting the free radical polymerisation of the acrylate functionality in EDMOA was investigated by applying a quartz plate on a thin film of EDMOA in the presence of DPI. Under these conditions dry films were produced and this may be ascribed to crosslinks being formed involving both the epoxide and acrylate components. The measurement of cure of both the acrylate and epoxide groups under anaerobic conditions, shown in Table I, were determined for 5 and 10 passes under the UV lamp. These results illustrate the detrimental effect oxygen has in the cure of thin films.

Table 1 Comparison of the UV cure response of EDMOA in the presence of DPI ( 0.047molkg<sup>-1</sup> ) under aerobic and anaerobic conditions

No. of passes	Percentage degree of cure			
	O <sub>2</sub> present		O <sub>2</sub> absent	
	acrylate	epoxide	acrylate	epoxide
5	0	48	43	47
10	0	89	96	94

### CONCLUSION

EDMOA containing DPI has been shown to cure when exposed to electron beam radiation and involves both the acrylate as well as the epoxide group. When DPI was absent electron beam radiation leads to the polymerisation of acrylate alone.

Exposure of EDMOA containing DPI to UV irradiation produces a wet film and spectroscopic evidence shows that the epoxide but not the acrylate groups reacted. The lack of reactivity of the acrylate group can be attributed to oxygen inhibition. This was shown to be the case by the finding that exposure of EDMOA containing DPI to UV radiation in the absence of oxygen, lead to film formation via consumption of both the acrylate and epoxide groups.

### ACKNOWLEDGEMENTS

I would like to thank Dr. R. J. Batten who prepared 6,7-epoxy-3,7-dimethyloctylacrylate, EDMOA.

## EXPERIMENTAL

### Materials

Diphenyliodonium hexafluorophosphate (Ciba Geigy) was used as received.

6,7-Epoxy-3,7-dimethyloctyl acrylate was prepared by Dr. R. J. Batten and dried over molecular sieves, 4A, (BDH Chemicals Ltd.). Aluminium foil (0.051mm gauge) (BDH Chemicals Ltd.) was used as a substrate for all coatings.

### Instrumentation

Electron beam curing was carried out using an Otto Durr ESH 150/130 electron beam unit under a nitrogen blanket. The operating voltage was maintained at 150kV and the beam current was adjusted for each applied dose.

UV curing was carried out using a Colordry curing unit situated 15cm above a moving belt which was calibrated in  $\text{mmmin}^{-1}$ .

Infrared spectroscopic data were obtained using a Digilab FTS-60 Fourier transform infrared spectrometer. The moving mirror velocity in the interferometer was  $0.16\text{cm}^{-1}$  and most of the spectra reported here were recorded at  $8\text{cm}^{-1}$  spectral resolution. Liquid samples were analysed using transmission infrared for 16 scans, while 'sticky' and tackfree films were recorded using a Digilab photoacoustic detector for 4096 scans.



### Preparation of thin films for electron beam curing

As described in previous section.

### Preparation of thin films for UV curing

As described in previous section.

### Analysis of infrared spectra obtained from films of EDMOA

The spectra of EDMOA obtained by both transmission and photoacoustic infrared are of excellent quality, and examples of which are shown in Appendix A. From a comparison of the spectra obtained from 3,7-dimethyloct-6,7-dienyl acrylate and that of EDMOA, showed the appearance of 2 new peaks located at  $871\text{cm}^{-1}$  and  $894\text{cm}^{-1}$  on epoxidation of the former compound. It was therefore assumed that these peaks were probably associated with the C-H deformation stretches of the epoxide. ON exposure to both electron beam and UV radiation the ring opening reaction of the epoxide was monitored by the peak at  $894\text{cm}^{-1}$ .

The growth of the hydroxyl content of the diepoxide film was monitored by the broad peak centred at  $3500\text{cm}^{-1}$  relevant to the O-H stretching frequency [60].

The peak centred at  $844\text{cm}^{-1}$  associated with the P-F stretching frequency [64] of the hexafluorophosphate anion was also measured. With the use of spectral subtraction the fate of the diphenyliodonium hexafluorophosphate initiator was determined.

The consumption of the carbon carbon double bonds

associated with the acrylate functionality was monitored by measuring the disappearance of the peaks at 1640/1620 $\text{cm}^{-1}$  due to the carbon carbon double bond stretching frequency and the 810 $\text{cm}^{-1}$  overtone frequency respectively [60].

The internal standard used to compensate for variation in film thicknesses was that absorption peak associated with the  $\text{CH}_3$ -twist [60].

The area associated with each peak was computed given a predefined baseline, from which peak ratio's were evaluated and the percentage change of a given peak calculated.

## REFERENCES

- [1] W.R. Watt, (1985). UV Curing : Science and Technology, Vol. II, S.P. Pappas, Ed., Technology Marketing Corp., Chap.6.
- [2] K. Meier and H. Zweifel, (1985). Radcure Europe, Munich, FC 85-417.
- [3] S. Paul, (1985). Surface coatings Science and Technology, Wiley - Interscience, Chap.2.
- [4] W.R. Watt, (1979). Epoxy Resin Chemistry, R.S. Bauer, Ed., ACS Symposium Series 114, Chap.2.
- [5] W.R. Watt, (1974). 14th Annual Coatings Symposium, North Dakota State.
- [6] Belgium Pat. 828,669 (1975) (to GE)
- [7] Belgium Pat. 828,841 (1975) (to 3M)
- [8] Belgium Pat. 837,782 (1976) (to ICI)
- [9] Belgium Pat. 828.668 (1975) (to GE)
- [10] Belgium Pat. 828,670 (1975) (to GE)
- [11] Belgium Pat. 833,472 (1976) (to ICI)
- [12] J.V. Crivello and J.H.W. Lam, (1976). J. Polym. Sci., Symposium No. 56, 383.
- [13] J.V. Crivello, J.H.W. Lam, J. Moore and S.H. Schroeter, (1978). J. Radiation Curing, 5 (1), 2.
- [14] A. M. Eastman, (1969). Encyclopedia of polymer science and technology, F. M. Herman, N. G. Gayland and N.M. Bikales, eds., Vol 2, Wiley-Interscience.
- [15] G. Odian, (1981). Principles of polymerisation, 2nd Ed., Mc Graw-Hill Publ. Corp., p.517

- [16] S. Penczek, P. Kubisa and K. Matyjaszewski, (1980) Advances in Polymer Science, 37, 52.
- [17] J.V. Crivello, (1978). UV Curing: Science and Technology, Vol. I, S.P. Pappas, Ed., Technology Marketing Corp., Chap.1.
- [18] A. Ledwith and D.C. Sherrington, (1974). Reactivity Mechanism and Structure in Polymer Chemistry, A.D. Jenkins and A. Ledwith, Eds., Wiley Interscience, Chap. 9.
- [19] R. Hoene and K.H.W. Reuchert, (1976). Makromol. Chem., 177, 3545.
- [20] F. Andruzzi, A.Prescia and G. Ceccarelli, (1975). Makromol. Chem., 176, 977.
- [21] A.G. Evans, G.W. Meadows and M. Polanyi, (1946). Nature (london), 158, 94.
- [22] K.C. Frisch and S.L. Reegan, (1976). Ring Opening Polymerisation, Marcel Dekker, Chap. 7.
- [23] J.J. Licari and P.C. Crepeau, US. 3,205,157 (1965).
- [24] M.P. Dreyfuss and P.Dreyfuss, (1965). Polymer, 6, 93.
- [25] M.P.Dreyfuss and P. Dreyfuss, (1966). J. Polym. Sci., PartA1, 4, 2179.
- [26] S.I. Schlesinger, (1974). Photogr. Sci. Eng., 18 (4), 387.
- [27] S.I. Schlesinger, (1974). Polym. Eng. Sci., 14 (7), 513.
- [28] R.O.C. Norman, (1978). Principles of Organic Synthesis, 2nd Ed., Chapman and Hall, p.438.
- [29] E.L. Meutterties, T.A. Bither, M.W. Forlow and D.D



- Coffman, (1960). J. Inorg. and Nucl. Chem., 16, 52.
- [30] F.W. Billmeyer, (1962). Textbook of Polymer Science, Wiley - Interscience.
- [31] R.C. Petterson, A. De Maggis, A.L. Herbert, T.J. Haley, J.P. Mykytka and I.M. Sarkar, (1971). J. Org. Chem., 36 (5), 631.
- [32] F.A.M. Abdul-Rasoul, A. Ledwith and Y. Yagci, (1978). Polymer, 19, 1219.
- [33] J.V. Crivello and J.H.W. Lam, (1976). J. Polm. Sci., Polym. Symp., 56, 383.
- [34] J.V. Crivello and J.H.W. Lam, (1977). Macromolecules, 10 (6), 1307.
- [35] J.V. Crivello, J.H.W. Lam and C.N. Volante, (1977). J. Radiat. Curing, 4 (3), 2.
- [36] J.V. Crivello and J.H.W. Lam, (1978). ACS Div. org. Coat. Plat. Chem., 39, 31.
- [37] J.V. Crivello and J.H.W. Lam, (1978). ACS Symp. Ser., 114, 1.
- [38] J.V. Crivello and J.H.W. Lam, (1979). J. Polym. Sci., Polym. Chem. Ed., 17 (4), 977.
- [39] H.J. Timpe, (1986). Pure Appl. Chem.,
- [40] J.W. Knapczyk and W.E. Mc Ewen, J. Org. Chem., 35 (8), 2539.
- [41] J.W. Knapczyk, J.J. Labinowski and W.E. Mc Ewen, (1972). Tet. Lett., (35), 3739.
- [42] J.V. Crivello, (1978). US 4,081,76.
- [43] R.S. Davidson and J.W. Goodin, (1982). Eur. Polym. J., 18, 589.

- [44] A. Ledwith, S. Al-Kass, D.C. Sherrington and P. Bonner, (1981). *Polymer*, 22 (2), 143.
- [45] S.P. Pappas, B.C. Pappas, L.R. Gatechair and W. Schnabel, (1984). *Polym. Chem. Ed.*, 22, 69,.
- [46] S.P. Pappas, B.C. Pappas, L.R. Gatechair, J.H. Jilek and W. Schnabel, (1984). *Polymer Photochem.*, 5, 1,.
- [47] A. Ledwith, (1982). *Preprints, 22nd. Fall Symp., Soc. Photograph. Sci. Eng., Arlington*, 44.
- [48] J.L. Dektar and N.P. Hacker, (1987). *J Chem. Soc., Chem. Comm.*, 1591.
- [49] J.V. Crivello and J.H.W. Lam, (1980). *J. Polym. Sci., Polym. Chem. Ed.*, 18 (8), 2677, 2697.
- [50] K. Chang and T. Chang, (1980). *US* 4,197,174.
- [51] J.V. Crivello, J.L.Lee and D.A. Conlon, (1980). *Makromol. Chem., Makromol. Suppl.*, 13/14, 145.
- [52] J.V. Crivello and J.H.W. Lam, (1978). *J. Polym. Sci., Polym. Chem. Ed.*, 16, 2441.
- [53] J.V. Crivello and J.H.W. Lam, (1979). *J. Polym. Sci., Poly. Chem. Ed.*, 17, 1059.
- [54] S.P. Pappas and J.H. Jilek, (1979). *Photogr. Sci. Eng.*, 23 (3), 140.
- [55] A. Ledwith, (1978). *Polymer*, 19, 1217.
- [56] S. Penczek and P. Kubisa, (1969). *Makromol. Chem.*, 130, 186.
- [57] T.P. Gill and K.R. Mann, (1980). *Inorg. Chem.*, 3007.
- [58] T.P. Gill and K. R. Mann, (1982). *Organomet.*,

- [59] Xiao-Hua Ma, Yukis Yamamoto and Koichio Hayaashi, (1987). *Macromol.* 20, 2703.
- [60] R. T. Conley, (1972). *Infrared spectroscopy*, Allyn and Bacon.
- [61] H. Pobiner, (1978). *Analytica Chim. Acta.*, 96, 153.
- [62] *Kobunshi Ronbunshu*, (1987). 44(10), 761.
- [63] J. V. Crivello, (1987). *Conf. Proc. Radcure Europe*, Munich, West Germany.
- [64] (1956). *J. Inorg. Nuclear Chem.*, 3, 326.
- [65] A. F. Holleman, (1985). *Lehrbuch der Anorganisches Chemie*, Wiberg.
- [66] Shahak, Manor and Bergman, (1968). *J. Chem. Soc.*, C 2129.
- [67] R.S. Davidson and S.a. Wilkinson. To be Published.
- [68] A. Ledwith and S. Al-Kass, (1981). *Polymer*, 22, 143.
- [69] *Tabulation of Infrared spectral data*, (1977). D. Dolphin and A. Wick, Eds., Wiley-Interscience.
- [70] G.H. Smith, (1973). US 3,741,769 (to 3M)
- [71] A. Kuneida, S. Kondo and K. Tsuda, (1974). *J. Polym. Sci., Polym. Lett. Ed.*, 12, 395.
- [72] A.D. Ketley and J. Tsao, (1979). *J. Radiation Curing*, 6 (2), 22.
- [73] J.V. Crivello and J.H.W. Lam, (1979). *J. Polym. Sci., Polym. Lett. Ed.*, 17, 759.
- [74] C.G. Roffey, (1982). *Photopolymerisation of Surface Coatings*, Wiley - Interscience, Chap.4.
- [75] A. J. Bard and H. Lund, (1978). *Encyclopedia of Electrochem. of the Elements. Organic section*, Vol.XIV, Marcel Dekker.